Investigating endocannabinoid signalling using a novel cell reporter assay

Lu, Leanne

Awarding institution:
King's College London

KING'S College LONDON

Institute of Psychiatry, Psychology & Neuroscience

Investigating endocannabinoid signalling using a novel cell reporter assay

A thesis for the degree of Doctor of Philosophy

Leanne Lu

Wolfson Centre for Age-Related Diseases

King's College London

Abstract

The endocannabinoid (eCB) system consists of cannabinoid receptors 1 and 2 (CB1 and CB2) that are activated by two well characterised lipid ligands, namely 2-arachidonoylglycerol (2-AG) and N-arachidonyl ethanolamine (AEA). 2-AG is synthesised by the diacylglycerol lipases (DAGLα and β), however these enzymes also synthesise other related lipids including 2-linoleoylglycerol (2-LG). The synthetic pathway for AEA synthesis is less clear. N-acylphosphatidylethanolamine-specific phospholipase D (NAPEPLD) is the most studied enzyme that can make AEA, however genetic knockout of NAPEPLD from animal models has little impact on AEA levels. More recently, a calcium activated N-acyl transferase (CaNAT) called PLA2G4E has been identified as a key regulatory enzyme in the AEA pathway.

In this thesis, three key questions have been addressed. Firstly, a detailed study using a CB1 reporter cell assay was undertaken to test whether 2-LG can signal via the CB1 receptor and/or modulate the activity of eCBs. The results clearly showed that 2-LG is a novel CB1 receptor partial agonist capable of signalling on its own, and also capable of modulating eCB signalling. Using the same human osteosarcoma reporter cell assay, the hypothesis that a nine amino acid peptide Hemopressin is an antagonist for the CB1 receptor was tested. Hemopressin failed to inhibit CB1 activation stimulated by a synthetic CB1 agonist, or the response stimulated by 2-AG and AEA. Finally, the CB1 reporter cell assay was utilised to measure activation of the receptor in response to stimulation by calcium or by direct activation of PKA or PKC, presumably as a consequence of the regulated synthesis of one or more eCBs. The CRISPR/Cas9 system was then used to systematically knockout the DAGLs that are involved in the generation of 2-AG. The results from this section confirmed that the DAGLs are responsible for over 90% of 2-AG synthesis in the cells and that in some circumstances they can contribute to eCB signalling. However robust eCB signalling is still found in their absence, possibly mediated by AEA. Interestingly, genetic deletion of NAPEPLD had no impact on AEA levels or eCB signalling. The cells do not express detectable levels of PLA2G4E suggesting that an as yet to be discovered enzyme is responsible for AEA synthesis in the cells. I identified PLA2G4B as a possible candidate, however genetic deletion of this also had no impact on AEA levels or eCB signalling.

Acknowledgements

This thesis is dedicated to Dr Fiona Howell and Henry Wong, both of whom gave me much hope and motivation during my studies and are both dearly missed.

I want to thank my supervisor Professor Pat Doherty for giving countless opportunities; pursuing this PhD, presenting my work at conferences and laying a foundation for my future career. I thank him immensely for his patience, guidance and support during the course of the PhD. I also thank my second supervisor Dr Gareth Williams for his insightful input into the work from which I have learnt a lot. Additionally, I want to thank Dr Michelle Roche and her staff for her assistance in mass spectrometry and Dr Mene Pangalos and Astra Zeneca for funding this project.

A big thank you to the members of the Doherty lab, I am especially grateful to Supanida Hompoonsup, a great friend who shared many joys and difficulties with me throughout our PhDs together. I am also very thankful to Dr Rachel Markwick for her assistance and companionship in the first stages of my PhD which gave me a great start. I also thank the previous members of lab – Dr Praveen Singh, Dr Ya Zhou and Dr Emma Williams and previous project students for their contribution and assistance towards the work.

I extend my thanks to my colleagues, the staff and students of the Wolfson CARD, members of Bateman lab, Steel lab and Raouf lab, Dr Caroline Formstone, Brenda Williams, John Chesson, Carl Hobbs and John Grist for their support in the last two years.

Finally, I would like to thank my King's College London friends for all their support during the PhD and during my undergraduate studies, which has made my years at King's very memorable. Lastly I would like to thank my family, particularly to my sister Joanne Lu who has always been there to encourage me and without whom none of this would have been possible.

Table of Contents

Table of Figures

Table of Tables

Abbreviations

A	AA	Arachidonic Acid
	ABHD4	α/β-Hydrolase 4
	ABHD6	αβ-Hydrolase Domain-Containing Protein 6
	ABPP	Activity-Based Protein Profiling
	AC	Adenylyl Cyclase
	ACEA	Arachidonyl-2'-Chloroethylamide (CB1 Agonist)
	2-AG	2-Arachidonylglycerol
	AM251	CB1 Antagonist
	AmpSeq	Amplification Sequence
	AEA	Anandamide or *N*-arachidonoylethanolamine
	ATP	Adenosine Triphosphate
B	Bla	β-lactamase gene
	bp	Base Pair
C	C2 Domain	Calcium-sensing domain
	Calcium-assisted RER	Calcium-assisted Receptor-driven Endocannabinoid Release
	CaER	Calcium-Driven Endocannabinoid Release
	CAMKIIa	Calcium/Calmodulin-dependent Protein Kinase IIa
	cAMP	Cyclic Adenosine Monophosphate
	CAMs	Cell Adhesion Molecules
	CaN	Calcineurin
	CaNAT	Calcium-sensitive *N*-acyltransferase
	Cas	CRISPR associated proteins
	CB	Cannabinoid
	CB1	Cannabinoid Receptor 1
	CB2	Cannabinoid Receptor 2
	CCF4-AM	LiveBLAzer™-FRET B/G
	cDNA	Complementary DNA
	CIP	Calf Intestinal Phosphatase
	CNS	Central Nervous System
	COX	Cyclooxygenase
	$cPLA_2$	Cytosolic phospholipase A2
	CRISPR	Clustered Regularly Interspaced Short Palindromic Repeats
	crRNA	CRISPR array
	Ctrl	Control
D	DAG	Diacylglycerol
	DAGL	Diacylglycerol Lipase
	DAGLα	Diacylglycerol Lipase α
	DAGLβ	Diacylglycerol Lipase β
	DiFMUO	6,8-Difluoro-4-Methylumbelliferyl Octanoate
	DNA	Deoxyribonucleic acid
	DSE	Depolarisation Suppression of Inhibition
	DSI	Depolarisation Suppression of Excitation

E	eCB	Endocannabinoid
	eCB-LTD	Endocannabinoid Mediated Long-Term Depression
	eCB-STD	Endocannabinoid Mediated Short-Term Depression
	ECL	Enhanced Chemiluminescence
	EDTA	Ethylenediaminetetraacetic acid
	EET-EAs	Epoxytrienoic Acid Ethanolamides
	EET-Gs	Epoxytrienoic Glyceryl Esters
	EPSCs	Excitatory Postsynaptic Currents
F	FABPs	Fatty Acid Binding Proteins
	FAC	Final Assay Concentration
	FAAH	Fatty Acid Amide Hydrolase
	FBS	Foetal Bovine Serum
	FGF2	Fibroblast Growth Factor 2
	FGFR	Fibroblast Growth Factor Receptor
	FLAT	FAAH-like Anandamide Transporter
	FokI	DNA endonuclease
	FRET	Fluorescence Resonance Energy Transfer
	FSK	Forskolin
G	GABA	Gamma-Aminobutyric Acid
	GAPDH	Glyceraldehyde 3-Phosphate Dehydrogenase
	GDE 1	Glycerophosphodiester Phosphodiesterase 1
	GPCR	G-Protein Coupled Receptor
	GP-AEA	Glycerophospho-*N*-Arachidonoyl Ethanolamine
	GPR55	G-protein coupled receptor 55
	GPR119	G-protein coupled receptor 119
	gRNA	Guide RNA
H	H460	Lung cancer cell line
	HDR	Homology Directed Repair
	HEK	Human Embryonic Kidney
	HEPES	4-(2-Hydroxyethyl)-1-Piperazineethanesulfonic Acid
	HETE-EAs	Hydroxy-Ethanolamines
	HETE-Gs	Hydroxyeicosatetraenoic Acid Glyceryl Esters
	HKG	Housekeeping Gene
	Hp	Hemopressin
	HSL	Hormone Sensitive Lipase
	HRASLS	HRAS-like suppressor
	HRP	Horse Radish Peroxidase
	HSP70	Heat Shock Protein 70
I	I_A	Inactivating A-type potassium current
	INAE	Inactivation No After-potential E
	iNAT	Calcium-insensitive N-acyl transferase
	Indels	Insertions/Deletions
	IP_3	Inositol Triphosphate
	IPSCs	Inhibitory Post-Synaptic Currents
	IsoLG-PE	Isolevuglandin-modified Phosphatidylethanolamine
J	JMJD7	Jumonji domain containing 7

	JNK	c-Jun N-terminal kinases
	JZL184	MAGL Inhibitor
	JZL195	Dual MAGL & FAAG Inhibitor
K	kDa	Kilo Daltons
	KO	Knockout
	KT109	DAGL inhibitor, more selective for DAGLβ
	KT172	DAGL inhibitor, equally selective for both DAGLs
L	2-LG	2-Linoleoylglycerol
	LPS	Lipopolysaccharide
	LOX	Lipoxygenase
	LRAT	Lecithin Retinol Acyltransferase
	LTD	Long-term Depression
	LTP	Long-term Potentiation
M	MAFP	Methoxy Arachidonyl Fluorophosphonate
	MAGL	Monoacylglycerol Lipase
	MAPK	Mitogen-activated protein kinase
	MCF7	Breast cancer cell line
	MFI	Median Fluorescence Intensity
	mGluR	Metabotropic Glutamate Receptor
	mRNA	Messenger RNA
	mtCB1	Mitochondrial CB1
N	N18TG2	Mouse neuroblastoma cell line
	NADA	*N*-arachidonoyl dopamine
	NAE	*N*-Acyl Ethanolamine
	N-acylPE	*N*-Acyl Phosphatidylethanolamine
	NAPE	*N*-Arachidonyl Phosphatidylethanolamine
	NAPEPLD	NAPE Phospholipase D
	NCAD	*N*-Cadherin
	NCAM	Neural Cell Adhesion Molecule
	NHEJ	Non-Homologous End Joining
O	OEA	*N*-Oleoyl Ethanolamide
	2-OG	2-Oleoylglycerol
	OMDM-188	THL analogue, DAGL inhibitor
P	P450	Cytochrome P450
	pAEA	Phosphor-AEA
	PAM	Protospacer Adjacent Motif
	PBS	Phosphate Buffered Saline
	PC	Phosphatidylcholine
	PCR	Polymerase Chain Reaction
	PE	Phosphatidylethanolamine
	PEA	*N*-Palmitoyl ethanolamide
	2-PG	2-Palmitoylglycerol
	PGE2	Prostaglandin E2
	PG-EA	Prostaglandin Ethanolamides
	PGD2	Prostaglandin D2

	PG-Gs	Prostaglandin Glyceryl Esters
	PI	Phosphatidylinositol
	PIP_2	Phosphatidylinositol 4,5-Bisphosphate
	PKA	Protein Kinase A
	PKC	Protein Kinase C
	PLA_2	Phospholipase A2
	PLA2G4	Cytosolic Phospholipase group IV
	PLA2G4E or $cPLA_2\varepsilon$	Phospholipase A2 group IVE
	PLAAT	Phospholipase A/Acyltransferase
	PLC	Phospholipase C
	PLD	Phospholipase D
	PMA	Phorbol 12-Myristate 13-Acetate
	PNPB	4-Nitrophenyl Butyrate
	pNAPE	*N*-acylethanolamine plasmalogen
	PPAR	Peroxisome Proliferators Activated Receptor
	PTPN22	Protein tyrosine phosphatase, non-receptor type 22
Q	qPCR	Quantitative PCR
R	RER	Receptor-Driven Endocannabinoid Release
	RMS	Rostral Migratory Stream
	RNA	Ribonucleic Acid
	rpm	Revolutions Per Minute
	RT-PCR	Reverse Transcription Polymerase Chain Reaction
S	SCP	Sterol carrier protein
	SDS	Sodium Dodecyl Sulfate
	SDS-PAGE	SDS-Polyacrylamide Gel Electrophoresis
	SEA	Stearoyl Ethanolamine
	SEM	Standard Error of the Mean
	sgRNA	Single Guide RNA
	SHSY5Y	Bone marrow Neuroblastoma
	SVZ	Sub-Ventricular Zone
	STD	Short Term Depression
T	TALENs	Transcription Activator-Like Effector Nucleases
	TAE	TRIS-Acetate-EDTA buffer
	TBI	Traumatic Brain Injury
	Δ^9-THC	Δ^9-Tetrahydrocannabiniol
	THL	Tetrahydrolipstatin
	tracrRNA	Trans-activating crRNA
	TRPV1	Transient Receptor Potential Vanilloid Type-1
	TXB2	Thromboxane B2
U	U2OS	Human Osteosarcoma Cell Line
	URB579	FAAH Inhibitor
	UTR	Untranslated Region
W	WT	Wild Type
Z	ZFNs	Zinc Finger Nucleases

Chapter 1. Introduction

1.1 History of cannabinoid research

1.1.1 Origins of cannabinoid research

Indigenous to central and South Asia, the cannabis plant *Cannabis sativa* has been used for cultural and religious purposes by numerous civilisations, with the earliest discovery of its cultural use dating back to around 2700 BC when it was found in a grave of a Chinese shaman (Russo et al., 2008). The earliest reference to its medicinal properties was described in a compendium dedicated to the Emperor of China Shen Nung (Li, 1974), but the therapeutic use of cannabis was introduced into western medicine by British physician William O'Shaughnessy (O'Shaughnessy, 1843). His observations of the analgesic, antiemetic and anticonvulsant properties of a local preparation of cannabis on rheumatism, tetanus and rabies led to the expansion of the therapeutic use of cannabis. Since then, medicinal cannabis has been used for the treatment of many ailments such as pain, asthma, and dysmenorrhea (Mikuriya, 1969; Baker et al., 2003).

The biological effects of cannabis are well known: cannabis induces a psychoactive effect with altered perception, euphoria and impairment of short-term memory. In some limited cases of chronic use, it can also induce anxiety, panic, and paranoia. Cannabis can also cause physiological effects such as an increase in heart rate, a lowering of blood pressure due to vasodilatation, appetite stimulation, dry mouth, and dizziness (Kumar et al., 2001). The psychoactive side-effects however limited the therapeutic potential of its use until the constituents of the plant were known.

1.1.2 Isolation of active phytocannabinoids

The effort to identify the active constituents of cannabis began in the late 20th century and the *Cannabis sativa* plant itself contains many different active compounds. Cannabis is a source of over 70 compounds now known as phytocannabinoids (ElSohly and Slade, 2005), but the major psychoactive ingredient Δ^9-tetrahydrocannabinol (Δ^9-THC) was first isolated by Gaoni and Mechoulam in 1964 in its pure form, and its structure was elucidated (Gaoni

and Mechoulam, 1964). Cannabidiol is one of the main non-psychoactive component of cannabis which may have therapeutic potential itself in the treatment of epilepsy and other neuropsychiatric disorders (Devinsky et al., 2014). Strains of cannabis plant with higher levels of Δ^9-THC and lower levels of cannabidiol tend to exert more negatively associated psychotropic effects when consumed (Watson et al., 2000), and through years of investigation the psychotropic effects of cannabis could indeed be attributed essentially just to Δ^9-THC (Hollister, 1974). Δ^9-THC also exerts effects on other biological systems other than the nervous system, such as the suppression of immune responses and causing vasodilatation in the cardiovascular system (Dewey, 1986). However, the mechanism of these actions of Δ^9-THC remained elusive for several years after its discovery due to the highly lipophilic properties of cannabinoids delaying experimental procedures.

1.1.3 Identification of cannabinoid receptors

The highly lipophilic properties of cannabinoids and Δ^9-THC were originally thought to be responsible for the effects of cannabis by interfering with membrane fluidity. However, the presence of a specific binding site for Δ^9-THC as the mechanism of action was proposed by several investigators in the 1970s. This was derived from the varying potencies of several structurally related cannabinoids and stereoisomers of Δ^9-THC, which are indicative of a specific and selective site-mediated response (Mechoulam et al., 1998). By the 1990's, novel potent and selective synthetic analogues of radiolabelled Δ^9-THC such as HU-210 (Mechoulam et al., 1990) and CP-55,940 (Pfizer in 1974) were developed. Radiolabelled CP-55,940 was found to bind in a highly specific and selective manner to cortical membrane preparations from rat brain (Devane et al., 1988), with dense binding of [^{3}H] CP-55,940 in the striatum of the basal ganglia, substantia nigra pars reticulata and globus pallidus, the cerebellum, the dentate gyrus of the hippocampus, as well as the cerebral cortex (Herkenham et al., 1990). This discovery was shortly followed by the cloning of the cannabinoid receptor 1 (CB1) from rat brain cDNA library (Matsuda et al., 1990) and from a human cDNA library (Gerard et al., 1991) and the cannabinoid receptor 2 (CB2) from a human leukemic cell line (Munro et al., 1993).

The cannabinoid receptors are seven transmembrane G-protein coupled receptors (GPCRs) and share approximately ~48% homology (68% identity for the TM domains) (Howlett, 2002). The downstream effects of cannabinoid receptor activation are mediated through the pertussis toxin-sensitive $G_{i/o}$ proteins. The G_i alpha subunit inhibits the production of cyclic

adenosine monophosphate (cAMP) by the inhibition of adenylate cyclase, which in turn causes increased mitogen-activated protein kinase (MAPK) activity, and this is the fundamental downstream signalling cascade of the cannabinoid receptors (Howlett et al., 1986). The second messenger cAMP also interacts in many other signalling proteins such as protein kinase A (PKA), protein kinase C (PKC), c-Jun N-terminal kinases (JNKs), as well as regulating calcium and potassium ion channels (Pagotto et al., 2006), linking the cannabinoid receptors to a wide range of cellular processes in many different cell types (Pertwee, 1997; Bosier et al., 2010).

The biological effects of certain cannabinoids are not fully mediated by classical CB1 or CB2 receptors, suggesting the presence of non-classical CB receptors (Di Marzo, 2018). These non-classical CB receptors are responsive to cannabinoids but do not necessarily share sequence homology to CB1 and CB2 receptors. Orphan GPCRs have been put forward as potential cannabinoid receptors: G-protein coupled receptor 18, 55 and 119 (GPR18, GPR55 and GPR119) (Morales and Reggio, 2017). GPR18 (McHugh et al., 2012), GRP55 (Baker et al., 2006; Ryberg et al., 2007) and GPR119 (Overton et al., 2006) are responsive to cannabinoid ligands, including Δ^9-THC, despite having low sequence homology to CB1 and CB2 receptors, however their physiological function requires further clarification. Other non-classical CB receptors include transient receptor potential of vanilloid type-1 (TRPV1) (Zygmunt et al., 1999; Smart et al., 2000) and the peroxisome proliferators activated receptors (PPAR) (Burstein, 2005; Rockwell et al., 2006).

1.2 Physiological functions of the CB receptors and eCB system

1.2.1 Cannabinoid receptor expression

The identification of the two cannabinoid receptors enabled further studies into the mechanisms behind the physiological effects of cannabinoids. The CB1 receptors from rat, mice and human species share 97-99% homology and is highly expressed in the mammalian central nervous system (CNS) (Herkenham et al., 1990; Howlett et al., 2002). In 1999, transgenic mice bearing genetic deletion of the CB1 receptor were generated (Ledent et al., 1999; Zimmer et al., 1999). The mice lacked responsiveness to cannabinoid drugs and the CB1 receptor was demonstrated to be a mediator of analgesia, hypotension and hypothermia as well as having an involvement in feeding behaviour and the motivational aspects of opiates.

CB1 is the most abundant GPCR in the mammalian brain. An immunohistochemical study using an antibody targeting the intracellular C-terminal tail of the receptor confirmed the expression of CB1 receptor in the cerebellum, hippocampus, basal ganglia, olfactory bulb and the neocortex in rat brain, which are mainly localised in nerve fibre systems and axon terminals (Egertova and Elphick, 2000). The expression of CB1 receptors in the brain correlate well with the well-known psychological effects of cannabis on motor coordination and short-term memory processing (Howlett et al., 2002). CB1 receptors are also expressed in non-neuronal CNS tissues in the periphery, including the neuromuscular junction and dorsal root ganglion cells where it may mediate pain sensation (Hohmann and Herkenham, 1999; Howlett, 2002) and also on peripheral organs such as the liver, small intestine and reproductive organs (Matias and Di Marzo, 2007).

The creation of a CB2 knockout (KO) mice revealed the CB2 receptor is predominantly expressed in tissues with immunological function such as in the spleen, tonsil and lymph nodes (Buckley et al., 2000). The CB2 receptor is abundantly expressed in B cells, monocytes, neutrophils and T cells where it may have a role in the regulation of immune responses and/or inflammatory reactions such as cytokine release (Munro et al., 1993; Galiegue et al., 1995; Howlett, 2002). It was originally thought that CB2 receptors have no functional role in the CNS, however lower levels of CB2 receptors are found in restricted areas in the CNS, for

example in microglial cells (Howlett et al., 2002; Pertwee, 2005) and also in neurons (Van Sickle et al., 2005; Gong et al., 2006; Li and Kim, 2015).

1.2.2 Discovery of the endocannabinoids

The identification and characterisation of the cannabinoid receptors implied the presence of endogenous cannabinoid ligands that could activate these receptors, leading to the search for endocannabinoids (eCBs). The lipophilic nature of the phytocannabinoids provided insight into the possible lipid nature of the eCBs and through studies using the lipid-soluble fractions of the brain, the first eCB was identified. Devane et al. (1992) found porcine brain fractions could compete with the binding of radiolabelled cannabinoid probe [^{3}H] HU-243 on rat synaptosomal membranes and subsequent chromatography of the brain fractions allowed them to isolate and identify the first putative eCB. This was the lipid N-arachidonyl ethanolamine (AEA), also known as anandamide from the Sanskrit word *ananda* meaning 'bliss' (Devane et al., 1992).

AEA belongs to a family of N-acyl ethanolamines (NAEs) which has been extensively studied and reviewed (Schmid and Berdyshev, 2002; Ueda et al., 2013). AEA bound to CB1 receptors potently (K_i = 52nM) and shared the ability with synthetic CB1 agonists to inhibit electrically evoked contractions of the mouse isolated vas deferens twitch assay. It was also demonstrated that AEA administrations reduces spontaneous motor activities, and results in immobility, hypothermia and analgesia in mice, very similarly to the effects of the phytocannabinoid Δ^9-THC (Devane et al., 1992). To date, many studies have shown AEA to exhibit a variety of effects via the CB1 receptor *in vitro* and *in vivo* (reviewed in Mechoulam et al., 1998; Sugiura et al., 2002).

However, there are some unresolved issues about the physiological role of AEA as an eCB to the CB receptors. For example, whilst AEA binds potently to the CB receptors, it acts as a partial agonist to the CB receptors in some studies which is unusual for an endogenous agonist (Mackie et al., 1993; Burkey et al., 1997; Sugiura et al., 2002). Indeed, AEA was later revealed to also act as a full agonist at TRPV1 receptors (Zygmunt et al., 1999; Smart et al., 2000). Furthermore, AEA did not fully recapitulate the behavioural effects of Δ^9-THC, being up to 18 times less potent than that of Δ^9-THC in behavioural assays (Smith et al., 1994). The endogenous levels of AEA are relatively low in fresh brain (in the order of pmol/g tissue) in comparison to the abundance of CB1 receptors in the brain, although it is possible that AEA

is localised to certain areas of the brain (Felder et al., 1996; Sugiura et al., 2002). There are multiple synthesis pathways of AEA (described further below) with no efficient or selective preference for synthesis (Liu et al., 2008) and stimulation of these pathways generate relatively low levels of AEA as there are low levels of the precursor to AEA (Sugiura et al., 1996). Thus, AEA may have a separate primary signalling role in addition to the activities at the CB receptors and the presence of other eCB(s) were postulated.

Shortly after the discovery of AEA, 2-arachidonoylglycerol (2-AG) was identified from canine gut and was demonstrated to bind to cell membranes overexpressing CB1 and CB2 receptors (Mechoulam et al., 1995). 2-AG is a monoacylglycerol and was originally thought to be part of the synthesis pathway for arachidonic acid (AA) (Prescott and Majerus, 1983). Phospholipase C (PLC) activity on inositol phospholipids generates 1,2-diacylglycerols (DAG) which is cleaved by diacylglycerol lipase (DAGL) to release 2-AG. 2-AG was reported to displace the radioactive cannabinoid probe [^{3}H]CP-55,940 from cannabinoid receptors in rat brain synaptosomes (Sugiura et al., 1995) and caused very similar responses to Δ^9-THC such as antinociception, immobility and reduction of spontaneous activity when administered *in vivo* in mice (Mechoulam et al., 1995; Di Marzo, 1998). 2-AG had the same effect as CB1 synthetic agonists in the hippocampus, whereby 2-AG inhibited long-term potentiation (LTP), an effect that could be blocked by CB1 antagonists (Stella et al., 1997). Despite the weaker binding affinity of 2-AG for the CB1 receptor (K_i = 472nM) in comparison to AEA, 2-AG has been argued to be the true endogenous ligand for CB receptors as the levels of 2-AG are considerably (>200x) higher than AEA in the brain and functions as a full agonist to the CB receptors (Sugiura et al., 1999). In peripheral organs such as the pancreas and spleen, 2-AG is accompanied by other monoacylglycerols such as 2-linoleoylglycerol (2-LG) and 2-palmitoylglycerol (2-PG) which have been reported to potentiate the activity of 2-AG (Ben-Shabat et al., 1998), suggesting a possible endogenous mechanism for the modulation of the activity of eCBs.

The umbrella term – the eCB system is generally used to collectively describe the two most well studied eCBs (AEA and 2-AG), their main target receptors (CB1 and CB2), as well as the enzymes involved in their synthesis and degradation which will be discussed further below. The discovery of the two major eCBs, along with several pharmacological tools, to the CB receptors have pioneered the characterisation of important functional roles of CB receptors during brain development as well as in the adult brain.

1.2.3 CB receptor functions in the CNS

The psychoactive properties of Δ^9-THC and the eCBs gave insight into certain neuropathways that are possibly modulated by the CB receptors. Expression of the CB1 receptor is detected both in the neonatal and postnatal brain with distinctively separate roles in brain development and function (Berrendero et al., 1998; Marsicano and Lutz, 1999; Wang et al., 2003; Begbie et al., 2004). Expression of CB2 receptors have been reported in restricted areas of the CNS in relatively much lower levels than CB1, such as rat dorsal root ganglia neurons and neuronal progenitors (Ross et al., 2001; Palazuelos et al., 2006) as well as in in brainstem, cerebellar and hippocampal pyramidal neurons of adult mammals (Van Sickle et al., 2005; Gong et al., 2006). However, the role of the CB2 receptor in CNS functions is not fully elucidated as the focus has mainly been placed on CB1 as the mediator of CNS functions.

Development axonal growth and guidance

The damaging effects of pre-natal exposure of cannabis on the neural development of offspring has been well documented (Keimpema et al., 2013). Exceptionally high levels of Δ^9-THC doses (>100 mg/kg) may induce *in utero* death (Harbison and Mantilla-Plata, 1972) and consumption of cannabis during pregnancy can cause growth impedance, damage to brain development, and adverse neurodevelopmental outcomes (Hurd et al., 2005; Spano et al., 2007; El Marroun et al., 2009; Psychoyos et al., 2012). It was therefore no surprise that the eCB system and the CB1 receptor is involved in the formation of the CNS. Both the eCB system and the CB1 receptor has been implicated in the development of the brain, through a variety of different processes including neural progenitor cell differentiation (Aguado et al., 2005; Compagnucci et al., 2013), cell migration (Song and Zhong, 2000; Zhou et al., 2014), synapse formation (Kim and Thayer, 2001) and axonal growth and guidance (Williams et al., 2003; Oudin et al., 2011b).

One significant role of the eCB system is in axonal growth and guidance, which is the process whereby neurons send out their axons to innervate their correct targets. Immunohistochemical studies have shown the expression of CB1 receptors are highly localised to the axons and growth cones of developing neurones, and are highly correlated with the expression of the DAGLs – the synthesising enzymes for 2-AG (Buckley et al., 2000; Bisogno et al., 2003; Berghuis et al., 2007) implying a possible autocrine signalling role in axonal development. Pharmacological and/or genetic disruption of the CB1 receptor has been shown to impair various axonal processes *in vivo* and *in vitro*. For example, the Harkany lab established that specific deletion of CB1 receptor from cortical GABAergic interneurons

results in impaired target selection *in vivo* (Berghuis et al., 2007). In other studies, both genetic and pharmacological ablation of the CB1 receptor led to abnormal axon growth of pyramidal neurons in embryonic and early postnatal mice (Mulder et al., 2008), and in corticothalamic and thalamocortical projections (Wu et al., 2010). Furthermore, both pharmacological studies in chick and morpholino knock down in zebrafish embryos show CB1 function is required for normal axonal growth and fasciculation in the early nervous system (Watson et al., 2008). These studies taken together support the role of the CB1 receptor as a modulator of axonal growth and guidance during brain development.

The CB1 receptors are localised primarily at the site of axonal growth, alongside the enzymes responsible for the generation of 2-AG, which is likely to be the eCB involved in the autocrine activation of CB1 receptors in this role (Watson et al., 2008). Although AEA is also present in the developing brain, levels of 2-AG are magnitudes higher and therefore it is postulated that 2-AG is the prime eCB in the developing brain (Harkany et al., 2008). Thus, the 2-AG synthesising enzymes – the DAGLs, are likely to be the connection between the eCB system and other signalling cues to regulate axonal growth and guidance (Bouquet and Nothias, 2007).

Pharmacological studies suggested that DAGL activity is required for axonal growth and guidance in a signalling cascade following activation of the fibroblast growth factor receptor (FGFR) (Williams et al., 1994a; Brittis et al., 1996). Activation of FGFR by certain cell adhesion molecules (CAMs) such as neural CAM (NCAM), N-cadherin (NCAD) and L1, or by direct activation by fibroblast growth factor 2 (FGF2) lead to downstream signalling cascades that culminate to calcium influx into the growth cone, promoting axonal growth and guidance (Figure 1.2.1) (Williams et al., 1994c; Walsh and Doherty, 1997; Williams et al., 2003). The DAGL inhibitor RHC-80267 inhibited FGFR mediated neurite outgrowth from cultured neurons, suggesting DAGL activity is present downstream of FGFR, but upstream of calcium influx (Williams et al., 1994b; Brittis et al., 1996). Further studies revealed that FGFR stimulates neurite outgrowth through the eCB system as this can be inhibited by CB1 antagonists, DAGL inhibitors RHC-80267 and tetrahydrolipstatin (THL), as well as a PLCγ inhibitor (Bisogno et al., 2003; Williams et al., 2003). In support of these findings is the observation that the expression of the 2-AG degrading enzyme monoacylglycerol lipase (MAGL) is excluded from the growth cone and is restricted to further back along the axon, thereby allowing 2-AG to be available to activate the CB1 receptor for neurite outgrowth (Keimpema et al., 2013).

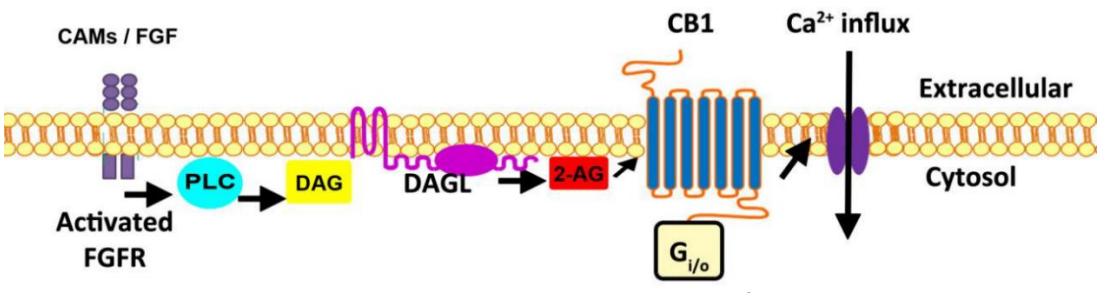

Figure 1.2.1. The role of the eCB system for axonal growth and guidance

A simplified schematic of the FGFR signalling cascade within the growth cone. Activation of FGFR by CAMs and/or FGF2 stimulates PLCγ to synthesise DAG, which in turn is hydrolysed by DAGL to generate 2-AG. This then acts on the CB1 receptor on the same growth cone leading to calcium influx via N- and L-type voltage gated calcium channels into the cell to promote motility and axonal growth.

Adapted from Zhou et al. (2014).

The role of the CB1 receptor in axonal growth and guidance has been the primary focus with the role of the CB2 receptor in the CNS in dispute. The CB2 receptor may be involved in neural stem cell proliferation in cell culture as well as in the adult mouse (Palazuelos et al., 2006; Molina-Holgado et al., 2007; Goncalves et al., 2008). It has also been recently reported that CB2 receptors may also have a modulatory role in axon guidance in retinal ganglion cells (Duff et al., 2013). Duff et al. (2013) reported CB2 receptor expression in the developing neurovisual system of mice, primarily located in the growth cones, filopodia and neurites of retinal ganglion cells. Unlike CB1 receptors, agonism of CB2 receptors caused a retraction of growth cone surface, reduced axonal growth and reduced filopodia, while antagonism of CB2 caused the converse, suggesting a contrasting modulatory effect to regulate axonal growth and guidance.

Taking together the pharmacological, genetic, and anatomical studies described above demonstrates the importance of eCB signalling and the CB receptors in axonal growth and guidance in the developing brain. After the establishment of synapses, expression of the eCB system shifts from an autocrine signalling system in axons and the growth cone to a retrograde signalling system, which correlates to a shift in function to modulation of synaptic signalling.

Synaptic plasticity and retrograde signalling

In the adult brain, both excitatory and inhibitory synapses can undergo changes and alter connection strengths between neurons. It is widely accepted that synapses strengthen or weaken over time in response to increases or decreases in their activity, and it is thought to be the underlying mechanism for learning and memory (Eccles and McIntyre, 1951; Holtmaat and Svoboda, 2009). Generally, synaptic plasticity can be divided into two forms: short-term synaptic plasticity which lasts from milliseconds to at most a few minutes, and long-term synaptic plasticity which can last from minutes to hours, or substantially longer (Citri and Malenka, 2008). Thus, there are numerous short-term and long-term changes to a synapse which can alter its connection, including the quantity of neurotransmitter released and the responsiveness of the postsynaptic site to the neurotransmitters. In the 1990s, retrograde signalling at synapses became a well-accepted phenomenon. This referred to the release of a signalling molecule from the depolarised postsynaptic site which then acts on the presynaptic terminal to suppress further neurotransmitter release (e.g. the inhibitory gamma-aminobutyric acid (GABA) and the excitatory glutamate). Retrograde signalling thus regulates release of neurotransmitters and thereby affects synaptic strength and plasticity (Regehr et al., 2009).

The development of CB1 antibodies and the generation of CB1 KO mice revealed the restricted expression of CB1 receptors to presynaptic terminals throughout the adult brain and spinal cord (Katona et al., 2006; Kawamura et al., 2006). Presynaptic expression of CB1 occurs at both excitatory and inhibitory synapses (Egertova and Elphick, 2000) which suggests the role of the CB1 receptor and eCB signalling in the regulation of synaptic function (Castillo et al., 2012; Kano, 2014).

Pharmacological studies have shown that activation of CB1 receptors can inhibit the release of various neurotransmitters (e.g. GABA, glutamate, acetylcholine) in cultured neurons as well as from slices from various parts of the brain including the hippocampus, cerebellum and the cerebral cortex (reviewed in Schlicker and Kathmann, 2001). For example, the cannabinoid agonist WIN55,212-2 was shown to suppress glutamatergic excitatory postsynaptic currents (EPSCs) which was sensitive to the CB1 antagonist SR141716A, confirming the involvement of CB1 receptors (Shen et al., 1996). Similarly, the inhibitory effects of cannabinoids on GABA release were first reported in neurons in the striatum (Szabo et al., 1998). In these neurons, WIN55,212-2 suppressed GABAergic inhibitory postsynaptic currents (IPSCs), but did not affect the postsynaptic response to exogenously

applied GABA, indicating a presynaptic site of action. The suppression of IPSCs were sensitive to the antagonist SR141716A which confirmed the involvement of CB1 receptors (Szabo et al., 1998).

Studies have shown that AEA and 2-AG can be released from postsynaptic neurons to act as retrograde messengers in distinct regions of the brain (Figure 1.2.2A) (Wilson and Nicoll, 2001; Alger, 2002). However, 2-AG is likely to be the primary eCB retrograde messenger for the CB1 receptor. The reasons for this are that the relative abundance of 2-AG is much higher in comparison to AEA, and the highly restricted positioning of the 2-AG synthesising enzymes in the postsynaptic density in close proximity to the CB1 receptors on the presynaptic density suggests 2-AG is well positioned to act as a retrograde messenger (Bisogno et al., 2003; Yoshida et al., 2006; Oudin et al., 2011a). Furthermore, inhibition of MAGL, the enzyme responsible for 2-AG degradation, but not AEA hydrolyzing enzyme fatty acid amide hydrolase (FAAH), can generally prolong the inhibition of neurotransmitter release (Hashimotodani et al., 2007).

Various stimuli can induce eCB production from the postsynaptic neuron. In 2001, several groups reported that depolarisation of the postsynaptic neuron results in suppression of the pre-synaptic release of inhibitory or excitatory neurotransmitters – termed depolarisation-induced suppression of inhibition/excitation (DSI and DSE) (Kreitzer and Regehr, 2001; Ohno-Shosaku et al., 2001; Wilson and Nicoll, 2001). This eCB mediated short-term depression (eCB-STD) was mediated by calcium influx in the depolarised postsynaptic cell which leads to the release of an eCB retrograde messenger through a yet unclarified mechanism and termed calcium-driven eCB release (CaER) (Figure 1.2.2A). CB1 antagonist AM251 blocked DSI/DSE whereas the CB1 agonist WIN55212-2 occluded DSI/DSE (Kreitzer and Regehr, 2001; Ohno-Shosaku et al., 2001; Wilson and Nicoll, 2001; Kano, 2014). In the same year, depolarisation-independent short-term depression of neurotransmitter release was also reported in the cerebellum (Maejima et al., 2001) and hippocampus (Varma et al., 2001). This was mediated by the activation of postsynaptic group 1 metabotropic glutamate receptors (mGluR1) which drives the generation of 2-AG and causes reduced neurotransmitter release in a CB1-dependent manner. This mechanism is termed receptor-driven eCB release (RER) and does not rely on a calcium influx to generate 2-AG, but activation of mGluR1 does enhance DSI/DSE (calcium-assisted RER) which can be blocked by CB1 and mGluR1 antagonists (Figure 1.2.2A) (Varma et al., 2001; Kano, 2014).

The mechanisms governing short term DSI/DSE (i.e. CaER, RER and calcium-assisted ER) also mediate long-term depression of synaptic transmission. Endocannabinoid mediated long-term depression (eCB-LTD) has been found in several areas of the brain at both excitatory and inhibitory synapses, causing long-lasting reduction in the efficiency of synapses (Heifets and Castillo, 2009). Repeated neuronal stimulation for lengthy periods (5-10 mins) causes prolonged eCB release and CB1 activation alongside additional presynaptic mechanism(s) such as presynaptic calcium influx to cause LTD (Figure 1.2.2B) (Collingridge et al., 2010; Kano, 2014). The presynaptic mechanisms of eCB-LTD have not been fully elucidated but inhibition of the downstream cAMP/PKA pathway seems to be crucial (Castillo et al., 2012; Ohno-Shosaku et al., 2012). For example, the presynaptic elevation of calcium can activate a phosphatase calcineurin which dephosphorylates target proteins (Figure 1.2.2B). In tandem, the activation of CB1 receptors causes a decrease in cAMP levels and PKA activity, leading to a reduction in phosphorylated target proteins. The resulting decrease in phosphorylation of target proteins causes suppression of transmitter release selectively from presynaptic terminals that have been active during CB1 activation (Heifets et al., 2008; Ohno-Shosaku et al., 2012).

Figure 1.2.2. Molecular mechanisms of eCB-STD and eCB-LTD

Schematic of the molecular mechanism of eCB-STD is shown in (A). Calcium-driven eCB release (a, CaER) occurs when a large calcium elevation is caused by activation of voltage-gated calcium channels or NMDAR and 2-AG is generated by DAGL-dependent manner. The method by which elevated calcium levels lead to 2-AG synthesis via DAGL remains unclear. Receptor-driven eCB release (b, RER) occurs through activation of $G_{q/11}$-coupled receptors. Upon receptor activation, PLCβ is stimulated to generate DAG, which is then converted to 2-AG by DAGL. Through the combination of subthreshold activation of $G_{q/11}$-coupled receptors and small calcium elevation, 2-AG is produced through the PLCβ-dependent pathway because the receptor-driven PLCβ stimulation is calcium dependent (c, Ca-assisted RER). 2-AG is released from postsynaptic neurons, activates presynaptic CB1 receptors, and induces transient suppression of transmitter release.

Schematic of the molecular mechanism of eCB-LTD is shown in (B). Stimulation of the post synaptic $G_{q/11}$-coupled receptors drives the generation of 2-AG synthesis through the PLCβ-DAGL pathway which can be enhanced by concomitant calcium elevation, but is not always necessary for eCB-LTD induction at some synapses. Activation of the presynaptic CB1 receptor by 2-AG inhibits adenylyl cyclase (AC), which decreases cAMP levels and reduces PKA activity. Presynaptic activity causes calcium elevation, which activates a phosphatase, calcineurin (CaN). In concert with reduced PKA activity, calcineurin dephosphorylates of target proteins (X), and induces persistent suppression of transmitter release, through yet unclarified mechanisms.

Adapted from Kano (2014).

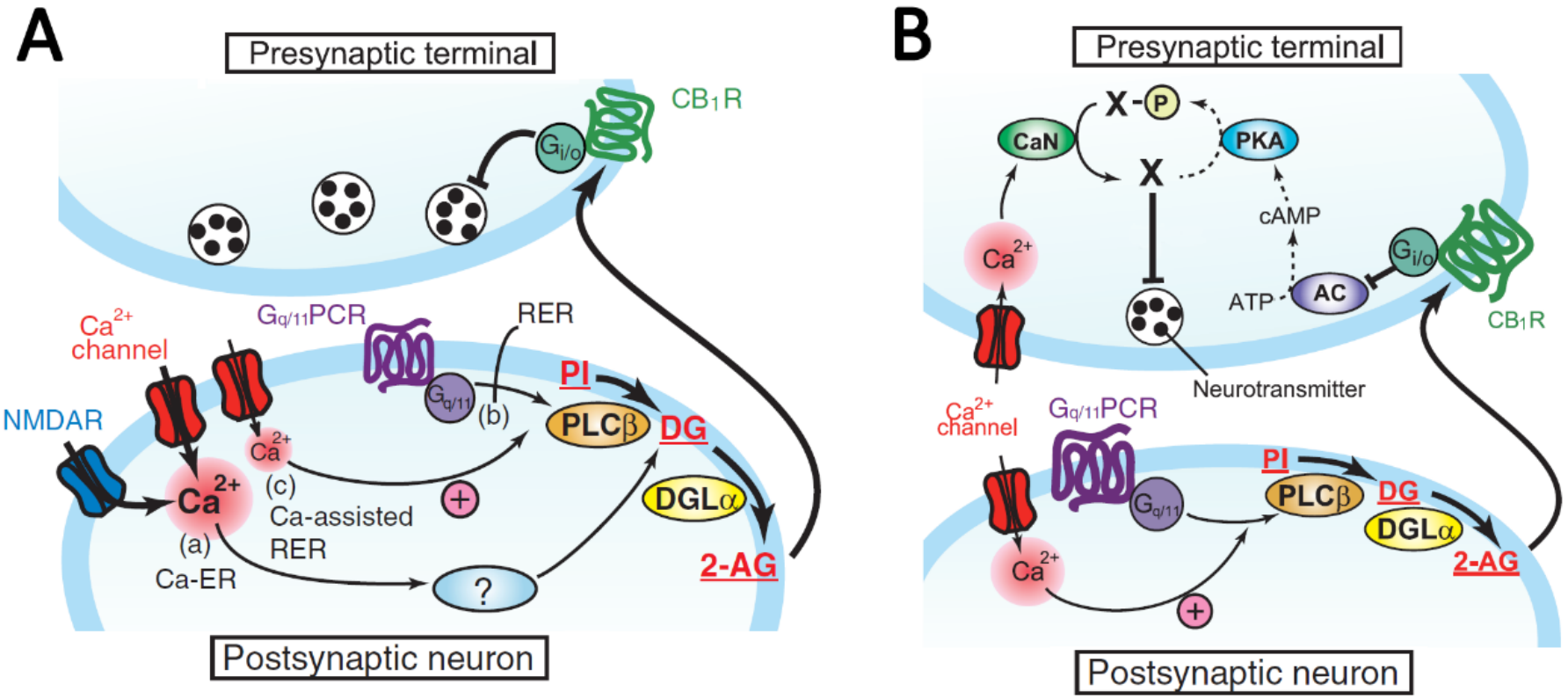
A
Presynaptic terminal
CB1R
Gi/o
Ca2+ channel
Gq/11PCR
RER
PI
NMDAR
Gq/11
(b)
PLCβ
DG
Ca2+
(c)
Ca-assisted RER
DGLα
Ca2+
(a)
Ca-ER
?
2-AG
Postsynaptic neuron
B
Presynaptic terminal
X-P
CaN
PKA
X
cAMP
Ca2+
Gi/o
ATP
AC
CB1R
Neurotransmitter
Ca2+ channel
Gq/11PCR
PI
Gq/11
PLCβ
DG
DGLα
Ca2+
2-AG
Postsynaptic neuron

It is possible that CB2 receptors may be present in distinct neuronal populations and play a similar but complementary role to CB1 receptor in modulating neurotransmitter release and hence, network activity. When CB2 receptors were expressed in cultured CB1 KO mice autaptic hippocampal neurones, DSE was restored indicating that CB2 receptors can also possess similar functions to CB1 receptors (Atwood et al., 2012). In support of this, CB2 receptors have been suggested to function in conjunction to CB1 receptors in the medial entorhinal area of rat brain in mediating DSI (Morgan et al., 2009). Genetic deletion of CB2 receptor in mice also revealed decreases in excitatory synaptic transmission and long-term potentiation in the hippocampus, which could suggest that CB2 might also have distinctly different synaptic functions to CB1 (Li and Kim, 2016). The precise location of endogenous CB2 receptors are reported to be present on postsynaptic densities in the hippocampus rather than presynaptic densities where CB1 receptors are primarily located (Brusco et al., 2008). However, due to the low level of expression of CB2 receptors in the CNS overall, the physiological contribution of CB2 to synaptic function is not fully elucidated.

Adult Neurogenesis

Neurogenesis is the generation of new functional neurons from neural stem cells and neural progenitors in the brain and are added to existing circuitry throughout life. This process is most active during prenatal CNS development, but declines rapidly after birth and is restricted to certain niches in the post-mitotic adult brain (Sanai et al., 2011). Adult neurogenesis was first described in the 1960s by Joseph Altman, who reported new neurons were generated in adult rat hippocampus (Altman and Das, 1965) and also subsequently reported neurogenesis in the adult olfactory bulb (Altman, 1969). After a contentious beginning, neurogenesis is now known to constitute a form of cellular plasticity in the developed brain that impacts on memory, depression and neurodegenerative diseases and thus, has wide therapeutic applications (Arvidsson et al., 2002; Zhao et al., 2008).

Neurogenesis occurs in mainly in two areas of the mammalian adult brain: in the sub-granular zone in the dentate gyrus of the hippocampus and in the sub-ventricular zone (SVZ) of the lateral ventricle (Alvarez-Buylla and Garcia-Verdugo, 2002; Vadodaria and Jessberger, 2014). In the adult hippocampus, the neural stem cells form dentate granule cells that integrate into the local circuitry associated with the formation of new memories and in the SVZ, stem cells produce migratory neurons which traverse through the rostral migratory stream (RMS) to the olfactory bulb where they integrate. In humans, adult neurogenesis has

been described in the hippocampus (Eriksson et al., 1998; Ihunwo et al., 2016), the lateral ventricles (Sanai et al., 2004) and more recently in the striatum (Ernst et al., 2014).

Several lines of study have implicated the eCB system to be involved in adult neurogenesis (reviewed in Prenderville et al., 2015). The expression of the CB receptors and the DAGLs are detected in the rat dentate gyrus and the SVZ (Morales and Backman, 2002; Goncalves et al., 2008; Xapelli et al., 2013). Neural progenitor cells and neural stem cells also express both CB1 and CB2 receptors (Aguado et al., 2005; Jiang et al., 2005; Molina-Holgado et al., 2007; Compagnucci et al., 2013; Xapelli et al., 2013) and both CB1 and CB2 agonists have been found to promote proliferation/neurogenesis in neural progenitor cells and neural stem cells *in vivo* and *in vitro*. For example, chronic administration of CB1/CB2 agonist HU-210 (Jiang et al., 2005) or CB2 selective agonist HU-308 (Palazuelos et al., 2012) enhances both proliferation and survival of cells in the rat dentate gyrus. This effect is reversed by CB1 and CB2 antagonists (Palazuelos et al., 2006; Molina-Holgado et al., 2007; Rubio-Araiz et al., 2008). The pharmacological inhibition of the 2-AG synthesising enzymes in adult mice over 7 days resulted in a significant decrease (~50%) in new neurons formed in the olfactory bulb post drug administration (Goncalves et al., 2008), indicating the effects of neurogenesis in the SVZ is mediated by the activity of the eCBs on the CB receptors.

Furthermore, a number of genetic studies have targeted enzymes involved in the biosynthesis and degradation of eCBs (Aguado et al., 2005; Gao et al., 2010), in addition to CB1 receptor (Jin et al., 2004) and CB2 receptors (Palazuelos et al., 2006), and have placed the eCB system as a key player in the processes underlying adult neurogenesis. The genetic knockdown of the enzyme responsible for AEA degradation increases cell proliferation (Aguado et al., 2005), whilst the KO of the 2-AG synthesising enzymes in adult mice reduced cell proliferation (~20-30%) in the hippocampus (Gao et al., 2010). A 50% reduction in adult neurogenesis was also observed in the dentate gyrus and SVZ of adult CB1 KO mice (Jin et al., 2004) whilst in CB2 KO mice showed ~50% decrease in proliferation rate (Palazuelos et al., 2006), indicating both CB receptors and eCBs are involved in mediating neurogenesis in the hippocampus and SVZ.

After the generation of new neuroblasts in the SVZ, these cells must migrate through the rostral migratory stream to the olfactory bulb and differentiate into mature neurons. Recently, the eCB system has also been shown to play a prominent role in neuroblast migration in the RMS of young adult mammals (Oudin et al., 2011b). Administration of CB1 and CB2 antagonists to cultured neuroblasts dramatically changed the morphology of the

migratory cells to a non-migratory phenotype. As well as this, DAGL inhibition caused shortening and branching of the leading process from the neuroblasts and decreased cell migration rates (Goncalves et al., 2008; Oudin et al., 2011b). Based on both pharmacological and KO studies, it has been demonstrated that the eCB system plays a fundamental role in adult neurogenesis in both the SVZ and hippocampus and neuronal migration in the SVZ which impacts on the number of proliferating neuronal stem cells in the adult brain.

Adult neurogenesis declines in the hippocampus (Marchalant et al., 2009) and in the SVZ with age in both the mouse (Goncalves et al., 2008) and the adult brain (Knoth et al., 2010), which may be due to an overall decline in eCB signalling that may account for age-related deterioration in neurogenesis. In support of this, 20-month-old mice – which have negligibly detectable levels of cell proliferation, were treated with CB1 agonist WIN55,212-2. The effects of WIN55,212-2 stimulated a ~6-fold increase in cell proliferation, returning proliferation levels to the levels of a 6-month old mouse (Goncalves et al., 2008). Furthermore, administration of WIN55,212-2 for 3 weeks partially restored neurogenesis in the hippocampus of aged rats (Marchalant et al., 2009). These experiments reveal the dependence of the eCB system in neurogenesis especially in old age and may be subject to influence from lifestyle circumstances such as diet. Therefore, targeting the eCB system is of therapeutic interest in the potential treatment of neurodegeneration.

1.2.4 Pathological and therapeutic perspective of the eCB system

The eCB system is involved in many roles throughout life, both within the CNS as previously described and in many peripheral physiological roles such as GI motility, modulation of the immune system and in the regulation of bone turnover (reviewed in Maccarrone et al., 2015). Therefore, abnormal regulation of the eCB system often results in disease phenotypes such as anxiety and depression, pain, fatty liver disease, obesity and osteoporosis (Di Marzo, 2008b; Sophocleous et al., 2017a; Capasso et al., 2018; Martin et al., 2018). Indeed, rare genetic variants of the CB1 receptor and the 2-AG synthesising enzyme DAGLα are associated with various neurological phenotypes in humans such as pain sensitivity (especially migraine), sleep and memory disorders and prevalence of seizures (Smith et al., 2017). Hence, it is not surprising that the eCB system provides a promising target for therapeutics in various disease states.

Brain injury and therapeutic potential

The eCB system has been reported to provide neuroprotective effects in cases of brain damage such as in ischemia or Alzheimer's disease (Fowler et al., 2010; Paloczi et al., 2017). Levels of AEA and 2-AG have been reported to be elevated after brain injury and damage (Natarajan et al., 1986; Hansen et al., 2001b; Panikashvili et al., 2001) which may reflect a self-neuroprotective response.

Exogenously applied CB receptor agonists have been shown to exert neuroprotection in various *in vitro* and *in vivo* models of neuronal injury (reviewed in Sarne and Mechoulam, 2005; van der Stelt and Di Marzo, 2005b). For example, 2-AG levels were elevated in the brains of mice following closed head injury and when synthetic 2-AG was administered, significant reductions in brain oedema and hippocampal cell death was observed with noticeable improved clinical recovery. These effects were dose dependent and could be antagonised by CB1 receptor antagonist SR1417161, indicating a protective role of the eCB system in damage and repair (Panikashvili et al., 2001). As well as this, application of AEA was found to reduce the infarct volume in an *in vivo* model of acute neuronal injury caused by ouabain-induced excitotoxicity (van der Stelt et al., 2001). AEA was also shown to be neuroprotective following inflammation-induced neuronal damage by engaging CB receptors on microglial cells which prevents their activation (Eljaschewitsch et al., 2006). Thus, levels of both eCBs are elevated in response to different brain injuries and may play a role in brain function homeostasis.

The neuroprotective effects of the eCBs can be attributed to the activity of the CB receptors. In CB1 receptor KO mice, more severe symptoms were present after cerebral ischemia, such as larger infarct size and a higher mortality rate (Parmentier-Batteur et al., 2002) and recovery from closed head injury was slower in CB1 receptor KO mice compared to wild type (WT) mice (Panikashvili et al., 2001). In experimental models of Alzheimer's disease, stimulation of CB1 and CB2 prevented microglial activation and microglia-mediated neurotoxicity and neurodegeneration (Ramirez et al., 2005). The activation of CB receptors have also been shown to be beneficial in other neurodegenerative diseases such as in Parkinson's disease, multiple sclerosis, and HIV-associated dementia (Centonze et al., 2007).

CB1 receptor mediated neuroprotective activity likely occurs via the prevention of excitotoxicity by the inhibition of glutamate release from neurones. However, other forms of eCB mediated neuroprotection that are independent of the CB1 receptor also exists. For example, 2-AG has antioxidant effects which suppresses the formation of reactive oxygen

species (McCarron et al., 2003). As mentioned previously, eCBs may activate CB receptors on microglial cells and prevent their activation; thus, supressing the inflammatory response and preventing further pathological cascades (Ramirez et al., 2005).

However, in some cases the eCB mediated mechanisms and the activation of CB1 receptors can have a neurotoxic effect as well. For example, activation of the CB1 receptors also exert detrimental effects on dopamine cell survival by potentiating the toxic effects of the TRPV1 agonist capsaicin (Kim et al., 2005). It is therefore conceivable that activation of both TRPV1 and CB1 receptors by AEA might contribute to Parkinson's disease pathophysiology by favouring apoptosis of dopamine neurons. As well as this, elevation of intracellular calcium levels is suggested to be one of the main causes for neuronal cell death, and cannabinoids can either stimulate or inhibit calcium entry into the cell, depending on their concentration. Low doses of cannabinoids will induce cell death, while high doses of cannabinoids will protect from neuronal loss, leading to a dual aspect of cannabinoid pharmacology (Sarne and Keren, 2004; Sarne and Mechoulam, 2005). Therefore, further research is needed to determine the subtle details of which aspects of eCB signalling are neuroprotective.

As well as neuroprotective effects of the eCB system in brain injury, the eCB system is involved in adult neurogenesis and can promote neuroblast migration, which may be of therapeutic interest as some studies have suggested that the progenitor cells produced by the SVZ can migrate out of the RMS to the site of brain injury (Arvidsson et al., 2002; Goings et al., 2004; Romanko et al., 2004; Sundholm-Peters et al., 2005). Overall, the eCB system is not only an attractive therapeutic target for early neuroprotection by reducing excitotoxicity and preventing microglial activation after injury, but also for replacing damaged neurones after injury or in neurodegenerative diseases.

TBI and osteoporosis

As mentioned above, levels of 2-AG and AEA are increased following neuronal injury which may have neuroprotective roles. Traumatic brain injury (TBI) is the disruption of brain activity due to an external force or violent blow to the head which can lead to a series of physical, cognitive, social, emotional, and behavioural impairments depending on the severity which is based on the length of time of lost consciousness (Yu et al., 2014). One interesting discovery from the studies of TBI in addition to neurological impairment is the dysregulation of peripheral bone turnover, which suggests the central involvement of the eCB system in bone maintenance. In fact, TBI is the beginning of an ongoing, and possibly lifelong, process

that impacts multiple organ systems including bone that can be distal to the site of injury (Bajwa et al., 2018).

Bone maintenance relies on the balanced action of osteoblasts – cells that form bone, and osteoclasts – cells that absorb bone (Manolagas, 2000). This balance is orchestrated through central control, mainly through the sympathetic nervous system which is partially regulated by the endocannabinoid system (Ishac et al., 1996; Idris and Ralston, 2012). CB2 receptors are present in osteoblasts and osteoclasts, stimulating bone formation and inhibiting bone resorption respectively in the cells when activated (Idris et al., 2008). CB1 expression is extremely low in bone cells but is expressed in bone sympathetic nerve fibres which innervate the cancellous bone (Tam et al., 2006). CB2 KO mice have a low bone mass phenotype, indicating the role of the CB2 receptor in bone formation (Ofek et al., 2006). The results from CB1 KO mice are more contentious: mice from a C57BL/6J background have low bone density, in part because of a substantial decrease in their bone formation (Tam et al., 2006) whilst mice from a CD1 background have a high bone density phenotype which is gender specific (Idris et al., 2005). The discrepancy could result from genetic differences between the background strains which can provide insight into a genetic basis of osteoporosis. Nonetheless, the results from the generation of KO mice revealed the involvement of CB receptors in the balance of bone remodelling.

In mice from a C57BL/6J background, there is mounting evidence linking the association between TBI and enhanced osteogenesis which leads to heterotopic ossification (the growth of bone tissue outside of the skeleton) and enhanced fracture healing and bone density (Melamed et al., 2002; Locher et al., 2015; Bajwa et al., 2018). The mechanisms underlying osteogenesis following TBI is not fully understood, but the involvement of the eCB system has been reported (Tam et al., 2008). Following TBI, the levels of eCBs 2-AG and AEA in cancellous bone increases, which may be from two sources: local production by bone cells which can produce comparable levels of 2-AG as in the brain, or from the release of eCBs from sympathetic nerve terminals following TBI damage. The release of eCBs from the sympathetic nerve cells could result from brain injury; hence, the mechanisms underlying the increase in both brain and bone eCBs levels after neuronal injury may be similar (Tam et al., 2008). The increase in eCB levels activate the CB1 receptors expressed on sympathetic nerve endings which inhibit the release of noradrenaline (Ishac et al., 1996). Noradrenaline released from sympathetic fibres inhibits bone formation and stimulates bone resorption

(Takeda et al., 2002). Therefore, activation of CB1 alleviates tonic inhibition of bone formation by the sympathetic nervous system leading to osteogenesis (Tam et al., 2008).

The discovery of the involvement of centrally and locally released eCBs following TBI in osteogenesis gives therapeutic potential to skeletal disorders such as osteoporosis. Whilst the evidence from animal studies are contentious depending on which model is used, observations in humans have shown that heavy use of recreational cannabis, which can activate both CB1 and CB2 receptors, is associated with low bone mineral density and increased bone turnover (Sophocleous et al., 2017b). As well as this, the loss of both CB1 and CB2 receptors in mice reduced age-related bone loss when compared with WT mice due to a reduction in osteoclast number (Sophocleous et al., 2017a). Further elucidation of the involvement of the eCB system in bone remodelling could provide interesting therapeutic targets, both centrally and locally, in the treatment of injury induced osteogenesis and age-related osteoporosis.

Given the importance of the roles of the eCB system in many physiological roles in the body and its therapeutic potential, a complete comprehension of the signalling pathway is needed to fully understand underlying mechanisms in disease phenotypes and for drug discovery efforts. Previous drug discovery efforts targeting the CB receptors are hindered by unwanted neurological side effects, for example the small molecule CB1 antagonist Rimonabant was approved for the treatment of obesity; however, it was later withdrawn due to depression and suicidal ideation (Moreira and Crippa, 2009). Thus, alternative targets which can modulate CB receptor activity, particularly of CB1 as it is involved in many neuronal roles, is particularly attractive but requires full understanding of the mechanisms of action. The work in this thesis will be focused on clarifying the involvement of natural ligands to the CB1 receptor in eCB signalling and the biosynthetic routes of these endogenous ligands.

1.3 Endogenous ligands to the CB receptors – Endocannabinoids

Much of what is known about the functions of the CB receptors and the roles of the eCB system has been through the discovery of the eCBs 2-AG and AEA. Unlike other neurotransmitters that are water-soluble and stored in vesicles prior to release, the eCBs are lipid based and synthesised and released "on demand" in response to cellular changes (Marsicano et al., 2003). 2-AG and AEA are the two main eCBs most extensively studied but both are members of wider families of structurally related molecules that may also have physiological roles and/or contribute to eCB signalling (Figure 1.3.4) (Schmid et al., 1990; Ben-Shabat et al., 1998). The processes that underlie the biosynthesis of eCBs have been extensively studied for 2-AG and AEA and will be described here.

1.3.1 Anandamide Synthesis

After the identification of AEA as the first eCB, speculation arose into the synthesis pathway of AEA. Two synthesis methods were reported for the generation of AEA. First, through the combination of ethanolamine and free arachidonate which may be energy-independent or catalysed by the backwards reaction of AEA hydrolysis (Devane and Axelrod, 1994; Ueda et al., 2000). Levels of ethanolamine and free arachidonate are low in neurones and many enzymatic steps are needed to generate the free molecules, which suggest that it is not likely to be the primary method of synthesis (Di Marzo et al., 1994). However as local levels may reach high enough concentrations, this pathway cannot be rigorously ruled out (Ueda et al., 2000). The second and most accepted pathway of AEA biosynthesis occurs by release from membrane phospholipid precursors (Di Marzo et al., 1994; Cadas et al., 1996). Di Marzo et al. (1994) used [^{3}H] ethanolamine labelled cultured neurons to demonstrate that the calcium ionophore ionomycin could stimulate the synthesis of AEA. This calcium stimulated AEA synthesis begins with the transfer of a fatty acyl chain from the *sn*-1 position of membrane phospholipids such as phosphatidylcholine (PC) to phosphatidylethanolamine (PE) by a calcium-sensitive N-acyltransferase enzyme (CaNAT). The activity of CaNAT leads to the formation of N-acyl phosphatidylethanolamine (N-acylPE), including arachidonoyl-containing N-arachidonyl phosphatidylethanolamine (NAPE) which is the precursor to AEA (Figure 1.3.1) (Cadas et al., 1997).

The calcium dependent formation of N-acylPEs was first noticed from dog tissues by Schmid's group (Natarajan et al., 1981; Natarajan et al., 1983; Reddy et al., 1983), but was later partially characterised by Piomelli's group with rat tissues (Cadas et al., 1997). Using neurones labelled with [^{3}H] ethanolamine or various [^{3}H] free fatty acids, ionomycin was able to induce the formation of various [^{3}H] N-acylPEs and the process was sensitive to the presence of EDTA (Cadas et al., 1996). Furthermore, activation of PKA to generate cAMP has also been shown to potentiate the activity of CaNAT, leading to the increased synthesis of AEA (Cadas et al., 1996; Cadas et al., 1997). However, the full identification of the CaNAT enzyme was proving problematic to elucidate due to purification difficulties and the lack of genetic advances. The identity of the CaNAT remained elusive for many years, until it was recently proposed to be PLA2G4E (also known as cPLA$_2\varepsilon$) which is part of the cytosolic PLA$_2$ group (PLA2G4) of enzymes. PLA2G4E was identified as possessing N-acyl transferase activity through the aid of activity-based protein profiling, as well as being calcium sensitive and could interact with PC and PE to generate NAPE when expressed in HEK293T cells (Ogura et al., 2016).

In the search to identify the elusive CaNAT, other enzymes with N-acyl transferase activity but lacking calcium sensitivity were also identified through the efforts of Ueda's group and termed calcium insensitive NAT (iNAT) (Jin et al., 2007; Jin et al., 2009). The search began with lecithin retinol acyltransferase (LRAT) which catalyses the transfer of the *sn*-1 acyl group from PC to vitamin A leading to the formation of retinyl ester, which is used in visual processes (Rando, 2002). This N-acyl transferase activity is similar to the N-acyl transferase activity of the partially characterised CaNAT, thus LRAT was the basis of a bioinformatics search for homologous enzymes that may have similar activity. This identified enzymes of the HRAS-like suppressor (HRASLS) subfamily (also known as phospholipase A/acyltransferase (PLAAT) 1–5) which are a family of class II tumour suppressors (Jahng et al., 2003; Golczak et al., 2012). In particular, HRASLS5 was cloned from rat cDNA library and expressed in COS7 cells where it showed ability to bind to PC and PE and catalysed a transfer of an acyl group to form NAPE. However, HRASLS5 showed little sensitivity to calcium and different expression profiles to CaNAT, but might be distinctive N-acyl transferases that could have a physiological role in the synthesis of N-acylPE (Jin et al., 2009).

Figure 1.3.1. Multiple pathways of AEA biosynthesis and degradation

The major pathway of AEA synthesis begins with the combination of phospholipids PC and PE by CaNAT or iNAT to generate NAPE. NAPE can release AEA from different pathways: (1) through one step hydrolysis by NAPEPLD, (2) through PLC to generate p-AEA which can be dephosphorylated by PTPN22, (3) through the action of ABHD4 or PLA_2 to generate lysoNAPE which can either be cleaved by lysoPLD to release AEA or undergo the combined action of ABHD4 and GDE1 to release AEA. AEA synthesis has also been described by cleavage of N-acylethanolamine plasmalogen (pNAPE) in NAPEPLD-dependent and independent manners. AEA is hydrolysed primarily by FAAH into AA and ethanolamine. AEA can also be oxygenated by: (1) COX-2 into prostaglandin ethanolamides (PG-EA), (2) LOXs into hydroxy-ethanolamines (HETE-EAs) and (3) P450s into epoxytrienoic acid ethanolamides (EET-EAs).

Adapted from Fezza et al. (2014).

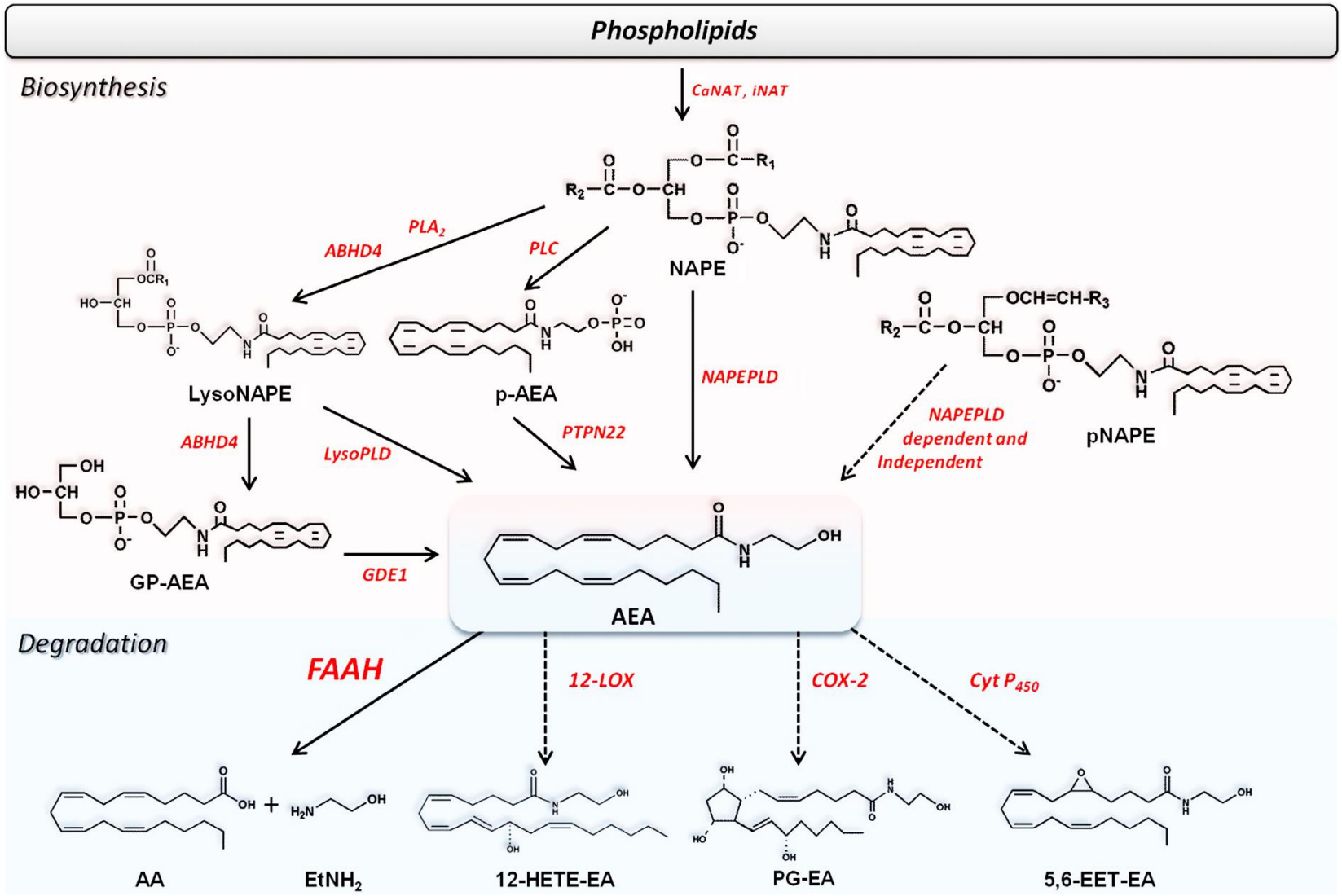
Phospholipids
Biosynthesis
CaNAT, iNAT
NAPE
PLA2
ABHD4
PLC
LysoNAPE
p-AEA
NAPEPLD
pNAPE
NAPEPLD dependent and Independent
ABHD4
LysoPLD
PTPN22
GP-AEA
GDE1
AEA
Degradation
FAAH
12-LOX
COX-2
Cyt P450
AA
EtNH2
12-HETE-EA
PG-EA
5,6-EET-EA

N-acylPE can then be hydrolysed to NAEs, by a calcium sensitive phospholipase D (PLD) activity (Di Marzo et al., 1994; Schmid, 2000). The NAPE-specific PLD (NAPEPLD) thought to be involved in the hydrolysis of N-acylPEs was then cloned (Okamoto et al., 2004) and was shown to be expressed ubiquitously, with high expression in the brain and is highly conserved between mammalians. Unlike other PLDs, NAPEPLD is part of the metallo-lactamase family of enzymes, show calcium sensitivity (Ueda et al., 2001) and when overexpressed in COS7 cells can hydrolyse N-acylPEs in NAEs, including NAPE into AEA. NAPEPLD was soon positioned as the likely primary enzyme in the generation of AEA despite no studies at the time demonstrating the direct involvement of NAPEPLD in AEA synthesis *in vivo* (Ligresti et al., 2005).

1.3.2 Generation of NAPEPLD KO mice

After the cloning of NAPEPLD, a NAPEPLD KO mice was generated to further characterise the activity of NAPEPLD *in vivo* (Leung et al., 2006). Levels of saturated and mono-unsaturated NAEs had decreased, with significant decreases in N-palmitoyl ethanolamine (PEA), N-stearoyl ethanolamine (SEA), and N-oleoyl ethanolamine (OEA). Surprisingly, there were no observable differences in the levels of AEA in the brains of WT and NAPEPLD KO mice. Brain homogenates did have reduced NAPE hydrolysis activity but a NAPEPLD-independent synthesis of AEA was still present at similar enzymatic rates as in WT mice. This suggested that NAPEPLD may have some preference for N-acylPEs and the generation of NAEs *in vivo*, with more preference for very long chain saturated NAEs. The results also suggested that there are other calcium-insensitive synthesis pathways of AEA involving other enzymes with potential to compensate for NAPEPLD.

Two other NAPEPLD KO mice were generated with comparable results. Tsuboi et al. (2011) reported the whole brain levels of AEA were lower in KO mice than in wild type mice but was not completely abolished. The levels of saturated and mono-unsaturated NAEs were more varied, as levels of PEA and OEA were significantly lower, as also observed by Leung et al. (2006), but levels of SEA remained unchanged. A third NAPEPLD KO mice was generated and had levels of NAEs and other structurally related lipid moieties measured from various brain regions (Leishman et al., 2016). In this comprehensive lipidomics profiling, levels of all NAEs were lower in the NAPEPLD KO mice in comparison to WT, including AEA, with surprisingly greater reductions in polyunsaturated NAEs in comparison to saturated and mono-unsaturated NAEs. The largest changes in AEA levels were observed in the striatum and

hippocampus of the KO mouse with ~3x reduction, but the levels were not completely abolished from other brain regions, suggesting perhaps a brain-region specific involvement of NAPEPLD in AEA synthesis.

At least two other synthesis pathways for AEA have been reported following the results from the studies with NAPEPLD KO mice (Figure 1.3.1). The remaining NAPEPLD independent generation of AEA was reported to be blocked by a broad serine hydrolase inhibitor methoxy arachidonyl fluorophosphonate (MAFP) (Simon and Cravatt, 2006). It was suggested that AEA synthesis can be mediated through the activity of a serine hydrolase catalysed double deacylation of NAPE to form lysoNAPE and subsequently generate glycerol-phospho-AEA (GP-AEA), followed by the phosphodiesterase-mediated cleavage of GP-AEA to release AEA. The serine hydrolase α/β-hydrolase domain containing 4 (ABHD4) which can selectively deacylate both NAPEs and lysoNAPEs prior to the generation of GP-AEA, was subsequently identified (Simon and Cravatt, 2006). The EDTA-sensitive conversion of GP-AEA to AEA was attributed to the metal-dependent glycerophosphodiester phosphodiesterase 1 (GDE1) (Simon and Cravatt, 2008). Both ABHD4 and GDE1 are expressed in various tissues including the brain, however the generation of GDE1 KO mice or double GDE1/NAPEPLD KO mice did not show significant decreases in AEA levels in the KO brain compared to WT (Simon and Cravatt, 2010). Furthermore, rat brain tissues have been shown to contain lysoPLD activity that can generate AEA from the intermediate lysoNAPE (Sun et al., 2004).

Another pathway was described in macrophages which produce AEA in response to stimulation by lipopolysaccharide (LPS). This pathway involves the actions of an unidentified PLC to generate phosphor-AEA (pAEA) and subsequent dephosphorylation by phosphatases such as phosphatase 22 (PTPN22) to release AEA (Figure 1.3.1). The LPS-induced synthesis of AEA in macrophages is mediated exclusively by this PLC/phosphatase pathway, which is up-regulated by LPS. Conversely, NAPEPLD is down-regulated by LPS and functions as a salvage pathway of AEA synthesis when the PLC/phosphatase pathway is compromised (Liu et al., 2006). In addition, a novel route was reported for AEA formation from N-acylethanolamine plasmalogen (pNAPE), one of the major classes of glycerophospholipids in mouse brain (Tsuboi et al., 2011).

Although it is accepted that NAPE is the precursor to AEA, the precise enzymatic steps leading to the generation of AEA remains unclear. The synthesis of AEA can also be elicited through the activities of PKA and PKA directly. Activation of PKA and PKC in HEK-293 cells and DRG neurones can increase the levels of AEA which is unaffected by the presence of a calcium

chelator (van der Stelt and Di Marzo, 2005a; Vellani et al., 2008). However, CaNAT is not directly responsive to kinase activation and requires calcium to function (Cadas et al., 1996) thus which of the pathways that might be affected by kinase activity has not been investigated. It is also unknown particularly how these pathways can selectively release AEA over other NAEs. KO studies so far have failed to identify a specific and selective pathway for the majority of AEA synthesis suggesting that different pathways can work in a co-operative and compensatory manner to maintain AEA levels in tissues. The global deletion of a widely expressed enzyme such as NAPEPLD may cause secondary pathways which may not normally be active to compensate. Pharmacological tools could be beneficial in determining the contribution of NAPEPLD by defining shorter end points in experiments, however currently no pharmacological tools have been developed for the inhibition of AEA synthesis. This may also help elucidate the contribution of the various pathways in basal AEA synthesis and "on-demand" stimulated AEA synthesis by calcium and LPS.

1.3.3 Anandamide Degradation

AEA signalling is terminated by its cellular uptake and subsequent catabolism into AA and ethanolamine. The primary enzyme responsible for the degradation of AEA in brain and peripheral tissues was cloned by Cravatt et al. (1996) from rat liver membranes and demonstrated its ability to hydrolyse AEA *in vitro*. FAAH is expressed in a wide range of tissues, especially in the brain and liver and is conserved in humans (Cravatt et al., 1996; Giang and Cravatt, 1997). The generation of a FAAH KO mouse showed barely any AEA hydrolysis activity and 15-fold higher brain levels of AEA compared to WT control. FAAH KO mice also displayed cannabimimetic behavioural effects that could be antagonised by the CB1 receptor antagonist SR141716A (Cravatt et al., 2001). Other genetic and pharmacological studies showed disruption of FAAH activity elevates brain levels of AEA and also displays CB1 dependent analgesia in multiple pain assays (Cravatt et al., 2001; Lichtman et al., 2004b; Lichtman et al., 2004a; Jhaveri et al., 2008; Ahn et al., 2009). In high concentrations of AA and ethanolamine, it has been shown that FAAH can catalyse the backwards reaction to generate AEA, but whether this function occurs physiologically is unclear (Ueda et al., 2000).

The intracellular endoplasmic reticulum location of FAAH suggested that transporters which uptake AEA into the cell and transport across the cytosol for degradation might exist (Di Marzo et al., 1994; Cravatt et al., 1996). Whilst AEA is lipid soluble and can freely diffuse

through membranes, evidence for transport-mediated uptake of AEA was described by Di Marzo et al. (1994) using exogenously applied [^{3}H] AEA to characterise the cellular uptake of AEA. The uptake of [^{3}H] AEA in neuronal cultures was rapid, temperature dependent, saturable at 37^{o}C but perturbed by the addition of non-radioactive AEA and finally selective as [^{3}H] PEA did not compete with the uptake of [^{3}H] AEA.

The identification of the transporters gained interest as a potential therapeutic target as it has been suggested that the cellular uptake of AEA is the rate limiting step to the termination of AEA signalling (Hillard and Jarrahian, 2000; Maccarrone et al., 2000b; Maccarrone et al., 2010). To date, several proteins capable of binding AEA have been identified which may have a role in the intracellular transport of AEA. For example, trafficking of AEA from the plasma membrane can be mediated by cytosolic carriers found in different cell types, including fatty acid binding proteins (FABPs) (Kaczocha et al., 2009), heat shock protein 70 (HSP70) and albumin (Oddi et al., 2009), FAAH-1-like AEA transporter (FLAT-1) (Fu et al., 2011), and potentially by sterol carrier protein 2 (SCP-2) (Liedhegner et al., 2014). These proteins may transport AEA via a non-vesicular mechanism or may interact with liposomes which have been shown to accumulate AEA (Oddi et al., 2008; Maccarrone et al., 2010). However, the roles of these proteins were elucidated through overexpression in recombinant systems and their functions have not been clarified *in vivo*. Thus, there still remains open questions about the specificity of these proteins in orchestrating AEA uptake and transport, and roles of AEA accumulation in different cell types (Maccarrone, 2017).

In addition to hydrolysis by FAAH, AEA can undergo oxygenation by cyclooxygenase-2 (COX-2) (Kozak et al., 2002; Rouzer and Marnett, 2011), 5-, 12- and 15-lipoxygenase (5-/12-/15-LOX) (Hampson et al., 1995; van der Stelt et al., 2002) as well as by several cytochrome P450 monooxygenases (P450) (Snider et al., 2010; Urquhart et al., 2015). Oxygenation by COX-2 turns AEA into prostaglandin ethanolamides (PG-EA), while LOXs convert AEA into hydroxy-ethanolamines (HETE-EAs), and P450s convert AEA into epoxytrienoic acid ethanolamides (EET-EAs) (Figure 1.3.1) (Urquhart et al., 2015). The oxygenated derivatives of AEA may have a biological activity of their own in mediating the inflammatory response, but their impact on human health and disease remains to be clarified.

1.3.4 2-AG Synthesis

2-AG is formed "on-demand" from AA-containing phospholipids in response to cellular responses. Phosphatidylinositol (PI) serves as the most preferred phospholipid substrate for 2-AG formation in the brain (Sugiura et al., 2006) with the main synthesis pathway of 2-AG release from PI through combined actions of PLC and the DAGLs. Following cellular stimulation such as receptor activation, the activity of PLC cleaves PI containing AA into inositol 1,4,5-trisphosphate (IP_3), and AA-containing DAG which is then subsequently hydrolysed by DAGL into 2-AG (Figure 1.3.2). PI containing other fatty acids in the *sn*-2 position are precursors to other 2-acylglycerols such as 2-LG, 2-PG and 2-oleoylglycerol (2-OG), which may also have physiological roles (Ben-Shabat et al., 1998). A secondary pathway was also described to occur through the activity of PLA_1 cleaving PI to release lysoPI, and the subsequent cleavage by lysoPI-specific PLC to release 2-AG (Figure 1.3.2) (Ueda et al., 1993).

DAG is an important second messenger in mammalian cells and is synthesised in response to cellular activation such as through the activation of various GPCRs (Brose et al., 2004). DAG can activate various downstream effectors, with the most prominent target being the PKC family of serine/threonine kinases which can subsequently activate various other effectors. The termination of DAG signalling generally occurs by the action of DAG kinase (Merida et al., 2008), so the activity of the DAGL was originally studied as an intermediate pathway to the release of AA (Prescott and Majerus, 1983). However, it was not until the discovery of 2-AG as an important signalling molecule in its own to the CB receptors (Mechoulam et al., 1995) that focus was placed on the synthesis steps of 2-AG as a signalling molecule by DAGLs.

After the discovery of 2-AG as an important eCB signalling molecule, many studies reported the abundance of 2-AG in many different tissues, including the highest levels in brain (Bisogno et al., 1997; Stella et al., 1997; Kondo et al., 1998). This places importance on elucidating the synthesis enzyme for the most abundant eCB in the brain. The DAGL activity was partially characterised in the context of AA synthesis pathway and found that the enzyme has an optimal pH of 7.0, and its action at the *sn*-1 position can lead to the downstream release of AA (Chau and Tai, 1981; Okazaki et al., 1981; Prescott and Majerus, 1983). The enzyme(s) responsible for the synthesis remained elusive until bioinformatics identification and cloning in 2003 (Bisogno et al., 2003).

Figure 1.3.2. Pathways of 2-AG biosynthesis and degradation

2-AG synthesis begins with activation of PLC following cell stimulation, which hydrolyses phospholipid PI to release DAG. DAG is further hydrolysed to 2-AG by DAGL. 2-AG can also be generated by a secondary pathway through the actions of PLA_1 to generate LysoPI and subsequent hydrolysis by PLC. 2-AG is degraded into glycerol and AA, the precursor to prostaglandin synthesis primarily by MAGL but ABHD6 and ABHD12 can also catalyse this process. 2-AG can also be oxygenated by: (1) COX-2 into prostaglandin glyceryl esters (PG-Gs), (2) LOXs into hydroxyeicosatetraenoic acid glyceryl esters (HETE-Gs), and (3) P450s into epoxytrienoic glyceryl esters (EET-Gs) (not depicted).

Adapted from Fezza et al. (2014).

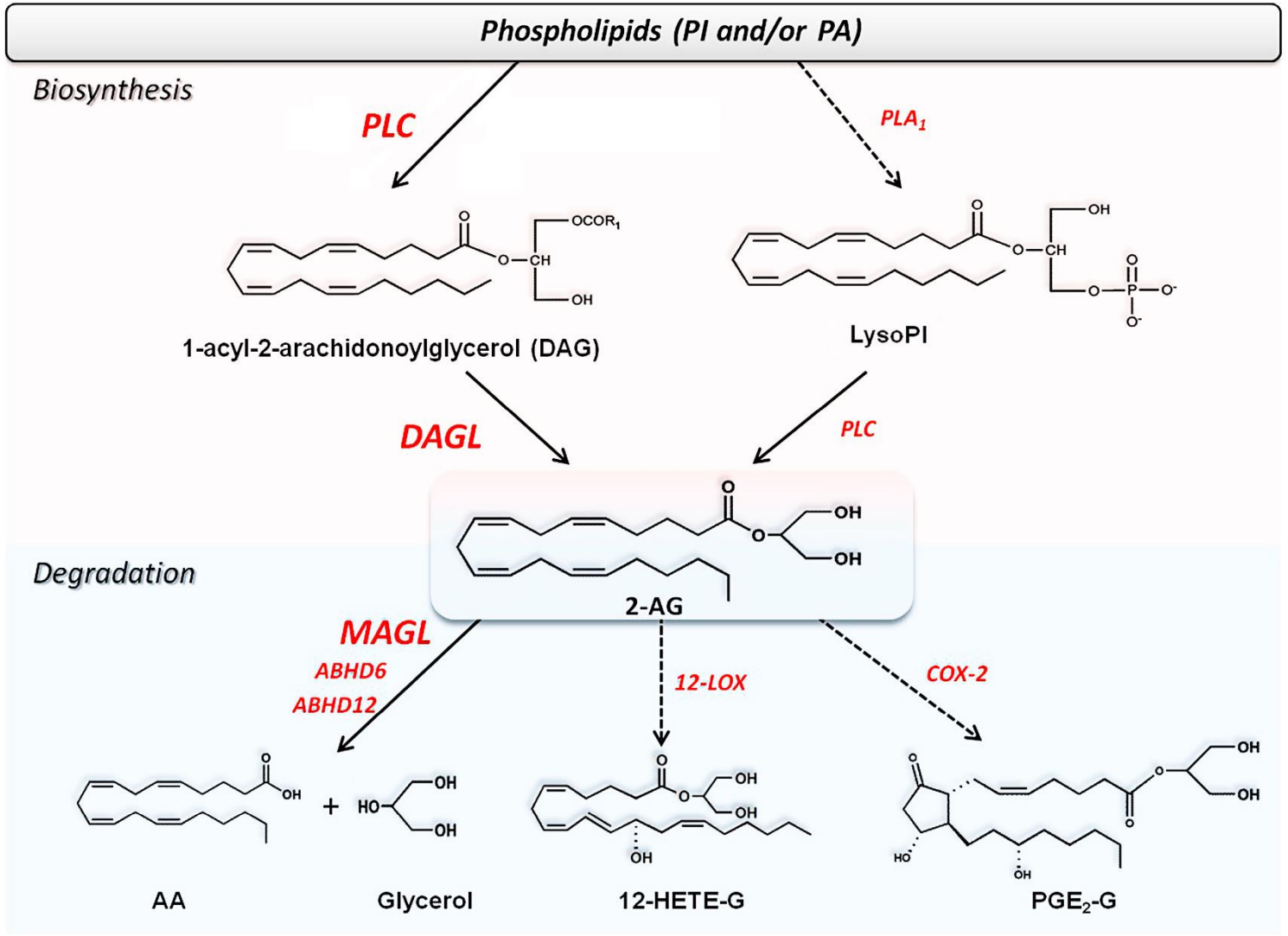
Phospholipids (PI and/or PA)
Biosynthesis
PLC
PLA1
1-acyl-2-arachidonoylglycerol (DAG)
LysoPI
DAGL
PLC
2-AG
Degradation
MAGL
ABHD6
ABHD12
12-LOX
COX-2
AA
Glycerol
12-HETE-G
PGE2-G

The gene encoding a known mono- and diacylglyceride hydrolysing enzyme in *Penicillium camembertii* fungus (Yamaguchi et al., 1991) was queried against mammalian genomes and clear homologues were identified. The two human homologues of DAGLs, diacylglycerol α (DAGLα) and diacylglycerol β (DAGLβ), were subsequently identified and cloned (Bisogno et al., 2003). These enzymes were highly specific and selective for the *sn*-1 position of DAG to release 2-acylglycerols, including 2-AG, in response to calcium influx, and could be inhibited by established DAGL inhibitors THL and RHC80267. Overexpression of these enzymes in COS7 cells also showed 3-fold greater lipase ability against 1-stearoyl-2-arachidonoy-sn-glycerol compared to untransfected cells (Bisogno et al., 2003). Furthermore, overexpression of DAGLα in Neuro-2A cells resulted in an increase in 2-AG and stearic acid and a decrease in 1-stearoyl-2-arachidonoyl-sn-glycerol (Jung et al., 2007).

Whilst on-demand 2-AG synthesis and release can be stimulated by calcium, the DAGLs do not seem to be directly activated by calcium (Farooqui et al., 1984; Moriyama et al., 1999; Rosenberger et al., 2007). The synthesis of 2-AG by the DAGLs therefore likely involves additional steps from calcium elevation that leads to the activation of DAGL (Reisenberg et al., 2012; Kano, 2014). DAGL from bovine brain microsomes can be directly activated by PKA (Rosenberger et al., 2007) and activation of PKA and PKC can both increase 2-AG synthesis in DRG neurons and HEK-293 cells (Vellani et al., 2008). Both PKA and PKC can also be activated by calcium (Steinberg, 2008; Dunn et al., 2009), thus it has been hypothesised that the activation of kinases may lead to the phosphorylation of DAGLs causing its activation as a way of regulating DAGL activity (Reisenberg et al., 2012).

Immunohistochemical studies showed that whilst DAGLα and DAGLβ were coexpressed in embryonic mice neurons correlating with the role in axonal growth and guidance, a developmental switch in expression led to the DAGLα isoform expression to be enriched in adult mouse brain and spinal cord. This suggested that DAGLα is the main isoform for the generation of 2-AG in the adult brain and that DAGLβ is downregulated during development. Expression of DAGLα is found in the high levels in the dendritic spines in adult neurones, also correlating well with eCB signalling in retrograde synaptic transmission (Bisogno et al., 2003). DAGLβ is expressed at lower levels in the CNS but at particularly high levels in macrophages and microglia which correlates well with its recently established role in inflammation (Bisogno et al., 2003; Hsu et al., 2012). These results demonstrated that the DAGLs were able to hydrolyse DAG to generate 2-AG *in vitro* and are positioned at the right place at the right time to mediate the well-established eCB signalling roles in the CNS and in the periphery.

1.3.5 Generation of DAGL KO mice

The generation of DAGLα and DAGLβ KO mice further supported the contribution of the DAGLs to the generation of 2-AG and clarified specific role differences between the two DAGLs. The role of DAGLα in retrograde eCB signalling in the CNS was also revealed by independent KO mice studies (Gao et al., 2010; Tanimura et al., 2010; Shonesy et al., 2014). In the brain and spinal cord of adult DAGLα KO mice, an astonishing 80% reduction of 2-AG levels was observed, establishing this enzyme as the major 2-AG synthesising enzyme in the CNS (Figure 1.3.3) (Gao et al., 2010). In a separate study, DAGLα KO mice also displayed an 80% reduction in 2-AG in the cerebellum, hippocampus and striatum, with little change to these brain regions in DAGLβ KO mice (Tanimura et al., 2010). Furthermore, DAGLα KO mice lost stimulus-induced increases in 2-AG in the brain and DSE and DSI in hippocampus, cerebellum and striatum were also lost, which is also observed in CB1 KO mice (Ohno-Shosaku et al., 2002; Tanimura et al., 2010). This loss of DSE and DSI was not observed in DAGLβ KO mice, indicating that DAGLα is principally involved in the generation of the retrograde messenger 2-AG for short term synaptic plasticity (Gao et al., 2010; Tanimura et al., 2010; Yoshino et al., 2011).

DAGLα KO mice displayed similar neurological phenotypes to mice with genetic deletion of the CB1 receptor. DAGLα KO mice showed increased emotional and stress-related behaviours such as anxiety and depressive-like behaviour in open-field tests (Shonesy et al., 2014; Jenniches et al., 2016) which was also observed in CB1 KO mice (Marsicano et al., 2002; Valverde and Torrens, 2012). In a separate study, DAGLα and CB1 KO mice showed similar anxiety behaviours in the hot plate, forced swim, tail suspension test and others, which were both statistically significantly different to WT mice (Powell et al., 2015). As well as this, CB1 KO mice display hypophagia and have a lean phenotype, which was also seen in DAGLα KO mice but not seen in DAGLβ or NAPEPLD KO mice (Powell et al., 2015). Finally, as mentioned previously, genetic mutations of CB1 and DAGLα are associated with similar neurological phenotypes in humans (Smith et al., 2017). Collectively, these results show the close behavioural phenotypes of DAGLα and CB1 KO mice, supporting the role of DAGLα as the predominant synthesising enzyme for the bulk of 2-AG required for eCB signalling at the CB1 receptor in the brain.

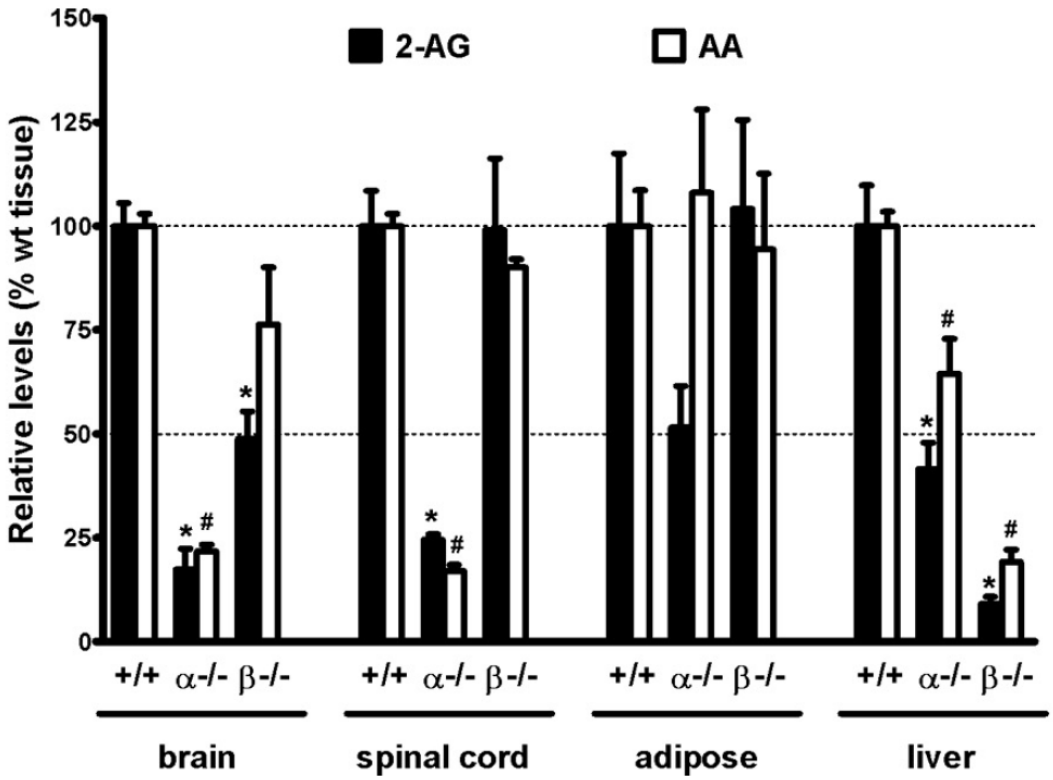

Figure 1.3.3. Comparison of 2-AG and AA levels in wild type and DAGL KO mice

2-AG and AA levels were measured in tissues of DAGLα KO (α-/-) and DAGLβ KO (β-/-) mice and compared to wild type (+/+) mice control. An 80% reduction of 2-AG levels was observed in the brains and spinal cord of adult DAGLα KO mice. A 50% reduction in 2-AG levels was observed in the brains of adult DAGLβ KO mice with no significant reduction in the spinal cord detected. In the adipose tissue, there was a 50% reduction in 2-AG in DAGLα KO mice while no significant reduction was observed in DAGLβ KO mice. In the liver, there was a 50% reduction in 2-AG in DAGLα KO mice, compared to a 90% reduction in the liver of DAGLβ KO mice. Reduction in AA levels changed in parallel with the reductions in 2-AG in the brain, spinal cord and liver, most notably was 80% reduction in AA levels in brain and spinal cord of DAGLα KO mice and a 90% reduction in AA in the liver of DAGLβ KO mice.

Adapted from Gao et al. (2010).

Interestingly, AEA levels were also affected in DAGLα KO animals. Levels of AEA were comparable to WT in DAGLβ KO mice brains but were reduced in the cerebellum and hippocampus of DAGLα KO mice (Tanimura et al., 2010). Furthermore, AEA levels were ~25-75% lower in the cortex, hippocampus and amygdala but not in the striatum of DAGLα KO mice (Jenniches et al., 2016). A separate report suggested a slight (~10%) reduction in AEA levels in the hippocampus of DAGLβ KO mice but this was more pronounced in DAGLα KO mice (~60%) (Yoshino et al., 2011). This crosstalk between 2-AG and AEA has been suggested to be a result of phospholipid remodelling in KO mice, which could affect the fatty acid composition of brain precursors for NAPE (Di Marzo, 2011) which can make it difficult to dissect the two synthesis pathways. Moreover, the relatively long-term loss of function in one pathway can lead to alterations in other pathways, thus genetic results should be interpreted with caution.

In adult DAGLβ KO mice, a 50% reduction in 2-AG levels was observed in the brains with no significant reduction in the spinal cord detected. However, a 90% reduction in 2-AG levels was observed in the liver of the DAGLβ KO mice, compared to a 60% reduction in the DAGLα KO mice (Figure 1.3.3). Interestingly, whilst DAGLα is attributed to most of generation of 2-AG in the brain, the KO of both DAGLα and DAGLβ collectively (DAGLα/β KO) in mice have even lower levels of 2-AG than in DAGLα KO alone across several areas of the brain (Yoshida et al., 2006). The loss of DAGLβ showed no impact on DSE/DSI whilst these were impaired in the loss of DAGLα, and had little impact in adult neurogenesis in the SVZ, but did show a ~30-40% reduction in the hippocampus (Gao et al., 2010; Tanimura et al., 2010). DAGLβ KO mouse peritoneal macrophages also show reductions in 2-AG, as well as AA and eicosanoids levels, and a reduction in LPS-induced TNF-α, supporting the role of DAGLβ in inflammation and as a key mediator in lipid metabolism (Hsu et al., 2012). These studies show that the individual contributions of the DAGLs to maintaining steady-state levels of 2-AG are different in different tissues, with the production of 2-AG in brain attributed to the activity of DAGLα. Furthermore, the DAGLs appear to maintain tissue 2-AG levels in a cooperative and compensatory manner.

The genetic deletion of the DAGLs revealed the interesting observation of a reduction in AA levels alongside reductions in 2-AG levels. 2-AG is the precursor to AA after hydrolysis by MAGL, however PLA2 was generally believed to be the primary enzyme involved in AA synthesis (Balsinde et al., 2002). DAGL KO studies showed AA was reduced by ~80% in the brain and spinal cord in DAGLα KO mice, as well as ~90% reduction in the liver of DAGLβ KO

mice which is in parallel to the reduction in 2-AG (Gao et al., 2010). This was also observed in DAGLβ KO mouse peritoneal macrophages (Hsu et al., 2012). Thus 2-AG appears to be the main precursor for AA and points to a role for DAGL activity in the regulation of AA synthesis.

1.3.6 2-AG Degradation

2-AG is degraded *in vivo* primarily by monoacylglycerol lipase (MAGL) which hydrolyses 2-acylglycerols to release a fatty acid and glycerol (Figure 1.3.2). MAGL was cloned from rat brain cDNA library and is widely expressed in the brain (Dinh et al., 2002). The overexpression of MAGL in HeLa cells showed markedly increased 2-AG hydrolysis (but not AEA hydrolysis) and resulted in reduced accumulation of 2-AG following stimulation of rat primary cortical neurons (Dinh et al., 2002). The inhibition of MAGL *in vivo* raises brain 2-AG concentrations by 8-10 fold (without altering AEA) and MAGL-inhibited mice exhibited much of the pharmacological behavioural responses typically seen with CB1 agonists (Long et al., 2009b; Schlosburg et al., 2010). Genetic deletion of MAGL in mice also exhibit elevated levels of 2-AG, but do not fully recapitulate the pharmacological behavioural responses seen with pharmacological blockade, possibly due to the desensitisation of the CB receptors (Taschler et al., 2011; Imperatore et al., 2015).

MAGL is considered to be responsible for ~85% of the 2-AG hydrolysing activity in the brain, with the remaining 15% of 2-AG hydrolysis being attributed to other serine hydrolases such as ABHD6, ABHD12 and FAAH (Figure 1.3.2) (Blankman et al., 2007). MAGL co-localises with CB1 in presynaptic terminals which positions MAGL as the main terminator of 2-AG-CB1 signalling (Kano et al., 2009). In a study by Marrs et al. (2010), the acute inhibition of ABHD6 in neuronal cultures led to activity-dependent accumulation of 2-AG. They described the post-synaptic location of ABHD6 which is well positioned to act as a guard to the intracellular pool of 2-AG, perhaps to control the seepage of 2-AG from the intended synaptic cleft. Furthermore, the inhibition of ABHD6 in cortical slices facilitated the induction of eCB-LTD with sub-threshold stimulation, placing ABHD6 as an important mediator of synaptic eCB signalling. The role of ABHD12 in eCB signalling is currently unclear, its 2-AG hydrolysing ability was discovered through activity-based protein profiling (ABPP) (Blankman et al., 2007) and is found to be expressed in microglia where it may have a role in mediating immune function in the CNS (Savinainen et al., 2012). FAAH can hydrolyse both AEA and 2-AG *in vitro*; however, the *in vivo* role of FAAH in 2-AG degradation is very minor in the brain and is much more involved in the hydrolysis of AEA *in vivo* (Blankman et al., 2007; Ueda et al., 2011).

Other pharmacological studies have since shown that MAGL is the key hydrolysing enzyme limiting 2-AG and CB1 signalling (Hashimotodani et al., 2007; Long et al., 2009b; Pan et al., 2009; Savinainen et al., 2012; Keimpema et al., 2013) making it a key regulator of eCB signalling.

In addition to hydrolysis by serine hydrolases, 2-AG can be oxygenated by many of the same enzymes described in AEA oxygenation (Kozak et al., 2002; Urquhart et al., 2015). Oxygenation by COX-2 turns 2-AG into prostaglandin glyceryl esters (PG-Gs), while LOXs convert 2-AG into hydroxyeicosatetraenoic acid glyceryl esters (HETE-Gs), and P450s convert 2-AG into epoxytrienoic glyceryl esters (EET-Gs) (Figure 1.3.2) (Urquhart et al., 2015). The oxygenation of the eCBs by these enzymes show the complexity of the eCB system and how it may influence the generation of potentially biologically active inflammatory mediators, some of which may be implicated in a range of neuroinflammatory diseases (reviewed in Turcotte et al., 2015).

1.3.7 Other putative eCBs and endogenous ligands to the CB receptors

Other structural analogues of AEA and 2-AG exist and may function as potential eCBs based on their structures (Figure 1.3.4). 2-AG ether (noladin) (Hanus et al., 2001; Fezza et al., 2002), AEA derivative O-arachidonoyl ethanolamine (virodhamine) (Porter et al., 2002) and N-arachidonoyldopamine (NADA) (Hu et al., 2009) have been reported to act as eCBs from various studies. Noladin was isolated from porcine brain and was shown to bind selectively to CB1 and CB2 receptors in mice causing sedation, hypothermia, intestinal immobility, and mild antinociception in mice (Hanus et al., 2001; Fezza et al., 2002). However, role of noladin as an eCB is disputed as some studies report the presence of noladin in the brain whilst others suggest endogenous levels of noladin in various mammalian species is not significant (Oka et al., 2003; Richardson et al., 2007). Porter et al. (2002) reported virodhamine is present in the human hippocampus at levels similar to AEA levels and in rat brain. It has been reported that virodhamine is an antagonist of CB1 but is an agonist of CB2 (Porter et al., 2002). NADA is detected in the brains of rats with especially high concentrations in the hippocampus, cerebellum and striatum (Huang et al., 2002). NADA has been shown to be an agonist to CB1 receptors inducing analgesia upon systemic administration and hyperalgesia when intradermally injected, but is also an agonist to the transient receptor potential of vanilloid type-1 (TRPV1) receptor (Bisogno et al., 1997; Huang et al., 2002). These putative

eCBs show activity towards the CB receptors in various studies but their full mechanism of action, the synthesis and degradation pathways and whether they are true eCBs in physiological systems remain elusive.

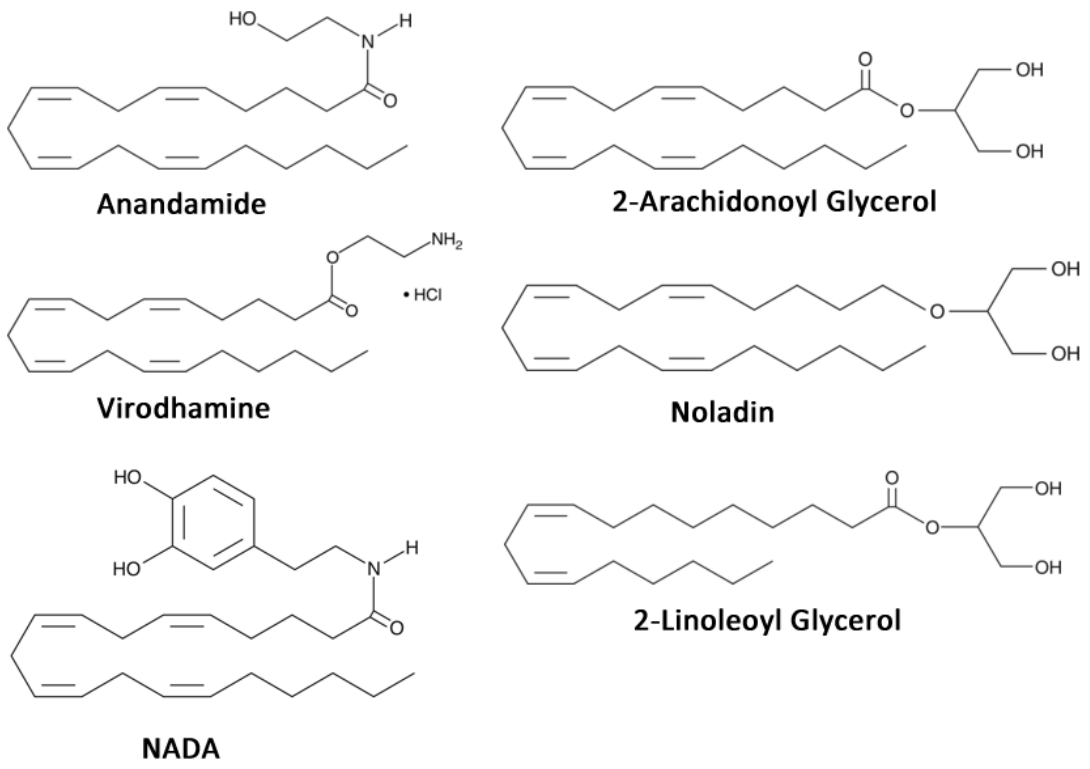

Figure 1.3.4. Structure of the Endocannabinoids

Structures of the two most well studied eCBs: 2-AG and AEA, three putative eCBs: virodhamine, noladin and NADA, and a putative entourage molecule 2-LG are presented above.

2-LG is structurally similar to 2-AG with a substitution of a linoleoyl group in place of arachidonoyl group (Figure 1.3.4) and could be generated by DAGL (Bisogno et al., 2003). 2-LG was profiled as the most abundant 2-acylglycerol in *Drosophila melanogaster* and may have a role in eCB signalling in invertebrates lacking arachidonic acid (Tortoriello et al., 2013).

2-LG is also detected in mammalian brain homogenate at around 10x lower concentrations than 2-AG (Richardson et al., 2007; Williams et al., 2007) and is in mouse spleen tissue (Ben-Shabat et al., 1998) and canine gut tissue (Mechoulam et al., 1995) in relatively high amounts compared to 2-AG. However, the physiological role of 2-LG is currently unclear. It was previously reported that whilst 2-LG is unable to directly activate mammalian CB receptors, it can potentiate the role of other eCBs, including 2-AG activation of CB1 receptors (Ben-Shabat et al., 1998). The mechanism for this potentiation is unknown, it has been suggested 2-LG may inhibit 2-AG breakdown by binding to MAGL (Ghafouri et al., 2004). However, a recent publication by Murataeva et al. (2016) showed 2-LG did not have an entourage effect but rather displayed antagonistic activity against 2-AG in a model of DSE, which would suggest that 2-LG can have direct ligand interaction with the CB1 receptor in order to antagonise 2-AG activity. Unlike the other putative eCBs, the synthesis and degradation pathways of 2-LG are known as they are likely to be the same pathways as 2-AG, and the levels of 2-LG are high enough to be physiologically relevant. Thus, 2-LG may have an active role in the eCB system which has not been fully elucidated and could be a novel eCB.

As well as novel agonists of the CB receptors, novel endogenous antagonists have also been described. The novel peptide hemopressin (Hp) is a 9-residue peptide derived from the α1 chain of haemoglobin which was extracted from rat brain homogenate and was found to be biologically active when injected *in vivo* (Rioli et al., 2003). Hp was shown to have hypotensive and antinociceptive effects when administered *in vivo* (Blais et al., 2005; Dale et al., 2005b) but the mechanism of its effects was unclear until Heimann et al. (2007) reported Hp as a selective antagonist to the CB1 receptor. Thus far, the ligands of the CB receptors have been lipid based, but the discovery of Hp garnered interest as a novel endogenous peptide cannabinoid ligand which would expand the repertoire of CB ligands and could be novel therapeutic targets. However, although some of its effects *in vivo* are reported to be mediated by CB1 receptor blockade (Dodd et al., 2010; Dodd et al., 2013; Zhang et al., 2016b), some studies have shown contentious findings that Hp does not exert its effects through the CB1 receptor (Lippton et al., 2006; Straiker et al., 2015; Dvoracsko et al., 2016). As well as this, evidence that Hp directly binds to CB1 has not been confirmed so far in laboratories other than the one that first described this activity (Heimann et al., 2007; Gomes et al., 2009). Finally, very little is known about the biosynthesis and inactivation of Hp, which makes any interpretation of its biological importance as an endogenous ligand to the CB1 receptor difficult.

1.4 Additional activities of the eCB system

DAGL and NAPEPLD have been studied extensively in the context of the generation of eCBs for eCB signalling. However, it is often overlooked that these enzymes are central to the generation of a range of other signalling moieties which could also have physiologically important roles, thus placing the synthesis enzymes as key modulators of many signalling systems.

1.4.1 Non-CB functions of 2-acylglycerols

The DAGLs are highly conserved between mammals and many species express some form of DAGL (Yuan et al., 2016). In some species such as *Drosophila*, a DAGL homologue is expressed in the absence of a homologue to the vertebrate CB receptors (Elphick and Egertova, 2001). This might suggest the DAGL homologue is relevant in non-eCB signalling contexts, for example it has been shown to be vital for visual processes in *Drosophila* (Leung et al., 2008). As well as this, *Drosophila* lacks an arachidonic acid pool but has a relatively abundant linoleoyl fatty acid pool. Therefore, the major 2-acylglycerol generated is 2-LG, which could have important physiological functions that are not mediated through CB receptors (Tortoriello et al., 2013).

Aside from the generation of 2-AG as the major eCB, the DAGLs can generate other 2-acylglycerols in mammals which have been suggested to function as entourage molecules of 2-AG (Ben-Shabat et al., 1998), or as ligands to other receptors, for example 2-OG is a proposed ligand for GPR119 which may have implications in diet and satiety (Hansen et al., 2011; Syed et al., 2012). Levels of 2-LG and 2-PG are in physiologically relevant levels in certain mammalian organs (Ben-Shabat et al., 1998), suggesting the DAGLs can generate steady state levels of these 2-acylglycerols, but their physiological function is not yet fully elucidated.

Furthermore, it has been reported that AA – which has no intrinsic activity at CB receptors, can modulate neuronal function by directly affecting voltage-dependent potassium channels (Figure 1.4.1) (Oliver et al., 2004; Meves, 2008; Carta et al., 2014). As 2-AG and AEA contain AA, they can also modulate the gating of ion channels in a CB-independent manner by entering the phospholipid bilayer directly (Oz, 2006; Gantz and Bean, 2017). 2-AG and AA has

been shown to accelerate firing of isolated midbrain dopamine neurones where expression of CB receptors is negligible (Herkenham et al., 1990). This occurs by the inhibition of Kv4.3 channels by interacting with the voltage sensing region of the channel which faces the lipid bilayer (Swartz, 2008). This in turn reduces the inactivating A-type potassium current (I_A) which leads to more rapid neuronal firing. The latter effect can be weakly enhanced by calcium influx from cell depolarisation but is more enhanced by activation of $G_{q/11}$ GCPRs (Gantz and Bean, 2017). In this context, 2-AG is able to modulate neuronal signalling through a CB receptor independent mechanism.

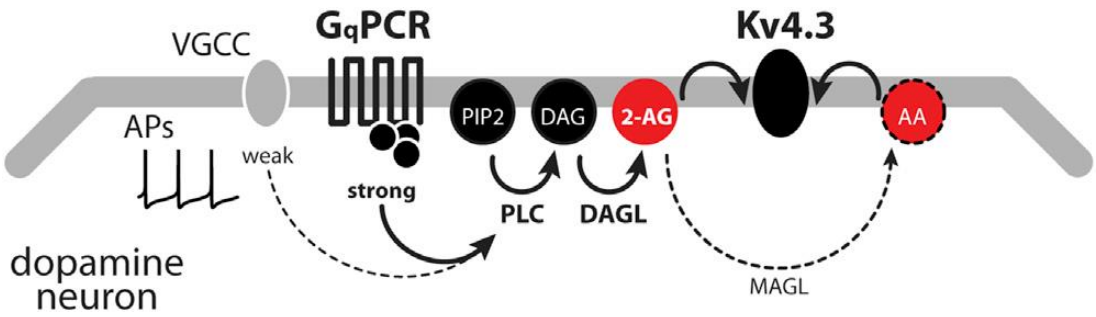

Figure 1.4.1. Schematic of the working model for the inhibition of A-type potassium current by 2-AG

Calcium entry during high-frequency action potential firing or activation of $G_{q/11}$ GPCRs mobilises 2-AG synthesis. 2-AG is generated through the activity of PLC to generate DAG, and conversion of DAG to 2-AG by DAGL. 2-AG may also be degraded by MAGL to release AA. 2-AG and AA inhibits I_A by lipid interaction with Kv4.3 channels. Inhibition of I_A enhances the excitability of dopamine neurons in an autocrine signalling manner.

Figure from Gantz and Bean (2017).

1.4.2 Eicosanoid signalling

The substantial reduction of AA in DAGL KO mice provides strong evidence for the DAGL/MAGL pathway as the major pathway for the release of AA (Gao et al., 2010). In this context, the role of DAGL would be to generate 2-AG as a substrate for MAGL rather than for eCB signalling. The role of MAGL therefore would be to hydrolyse 2-AG to maintain levels of AA for generation of eicosanoids instead of terminating the signalling action of 2-AG. This pathway would serve to maintain steady-state levels of AA and serve as a response pathway to generate signalling pools of AA in inflammatory states.

In support of this DAGL/MAGL mediated generation of AA, MAGL inhibition *in vivo* resulted in an increase in 2-AG levels coupled with a complimentary decrease in AA levels in mouse brain, spinal cord, liver, spleen, and lung (Nomura et al., 2008). In the brain, inhibition of MAGL with specific inhibitor JZL184 is associated with substantial decreases of AA (Long et al., 2009b). Furthermore, in animal models of cerebral artery occlusion stroke, administration of JZL184 reduced brain levels of AA levels and inflammatory cytokine TNF-α but increased brain levels of anti-inflammatory cytokine IL-10 (Rahmani et al., 2018). Similarly, in a separate study of ischemic stroke, JZL184 suppressed the inflammatory response, decreased the number of degenerating neurons as well as reducing brain oedema and improving behavioural functions which resulted in neuroprotective effects (Choi et al., 2018). These neuroprotective effects of MAGL inhibition were not fully antagonised by antagonists of CB receptors, indicating that the anti-inflammatory effects are likely caused by inhibition of eicosanoid production rather than by CB receptor activation.

In the brains of MAGL KO animals, a 5-fold decrease in AA was observed but also a decrease in levels of eicosanoids like prostaglandin E2 (PGE2), prostaglandin D2 (PGD2) and thromboxane B2 (TXB2) (Nomura et al., 2011). MAGL inhibition also reduced LPS-stimulated inflammatory cytokine levels by ~4-8 fold in a CB1/2 independent manner, as well as supressing microglial activation (Nomura et al., 2011). In support of the hypothesis that MAGL makes a much more substantial contribution to the generation of AA than the classically described pathway of release by PLA_2, basal levels of AA and eicosanoids remain unaltered in PLA2G4A ($cPLA_2$) KO mice, which is in contrast a 5 to 10-fold reduction in MAGL KO mice or following MAGL inhibition. Furthermore, only a 20% reduction in LPS-induced prostaglandins production was detected in brains of PLA2G4A KO mice which is modest when compared to a >3-fold reduction in MAGL KO mice. In addition to this, a clear partitioning of function between MAGL and PLA2G4A was uncovered: MAGL was mainly responsible for

regulating basal and LPS-stimulated levels of AA and prostaglandins in the liver and lung, whereas PLA2G4A regulated these lipids more in the gut and spleen (Nomura et al., 2011).

These studies, alongside DAGL KO studies reveal the large contribution of DAGL/MAGL signalling to the production of AA and downstream eicosanoids. The KO of MAGL in the liver reduced AA levels by around 50% (Nomura et al., 2011), whereas the KO of DAGLβ revealed a 90% reduction of AA in the liver (Gao et al., 2010), suggesting that the bottleneck of AA synthesis is likely to be the DAGL step in certain areas of the body. The reduction of downstream eicosanoids implicate a role of DAGL/MAGL as mediators of inflammation. In support of this, DAGLβ is expressed primarily in immune cells where a substantial reduction in 2-AG, AA and eicosanoids were observed in DAGLβ deficient macrophages (Hsu et al., 2012). The reduction of eicosanoids associated with decreases in AA following disruption of DAGL or MAGL further confirms that the release of AA is not simply a by-product of 2-AG hydrolysis, but may have implications in the regulation of inflammatory responses.

1.4.3 Synthesis and Functions of NAEs

N-acylPEs containing various fatty acid side chains can be generated by the transferase activity of CaNAT and the hydrolysis of N-acylPEs generate NAEs (Ueda et al., 2010). It is generally accepted that N-acylPEs and NAEs occur in low levels ubiquitously in many organisms and have a variety of functions (Schmid and Berdyshev, 2002).

Various NAEs have been functionally characterised, with AEA being the best characterised as an agonist to the CB receptors and the TRPV1 receptor (Devane et al., 1992; Smart et al., 2000). PEA has been reported to exhibit pharmacological activities such as anti-inflammatory, analgesic, and neuroprotective actions through agonistic activity toward the PPARα receptor (Hansen, 2010; Petrosino et al., 2010). OEA is known to exert an anorexic action, which appears to be mediated largely by its binding to GPR119, but could also act through PPARα and TRPV1 receptors (Fu et al., 2003; Piomelli, 2003; Movahed et al., 2005; Overton et al., 2006). SEA has been reported to have pro-apoptotic activity through CB and TRPV receptor independent mechanisms (Terrazzino et al., 2004) also possesses anti-inflammatory and anorexic properties (Astarita and Piomelli, 2009). The activity of these NAEs are mediated through non-CB receptors but the physiological roles of these NAEs have not yet been fully characterised.

Whilst endogenous levels of NAEs are generally at a low level, NAEs have been of interest as they are shown to be more highly detected following tissue injury in different organs, including the brain (Hansen et al., 2001a; Hansen, 2010). Different species of NAEs have shown protective properties, for example through the activation of CB receptors by AEA to prevent excitotoxicity (Eljaschewitsch et al., 2006) or through non-CB related mechanisms by the other NAEs. NAEs can also protect cells in different ways, for example through the antioxidative properties of saturated NAEs, by monounsaturated NAEs preventing calcium leakage from mitochondria, and by inhibiting release of mediators that promote necrosis and inflammation (Hansen et al., 2000; Esposito et al., 2014). The accumulation and protective properties of NAEs following injury are of interest as potential future therapeutics for brain injury and neurogenerative diseases.

These NAEs have been shown to be generated by NAPEPLD *in vitro* showing that NAPEPLD is not selective for the fatty acyl chain (Okamoto et al., 2004). However, the KO of NAPEPLD in mice show the largest changes in saturated and monounsaturated NAEs over polyunsaturated NAEs (Leung et al., 2006). The partiality of NAPEPLD *in vivo* for the generation of saturated and monounsaturated NAEs over polyunsaturated NAEs such as AEA raises questions about the primary role for NAPEPLD and its contribution to eCB signalling.

1.5 Aims and Objectives

After 25 years since the identification of the two major endocannabinoids, many studies have established the importance of the role of the eCBs and the CB receptors in eCB signalling for many brain processes in neonatal neuronal development, in postnatal synaptic retrograde signalling and neurogenesis. The eCB system also plays important roles in maintaining the physiological functions of peripheral systems such as GI mobility and bone maintenance. As well as this, the eCB synthesis enzymes might also have distinct roles outside of eCB signalling. Given these important roles of the eCB system, a full understanding of the synthesis and signalling pathways of endogenous ligands to the CB receptors is needed. However, there are still many unanswered questions about the endogenous ligands of the CB receptors.

Aside from the two major eCBs, little is known if there are any other endogenous eCBs or molecules that may modulate eCB signalling. The unclear role of 2-LG as an entourage for 2-AG or as a CB1 antagonist warrants further investigation as 2-LG can be detected at physiologically relevant levels and the synthesis and degradation pathways are already elucidated. Hp, the first proposed endogenous peptide antagonist of the CB1 receptor could be a promising pharmacological tool or for potential therapeutics. However, conflicting reports of its activity at the CB1 receptor and disputed presence of its synthesis and degradation pathways would require further clarification prior to further drug discovery efforts.

There also remains questions regarding the generation of the major eCBs 2-AG and AEA through the actions of DAGLα/DAGLβ and NAPEPLD, respectively. The contribution of the DAGLs in retrograde eCB signalling in the brain has been very well characterised. However, the DAGLs have also been shown to be involved in autocrine signalling and non-CB signalling roles. Unlike neurons, 2-AG synthesis in these roles may not be stimulus-induced and the contributions of DAGL and 2-AG to eCB signalling in these instances are less well characterised. A full understanding of AEA synthesis is still elusive given the redundancy of AEA synthesis pathways. Despite this, the two main enzymes currently accepted to be the main enzymes synthesising AEA are NAPEPLD and CaNAT. Therefore, it is of interest to elucidate the contribution of NAPEPLD and the recently discovered CaNAT enzyme PLA2G4E have in AEA synthesis and eCB signalling.

The CB1-Tango assay is an industry standard cell-based reporter assay system that gives quantitative activation of the CB1 receptor (van der Lee et al., 2009) and was adopted as the model system for the study of novel CB ligands and eCB signalling.

The CB1-Tango assay was used to address the following questions:

- Does 2-LG have direct activity on the CB1 receptor or is it an entourage for 2-AG?
- Is the Hp peptide a CB1 receptor antagonist and can it modulate eCB signalling?
- Can the CB1-Tango assay be adapted to measure eCB signalling?
- Does DAGL generate 2-AG for eCB signalling in the CB1-Tango cells?
- To what extent is NAPEPLD required for AEA synthesis and eCB signalling?
- Is the recently described PLA2G4E enzyme the elusive CaNAT and are there other obvious candidate enzymes for the synthesis of AEA?

Chapter 2. Materials and Methods

2.1 Materials

2.1.1 Cell Culture

Phosphate Buffered Saline (PBS)

Ten Dulbecco 'A' tablets from Oxoid (*Cat No: BR0014*) dissolved in 1 litre of distilled water and autoclaved. 1 litre of PBS contains sodium chloride (8.0g/l), potassium chloride (0.2g/l), disodium hydrogen phosphate (1.15g/l) and potassium dihydrogen phosphate (0.2g/l)

PBS-EDTA

PBS with 0.5mM Ethylenediaminetetraacetic acid (EDTA) at pH 8.0

Trypsin

2.5% Trypsin in PBS-EDTA from Gibco (*Cat No: 15090046*) diluted with PBS-EDTA to desired concentration

Cell culture plastics from Thermofisher Scientific

Polystyrene Nunclon™ Delta Surface 10 cm cell culture dishes (*Cat No: 150350*)

Nunc Polystyrene T75 cell culture flask (*Cat No: 156499*)

Transfection Reagent

FuGene HD Transfection Reagent from Promega (*Cat No: E2311*)

Puromycin selection

Puromycin (hydrochloride) from Cayman Chemicals (*Cat No: 13884-25mg-CAY*) diluted in sterile water and added to cell growth media at the concentration of 3μg ml^{-1}

2.1.2 CB1-TANGO Assay

CB1-TANGO Cells

TANGO™ CNR1-bla U2OS cell line from Invitrogen, Life Technologies (*Cat No: K1513*)

CB1-TANGO Growth Media

McCoy's 5A Medium (*Cat No: 26600-023*) with 10% dialysed FBS (*Cat No: 26400-036*), 0.1M NEAA (*Cat No: 11140-050*), 25mM HEPES (pH 7.3) (*Cat No: 15630-080*), 1mM Sodium Pyruvate (*Cat No: 11360-070*), 100µg/ml Penicillin/Streptomycin (*Cat No: 15140-122*), 200µg/ml Zeocin™ (*Cat No: R250-01*), 50µg/ml Hygromycin (*Cat No: 10687-010*) and 100µg/ml Geneticin (*Cat No: 10131-027*), all from Invitrogen, Life Technologies

0.5% FBS McCoy's Assay Medium

McCoy's 5A Medium supplemented with 0.5% FBS, 0.1M NEAA, 25mM HEPES (pH 7.3), 1mM Sodium Pyruvate, 100µg/mL Penicillin/Streptomycin, all from Invitrogen, Life Technologies

Freestyle Assay media

Freestyle 293 expression media Invitrogen, Life Technologies (*Cat No: 12338-018*)

No Starve Freestyle Assay media

Freestyle 293 expression media supplemented with 2mM sterile $CaCl_2$ from Sigma (*Cat No: 21114-1L*) and 100nM JZL195.

Tango Assay Plates

Costar 96-well black clear bottom polystyrene plates, from Fisher Scientific (*Cat No: 10530753*)

Detection reagent

LiveBLAzer™-FRET B / G Loading Kit, from Life Technologies (*Cat No: K1096 and K1156*)

Fluorescent Reader

FlexStation® Microplate Reader, from Molecular Devices

Compounds

COMPOUND	DESCRIPTION	SUPPLIER
ARACHIDONYL-2'-CHLOROETHYLAMIDE (ACEA)	CB1 receptor agonist	Sigma (*Cat No: A9719-25MG*)
AM251	CB1 receptor inverse agonist	Sigma (*Cat No: A6226-10MG*)
IONOMYCIN	Ca^{2+} ionophore	Cambridge Biosciences (*Cat No: 10004974-10 mg-CAY*)
TETRAHYDROLIPASTATIN (THL)	Serine lipase inhibitor	Tocris (*Cat No: 3540*), Sigma (*Cat No: O4139 SIGMA*)
KT109	DAGLβ inhibitor	Cravatt compounds, Sigma (*Cat No: SML1364*)
KT172	DAGLα and DAGLβ inhibitor	Cravatt compounds, Sigma (*Cat No: SML1688*)
JZL195	Dual MAGL and FAAH inhibitor	Sigma (*Cat No: SML0257-5MG*)
FORSKOLIN (FSK)	Adenylyl Cyclase activator	Sigma (*Cat No: F6886*)
PHORBOL 12-MYRISTATE 13-ACETATE (PMA)	PKC activator	Sigma (*Cat No: P1585-1MG*)
2-LINOLEOYL GLYCEROL (2-LG)	Lipid containing linoleoyl glycerol	Cambridge Biosciences (*Cat No: 62260-1 mg-CAY*)
2-ARACHIDONOYL GLYCEROL (2-AG)	CB1 receptor agonist	Cambridge Biosciences (*Cat No: 62160-1 mg-CAY*)
ANANDAMIDE (AEA)	CB1 receptor agonist	Cambridge Biosciences (*Cat No: 90050-5 mg-CAY*)
HEMOPRESSIN (HP)	Putative CB1 receptor antagonist	(1) Tocris (*Cat No: 3791/1*) (2) Cambridge Biosciences (*Cat No: 10011038-1 mg-CAY*) (3) Sigma (*Cat No: H3042-1MG*)

Table 2.1.1. Drug compounds used in Tango assay characterisation

2.1.3 Multiplex Assay

Multiplex bead and probe set

Quantigene Multiplex set from Affymetrix (*Cat No: QP1013 and QGP-113*)

Multiplex Analysis System

MAGPIX® multiplex system from Luminex

Total RNA Samples

Total human RNA of cerebellum and hippocampus from Takara Bio Europe (*Cat No: 636535 and 636593*) and skin from AMS Biotechnology Ltd (*Cat No: R1234218-50*) were purchased and diluted to desired concentration using nuclease free water and used in the Magpix beads assay.

2.1.4 Molecular Biology for CRISPR

Plasmids and Oligomers

pSpCas9(BB)-2A-Puro (PX459) was a gift from Feng Zhang (*Addgene plasmid #48139*)

Primers and oligomers were ordered from Sigma Aldrich and diluted in deionised water.

DAGLα CRISPR gRNA oligomers:	
DAGLα Exon 14 gRNA 1	5'– CGGAACCAAACACTACGGCC –3'
DAGLα PCR reaction primers:	
DAGLα Exon 14 Intron FWD	5'– AGCAAGGTTTGGAAGCGTAA –3'
DAGLα Exon 14 Intron REV	5'– CAGACCTCCATGTGACCAGA –3'
DAGLβ CRISPR gRNA oligomers:	
Exon 9 gRNA 1	5'– GTCAGCGGAGAGTGAGGTGC –3'
Exon 9 gRNA 2	5'– GGTGCTGGACGTGGAGTGTG –3'
Exon 9 gRNA 3	5'– GTGTGAGGTGCAGGACCGCC –3'
Exon 9 gRNA 4	5'– GCACCTCACTCTCCGCTGAC –3'
Exon 10 gRNA 1	5'– GATACGTTTACCAACGACTC –3'
Exon 11 gRNA 1	5'– GAGCCGCCTACCCGCAGGTC –3'
Exon 11 gRNA 2	5'– GGGCGGGGCGGCCGCCCTGC –3'
Exon 11 gRNA 3	5'– GTAGCACCTGACCTGCGGGT –3'
Exon 11 gRNA 4	5'– GTCATAGTGGGCCACAGCCT –3'
Cell assay PCR primers (in introns):	
DAGLβ Ex9 intron FWD	5'–CGCTGGGTTTCCCTCTTTAG –3'
DAGLβ Ex9 intron REV	5'–GTCAGCATTCACAGGCAAGA –3'
DAGLβ Ex10 intron FWD	5'–GCAGTCTCAGATCCCAGGAG –3'
DAGLβ Ex10 intron REV	5'–CAGCTCCAAAGAGGACAAGG –3'
DAGLβ Ex11 intron FWD	5'–CCTTGTCCTCTTTGGAGCTG –3'
DAGLβ Ex11 intron REV	5'–AGCAGGAAAACAAAGGCTCA –3'
DAGLβ PCR reaction primers:	
DAGLβ Exon 9 Intron FWD	5'– CGCTGGGTTTCCCTCTTTAG –3'
DAGLβ Exon 9 Intron REV	5'– GTCAGCATTCACAGGCAAGA –3'
NAPEPLD CRISPR gRNA oligomers:	
Exon 3 gRNA 1	5'– GATAAGGACCGCATCTATTGG –3'
Exon 3 gRNA 2	5'– GCTTCACCATCGCAGTACAT –3'
Exon 3 gRNA 3	5'– GAAGTGACCTTATCATGTCCG –3'
Exon 3 gRNA 4	5'– GGGGAACGACGAAATCGCTT –3'
NAPEPLD PCR reaction primers:	
NAPEPLD Exon 2 FWD	5'– TTCCGGAGCAAGTGATTCTT –3'
NAPEPLD Exon 4 REV	5'– CCACCTCGGTTCATAAGCTC –3'
PLA2G4B CRISPR gRNA oligomers:	

PLA2G4B Exon 13 gRNA 1	5'– GCTATTATGGCCACTGGTGGT –3'
PLA2G4B Exon 13 gRNA 2	5'– GCTATTATGGCCACTGGTGG –3'
PLA2G4B Exon 19 gRNA 3	5'– GCAGGCACAGGTGGGGCTCCG –3'
PLA2G4B Exon 19 gRNA 4	5'– GCACCTGTGCCTGCTGGATGT –3'
PLA2G4B PCR reaction primers:	
PLA2G4B Exon 13 Intron FWD	5'– CTGGTCCCAAGACCTGTGAT –3'
PLA2G4B Exon 19 Intron REV	5'– AGGGGACCCAGCTACAAGAT –3'

Table 2.1.2. Table of oligomers and primers

Enzyme Kits

T4 DNA Ligase kit *(Cat No: M0202S)*, T4 Polynucleotide Kinase *(Cat No: M0201S)*, BbsI Restriction Enzyme kit *(Cat No: R0539S)* and Calf Intestinal Phosphatase (CIP) kit *(Cat No: M0290S)* were ordered from New England Biolabs and used following manufacturer's instructions.

DNA Processing and Purification Kits

QIAprep Spin Mini Prep Kit *(Cat No: 27104)*, QIAamp DNA Mini Kit *(Cat No: 51304)* and QIAquick Gel Extraction Kit *(Cat No: 28704)* were from Qiagen

Qiashredder *(Cat No: 79654)*, RNeasy Mini Kit *(Cat No: 74104)* and RNase-free DNase Kit *(Cat No: 79254)* for RNA extraction were from Qiagen

High-Capacity RNA to cDNA Kit *(Cat No: 4387406)* from Thermo Fisher Scientific

Competent cells for transformation

NEB 10-beta Competent *E. coli* (High Efficiency) (*Cat No: C3019I*) from New England Biolabs

2.1.5 Polymerase Chain Reaction (PCR)

Polymerase Chain Reaction

Phusion Green Hot Start II High-Fidelity DNA Polymerase (*Cat No: F-537S*) from Thermo Scientific

1% Agarose

Agarose from Eurogentec (*Cat No: EP-0010-05*) dissolved in 1X TAE buffer – 40mM Tris, 20mM acetic acid, and 1mM EDTA, pH 8.4

DNA Ladders

Quick-Load 1 kb DNA Ladder (*Cat No: N0468S*) and Quick-Load 100bp DNA Ladder (*Cat No: N0467S*) from New England Biolabs

Visualiser

Molecular Imager® Gel Doc™ XR+ System and Quantitiy One software v4.6.5, from Bio-Rad

Spectrophotometer

Nanodrop ND-1000 from Thermo Scientific

2.1.6 Protein Assays

Membrane Preparation Lysis Buffer

20mM HEPES pH 7.0 (*Cat No: H3375*), 2mM DTT (*Cat No: 443853B*), 0.25M Sucrose (*Cat No: S0389*), 10mM NaF (*Cat No: S7920*), 1mM Na_3VO_4 (*Cat No: S6508*) with Complete Protease Inhibitor (Roche) (*Cat No: 04693116001*) made up in deionised water. Sucrose free lysis buffer is used for the final resuspension.

Cell Lysate Buffer

RIPA Lysis Buffer (Millipore) (*Cat No: 20-188*) diluted to 1x concentration and supplemented with Complete Protease Inhibitor (Roche).

Homogeniser

POLYTRON PT 1200 E handheld homogeniser from Kinematica

Protein Quantification Assays

Pierce BCA Protein Assay Kit (*Cat No: 23227*) from Thermo Scientific

Pierce Coomassie® Plus Protein Assay (*Cat No: 23200*) from Thermo Scientific

Absorbance Reader

SpectraMax Plus384 Absorbance Microplate Reader, from Molecular Devices

2.1.7 Western Blot

Gels and membranes

Mini-PROTEAN® TGX™ Precast Gels 7.5% (*Cat No: 4561023*) and 10% (*Cat No: 4561033*) from Bio-Rad

Amersham™ Hybond ECL Nitrocellulose Blotting Membrane (0.45μm) (*Cat No: RPN78D*) from GE Healthcare

Antibodies

ANTIBODY	WESTERN BLOT DILUTION	SPECIES	SUPPLIER
ACTIN	1:10,000	Mouse	Millipore (*Cat No: MAB1501*)
DAG LIPASE B (D4P7C)	1:2500	Rabbit	Cell Signaling (*Cat No: 12574S*)
ALEXA FLUOR 700 ANTI-MOUSE (SECONDARY)	1:5000	Goat	Invitrogen (*Cat No: A21036*)
IRDYE 800CW ANTI-RABBIT (SECONDARY)	1:5000	Goat	Licor (*Cat No: 925-32211*)
PEROXIDASE ANTI-RABBIT IGG (H+L) (SECONDARY)	1:3000	Goat	Vector Laboratories (*Cat No: PI-1000*)

Table 2.1.3. Antibodies used in western blot analysis

ECL Reagent

Pierce® ECL Western Blotting Substrate (*Cat No: 32209*) from Thermo Scientific

Imaging Systems

Odyssey Infrared Imaging System V3.0.25 from LI-COR

UVP™ BioSpectrum 810 Imaging System from Fisher Scientific

2.2 Methods

2.2.1 Passage of Cell Cultures

When cells were around 90% confluent, they were passaged using aseptic techniques. Cell culture medium was removed by aspiration and cells were washed with PBS-EDTA to remove residual serum before treatment with 0.05% trypsin in PBS-EDTA for 3-5 minutes in the incubator. Equal volume of media containing 10% serum was then added to inactivate the trypsin, and the cells were centrifuged at 1000rpm for 3 minutes. The cell pellet was resuspended in media and the density of cells were determined before seeding into appropriate dishes. Plated cells were incubated at 37^{o}C in a humid atmosphere with 5% CO_2 content.

2.2.2 CB1-Tango Assay

CB1-Tango cells were seeded in a 96 well black assay plate at a density of 30,000 cells per well in 100μl of 0.5% FBS McCoy's media or Freestyle media and incubated in 37^{o}C, 5% CO_2 incubator for 24 hours. Drug compounds were made up in plating media in 6x concentrations, and 50μl of total drug volume was added to appropriate wells (25μl of agonist plus 25μl of media, or 25μl of agonist and 25μl antagonist) and returned to the incubator for 4 hours. 6x concentration of LiveBLAzer™-FRET B/G (CCF4-AM) TANGO substrate (Invitrogen) was prepared according to manufacturer's instructions and 30μl was added to each well. The plate was left in the dark for 90 minutes at room temperature and then read on the Flexstation microplate reader (Molecular Devices). CB1 activation is measured as the fluorescence ratio between fluorescent blue channel (excitation 409nM, emission 460nM) from the cleaved substrate and FRET signal in green channel (excitation 409, emission 530nM) from the intact substrate using SoftMax Plus software). Ratios were normalised to control wells (set as 100%) where no agonists or antagonists were added; to wells with antagonist AM251; or by subtracting control wells from treatment wells and normalising to the maximal response of agonist.

2.2.3 Multiplex Assay

QuantiGene Multiplex assay system is a high-throughput profiling technology that enables gene expression quantitation of up to 50 different genes simultaneously. Sample cells were trypsinised and centrifuged to remove all media for RNA extraction. RNA was extracted from the cell lines using the Qiashredder (Qiagen) and RNeasy Mini Kit (Qiagen) according to manufacturer's instructions with additional β-mercaptoethanol added during cell lysis, plus digestion of genomic DNA with RNase-free DNase (Qiagen). Other RNA from tissues were purchased (Takara Bio Europe and AMS Biotechnology Ltd) and diluted with nuclease free water. A fixed concentration of RNA was processed with the Quantigene Plex Assay kit according to manufacturer's instructions. In brief, probe sets are generated against specific gene transcripts of interest which are coupled to magnetic beads with unique identification ratios of red and far-red light emissions. These are incubated with RNA samples overnight shaking at 600rpm at 54°C in a 96 well plate. The next day the hybridised samples and beads were washed and amplifier solutions were added to amplify the signal from the beads. The beads were then washed and read on the MAGPIX® multiplex system (Luminex) immediately. The median fluorescent intensity (MFI) was collected from each well for each bead type and the background was subtracted to get the Net MFI value. When comparing across cell lines, Net MFIs were normalised to the GEO means of two housekeeping genes (HKGs) HLCS and FOXJ2 and averaged. Analysis was carried out in Excel.

2.2.4 Molecular Biology for CRISPR

Designing gRNA Oligomers

pSpCas9(BB)-2A-Puro (PX459) Version 2 plasmid (Ran et al., 2013) is a cloning backbone plasmid for single guide RNA (sgRNA) and encodes Cas9 endonuclease from *S. Pyogenes* with Puromycin resistance (Figure 2.2.1). Guide RNA (gRNA) targeting specific DNA sequences can be cloned into the plasmid between two BbsI restriction sites located subsequent to the U6 promoter. The plasmid can then be transfected into mammalian cell lines for targeted gene editing. Oligomers targeting the catalytic domain of DAGLβ, NAPEPLD and PLA2G4B (listed in Materials Table 2.1.2) were designed for the PX459 plasmid with BbsI restriction enzyme overhangs.

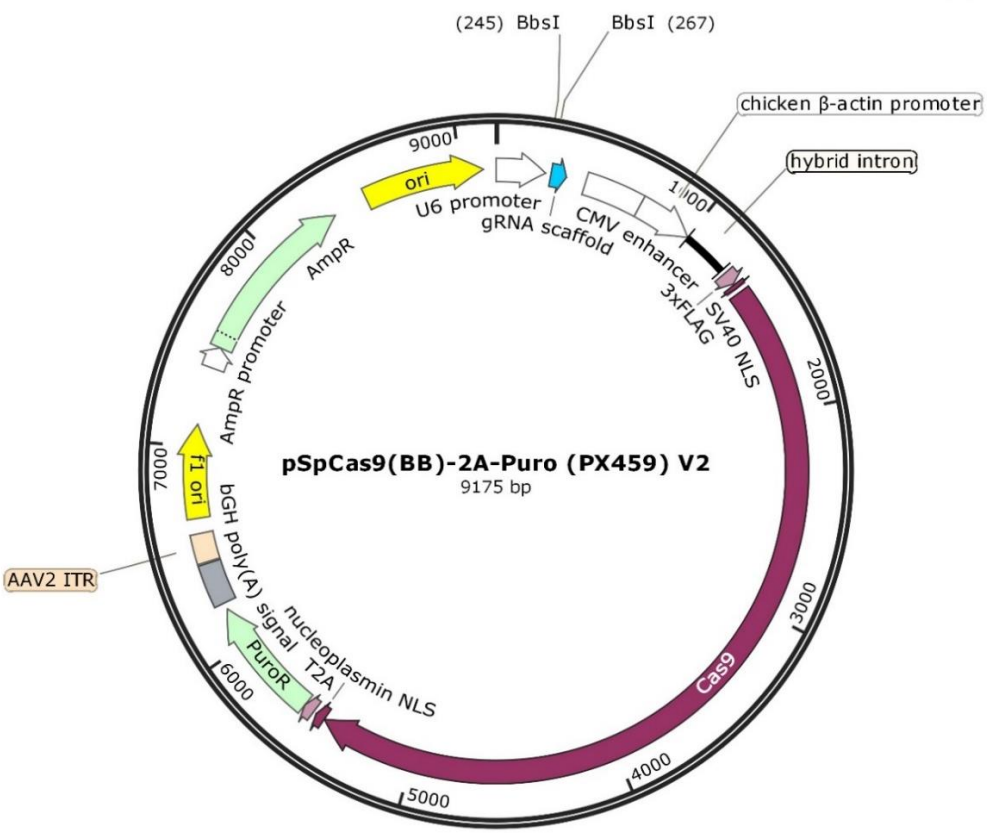

Figure 2.2.1. Vector map of pSpCas9(BB)-2A-Puro (PX459) Version 2 plasmid

Vector map of PX459 Version 2 plasmid (a gift from Feng Zhang (Ran et al., 2013)) with gene features was created on SnapGene Viewer. The restriction enzyme sites that are digested by BbsI are indicated downstream of the U6 promotor region and upstream of the gRNA scaffold.

Annealing oligomers

Oligomers were diluted to 100μM in sterile deionised water. The pairs of oligomers were then phosphorylated and annealed in one reaction.

COMPONENT	VOLUME (μL)
Forward Oligomer (100μM)	1
Reverse Oligomer (100μM)	1
10X T4 Ligation Buffer	1
T4 PNK	1
H_2O	6
TOTAL	**10**

The reaction was carried out in a thermocycler using the following parameters:

STEP	TEMPERATURE (^oC)	TIME
1	37	30 min
2	95	5 min
3	95 to 25	Ramp down at 5°C/min

After annealing, the oligomers were diluted 1:200 with deionised water to give a concentration of 50nM.

BbsI digest and dephosphorylation of PX459 plasmid

Digestion of the plasmid was carried out using the following reaction mix:

COMPONENT	VOLUME
PX459 Vector	1μg
BbsI enzyme	1μl
10x BbsI buffer	5μl
H_2O	Quantity Sufficient
TOTAL	**50μL**

The reaction mix was incubated at 37°C for 30 minutes. After incubation, 1 unit of CIP was added and the reaction was incubated again at 37°C for 60 minutes. The digested PX459 was then loaded with 6X loading dye and run on 1% TAE agarose gel and purified using QIAquick Gel Extraction Kit using a microcentrifuge (Qiagen) following manufacturer's instructions.

Ligation of oligomers and PX459 plasmid

Oligomers and PX459 plasmid were incubated together at 16°C for 2 hours using the following reaction mix:

COMPONENT	VOLUME
10X T4 Ligase Buffer	2μl
Digested PX459 Vector	50ng
Annealed Oligomer pair	1μl
T4 Ligase	1μl
H_2O	Quantity Sufficient
TOTAL	**20μL**

The mix was then heat inactivated at 65°C for 10 minutes, and then chilled for transformation.

Transformation into E.coli DH5α

25μl of competent *E.coli* cells (New England Biolabs) were thawed on ice for 10 minutes before adding 4μl of ligated CRISPR vector and incubated on ice for 30 minutes. The cells were then heat-shocked at 42°C for 1 minute and replaced immediately on ice. 250μl of S.O.C medium was added to the cells and incubated at 37°C, shaking at 250rpm for 1 hour. Cells were then plated on 100μg/ml ampicillin selective LB agar plates and incubated at 37°C overnight.

Individual colonies grown on LB agar plates were selected with a sterile loop and placed into 5ml LB broth containing 100μg/ml ampicillin in a culture tube. The tube was incubated in a 250rpm shaker at 37°C overnight. The plasmid was then extracted from the *E.coli* cells with QIAprep Spin Miniprep Kit (Qiagen) according to manufacturer's instructions.

Transfection

Cells were plated in 6-well plates at a density of around 80% confluency and were transfected the following day with plasmid DNA using FuGene HD Transfection Reagent (Promega) according to manufacturer's instructions. In brief, plasmid DNA was diluted in sterile water to the concentration of 0.02μg/μl and 12μl of FuGENE reagent was added and incubated for 15 minutes at room temperature. The complex was then added to cells and the cells were returned to the 37°C incubator for 24 hours. Cells were either trypsinised for the SURVEYOR Nuclease assay or the media was changed with puromycin antibiotic selection for 24 hours for clonal expansion.

SURVEYOR Nuclease Assay

Surviving transfected cells were trypsinised and pelleted by centrifuging and the remaining medium was removed. Genomic DNA was extracted from the cells using Puregene Core Kit B (Qiagen) according to manufacturer's instructions.

Surveyor nuclease assay verifies the presence of indel mutations by hybridising indel mutated DNA with wild type DNA and cleaving mismatched hetero-duplexes. The CRISPR site is amplified by PCR from the pooled genomic DNA and half is run on 1% agarose gel to check for successful PCR reaction. The remaining PCR reaction mix is heated and cooled to allow annealing to form heteroduplexes: 95°C for 10 min; ramping down at a rate of -0.3°C s^{-1} to 85°C and holding for 1 min; continuing ramping down -10°C at a time and holding for 1 min until 25°C; and 25°C hold for 1 min and finally hold at 4°C. After re-annealing, 10µl of PCR products were treated with 1µl of Surveyor nuclease and 1µl of enhancer (supplied with the kit) and incubated at 42°C for 40 minutes. Finally the PCR mix is run on 2% agarose gel to visualise any smaller cleaved bands.

Clonal isolation and expansion

Surviving cells that were transfected with CRISPR vector after puromycin treatment were trypsinised – ensuring cells are fully dissociated from each other, and split into a large 150mm cell culture dish with varying densities of cells to ensure cells are isolated for clonal expansion. Cells are left to grow for 2-3 weeks in a 37°C incubator. Individual colonies of cells were selected with cloning discs (Sigma Aldrich) and placed into separate wells in 24 well plates for expansion. The discs were removed after 24 hours and the cells were left to grow until around 50% confluent and then transferred to larger vessels.

2.2.5 PCR and RT-PCR

For mutation analysis in CRISPR treated cells, both genomic PCR and RT-PCR were carried out on the cell lines. Genomic DNA was extracted using the QIAamp DNA Mini Kit (Qiagen) according to manufacturer's instructions. RNA were extracted from sample cell lines using RNeasy Mini Kit (Qiagen). Conversion of RNA to cDNA was carried out using High Capacity RNA-to-cDNA Kit (Thermo Fisher Scientific) according to manufacturer's instructions. PCR reactions of CRISPR sites were carried out with primers (Sigma Aldrich) located before and after the CRISPR mutation site.

PCR was carried out using Phusion Polymerase (ThermoScientific) with the following components:

COMPONENT	VOLUME
Genomic DNA or cDNA	1µg
100µM Primer FWD	1µl
100µM Primer REV	1µl
5X HF Buffer	4µl
50mM dNTPs	0.08µl
Phusion Polymerase	0.2µl
H_2O	Quantity Sufficient
TOTAL	**20µL**

STEP	TEMPERATURE (^oC)	TIME (SECONDS)
1	98	30
2	98	5
3	63	10
4	72	30
5	Go to step 2 for 30 cycles	
6	72	60
7	12	Hold

The samples were run on 1% or 2% agarose gel at 90V for 45 minutes. The PCR product was purified from the gel using QIAquick Gel Extraction Kit using a microcentrifuge (Qiagen) following manufacturer's instructions and then sent for Sangar sequencing (Source Biosciences).

2.2.6 Protein Assays

Cell Membrane Preparations

Cells were grown in 10cm dishes until confluent. The media was removed and cells were washed in cold PBS before adding 600µl of lysis buffer to each dish and left to stand for 1 minute. The cells were harvested using a cell scraper and collected into an eppendorf tube on ice. Cells were then homogenised in 7 second bursts at 10 second intervals, repeated 3 times using the POLYTRON PT 1200 homogeniser (Kinematica). The homogenate was then centrifuged at 53,000rpm for 30 minutes at 4^{o}C to pellet the membranes. The supernatant was removed and pellet resuspended in 200µl of sucrose-free lysis buffer, and homogenised again in 7 second bursts at 10 second intervals, repeated 3 times. Protein concentration was determined using Bradford Coomassie assay (Thermo Fisher Scientific). Remaining aliquots of membranes were stored at -80^{o}C.

Whole Cell Lysates

Media was removed from cells and washed in cold PBS before 600µl of RIPA buffer containing protease inhibitors were added to the plate. The cells were harvested using a cell scraper and collected into an eppendorf tube and placed on a rocker at 4°C for 30 minutes. The lysed cells were then spun at 3000rpm for 5 minutes at 4°C and the supernatant was collected. Protein concentration was determined using Bradford BCA assay (Thermo Fisher Scientific). Remaining aliquots of cell lysates were stored at -20°C.

Crude brain lysate

Mice brains were kindly provided by Karen Steel's group. Wild type C57BL/6 male mice were culled at P50 and the whole brain plus cerebellum were collected and lysed in lysis buffer containing 0.2% SDS, 0.01M EDTA pH8.0 and 1x Protease inhibitor cocktail (Roche). Cells were then homogenised in 7 second bursts at 10 second intervals, repeated 3 times using the POLYTRON PT 1200 homogeniser (Kinematica). The homogenate was then centrifuged at 13,000g for 15 minutes at 4°C and the supernatant was collected. Protein concentration was determined using Bradford BCA assay. Remaining aliquots were stored at -20°C.

Western Blot

Cell membrane preps and whole cell lysate samples containing 1µg/µl of protein were prepared by adding 5x protein loading buffer, boiled for 5 minutes at 100°C and then loaded into precast gels. The gel was run for 1 hour at 100V. The gel was then transferred onto nitrocellulose membrane at 100V for 1 hour. The membrane was then blocked with 5% milk in PBS and then washed in PBS-T before incubating with primary antibody in 2% milk in PBS-T overnight in 4°C. The primary antibody was then removed with PBS-T wash and the membrane was then incubated with fluorescent secondary antibody in 2% milk in PBS-T for 1 hour in the dark. The blot was then visualised using Odyssey Infrared Imaging System V3.0.25 (LI-COR).

For enhanced chemiluminescence (ECL) detection of horse radish peroxidase (HRP), the blot was treated as above with the exception of peroxidase conjugated antibody as the secondary antibody. The substrate was then mixed according to manufacturer's instructions and applied to the blot. The blot was then visualised using UVP™ BioSpectrum 810 Imaging System (Fisher Scientific).

2.2.7 Data Analysis

Data collected was analysed using Graph Pad Prism 5.0 or Microsoft Excel.

CB1-Tango Assays

Ratios obtained from CB1-Tango assays were averaged across technical repeats and normalised to average control ratios set as 100% stated in each experiment (control determined as either in the absence of any pharmacological drugs or in the presence of AM251 only). Normalised data were then averaged across independent experiments and plotted on Graph Pad Prism. Log EC_{50} values were obtained from non-linear regression curve fitted to the data points generated by Graph Pad Prism and averaged across experiments.

QuantiGene Multiplex Assays

The Median Fluorescent Intensity (MFI) was collected for each gene which is proportional to the abundance of the RNA for that gene and averaged across technical repeats. The MFI from the background wells were subtracted from the sample data to give the Net MFI. The Net MFIs of each gene were plotted in Graph Pad Prism when comparing within a cell type. When comparing across cell types, the Net MFIs of each gene were normalised to the GEO mean of two housekeeping genes: HLCS and FOXJ2. The relative expression of the genes to the housekeeping genes are then graphed in Graph Pad Prism.

Student's two-tailed T-test and One Way or Two Way ANOVA followed by Dunnett's multiple comparison test or Bonferroni's multiple comparison test used for all statistical analysis. Statistical significance is defined as: *p<0.05; **P<0.01; ***p<0.001. n refers to number of independent experiments.

Chapter 3. Results 1 - 2-LG as a novel eCB

3.1 Introduction

The two human DAGLs, DAGLα and DAGLβ, were first discovered using a bioinformatics approach. The gene encoding a known mono- and diacylglyceride hydrolysing enzyme in *Penicillium camembertii* fungus (Yamaguchi et al., 1991) was queried against mammalian genomes and clear homologues were defined. The human homologues were subsequently identified and cloned (Bisogno et al., 2003). The DAGLs have a high degree of conservation in mammals and are expressed in a wide range of species including fungi, invertebrates and vertebrates (Yuan et al., 2016). The DAGLs are *sn*-1 specific and can produce 2-acylglycerols with varying lengths of fatty acids in the *sn*-2 position, including linoleic, oleic, arachidonic and stearic acid (Bisogno et al., 2003). 2-AG is synthesised primarily by DAGL and has an important role as the major endocannabinoid in activating CB1 and CB2 receptors (Mechoulam et al., 1995; Sugiura et al., 1995). However, other structurally related lipids such as 2-LG, 2-OG and 2-PG generated by DAGL are less well studied. Knockout experiments in mice have shown that the DAGLs are required for all of the well-established eCB functions and for the synthesis of nearly all of the 2-AG in tissues (Gao et al., 2010; Tanimura et al., 2010; Shonesy et al., 2014; Jenniches et al., 2016); this supports the hypothesis that 2-AG is the major eCB in the body, but it leaves speculation for other DAGL derived lipids playing minor roles.

Despite *Drosophila melanogaster* lacking the expression of functional CB receptors (Elphick and Egertova, 2001; McPartland et al., 2001; McPartland, 2004), DAGL homologue Inactivation No After-potential E (INAE) is expressed and presumably has a non-cannabinoid signalling role. INAE activity is required to couple photo-excitation of rhodopsin to the opening of TRP/TRPL channels in photoreceptors (Leung et al., 2008) and is able to generate 2-acylglycerols primarily containing linoleic acid, as *Drosophila* lacks an arachidonic acid pool (Shen et al., 2010). 2-LG is in relatively high abundance in *Drosophila*, and has been postulated as an active signalling ligand for the activation of photoreceptors via the action of INAE (Tortoriello et al., 2013). However, these findings have been challenged, (Hardie and Franze, 2012; Randall et al., 2015) suggesting an alternative function for 2-LG.

In recent collaborative experiments, the Doherty and Harkany labs have seen up to 50% reductions in 2-LG in *Drosophila* that have had INAE/DAGL knocked out (unpublished observation). Homologues of CB1 receptors have been described in various species including *Hydra vulgaris* (De Petrocellis et al., 1999), the mollusc *Mytilus edulis* (Stefano et al., 1996), and in some *Crustaceans* (McPartland et al., 2006). Insects likely emerged from a C*rustacean*-like ancestor expressing a CB1 homologue (Abzhanov and Kaufman, 2000; Regier et al., 2010) so the reason for their unique lack of expression of CB receptors is open for conjecture. A pragmatic explanation of a "secondary loss" of CB receptors could be due to various evolutionary pressures, for example, the toxicity of phytocannabinoids (McPartland, 2004). This raises an interesting, albeit speculative, concept that 2-LG could be an ancestral eCB.

2-LG is present in mammalian brain homogenate (Richardson et al., 2007; Williams et al., 2007) and mouse hippocampal neurones (Murataeva et al., 2016) at around 10x lower concentration than 2-AG. 2-LG is also found in mouse spleen tissue (Ben-Shabat et al., 1998) and canine gut tissue (Mechoulam et al., 1995) in relatively high amounts compared to 2-AG. Despite the physiologically detectable levels of 2-LG, its physiological role is undetermined. It has been previously reported that 2-LG is unable to directly activate mammalian CB receptors but instead can potentiate 2-AG activation of CB1 receptors in behavioural assays (Ben-Shabat et al., 1998; Gallily et al., 2000). The mechanism for this potentiation is not clear. It has been suggested that 2-LG may limit 2-AG breakdown by occupying MAGL with similar affinities (Ghafouri et al., 2004), thus prolonging 2-AG signalling leading to an 'entourage effect'. Conversely, experiments in autaptic mouse hippocampal neurons show that 2-LG does not have an entourage effect on the action of 2-AG on CB1 dependent DSE, but instead 2-LG displays an antagonistic effect in this study (Murataeva et al., 2016). One explanation for the antagonistic effect seen by Murataeva et al could be due to 2-LG acting as a partial agonist which can behave as an antagonist in the presence of a full agonist (Calvey and Williams, 2008). Therefore, 2-LG might have a wider role in eCB signalling. With the above studies in mind, we decided to directly test the hypothesis that 2-LG is a partial CB1 receptor agonist by using a sensitive industry standard cell-based CB1 receptor reporter assay.

The CB1-Tango assay is a recombinant cell-based assay that utilises the commercially available Tango™ CNR1-bla U2OS cell line from Invitrogen. The assay allows us to study CB1 signalling via a β-lactamase reporter gene in a human osteosarcoma cell line (Barnea et al., 2008; van der Lee et al., 2009). The cell line stably expresses human CB1 receptors that are

linked at the C terminus to a TEV protease site and a Gal4-VP16 transcription factor. This parental cell line also stably expresses the β-arrestin protein fused to a TEV protease, and a β-lactamase reporter gene under the control of a UAS response element (Figure 3.1.1). Upon activation of the CB1 receptor, β-arrestin is recruited to the CB1 receptor C terminus where it cleaves the transcription factor. The transcription factor is then transported to the nucleus and activates the β-lactamase reporter gene which is non-native to a human cell line and therefore provides a level of specificity. Levels of β-lactamase enzyme can be detected by application of the ester CCF4-AM FRET substrate ("LiveBLAzer") which emits fluorescence at 530nM when intact. Once cleaved by β-lactamase, FRET transfer is not able to occur, resulting in a different emission at 460nM. Therefore, the ratio of green (530nM) to blue fluorescence (460nM) will directly correlate to the activation of CB1.

In this chapter, I will report on the successful utilisation of the CB1-Tango assay to assess the activity of a small molecule CB1 agonist (ACEA) and antagonist (AM251) on the CB1 receptor and to directly compare the activity of 2-LG with that of 2-AG and AEA on the CB1 receptor. I will also derive some insights into the activity of 2-LG as a potential eCB and its relevance as an entourage molecule in physiological conditions.

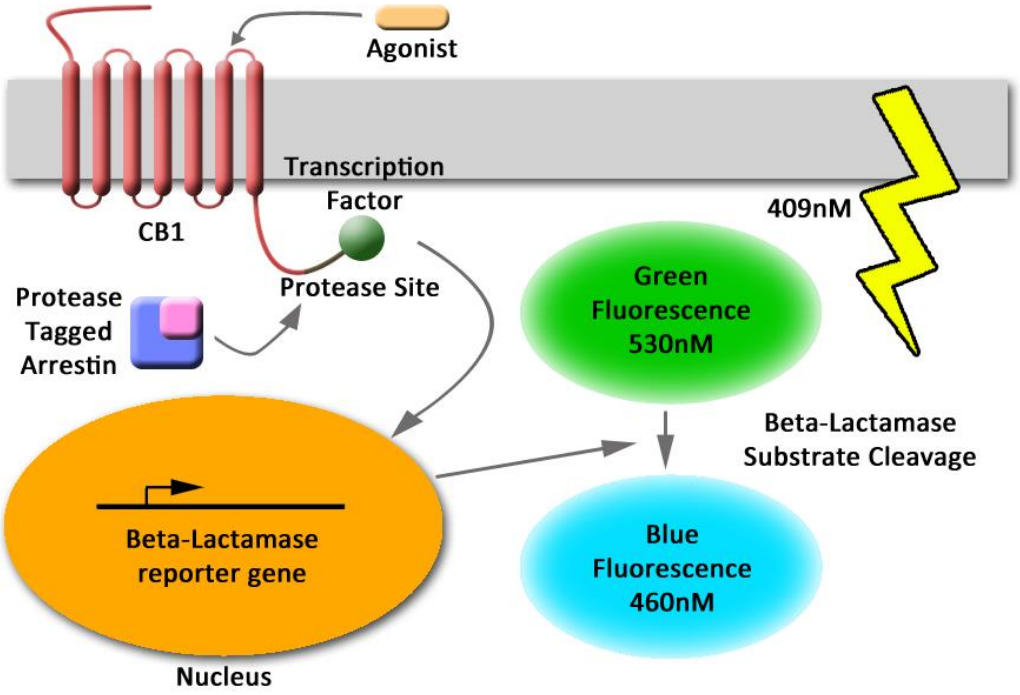

Figure 3.1.1. Schematic overview of the Tango Assay system

The CB1 receptor is extended at the C-terminus with a non-native transcription factor by a linker that contains a protease cleavage site. β-Arrestin-2 is fused to a TEV protease. Upon CB1 activation by agonist(s), β-arrestin-2 is recruited to the receptor. Close proximity of the protease and the cleavage site allows the transcription factor to be released, which activates transcription of β-lactamase reporter gene in the nucleus. Activity of the β-lactamase enzyme is detected with the fluorogenic membrane-permeable substrate ester CCF4/AM, which is cleaved by the β-lactamase enzyme resulting in blue fluorescence. The ratio of green (530nM) to blue fluorescence (460nM) will directly correlate to the activation of CB1.

3.2 Results

The use of ACEA as a control agonist and AM251 as a control antagonist in the CB1 reporter assay

In order to establish baseline positive controls, we tested the response of the CB1-Tango cells to the potent and selective CB1 agonist arachidonyl-2'-chloroethylamide (ACEA) (K_i = 1.4nM) (Hillard et al., 1999) as well as the potent and selective CB1 antagonist AM251 (K_i = 7.49 nM) (Lan et al., 1999). CB1-Tango cells were plated in Freestyle Media as described in Methods. The cells were incubated in 37°C incubator overnight and starved (Freestyle media is serum free) to reduce the background signal in the assay. The cells were then treated with a serial dilution of ACEA (0.04 – 25μM, 1:5 dilution) in the presence and absence of 10μM AM251 to ensure a molar excess over the highest concentration of ACEA (all concentrations in this and all other experiments relate to the final concentration during the assay period). The assay was carried out as described in Methods. The fluorescence ratio between blue and green excitation wavelengths was calculated and the data was normalised to control wells which have not been treated with any drugs.

The results from a representative experiment are shown in Figure 3.2.1. A robust CB1 response can be readily detected at all tested concentrations of ACEA with relatively low SEMs (SEMs were below 2.5% of control) which is statistically significantly different to the control values from 0.04μM ACEA (185.5% ± 1.8% of control, $p<0.001$) indicating the sensitivity of the assay. This response is concentration dependent, as CB1 response increases with increasing concentrations of ACEA, until the maximal response of 259.2% ± 2.5% of control levels at around 5μM is reached. Thus, this confirms the cells' ability to respond to CB1 activation by a synthetic CB1 agonist. Importantly, no significant response to ACEA was seen when AM251 was present ($p>0.05$), which indicated that AM251 successfully antagonised the CB1 responses. In further studies AM251 was seen to fully inhibit the 5μM ACEA response when used at 2.5μM. These concentrations were then generally used in subsequent experiments throughout as positive controls (unless otherwise stated). It is important to note that on its own AM251 did not have any effect in the assay; this shows that under the normal assay conditions there is no basal CB1 dependent signalling (Figure 3.2.1). The EC_{50} obtained from a series of concentration response experiments carried out for ACEA was 0.018μM (Log EC_{50} = -7.735 ± 0.37, n = 5) (Figure 3.2.7).

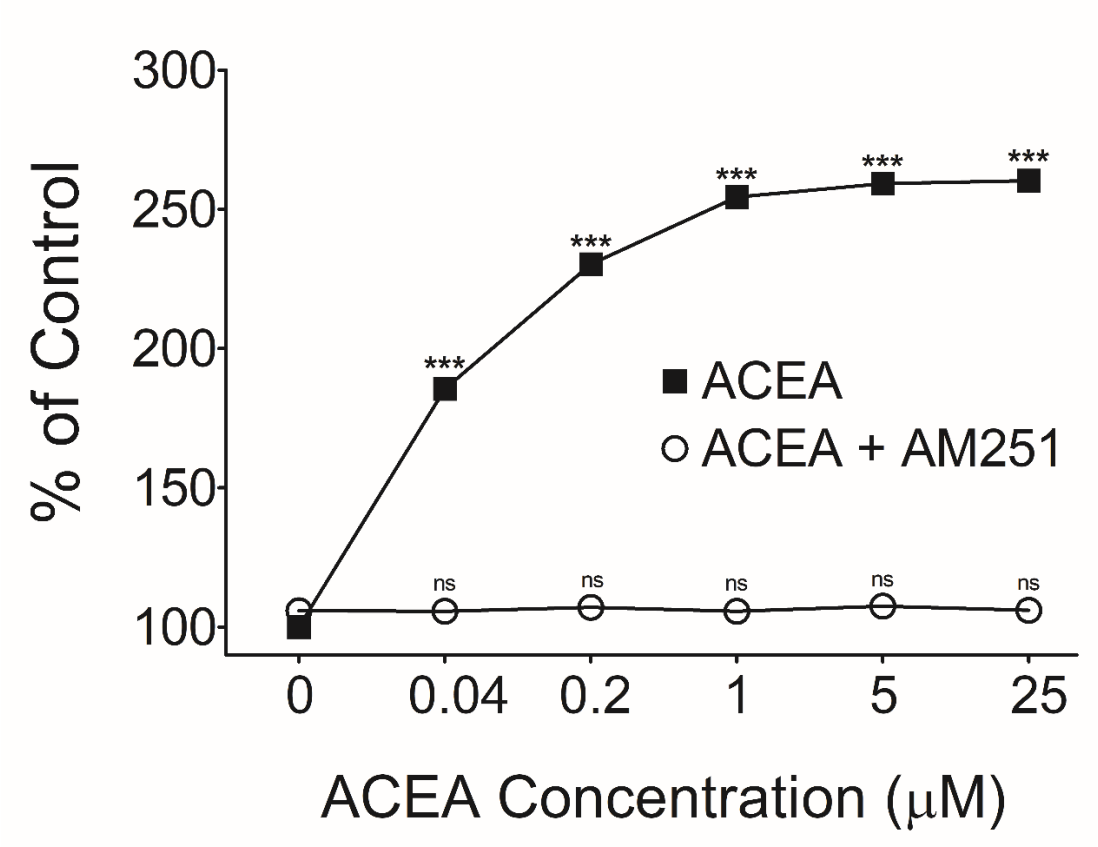

Figure 3.2.1. Small molecule agonist ACEA elicits CB1-dependent responses in CB1-Tango cells in a concentration dependent manner

CB1-Tango cells were seeded at 30,000 cells per well in Freestyle expression media for 24 hours in clear bottom black plates. CB1 response was established by adding ACEA (final top concentration 25μM, 1:5 serial dilutions) in the absence and presence of AM251 (final concentration 10μM). Drug compounds were left for 4 hours for the accumulation of β-lactamase enzyme before, 6x concentration of β-lactamase substrate was added to the wells for 90 minutes. Green and blue fluorescence detection of the cleavage of the β-lactamase substrate was measured. Fluorescence ratio between green and blue channels were calculated and values were normalised to the control wells (set as 100) as % of control. Graph shows means of 8 replicates from a single representative assay. In this experiment, SEMs of the data points were relatively narrow (<2.5%) and for this reason are not evident on the graph. Statistical significance of ACEA responses compared to the control in the absence of ACEA, and ACEA responses in the presence of AM251 compared to AM251 only control, were established with One Way ANOVA.

ns $p>0.05$; ***$p<0.001$; One Way ANOVA, Dunnett's post-test.

Characterisation of 2-AG and AEA responses in the CB1-reporter assay

We next wanted to determine the cellular response to the two major established eCBs: 2-AG (K_i = 472nM) (Mechoulam et al., 1995) and AEA (K_i = 52nM) (Devane et al., 1992), and to confirm that AM251 is able to antagonise the responses to the native ligands. Cells were treated with a range of concentrations of 2-AG (0.04 – 25μM, 1:5 dilution) in the absence or presence of AM251 (FAC 2.5μM). The result from a representative experiment is shown in Figure 3.2.2. Detectable CB1 responses are observed at all tested concentrations of 2-AG, with a statistically significant responses detected from 0.04μM (140.6% ± 2.0% of control, $p<0.001$). With increasing concentrations of 2-AG the CB1 response increased, reaching a maximal activation between 5μM (318.4% ± 9.0% of control response) and 25μM (325.5% ± 9.2% of control response). Quite notably, 2.5μM AM251 is able to fully inhibit the response to all tested concentrations of 2-AG confirming that the response is indeed CB1 dependent.

Similarly, the second major eCB AEA was also tested on the CB1-Tango cells for its ability to activate the CB1 receptor (Figure 3.2.3). A range of AEA concentrations (0.0025 – 5μM) was used to treat the CB1-Tango cells. AEA was observed to elicit a normal concentration response curve with significant responses apparent at as little as 0.025μM (119.4% ± 2.4% of control, $p<0.001$), reaching the maximal response at around 2.5 - 5μM (242.0% ± 3.0% of control). Importantly, there were no statistically significant AEA responses observed when 2.5μM AM251 was present across all concentrations ($p>0.05$). This confirms that the response to AEA is CB1 dependent. The assay is sensitive to the response of the agonists as it is able to detect responses from low concentrations of drugs (40nM ACEA and 2-AG; 25nM AEA).

Based on a series of independent concentration response curves, the EC_{50} for 2-AG was 1.17μM (Log EC_{50} = -5.930 ± 0.42 SEM, n = 4) as compared with 0.057μM for AEA (Log EC_{50} = -7.242 ± 0.35 SEM, n = 6) (Figure 3.2.7).

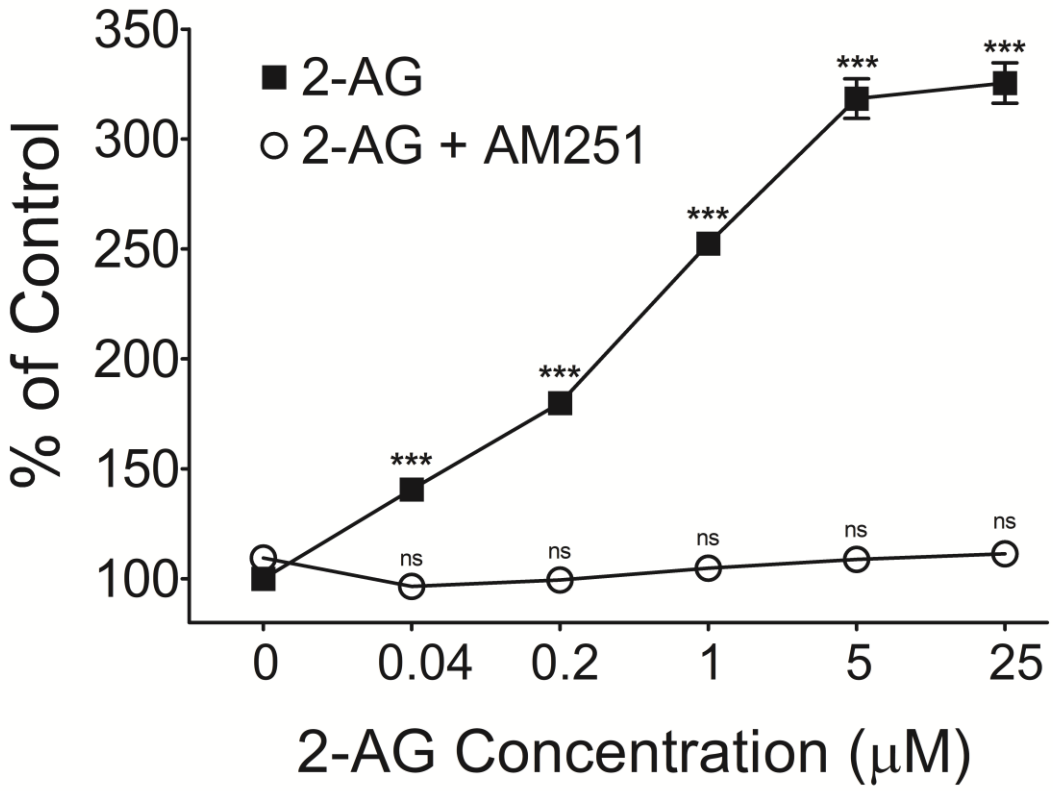

Figure 3.2.2. The eCB 2-AG stimulates CB1-dependent responses in CB1-Tango cells in a concentration dependent manner

30,000 CB1-Tango cells were seeded per well in Freestyle media in clear bottom black plates for 24 hours. Serial dilutions of 2-AG (final top concentration 25μM, 1:5 dilution) in the presence and absence of AM251 (final concentration 2.5μM) were made up in Freestyle media. Drug compounds were left for 4 hours for the accumulation of β-lactamase enzyme before 6x concentration of β-lactamase substrate was added to the wells for 90 minutes. Green and blue fluorescence detection of the cleavage of the β-lactamase substrate was measured. Fluorescence ratio between green and blue channels were calculated and values were normalised to the control wells (set as 100) as % of control. Graph shows means and bars represent SEMs of 8 replicates from a single representative assay. Statistical significance of 2-AG responses compared to the control in the absence of 2-AG, and 2-AG responses in the presence of AM251 compared to AM251 only control were established with One Way ANOVA.

ns $p>0.05$; ***$p<0.001$; One Way ANOVA, Dunnett's post-test.

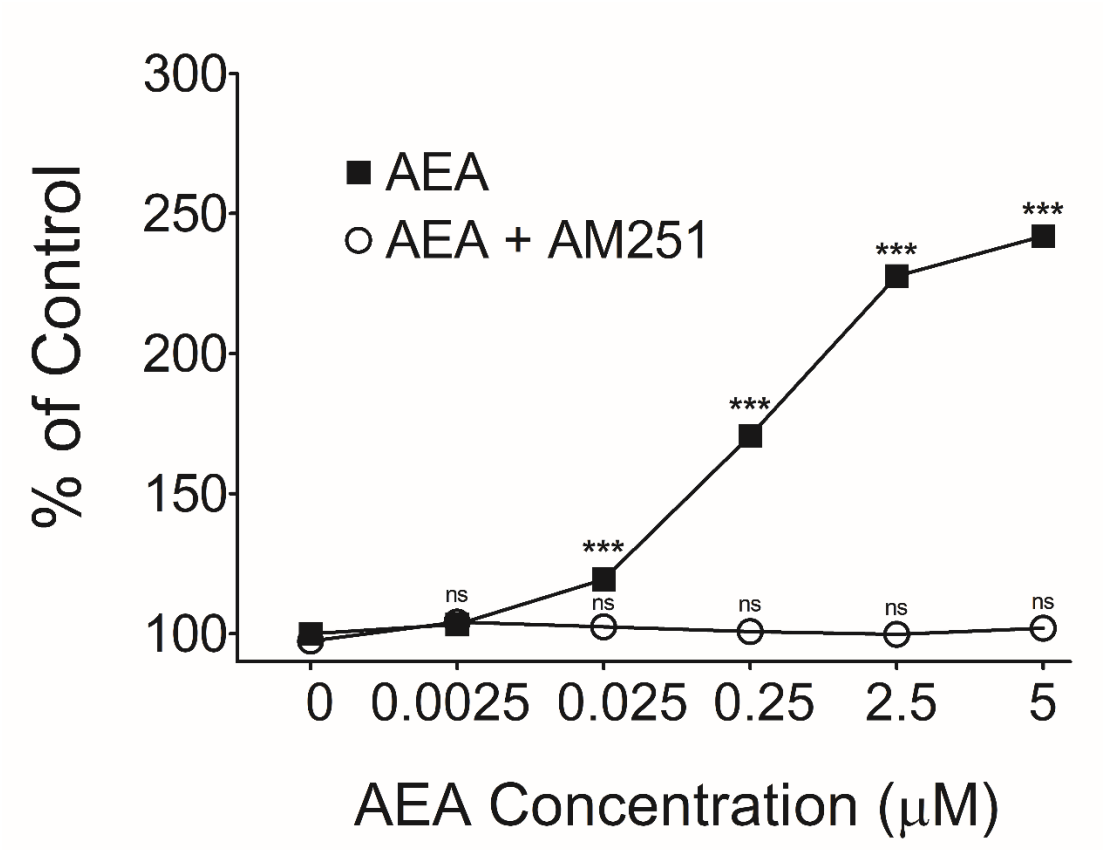

Figure 3.2.3. The eCB AEA stimulates CB1-dependent responses in CB1-Tango cells in a concentration dependent manner

30,000 CB1-Tango cells were seeded per well in Freestyle media in clear bottom black plates for 24 hours. A varying range of concentrations of AEA (final top concentration 5μM, 1:2 and 1:10 dilutions) in the presence and absence of AM251 (final concentration 2.5μM) were made up in Freestyle media. Drug compounds were left for 4 hours for the accumulation of β-lactamase enzyme before 6x concentration of β-lactamase substrate was added to the wells for 90 minutes. Green and blue fluorescence detection of the cleavage of the β-lactamase substrate was measured. Fluorescence ratio between green and blue channels were calculated and values were normalised to the control wells (set as 100) as % of control. Graph shows means of 8 replicates from a single representative assay. SEMs of the data points were relatively narrow (<3.4%) and are not evident on the graph. Statistical significance of AEA responses compared to the control in the absence of AEA, and AEA responses in the presence of AM251 compared to AM251 only control were established with One Way ANOVA.

ns $p>0.05$; ***$p<0.001$; One Way ANOVA, Dunnett's post-test.

2-LG exhibits an eCB like activity in the reporter assay, but only in the presence of a hydrolase inhibitor

The CB1-Tango cells are viable and are able to detect CB1 activation by synthetic and natural ligands. Furthermore, signalling can be blocked by a robust synthetic CB1 antagonist. Since 2-LG is structurally similar to 2-AG and for reasons discussed above, we have postulated that it might serve as a partial agonist at the CB1 receptor. We have utilised the CB1-Tango assay to test this hypothesis.

To test whether 2-LG has agonist-like activity at the CB1 receptor, CB1-Tango cells were plated as previously described and treated with varying concentrations of 2-LG on its own over a 1 - 50μM range for 4 hours. Initial experiments indicated 2-LG could induce a modest concentration dependent CB1 response on the cells across all concentrations, but the response was limited and relatively variable across a large number of independent experiments, even at higher concentrations of 2-LG (Figure 3.2.4). In brief, the results "tended" towards a concentration dependent response, but even at 25μM, whilst statistically significant to the control (134.3% ± 4.18% of control, $p<0.001$), the response was at best only 34% higher than control and only around 10-15% of the response seen with maximally active concentrations of 2-AG or AEA (Figure 3.2.2 and Figure 3.2.3).

Initially, the above results do not support the hypothesis that 2-LG is a partial agonist of the CB1 receptor, but if 2-LG is unstable we have perhaps not actually tested the hypothesis critically. We reasoned that the CB1-Tango cells are likely to express eCB degrading enzymes MAGL, FAAH and ABHD6 which may contribute to the early and rapid termination of any 2-LG elicited signalling or other eCB signalling that 2-LG may be potentiating. Thus, 2-LG concentrations were again tested on CB1-Tango cells but in the presence of 100nM of JZL195 – a MAGL, FAAH and ADBH6 inhibitor (Long et al., 2009a) (Figure 3.2.4).

The first important observation that we need to consider is that when added at 100nM, JZL195 on its own stimulated a small response to 112.3% ± 3.65% of control. Experiments to be discussed later suggest that this reflects a small but significant increase in a basal eCB tone in the cells as it is not seen in the presence of AM251. However, in the presence of 100nM JZL195, 2-LG elicited a very clear concentration dependent response with a maximal effect between 25μM (169.4% ± 7.13% of control) and 50μM (175.4% ± 8.30% of control) (Figure 3.2.4). When JZL195 is present, a significant response is reached at 12.5μM (145.0% ± 14.48% of control) which is not significant in the absence of JZL195. The responses at 25μM

and 50μM 2-LG are much higher when compared to the equivalent concentration in the absence of JZL195. This suggests that one or more eCB degrading enzymes (MAGL, FAAH and ABHD6) might limit the action of 2-LG in the assay. In other experiments, a MAGL specific inhibitor JZL184 (Long et al., 2009b) and a FAAH specific inhibitor URB597 (Mor et al., 2004) did not significantly enhance 2-LG signalling when added alone or in combination, suggesting the involvement of all three eCB degrading enzymes (data not shown). Nonetheless the above results support the hypothesis that 2-LG is a partial agonist at the CB1 receptor, but firm conclusions on this point are tempered by the fact that JZL195 has to be present to fully reveal that activity.

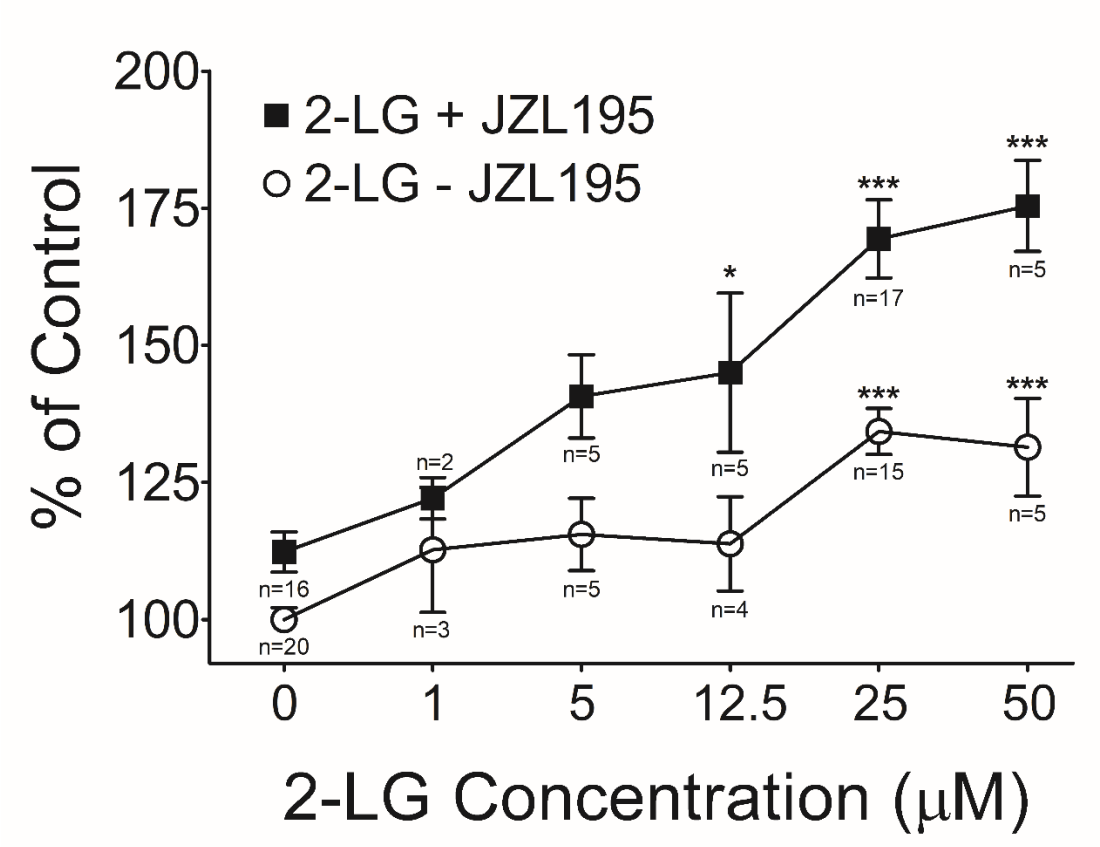

Figure 3.2.4. 2-LG mediated response is detectable but full response requires JZL195

30,000 CB1-Tango cells were plated into black 96 well plates in Freestyle media as described previously. The cells were treated with varying concentrations of 2-LG (50μM – 0μM) in the presence and absence of JZL195 (100nM) for 4 hours. Responses were measured as described previously and normalised to the control wells in the absence of JZL195 and 2-LG (set to 100) as % of control. Graph shows means and bars represent SEMs of pooled independent experiments (n indicated on the graph) with 8 replicates in each experiment. Statistical significance of 2-LG responses in the absence of JZL195 compared to its control, and 2-LG responses in the presence of JZL195 compared to JZL195 only control were established with One Way ANOVA.

*p<0.05; ***p<0.001; One Way ANOVA, Dunnett's post-test.

The 2-LG effects are fully inhibited by AM251

The experiments in Figure 3.2.4 show the effects of 2-LG and JZL195 relative to the control that has neither agent present. Most of the experiments had also in parallel, the same conditions in the presence of AM251 to determine if the response was dependent on CB1 receptor function. In this section, all of the data has been plotted as a percentage of the control value obtained in the presence of JZL195 (the JZL195 control). When plotted in this way, 2-LG still demonstrated a concentration dependent response with statistically significant responses to the JZL195 control apparent at 12.5μM (129.1% ± 12.9% of control) (Figure 3.2.5). 2-LG was maximally active at concentrations between 25μM (150.9 ± 6.4% of control) and 50μM (156.3% ± 7.4% of control). The EC_{50} for 2-LG calculated from these series of experiments was 16.56μM (Log EC_{50} = -4.781 ± 0.19 SEM) (Figure 3.2.7). When plotted in this manner, AM251 on its own reduces the control value to 87.7% ± 3.4%, a small yet highly significant ($p=0.002$, Students' unpaired T-Test) response that presumably reflects inhibition of a low level of eCB tone consequential to JZL195 treatment. Importantly, 2-LG failed to stimulate any response when AM251 is present ($p>0.05$), confirming that the response seen in the presence of JZL195 is CB1 dependent. Thus, when plotted against the JZL195 control, the data still support the hypothesis that 2-LG has concentration dependent agonist-like activity at the CB1 receptor.

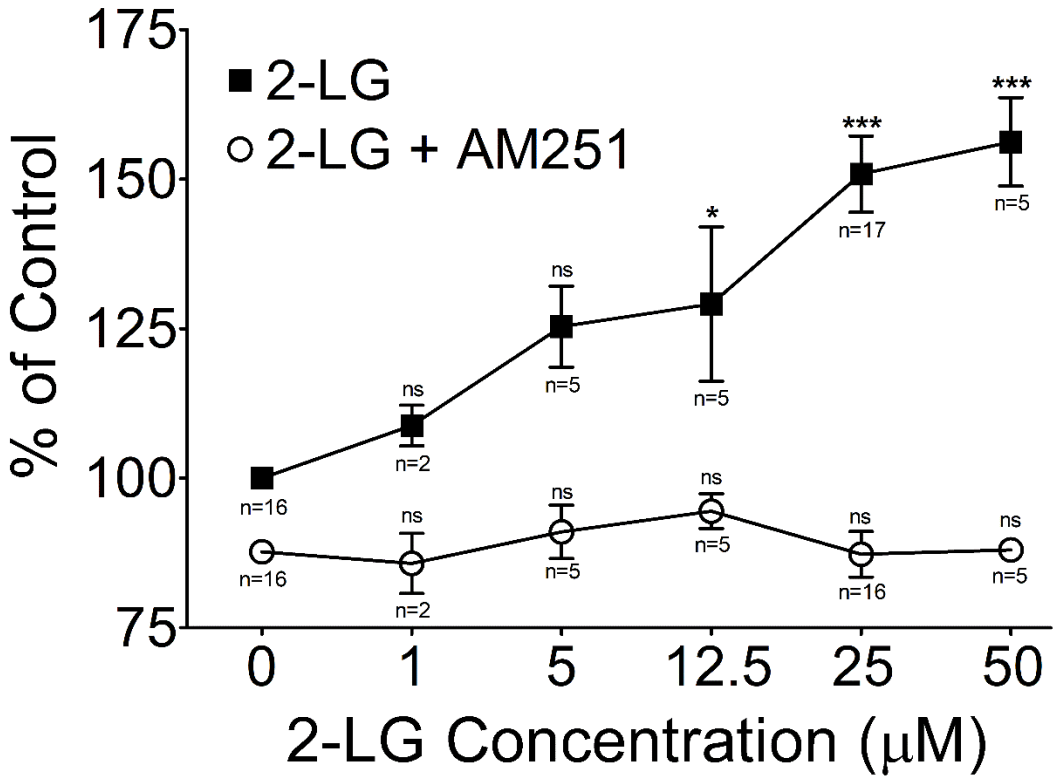

Figure 3.2.5. 2-LG activates a CB1-dependent response in a concentration dependent manner

30,000 CB1-Tango cells were seeded overnight in Freestyle media into black 96 well plates. The cells were treated with varying concentrations of 2-LG (50μM – 0μM) in the absence or presence of CB1 antagonist AM251 (2.5μM) in Freestyle media with 100nM JZL195 present to prevent the hydrolysis of 2-LG. The compounds were incubated for 4 hours before detecting β-lactamase expression by addition of a FRET-enabled substrate, as per manufacturer's protocol. The data has been normalised to control wells (set to 100) as % of control. Graph shows means and bars represent SEMs of pooled independent experiments (n indicated on the graph) with 8 replicates in each experiment. Statistical significance of 2-LG responses in the absence of AM251 compared to its control, and 2-LG responses in the presence of AM251 compared to AM251 only control were established with One Way ANOVA.

ns $p>0.05$; * $p<0.05$; *** $p<0.001$; One Way ANOVA, Dunnett's post-test.

2-LG shows submaximal CB1 receptor activation

The maximum response of 2-LG was compared to the maximal response of ACEA, 2-AG and AEA over a large number of independent experiments. These agonists were used at their maximally active concentrations (2LG – 25μM, ACEA – 5μM, 2-AG – 25μM, AEA – 5μM) to treat the CB1-Tango cells as previously described and JZL195 was included in all 2-LG experiments to prevent the breakdown of 2-LG. 2-LG shows submaximal activation of the CB1 receptor, giving rise to around 163.1% ± 4.5% of control response whilst the full agonists give around 300% of the control response (ACEA = 320.0% ± 12.5%; 2-AG = 300.2% ± 14.2%; AEA = 299.5% ± 26.4%) (Figure 3.2.6). The full agonists each have a significant difference in their responses when compared to 2-LG ($p<0.001$), but are not statistically different in comparison to each other, suggesting their maximal responses are all similar in the full occupation and activation of CB1 receptors (One Way ANOVA, Bonferroni Multiple Comparison post-test). AM251 in control conditions did not significantly inhibit baseline levels. However, in the presence of JZL195, AM251 on its own reduced the baseline to around 90% of control values across the experiments (data not shown), as demonstrated in previous experiments (Figure 3.2.5). All CB1 responses elicited were antagonised in the presence of 2.5μM AM251 to near control levels (2-LG = 91.7%, ACEA = 92.2%, 2-AG = 106.7%, AEA = 107.0% of control), demonstrating the ability of AM251 to robustly antagonise activation of the CB1 receptor by all tested agonists.

The log concentration response curves for all 4 tested agonists pooled across experiments are displayed in Figure 3.2.7. Comparing the previously mentioned EC_{50} values for ACEA, 2-AG and AEA from Figure 3.2.7, ACEA and AEA have similar values of under 0.1μM, while 2-AG has a slightly higher EC_{50} value at just above 1μM. 2-LG has an EC_{50} value of around 18.03μM in the absence of JZL195 (not displayed) and has an EC_{50} value of 16.56μM in the presence of JZL195 (Figure 3.2.7) from our experiments, suggesting that 2-LG is a much less potent agonist and requires the presence of JZL195 to exhibit a more pronounced response.

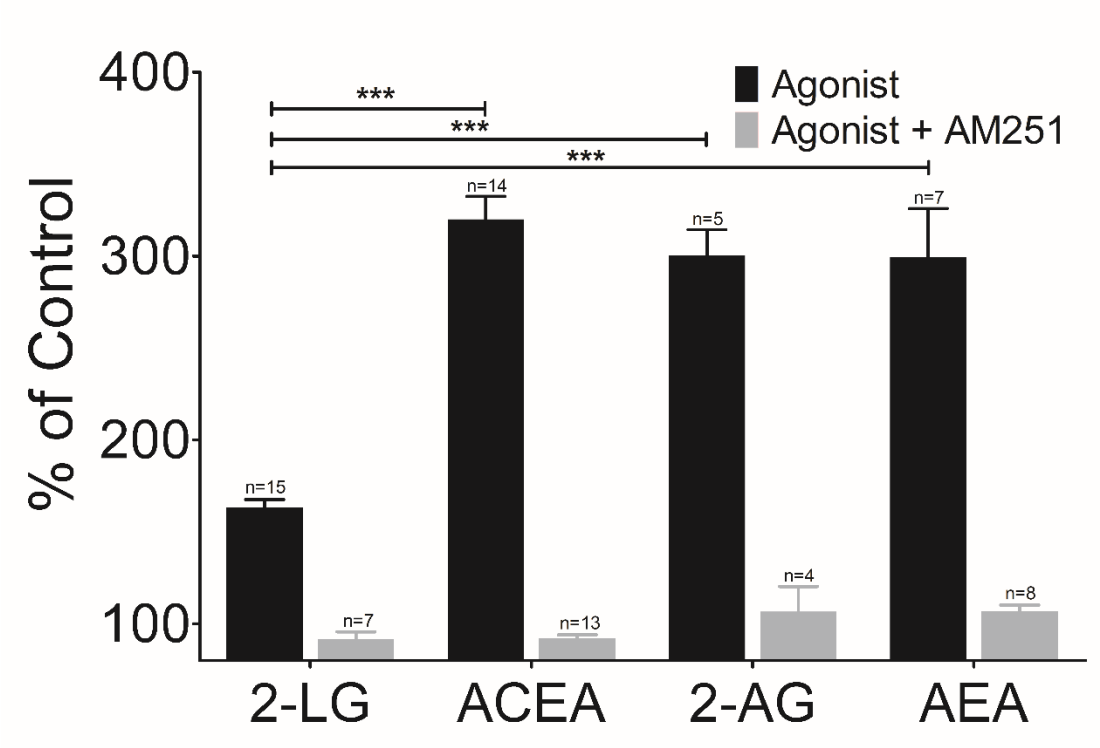

Figure 3.2.6. 2-LG is a partial agonist in comparison to full CB1 agonists

30,000 CB1-Tango cells were plated in 100μl Freestyle media for 24 hours overnight as described previously. Drugs were diluted in Freestyle media (final assay concentrations of 2LG – 25μM, ACEA – 5μM, 2-AG – 25μM, AEA – 5μM) in the presence and absence of 2.5μM FAC AM251. 100nM JZL195 was included in all 2-LG wells and experiments. Drugs were added to the cells for 4 hours before responses were measured as described previously. For each agonist experiment group, responses were normalised to the control wells in the absence of agonist or antagonist drug (set to 100) as % of control. Graph shows means and bars represent SEMs of pooled independent experiments (n indicated on the graph) with 8 replicates in each experiment. Significance between groups was established with One Way ANOVA.

***p<0.001; One Way ANOVA, Bonferroni Multiple Comparison post-test.

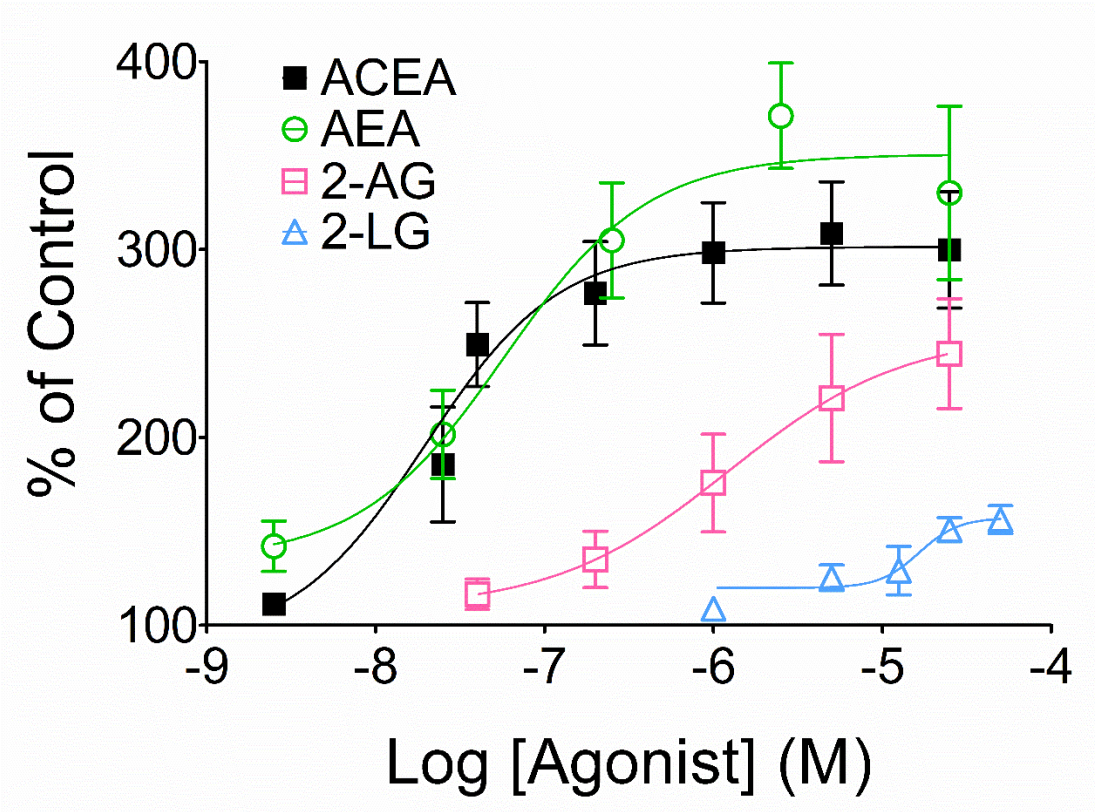

Figure 3.2.7. Log concentration response curves of eCBs, CB1 agonists and 2-LG

Log concentration response curves for CB1-Tango cells treated with CB1 agonists ACEA, 2-AG, AEA and 2-LG (2-LG in the presence of 100nM JZL195), generated according to Methods. Data was pooled across several independent experiments: ACEA n = 5, 2-AG n = 4, AEA n = 6, 2-LG n = 2 to 17 independent experiments. Points represent the means and bars represent SEMs of pooled data. Non-linear regression curve was fitted to the data points and log EC_{50} values were calculated from this graph by Graph Pad Prism.

The 2-LG response remains in the presence of DAGL inhibitors

As mentioned before, the presence of JZL195 will likely prevent the hydrolysis of other eCBs present in the system, causing those eCBs to also activate CB1 as a basal tone. This is evident in Figure 3.2.4 and Figure 3.2.5, where JZL195 has been included in the CB1-Tango assay. Thus, a component of the 2-LG effect might reflect potentiation of this eCB tone by 2-LG rather than a direct action on the CB1 receptor, akin to a positive allosteric modulator.

In order to investigate this, we sought to determine the effects of 2-LG in the presence of DAGL inhibitors, as 2-AG is perhaps the most likely "entourage" candidate (Ben-Shabat et al., 1998). CB1-Tango cells were treated with 25μM 2-LG in the presence of DAGL specific inhibitors KT109 and KT172 (Hsu et al., 2012) and broad serine lipase inhibitor THL (Bisogno et al., 2006) to inhibit the synthesis of 2-AG (Figure 3.2.8). 100nM JZL195 was again included in the wells and the data has been normalised to this JZL195 control. An AM251 control was also included and reduced the tone to 92.2% ± 0.22% of the control response (data not shown), consistent with data obtained from previous experiments. The two DAGL specific inhibitors on their own do not inhibit the basal response to below control levels as AM251 does (KT109 = 104.9% ± 4.4% of control; KT172 = 98.7% ± 4.8% of control) suggesting the basal eCB activity is not due to DAGL contribution (Figure 3.2.8). THL however, does have a significant effect on the control levels and inhibits the value to 90.2% ± 2.3%, this could be due to THL reducing the control eCB tone via an unknown or a non-specific mechanism.

Importantly there is still a significant response caused by 2-LG activation in the presence of DAGL inhibitors. For example, although the 2-LG response in the presence of KT109 (154.0% ± 10.5% of control) and KT172 (147.9% ± 7.3% of control) were slightly lower than control 2-LG responses (171.7% ± 9.4% of control) these differences were not statistically different to the control 2-LG response, but are significantly different to responses with KT109 and KT172 alone.

The results in the presence of THL are more difficult to interpret, as THL reduces the control value to 90.2% ± 2.3%. However, 2-LG in the presence of THL is still eliciting a statistically significant response to 131.7% ± 2.8% of the control. Furthermore, if the 2-LG response is normalised to the THL control, the response increases to almost 150%, which is essentially the same as that seen in the presence of the KT compounds. Thus, we can conclude that the 2-LG response is not obviously suppressed when DAGL activity is inhibited.

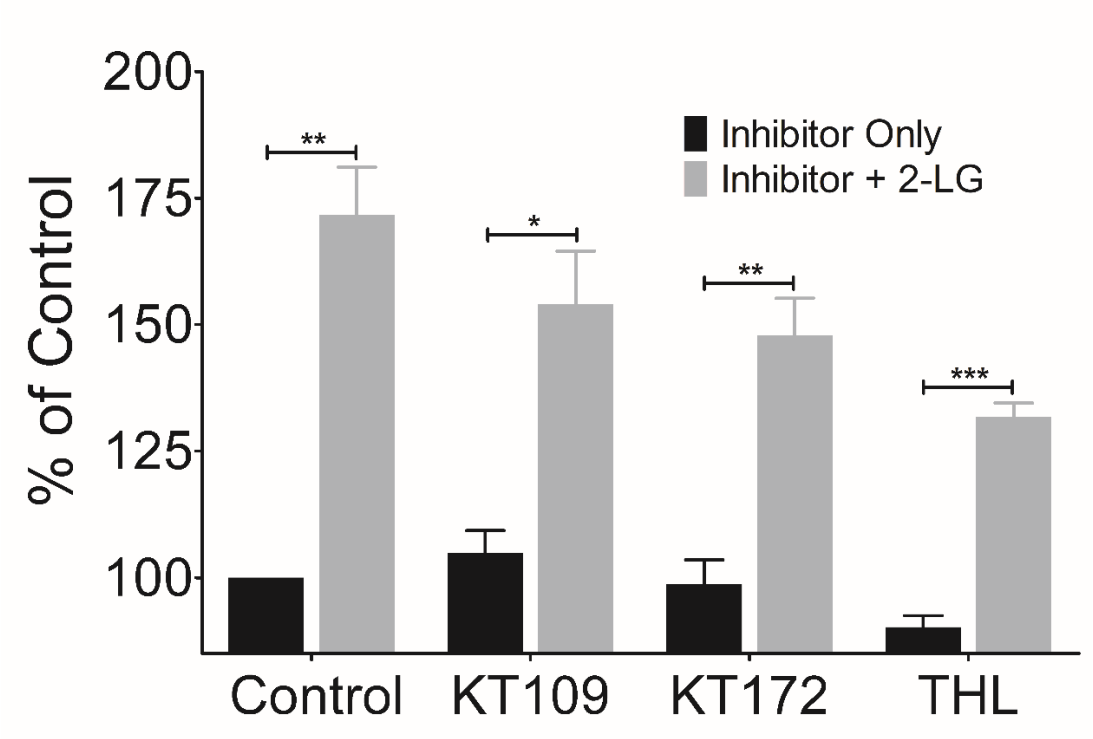

Figure 3.2.8. 2-LG signalling is still present in the presence of DAGL inhibitors

30,000 CB1-Tango cells were plated into black 96 well plates in Freestyle media as described previously. The cells were treated with DAGL inhibitors KT109 (FAC 1μM), KT172 (FAC 1μM) and THL (FAC 20μM) in the presence and absence of 25μM 2-LG for 4 hours. 100nM JZL195 was included in all wells. CB1 responses were measured as described previously and normalised to the control wells in the absence of inhibitors and 2-LG (set to 100) as % of control. Graph shows means and bars represent SEMs of 3 independent experiments, 8 replicates in each experiment. Significance of responses over respective control wells was established with Student's T-test.

*p<0.05; **p<0.01; ***p<0.001, Student's T-test.

Fixed concentrations of 2-LG show antagonist activity against eCBs 2-AG and AEA

A CB1 receptor dependent response is still elicited by 2-LG in the presence of DAGL inhibitors, indicating 2-LG alone can induce a CB1 signal when production of 2-AG is suppressed. However, this does not clarify if 2-LG could still function as a positive allosteric modulator or "entourage" molecule for the potentiation of 2-AG or other eCBs, as the presence of JZL195 would occlude any potentiation by 2-LG. To directly test the effects that 2-LG has on the eCBs 2-AG and AEA, concentration response curves of 2-AG and AEA were determined in the presence of a fixed concentration of 2-LG in the absence of JZL195.

CB1-Tango cells were treated with a range of concentrations of 2-AG (FAC 0.2 – 50μM) in the absence and presence of 2-LG (FAC 20μM) for 4 hours. The control wells were subtracted and data was normalised to the maximum 2-AG response obtained and the results are shown in Figure 3.2.9. In the absence of 2-LG, detectable CB1 responses are seen at all tested concentrations of 2-AG similarly to previous results and a normal concentration response curve is obtained. 2-LG on its own gave a CB1 activation 31.7% ± 1.5% of the maximal 2-AG response, similar to previous results. The 2-LG responses occlude the increases in CB1 activation as the concentration of 2-AG increases, suggesting little "additive" effect of 2-AG and 2-LG together. At 5μM of 2-AG and above, the responses of 2-AG in the presence of 2-LG are lower than that in the absence of 2-LG; this is not characteristic of the activity of a positive allosteric modulator or an entourage molecule, which should potentiate the 2-AG response at the same concentration. Finally, at the highest concentrations of 2-AG, rather than potentiating the 2-AG response, the presence of 2-LG instead inhibits the maximal 2-AG response and causes a lower maximal plateau which is statistically significant ($p<0.01$).

Similarly, the second major eCB AEA was also tested on the CB1-Tango cells in the absence or presence of 2-LG (Figure 3.2.10). A range of AEA concentrations (FAC 0.0025 – 5μM) was used to treat the CB1-Tango cells in the absence or presence of 2-LG (FAC 20μM). In the absence of 2-LG, AEA was able to elicit a normal concentration response curve, reaching the maximal response at around 2.5μM, similarly to previous results. 2-LG on its own again elicited a CB1 dependent response that is ~30% of the maximal response of AEA, but occluded the responses of increasing concentrations of AEA, as with 2-AG. At 0.025μM of AEA, there is no additive response of AEA and 2-LG and no potentiation effect, but rather the AEA response is lower in the presence of 2-LG. At the higher concentrations of AEA, 2-LG significantly ($p<0.05$) inhibits the maximal AEA response, leading to a submaximal plateau as

with 2-AG. 2-LG therefore has similar antagonistic effects on both 2-AG and AEA concentration curves.

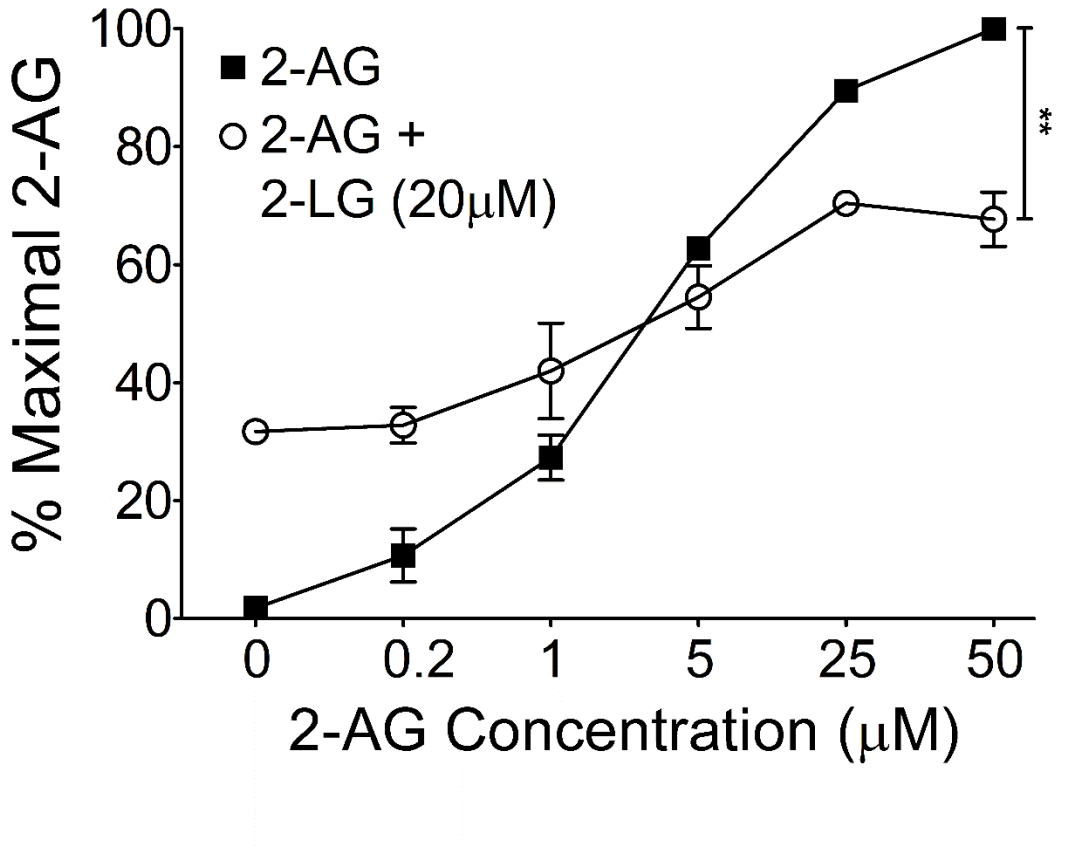

Figure 3.2.9. Effect of 2-LG on 2-AG concentration response curve

30,000 CB1-Tango cells were seeded per well in Freestyle media in clear bottom black plates for 24 hours. Serial dilutions of 2-AG (final top concentration 50μM, 1:2 and 1:5 dilutions) in the presence and absence of 2-LG (FAC 20μM) were made up in Freestyle media. Drugs were added to the cells for 4 hours before CB1 responses were measured as described previously. The background was subtracted and data were normalised to the maximal 2-AG response (set to 100) as % maximal 2-AG response. Graph shows means and bars represent SEMs of 2 independent experiments, 6 replicates from each experiment. Significance between the responses at the highest concentrations was established with Student's T-test.

**p<0.01, Student's T-test.

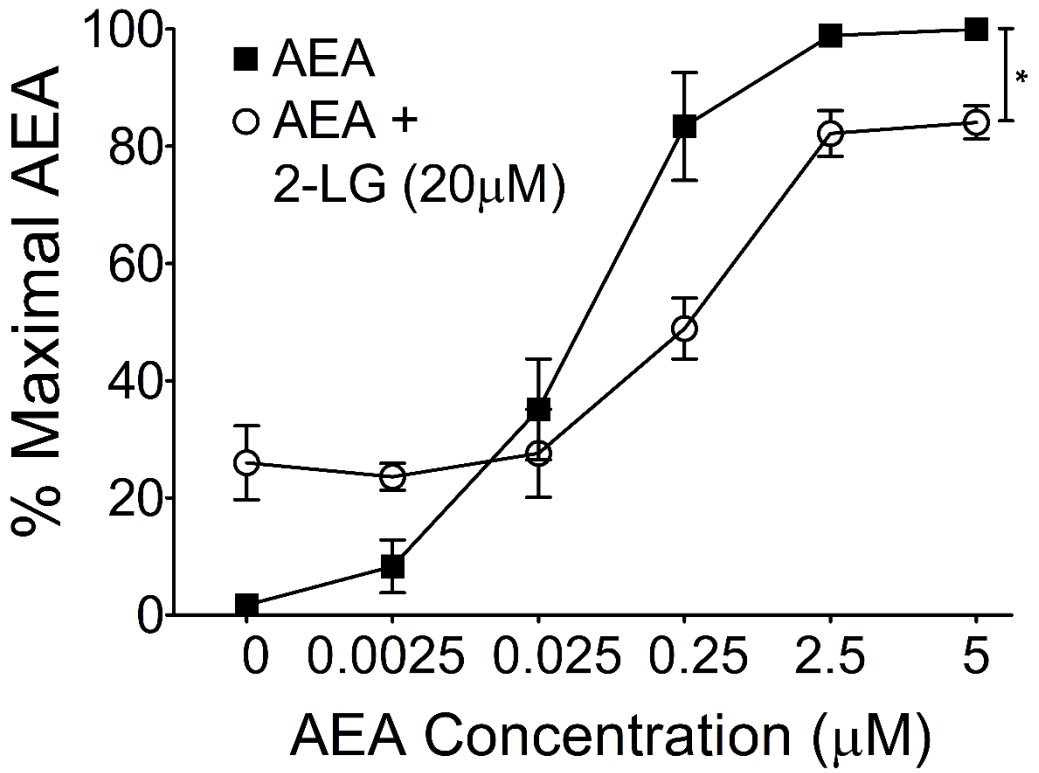

Figure 3.2.10. Effect of 2-LG on AEA concentration response curve

30,000 CB1-Tango cells were seeded per well in Freestyle media in clear bottom black plates for 24 hours. Serial dilutions of AEA (final top concentration 5μM, 1:2 and 1:10 dilutions) in the presence and absence of 2-LG (FAC 20μM) were made up in Freestyle media. Drugs were added to the cells for 4 hours before CB1 responses were measured as described previously. The background was subtracted and data were normalised to the maximal AEA response (set to 100) as % maximal AEA response. Graph shows means and bars represent SEMs of 2 independent experiments, 6 replicates from each experiment. Significance between the responses at the highest concentrations was established with Student's T-test.

*$p<0.05$, Student's T-test.

3.3 Discussion

The DAGLs are able to generate the main eCB 2-AG, but also a wide range of 2-acylglycerols, some of which may have a role in the larger eCB signalling pool. The presence of 2-LG in mammalian tissue has raised interest in its biological importance to eCB signalling. The aim of this chapter was to evaluate the activity of 2-LG on the CB1 receptor as a potential eCB, as conflicting reports of the entourage effect of 2-LG have emerged (Ben-Shabat et al., 1998; Murataeva et al., 2016).

There are many functional assays that have been used to test for activity of ligands at the CB1 receptor. For example, the inhibition of the vas deferens twitch response was used to identify the two major eCBs (Devane et al., 1992; Mechoulam et al., 1995; Zhang and Xie, 2012). However, these methods are usually low throughput, expensive and are subject non-specificity and other limitations. We have opted for a 96-well microtiter cell-based assay system to study the direct effect of 2-LG on the CB1 receptor, which has been extensively characterised in previous studies with other CB1 pharmacological tools (van der Lee et al., 2009). The main advantage of this cell-based assay system is that the measured response is mediated only through the constructed CB1 receptor linked to a non-mammalian β-lactamase reporter system and thereby removing any interference from activation of other endogenous receptors (Barnea et al., 2008).

We first confirmed the CB1-Tango cells were sensitive to an established CB1 agonist and antagonist. We obtained CB1-dependent concentration response curves to ACEA, 2-AG and AEA and the EC_{50} values were compared to published EC_{50} values obtained from [^{35}S]GTPγS binding assays (Hillard et al., 1999; Ryberg et al., 2007; Pertwee, 2015). Values vary across preparations, species and methods used. However, the EC_{50} values obtained from the CB1-Tango assay were all within the published range and towards the lower side (Pertwee, 2015). Our EC_{50} values obtained were lower than those published by Hillard et al (1999) for ACEA (51 ± 6nM). The values for AEA were comparable to EC_{50} values (31 ± 6nM) published by Ryberg et al (2007), who published the lowest EC_{50} values for 2-AG and AEA as reviewed by Pertwee (2015). This indicates the sensitivity of the assay as the pathway is not affected by other metabolic processes that may be active within the cell. The EC_{50} value of 2-AG obtained in this set of experiments is noticeably higher than reported by Ryberg (2007) (519 ± 48nM). A possible explanation for this could be due to the spontaneous isomerisation of 2-AG to 1-

AG which is inactive at the CB1 receptor (van der Stelt et al., 2002), thus decreasing the effective concentrations of 2-AG. This spontaneous isomerisation is difficult to prevent due to the long incubation time at 37°C. However, our values still lie within the range of published EC_{50} values (Pertwee, 2015).

In Figure 3.2.1, Figure 3.2.2 and Figure 3.2.3, there are no noticeable differences in the responses produced by the AM251 treated cells and control cells, suggesting that in control conditions there is no eCB signalling at the CB1 receptor. This may be due to the lack of substrate available under the growth conditions, as the CB1-Tango assay requires the cells to be starved in Freestyle expression media to reduce background noise. The manufacturer has confirmed that the media is serum free and calcium free but do not reveal the composition of the media, suggesting the cells may not have necessary components to drive eCB signalling. The absence of basal activity could also be possibly due to the function of eCB degrading enzymes acting in a "gatekeeper" role to prevent eCB from activating the CB1 receptor. The gatekeeping role has been previously described in developing neurones where MAGL is not expressed in the growth cone but has increased expression on axons, thus restricting eCBs to only accumulate locally on the growth cone to promote CB1 activation, but terminates any signalling along the axon (Keimpema et al., 2013). When MAGL, FAAH and ABHD6 activity was inhibited by JZL195, there was around 10% increase of the basal response and this can be antagonised by AM251, indicating some tonal eCB is signalling at the CB1 receptor when JZL195 is present. This suggests that small amounts of eCBs are produced under control conditions but are not signalling through the CB1 receptor due to the actions of the eCB hydrolysing enzymes. From previous results in our lab, it has been shown that inhibition of MAGL alone with MAGL specific inhibitor JZL184 alone does not reveal an eCB tone, but inhibition of both MAGL and FAAH with JZL195 can reveal the presence of a low, but statistically significant eCB tone (thesis of Rachel Lane Markwick, 2015). This is possibly due to compensation of both hydrolysis enzymes or there is more than one component to the eCB tone, namely the presence of both 2-AG and AEA. In further chapters, the nature of this eCB tone will be explored.

2-LG was also tested in the assay and has demonstrated CB1 activation ability in our experiments but only at around half of the maximal activation elicited by the other established agonists. This ability is only revealed at high concentrations of 2-LG or when JZL195 is included to mitigate against 2-LG hydrolysis (Figure 3.2.6). However as mentioned previously, the inclusion of JZL195 reveals the presence of a small basal eCB tone which may

contribute to the activation of the CB1 receptor, casting uncertainty on whether the observed effect of 2-LG is direct on the CB1 receptor, in combination with the eCBs or through positive allosteric modulation to potentiate the activity of the eCBs produced. Since 2-AG is the likely molecule for the entourage effect of 2-LG and pharmacological tools are available to target DAGL, 2-AG synthesis was inhibited with DAGL inhibitors to discern whether the effect of 2-LG is direct (Figure 3.2.8).

The DAGL inhibitors KT109 and KT172 alone did not inhibit the basal eCB tone to below control levels suggesting the basal eCB activity is not due to DAGL. THL was able to elicit a very small response in the assay, reducing the control value by around 10%. THL has previously been shown to have inhibitory effects against several serine lipases, some with greater affinity than DAGL (Hoover et al., 2008). Therefore, the small inhibition of the control value may not be due to the blockade of DAGL alone. If the controls were redefined as the wells in the presence of DAGL inhibitors and the data was normalised to these controls, the 2-LG response is consistent in the presence of all three inhibitors at around 150%, suggesting the activity of 2-LG is not affected by the presence of the DAGL inhibitors. In the presence of the DAGL inhibitors, the total 2-LG response is around 20% lower for all three inhibitors than the 2-LG control response, suggesting that part of the total response might be due to the activity of 2-AG, but the remaining response is likely to be attributed to the activity of 2-LG or other eCBs on the CB1 receptor.

Unfortunately there are currently no effective pharmacological inhibitors of AEA synthesis due to redundancy of possible pathways that can generate AEA (Liu et al., 2008; Ueda et al., 2013; Maccarrone, 2017). It is not known whether 2-LG can potentiate AEA, but it can be reasoned that since AEA is also broken down by a crossover of MAGL and FAAH (Cravatt et al., 1996), and is also structurally similar to 2-AG and 2-LG, it is conceivable that 2-LG could also potentiate AEA by the same manner proposed for 2-AG. Ben-Shabat et al (1998) have shown that 2-LG is the 2-acylglycerol that primarily slows the hydrolysis of 2-AG, likely by preventing the breakdown of 2-AG by occupying and blocking access to the active site on degrading enzymes and therefore increasing the presence of 2-AG to activate the CB1 receptor. The potentiation of AEA was not tested by the group but our experiments show that blocking eCB degradation with JZL195 has no effect on the activity of 2-LG, thus ruling out the AEA potentiation hypothesis.

It has also been suggested that 2-LG may work via different mechanisms to potentiate the activity of eCBs, for example via positive allosteric modulation of the CB1 receptor or perhaps

2-LG could have activity on other GPCRs such as GPR119, in the same way that 2-OG and 2-PG may be endogenous ligands for GPR119 (Hansen et al., 2011; Syed et al., 2012). 2-LG was not shown to enhance direct 2-AG binding to CB1, but 2-PG did potentiate the direct binding of 2-AG to receptors. This binding potentiation occurs through currently unknown mechanisms; perhaps through allosteric modulation or through inhibition of 2-AG binding to plasma proteins. Nonetheless, full potentiation effect is achieved by a mix of the two 2-acylglycerols (Ben-Shabat et al., 1998). Whilst 2-LG being an active ligand to other receptors is not refuted by our results, the coupling of the protease-fused arrestin to the non-native transcription factor ensures specificity of the CB1-Tango assay and is therefore unaffected by activation of other GPCRs (Barnea et al., 2008). The results we obtained in this set of experiments therefore only show the activity of 2-LG at the CB1 receptor, but perhaps 2-LG can also have effects at other GPCRs.

Antagonistic properties of 2-LG were observed by Murataeva et al (2016) in DSE experiments with pre-incubation of 5μM 2-LG for 5 minutes, crucially without JZL195. In experiments described here, 5μM of 2-LG without JZL195 in a 4 hour assay gave rise to a CB1 response around 15% above control levels (Figure 3.2.4), which was not statistically significant. In the presence of JZL195, this rises to around 25% above control levels (Figure 3.2.5) but is also not statistically significant, suggesting 2-LG is indeed occupying CB1 receptors but has low intrinsic activity. In the presence of endogenously released 2-AG from the stimulation of autaptic hippocampal neurones, 2-LG may compete with the full agonist, but with low efficacy for the receptor and therefore acting as an antagonist with small non-significant activation of the receptor (Ariuens and Simonis, 1964; Calvey and Williams, 2008).

Submaximal concentrations of 2-LG (20μM) was included in the concentration response curves for both 2-AG and AEA and showed notable partial agonism effects as described by Calvey and Williams (2008). In the absence of the full agonist, 2-LG elicits a small response on its own. In small concentrations of full agonist, there is little additive effect observed as the effect of the agonist is occluded by the response from 2-LG. When the response to 2-AG or AEA equals the maximal response of 2-LG, there is no additive or inhibitory effect and 2-LG does not seem to have any effect on the response that occurs around 5μM for 2-AG and 0.025μM for AEA. Finally, at higher concentrations of 2-AG and AEA, 2-LG acts as a antagonist and reduces the response to the full agonist. This indicates that 2-LG can bind to the same binding site as 2-AG and AEA on the CB1 receptor, causing an inhibition of the CB1 response elicited by the eCBs. Furthermore, a submaximal concentration of 2-LG was used which is

not likely to cause saturation of MAGL/ABHD6 in the absence of JZL195, as JZL195 can enhance the 2-LG response as observed in Figure 3.2.4. This submaximal concentration of 2-LG caused sufficient inhibition of the eCB responses, indicating that lower concentrations of 2-LG is able to modulate the responses to the eCBs and that 2-LG is not saturating the active sites of MAGL/ABHD6 to cause an entourage effect. Lastly, the antagonist effect of 2-LG to high concentrations of eCBs is evidence against 2-LG acting as a positive allosteric modulator and could explain the antagonistic effect observed by Murataeva et al. (2016), and the partial agonism effect could also explain the additive entourage effect observed by Ben-Shabat et al. (1998).

Physiologically, 2-LG is present in mammalian the brain at levels much lower than 2-AG, suggesting that it is not likely to function as an agonist in retrograde eCB signalling (Murataeva et al., 2016). In our results, significance was reached at only the higher concentrations of 2-LG without JZL195 present, supporting the notion that 2-LG may not be physiologically relevant in the brain for the entourage of 2-AG. It could be more likely that the role of 2-LG is subtler in the brain and rather than behaving as a partial agonist, may act as an endogenous antagonist to modulate eCB signalling. However, further clarifications of its role will need to be explored. Importantly, in the experiments conducted by Ben-Shabat et al (1998) and Gallily et al (2000), it was noted that the potentiation effect of 2-LG, in conjunction with 2-PG, on 2-AG was maximal in ratios close to what is found physiologically in the spleen, where levels of 2-LG are around 12x higher than levels of 2-AG. This ratio of 2-LG to 2-AG was shown to have the most profound entourage effect and thus may be physiologically relevant to the biological activity of 2-LG in areas of the body where 2-LG is in relatively high abundance (Mechoulam et al., 1995; Ben-Shabat et al., 1998).

In conclusion, this chapter has shown that through our CB1-Tango assay system, 2-LG has partial agonist activity at the CB1 receptor, which is independent of the entourage of 2-AG, but whether this is physiologically relevant in the mammalian brain remains to be elucidated. This signalling activity is limited by the function of eCB hydrolysing enzymes, which can also conceivably hydrolyse 2-LG. The inhibition of these eCB hydrolysing enzymes thus enhances 2-LG signalling, but in turn also reveals a basal eCB tone. From this, we postulate that the eCB tone consists of 2-AG and AEA and go on to explore this in further chapters. We have successfully utilised the CB1-Tango assay to elucidate the activity of a potential CB1 agonist and will go on to use this assay system to next look at the effects of a putative endogenous CB1 antagonist.

Chapter 4. Results 2 – The activity of Hp as a CB1 antagonist

4.1 Introduction

The eCB system has been studied extensively in many disease states, including in the fields of pain, cardiovascular disease and neurodegenerative disease (Di Marzo and Petrosino, 2007; Fine and Rosenfeld, 2013; Sierra et al., 2017). The CB1 receptor is able to modulate pain nociception and appetite (Salamone et al., 2007; Pernia-Andrade et al., 2009) and novel antagonists targeting CB1 for the treatment of pain or obesity have been under investigation. However, drugs targeting CB1 receptors, such as Rimonabant, often display side effects due to the expression of CB1 in the CNS associated with mood and cognition (e.g. limbic system and prefrontal cortex) (Zarate et al., 2008; Heng et al., 2011). In 2009 Rimonabant was withdrawn as an appetite suppressant to treat obesity following reports of unwarranted side effects such as severe depression and suicide ideation (Christensen et al., 2007; Moreira and Crippa, 2009). These side effects limit the therapeutic targeting of the CB1 receptor to modulate the eCB system (Herkenham et al., 1990; Svendsen et al., 2004), warranting the need to identify drug targets without such severe side effects.

Canonically, CB1 ligands are lipid based, with the two major eCBs being derived from membrane phospholipids. CB1 drugs are also often hydrophobic, which can cause difficulties with drug delivery and may cross the BBB. A lot of interest was therefore raised when a publication by Heimann et al. (2007) claimed an endogenous peptide could serve as a CB1 ligand; this not only suggested a whole new field of study on the physiological function of the peptide in the eCB system, it also raised hopes of developing a completely new drug class to target the eCB system. Hemopressin (Hp) is a 9-residue peptide derived from the α_1 chain of haemoglobin (Table 4.1.1), first discovered from crude rat brain extracts using a substrate-capture assay of catalytically dead endopeptidases (Rioli et al., 2003). A homology search showed that Hp is part of the α1 chain of haemoglobin and highly conserved across species, except for one amino acid substitution found in the rat orthologue, suggesting a potentially important biological function (Table 4.1.1) (Dale et al., 2005a). Mass spectrometry of homogenised brain regions using extraction methods with low proteolytic activity were able

to detect levels of Hp and two N-terminally extended forms of Hp (VD-Hpα and RVD-Hpα), which have also been reported to have activity on the CB1 receptor, giving rise to a prospective family of endogenous peptide CB1 modulators (Heimann et al., 2007; Gomes et al., 2009).

SPECIES	SEQUENCE
RAT	-AHKLRVD PVNFKFLSH SLLVTLA-
HUMAN	-AHKLRVD PVNFKLLSH SLLVTLA-
MOUSE	-AHKLRVD PVNFKLLSH SLLVTLA-
PIG	-AHKLRVD PVNFKLLSH SLLVTLA-

Table 4.1.1. Amino acid sequences of hemopressin in different mammalian species

The sequence of Hp within the a_1 haemoglobin sequence is displayed from various species. Hp sequence is underlined and residues in red represent the singular amino acid differences. Adapted from Dale et al. (2005a).

One of the key assays suggesting Hp could to bind to CB1 receptors was an ELISA on dried SK-N-SH cells with conformation-sensitive antibodies generated to the extracellular N-terminal portion of CB1 receptors (Gupta et al., 2007). The presence of CB1 agonist Hu-210 enhanced antibody binding and CB1 antagonist SR141716 (Rimonabant) reduced antibody binding. Hp reduced CB1 antibody binding to the same level as SR141716 and did not display the same effect to similarly generated antibodies against other related receptors including CB2 (Heimann et al., 2007). Hp was also tested in [^{35}S]GTPγS binding and adenylyl cyclase assays for any biological activity. On HEK cells expressing CB1 receptors, Hp showed antagonist activity against Hu-210 and inverse agonist activity in the absence of any agonist akin to SR141716. This effect was not seen in HEK cells expressing CB2 receptors, suggesting that Hp shows specificity to CB1 receptors (Heimann et al., 2007). Hp also demonstrated marked analgesic effects when administered to animal models of inflammatory pain, on a comparable level to the CB1 antagonist AM251 and was active independently of administration route (oral, local or intrathecal) (Heimann et al., 2007). This analgesic effect is also effective with shorter lengths of Hp (Hp1-6 [PVNFKF] and Hp1-7 [PVNFKFL]) (Dale et

al., 2005b). However, there was no direct evidence that the peptides worked via a CB1-dependent mechanism in these pain models.

Nonetheless, additional studies have supported the hypothesis that the antagonist activity of Hp might be attributable to binding to CB1 receptors. For example, *in silico* molecular docking assays have predicted that Hp has the potential to bind to the same pocket as the classic CB1 agonist SR141716 and moreover, the first 6 amino acids of Hp are necessary for this *in silico* binding. This is in keeping with the indication that Hp fragments are also biologically active (Scrima et al., 2010). Hp was also able to block CB1 receptor internalisation induced by WIN55,212-2 similarly to AM251 in CB1-transfected cells, and reduce animal feeding in WT but not in $CB1^{-/-}$ KO mice (Dodd et al., 2010). Mice models of memory also showed Hp acts very similarly to AM251 in preventing CB1 induced memory loss (Zhang et al., 2016b). In experiments measuring c-Fos expression as an indicator for neuronal firing, Hp and AM251 both increased c-Fos expression in WT but not $CB1^{-/-}$ KO mice suggesting activity as a CB1 antagonist, albeit in distinctly different areas of the brain (Dodd et al., 2013). These studies support the hypothesis that Hp is a CB1 antagonist but importantly they are based on *in silico* models and/or indirect assays.

Indeed, other studies have utilised Hp as a CB1 antagonist without actually directly testing if Hp directly and/or solely acts at CB1 receptors. These have uncovered various physiological effects of Hp, for instance its analgesic effects in certain animal models of pain (Dale et al., 2005b; Hama and Sagen, 2011b; Petrovszki et al., 2012; Toniolo et al., 2014); its ability to promote the differentiation of oligodendrocytes and the maturation of sub ventricular zone progenitor cells (Xapelli et al., 2014) and its ability to slow GI transit (Li et al., 2016). Again, although these effects might reflect activity at the CB1 receptor, they might conceivably be attributable to other indirect mechanisms. One prominent paper has used the failure of Hp to mimic AM251 in blocking a biological response to argue that the response must be mediated by intracellular CB1 receptors on mitochondria that can be accessed by AM251 – which is hydrophobic, but not by Hp (Ma et al., 2015). Other studies have also implicated mitochondrial CB1 function in the thalamic paraventricular nucleus neurons based on the use of Hp as a specific and selective CB1 receptor antagonist, again with little regard for the possibility that Hp might have other actions (Zhang et al., 2015, 2016a).

Several other studies have shown that Hp has pronounced activities that are independent of the CB1 receptor or activities that do not mimic the effects of established CB1 antagonists. For example, Hp displays hypotensive effects that do not seem to be mediated through CB1 receptors, as established CB1 antagonists or genetic KO of CB1 receptors from mice models have little effect on blood pressure (Jarai et al., 1999; Ledent et al., 1999; Lippton et al., 2006). Hp also did not antagonise the analgesic effect of the CB1 agonist WIN55,212-2 in a spinal cord injury model, in contrast to SR141716 which did antagonise the WIN55,212-2 response (Hama and Sagen, 2011a). Likewise, Hp has not shown CB1 antagonist-like activity in other models of chronic pain (Petrovszki et al., 2012; Toniolo et al., 2014). The effects of Hp on autaptic mouse hippocampal neurons on CB1-dependent DSE have also been reported; these studies also failed to show Hp antagonism against 2-AG activity on CB1 receptors (Straiker et al., 2015). In support Dvorácskó et al (2016) have reported Hp binding to as-yet-to-be identified targets in $CB1^{-/-}$ KO mice brain homogenate. Many of these studies indicate Hp having no activity at the CB1 receptor and/or acting at sites other than the CB1 receptor.

The contradictory results of the activity of Hp need to be clarified if Hp is to be of interest therapeutically in the wider eCB drug discovery effort, or for it to be seriously considered as an endogenous and selective CB1 receptor antagonist. A recent Pubmed search (accessed 2nd February 2018) identified 58 publications that mention Hp with no less than 38 of these also mentioning the CB1 receptor. Many of the publications draw conclusions based on the premise that Hp is a selective CB1 antagonist, yet this conclusion is largely based on a number of indirect experiments published in a single paper. Given the increasing volume of the literature that used Hp as a tool compound, it is very important to determine if it is or is not an effective and selective CB1 antagonist.

In this chapter I have directly tested if three independently sourced preparations of Hp display antagonistic activity towards the CB1 receptor. In this context, in the previous chapter I have shown that the recombinant cell line CB1-Tango can be used to quantify responses from the synthetic CB1 agonist ACEA and from the two best characterised eCBs 2-AG and AEA. Furthermore, this reporter cell line approach has provided the first direct evidence for 2-LG acting as a partial CB1 receptor agonist. In this chapter I have utilised the CB1-Tango assay to directly test if Hp, sourced from three independent companies, can antagonise the activity of the above four CB1 agonists.

4.2 Results

Hemopressin does not exhibit antagonist activity against CB1 agonist ACEA

Most of the published literature has reported on the effects of the rodent Hp (rHp) peptide in assays against the rodent CB1 receptors, with contradicting reports of Hp antagonism. As of yet, there are no publications based on the activity of human Hp (hHp) on human CB1 (hCB1) receptors. To determine if hHp acts as an antagonist of the hCB1 receptor, we have tested it on agonist responses in the CB1-Tango assay. This hHp peptide was purchased from Cayman Chemicals and is designated as Hp1.

The activity of Hp1 was initially tested in the CB1-Tango assay by determining if it could inhibit the activity of CB1 agonist ACEA. The CB1-Tango cells were plated in Freestyle media as described in methods and after 24 hours, ACEA was added at a range of concentrations (FAC 0.0025 – 25μM) for 4 hours in the presence and absence of 10μM of the Hp1. Control experiments established that Hp1 on its own did not exhibit any effect on the basal activity of the assay over a concentration range of 0.4μM – 20μM (data not shown). A robust concentration-dependent ACEA response was obtained with a maximal response detected at 2.5μM (457.4% ± 16.6% of control) (Figure 4.2.1) similarly to previous experiments with an EC_{50} value of 0.045μM (log EC_{50} = -7.34 ± 0.07 SEM). 10μM Hp1 was unable to significantly affect ACEA responses across the full range of ACEA concentrations tested. The EC_{50} value for the ACEA response curve in the presence of Hp1 was 0.051μM (log EC_{50} = -7.29 ± 0.07 SEM) which was not significantly different to ACEA response curve on its own ($p>0.05$, Student's unpaired T-Test). Multiple experiments were carried out and the log EC_{50} values were pooled across experiments. Statistical analysis comparing the effect of Hp1 has shown it was unable to affect the log EC_{50} values of ACEA (Table 4.2.1).

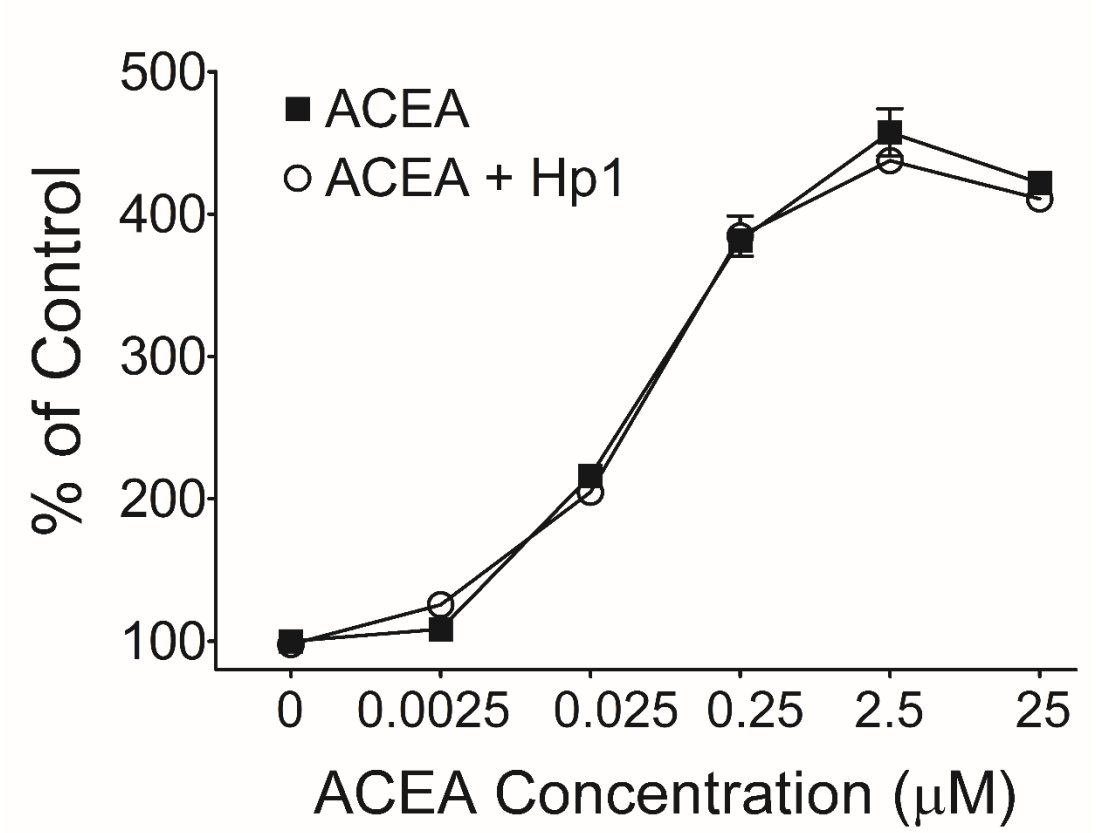

Figure 4.2.1. Human hemopressin 1 (Hp1) does not antagonise a range of ACEA concentrations

CB1-Tango cells were seeded at a density of 30,000 cells per well in Freestyle media overnight as described in methods. The following day, varying concentrations of ACEA were added to the cells (FAC of 25μM, 1:10 dilution) in the presence and absence of 10μM human hemopressin (Hp1) for 4 hours. Assay substrate was added for 90 minutes and read on the Flexstation. Data was normalised to control wells without any drugs (set to 100) as % of control. Graph shows means of 8 replicates and bars represent SEMs, from a single representative assay.

Preparations of rodent Hp do not antagonise CB1 responses

Initially human Hp peptide was tested for its ability to antagonise the ACEA response, however, most publications have used the rat form of Hp which has a one amino acid difference (Table 4.1.1) to the human form (Dale et al., 2005a). The one amino acid substitution of Hp itself does not seem to make much difference in activity when tested in rabbits, rats and mice (Blais et al., 2005) but may have an effect on the activity of Hp on the hCB1 receptor. Rodent versions of Hp (rHp) were purchased from separate companies and designated as Hp2 from Cayman Chemicals and Hp3 from Sigma Aldrich. Both preparations were tested against the maximal ACEA response to determine if they could antagonise responses at the hCB1 receptor.

The ability of all three preparations of Hp to antagonise the maximal ACEA response was compared to the inhibition seen with the established CB1 antagonist AM251 (Figure 4.2.2). The CB1-Tango cells were treated with 5μM ACEA in the absence and presence of 20μM of either Hp1, Hp2, Hp3 or 10μM AM251. The maximal ACEA response obtained across experiments was 416.0% ± 18.6% of control (data not shown) which is of similar magnitude to results reported in the previous chapter. To best present the inhibitory effects of the antagonists, the background well levels were subtracted and all data was normalised to the maximal ACEA response (set to 100) as % of ACEA response.

All three preparations of Hp and AM251 did not exhibit any significant effects on the baseline when added by themselves to cultures for the standard 4 hour assay period (Hp1 = 100.4%; Hp2 = 97.7%; Hp3 = 101.0%, AM251 = 105.1% of the control, data not shown). AM251 (10μM) essentially fully inhibited the ACEA (5μM) response (Figure 4.2.2), similarly to experiments reported in the previous chapter. In marked contrast when added at 20μM; Hp1, Hp2 and Hp3 did not significantly antagonise the ACEA response and there were no differences between different preparations of Hp ($p>0.05$, Bonferroni's Multiple comparisons test).

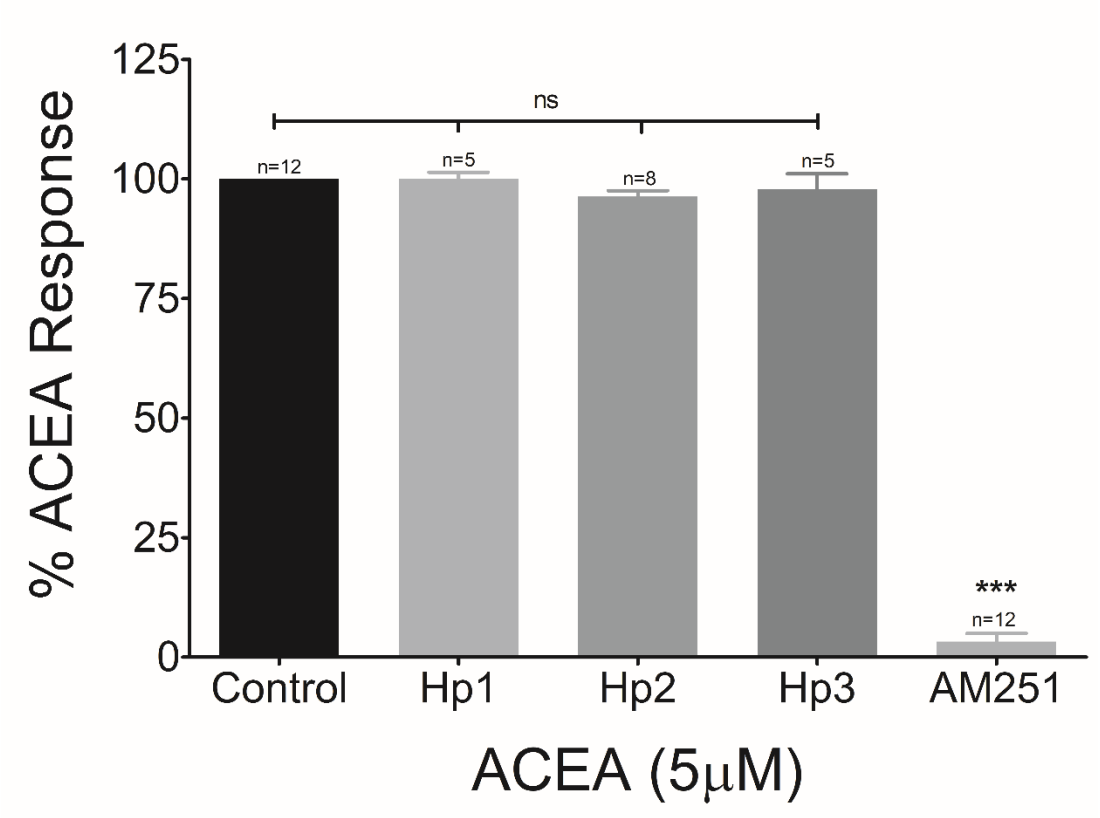

Figure 4.2.2. Comparison of the inhibition of ACEA between Hp from different sources and AM251

CB1-Tango cells were seeded at a density of 30,000 cells per well in Freestyle media overnight as described in methods. FAC of 5μM ACEA were added to the cells in the absence or presence of 10μM AM251, 20μM Hp1 (Tocris), Hp2 (Cayman Chemical) or Hp3 (Sigma) for 4 hours. Assay substrate was added for 90 minutes and read on the Flexstation. To show the full ACEA elicited CB1 response, control well ratios were subtracted from the sample well ratios and the data was then normalised to the maximal ACEA response (set to 100) and displayed as % of ACEA response. Graph shows means and bars represent SEMs of pooled independent experiments, with 8 replicates in each experiment. Significance of the responses was compared to ACEA control using One Way ANOVA.

ns $p>0.05$; ***$p<0.001$, One Way ANOVA, Bonferroni's Multiple Comparison Test.

Hemopressin does not exhibit antagonism against eCBs

AM251 has been shown to be a robust CB1 receptor antagonist against the synthetic agonist ACEA and the major eCBs in the previous chapter. However, AM251 is synthetic and cell permeable and so might differ in its mode of action from Hp, which is not cell permeable (Rozenfeld and Devi, 2008; Benard et al., 2012). It has also been proposed previously that the effects of Hp may not be as effective against synthetic agonists such as WIN55,212-2 versus endogenous agonists such as 2-AG and this could explain some differences in Hp activity reported in the literature (Petrovszki et al., 2012). It was therefore important to test whether Hp can antagonise the activation of the CB1 receptor stimulated by the natural ligands 2-AG and AEA.

In a series of experiments, a range of concentrations of the eCBs 2-AG (FAC 0.04 – 25μM) and AEA (FAC 0.0025 – 25μM) were tested for their ability to activate the CB1 receptor in the absence and presence of Hp1 with the results summarised in Figure 4.2.3 and Figure 4.2.4. 2-AG-elicited a concentration-dependent response reaching a maximal stimulation to 216.3% ± 14.8% of control at 25μM (Figure 4.2.3) with an EC_{50} value of 1.84μM (log EC_{50} = -5.74 ± 0.19 SEM, n = 3) (Table 4.2.1). In the presence of 10μM Hp1, the 2-AG responses remain unchanged at all tested concentrations. The pooled EC_{50} value for 2-AG in the presence of Hp1 was 2.30μM (log EC_{50} = -5.64 ± 0.13 SEM, n = 3) and this was not significantly different from that seen in the absence of Hp1.

Likewise, AEA elicited a concentration-dependent response with a maximum stimulation seen at 2.5μM (288.1% ± 25.8% of control) but at the highest tested concentration of 25μM, the response was slightly (but not significantly) reduced (260.1% ± 37.1% of control). When added at 10μM, Hp1 does not significantly antagonise AEA at all concentrations tested. The EC_{50} value of AEA alone was 0.11μM (log EC_{50} = -6.97 ± 0.34 SEM, n = 3), which is similar to the EC_{50} values obtained in the previous chapter. In comparison, the EC_{50} value of AEA in the presence of Hp1 was 0.092μM (log EC_{50} = -7.04 ± 0.31 SEM, n = 3) and this is not statistically different to AEA alone (Table 4.2.1).

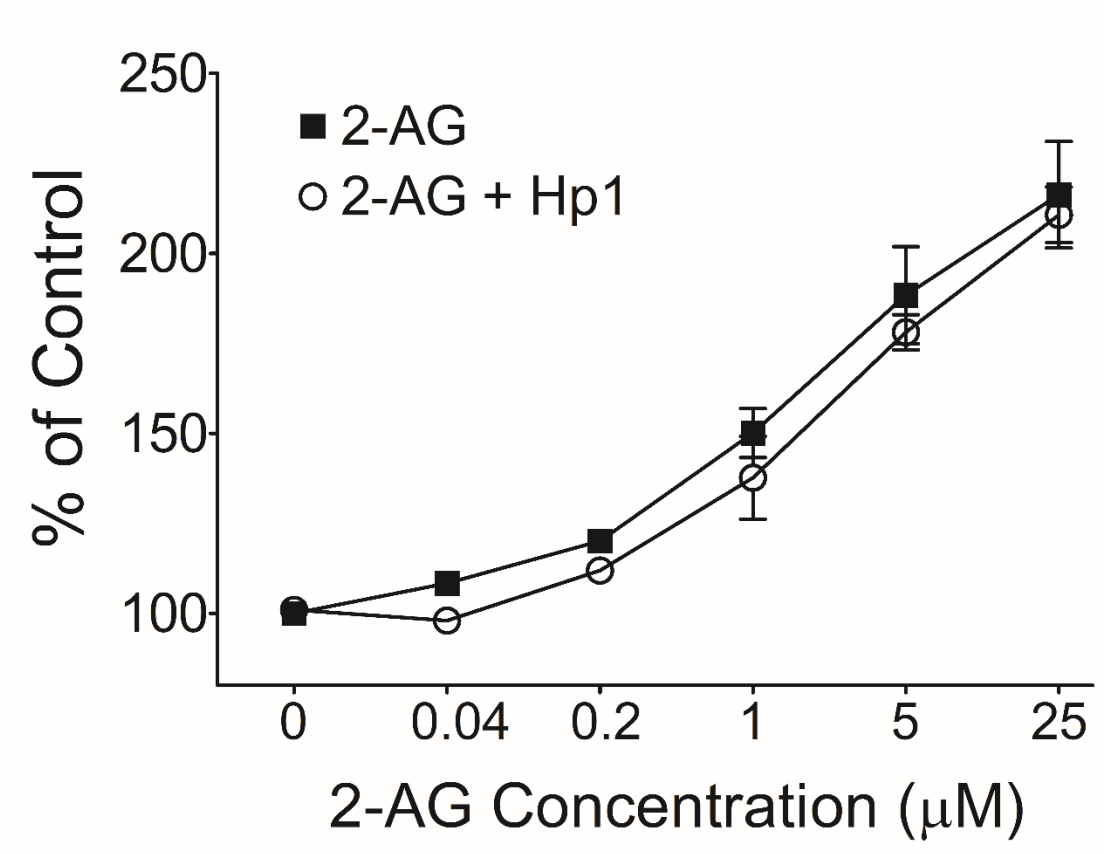

Figure 4.2.3. Hp1 does not antagonise a range of 2-AG concentrations

30,000 CB1-Tango cells were seeded per well in black 96 well plates in Freestyle media overnight. Varying concentrations of 2-AG (final top concentration 25μM, 1:5 dilution) were diluted in Freestyle media and added to the cells in the presence and absence of 10μM Hp1 for 4 hours incubating at 37°C. FRET substrate was added for 90 minutes after incubation and read on the Flexstation. Data was normalised to control wells (set to 100) as % of control. Graph shows means and bars represent SEMs of 3 independent experiments, 8 replicates in each individual experiment.

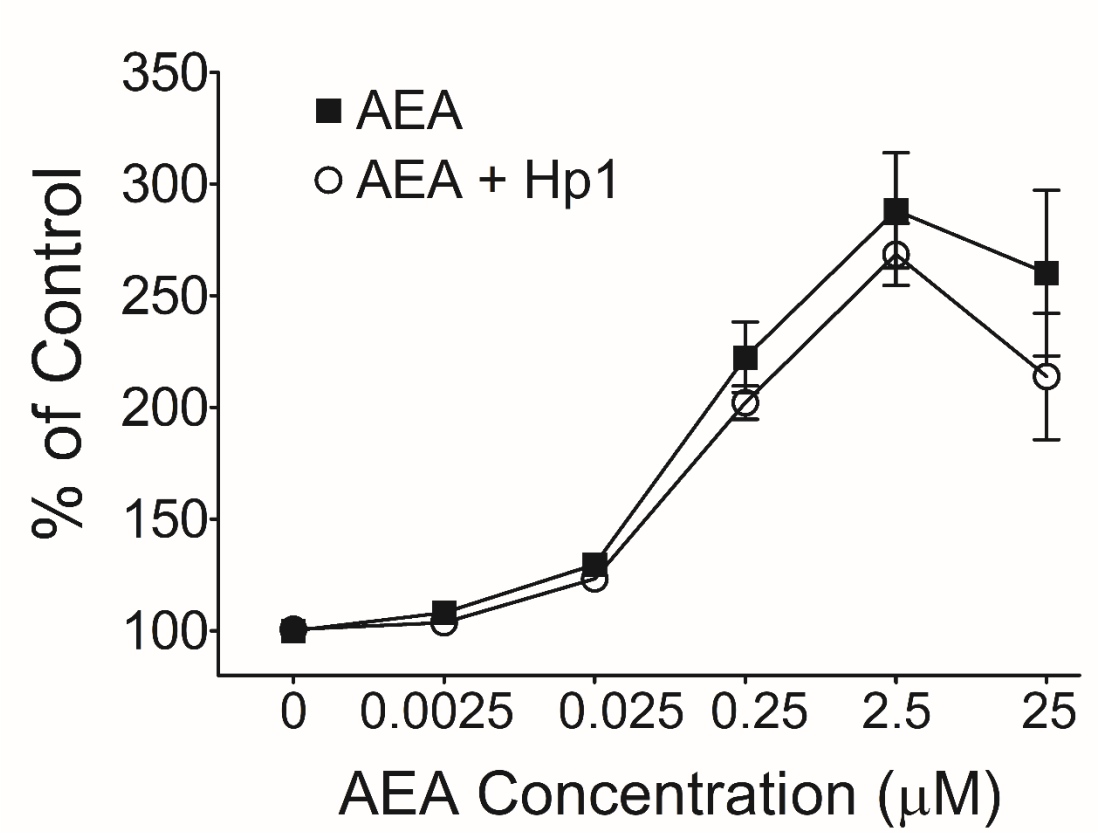

Figure 4.2.4. A range of AEA concentrations is not inhibited by Hp1

30,000 CB1-Tango cells were seeded per well in Freestyle media overnight. The following day, varying concentrations of AEA were added to the cells (final top concentration of 25μM, 1:10 dilution) in the presence and absence of 10μM Hp1 for 4 hours incubating at 37°C. Assay substrate was added for 90 minutes and read on the Flexstation. Data was normalised to control wells (set to 100) as % of control. Graph shows means and bars represent SEMs of 3 independent experiments, 8 replicates in each individual experiment.

Rodent hemopressin does not antagonise eCBs

In the above experiments we have established that when used at 10μM, human Hp1 did not significantly inhibit the activity of 2-AG or AEA at any of the tested concentrations of the eCBs. As mentioned previously, the amino acid substitution in the rat orthologue could be the key residue that is responsible for the activity of Hp at the CB1 receptor. We therefore again tested the two independently sourced preparations of the rat variant of Hp alongside the human Hp and AM251 against the responses elicited by 5μM 2-AG and AEA to determine if rHp has antagonist effect against these eCBs.

The 2-AG response was averaged at 250.6% ± 15.3% of control and this has been normalised as the maximal 2-AG response (set at 100%) as described previously. Similarly to the experiments with ACEA, AM251 inhibited the 2-AG response by approximately 90% across this series of experiments (Figure 4.2.5). In contrast 10μM Hp1, Hp2 and Hp3 had no significant effect on the 2-AG response. There is perhaps a trend towards a very minor inhibition with Hp2 inhibiting the 2-AG response by 12.1%, nonetheless this is a marginal response and it was not a significant inhibition.

Next, AEA similarly averaged a response at 383.1% ± 20.8% of control and is displayed as 100% of AEA response as described previously. AM251 inhibited the AEA responses by ~93% across this series of experiments (Figure 4.2.6). Again none of the Hp preparations used at the same concentration had a significant effect on the AEA response but there was again perhaps a trend towards a very small, but not significant effect with Hp2 reducing the response by ~10%.

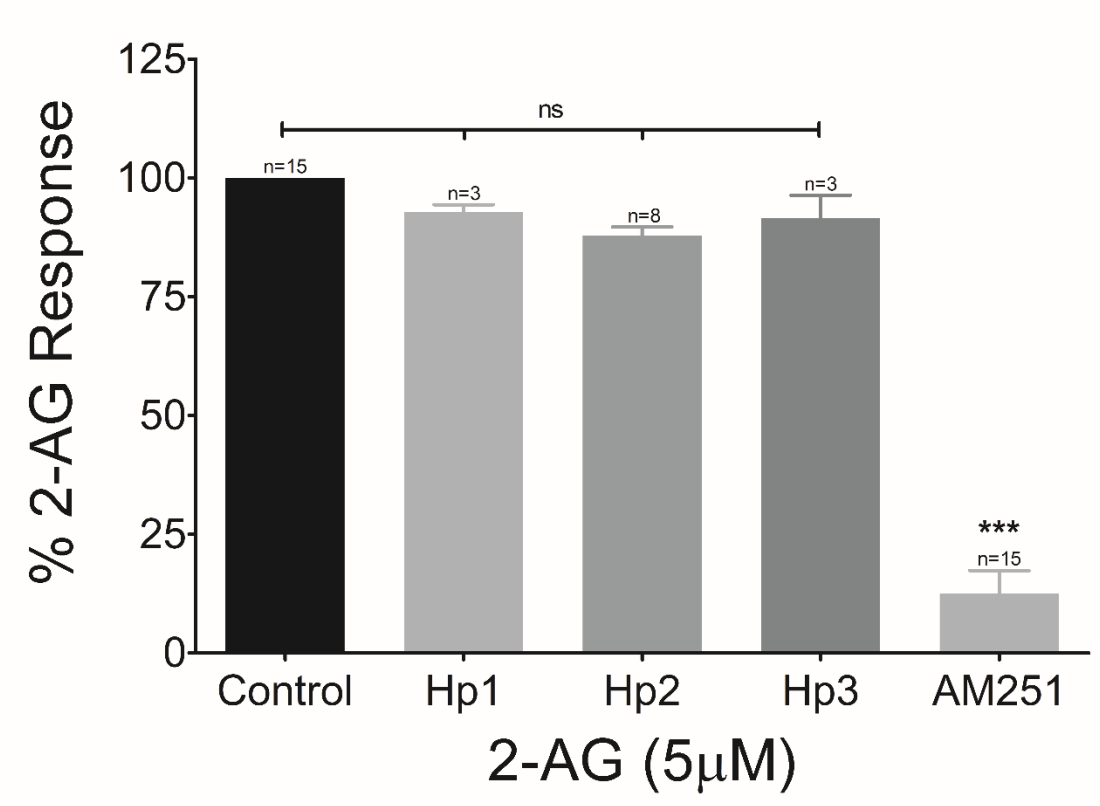

Figure 4.2.5. Comparison of the inhibition of 2-AG between Hp from different sources and AM251

CB1-Tango cells were seeded in black 96 well plates in Freestyle media overnight. Final assay concentration of 5μM 2-AG was added to the cells in the absence or presence of 10μM AM251, 10μM Hp1 (Tocris), Hp2 (Cayman Chemical) or Hp3 (Sigma) for 4 hours. Assay substrate was added for 90 minutes and read on the Flexstation. To show the full 2-AG elicited CB1 response, control well ratios were subtracted from the sample well ratios and the data was then normalised to the maximal 2-AG response (set to 100) and displayed as % of 2-AG response. Graph shows means and bars represent SEMs from pooled independent experiments, 8 replicates in each experiment. Significance of responses were compared to 2-AG control using One Way ANOVA.

ns $p>0.05$; ***$p<0.001$, One Way ANOVA, Bonferroni's Multiple Comparison Test.

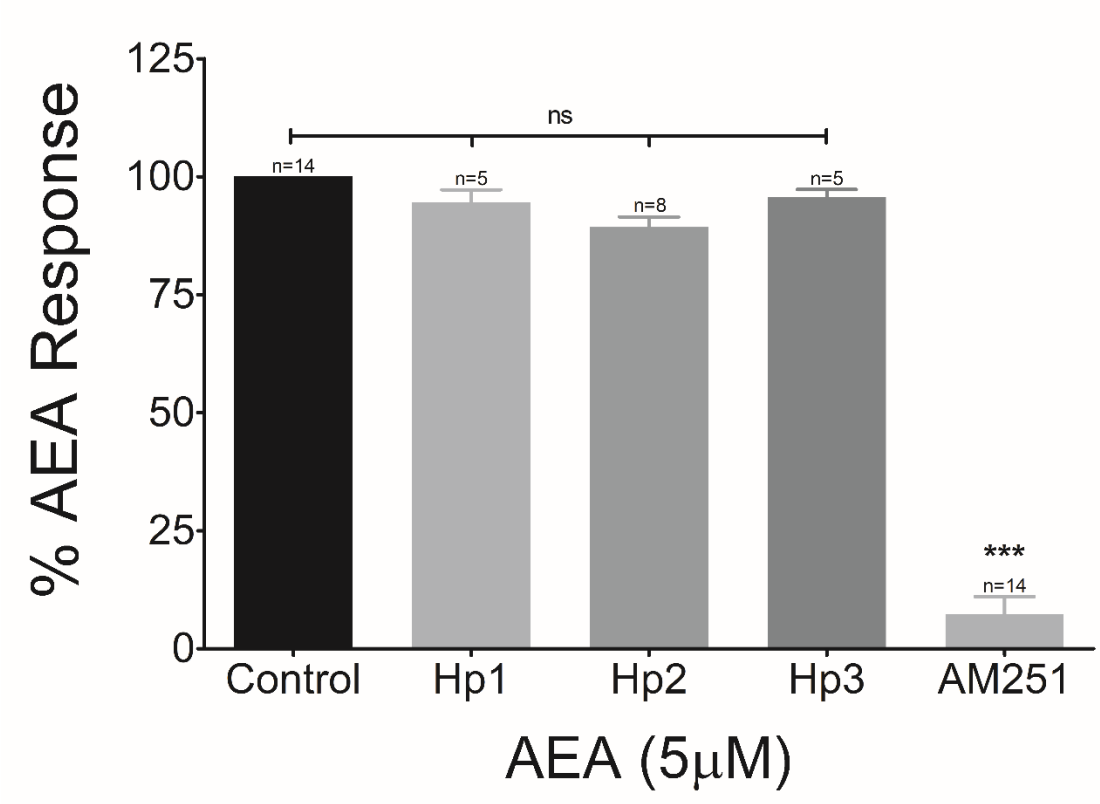

Figure 4.2.6. Comparison of the inhibition of AEA between Hp from different sources and AM251

CB1-Tango cells were seeded in black 96 well plates in Freestyle media overnight. Final assay concentration of 5μM AEA was added to the cells in the absence or presence of 10μM AM251, 10μM Hp1 (Tocris), Hp2 (Cayman Chemical) or Hp3 (Sigma) for 4 hours. Assay substrate was added for 90 minutes and read on the Flexstation. To show the full AEA elicited CB1 response, control well ratios were subtracted from the sample well ratios and the data was then normalised to the maximal AEA response (set to 100) and displayed as % of AEA response. Graph shows means and bars represent SEMs from pooled independent experiments, 8 replicates in each experiment. Significance of the responses was compared to AEA control using One Way ANOVA.

ns $p>0.05$; ***$p<0.001$, One Way ANOVA, Bonferroni's Multiple Comparison Test.

2-LG response remains in the presence of hemopressin

In contrast to AM251, three independent preparations of Hp (one human and two rat) failed to significantly inhibit the response to ACEA, 2-AG and AEA tested over a wide-range of concentration of the three agonists. In the previous chapter we have provided the first clear evidence that 2-LG can function as a partial agonist at the CB1 receptor, identifying it as a putative novel endogenous ligand for the CB1 receptor. For this reason, we decided to test the effects of Hp on the 2-LG response.

The maximal response to 2-LG is revealed when JZL195 is included to mitigate against the hydrolysis of 2-LG, and it was again added in this series of experiments. As before, 2-LG (FAC 6.25 – 50μM) elicited a concentration-dependent and saturable CB1-dependent response (Figure 4.2.7), reaching a maximum at 25μM (160.4% ± 4.8% of control). AM251 was shown to reveal an eCB tone when JZL195 was present previously, however, Hp1 on its own did not have any effect on baseline value (data not shown). The 2-LG response is not inhibited by the presence of 10μM Hp1 at all tested concentrations of 2-LG. The EC_{50} values for 2-LG concentration response curve was 2.28μM (log EC_{50} = -5.64 ± 1.74 SEM, n = 2) and 3.70μM (log EC_{50} = -5.43 ± 1.89 SEM, n = 2) in the absence and presence of 10μM Hp1 respectively. When comparing the log EC_{50} values, the difference is not statistically significant (Table 4.2.1).

We next compared the activity of the independent preparations of Hp with AM251 on the maximal 2-LG response. The average 2-LG response across this series of experiments was a stimulation to 179.3% ± 10.6% relative to control, in line with the results from the previous chapter. The 2-LG response was expressed as 100% by subtracting the background ratios and normalising the data to the maximal 2-LG response. As before, AM251 revealed a small eCB tone induced by the presence of JZL195 throughout the assay period and this explains why AM251 reduces the signal to a value below the control in Figure 4.2.8.

The three independently sourced preparations of Hp alone did not have an effect on the baseline value seen in the presence of JZL195 (Hp1 = 100.3% ± 1.6%, Hp2 = 98.5% ± 1.1%, Hp3 = 99.4% ± 1.6% of control) unlike AM251 which consistently and significantly reduces the baseline value by ~10%. This reinforces the observation that the Hp preparations do not display AM251-like CB1 antagonism, in this case against a small but significant tone induced by JZL195. The 2-LG response in the presence of all three Hp preparations was reduced by

around 10% of the full response (Hp1 = 88.5%, Hp2 = 87.6%, Hp3 = 87.1% of 2-LG response) but this was not significantly different to the control maximal 2-LG response nor significantly different from each other ($p>0.05$, Bonferroni's multiple comparison test). As expected, AM251 fully inhibited the 2-LG response, taking the basal value down to the same level seen in the absence of 2-LG which is ~90% of the basal control as a consequence of the presence of JZL195 in the assay medium (-10.8% ± 5.6%).

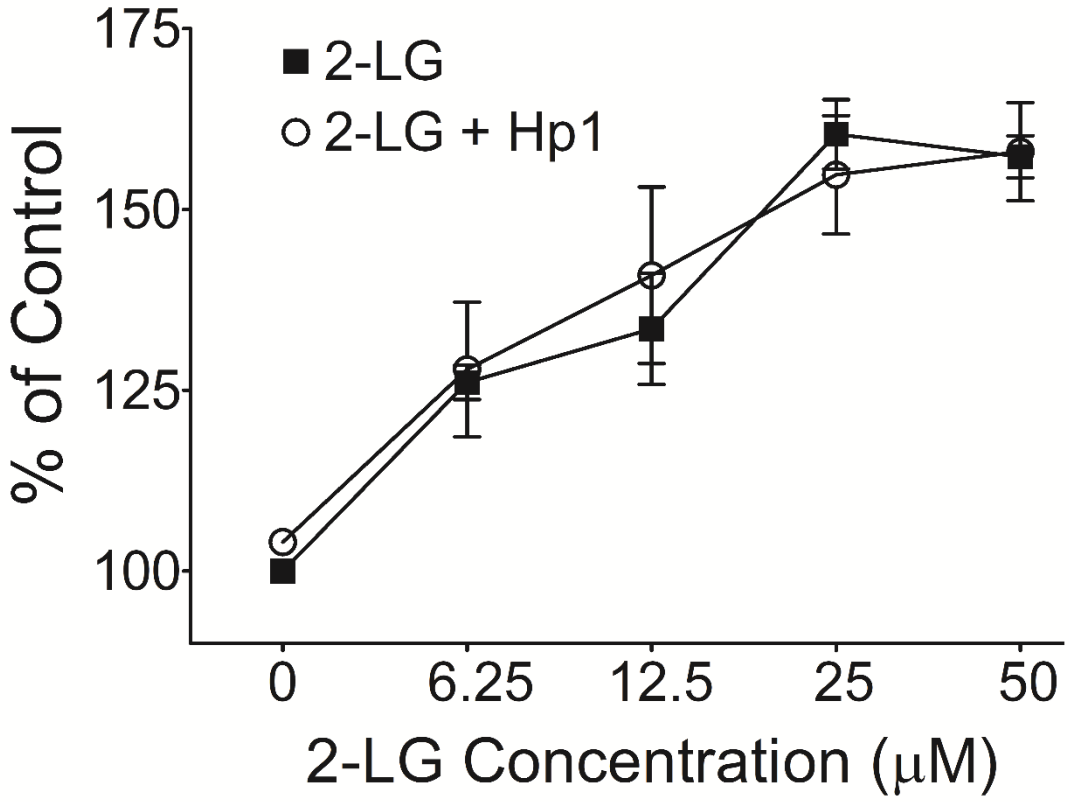

Figure 4.2.7. 2-LG concentration response curve is not inhibited by Hp1

30,000 CB1-Tango cells were plated in Freestyle media overnight. Drugs were diluted in Freestyle media and the cells were treated with a range of concentrations of 2-LG (final top concentration 50μM, 1:2 serial dilutions) in the presence and absence of 10μM Hp1 for 4 hours in a 37°C incubator. 100nM JZL195 was also present in all wells. Assay substrate was added for 90 minutes and read on the Flexstation. Data was normalised to control wells (set to 100) as % of control. Graph shows means and bars represent SEMs for 2 independent experiments, 8 replicates in each experiment.

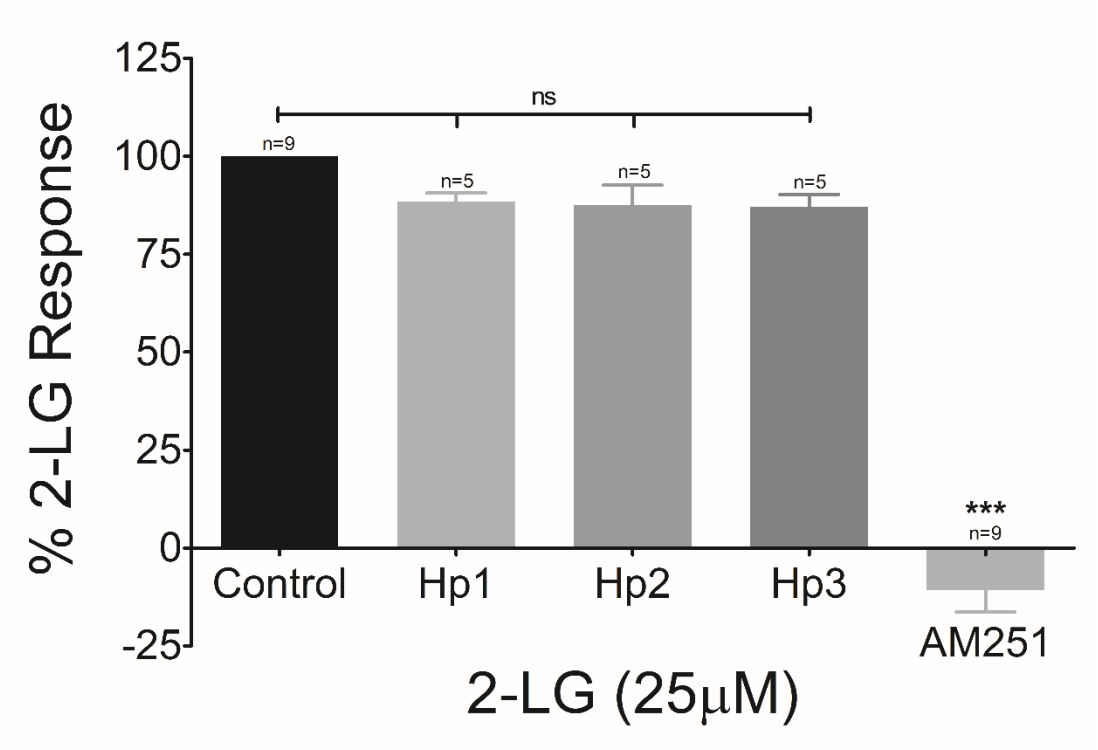

Figure 4.2.8. Comparison of the inhibition of 2-LG between Hp from different sources and AM251

CB1-Tango cells were seeded in black 96 well plates in Freestyle media overnight. Final assay concentration of 25μM 2-LG was added to the cells in the absence or presence of 10μM AM251, 10μM Hp1 (Tocris), Hp2 (Cayman Chemical) or Hp3 (Sigma) for 4 hours. 100nM JZL195 was included in all wells in all experiments. Assay substrate was added for 90 minutes and read on the Flexstation. To show the full 2-LG elicited CB1 response, control well ratios were subtracted from the sample well ratios and the data was then normalised to the maximal 2-LG response (set to 100) and displayed as % of 2-LG response. Graph shows means and bars represent SEMs of pooled independent experiments, 8 replicates in each experiment. Significance of the responses was compared to 2-LG control using One Way ANOVA.

ns $p>0.05$; ***$p<0.001$, One Way ANOVA, Bonferroni's Multiple Comparison Test.

AGONIST	CONTROL LOG EC_{50}	+ HP1 LOG EC_{50}	P VALUE	SIGNIFICANCE
ACEA	-7.74 ± 0.37	-7.67 ± 0.22	0.8664	ns
2-AG	-5.74 ± 0.19	-5.64 ± 0.13	0.7235	ns
AEA	-6.97 ± 0.34	-7.04 ± 0.31	0.8912	ns
2-LG	-5.64 ± 1.74	-5.43 ± 1.89	0.9513	ns

Table 4.2.1. Comparison of log EC_{50} values obtained of CB1 agonists in the absence and presence of Hp1

Log EC_{50} values of agonist alone and agonist with Hp1 concentration response curves were obtained from each experiment and were pooled together. Statistical analysis was carried out to determine if the log EC_{50} values were significantly different to each other. Unpaired Student's T-Test, two tailed.

4.3 Discussion

The CB1 receptor is an attractive target for therapeutics as it mediates many physiological processes including pain and appetite (Salamone et al., 2007; Davis, 2014). According to the World Health Organisation, obesity is becoming a major epidemic with increasing prevalence in a number of obesity-related diseases in many countries worldwide (Segula, 2014). Evidence in the literature supports the appetite reducing effects of CB1 antagonists (Rinaldi-Carmona et al., 1994; Colombo et al., 1998) and Rimonabant, a CB1 specific antagonist, was approved for medical use as an anti-obesity drug receptor (Pi-Sunyer et al., 2006). Rimonabant, however, was promptly removed from the market as its ability to cross the blood brain barrier caused an increased risk of centrally mediated side effects such as depression and suicide ideation. This lead to a fall in interest in the development of other CB1 antagonists (Moreira and Crippa, 2009). However, blockade of peripherally located CB1 receptors has demonstrated similar, albeit smaller, weight loss (Pavon et al., 2008) and analgesic effects (Agarwal et al., 2007) with reduced central activity. Therefore, peripherally restricted CB1 antagonists are being pursued as potential therapeutics (Kunos et al., 2009). In this context, the claim that the 9 amino acid peptide Hp functions as a CB1 antagonist was of considerable interest (Heimann et al., 2007) as it might be, or might be modified to be, peripherally restricted.

Many companies currently sell Hp as a CB1 antagonist based upon these studies utilising Hp as a CB1 antagonist. However with contradictory reports emerging negating the claim that Hp is a true CB1 receptor antagonist (Hama and Sagen, 2011a; Straiker et al., 2015; Dvoracsko et al., 2016), it is important to resolve the direct effects of Hp on the CB1 receptor. In this chapter the direct antagonistic activity of three independently sourced preparations of Hp, one human and two rat, was tested using the CB1-Tango assay against three full CB1 agonists ACEA, 2-AG and AEA and one novel partial agonist, 2-LG.

Hp1 was tested over the range of 0.4μM – 20μM and failed to inhibit the response to CB1 agonists (data not shown). The agonists produced a CB1-dependent response with EC_{50} values similar to those reported in the previous chapter, indicating reproducibility of the assay. When tested at a fixed concentration (10μM), Hp1 failed to inhibit the activity of any of the CB1 agonists over their full concentration-response range (Figure 4.2.1, Figure 4.2.3 and Figure 4.2.4). This concentration was selected as it was in excess to what is published in

literature and used *in vitro* assays (1μM) (Heimann et al., 2007). There is no statistically significant difference between the log EC_{50} values (Table 4.2.1); and no difference in the maximal responses of the concentration response curves of all tested agonists in the absence and presence of Hp1, indicating no antagonism or allosteric modulation of the agonists.

Hp was reported to be able to antagonise synthetic CB1 receptor ligand Hu-210 and acted similarly to CB1 antagonist SR141716 in displaying both antagonist and inverse agonist activity (Heimann et al., 2007). Here, Hp was hypothesised to bind to the same pocket as SR141716 on the CB1 receptor, thus explaining the similar activity profiles of Hp and SR141716 (Scrima et al., 2010). AM251 is structurally closely related to SR141716 (Lan et al., 1999), which we utilised in our experiments to compare to the activity of Hp. 1μM of Hp was shown to be sufficient to demonstrate antagonism of the CB1 receptor at similar activity levels to 1μM of SR141716 (Heimann et al., 2007). In our results from the previous chapter, molar excess of AM251 was able to antagonise all CB1 ligands and natural eCBs fully whilst molar excess of Hp was unable to show any antagonism. We also utilised AM251 at its maximally active concentration of 2.5μM in the previous chapter whilst Hp showed no discernible antagonism at 2.5μM against the tested CB1 agonists (data not shown). The activity of Hp was therefore significantly different to AM251 in our assay system.

The effects of Hp have largely been demonstrated with the rat orthologue and Hp was originally tested in rodent models (Heimann et al., 2007). The one amino acid difference between rat and human Hp might conceivably have an effect on the antagonist activity of the peptide against CB1 receptors from different species. For this reason, we tested different sources of Hp (one human Hp and two rat Hp) and found there was no significant difference between the three independently sourced batches of Hp and no difference between the actions of human Hp and rodent Hp against four CB1 agonists; including 2 eCBs. Our inability to detect any significant inhibition in the CB1-Tango assay is not in keeping with the proposed function of Hp as a CB1 antagonist.

Our results are in agreement with the results reported by Straiker et al (2015) who tested 2μM Hp against endogenously produced 2-AG in autaptic hippocampal neurones and did not see any antagonism by Hp when applied both extracellularly and intracellularly. Likewise other scientific groups have failed to find any evidence for Hp acting as a CB1 antagonist in their assays (e.g. Tibor Harkany group, unpublished observations). A lack of CB1 antagonism

against the antinociceptive effect of centrally administered WIN55,212-2 by Hp was also reported by Hama and Sagen (2011a). Finally, Dvorácskó et al (2016) have shown truncated [^{3}H]Hp(1-7) displaying saturable binding to an as-yet-to-be identified target in CB1$^{-/-}$ KO mice which cannot be displaced by conventional CB1 ligands SR141716, AM251 or JWH-018 but can be displaced by full length Hp. Thus it is reasonable to conclude that Hp may not have CB1 antagonist activity and can bind to and perhaps signal via a non-CB1 receptor.

These findings are in contrast to the original study by Heimann et al (2007) who first reported the activity of Hp on the CB1 receptor. The conformation-sensitive antibodies generated to the N-terminus of the CB1 receptor used in the ELISA assay are reported to only bind to the activated CB1 receptor (Gupta et al., 2007). The antibodies were produced in-house by the same group and the anti-CB1 antibody have as yet not been validated by other groups. Interestingly the antibody is reported to bind to an epitope in the N-terminal region of the CB1 receptor that is not actually involved in CB1 receptor activation; in fact deletion of up to 89 amino acids of the N-terminal region (including the epitope used for antibody recognition) showed no difference to activation by CB1 agonist CP-55,940 (Andersson et al., 2003). In the preliminary verification of the antibodies by Gupta et al (2007), receptor internalisation was intentionally compromised in the whole cell and membrane assays, which could have led to false positive antibody binding due to the overexpression of the target receptor and other receptors. As well as this, the antibodies in the presence of 1μM SR141716 did not originally reduce antibody binding to CB1 receptor, in contrary to the study by Heimann et al (2007) which did show a reduction in antibody binding in the presence of 1μM SR141716 despite using the same assay set up. This suggests that the antibody might not be indicative of changes in CB1 conformation.

Furthermore, the [^{35}S]GTPγS binding assay and adenylyl cyclase assays are also indirect measures of ligand activity to transfected CB1 receptors and these assays can be subject to false positives through influence from other receptors that are expressed. In fact, in the [^{35}S]GTPγS binding assay, Heimann et al (2007) originally saw a decrease in binding in the presence of 1μM Hp in the same manner as SR141716. However, in separate studies, Szlavicz et al (2015) and Dvorácskó et al (2016) saw a slight increase in [^{35}S]GTPγS binding in the presence of 1μM Hp and did not exhibit the same activity as SR141716 in their binding assays. In contrast to assays which measure secondary effectors as an indirect measurement of receptor activity, the CB1-Tango assay is a direct receptor activation assay system that is not

influenced by the expression or activation of other GPCRs. The response is also not altered or terminated by endogenous cellular metabolism during incubation time, thus allowing direct measurement of CB1 receptor activation and antagonist modulation (Barnea et al., 2008). Other receptors could form heterodimers with the CB1 receptor to modulate signalling (Birdsall, 2010) but it is unknown whether this occurs in the CB1-Tango assay. Since there is little change in the concentration response curves of 4 different CB1 agonists and little difference between the log EC_{50} values of these agonists in the presence of Hp, it is not very likely that there is modulation of CB1 receptors through heterodimer formation.

Hp has in fact displayed opposing differences in mechanism of action both *in vitro* (as mentioned above) and *in vivo*. In some animal studies, Hp has no discernible difference to other CB1 agonists. Hp has shown antinociceptive effects similarly to CB1 agonists (WIN55,212-2 and VD-Hp) and animal models show cross-tolerance to the three treatments (Pan et al., 2014). Hp has also shown ability to slow gut motility which can be blocked by AM251 in a similar fashion to WIN55,212-2 and VD-Hp (Li et al., 2016).

Variability between results might conceivably be related to peptide solubility, *in vitro* systems such as the CB1-Tango assay or autaptic hippocampal neuron cultures rely on cell culture media, which may affect the ability of Hp to stay in monomeric form. In fact, Bomar et al (2012) has shown that Hp aggregates in physiologically relevant conditions at high concentrations (>1mM) and that hHp tend to aggregate more than rHp (Song et al., 2015), this could account for the variability of activity across experiments. At physiological levels, Hp is able to bind to metal ions which could have an effect on its mechanism of action *in vivo* (Remelli et al., 2016) or perhaps protein chaperones or local release of low concentrations of Hp can prevent aggregations *in vivo* (Gomes et al., 2010). However, physiological implications of the self-assembly remain unclear and even in some *in vivo* studies, Hp showed opposing effects or has been unable to antagonise CB1 receptors (Hama and Sagen, 2011a; Petrovszki et al., 2012). In our studies Hp was readily soluble in all media and there was no indication of Hp aggregates or precipitation in the media.

Further studies have indicated Hp exerts non-CB1 mediated effects. Administration of Hp to anesthetised rats causes dose-dependent hypotension caused by reduction in systemic vascular resistance (Lippton et al., 2006). This hypotensive effect was also seen across different species of mammals (Blais et al., 2005) and the mechanism behind the effects were

unclear but was thought to be through the release of nitric oxide (Lippton et al., 2006). Hp has also recently been shown to be able to stimulate μ-opioid receptor and is antagonised by broad opioid antagonist naloxone (Szlavicz et al., 2015) despite previous studies indicating that Hp does not induce opioid-mediated analgesia (Dale et al., 2005b; Heimann et al., 2007). Hp has also been linked to activity on the TRPV1 receptor; rats treated with Hp displayed anxiogenic behaviour which was prevented by TRPV1 antagonists but not by CB1 antagonists (Fogaca et al., 2015; Leone et al., 2017).

Studies which have utilised Hp as a CB1 antagonist but did not see CB1 antagonism when applied extracellularly have accredited this result to intracellularly located CB1 receptors on the mitochondria (mtCB1) (Zhang et al., 2015, 2016a). Zhang et al. reported no CB1 antagonism when Hp was applied extracellularly whilst conventional CB1 antagonists, such as AM251 and SR141716, show typical CB1 antagonism. This result was hypothesised to be due to conventional CB1 antagonists being cell permeable whilst Hp cannot cross the plasma membrane (Rozenfeld and Devi, 2008). This led to the conclusion that the effect seen by conventional CB1 antagonists must be due to intracellular mtCB1 receptors. Applying Hp intracellularly through the recording pipette solution showed more noticeable effects, supporting this claim of modulation by mtCB1. However, when Straiker et al (2015) applied 2μM Hp intracellularly in autaptic mouse hippocampal neurons in DSE experiments, they observed no CB1 antagonism. In comparison to the studies by Straiker et al. (2015), Zhang et al. (2015, 2016a) applied higher intracellular concentrations of Hp (10-20μM). As mentioned previously, high concentrations of Hp may form aggregates. However, when applied intracellularly, the presence of proteases and other metabolic enzymes may degrade Hp aggregates and cause non-specific effects in the cell. This may have been interpreted as a response mediated by mtCB1. The use of Hp as a CB1 antagonist therefore has posed a problem in literature where mistaken conclusions might have been drawn if, as this and other studies suggest, Hp is not actually a CB1 antagonist.

The physiological relevance of Hp as a biological signalling molecule has also been questioned. Although it could be extracted from tissues and, on this basis, was postulated to be an endogenous signalling molecule, it is not known exactly where and how it is produced. Mass spectrometry originally suggested that Hp is detected in the brain thus is endogenously produced, but speculation arose that Hp could be an artefact of hot acid extraction which can cleave D-P bonds from longer peptides (RVD-Hp) to produce Hp (Bomar and Galande,

2013). More recent studies using mass spectrometry without hot acid extraction method in mice brains failed to detect fragments of Hp shorter than RVD-Hp (Gomes et al., 2009; Gelman et al., 2013). This was further supported by Bauer et al (2012), who only detected RVD-Hp from mice brain homogenate using antibodies raised against the C terminus of Hp, suggesting that only RVD-Hp is produced endogenously but not Hp. These publications suggest Hp does not exist as an endogenous free peptide in the body, plus research shown through the CB1-Tango assays and other studies indicate that even as a free peptide, Hp does not function as an endogenous ligand for the CB1 receptor.

Interestingly, N-terminally extended peptides containing the Hp sequence of up to 23 amino acids long can be extracted from tissues (Bauer et al., 2012), with the best characterised of these being RVD-Hp and VD-Hp (Gomes et al., 2009). Of the related peptides, VD-Hp has been proposed to be a CB1 receptor agonist (Han et al., 2014), while RVD-Hp was initially suggested to act as a CB1 agonist (Gomes et al., 2009) but later studies then showed RVD-Hp exhibited negative allosteric modulation at CB1 receptors (Bauer et al., 2012) and positive allosteric modulation at CB2 receptors (Petrucci et al., 2017). It has been suggested that RVD-Hp and VD-Hp interact with the CB1 receptor in a distinctively different manner to the lipid eCBs (Gomes et al., 2009), perhaps due to binding to an allosteric site (Bauer et al., 2012). In these models one would assume that Hp is likely to bind to the same pocket as its related longer peptides suggesting it could be a better antagonist for Hp related peptides and not endogenous eCBs. To this end the activity of RVD-Hp and VD-Hp has not been tested in the CB1-Tango assay system, so no comment can be made on whether they truly have activity at the CB1 receptor.

Taking together many of the studies highlighting the non-CB1 mediated activity of Hp and that Hp can bind to potential unidentified targets in $CB1^{-/-}$ KO mice brain homogenate, it is possible that Hp is biologically active *in vivo* through different receptor(s). On that basis, even if Hp was a CB1 antagonist, any results obtained need to be interpreted with caution given that Hp clearly has the potential to have major "off-target" effects relative to any CB1 activity. Based on these observations together with the research conducted in this thesis and in literature mentioned earlier in support of these findings, Hp is clearly not a specific CB1 antagonist. This puts into question whether publications that have used Hp on the basis it is a CB1 antagonist also considered these factors as this causes a serious risk of reaching false conclusions. In modern day science, there is a worrying reproducibility crisis in the biological

sciences (see Begley and Ellis, 2012; Baker, 2016). This is likely, or at least partly, due to some compounds such as Hp being marketed as having selective activities, which upon closer inspection, they do not possess. Unfortunately, the consequence of this is we end up in a vicious cycle where the more often the compound is used as a "selective antagonist", the more it is adopted by others for the same purpose.

In summary, the CB1-Tango assay system was utilised to test if three independently sourced preparation of Hp can inhibit the ability of a wide range of agonists to activate the CB1 receptor. The results show no marked antagonism by Hp of any CB1 ligands used at a range of concentrations. This is supported by several other publications and is contradictory to the conclusions reached in the original publication. The question as to why others have concluded that Hp is a true CB1 antagonist might be related to Hp having actions at other receptors that in turn can modulate CB1 function via indirect mechanisms. Furthermore, it would now appear that Hp does not exist as a free endogenous peptide but is actually an artefact of hot acid extraction. Taking together the direct *in vitro* assay results and the published literature data, it can be concluded that Hp is not an endogenous CB1 antagonist. Moreover, the fact that Hp appears to have significant activity at targets other than the CB1 receptor questions its value in any assay, as based on these observations there is no basis for using it as a selective CB1 antagonist.

Chapter 5. Results 3 – Development of a cell-based model of eCB signalling

5.1 Introduction

The two established eCB ligands are 2-AG and AEA (Devane et al., 1992; Mechoulam et al., 1995) and both have been extensively studied since their discovery (Iannotti et al., 2016). In the context of retrograde synaptic signalling, the ligands are thought to be synthesised "on-demand" from membrane lipids in response to cellular signalling rather than being premade and stored in vesicles like other neurotransmitters (Marsicano et al., 2003; Piomelli, 2003). The process underlying the generation of 2-AG and AEA for retrograde synaptic signalling have been comprehensively studied and several stimuli, such as membrane depolarization, increases in intracellular calcium levels and specific receptor stimulation can increase the cellular release of 2-AG and AEA for eCB signalling (Williams et al., 2003; Di Marzo, 2008a, b; Wang and Ueda, 2009). However, in non-synaptic forms of eCB signalling, such as autocrine signalling that is believed to be important for adult neurogenesis and axonal growth and guidance (Gao et al., 2010; Oudin et al., 2011b; Oudin et al., 2011a; Maccarrone et al., 2014), there is no simple consensus on how these two eCB signalling pathways are regulated.

Several stimuli like ionomycin can increase 2-AG and AEA levels in cells and tissues, but it is not always clear as to whether the measured eCBs are from a signalling pool that can contribute to eCB signalling or a general metabolic pool as they are usually quantified from homogenates of cells and/or tissues (Devane et al., 1992; Bisogno et al., 1997; Stella et al., 1997). Besides monitoring physiological responses like DSI/DSE for 2-AG signalling, studying eCB activity relies heavily on mass spectrometry quantification, which requires an elaborate laboratory setup, specialised equipment and tends to be low throughput (Balgoma et al., 2013). Thus, it is often difficult to study stimuli-induced eCB signalling, especially for AEA.

As hinted at above, it is unclear if the 2-AG and AEA measured in many studies is reflective of a signalling pool of the lipid, as opposed to a general metabolic pool. A bottle neck in our understanding of the synthesis of eCBs is the lack of simple cellular models that report directly on eCB signalling. In the first two chapters of the thesis we have shown the value of

the CB1-Tango cells for addressing the question as to whether Hp might be a novel endogenous CB1 antagonist, and whether 2-LG might be a novel eCB. CB1-Tango cells are genetic variants of the U2OS human osteosarcoma cell line (Ponten and Saksela, 1967) where eCB signalling is important for bone development and maintenance (Tam et al., 2008; Idris and Ralston, 2012) and thus the CB1-Tango cells could potentially produce eCBs for eCB signalling.

5.1.1 Aims

We reasoned that this human osteosarcoma cell line might provide an opportunity to address some fundamentally important questions that relate to eCB signalling. However, to be of value to eCB signalling, the cells would need to express the key enzymes thought to be involved in the synthesis and breakdown of 2-AG and AEA, and moreover pathways that are established to activate eCB signalling would need to be functional and report via CB1 receptor activation in the CB1-Tango cell line. It follows that if the osteosarcoma cell line expresses the key enzymes and the pathways are active and can be detected by the CB1-Tango assay, pharmacological and genetic tools (e.g. CRISPR) can be employed to critically test the requirement of individual components for both 2-AG and AEA synthesis, as well as eCB signalling. With this in mind the aims of this chapter are to:

- Profile the level of transcript expression of the major known enzymes implicated in eCB signalling in the CB1-Tango cells and compare the individual transcript levels in the CB1-Tango cells to the levels found in a variety of tissues to see if each is within a range expected for a role in eCB signalling
- Adapt the CB1-Tango assay to produce and detect an eCB tone using different pharmacological stimuli that activate key enzymes in the signalling pathways

5.2 **Results 3A**. Are the CB1-Tango cells a suitable model to study eCB signalling?

5.2.1 **Results 3A.** Introduction

In previous chapters, the CB1-Tango cells have been shown to be able to generate a measurable and reliable CB1-dependent response to exogenously applied CB1 agonists and have reduced responses in the presence of CB1 antagonists. The use of the FAAH and MAGL inhibitor JZL195 in the previous chapters reveals an eCB tone which can be antagonised by AM251. In the absence of JZL195, there is no eCB tone revealed by AM251, suggesting that the eCB degrading enzymes are acting as gate keepers to prevent a relatively low level of signalling at the CB1 receptor under the manufacturer's recommended conditions. CB1-Tango cells therefore are able to synthesise and hydrolyse eCBs, albeit the eCB tone revealed by JZL195 is very modest relative to the response elicited by a maximally active concentration of ACEA, or by exogenously applied 2-AG or AEA.

To fully understand the nature of the eCB system in the CB1-Tango cells, it was prudent to profile the cells to determine specifically which of the eCB synthesis and degrading enzymes were expressed and whether these were expressed to physiologically relevant levels as cancer cell lines may have irregularly upregulated or downregulated genes. In the context of the DAGL and 2-AG pathway, western blotting analysis was carried out by previous members of the lab and detected the presence of both the DAGLs and MAGL proteins in the CB1-Tango cells, but was unable to detect FAAH (thesis of Praveen K Singh, 2013). As well as this, in previous qPCR experiments carried out in the lab, endogenous expression of DAGLα and DAGLβ transcripts were detected; DAGLβ RNA transcripts were around 2.5x higher than DAGLα (thesis of Rachel Lane Markwick, 2015). At the time, the AEA pathway was not characterised in the CB1-Tango cells, however focus has been placed on the AEA pathway as an important signalling molecule in peripheral systems such as cardiovascular system, gastrointestinal tract and bone maintenance (reviewed in Maccarrone et al., 2015). Therefore, AEA is likely to be relevant in eCB signalling in our cell line.

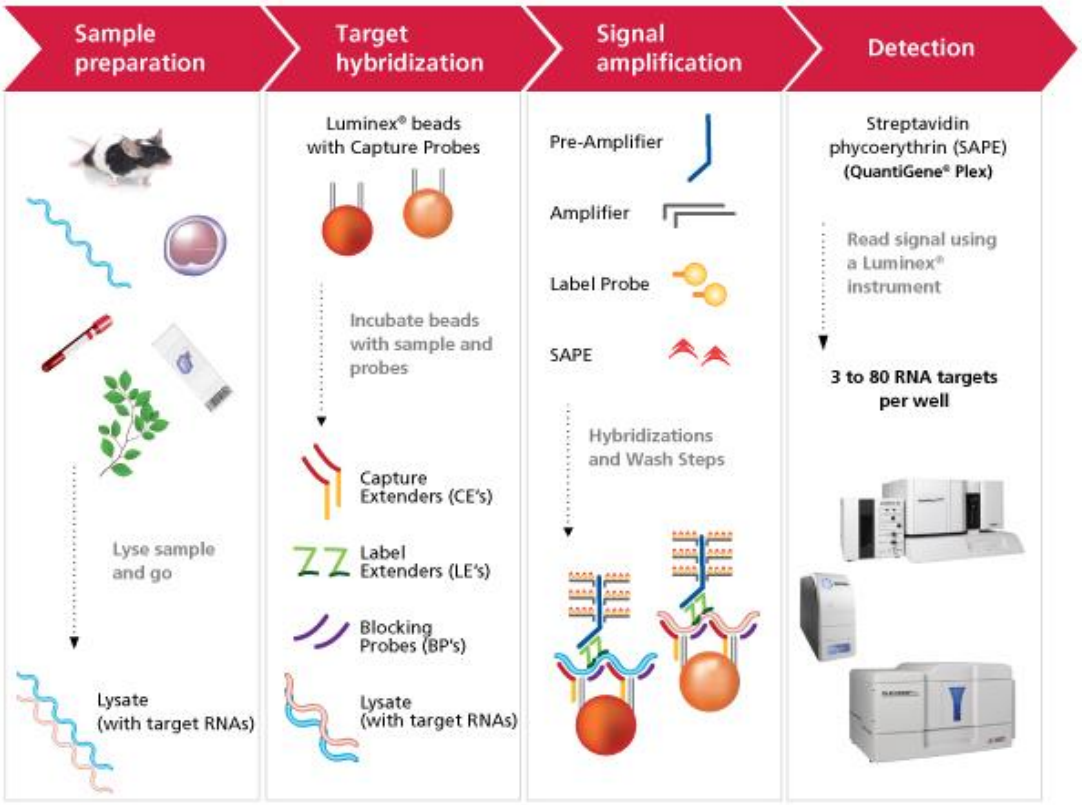

Figure 5.2.1. Workflow of the QuantiGene Multiplex assay system

Image from QuantiGene Multiplex assay user manual, Thermofisher Scientific.

The amount of RNA bound to each bead is quantified using branched DNA technology, where the pre-amplifier DNA molecules bind to each bound RNA sample. Signal amplification is based on the DNA branch structures capturing multiple labels rather than RNA being amplified as in standard microarray platforms, which may lead to bias (Boelens et al., 2007). Finally, an R-Phycoerythrin conjugate is added to give a detectable fluorescence emission and the intensity of the emission is collected. The Median Fluorescent Intensity (MFI) is collected for each gene which is proportional to the abundance of the RNA for that gene. The MFI from background wells is subtracted from the sample data giving the Net MFI.

To quantitatively determine the expression of the necessary synthesis and degrading enzymes required for both the 2-AG and AEA pathway, we have utilised a more robust multiplex assay system to detect the RNA transcripts of major eCB components and their relative transcript expression. The QuantiGene Multiplex assay system can quantitatively measure gene transcripts of up to 50 different genes simultaneously (Figure 5.2.1). Several bespoke capture extender probes are designed to unique sequence areas of RNA on a given target gene to improve specificity of binding. Other probes (label extenders and blocking probes) are also designed in the probe set alongside the capture probes to further reduce off target binding. The probes are coupled to magnetic beads labelled with unique identification ratios of red and far-red light emissions and each probe set per gene is coupled to only one colour bead to identify specifically which gene is being detected.

In this section, I will report on the selection and bespoke design of the probes for a panel of eCB genes, the optimisation of the QuantiGene Mulitplex assay system and utilisation of the assay to quantify the expression of the eCB panel of genes in the CB1-Tango cell line and for comparison to other cell lines and total RNA from human tissues. This is an important basis to determine whether the CB1-Tango assay can be adapted to address some fundamental question relating to eCB signalling in general, and more specifically eCB signalling in a human cancer cell line.

5.2.2 **Results 3A**. Results

Design of the eCB panel of genes

For the eCB panel, we designed probes to the gene transcripts of two established CB receptors, the major eCB synthesis enzymes and the major eCB degrading enzymes listed (Table 5.2.1). In brief we wanted to profile the cells for the transcript level of the CB1 and CB2 receptors, the enzymes implicated in 2-AG synthesis (DAGLα, DAGLβ), the enzymes postulated to regulate AEA levels (NAPEPLD and PLA2G4E) and the main enzymes that degrade 2-AG and/or AEA (MAGL, FAAH and ABHD6). In addition, we also decided to profile PLA2G4B as although it has not been implicated in AEA synthesis, it is structurally very closely related to PLA2G4E and its expression matches more closely with CaNAT and on that basis worthy of some investigation.

The probes for each transcript are generated in tandem on a single stretch of sequence (Figure 5.2.2). There are several capture extender probes generated along the region and the redundancy of the probes increase the specificity of binding to the RNA samples. The blocking probes and label extenders are generated around the capture extender probes in order to form a steric complex that amplifies only the specific signal of the bound RNA, again to increase specificity of the signal produced and reduce off target binding.

The probes were largely generated to stretches of unique sequences that share little homology to other genes in order to reduce off-target binding (Table 5.2.1). For some genes however, the probes were designed to catalytic regions of interest, for instance in the case of DAGLα and DAGLβ, the probes were designed to the exons of the catalytic regions of each gene (Reisenberg et al., 2012). The NAPEPLD probes were also designed to exon 3, which is the largest exon, and harbours the catalytic motif (Daiyasu et al., 2001; Tsuboi et al., 2011) and PLA2G4E and PLA2G4B probes were designed to their respective catalytic regions (Song et al., 1999; Ogura et al., 2016). The design of the probes to the catalytic region serves two purposes. Firstly, there are different splice variants of these genes, and though it is common practice to generate probes to areas that span all splice variants, not all splice variants are enzymatically active and consequently such probes are not necessarily reflective of enzymatically active protein expression. It is therefore more reflective of functional protein expression to generate probes to the catalytic regions.

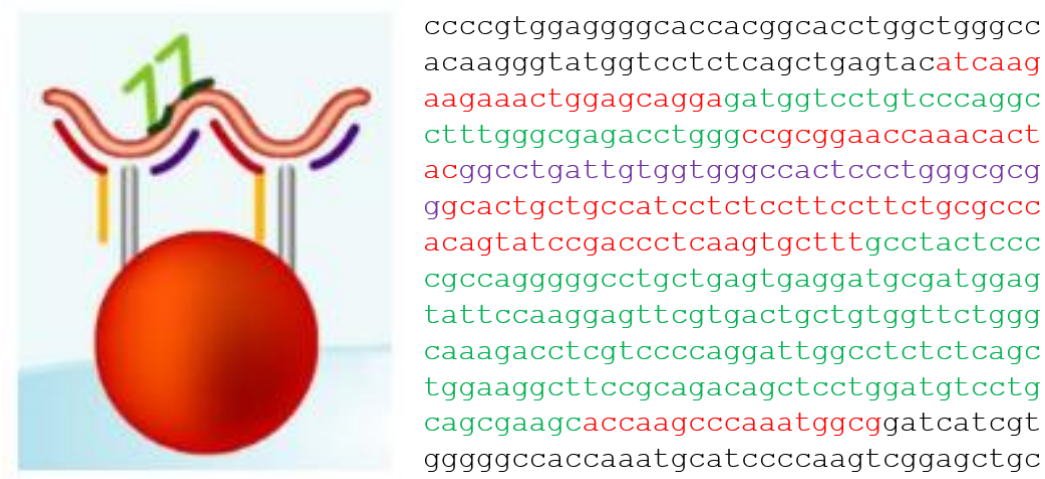

Figure 5.2.2. Example of the design of probe sets against the panel of eCB genes

Schematic of the probe set interacting with the sample RNA and forming a bead complex. Probe sets were designed to each gene in the panel. Example shown in the figure of DAGLβ gene on the right, red sequence corresponds to capture extender probes, green sequence corresponds to label extenders and purple corresponds to blocking probes which are schematically displayed on the left.

GENE	ROLE IN eCB SIGNALLING	REGION OF GENE TARGETED
CNR1	Cannabinoid Receptor 1	Exon 2 – UTR (532bp)
CNR2	Cannabinoid Receptor 2	Exon 2 (368bp)
DAGLα	Key 2-AG synthesising enzyme	Exon 13 – Exon 17 (347bp)
DAGLβ	Key 2-AG synthesising enzyme	Exon 7 – Exon 11 (400bp)
NAPEPLD	Key AEA synthesising enzyme	Exon 3 (486bp)
ABHD6	eCB hydrolysing enzyme	Exon 5 – Exon 9 (511bp)
MGLL	eCB hydrolysing enzyme	Exon 7 – UTR (563bp)
FAAH	eCB hydrolysing enzyme	Exon 5 – Exon 10 (463bp)
PLA2G4E	Putative CaNAT enzyme	Exon 13 – Exon 16 (430bp)
PLA2G4B	Candidate CaNAT enzyme	Exon 16 – Exon 18 (413bp)
HLCS	Housekeeping gene	Exon 5 (572bp)
FOXJ2	Housekeeping gene	Exon 2 – Exon 6 (425bp)

Table 5.2.1. List of genes included in the eCB panel of probes for the QuantiGene Multiplex assay

Secondly, we wanted to design probes that would not only report on transcript levels in parental cell, but could also be used in screening assays where strategies have been adopted to delete the catalytic sites from each of the key genes. This would allow us to use the multiplex system as a fast and convenient validation tool to characterise the KO of genes, if the deleted region of the gene is the region where the probes are targeting, then there will be no signal from the beads assay. As a result, we have specifically designed the probes to catalytic regions that could be targeted with gene editing tool CRISPR in the future. In later experiments, we use CRISPR to genetically KO genes for the characterisation of the 2-AG and AEA pathway and to KO candidate genes for validation of the putative CaNAT enzymes.

Probes to two housekeeping genes HLCS and FOXJ2 were also generated, these housekeeping genes were selected based on data analysed across published microarray studies, due to their low variability across different cell lines and conditions (Gareth Williams, unpublished data). In summary, the probes were generated to this panel of genes for both the determination of transcript level in the CB1-Tango cells and as tools to validate disruption of the catalytic region of each gene in genetic KO studies.

Optimisation of the Magpix Beads assay

We wanted to quantitatively confirm the expression of the eCB gene transcripts in the CB1-Tango cells using the multiplex system. We extracted RNA from CB1-Tango cells grown under normal culturing conditions in a T-75 flask. Preliminary experiments were carried out using the manufacturer's recommended serial dilution of 50 – 500ng of total RNA from the CB1-Tango cell line as described previously in methods. For each individual gene, the linear relationship between the RNA concentration and net MFI was calculated. A representative graph of DAGLβ is shown in Figure 5.2.3. The results show a good linear relationship when the net MFI lies within the dynamic detectable range of 10-20,000/30,000 MFI (3.5 log units). For some gene transcripts, particularly at lower concentrations, the net MFI lies outside the dynamic range which reduces the strength of the linear relationship (data not shown). Our highest net MFI reading from the eCB beads set was from 500ng of DAGLβ at 1780 ± 45.3 net MFI (Figure 5.2.3), which is within the dynamic detectable range but is rather low within the range. Also, signals that are about 3 standard deviations above background levels are typically considered a "real" signal from the noise and 5 of our genes were below this threshold even at 500ng (data not shown). This indicated that even the highest recommended RNA concentration would not give us enough signal to robustly detect the eCB gene transcripts from the CB1-Tango cells.

For these reasons it was decided to increase the amount of RNA in the wells from 500ng to 7500ng so that the net MFI signals lie more within the detectable range of the assay. The plot of the correlation of both RNA concentrations is shown in Figure 5.2.4. There is a strong positively linear relationship between the relative net MFIs of the genes from both RNA concentrations (Figure 5.2.4). The higher concentration of RNA also boosted the less expressed gene transcripts to give a better signal compared to background signal, and only two gene transcripts remained below the detection threshold. The relative expression and ranking of the eCB gene transcripts are maintained even at the higher concentration, which is also displayed in Figure 5.2.5. The higher concentration is therefore useful for detecting less highly expressed gene transcripts and is very consistent detecting the relative expression of the transcripts within a wide range of concentrations of RNA.

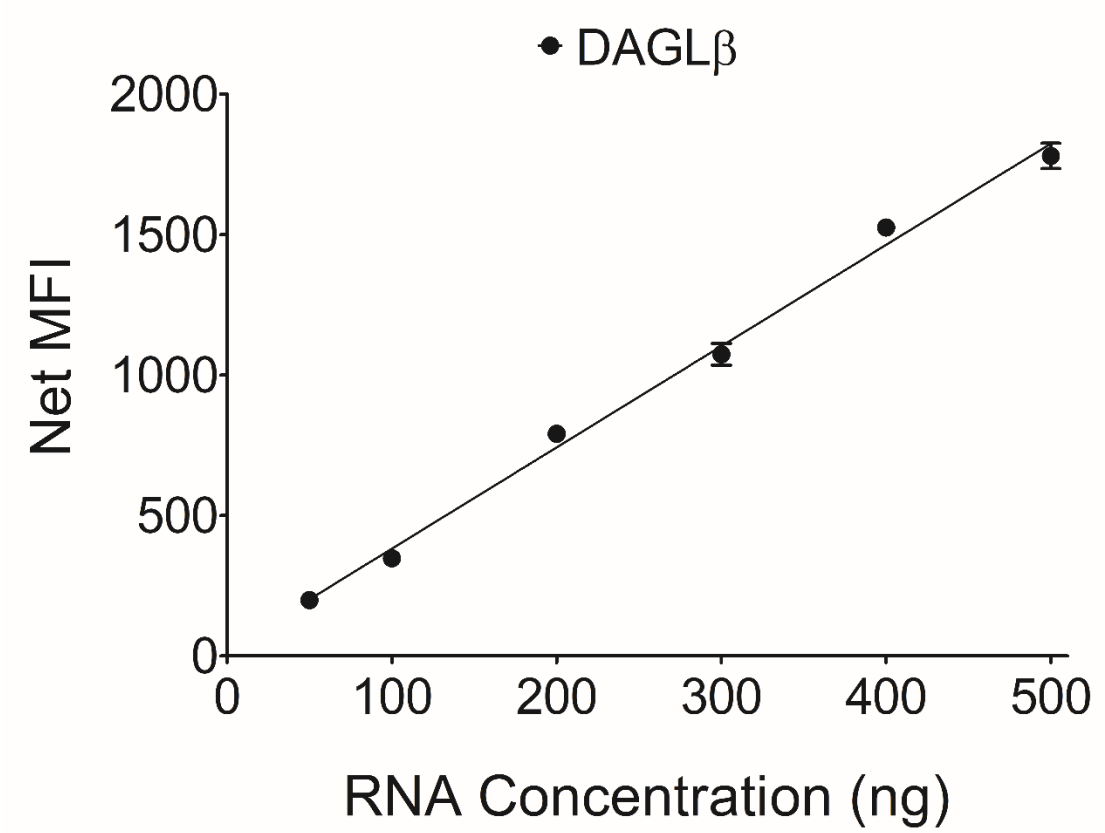

Figure 5.2.3. RNA concentration-intensity relationship of serial dilutions of CB1-Tango cell RNA

CB1-Tango cells were grown until 90% confluent in T-75 flasks and RNA was extracted according to manufacturer's instructions. The RNA was serially diluted to 50, 100, 200, 300, 400 and 500ng in 20μl. Nuclease free water was added in control wells instead of RNA samples. The RNA was then incubated with the probe sets designed to genes in the eCB signalling pathway and magnetic beads for at least 18 hours at 54°C shaking at 600rpm. The next day, the beads were washed and amplifying mixtures were added according to manufacturer's instructions. The beads were read on the Magpix multiplex system (Luminex) and the Net MFI was calculated by removing background readings from the sample readings. Graph shows a single representative assay of DAGLβ, points represent means and bars represent SEMs of 5 technical replicates.

Figure 5.2.4. Comparison of signal amplification between 500ng RNA to 7500ng RNA

CB1-Tango cells were grown until 90% confluent in T-75 flasks and RNA was extracted according to manufacturer's instructions. In order to amplify the signal, RNA was diluted to 7500ng in 20μl (concentration of 375ng/μl) and to 500ng in 20μl (concentration of 25ng/μl). Nuclease free water was added in control wells instead of RNA samples. The RNA was then incubated with the probe sets designed to genes in the eCB signalling pathway and magnetic beads for at least 18 hours at 54^{o}C shaking at 600rpm. The next day, the beads were washed and amplifying mixtures were added according to manufacturer's instructions. The beads were read on the Magpix multiplex system (Luminex) and the Net MFI was calculated by removing background readings from the sample readings. Graph shows plots of means of 5 replicates of 7500ng against 500ng RNA of (A) all eCB components, (B) expanded view of box in A, from a single representative assay.

(A)

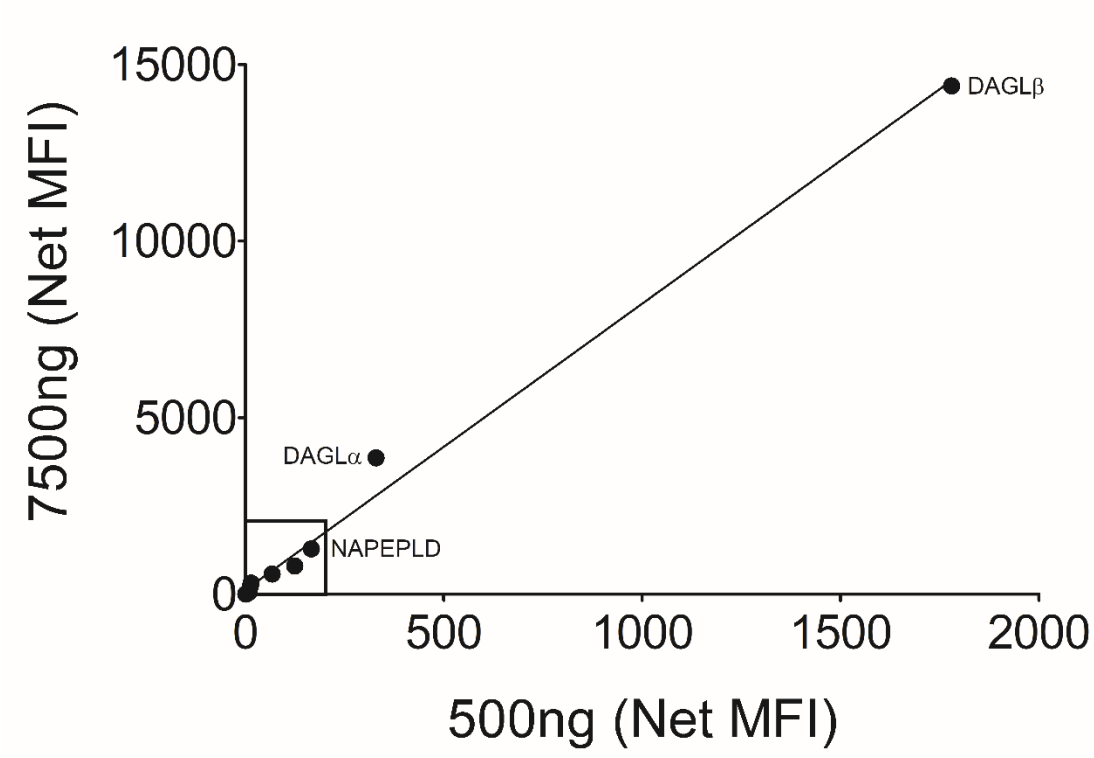
15000
10000
5000
0
7500ng (Net MFI)
DAGLβ
DAGLα
NAPEPLD
0
500
1000
1500
2000
500ng (Net MFI)

(B)

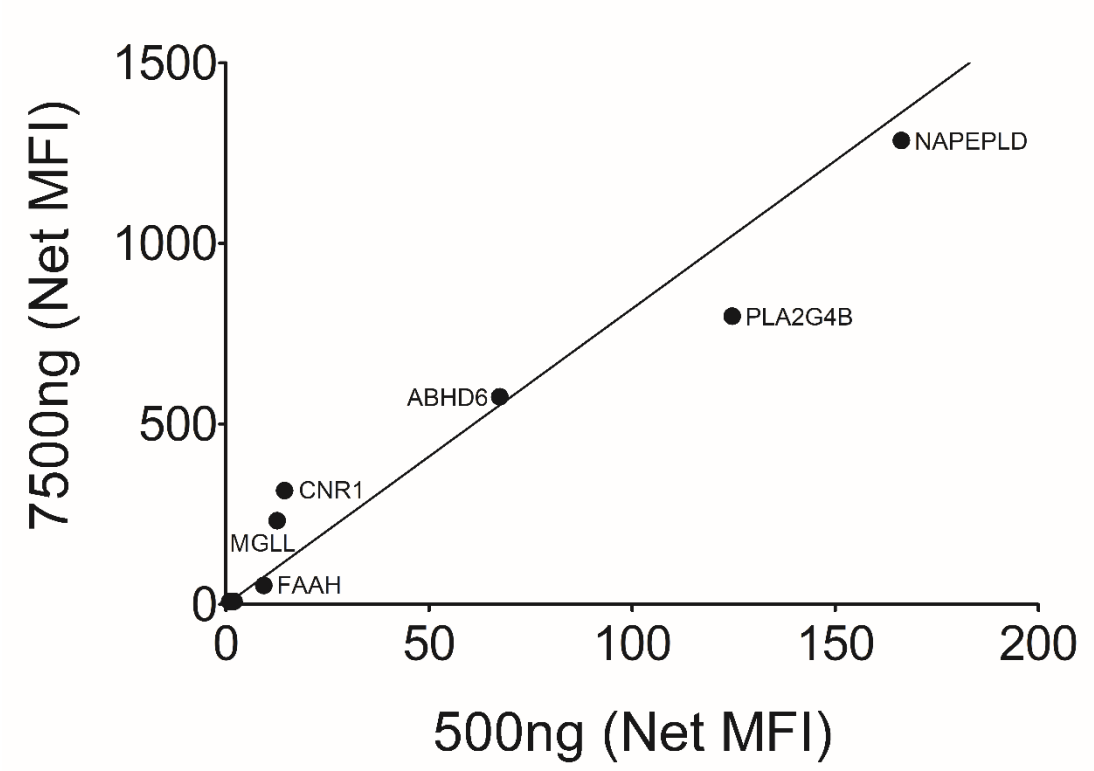
1500
1000
500
0
7500ng (Net MFI)
NAPEPLD
PLA2G4B
ABHD6
CNR1
MGLL
FAAH
0
50
100
150
200
500ng (Net MFI)

Relative expression of eCB components in the CB1-Tango cells

Net MFIs obtained for each gene at 7500ng are plotted according to relative expression levels in Figure 5.2.5. The highest net MFI was again from DAGLβ transcripts, giving a net MFI at 14388.8 ± 456.4, which lies within the upper range of the dynamic detectable range, whilst the two lowest gene transcripts gave the measurements at just under 10 net MFI. The DAGL transcripts are both very highly expressed in CB1-Tango cells, DAGLβ transcripts were around 4x higher than DAGLα transcripts, and ~10x higher than NAPEPLD transcripts. These results are generally in keeping with the previous qPCR results from CB1-Tango cells carried out by other members of our lab, where endogenous DAGLβ transcripts were more highly detected than DAGLα transcripts (thesis of Rachel Lane Markwick, 2015).

The assay detected the transcripts for the major eCB degrading enzymes present in the cells, ABHD6 and MGLL. The ABHD6 transcript signal was around 2.5x higher than MGLL in the CB1-Tango cells. Low levels of FAAH transcripts were also detected and this can be viewed as perhaps supporting a low level of protein expression, as suggested by previous western blot analysis. As well as this, both MAGL and FAAH inhibitors are needed to reveal a low eCB tone in the cell line (thesis of Rachel Lane Markwick, 2015), indicating the expression of both enzymes in the cell line and some degree of crossover.

CNR1 transcripts are also detected but it is unsure what proportion of the signal is from the cells' own endogenous expression of the native CB1 or from the chimeric human CB1 from the assay system. It has been previously published in a few independent microarray studies that there is hardly any detectable native CNR1 transcripts found in U2OS cells (Kim et al., 2007; Sadikovic et al., 2008; Abbas et al., 2010). It is therefore likely that the detected CNR1 signal is reflective of the chimeric CB1 receptor only, however there still is relatively low CNR1 transcript levels in the CB1-Tango cells despite the gene being expressed under a strong cytomegalovirus promoter (Barrow et al., 2006). This might be due to the probe design targeting partially to the 3'-UTR of the CNR1 gene which would not be present in the pTangoCNR1 plasmid that the CB1-Tango cells are expressing, thus reducing some of the signal obtained. CNR2 transcripts are scarcely detectable in the assay when 15x concentrated RNA was used giving a net MFI reading of 8.1 ± 1.3. Nonetheless, the results do show that a relatively low level of transcript for the CB1 receptor is still sufficient for the cells to express functionally important levels of receptor as the cells are highly responsive to all of the exogenous CB1 agonists.

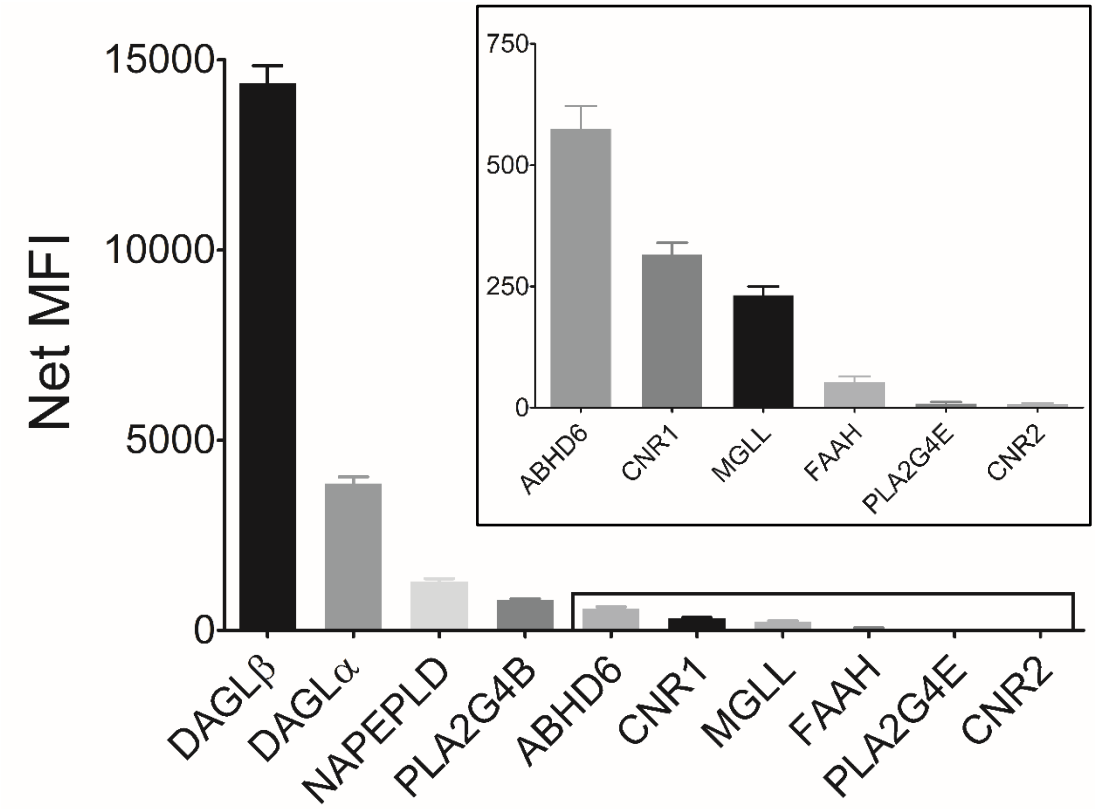

Figure 5.2.5. Detection of key eCB signalling components in CB1-Tango cells using Magpix beads assay

CB1-Tango cells were grown until 90% confluent in T-75 flasks and RNA was extracted according to manufacturer's instructions. In order to amplify the signal, RNA was diluted to 7500ng in 20μl (concentration of 375ng/μl). Nuclease free water was added in control wells instead of RNA samples. The RNA was then incubated with the probe sets designed to genes in the eCB signalling pathway and magnetic beads for at least 18 hours at 54°C shaking at 600rpm. The next day, the beads were washed and amplifying mixtures were added according to manufacturer's instructions. The beads were read on the Magpix multiplex system (Luminex) and the Net MFI was calculated by removing background readings from the sample readings. Graph shows means and bars represent SEMs of 5 replicates of each eCB component, insert shows expanded view of the 6 lowest detected eCB components indicated in a box, from a single representative assay.

Transcripts for the recently identified CaNAT PLA2G4E are essentially undetectable in the CB1-Tango cells (8.8 ± 3.8 net MFI). This low level of detection is out of the detectable dynamic range, even at very high concentrations of RNA at 7500ng. Interestingly, the transcripts for the structurally related (but functionally uncharacterised) PLA2G4B were readily detected.

These results from the QuantiGene multiplex assay are further supported by "The Human Protein Atlas" (Thul et al., 2017). This is a project focused on profiling the human proteasome using antibody-based imaging and mRNA transcriptomics. Analysis of human tissues and several cell lines have been carried out and are publicly available online (https://www.proteinatlas.org/). In U2OS cells, expression of DAGLβ has been classified as high abundance; DAGLα, NAPEPLD, ABHD6 and MGLL are classified as medium abundance; and PLA2G4B, PLA2G4E, FAAH, CNR1 and CNR2 are classified as low abundance which is generally in agreement with our results.

We can conclude that the CB1-Tango cells in general express high level of transcripts for the synthesis enzymes for eCBs, moderate levels of the degrading enzymes and low levels of CB receptor gene transcripts and this is in keeping with the western blot analysis and qPCR results obtained previously in our lab and of publicly available mRNA data of U2OS cells from microarray and the Human Protein Atlas. However, they do not appear to express PLA2G4E transcripts or CB2 transcripts.

Expression of eCB components in CB1-Tango cells compared to other cell lines and tissues

Whilst we are able to detect RNA transcripts of key eCB genes from our CB1-Tango cells, we were unsure whether this was at physiologically relevant signalling levels. The U2OS host cell line (CB1-Tango cell background) is a cancer cell line and thus many genes may be up or downregulated abnormally to ensure survival of the cells. On top of this, the cells are overexpressing many non-native constructs and proteins for the Tango system – particularly of CB1, therefore it was prudent to evaluate the relative levels of transcripts of the eCB components with other human immortalised cell lines and human total RNA from relevant tissues.

Total RNA from 3 human cancer cell lines in addition to CB1-Tango cells were extracted, and total RNA from cerebellum, hippocampus and skin from human donors was purchased. Due

to the limited resource of human RNA from cerebellum and hippocampus, the RNA from all samples were used at 500ng in the assay. The RNA samples were incubated along with the magnetic beads and probe sets and the assay was carried out as described in Methods. The net MFI was calculated and then normalised to the GEO mean of the two housekeeping genes: HLCS and FOXJ2. The relative expression of the eCB genes to the housekeeping genes are graphed and the results are shown in Figure 5.2.6.

The CNR1 transcript is expressed very highly in the cerebellum and hippocampus, as expected where it plays an important role in many synaptic functions (Kawamura et al., 2006). CNR1 transcript expression is not reliably detected in the tested cancer cell lines (net MFI readings of <5) and is detected in the CB1-Tango cells (see above). Similarly, across all tested samples, CNR2 transcripts were not reliably detected (net MFI readings of <3).

The DAGLα transcript levels in our CB1-Tango cells are comparable to the levels found in the cerebellum and hippocampus where it is established as the major enzyme regulating eCB synthesis that functions in retrograde synaptic transmission (Tanimura et al., 2010). Out of all 4 tested cancer cell lines, CB1-Tango cells express the highest amount of DAGLα transcripts. These results clearly point to DAGLα being functional in the CB1-Tango cells. Remarkably, the DAGLβ transcript is expressed at considerably higher levels (4-8 fold) in Tango cells than the other cell lines and tissues, clearly pointing to an important function for this enzyme in these cells. NAPEPLD transcript levels are relatively similar in the CB1-Tango cells to other cancer cell lines, but the transcript is clearly more highly expressed in cerebellum and hippocampus, again where the eCB system is predominantly active in retrograde signalling in synapses (Egertova et al., 2008). These results would support all three enzymes being functional and potentially contributing to eCB signalling in Tango cells.

Remarkably, PLA2G4E transcripts were not detected in any of the cancer cell lines (including the Tango cells – see above), but was found at relatively high levels in the skin. This observation clearly raises question as to whether this enzyme can be considered as the key CaNAT that generally regulates AEA synthesis. Interestingly, the structurally related PLA2G4B had robust expression of transcripts in most of the cell lines (the exception being MCF7 cells) and in all three tissues, with transcript levels in the skin again being relatively high. Thus if this enzyme also has CaNAT activity it might be better placed than PLA2G4E to play a general role in AEA synthesis.

Finally, the levels of MGLL and ABHD6 transcripts in the Tango cells were as high (or higher) than those seen in the other cancer cell lines and only 2-3 times lower than levels seen in the cerebellum and/or hippocampus. The highest levels were seen in the hippocampus, the tissue that also had the highest levels of DAGLα and NAPEPLD transcripts. Interestingly, although clearly detectable in Tango cells (see above), FAAH transcript levels were really very low in these cells relative to the levels seen in the MCF7 cell line and the three tissues. These results would be consistent with all three enzymes being involved in eCB turnover in Tango cells, but would perhaps point to MGLL and ABHD6 being more important.

Figure 5.2.6. Comparison of eCB component expression in CB1-Tango cells and other cell lines

RNA was extracted from immortalised cell lines: CB1-Tango, SHSH5Y, MCF7 and H460 lines and eluted in nuclease free water. Total RNA from cerebellum, hippocampus and skin were purchased and all RNA were diluted in nuclease free water to recommended amount of 500ng in 20μl (concentration of 25ng/μl). Nuclease free water was added in control wells instead of RNA samples. The RNA was then incubated with the probe sets designed to genes in the eCB signalling pathway and magnetic beads for at least 18 hours at 54^{o}C shaking at 600rpm. The next day, the beads were washed and amplifying mixtures were added according to manufacturer's instructions. The beads were read on the Magpix multiplex system (Luminex) and the relative expression was calculated by removing background readings from the sample readings and normalising to the GEO means of 2 housekeeping genes. Graph shows means and bars represent SEMs of 5 replicates of each normalised eCB component from each cell line, from a single representative assay.

(A)

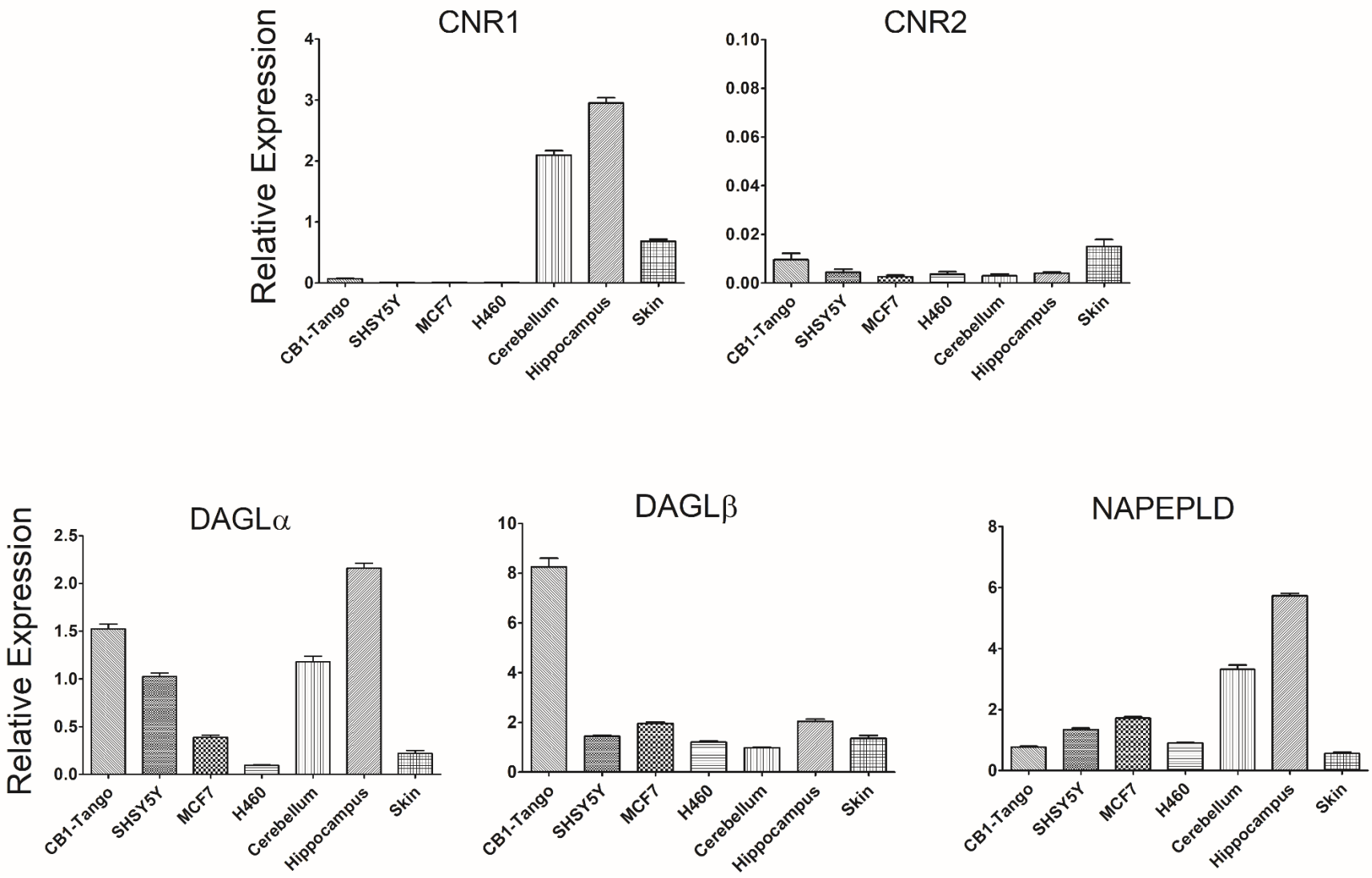
CNR1
Relative Expression
0
1
2
3
4
CB1-Tango
SHSY5Y
MCF7
H460
Cerebellum
Hippocampus
Skin
CNR2
0.00
0.02
0.04
0.06
0.08
0.10
DAGLα
0.0
0.5
1.0
1.5
2.0
2.5
DAGLβ
0
2
4
6
8
10
NAPEPLD
0
2
4
6
8

(B)

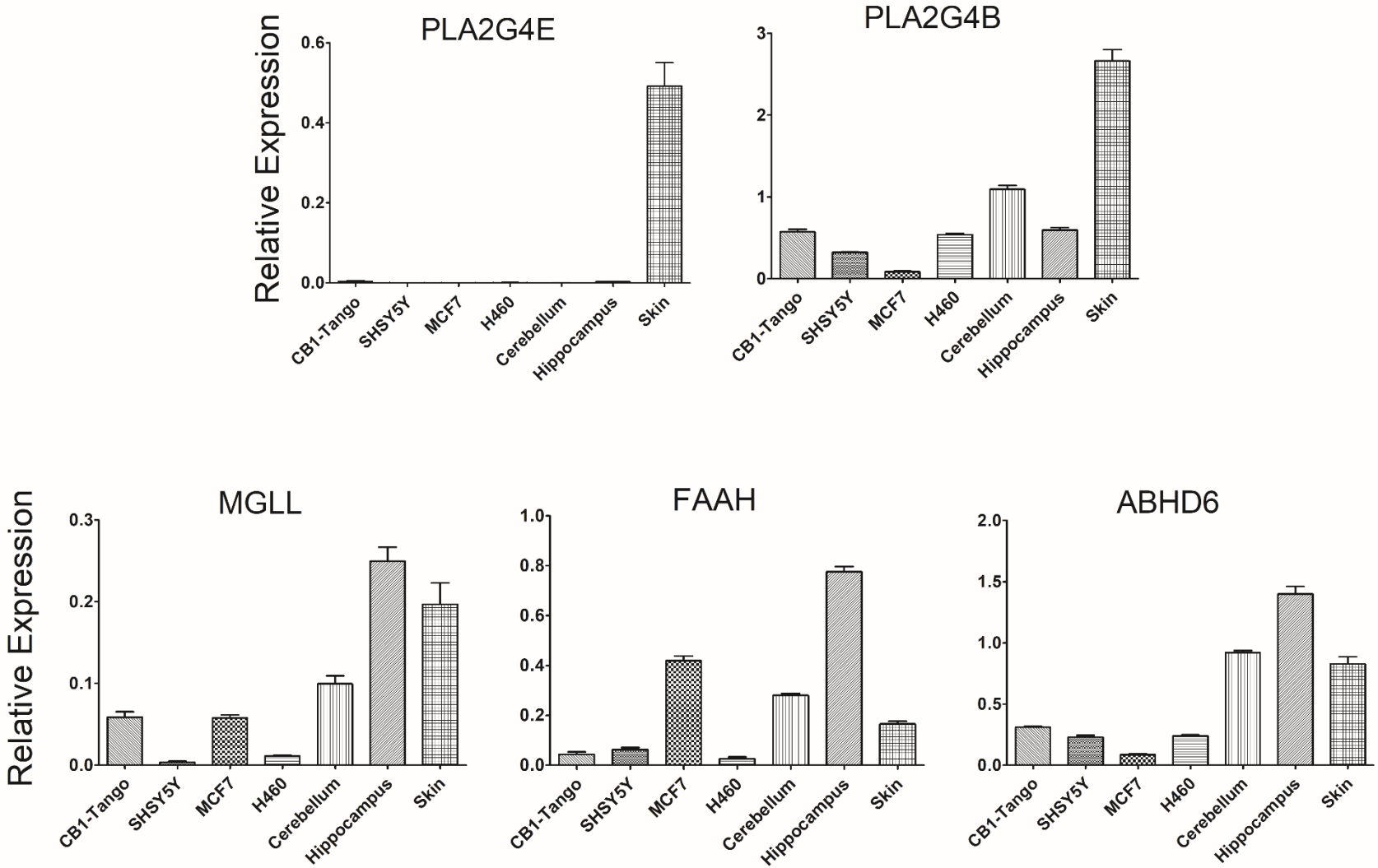
PLA2G4E
Relative Expression
0.6
0.4
0.2
0.0
CB1-Tango
SHSY5Y
MCF7
H460
Cerebellum
Hippocampus
Skin
PLA2G4B
3
2
1
0
CB1-Tango
SHSY5Y
MCF7
H460
Cerebellum
Hippocampus
Skin
MGLL
Relative Expression
0.3
0.2
0.1
0.0
CB1-Tango
SHSY5Y
MCF7
H460
Cerebellum
Hippocampus
Skin
FAAH
1.0
0.8
0.6
0.4
0.2
0.0
CB1-Tango
SHSY5Y
MCF7
H460
Cerebellum
Hippocampus
Skin
ABHD6
2.0
1.5
1.0
0.5
0.0
CB1-Tango
SHSY5Y
MCF7
H460
Cerebellum
Hippocampus
Skin

5.2.3 **Results 3A.** Summary & Conclusions

In order to establish a reporter cell assay system tailored to answering some fundamentally important questions relating to eCB synthesis and signalling, we must first establish if the reporter cells express the enzymes that are necessary for the generation and degradation of the two well established eCBs, namely 2-AG and AEA. Probes were generated to a panel of eCB genes for use in the QuantiGene multiplex assay system for the purposes of profiling the transcriptome of CB1-Tango cells for the expression of eCB related enzyme transcripts, and for further downstream validation profiling of successful genetic KO of candidate enzymes.

The QuantiGene assay system is a relatively simple and effective assay to profile the transcripts of a panel of genes in comparison to microarray which may introduce bias and false positives (Boelens et al., 2007) and is not as costly and time consuming as RNA sequencing (Wang et al., 2009). The customisable design of probes has the advantage of detecting catalytic regions of gene transcripts to reflect functional protein expression more closely, and this also allows the bead assay system to be used as a verification system for genetic deletion of catalytic regions of candidate genes using gene editing technique CRISPR. The results are generally easily scalable, particularly if some gene transcripts are on the threshold of detectability, whilst still retaining a good noise to background ratio. Finally the transcript levels detected corroborate well with already published data from publicly available databases.

The bead assay confirmed previous conclusions reached by members of the lab that the CB1-Tango cells express both DAGLs and MAGL at protein level, and that DAGLβ was expressed more highly than DAGLα from qPCR results. There are low levels of transcripts for CNR1 and CNR2 in comparison to the high level of transcripts for DAGLα, DAGLβ and NAPEPLD. This might suggest that the cells could be generating eCBs for signalling to other cells in an autocrine/paracrine system, or as highlighted before, it could be that the DAGLs and NAPEPLD have secondary roles in these cells. For example, the DAGL/MAGL pathway may also be responsible for the generation/maintenance of AA levels which can affect bone remodelling via the action of prostaglandins generated from AA (Kruger et al., 2010). NAPEPLD is not selective for its substrates (Ueda et al., 2013) and other NAEs produced by NAPEPLD can have a wide range of functions, including anti-inflammatory and anorexic effects (Rahman et al., 2014). Additionally, NAPEPLD$^{-/-}$ mice have also shown reductions in 2-AG and 2-LG levels, suggesting biosynthesis and metabolic crosstalk between lipid species (Leishman et al., 2016), perhaps in the maintenance of the lipid pool.

Generally, the CB1-Tango cells have similar transcript expression of the eCB components to other human cancer cell lines tested, however the most obvious difference is the substantially higher levels of DAGLα and DAGLβ transcripts and comparable levels of NAPEPLD transcripts in the CB1-Tango cells, signifying that the U2OS cells are a good host line for the potential generation of eCBs. In comparison to relevant RNA from brain tissues where eCBs are known to be synthesised and functional in important roles, the CB1-Tango cells have comparable levels (or even higher levels in the case of DAGLβ) transcript levels of the eCB synthesising enzymes which would support all three enzymes potentially contributing to eCB signalling in the CB1-Tango cells.

The recently identified CaNAT PLA2G4E was included in our panel of genes along with PLA2G4B which was also uncharacterised within the PLA2 family. Of the PLA2G4 family, PLA2G4A is the most well characterised as an enzyme involved in hydrolysis membrane phospholipids to release AA for the generation of eicosanoids to link oxidative events to inflammatory responses (Burke and Dennis, 2009; Niknami et al., 2009; Sun et al., 2010). Members of the PLA2G4 family are all cytosolic proteins, display calcium sensitivity (except PLA2G4C), and are likely to have similar function and activity to PLA2G4A which can also be activated by phosphorylation (Ghosh et al., 2006). PLA2G4D and PLA2G4F are also poorly characterised, but expression patterns showed abundancy in skin and reproductive organs but was not detected in RNA sequencing of various brain cells (Zhang et al., 2014).

PLA2G4E was previously thought to be involved in recycling through an clathrin-independent endocytic route (Capestrano et al., 2014) and PLA2G4B does not currently have a defined function but has been linked to neuronal case studies including schizophrenia (Tao et al., 2005) autism (Matsunami et al., 2014) and reading disability (Morris et al., 2004). Interestingly, tissues may also express a readthrough transcript of an upstream jumonji domain containing 7 (JMJD7) gene into the PLA2G4B gene, creating a conjoined JMJD7-PLA2G4B transcript which may have implications in head and neck squamous cell carcinoma survival (Cheng et al., 2017).

The Human Protein Atlas has documented very high expression of PLA2G4E transcripts in skin despite its unidentified function in the skin, which was reflected in our results obtained here. However, PLA2G4E transcripts were surprisingly below threshold in cancer cell lines and in human cerebellum and hippocampal RNA where NAPEPLD is known to be expressed and AEA is synthesised (Di Marzo et al., 1994; Egertova et al., 2008). PLA2G4E was suggested to be in abundance in rat and mouse brain (Hussain et al., 2018) however the lack of

transcripts in human brain RNA raises the possibility that other enzymes responsible for the generation of NAPE may exist. PLA2G4B transcripts were readily detected in the human brain RNA most of the cancer cell lines including the CB1-Tango cells, and have previously been documented to be highly expressed in the cerebellum (Pickard et al., 1999), and from the Human Protein Atlas it is in abundance in skin and GI tract and is rather ubiquitous in the human body (Uhlen et al., 2015).

The eCB degrading enzymes transcripts are also detected at moderate levels in the CB1-Tango cells but are expressed much more highly in RNA extracted from cerebellum and hippocampus where eCB signalling activity is high and degradation of eCBs is a way of regulating retrograde signalling activity (Marrs et al., 2010; Savinainen et al., 2012; Tanimura et al., 2012), which might not be necessarily relevant in autocrine/paracrine signalling conditions. The eCB degrading enzymes are indeed functional in the CB1-Tango cells as pharmacological blockade of them with JZL195 results in an increased eCB tone that activates the CB1 receptor. The CB1-Tango cells therefore are a good cell line to study the regulation of eCB signalling in the context of autocrine/paracrine eCB signalling that is involved in important developmental and maintenance processes in the body.

5.3 **Results 3B**. Can we establish eCB assays?

5.3.1 **Results 3B.** Introduction

In the previous section it has been established that the CB1-Tango cells express the necessary machinery for the generation and degradation of the two major eCBs 2-AG and AEA. Expression levels of the synthesis enzymes DAGLs and NAPEPLD as well as the eCB hydrolysing enzymes are present at comparable levels to RNA extracted from areas of the brain where eCB signalling is predominant. Interestingly, the CB1-Tango cells actually express elevated levels of the DAGLs when compared to other possible host cell lines, which is favourable for evoking eCB signalling in the CB1-Tango cells.

The CB1-Tango assay had been used in previous chapters to study exogenously applied CB1 ligands, but seeing as they express the components for eCB signalling, it should be feasible to adapt the assay to study eCB signalling by stimulating the generation of eCBs with different assay conditions and stimuli. Currently, the methods used to monitor eCB signalling rely on electrophysiological responses such as DSI/DSE experiments or quantification of eCB levels following cell stimulation. Quantification of eCBs using mass spectrometry relies on an expensive laboratory set up and specialised equipment which tends to be low throughput (Balgoma et al., 2013). As well as this, it is unclear if the measurement of the eCBs from mass spectrometry studies reflect the presence of a signalling pool of eCB or a general metabolic pool which may contribute to a physiological eCB tone under resting conditions (Howlett et al., 2011); this is particularly relevant of AEA which has been suggested to be present in intracellular stores prior to signalling (Maccarrone et al., 2010). Our aim was therefore to adapt the CB1-Tango assay to more easily detect eCB-dependent CB1 activation which would furnish us with a simple cellular assay amenable from moderate to high throughput studies.

The use of MAGL, FAAH and ABHD6 inhibitor JZL195 in the CB1-Tango assay highlighted the presence of at least a modest eCB tone, which is constitutively generated but not signalling at the CB1 receptor under normal conditions due to the gate keeping activity of the eCB hydrolysing enzymes. Importantly, the modest tone revealed by JZL195 is seen under conditions where there is no obvious eCB drive. The primary enzymes which can degrade 2-AG and/or AEA are MAGL (Dinh et al., 2002; Makara et al., 2005) and FAAH (Giang and Cravatt, 1997; Cravatt et al., 2001) but these enzymes may have a degree of crossover between substrates and can also hydrolyse other possible monoacylglycerols and N-

acylethanolamines (Cravatt et al., 1996; Long et al., 2009a). ABHD6 and ABHD12 can also hydrolyse 2-AG but are responsible for only around 15% of 2-AG hydrolysis and ABHD12 is not currently recognised as a *bona fide* eCB component (Blankman et al., 2007; Savinainen et al., 2012). JZL195 has been shown to block MAGL, FAAH and ABHD6 but the study did not mention ABHD12 (Long et al., 2009a), nonetheless JZL195 can reveal a significant eCB tone by inhibiting eCB degradation; however it would be difficult to draw any conclusion as to the nature of the responsible eCBs.

Several stimuli can evoke eCB signalling in neuronal cells, including elevated calcium levels (Di Marzo et al., 1994; Stella et al., 1997), activation of post synaptic GPCRs (Jung et al., 2007) and activation of PKA and PKC (Rosenberger et al., 2007; Vellani et al., 2008). Calcium elevation in neurons has long been shown to stimulate the release of the established eCBs 2-AG and AEA (Di Marzo et al., 1994; Stella et al., 1997). In mouse neuroblastoma (N18TG2) cells, 2-AG was released into cell culture media following addition of the calcium ionophore ionomycin in a concentration dependent manner which is sensitive to the presence of EDTA (Bisogno et al., 1997). In the context of retrograde signalling, activation of post-synaptic glutamate receptors leads to increases in intracellular calcium and causes 2-AG synthesis via the activity of DAGLα (reviewed in Kano, 2014).

However, how elevated calcium levels can lead to 2-AG synthesis via DAGL remains unclear as the DAGLs do not show direct calcium sensitivity (Farooqui et al., 1984; Moriyama et al., 1999). The current consensus is there are additional steps subsequent to an increase in calcium that are required for full eCB mobilisation. (Reisenberg et al., 2012; Kano, 2014; Ohno-Shosaku and Kano, 2014). It has been hypothesised that the activation of kinases may lead to the phosphorylation of DAGLs causing its activation and stimulating 2-AG synthesis (Reisenberg et al., 2012). Indeed, it has been reported that activation of PKA and PKC leads to the synthesis of 2-AG (Rosenberger et al., 2007; Vellani et al., 2008) and both PKA and PKC can be activated by an elevation in calcium (Steinberg, 2008; Dunn et al., 2009).

The generation of AEA can also be stimulated by calcium and PKA and PKC. AEA is formed and released from cultured brain neurones in a calcium-dependent manner using ionomycin (Di Marzo et al., 1994) and the presence of extracellular calcium is necessary to generate AEA as release of intracellular calcium alone does not promote AEA synthesis (Placzek et al., 2008). However, this is complicated by the fact that calcium has many direct as well as indirect effects in cells that include the release of other monoacylglycerols (Kondo et al., 1998) or other potential eCBs such as 2-LG (Ben-Shabat et al., 1998), virodhamine (Porter et

al., 2002), noladin ether (Hanus et al., 2001; Fezza et al., 2002) and others, although the full details on the synthesis of these lipids have yet to be elucidated. Therefore, it is likely that other levels of regulation exist to activate AEA synthesis.

Activation of PKA and PKC in HEK-293 cells DRG neurones can also increase the levels of AEA which is unaffected by the presence of a calcium chelator, suggesting the presence of a calcium-insensitive synthesis pathway of AEA (van der Stelt and Di Marzo, 2005a; Vellani et al., 2008). The activity of CaNAT can be potentiated by PKA activation, leading to the increased synthesis of AEA, however CaNAT requires calcium for its activity and is not reported to be directly sensitive to PKA phosphorylation in the absence of calcium (Cadas et al., 1997). Thus, the target of PKA and PKC phosphorylation in the calcium-insensitive generation of AEA is currently unknown.

As the CB1-Tango cells are a non-neuronal cell line, it is not clear how the synthesis of eCBs are stimulated and regulated, and whether the same type of stimulation that neuronal cells experience could also elicit eCB signalling in the CB1-Tango cells. As the U2OS cells are of a bone origin (Ponten and Saksela, 1967), it is likely that the high levels of calcium in cancellous bone matrix may have a role in the generation of eCBs. Indeed, 2-AG and AEA are both found in levels comparable to brain levels in cancellous bone tissue and are involved in bone maintenance (Bab et al., 2008; Tam et al., 2008; Maccarrone et al., 2015). The rapid generation of eCB signalling in synapses and the slower long-term generation of eCB in peripheral systems like in cancellous bone differs through environmental conditions as a way of regulating of eCB synthesis. We adapted the CB1-Tango assay to report on both rapid increases in calcium induced by ionomycin akin to neuronal signalling and through passive elevated extracellular calcium found in bone matrix to determine if eCB signalling can be stimulated in one cell line using different conditions.

In this chapter I report on the use of three distinct stimuli to elicit a robust eCB response from the CB1-Tango cells. To establish which eCB pathway is dominant in the production of the eCB response, we utilised pharmacological tools to establish whether eCB signalling in the cells is likely to be DAGL dependent or due to the production of AEA or other possible eCBs. As there are currently no pharmacological tools to target AEA synthesis, it is not possible to pharmacologically isolate AEA synthesis from the overall eCB tone. Therefore, genetic intervention is considered to complement the pharmacological approach to test the involvement of candidate enzymes in the step that leads to eCB signalling in the cells.

5.3.2 **Results 3B.** Results

The CB1-Tango assay is functional in a more physiological medium

It has been highlighted that the cells' own endogenous eCB production is active in the CB1-Tango cells, but the assay requires the cells to be starved for 24 hours in the presence of serum free and calcium free Freestyle media, thus the background activity of eCB production is muted to reduce background noise. The assay was originally developed for the purposes of drug discovery of agonists and antagonists to the CB1 receptor so would not necessarily contain any factors needed for the synthesis of eCBs in the cells. The manufacturers do not fully disclose the contents of the media except confirming that it is calcium and serum free.

Therefore, to fully assess whether we can stimulate robust eCB signalling in these CB1-Tango cells, preliminary tests in the lab determined that the cells were healthy and viable over a 48 hour period when cultured in 0.5% FBS in McCoy's assay media. This media was selected as its full contents are known and we found a good signal to noise ratio in the standard reporter cell assay. This media is modified to a reduced serum content of 0.5% from 10% to reduce metabolic processes in the cells and without antibiotics to reduce stress on the cells. As McCoy's media contains around 1mM calcium, it allows for paradigms where the eCB system might be activated by the influx of extracellular calcium into the cells.

To test that the CB1-Tango assay system is functional in the McCoy's assay media, an ACEA concentration response curve in the presence of AM251 was carried out similarly to previous experiments. CB1-Tango cells were plated in 100μl of McCoy's assay media for 24 hours. A range of ACEA concentrations were added to the cells in the presence and absence of AM251 for 4 hours before beta-lactamase substrate was added for 90 minutes and read on the Flexstation. A representative experiment is graphed in Figure 5.3.1. ACEA elicited a CB1 dependent response at all tested concentrations (0.008 – 5μM), with statistically significant levels detected at the low concentration of 0.008μM. At 5μM, the response reached 265.3% ± 5.4% of control levels, which is of a similar magnitude to the maximal CB1 activation levels detected in Freestyle media (259.2% ± 2.5% of control). Despite not reaching a plateau at 5μM ACEA in our representative assay, it was used at that concentration for the remaining experiments as a positive control. AM251 on its own in this representative experiment was not statistically significantly different to the control in the absence of AM251 ($p>0.05$), indicating little if any basal eCB tone in McCoy's assay medium despite the presence of 0.5% serum. The ACEA responses were all antagonised by AM251 to basal levels. Thus, we can

conclude that the assay can be performed in modified tissue culture media, and that the cells remain highly sensitive to ACEA.

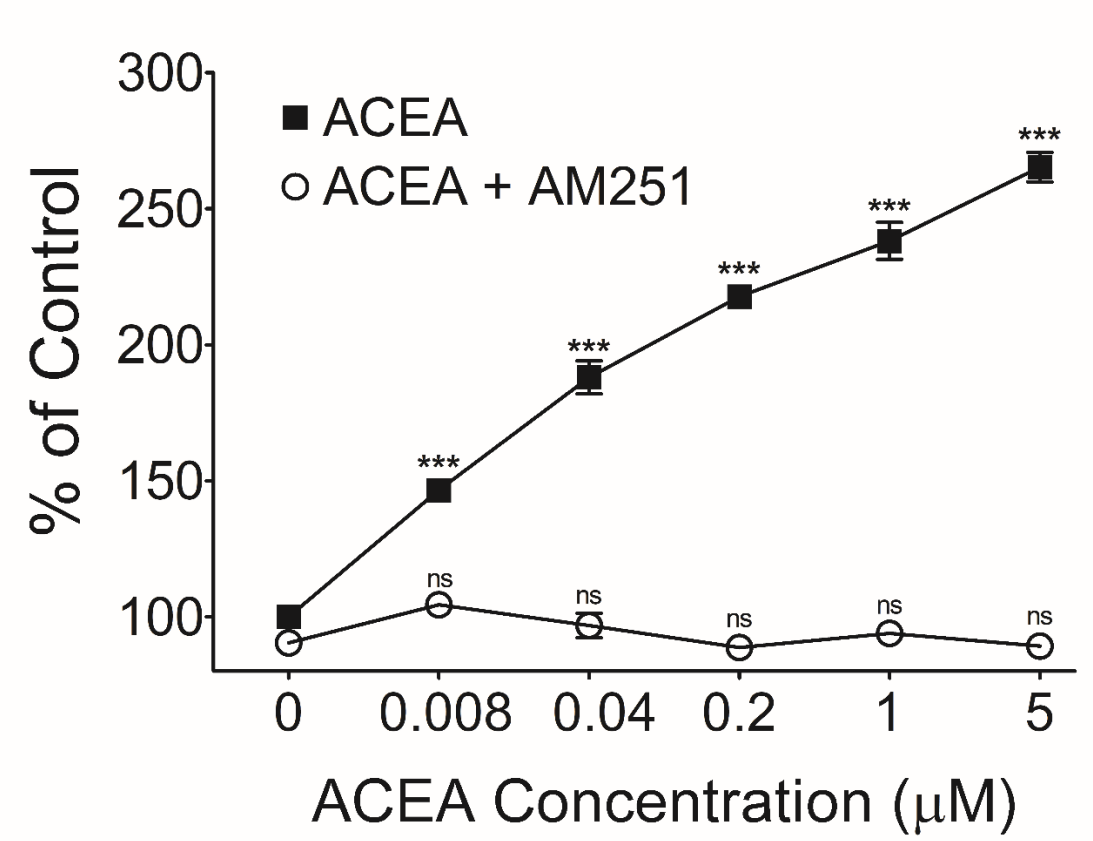

Figure 5.3.1. Tango assay responses to ACEA and AM251 are similar in McCoy's media supplemented with 0.5% FBS

CB1-Tango cells were seeded 30,000 cells per well in McCoy's media supplemented with 0.5% FBS for 24 hours in clear bottom black plates. CB1 response was established by adding ACEA (5μM top concentration, 1:5 serial dilutions) in the absence and presence of AM251 used in molar excess (10μM). Drug compounds were left for 4 hours before green and blue fluorescence detection of β-lactamase reporter gene was measured using a FRET-enabled substrate. Fluorescence ratios between green and blue channels were calculated and values were normalised to control well conditions (defined as 100) as % of control. Graph shows means and bars represent SEMs of 8 replicates from a single representative assay. Statistical significance of ACEA responses and ACEA responses in the presence of AM251 compared to the control in the absence of ACEA were established with One Way ANOVA.

ns $p>0.05$; ***$p<0.001$; One Way ANOVA, Dunnett's post-test.

Detection of eCB tone with JZL195 in Freestyle and 0.5% FBS McCoy's assay medium

The McCoy's assay medium is a more physiological medium for the CB1-Tango assay and the effects of ACEA and AM251 similarly elicit CB1 responses as in Freestyle media. There is no significant eCB tone in this assay media as treatment with AM251 has no significant effect on its own (Figure 5.3.1). This is comparable to Freestyle media where responses in cells to the presence of AM251 are not statistically different to control responses across several experiments (Figure 5.3.2). Likewise, in McCoy's assay media, there was no statistically significant difference between control and AM251 treated cells across experiments as shown in Figure 5.3.2, suggesting no significant eCB tone in both media.

The addition of JZL195 in previous experiments in Freestyle media revealed the presence of an eCB tone. When pooled across experiments, AM251 reduces the response in Freestyle media to around 15% below control levels in the presence of JZL195 (86.3% ± 2.40% of control, Figure 5.3.3). This eCB tone is also revealed in McCoy's media, in the presence of JZL195 a significant eCB tone is revealed by AM251 across independent experiments (Figure 5.3.3). The eCB tone in McCoy's media is of a similar magnitude to that in Freestyle media (81.8% ± 2.03% of control), signifying the cells in 0.5% FBS McCoy's media are capable of generating similarly low levels of eCBs in comparison to Freestyle media conditions, but JZL195 is required to reveal this basal eCB tone.

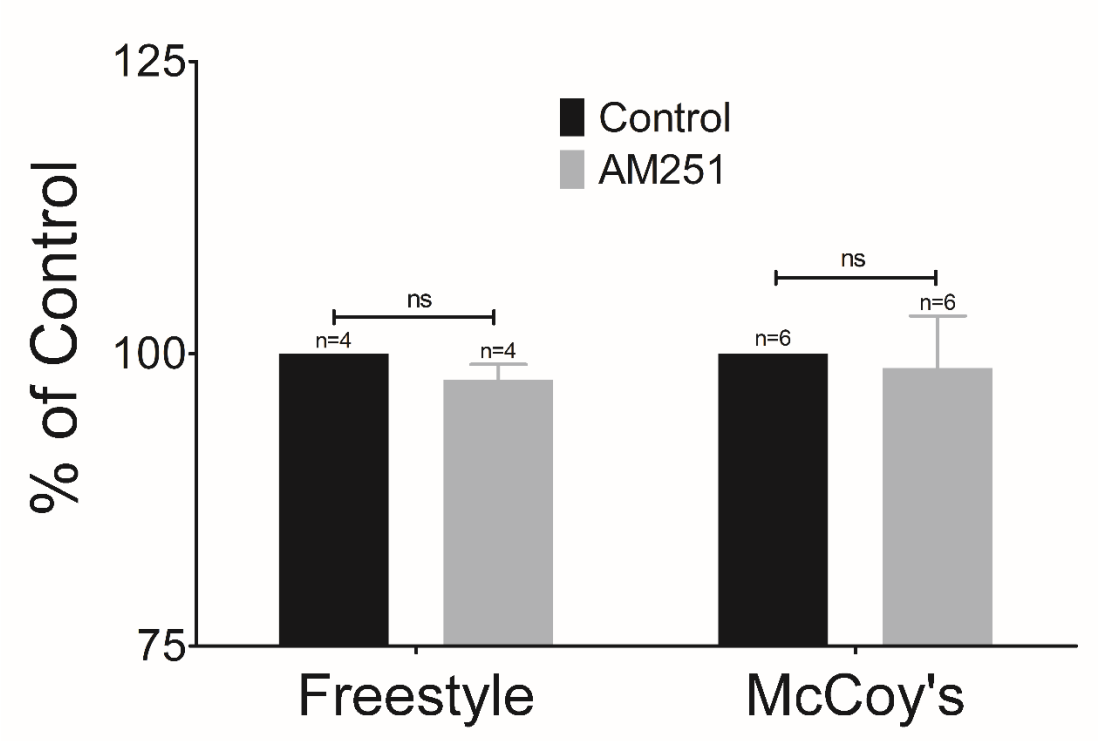

Figure 5.3.2. CB1-Tango cells lack basal eCB tone in Freestyle and McCoy's media in control conditions

30,000 CB1-Tango cells were plated in Freestyle media or McCoy's medium supplemented with 0.5% FBS and maintained for 24 hours. Half the cells were treated for a total of 4 hours with AM251 (10μM) diluted in the same medium. CB1 activation was then measured by the β-lactamase assay, as described previously and the fluorescence ratio between green and blue channels was calculated. Data was normalised to the control wells without the presence of any drugs (set to 100) as % of control. The graph presented shows means and bars represent SEMs of pooled independent experiments (number of experiments indicated on the graph) with 8 replicates in each experiment. Significance between control and AM251 was calculated using Student's T-test.

ns $p>0.05$; Paired Student's T-test, two-tailed.

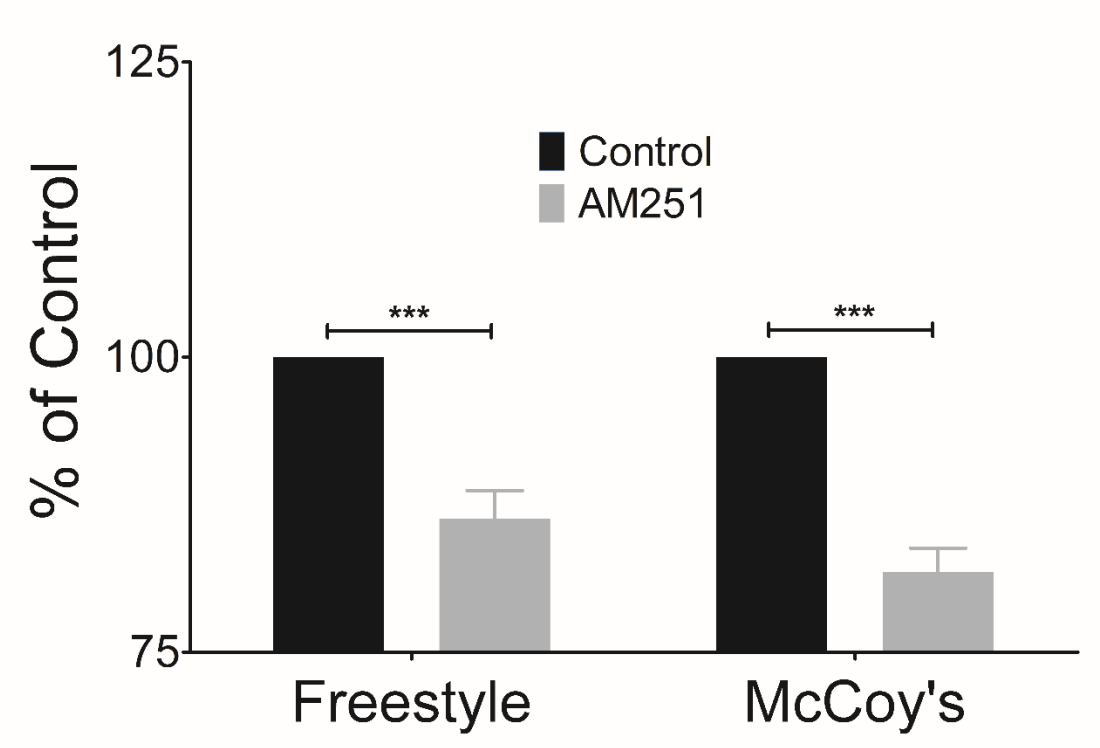

Figure 5.3.3. Basal eCB tone in McCoy's and Freestyle media is revealed in the presence of JZL195

30,000 CB1-Tango cells were plated in Freestyle media or McCoy's medium supplemented with 0.5% FBS and maintained for 24 hours. Cells were treated for a total of 4 hours in the presence or absence of AM251 (FAC 10μM) with 100nM JZL195 present in all wells. CB1 activation was then measured by the β-lactamase assay, as described previously. Data was normalised to control wells with JZL195 present (set to 100) as % of control. The graph presented represents the mean and bars represent the SEMs of 8 pooled independent experiments, 8 replicates in each individual experiment. Significance between groups was calculated using Student's T-test, as indicated below.

***p<0.001; Paired Student's T-test, two-tailed.

Calcium ionophore ionomycin elicits an eCB response that is partially DAGL dependent

Calcium has been documented to be able to stimulate release of both 2-AG and AEA, and calcium ionophore ionomycin has been used previously to elicit the synthesis of these eCBs (Di Marzo et al., 1994; Bisogno et al., 1997). The presence of calcium in McCoy's assay media allows us to be able to increase the concentration of intracellular calcium with ionomycin, similarly to physiological conditions i.e. in neuronal cells. We therefore tested the CB1-Tango cells in McCoy's media with ionomycin, to see if we could elicit an eCB-dependent CB1 response.

The CB1-Tango cells were plated in McCoy's assay medium and treated with a range of concentrations of ionomycin (FAC 0.5 – 4μM) in the presence or absence of AM251 for 4 hours as described in methods. A clear concentration-dependent increase in CB1 response was measured at all concentrations, reaching statistically significance at 2μM ionomycin. The responses are largely blocked by 10μM AM251 at an ionomycin concentration of up to 2μM. However, at the highest concentrations of ionomycin (4μM), AM251 does not fully antagonise the response to baseline levels and there is still a significant response detected, perhaps indicating a non-specific component within the response (Figure 5.3.4).

When pooled from a number of independent experiments, the CB1 response obtained at 4μM ionomycin (242.7% ± 14.0% of control) is comparable to the maximal ACEA response in these cells (254.7% ± 12.0% of control) (Figure 5.3.5), indicating that ionomycin can elicit robust CB1 activation via eCB signalling. AM251 substantially (~75%) but not completely blocked the ionomycin response at 4μM (135.0% ± 6.5% of control), this is likely due to a non-specific component at the high concentration of ionomycin as it is not mediated through CB1 activation. Thus, for further experiments, to mitigate against the presence of the non-specific component, ionomycin was generally used at 2μM which gives a clearer window of eCB signalling.

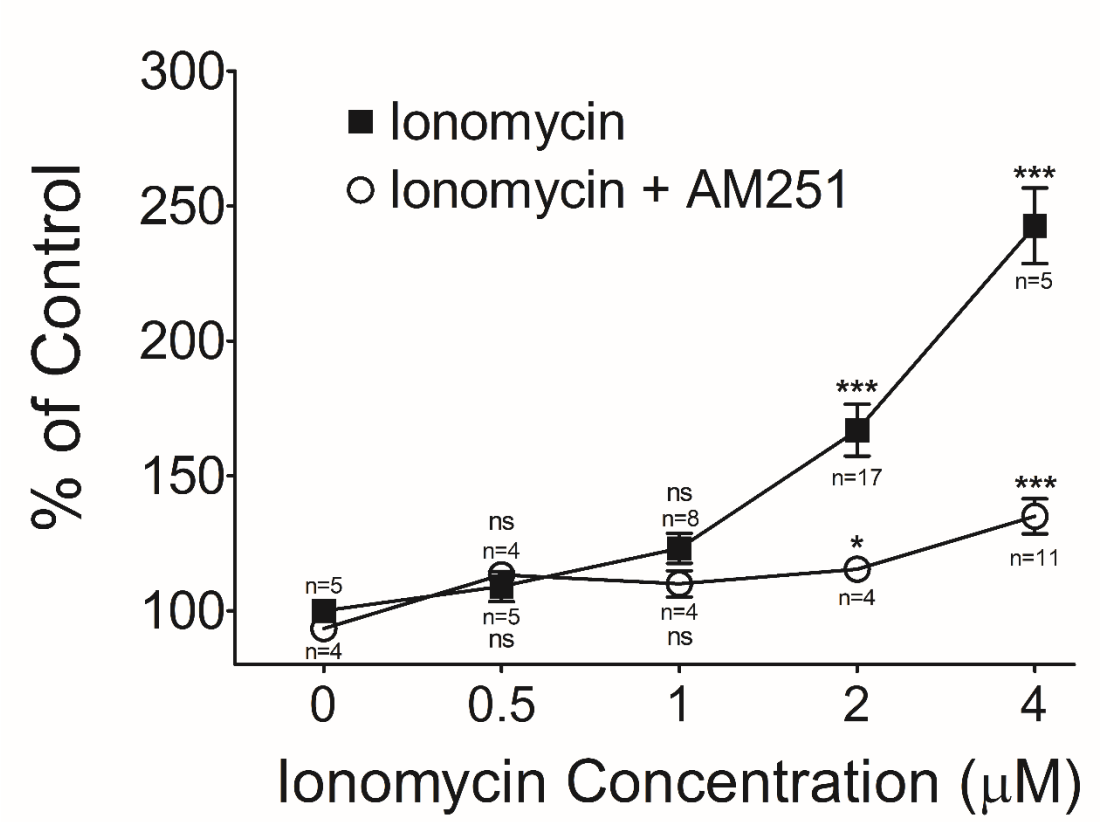

Figure 5.3.4. Ionomycin treatment activates CB1 on CB1-Tango cells

30,000 CB1-Tango cells were plated in clear bottom black plates and maintained in 0.5% FBS McCoy's medium for 24 hours. Ionomycin was diluted in the same medium (FAC 4μM top concentration, diluted 1:2) and cells were treated with the indicated concentrations of ionomycin in the presence or absence of AM251 (FAC 10μM) for 4 hours. CB1 activation was then measured by the β-lactamase assay as described in the methods. Results were normalised to the control wells (set to 100) as % of control. Graph shows means and bars represent SEMs of pooled independent experiments (n indicated on graph) with 8 replicates in each individual experiment. Statistical significance of ionomycin responses in the absence of AM251 compared to its control, and ionomycin responses in the presence of AM251 compared to AM251 only control were established with One Way ANOVA, as indicated below.

ns $p>0.05$; * $p<0.05$; *** $p<0.001$; One Way ANOVA, Dunnett's post-test.

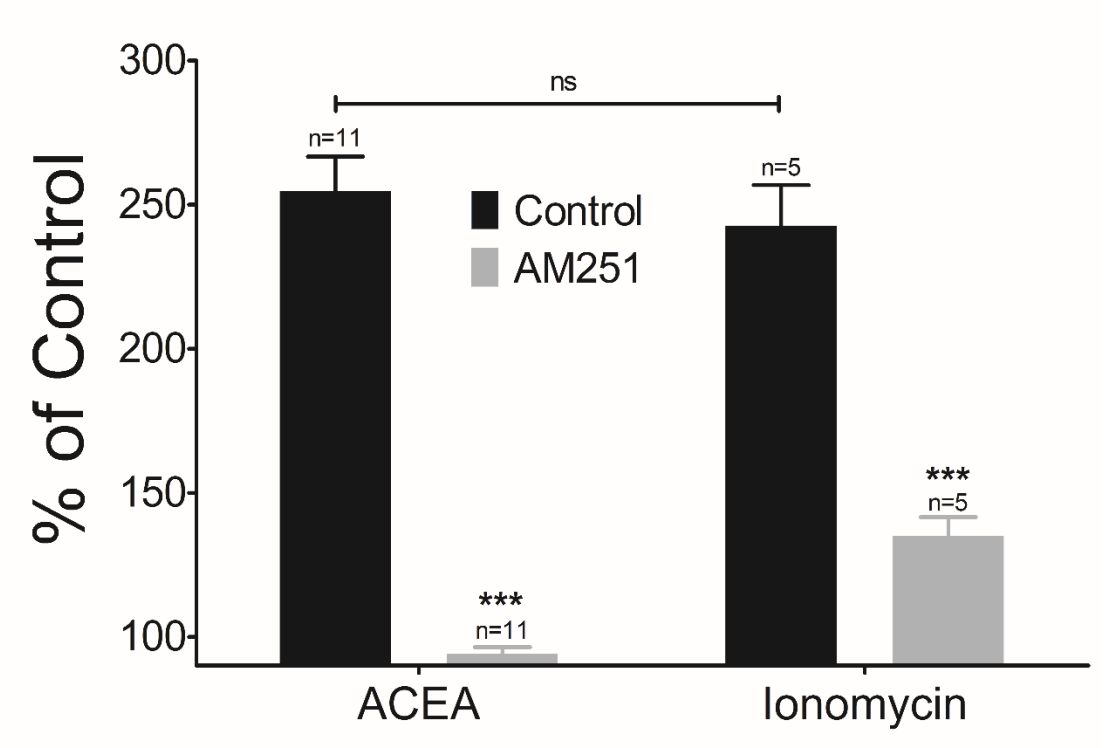

Figure 5.3.5. Ionomycin-induced CB1 activation is comparable to full activation of CB1 by ACEA

30,000 CB1-Tango cells were plated in 0.5% FBS McCoy's medium on clear bottom black plates for 24 hours. Cells were treated with either ACEA (FAC 5μM) or ionomycin (FAC 4μM) in the presence or absence of AM251 (FAC 10μM) for 4 hours. CB1 activation was then measured by the β-lactamase assay as described in the methods. Results were normalised to the control CB1 response (set as 100) and expressed % of control. Graph shows means and bars represent SEMs of pooled independent experiments (n indicated on the graph, 8 replicates in each individual experiment). Significance between the two agonists, and significance between agonist and AM251 was established using the Two Way ANOVA, as indicated below.

ns $p<0.05$; ***$p<0.001$; Two Way ANOVA, Bonferroni's post-test.

The above experiments indicate that ionomycin can elicit eCB signalling from the CB1-Tango cells, however the response is likely to be limited by MAGL, FAAH and ABHD6. To test this, the ionomycin concentration response was repeated in the presence of JZL195.

To this end, the CB1-Tango cells were plated in McCoy's assay medium and treated with a range of concentrations of ionomycin (FAC 0.25 – 4μM) in the presence or absence of AM251 for 4 hours as described in methods. 100nM JZL195 was included in all the wells and graphed in Figure 5.3.6. On its own AM251 in the presence of JZL195 inhibited the control response significantly to 81.6% ± 2.6% of control, as expected and in line with the results from Figure 5.3.3. A clear concentration-dependent increase in CB1 response was measured at all concentrations of ionomycin, reaching statistical significance at 1μM ionomycin and is maximally active at 2μM (247.7% ± 20.6% of control). The responses are largely (~90%) blocked by 10μM AM251. Previous results from the lab have shown that inhibition of MAGL and FAAH separately do not potentiate the ionomycin induced response (thesis of Rachel Lane Markwick, 2015), therefore the ionomycin response can be potentiated by the inhibition of MAGL, FAAH and ABHD6 together, indicative of eCB signalling.

As the levels of both 2-AG and AEA are likely to be stimulated by elevated levels of calcium in the cells, it was of interest to determine which pathway may be responsible for the response. At this time, no AEA pathway inhibitors are available and the complexity of the AEA pathway hinders the use of pharmacological tools to dissect the pathway. We therefore considered the pharmacological blockade of the DAGL pathway with DAGL inhibitors which were used previously. THL inhibits DAGL but can also inhibit a wide range of lipases (Borgstrom, 1988), we therefore in addition tested two more specific DAGL inhibitors KT109 and KT172 which reportedly have high selectivity for the DAGLs (Hsu et al., 2012). The compounds were used at concentrations which are likely to fully block both DAGLα and DAGLβ. Using these two specific DAGL inhibitors should confirm if part of the ionomycin induced CB1 response is DAGL dependent.

CB1-Tango cells were plated in McCoy's 0.5% FCS media and starved for 24 hours before treating with 20μM THL, 2μM KT109 and 2μM KT172 in the presence and absence of 2μM ionomycin (Figure 5.3.7A). These inhibitors alone did not significantly affect base level signalling in the absence of ionomycin, reconfirming the effectiveness of the McCoy's assay medium in starving the cells. 2μM ionomycin elicited a response that is comparable to previous results in Figure 5.3.4 and in the presence of DAGL inhibitors, there was no statistically significant inhibition of the ionomycin response by any of the DAGL inhibitors.

This result was unexpected as the DAGLs are highly expressed in the CB1-Tango cells and it clearly points to the response being mediated by a DAGL independent pathway.

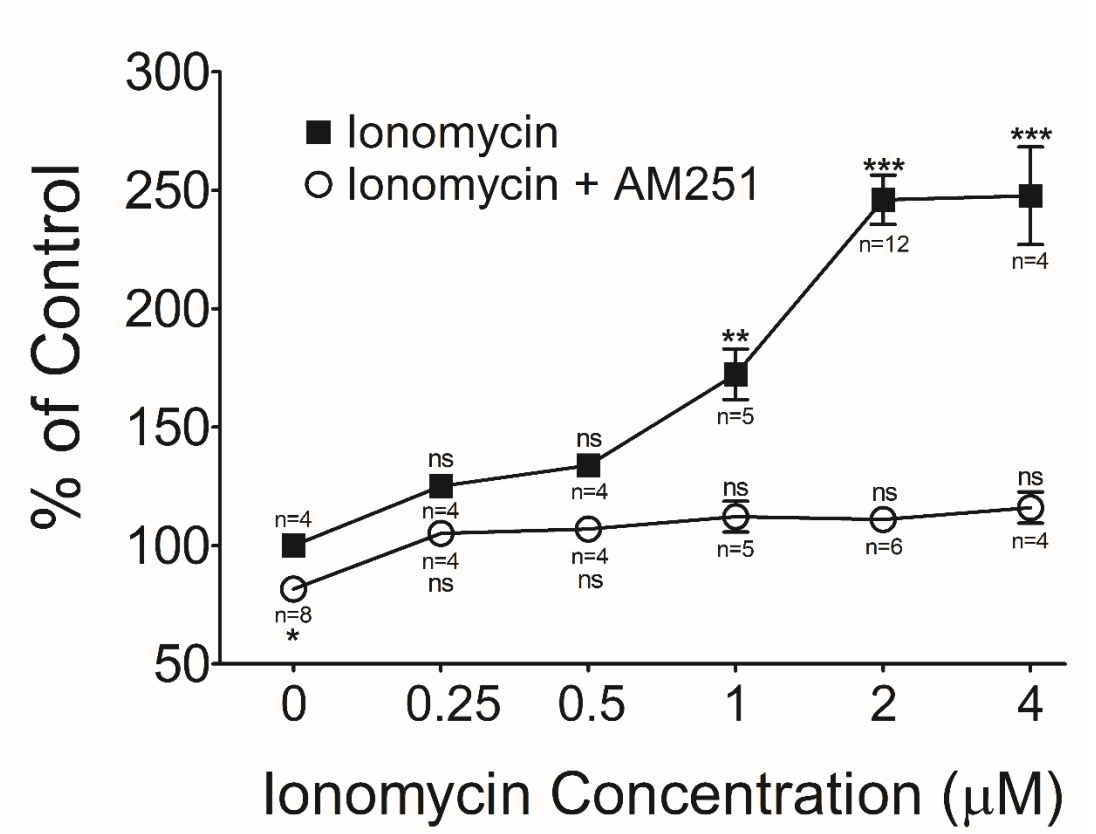

Figure 5.3.6. Ionomycin induced CB1-Tango response is potentiated by JZL195

30,000 CB1-Tango cells were seeded and maintained in 0.5% FBS McCoy's assay media for 24 hours. The cells were treated with varying concentrations of ionomycin (4μM top concentration, 1:2 dilution) in the presence and absence of AM251 (FAC 10μM), 100nM JZL195 was included to prevent eCB hydrolysis. CB1 activation was then measured by the β-lactamase assay as described in the methods. Ratios were normalised to the control wells with JZL195 present (set to 100) as % of control. Graph shows means and bars represent SEMs of pooled independent experiments (n indicated on the graph) with 8 replicates in each individual experiment. Significance over the control was established using One-way ANOVA, as indicated below.

ns p>0.05; ns *<0.05; **p<0.01; ***p<0.001; One-way ANOVA, Dunnett's post-test.

We next wanted to test if the DAGL activity is required for the small basal eCB tone that is revealed when JZL195 is present. To this end we tested the effect of the KT compounds and THL on the cells in the presence of JZL195. In the presence of JZL195, but absence of ionomycin (Figure 5.3.8A) a slight but significant inhibition of the basal tone by THL (84.61% ± 4.61% of control) was seen. Whilst KT172 has a small significance relative to control and KT109 does not, the effect of the two are not significantly different from each other. The KT compounds had at best a 5% inhibition, which suggests that if DAGL is contributing to the JZL195 tone it does so in a very minor manner; the significant effect of THL (~15% inhibition) is similar to the effect seen with AM251 and might be explained by the fact that it can inhibit several serine hydrolases, or it might be a non-specific effect.

Interestingly in the presence JZL195, the ionomycin response is substantially potentiated (from 177.4% ± 12.1% in control to 258.8% ± 12.6% with JZL195) and in this circumstance KT109, KT172 and THL all inhibited the 2μM ionomycin response similarly by around 50% of the full response, indicating that around half of the full ionomycin response is mediated by the DAGLs but this was not revealed previously due to the rapid activity of the eCB degradation enzymes (Figure 5.3.8B). Therefore, in the presence of JZL195, the ionomycin response is partially mediated by DAGL and 2-AG.

Figure 5.3.7. Ionomycin induced CB1-Tango response remains in the presence of DAGL inhibitors in CB1-Tango cells

Tango assay plate was set up with 30,000 CB1-Tango cells maintained in 0.5% FBS McCoy's assay media for 24 hours. The cells were treated with DAGL inhibitors KT109 (FAC 2μM), KT172 (FAC 2μM) or THL (FAC 20μM) in the (A) absence or (B) presence of ionomycin (FAC 2μM) for 4 hours. CB1 activation was then measured by the β-lactamase assay as described in the methods. Results were normalised to control response (set as 100) as % of control. Graphs show mean and bars represent SEMs across pooled independent experiments (n indicated on graph) with 8 replicates in each individual experiment. Significance across groups was calculated using One Way ANOVA, as indicated below.

ns $p>0.05$; One Way ANOVA, Dunnett's post-test.

(A)

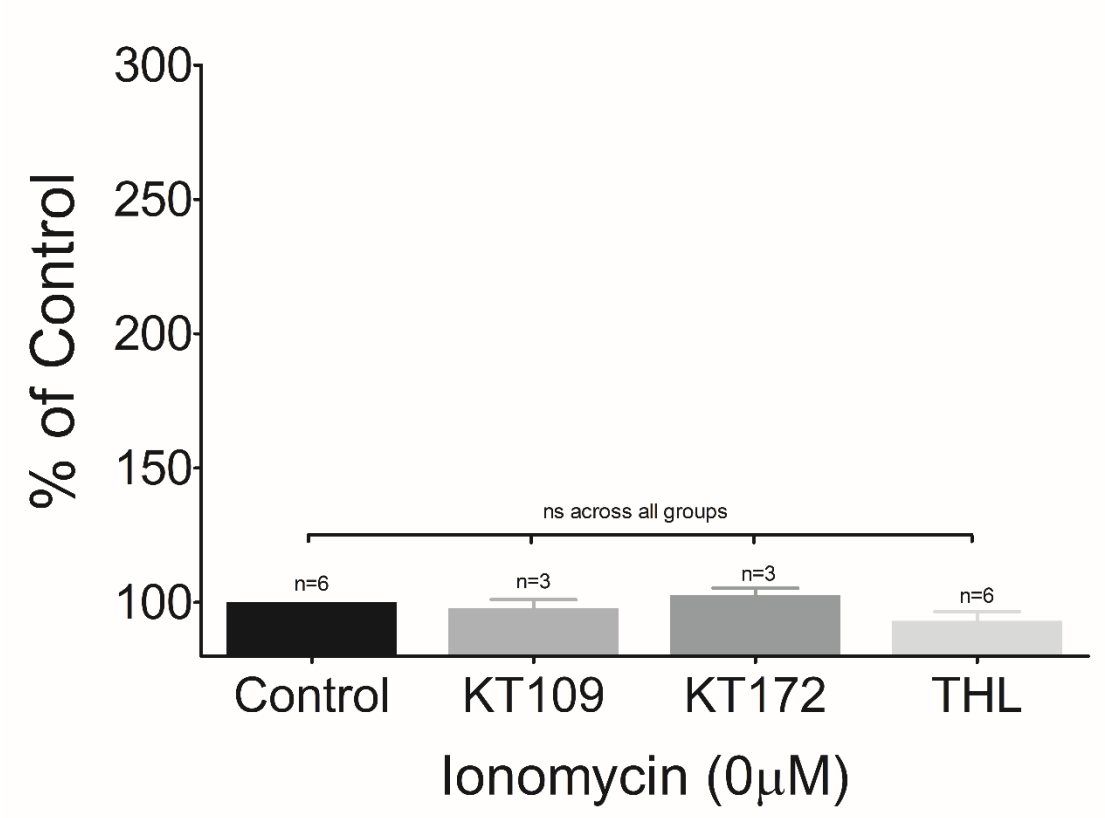
300
250
200
150
100
% of Control
ns across all groups
n=6
n=3
n=3
n=6
Control
KT109
KT172
THL
Ionomycin (0μM)

(B)

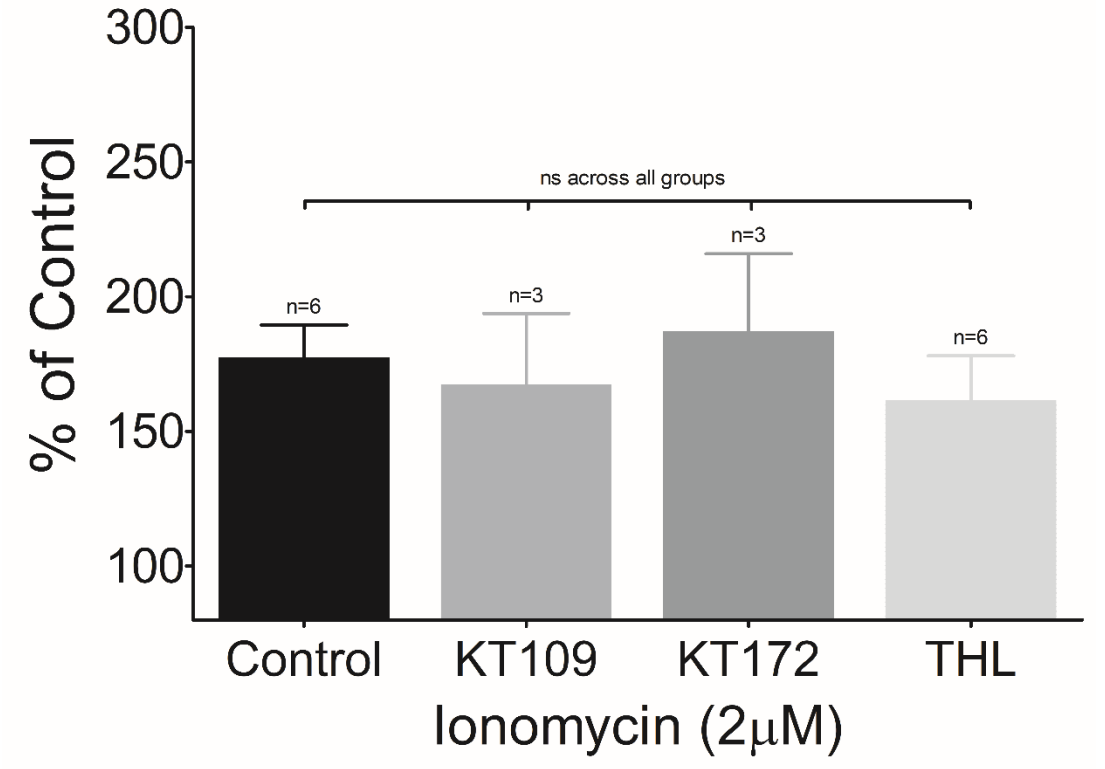
300
250
200
150
100
% of Control
ns across all groups
n=6
n=3
n=3
n=6
Control
KT109
KT172
THL
Ionomycin (2μM)

Figure 5.3.8. JZL195 reveals DAGL dependent component in ionomycin-induced CB1-Tango response in CB1-Tango cells

30,000 CB1-Tango cells were plated into 96 well assay plate and maintained in McCoy's medium containing 0.5% FBS for 24 hours. The cells were then treated with DAGL inhibitors KT109 (FAC 500nM), KT172 (FAC 500nM) or THL (FAC 10μM) in the (A) absence or (B) presence of ionomycin (FAC 2μM) for 4 hours. FAC 100nM JZL195 was included in the wells. CB1 activation was then measured by the β-lactamase assay as described in the methods. Results were normalised to control wells with JZL195 present (set as 100) as % of control. Graphs show mean and bars represent SEMs of pooled independent experiments with 8 replicates in each individual experiment. Significance was established against control or ionomycin control using One Way ANOVA, as indicated below.

ns $p>0.05$; *$p<0.05$; ***$p<0.001$; One Way ANOVA, Dunnett's post-test.

(A)

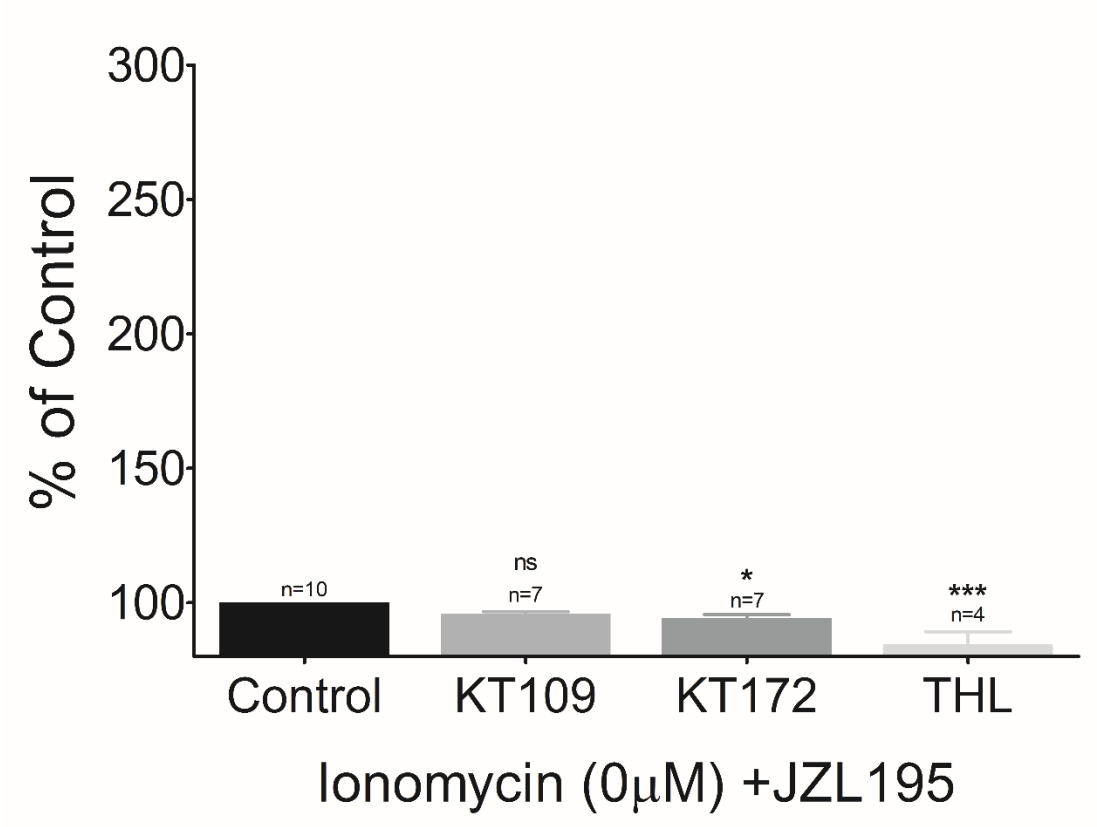
300
250
200
150
100
% of Control
n=10
ns
n=7
*
n=7
***
n=4
Control
KT109
KT172
THL
Ionomycin (0μM) +JZL195

(B)

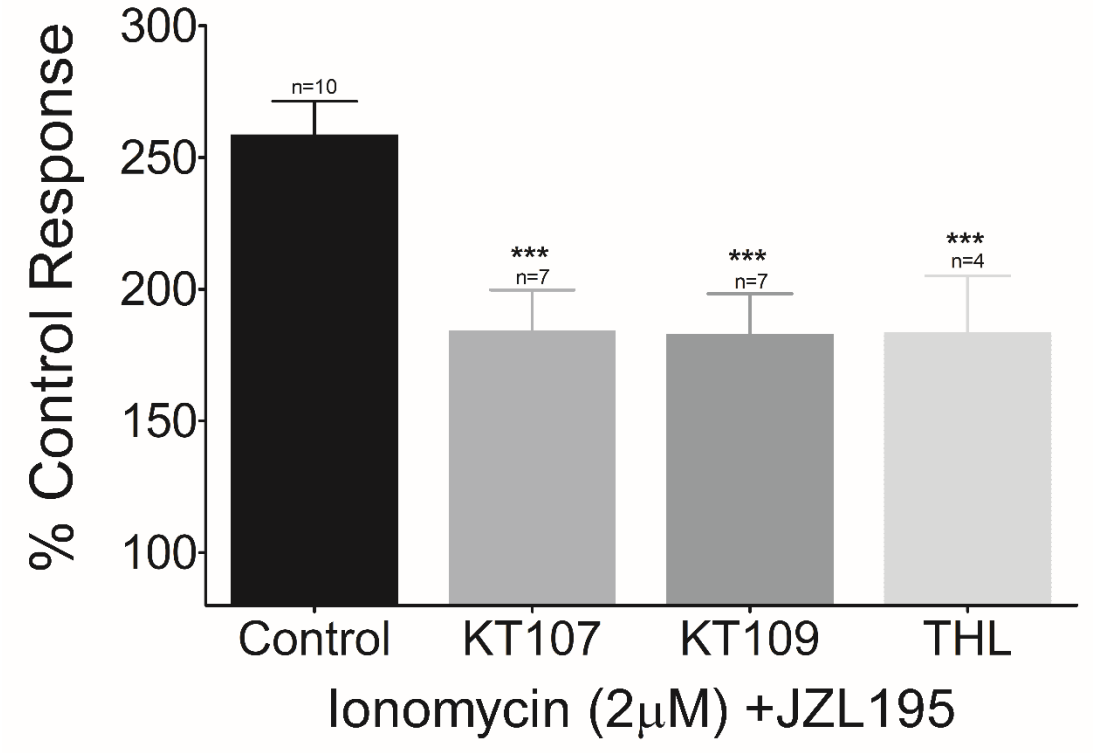
300
250
200
150
100
% Control Response
n=10
***
n=7
***
n=7
***
n=4
Control
KT107
KT109
THL
Ionomycin (2μM) +JZL195

Increased calcium levels in Freestyle media generates a substantial eCB tone

The physiological level of extracellular calcium is in the low mM range, and a high amount of extracellular calcium in cancellous bone may have a role in the maintenance of an eCB tone for bone growth and remodelling (Bab et al., 2008; Tam et al., 2008). The Freestyle media recommended for the standard CB1-Tango cell assay is serum and calcium free, we reasoned that the simple addition of calcium into the cell media for the duration of the assay might stimulate a significant basal eCB tone.

Currently, overnight starvation in Freestyle media followed by a 4 hour drug treatment with JZL195 reveals an eCB tone that is around 15% of the control which suggests a relatively low basal turnover of the eCBs. The recommended 4 hour window for the activation of the CB1 receptor is sufficient for drug discovery efforts which aim to act on the CB1 receptor directly, but the generation of eCBs for signalling at the CB1 receptor is likely to be much slower and exceed the 4 hour assay window, particularly if the cells have been starved beforehand to reduce eCB generation to a minimum. We adapted the assay by removing the overnight starvation period and adopted a 24 hour (rather than a 4 hour) assay period to determine if this would result in a more substantial eCB tone.

First it was important to ensure the CB1-Tango assay is properly functional in this novel Freestyle condition using the CB1 agonist ACEA. The CB1-Tango cells were cultured and plated in Freestyle media as described in methods, however drug treatments were added immediately after the cells were plated. 100nM JZL195 was included in all wells and experiments to prevent the degradation of any eCBs synthesised during the assay period. AM251 (FAC 2.5μM) was included as a very important control in all experiments to block all signalling at the CB1 level and thereby reveal a key basal control value. In the following set of experiments all results were expressed as a % of this basal control value (set to 100). The plate was then incubated for 24 hours in 37^{o}C; after which the β-lactamase substrate was added for 90 minutes and responses were measured in the Flexstation.

The cells were also treated with a maximally active concentration of ACEA (FAC 5μM) in the presence or absence of AM251 (FAC 2.5μM). A very substantial ACEA response was apparent under the new assay condition (477.1% ± 27.7% of the basal AM251 control) (Figure 5.3.9). This ACEA response is much more robust after 24 hour drug treatment in comparison to 4 hour treatments. AM251 was also able to largely block the ACEA response back to close to baseline value (142.8% ± 10.9% of AM251 control) but a small amount of CB1 activation was still present, likely due to the prolonged exposure of the cells to ACEA.

Next, the effect of the addition of calcium into Freestyle media for the duration of the 24 hour incubation period on this eCB tone was tested. Across separate experiments, the CB1-Tango cells were plated in Freestyle media supplemented with 100nM JZL195 with or without 2mM $CaCl_2$ and with and without AM251 (FAC 2.5μM). After 24hrs the substrate was added to determine the level of CB1 activation, with the data normalised to the basal AM251 control value and is shown in Figure 5.3.10. Even in the absence of added calcium, the presence of AM251 revealed a substantial eCB tone that was 199.8% ± 20.0% of basal control. This was substantially larger than the equivalent tone seen in the 4 hour assay that followed a starvation period (116.6% ± 3.37% of the AM251 basal control (Figure 3 data normalised to the basal AM251 control)). The presence of 2mM calcium enhanced the eCB tone significantly by around 50% compared to the same conditions in the absence of calcium (Figure 5.3.10). This enhancement of the eCB tone suggests that the addition of extracellular calcium can affect the production of eCBs, likely through the increased basal activity of the eCB synthesising enzymes. For this reason, the following experiments include the addition of 2mM calcium into Freestyle media along with 100nM JZL195.

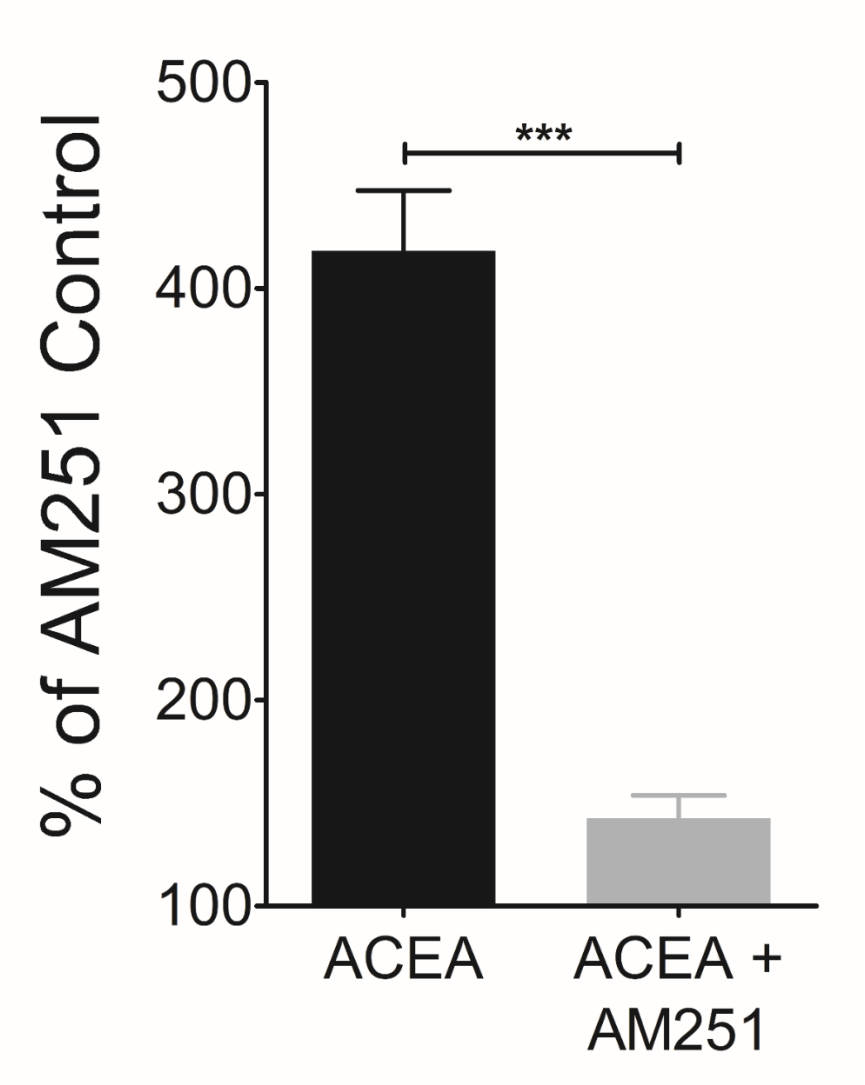

Figure 5.3.9. ACEA still elicits a robust CB1 dependent response in No Starve Freestyle conditions

CB1-Tango cells were plated in 96 well plates at a density of 30,000 per well in Freestyle media supplemented with FAC 100nM JZL195. Immediately after plating, the cells were treated with ACEA (FAC 5μM) in the presence and absence of AM251 (FAC 2.5μM) diluted in the same medium and incubated for 24 hours. Control wells contained media only and no AM251. CB1 activation was then measured by the β-lactamase assay as per manufacturer's protocol. The data collected were normalised to wells containing AM251 only (set at 100) as % of AM251 control. The graph presented represents the mean and bars represent the SEM of n = 3 independent experiments, 8 replicates in each individual experiment. Significance was established using Student's T-test, as indicated below.

* $p<0.05$; unpaired Student's T-test, two-tailed.

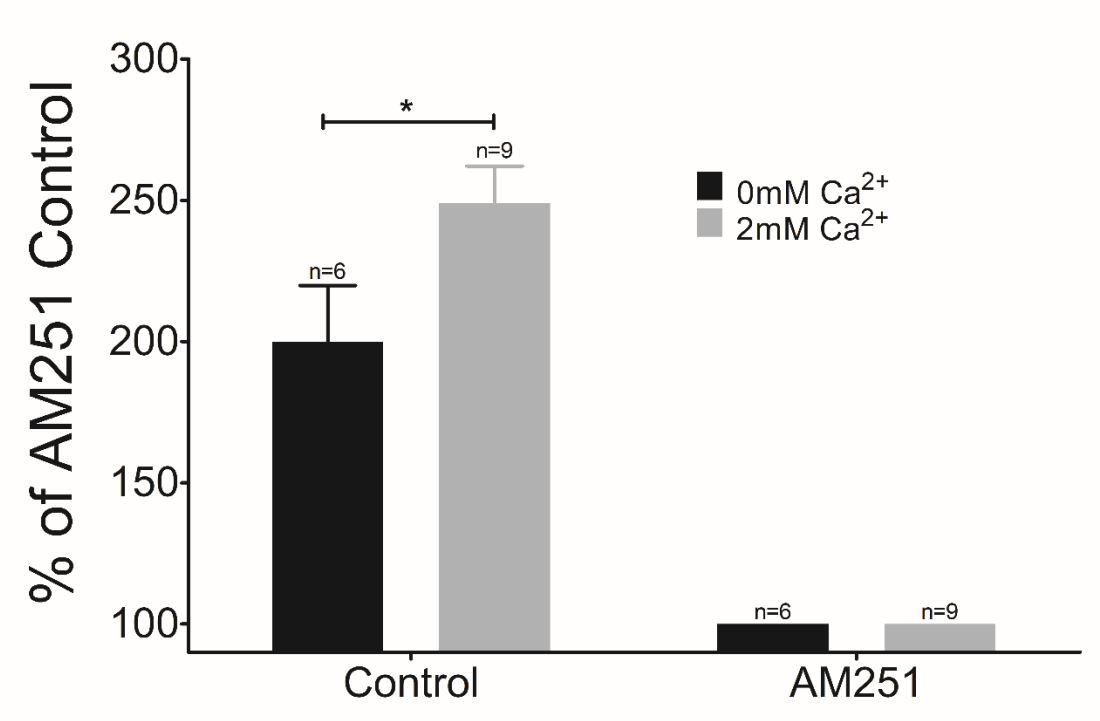

Figure 5.3.10. Reducing starvation time in Freestyle media and overnight treatment with JZL195 and calcium enhances eCB tone

CB1-Tango cells were plated in 96 well plates at a density of 30,000 per well in Freestyle media supplemented with FAC 100nM JZL195 in the absence or presence of 2mM $CaCl_2$. Cells were treated with AM251 (2.5μM) diluted in the same medium as a control immediately after plating and incubated for 24 hours. Control wells contained media only and no AM251. CB1 activation was then measured by the β-lactamase assay as per manufacturer's protocol. The data collected were normalised to wells containing AM251 (set at 100) as % of AM251 control. The graph presented represents the mean and bars represent the SEM of pooled independent experiments (n indicated on graph), 8 replicates in each individual experiment. Significance was established using Student's T-test, as indicated below.

*$p<0.05$; unpaired Student's T-test, two-tailed.

PKA activation by forskolin generates an eCB dependent response

Likely targets of calcium elevation in both rapid and long term eCB signalling are kinases which can regulate activity of other enzymes by phosphorylation. Based on the hypothesis that the DAGLs and the CaNAT are likely to be the targets of activation by PKA and/or PKC, we reasoned that direct activation of PKA and PKC in the CB1-Tango cells would activate eCB signalling which would be measurable in the CB1-Tango cells.

Forskolin (FSK) has been reported to activate adenylyl cyclase which increases intracellular levels of cAMP leading to the activation of PKA (Seamon and Daly, 1986). CB1-Tango cells were plated in Freestyle media supplemented with 2mM calcium and 100nM JZL195 as described previously. Immediately after plating, the cells were treated with FSK at the final assay concentration of 10μM, in the presence and absence of AM251 (FAC 2.5μM). The responses were normalised to the basal control value (Figure 5.3.11). FSK elicited a robust CB1 response (656.8% ± 40.1% of AM251 control) which was essentially fully inhibited by the presence of AM251 (138.6% ± 3.9% of AM251 control), indicating CB1-dependent signalling. The FSK response is of a similar magnitude to a maximally active concentration of ACEA tested in the same assay conditions (612.8% ± 30.6% of AM251 control, data not shown).

PKC activation by PMA generates an eCB dependent response

Similarly to PKA, PKC has also been suggested to be able to activate the synthesis of 2-AG and AEA (Vellani et al., 2008). Based on publicly available databases from mass spectrometry studies DAGLs contain proposed PKC phosphorylation sites that are located in/around the regulatory loop (Reisenberg et al., 2012). AEA levels can also be enhanced by PKC activation in both HEK-293 cells and sensory neurons but by what mechanism this occurs has not been investigated (van der Stelt and Di Marzo, 2005a). Phorbol 12-myristate 13-acetate (PMA), is a potent tumour promoter and an activator of PKC due to its structural similarity to DAG (Castagna et al., 1982). Like FSK, we hypothesised that PMA could induce eCB signalling in the CB1-Tango cells by activation of PKC that may activate DAGLs and/or CaNAT.

Cells were plated as above in Freestyle media (with 2mM calcium and JZL195) with PMA then added for 24 hours (FAC 25nM) in the presence and absence of AM251 with the results summarised in (Figure 5.3.12). PMA was able to elicit a CB1 dependent response reaching a mean of 383.2% ± 7.7% of AM251 control; while this is a considerable response, it is much lower than the maximal activity shown by ACEA and FSK. The PMA response was mostly blocked by AM251 but did show a small residual component, which could not be inhibited by 2.5μM AM251 (169.2% ± 4.2% of AM251 control).

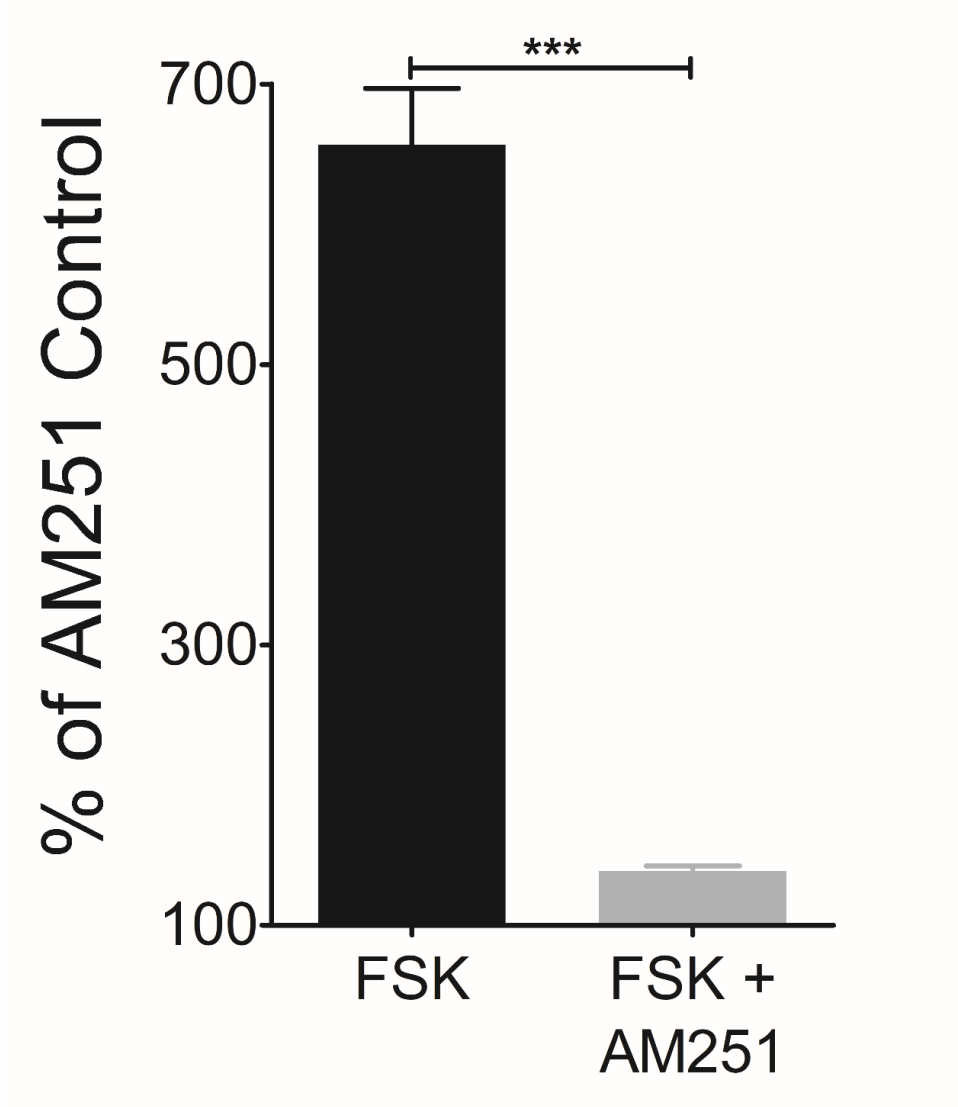

Figure 5.3.11. PKA activation stimulates an eCB response in the CB1-Tango cells

CB1-Tango cells were plated in 96 well plates at a density of 30,000 per well in Freestyle media supplemented with FAC 100nM JZL195 in the presence of 2mM $CaCl_2$. Immediately after plating, the cells were treated with FSK (FAC 10μM) in the presence and absence of AM251 (FAC 2.5μM) diluted in the same medium and incubated for 24 hours. CB1 activation was then measured by the β-lactamase assay as per manufacturer's protocol. The data collected were normalised to wells containing AM251 (set at 100) as % of AM251 control. The graph presented represents the mean and bars represent the SEM of 3 independent experiments, 8 replicates in each individual experiment. Significance was established using Student's T-test, as indicated below.

*** $p<0.001$; unpaired Student's T-test, two-tailed.

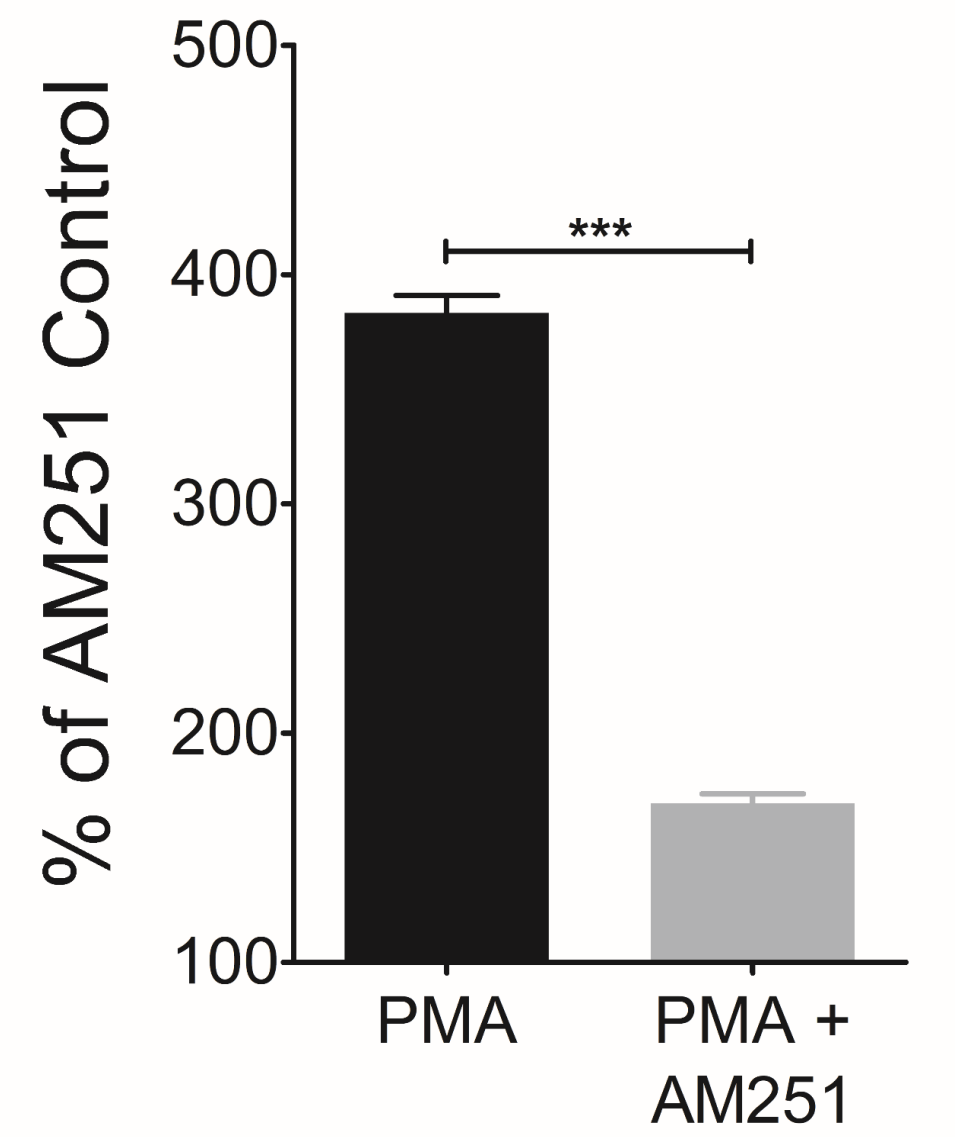

Figure 5.3.12. PKC activation stimulates an eCB response in the CB1-Tango cells

CB1-Tango cells were plated in 96 well plates at a density of 30,000 per well in Freestyle media supplemented with FAC 100nM JZL195 in the presence of 2mM $CaCl_2$. Immediately after plating, the cells were treated with PMA (FAC 25nM) in the presence and absence of AM251 (FAC 2.5μM) diluted in the same medium and incubated for 24 hours. CB1 activation was then measured by the β-lactamase assay as per manufacturer's protocol. The data collected were normalised to wells containing AM251 (set at 100) as % of AM251 control. The graph represents the mean and bars represent the SEM of 4 independent experiments, 8 replicates in each individual experiment. Significance was established using Student's T-test, as indicated below.

*** $p<0.001$; unpaired Student's T-test, two-tailed.

5.3.3 **Results 3B.** Summary & Conclusions

The aim of this section was to determine if the CB1-Tango assay can be adapted with different assay conditions and stimuli to maximise the eCB response from the CB1-Tango cells. Various conditions have been tested in our lab previously and have successfully evoked eCB signalling in many of the conditions, for example various media and growth supplements, starvation times and assay times (unpublished observations). Here I have reported the adaptation of the CB1-Tango assay in two ways to generate eCB signalling: (1) in a modified 0.5% FBS McCoy's assay medium which allows for rapid intracellular increases of calcium in the cells by ionomycin, and (2) in Freestyle media supplemented with 2mM calcium and JZL195 with no starvation period and a 24 hour drug treatment to promote accumulation of eCBs over the drug treatment period. These two paradigms allow the use of pharmacological tools to evoke eCB signalling in conditions akin to neuronal signalling and in bone matrix.

In McCoy's assay media, no eCB tone is present in control conditions, indicating the assay media is sufficient to reduce basal activity of the cells. A small eCB tone can be revealed by JZL195 in McCoy's media, similarly to standard Freestyle media, indicating a low turnover of eCBs is present. A more enhanced eCB tone can be generated in No starve Freestyle media in an overnight assay where the breakdown of eCBs are prevented. The addition of extracellular calcium into No Starve Freestyle media alone was sufficient to significantly enhance the basal production of the eCBs, suggesting that extracellular calcium in cancellous bone (and indeed other tissues) may indeed affect basal eCB generation (Idris and Ralston, 2012).

The presence of physiologically relevant levels of calcium in McCoy's assay media allowed us to utilise ionomycin as a rapid elevator of intracellular calcium for the activation of eCB synthesis. Ionomycin increases calcium flux across the plasma membrane but also depletes intracellular calcium stores for a rapid increase in intracellular calcium (Kao et al., 1990). This rapid increase in calcium caused a concentration-dependent CB1 response that could be inhibited by AM251 and was enhanced by JZL195. It is noteworthy that when used at 4μM in the absence of JZL195, a component of the ionomycin response was not inhibited by 10μM AM251. This might reflect a non-specific activation of the pathway, perhaps by calcium activated proteases releasing the signalling moiety from the CB1 receptor. However, it might also reflect the fact that AM251 is a competitive inhibitor that might simply have failed to

fully block an eCB response. Unfortunately, this could not simply be tested by increasing AM251 concentration as a precipitate was formed in the media at higher concentrations.

The use of DAGL inhibitors showed surprisingly that the ionomycin response is independent of DAGL activity, despite the prominent levels of DAGL transcripts detected in the cells. Only in the presence of JZL195 is the response revealed to be only partially DAGL mediated by various DAGL inhibitors. Similar results have been obtained previously by other members of the lab using THL and another reported DAGL inhibitor OMDM-188 (an analogue of THL) (Ortar et al., 2008). Both THL and OMDM-188 inhibited a 2μM ionomycin response in the presence of JZL195 by ~50% (thesis of Rachel Lane Markwick, 2015), consistent with the results of independent experiments reported here. The remaining response is likely to be attributed to other eCBs produced and suggests the activity of ABHD6 and MAGL are likely to limit 2-AG signalling.

The mechanism for the elevation of calcium evoking eCB signalling is unclear; it is likely that calcium can stimulate the production of NAPE and subsequently AEA by activation of CaNAT directly (Cadas et al., 1997), but for the generation of 2-AG there are likely to be additional steps following on from calcium elevation (Reisenberg et al., 2012; Kano, 2014). A study has shown calcium can modulate DAGLα activity via calcium/calmodulin-dependent protein kinase IIa (CAMKIIa) activity (Shonesy et al., 2013). Activated CAMKIIa has been shown *in vitro* to interact with the C-terminal tail of DAGLα, can phosphorylate two serine residues and reduce DAGLα activity by ~40%. Genetic deletion of CAMKIIa in mice models increased DAGL activity in striatal glutamatergic synapses leading to increased short term retrograde signalling. This suggests that calcium influx can modulate activity of CAMKIIa and subsequently DAGLα to modulate retrograde synaptic signalling (Shonesy et al., 2013). However, the generation of eCB signalling in the CB1-Tango cell line is not likely to be mediated through a CAMKIIa dependent mechanism as the influx of calcium in our cell line increases the generation of eCBs for signalling rather than reducing the generation of 2-AG by inhibiting DAGLα activity. The C-terminal tail of DAGLα is dispensable for the catalytic activity of DAGLα (Pedicord et al., 2011), thus the interaction of CAMKIIa and the DAGLα tail is more likely to modulate activity in post synaptic densities with the aid of other anchoring proteins for DAGLα recycling (Zhou et al., 2016). As well as this, a key difference between DAGLα and DAGLβ is the absence of a long C-terminal tail in DAGLβ (Reisenberg et al., 2012) thus is it not likely that DAGLβ is modulated by CAMKIIa in the same way DAGLα is (Shonesy

et al., 2013). This points to the involvement of other calcium-activated moieties in the CB1-Tango cells for the generation of eCB signalling.

As the DAGLs do not seem to have direct calcium sensitivity (Farooqui et al., 1984; Moriyama et al., 1999; Rosenberger et al., 2007), it has been hypothesised that the DAGLs are regulated by phosphorylation, similarly to the structurally-related hormone sensitive lipase (HSL) (Lampidonis et al., 2011). Using phosphorylation databases which curate experimentally observed phospho-sites identified from published sources, a predicted phosphorylation map of the DAGLs were generated (Reisenberg et al., 2012; thesis of Rachel Lane Markwick, 2015). Of all the predicted phosphorylation sites, sites which were detected independently more than 3 times and were detected in more than one database were included. Using these parameters, one site was present on the DAGLα regulatory loop, along with several sites on the C-terminal tail. The site on the regulatory loop was predicted to be phosphorylated by PKC or cdc2. The tail of DAGLα seems to be heavily phosphorylated by kinases other than CAMKIIa and is likely to play a role in the subtle modulation of DAGLα activity and expression; in fact DAGLα recycling seems to be dependent on PKC activity (Zhou et al., 2016). DAGLβ was also subject to the same analysis and only one site was present which was predicted to be phosphorylated by a range of kinases including PKA, PKC and cdc2 (thesis of Rachel Lane Markwick, 2015).

Indeed, aside from calcium, activation of PKA and PKC can also reliably stimulate eCB signalling in the CB1-Tango cells in different media conditions. FSK had been used previously in the CB1-Tango assay in McCoy's assay medium for 4 hours (thesis of Rachel Lane Markwick, 2015). The results showed that 10μM FSK could induce a modest response when applied alone (~110% of control) which was potentiated by the presence of JZL195 (~115% of control). These responses could be fully inhibited by AM251, indicating CB1-dependency. The FSK responses were much more robust when the cells were incubated in the drugs for 18 hours overnight than for 4 hours (FSK alone = ~137% and FSK + JZL195 = ~196%).

PMA was also used in McCoy's assay medium in a 4 hour assay system (thesis of Rachel Lane Markwick, 2015). In the absence of JZL195, 25nM PMA had little effect in the CB1-Tango assay; a small response was measured (~110% of control) but was not inhibited by AM251, indicative of a non-specific effect and could not be taken as an eCB response. In the presence of 100nM JZL195, PMA gave a slightly more substantial response (~145% of control) and this was fully inhibited by AM251. In overnight assays, the PMA response was much more robust but introduced a lot of variation and non-CB1 dependent responses.

CB1 responses evoked by PKA and PKC are much more enhanced and stable in Freestyle media in the presence of calcium and JZL195 with no cell starvation time. This might partially be due to the increased calcium concentration in the media which enhances basal eCB tone. Whilst PKA activation by FSK gives a full eCB response, PKC activation by PMA gave only about 50% of full CB1 activation. Whilst the responses were originally thought to be DAGL dependent, in other similar paradigms tested by members of the lab, THL inhibited about half of the FSK response in Freestyle media plus JZL195, but OMDM-188 and KT compounds did not significantly inhibit the FSK response (unpublished observations, Emma Williams). This result was surprising; THL is likely to have non-specific effects however the lack of inhibition by other DAGL inhibitors would suggest the response is indeed largely DAGL independent. This may in part be due to low substrate (DAG) availability in Freestyle media thus limiting DAGL activity and driving other synthesis pathways, or PKA and PKC activation could stimulate the release of more than one eCB.

It is not clear whether AEA synthesis is regulated by phosphorylation. It is possible that activation of PKA and PKC can generate AEA through the activity of CaNAT. CaNAT is the most likely candidate to be modulated by phosphorylation as NAPE generation was reported to be enhanced by FSK, despite FSK not directly activating CaNAT (Cadas et al., 1996). FSK has been shown to be able to generate AEA in the presence of a calcium chelator (Vellani et al., 2008) which might point to the involvement of iNAT, but it is unknown whether iNAT is regulated by phosphorylation (Jin et al., 2007; Jin et al., 2009). The hydrolysis of NAPE to AEA by NAPEPLD is currently considered to be constitutively active and the presence of multiple pathways of AEA synthesis is likely to occlude any regulatory step, but it is not ruled out that NAPEPLD may be regulated or modulated by phosphorylation. As well as this, the NAPEPLD-independent generation of AEA relies on multiple enzymes, often consisting of more than two reaction steps and the enzymes are likely to have other functional roles; thus, it difficult to discern the phosphorylation sensitive enzymes and if they will generate AEA for eCB signalling following phosphorylation.

However, during the development of the assay system, the activity of the DAGL inhibitors were tested on the CB1-Tango cells in the No Starve Freestyle conditions to elucidate what portion of eCB signalling is attributable to DAGL and other eCBs. Preliminary results tested THL, OMDM-188, KT109 and KT172 on the CB1-Tango cells in the presence of a maximally active concentration of ACEA. As ACEA maximally activates the CB1 receptor pool directly, any effect on the ACEA response is generally indicative of a non-specific effect on the cells

viability. In most experimental paradigms, the ACEA response was generally not inhibited by the DAGL inhibitors. However, in the presence of the 4 DAGL inhibitors in the No Starve Freestyle conditions, the ACEA response had a reduction of between 20 – 50% of the full ACEA response (results not shown). Some of the DAGL inhibitors also display non-specific activity on the AM251 control of the cells, perhaps through a non-specific effect affecting the viability of the cells and expression of CB1 receptors. The reason for this effect is unknown; the DAGL inhibitors can inhibit other enzymes (Hoover et al., 2008; Ortar et al., 2008; Hsu et al., 2012) and perhaps the long incubation period with DAGL inhibitors affects the overall metabolic activity of the cells. For this reason, the DAGL inhibitors were not used to determine the DAGL proportion of eCB signalling in the No Starve Freestyle conditions and genetic intervention would be required to perturb the expression of the DAGLs.

As pharmacological blockade of eCB synthesis is limited in the new No Starve Freestyle paradigm and there are currently no pharmacological tools to separate the multiple pathways for anandamide synthesis, genetic disruption of key eCB synthesis enzymes would be required to further characterise the eCB responses to ionomycin, FSK and PMA, and more specifically to determine the absolute requirement for all of the known eCB synthetic enzymes for these responses.

Chapter 6. Results 4 – Dissection of eCB signalling in the CB1-Tango cells

6.1 Introduction

The CB1-Tango cells in the previous chapter have demonstrated inducible eCB signalling in two different assay conditions in response to calcium, PKA and PKC activation. Both 2-AG and AEA have been shown to be synthesised "on demand" by these stimuli by the proposed activation of the respective synthesis enzymes which will be briefly described here. The synthesis enzymes that can be activated by these stimuli are likely to be regulated in this manner *in vivo* and thus are the focus of this chapter.

6.1.1 Activation and regulation of the production of 2-AG

The signalling pathway for 2-AG begins with the generation of DAG by a PLC following cellular stimulation in the first step, and subsequent hydrolysis of DAG by DAGL at the *sn*-1 position leading to the release of 2-AG for signalling in the second step (Figure 6.1.1). 2-AG signalling is then terminated by the activity of MAGL/ABHD6 to AA and glycerol. As mentioned previously, several studies have reported increases in 2-AG signalling in response to a range of stimuli (Williams et al., 2003; Di Marzo, 2008a). These increases in 2-AG signalling can partially be explained by increased substrate availability due to the associated increase in activity of PLCβ/γ, however PLC-independent 2-AG release (CaER) also exists (Hashimotodani et al., 2005; Tanimura et al., 2010). This would suggest that the regulation step of 2-AG synthesis may not lie in the generation of DAG but rather at the level of 2-AG synthesis by the DAGLs.

Studies of DAGL KO mice have shown that DAGLα and DAGLβ are responsible for the production of virtually all 2-AG levels in the brain and other tissues, for example loss of DAGLα has a dominant impact on brain and loss of DAGLβ has a dominant impact in the liver (Gao et al., 2010; Tanimura et al., 2010). Importantly from these studies, stimulus-induced increases in 2-AG are absent in all of the three forms of eCB-mediated retrograde signalling in DAGLα KO mice brain, indicating the importance of DAGLα for calcium-driven eCB

signalling (Tanimura et al., 2010). DAGLα and DAGLβ both exhibit distinct contributions to the cellular levels of 2-AG and AA, for instance DAGLα is primary responsible for CB1 signalling at the neuronal synapse whilst recent studies have indicated DAGLβ as a key enzyme within the lipid network for the generation of proinflammatory molecules for immune responses within macrophages and microglia (Hsu et al., 2012). Importantly, the DAGL KO studies also showed the levels of AA to be substantially reduced alongside 2-AG reductions (Gao et al., 2010); AA had been thought to be generated largely through the activity of PLA2 (Balsinde et al., 2002), however this highlights that the DAGL/MAGL pathway may have a bigger role for the generation/regulation of AA levels (Figure 6.1.1). These studies highlight the importance of the DAGLs as major regulators of eCB signalling, 2-AG synthesis and the AA pool; this would suggest that a level of regulation is needed, however it is unclear how the DAGLs are regulated.

The increased release of 2-AG following calcium elevation suggests that calcium is involved the regulation of the production of 2-AG. The DAGLs however, which catalyse the generation of 2-AG, do not appear to be directly sensitive to calcium (Farooqui et al., 1984; Moriyama et al., 1999). A simple model of explanation would be that increases in calcium levels can stimulate 2-AG generation via the DAGL pathway by indirect mechanisms that might involve an increased synthesis of substrate via PLC activation and/or the activation of DAGLs via a kinase network (Reisenberg et al., 2012).

In the above context, the DAGLs are structurally similar to HSL which contains a module that is regulated through phosphorylation (Lampidonis et al., 2011). The DAGLs have a structurally related 50-60 amino acid insert in the catalytic domain, likely to be a regulatory loop positioned to restrict access of the substrate to the catalytic site. Various phosphorylation sites have been identified within this regulatory loop, suggesting conformational changes of the regulatory loop by phosphorylation to be a rate-limiting mechanism (Reisenberg et al., 2012). Indeed, DAGL from bovine brain microsomes can be directly activated by a cAMP-dependent protein kinase (Rosenberger et al., 2007), and activation of PKA and PKC can both increase 2-AG synthesis (Vellani et al., 2008). Both PKA and PKC can also be activated by calcium (Steinberg, 2008; Dunn et al., 2009). Our working hypothesis therefore is that the DAGLs are regulated by phosphorylation by calcium activated kinases with phosphorylation of the regulatory loop resulting in a structural change that facilitates substrate access to the catalytic domain, thus the regulation step of 2-AG synthesis is likely to occur at step 2 at the level of the DAGLs (Figure 6.1.1).

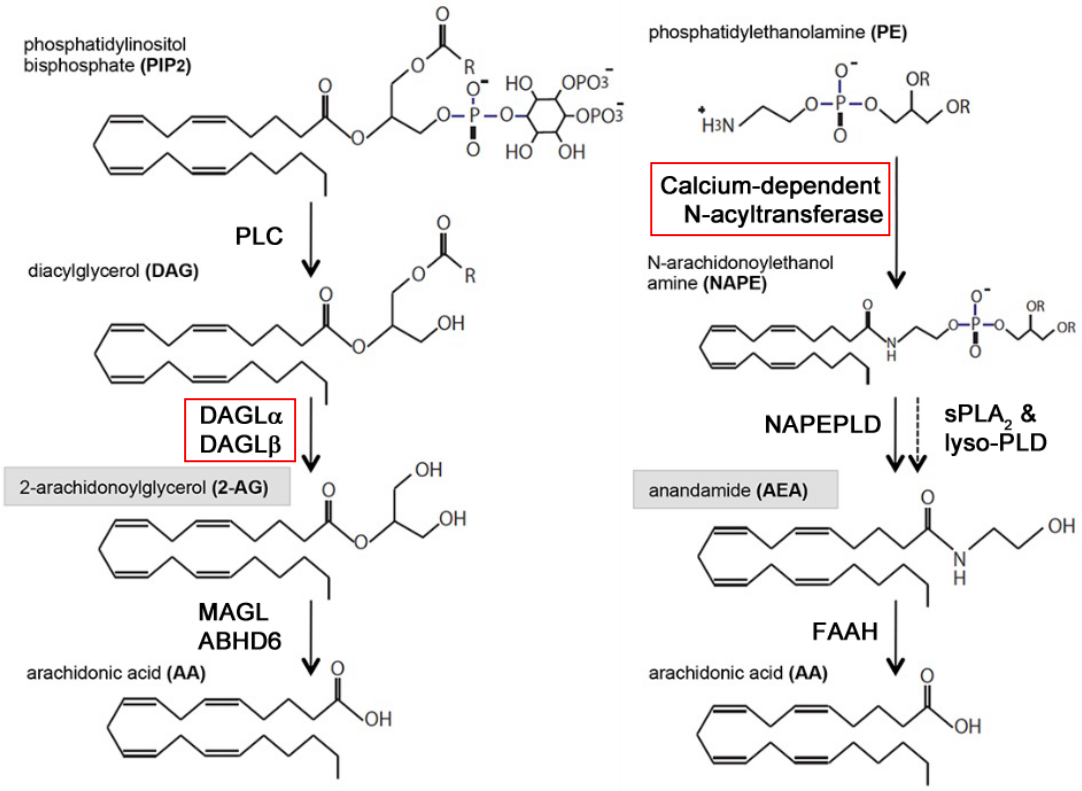

Figure 6.1.1. Simplified schematic of the main biosynthesis and hydrolysis pathways of eCBs 2-AG and AEA

The generation of 2-AG begins with a PLC hydrolysing *sn*-2-arachidonoyl PIP_2 to release DAG (Step 1). DAG is then cleaved by *sn*-1-specific DAGLs (DAGLα and DAGLβ) to release 2-AG (Step 2). Finally, MAGL hydrolyses most of the 2-AG in the brain, and ABHD6 also catalyses residual 2-AG at the post synaptic compartment (Step 3).

AEA synthesis starts with the formation of arachidonoyl-containing NAPE using PE and PC catalysed by a CaNAT (Step 1). Multiple synthetic pathways of AEA release from NAPE are postulated (Step 2). The consensus pathway posits that NAPE is hydrolysed in one step to release AEA by NAPEPLD, with secondary pathways containing the action of several enzymes including $sPLA_2$ and lysoPLD which can also release AEA from NAPEPLD – explained in more detail in Introduction. Finally, FAAH hydrolyses AEA to AA and ethanolamine (Step 3).

The hypothesised regulatory steps in 2-AG and AEA synthesis are highlighted in a red box.

Adapted from Kouchi (2015).

6.1.2 Role of NAPEPLD in AEA synthesis

Whereas we now have a clearer understanding of 2-AG synthesis, the pathways that regulate the synthesis of AEA appear to be much more complex. The "model" view of AEA synthesis begins with generation of NAPE from PC and PE through a CaNAT enzyme that had until recently remained elusive (Ogura et al., 2016). The precursor NAPE is then hydrolysed by NAPEPLD in the second step to release AEA (Di Marzo et al., 1994; Liu et al., 2008). Finally, AEA is hydrolysed by FAAH to release AA and ethanolamine (Figure 6.1.1).

However, some studies from NAPEPLD KO mice have shown that AEA levels were reduced slightly but not completely depleted in the brain (Leung et al., 2006; Tsuboi et al., 2011; Leishman et al., 2016). This highlights the presence of other biochemical pathways synthesising AEA from NAPE which are not necessarily NAPEPLD dependent, depicted in Figure 6.1.1 (Liu et al., 2006; Simon and Cravatt, 2006). Activation of PKA and PKC with FSK and PMA can also increase the levels of AEA in DRG neurones which is unaffected by the presence of a calcium chelator (Vellani et al., 2008). NAPEPLD also does not distinguish among other NAPEs containing different N-acyl substituents which are present even in unstimulated neurones (Ueda et al., 2013), while NAPE containing N-arachidonoyl, the precursor to AEA, is low in resting conditions but rapidly increases when neurones are exposed to stimuli that elevate intracellular calcium (Di Marzo et al., 1994; Cadas et al., 1996; Cadas et al., 1997). The redundancy of NAPEPLD for AEA synthesis and the presence of calcium-dependent and -independent pathways indicate that the regulatory step in the pathway of AEA synthesis does not lie with NAPEPLD but rather with the generation of N-arachidonoyl containing NAPE.

6.1.3 Identity of the putative CaNAT

The regulatory step of AEA synthesis is likely to be through the generation of the precursor NAPE from membrane phospholipids. The enzyme responsible for this generation of NAPE was crudely purified and showed sensitivity to calcium in eCB enriched areas such as the brain and testes (Natarajan et al., 1983; Schmid et al., 1990; Cadas et al., 1997). The activity of the CaNAT can also be enhanced by cAMP elevating agents such as FSK but as addition of FSK does not directly generate NAPE itself, the target of cAMP leading to enhancement of NAPE production remains unclear (Cadas et al., 1996). A calcium-insensitive NAT (iNAT) enzyme had been identified as part of the HRASLS family of genes and was related to the N-acyltransferase lecithin retinol acyltransferase (LRAT) (Jin et al., 2007), however this enzyme

did not match the enzymological or expression profile of the CaNAT which had been extensively profiled (Ueda et al., 2010).

The CaNAT was only recently proposed to be the poorly characterised serine hydrolase PLA2G4E, part of the PLA2 family of genes (Ogura et al., 2016). Of the PLA2G4 family, PLA2G4E and related enzyme PLA2G4B are both poorly characterised in terms of function. PLA2G4E exhibited calcium-dependent activity and could generate the NAPE precursor to AEA, along with other N-acylPE to NAE derivatives in mouse brain homogenate and in transfected mammalian cells. RT-PCR revealed expression of PLA2G4E in mouse brain and testis which generally matched areas of CaNAT activity but is also detected predominantly in heart, skeletal muscle, and thyroid (Ohto et al., 2005). The human orthologue of PLA2G4E has recently been functionally characterised in COS7 cells and also exhibit calcium-sensitive NAPE generation (Hussain et al., 2018).

NAPEPLD expression is present in almost all organs but is predominantly higher in brain, kidney and testis in mice (Okamoto et al., 2004), which does not corroborate exactly with PLA2G4E expression. Comparison of RNA-Seq data from purified sub-populations of cells from mouse cerebral cortex show high transcript expression of PLA2G4E in neurones only, whilst NAPEPLD transcripts are more ubiquitous but are highly detected in myelinating oligodendrocytes and endothelial cells (Zhang et al., 2014). AEA can be produced in astrocytes for example (Walter et al., 2002) but the lack of PLA2G4E transcripts detected in astrocytes (Zhang et al., 2014) raises the possibility that other functionally related enzymes to PLA2G4E may also generate NAPE and contribute to AEA synthesis in cells and tissues where PLA2G4E appears to be absent. PLA2G4B is currently poorly characterised in terms of function but show high expression in cerebellum, heart, pancreas and liver in mice (Ghosh et al., 2006); has homology (~45-50%) and similar calcium sensitivity to PLA2G4E; and data from RNA-seq show the presence of PLA2G4B is also rather ubiquitous in mouse cerebral cortex but is more highly detected in astrocytes, neurons and oligodendrocyte precursor cells (Zhang et al., 2014) which is more in line with NAPEPLD expression and regions of AEA production.

At this time, PLA2G4E expression in human tissues and proof-of-principle testing of PLA2G4E as the CaNAT responsible for the generation of NAPE for AEA signalling has not been established. In this section, the expression of PLA2G4E in our CB1-Tango cells will be questioned, as will whether PLA2G4E, and its related enzyme PLA2G4B, have a role in AEA synthesis in our cell line.

6.1.4 Aims

From the above studies we can be sure that the DAGLs play an essential role in eCB signalling via the synthesis of 2-AG, but the role that NAPEPLD and PLA2G4E play in AEA synthesis remains unclear. The adaptation of the CB1-Tango assay to measure eCB signalling in the previous chapter revealed different stimuli and physiologically emulated conditions are able to elicit robust eCB dependent CB1 activation on par with that seen with a maximally active concentration of a synthetic CB1 agonist. However, the use of various DAGL inhibitors revealed that DAGLs are at best only partially responsible for eCB signalling, raising the prospect that other eCBs are primarily responsible for eCB signalling in the CB1-Tango cells, with the second most characterised eCB, AEA, being the most likely candidate. There are some reasonable pharmacological tools to inhibit 2-AG synthesis, but none to inhibit AEA synthesis due to the presence of multiple synthesis pathways and no inhibitors have been generated yet for the novel CaNAT (Hoover et al., 2008; Liu et al., 2008). As well as this, long-term use of DAGL inhibitors in certain conditions causes non-specific inhibition of other enzymes. We therefore wanted to complement the pharmacological studies with genetic KO studies to determine the contributions of the DAGLs, NAPEPLD, PLA2G4E and candidate CaNAT enzyme PLA2G4B to eCB in the CB1-Tango cells. The aims of this chapter are to:

- Utilise gene editing tool CRISPR to systematically KO individual known components for 2-AG and AEA synthesis: DAGLs, NAPEPLD and PLA2G4B
- Characterise the effect of the systematic KO of eCB components on the eCB tone

6.2 **Results 4A**. To what extent is DAGL activity required for 2-AG synthesis and eCB signalling in this model?

6.2.1 **Results 4A.** Introduction

The first eCB synthesising enzymes to be targeted by CRISPR are the DAGLs as they have been shown previously to be major 2-AG synthesising enzymes *in vivo* (Gao et al., 2010; Tanimura et al., 2010) and the disruption of both DAGLs in animal KO studies have shown both enzymes are responsible for ~90% of 2-AG synthesis in the brain (Yoshino et al., 2011). The disruption of the DAGLs would eliminate the contribution of 2-AG to the eCB tone and provide a good basis for the study of the AEA pathways. DAGLα and DAGLβ transcripts are detected at higher levels than NAPEPLD transcripts in the CB1-Tango cells despite only contributing to around half of the eCB tone and the relative contribution of the individual DAGLs to the generation of 2-AG in the cells are unknown. Thus, to determine which of the separate DAGLs are involved in the generation of 2-AG, DAGLα and DAGLβ will be targeted separately to generate two KO lines. Furthermore, to ensure that the 2-AG pathway does not contribute to the eCB tone and for the purposes of elucidating how DAGL-independent eCB signalling is regulated in the CB1-Tango cells, a cell line with disruptions to both DAGLs will be generated using genetic tools.

Recent advances in gene editing techniques have allowed for precise DNA cleavage in a site-specific manner leading to many advances in the modelling of genetic causes of diseases and is a valuable tool for the manipulation of endogenous genes. Commonly used techniques include Zinc Finger Nucleases (ZFNs), Transcription Activator-like Effector Nucleases (TALENs) and RNA-guided Clustered Regularly Interspaced Short Palindromic Repeats (CRISPR) and CRISPR Associated (Cas) nuclease system. ZFNs and TALENs are DNA binding proteins that can be modified in their DNA binding domains to be able to bind to any desired portion of DNA (Durai et al., 2005; Gaj et al., 2013). ZNFs and TALENS are combined with a DNA cleavage domain (FokI) which dimerises to induce double strand breaks at the site of interest (Bitinaite et al., 1998). Although ZFN and TALENs have proven to be successful for gene editing, the requirement for two ZNFs or TALENs to be generated in near proximity for specificity and the generation of new proteins for each DNA site has proven to be time

consuming and costly. CRISPR-Cas9 is an RNA-guided nuclease system, where the straightforward design of a guide RNA sequence can target the nuclease to any desired portion of DNA, thus making for a much faster, more efficient and cost-effective genome editing technique.

CRISPR-Cas system is a bacterial and archaeal adaptive immune system that uses RNA-guided nucleases to cleave foreign genetic elements such as viral DNA (Barrangou et al., 2007; Deveau et al., 2010). Different types of CRISPR systems have been identified across a range of bacterial and archaeal hosts (Makarova et al., 2011; Koonin et al., 2017) but the most characterised system is Type II CRISPR from *Streptococcus pyogenes* (Garneau et al., 2010; Deltcheva et al., 2011; Jinek et al., 2012). In brief, stretches of sequences with homology to foreign DNA incorporated into bacterial DNA are separated by short palindromic repeat sequences in a CRISPR array (crRNA). The array is transcribed and processed into individual crRNAs by RNase III and special trans-activating crRNA (tracrRNA) with homology to the short palindromic repeats. Cas9 enzymes are recruited and form Cas9:crRNA complexes with individual cRNAs. These complexes target foreign genomic DNA sequences which are complementary to the crRNA and induce a double strand break. In Type II CRISPR systems, the target sequence must contain a Protospacer Adjacent Motif (PAM) directly downstream of where the crRNA would bind (5'-NGG).

The Type II CRISPR system was adapted for precise genome editing in mammalian systems (Jinek et al., 2013; Mali et al., 2013; Ran et al., 2013). The system utilises *Streptococcus pyogenes* endonuclease Cas9 which has been codon-corrected for mammalian expression, and the crRNA and tracrRNA are fused together to create a chimeric, single-guide RNA (sgRNA) which is linked to the Cas9 nuclease (Figure 6.2.1). A 20-nucleotide guide RNA (gRNA) sequence within the sgRNA can be designed to a genomic target site preceding a PAM site to cleave the double-stranded DNA at that site. Upon causing a double stranded break, two possible mechanisms for DNA repair are triggered: Non-Homologous End Joining (NHEJ) and Homology Direct Repair (HDR) leading to mutations within genomic DNA (Jinek et al., 2012; Jinek et al., 2013).

Intrinsically within mammalian cells, NHEJ is the default pathway of repair when there is an absence of a homology repair template. In this circumstance, repair machinery within the cell recognises the double strand break and attempt to repair the break where compatible

overhangs allow. When there are no compatible overhangs, the error-prone pathway introduces additional nucleotides or removes nucleotides at the breakage site which causes insertion/deletion mutations (indel mutations). Indel mutations often lead to premature stop codons and truncated proteins (Moore and Haber, 1996; Pardo et al., 2009). HDR on the other hand allows for precise genomic editing when a repair template is introduced to the cell with homology arms flanking the CRISPR site (Pardo et al., 2009). For the purposes of genetic KO of candidate genes, we have utilised NHEJ as the preferred method to introduce frameshift mutations in the catalytic regions of the genes as homology directed repair showed lower success rate (thesis of Rachel Lane Markwick, 2015).

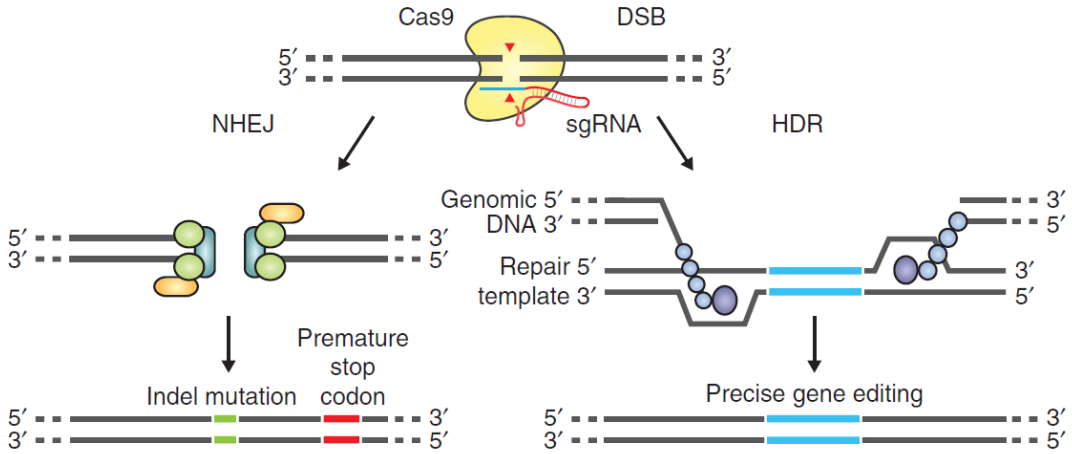

Figure 6.2.1. Schematic overview of CRISPR/Cas9 causing double stranded breaks in gene editing

Cas9 endonuclease (yellow) is guided by sgRNA to the correct cleavage site which is directly upstream a 5'-NGG PAM sequence and induces a double strand break in the genomic DNA. Double strand breaks can be repaired in one of two ways: NHEJ and HDR. NHEJ utilises the endogenous repair mechanism in the cell to rejoin the two strands which can be error prone and introduce random indel mutations at the site, which in the coding frame could lead to frameshift mutations or premature stop codons. HDR uses a homology repair template in the form of a plasmid or single stranded oligonucleotides introduced into the cell to allow precise gene editing. Adapted from Ran et al. (2013).

It has been established in previous chapters that endogenous DAGLα and DAGLβ transcripts are detected in CB1-Tango cells at relatively high levels but that their enzymatic products are not likely to be solely responsible for eCB signalling in the CB1-Tango cell line. To try to strip back the eCB tone detected in the CB1-Tango cells, we aimed to systematically eliminate key enzymes that are likely to contribute to eCB synthesis. We first targeted the DAGLs separately with CRISPR to determine the relative contributions of the DAGLs to 2-AG generation in the CB1-Tango cells, and then disrupted both genes to generate a cell line that would allow us to study DAGL-independent eCB pathways. Three cell lines were generated: a DAGLα knock out cell line, a DAGLβ knock out cell line and a dual DAGL knock out cell line. I will describe the generation of a DAGLβ knock out line and the characterisation of the dual DAGLα/β KO line which was generated in tandem by other members of the lab (thesis of Rachel Lane Markwick, 2015). The eCB levels of the three KO cell lines were measured to determine the contribution of each of these enzymes to 2-AG synthesis in the CB1-Tango cells and finally the DAGLα/β KO line was tested in the CB1-Tango assay to determine if eCB signalling can still be elicited.

6.2.2 **Results 4A.** Results

Design of gRNAs to the catalytic regions of DAGLβ

To introduce the CRISPR/Cas9 system to the CB1-Tango cells, we used the pSpCas9(BB)-2A-Puro (PX459) backbone plasmid which was deposited on Addgene by the Feng Zhang lab (Ran et al., 2013). This plasmid contains all the necessary components for the expression of Cas9 gene (4272 bp) with nuclear localization signal for eukaryotic expression, U6 promoter and allows insertion of the desired gRNAs using a restriction enzyme digest and ligation step (Figure 2.2.1). The plasmid also contains puromycin antibiotic resistance which allows for selection of successfully transfected cells.

The catalytic region of the candidate genes were targeted as frameshift mutations in the region would disrupt the catalytic activity of the enzymes even if various splice variants of the enzymes are made. The genomic sequences for the genes were obtained from Ensembl Genome Browser (ensembl.org). The catalytic triad crucial for DAGLβ activity consists of a serine residue in exon 11, aspartic acid residue in exon 12 and a histamine residue in exon 15. As the deletion of serine renders the enzyme catalytically dead (Bisogno et al., 2003) and is the most upstream of the three catalytic residues, we chose to design gRNAs in exon 11, 10 and 9 in hopes of a frameshift mutation that would affect serine and also further downstream catalytic residues.

To generate the gRNAs, the genetic sequence of DAGLβ catalytic domain was uploaded onto publicly available software to generate CRISPR guides. 20 nucleotide long sequences were selected using software available on ZiFiT (http://zifit.partners.org/ZiFiT/) (Sander et al., 2010) and cross-referenced with nucleotides generated from ATUM CRISPR design tool (https://www.atum.bio/eCommerce/cas9/input). We chose 9 different gRNAs to target exon 9, 10 and 11 of DAGLβ (Table 2.1.2 and Figure 6.2.2). The gRNA and complementary oligonucleotides were ordered as single strands with additional modifications: a starting 5'–G nucleotide as transcription initiation has requirement of a 'G' base for the human U6 promoter (Cong et al., 2013), and with BbsI restriction enzyme overhangs for annealing and ligating to the PX459 backbone vector (Ran et al., 2013).

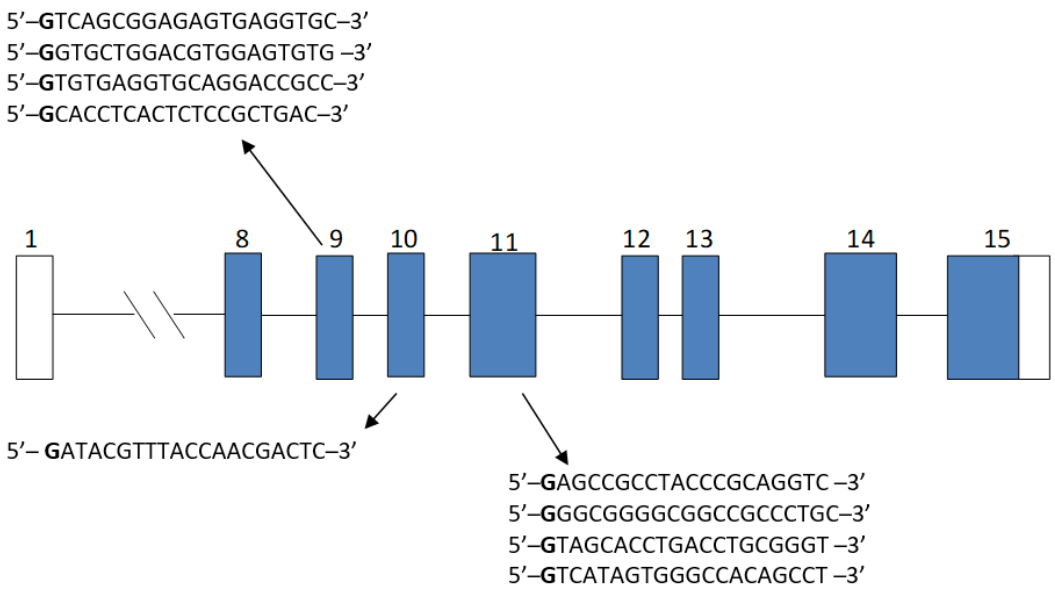

Figure 6.2.2. gRNA sequences selected for Cas9 recognition of DAGLβ catalytic domain

Schematic representation of the human DAGLβ sequence, indicating exons (numbered) which harbour the catalytic domain (blue). There are many predicted splice variants of DAGLβ with this diagram representing the longest predicted transcript (and exons that cross most predicted variants). Sequences for gRNAs begin with G (bold) for U6 promotor recognition (Ran et al., 2013).

Cloning and validation of constructs and generation of DAGLβ KO line

The vectors were constructed to contain the custom gRNA oligonucleotides into the PX459 backbone vector. In brief, the backbone vector was digested by the restriction enzyme BbsI, dephosphorylated and purified after separation on an agarose gel. The complementary pair of oligonucleotides were annealed together and phosphorylated, and then ligated to the purified backbone. Once the 9 complete vectors were constructed, the vectors were individually transfected into separate pools of CB1-Tango cells for transient expression of Cas9 nuclease.

It is important that the gRNA has been ligated into the vector in the correct place and orientation, and thus produce active Cas9 to cleave genomic DNA and introduce indel mutations. To test the efficiency of each gRNA we designed, the Surveyor Nuclease assay (Qiu et al., 2004) was used to detect mismatched base pairs that have been caused by indel mutations within the alleles of DAGLβ gene. In brief, hybridising PCR amplicons containing indel mutations with wild-type PCR amplicons that do not contain the CRISPR indels causes a mismatch in base pairs which Surveyor nuclease detects and cleaves apart, resulting in smaller sized fragments (Figure 6.2.3). This can easily be visualised by gel electrophoresis, indicating whether CRISPR treatment has been successful.

The genomic DNA for the pool of transfected cells were extracted and PCR amplification of the CRISPR site was carried out using primers flanking each exon (Table 2.1.2) and half of the reaction mix was visualised on 2% agarose gel (Figure 6.2.4A). PCR amplifications of the regions were very clean at the correct band size with the exception of exon 10 PCR product which seemed to have a higher molecular weight band above the expected band size. Since this was seen in both the untransfected and transfected cells, for the purposes of the Surveyor nuclease assay, it would not affect the formation of hetero-duplexes and cleavage of the mismatched nucleotides.

The remaining PCR mix was boiled and reannealed to form mismatched hetero-duplexes then Surveyor nuclease enzyme was added to the mix for the cleavage of mismatched pairs. The remaining products were then run on 2% agarose gel (Figure 6.2.4B). Untransfected CB1-Tango cells did not show any signs of mismatch cleavage which indicates that within the CRISPR region there are no endogenously mismatched pairs. Upon comparison of the PCR products of transfected cells with untransfected cells, certain vectors show additional smaller sized fragments under the large band size (indicated by asterisks in Figure 6.2.4B). This indicated that the vector could introduce indel mutations via NHEJ. For our further experiments, CRISPR vector 9.2 was used which had the most prominent cleaved bands.

Figure 6.2.3. Schematic of Surveyor nuclease cleavage of mismatch heteroduplexes of DNA

Extraction of genomic DNA and PCR amplification of the region of known indel formation by CRISPR (indicated in red) was carried out on a pool of transfected cells (DNA indicated by black lines) and untransfected cells (DNA indicated by blue lines) (step 1). PCR products were heated to separate the DNA strands and slowly cooled to promote annealing of heteroduplexes of mismatched DNA (step 2). Surveyor nuclease (indicated in green) then cleaves mismatched DNA strands into smaller fragments (step 3) which can be visualised by gel electrophoresis (step 4). This allows identification of indel formation by CRISPR.

Step 1. PCR amplify sample DNA.

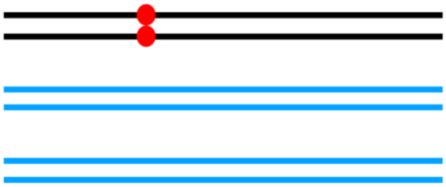

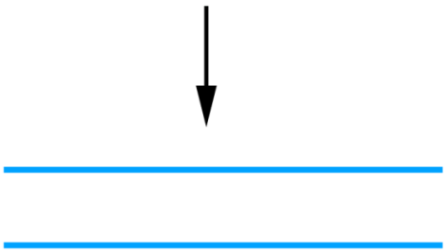

Step 2. Heat/Cool to form heteroduplexes.

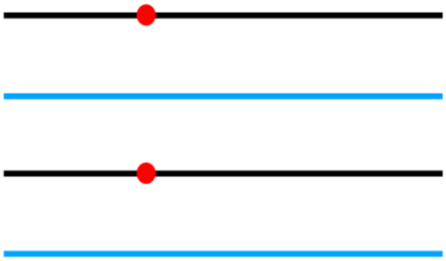

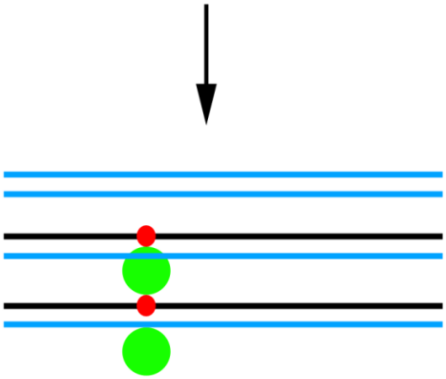

Step 3. SURVEYOR Nuclease cleavage of mismatched pairs.

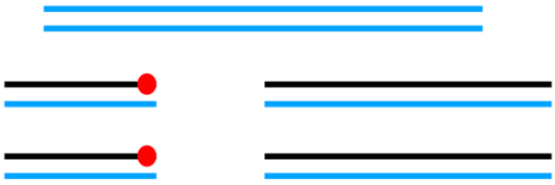

Step 4. Size-based fragment analysis.

(A)

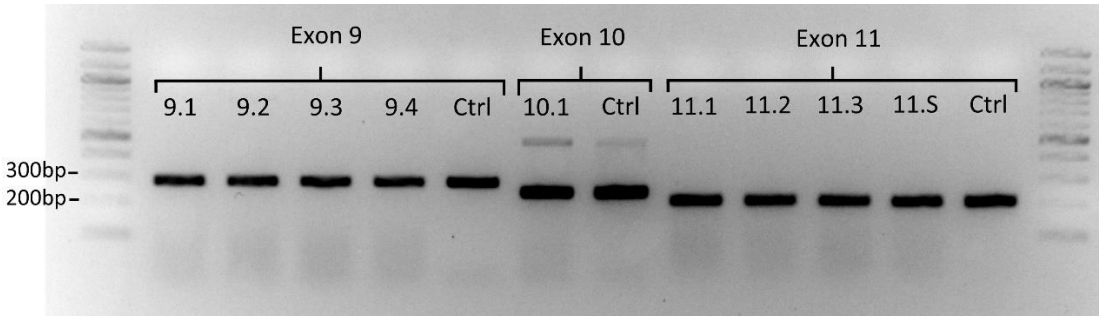

(B)

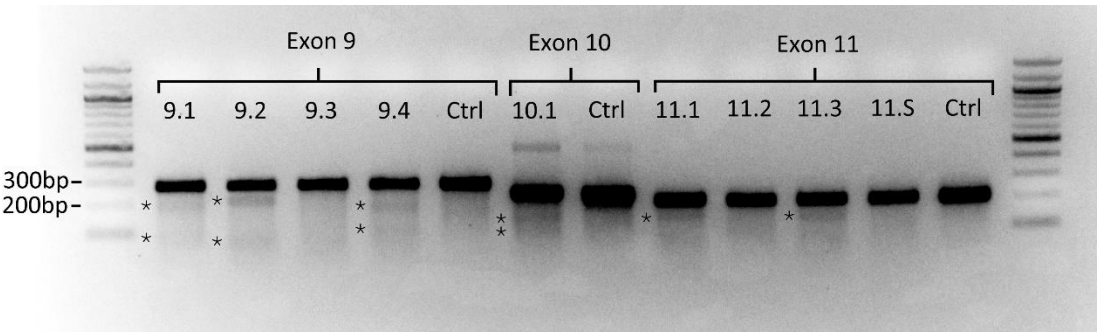

Figure 6.2.4. PCR amplification of DAGLβ catalytic domain exons from transfected CB1-Tango cells (A) and Surveyor Nuclease digestion products of PCR products (B).

CB1-Tango cells were seeded on 6 well dishes and transfected with CRISPR vectors 24 hours after. Genomic DNA from the pool of cells in each well was extracted using Puregene Core Kit B (Qiagen) after 24 hours of transient expression of the vector. PCR amplification of exon 9 (284bp), exon 10 (246bp) and exon 11 (210bp) of DAGLβ catalytic domain was performed from extracted genomic DNA from transfected CB1-Tango cells and untransfected CB1-Tango cells (Ctrl). Half the volume of PCR products were run on 2% agarose gel (A) and Surveyor enhancer S and Surveyor nuclease were added to the remaining PCR product mixture before incubating at 42°C for 1 hour and run on 2% agarose gel (B). Asterisks indicate digested products of mismatched PCR products.

RT-PCR and sequencing show genetically disrupted DAGLβ transcripts

After transfection of parental CB1-Tango cells with vector CRISPR 9.2 and treatment for 24 hours with the selection agent puromycin, cells were reseeded at very low density and cell colonies were left to grow for 3 weeks before being selected for cell expansion. It was hoped that these would be clonal, but we could not exclude the possibility that a more careful cloning step would be required further down the line. Once sufficient numbers of cells had grown, RNA was extracted from each colony pool and converted to cDNA before PCR amplification of DAGLβ gene between exons 8 – 10 (Figure 6.2.5).

Certain colony lines had observable differences from untransfected parental CB1-Tango cells (marked with an asterisk) and others had no observable differences, perhaps due to the introduction of very subtle mutations. The PCR for all the knock out cell lines and untransfected cells were carried out using the same primers simultaneously, therefore any observable differences are a result of the differences caused by CRISPR indel mutations.

For further analysis, certain candidate knock out cell lines were picked based on their observable differences – F and C3, but we also selected lines with no observable differences – H and G2. The PCR product of RT-PCR of these cell lines were ligated into a TOPO-cloning expression vector and transformed into *E. coli*. 24 bacterial *E. coli* colonies were picked from each knock out line and sent for sequencing.

Sequences of DAGLβ RT-PCR from selected knock out cell lines were analysed and compared to wild type DAGLβ sequence. Ideally, both alleles of DAGLβ in the cell lines would have undergone NHEJ and repaired in slightly different ways; with both alleles containing indel mutations leading to truncated protein. We therefore expected at least two transcripts arising from sequencing results of each knock out line. The results from the first round of sequencing are listed in Table 6.2.1.

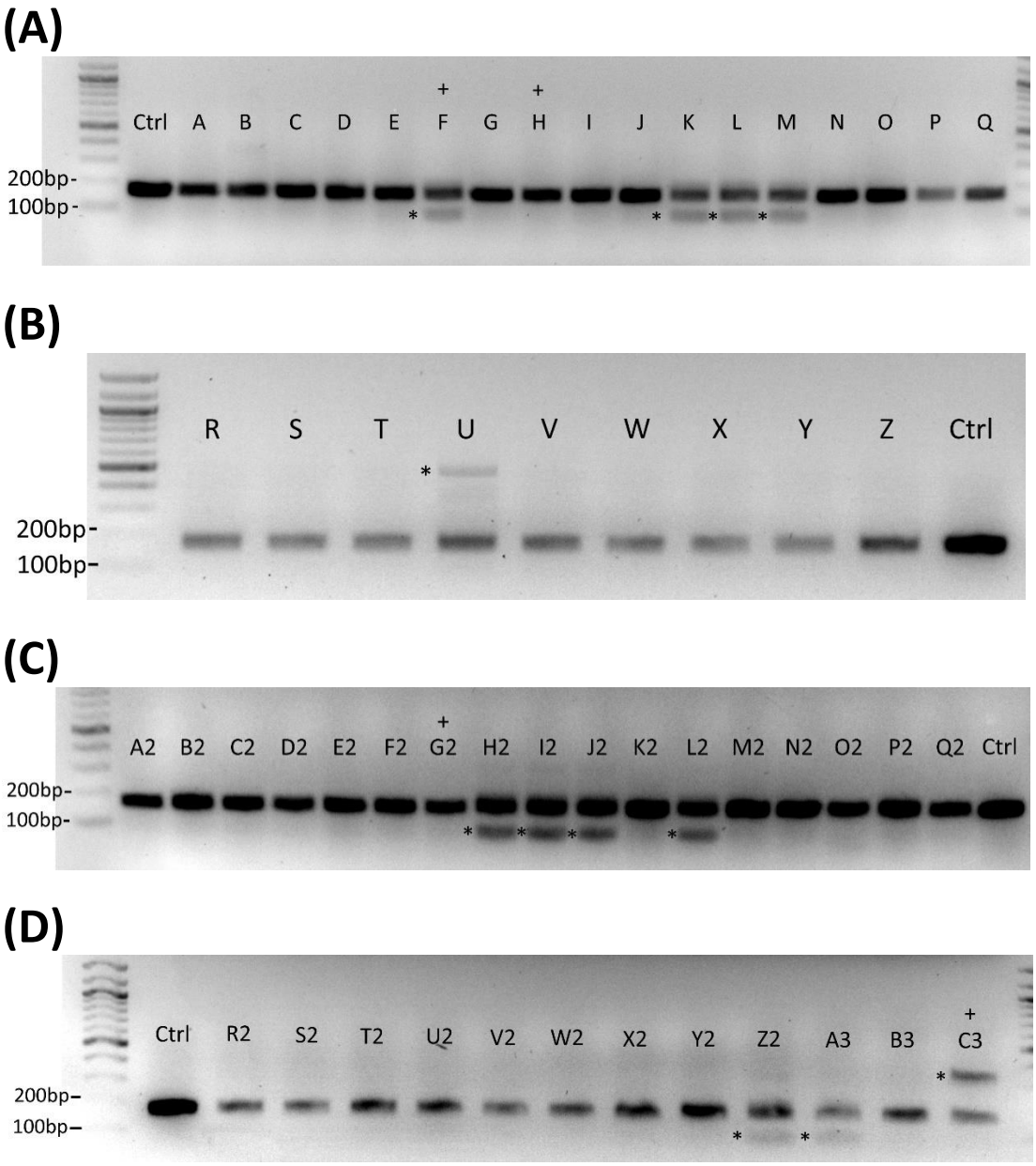

Figure 6.2.5. Reverse Transcription PCR amplification of DAGLβ CRISPR site of CRISPR knock out lines.

RNA from selected CRISPR knock out lines and parental CB1-Tango cells (Ctrl) were extracted and converted to cDNA. PCR amplification of cDNA surrounding the CRISPR site was performed with primers spanning exons 8 to 10. The PCR products were run on 2% agarose gel and visualised. Knock out cell lines with observable differences from parental CB1-Tango cells have been highlighted with an asterisk and lines taken for further analysis are indicated by a plus symbol above the letter name.

CELL LINE	MUTATION	FREQUENCY
COLONY F	1bp insertion (CRISPR site)	15/24
	78bp deletion * (Exon 9)	3/24
	299bp insertion (Retained intron 8-9)	1/24
COLONY H	1bp insertion (CRISPR site)	23/24
	1bp insertion (CRISPR site) & 1bp deletion * (upstream of CRISPR site)	1/24
COLONY G2	1bp insertion (CRISPR site)	23/24
	Wild type sequence	1/24
COLONY C3	1bp insertion (CRISPR site)	13/24
	178bp insertion (CRISPR site)	6/24
	1bp deletion (CRISPR site)	2/24

Table 6.2.1. Sequencing results of DAGLβ catalytic domain exon 8-10 in selected CRISPR lines.

PCR amplified cDNA between exons 8 to exon 10 of DAGLβ in CRISPR knock out lines F, H, G2 and C3 were cloned into TOPO vector and sent for sequence analysis. The types of indel mutations and locations of these mutations were categorised and tallied as listed in the table. Asterisk indicates in-frame deletions.

CELL LINE	MUTATION	FREQUENCY
COLONY H	1bp insertion (CRISPR site)	14/21
	1bp insertion & 128bp deletion (Exon 11)	3/21
	1bp insertion & 41bp deletion (End of exon 14)	2/21
	1bp insertion & 209bp deletion (Exons 10 & 11)	1/21
	1bp insertion & 1bp deletion *† (Within exon 14)	1/21

Table 6.2.2. Sequencing results of DAGLβ catalytic domain exon 8-15 in selected CRISPR lines.

PCR amplified cDNA between exons 8 to exons 15 of DAGLβ in knock out cell line H were cloned into TOPO vector and sent for sequence analysis. The types of indel mutations were categorised and tallied as listed in the table. * indicate in frame mutations. † indicates the deleted nucleotide is different to the one listed in Table 6.2.1.

The promising result from Table 6.2.1 was knock out line H, which has only 2 different sequencing reads from the total of 24, other cell lines either had more than two reads or the presence of a wild type sequence. However, one of the transcripts from knock out line H had a 1bp insertion & 1bp deletion within the same read, which would put the sequence back in frame as a stop codon was not reached before the sequence shifted back in frame. We were unsure if this mutation affected the catalytic domain which was further downstream as sequencing was carried out between exon 8 – 10 which did not span the catalytic triad of DAGLβ. To ensure that the catalytic triad of DAGLβ is disrupted a longer PCR product for the second round of sequencing was carried out from exon 8 – 15, summarised in Table 6.2.2.

Longer sequencing reads of knock out line H have shown that there were more than two types of transcript present, where the majority of deletions occur after exon 10 which includes deletion of the catalytic triad. In the second round of sequencing, the same 1bp insert that would cause an in-frame read was not detected and no wildtype sequence was detected. When converting the sequences of the transcripts to protein sequences, all detected KO line H transcripts gave disrupted protein sequences with a premature stop codon after the 1bp mutation at the CRISPR site. To see whether this translates to disrupted protein expression, western blot analysis was carried out in the 4 CRISPR treated cell lines.

Western blot analysis shows disrupted DAGLβ protein in CRISPR treated cells

To determine if mutations seen within the genome corresponded to subsequent knock down of DAGLβ protein, membrane preparations and cell lysates of four DAGLβ knock out lines: F, H, G2 and C3 were analysed on a western blot as described in methods (Figure 6.2.6). The DAGLβ antibody was generated using an epitope corresponding to residues surrounding Leu505 in exon 13 of human DAGLβ protein. Wild type DAGLβ is around 73kD and expression is concentrated in the cell membrane, and thus produces a more prominent band in the membrane preparation compared with cell lysates (Figure 6.2.6A). DAGLβ expression in membrane preparations of the knock out lines is reduced to essentially undetectable levels, which is mirrored in the cell lysates blot (Figure 6.2.6B).

Taking together the sequencing results with the western blotting results, we can conclude that CRISPR has clearly disrupted essentially all of the DAGL transcripts in the selected cell colonies, and perhaps more importantly we cannot detect the expression of DAGLβ protein in any of the colonies. We therefore will take forward line H as the DAGLβ knock out cell line.

Figure 6.2.6. Western blot analysis of DAGLβ expression in CRISPR DAGLβ knock out cell lines.

Membrane preps and cell lysates were prepared of parental CB1-Tango cells (Ctrl) and DAGLβ knock out lines F, H, G2 and C3. 20μg of protein was loaded and run on SDS-PAGE gel before transferring onto nitrocellulose membrane and probed for DAGLβ expression (~73kD). Bands were visualised using ECL analysis in membrane preparations (A) and whole cell lysates (B).

(A)

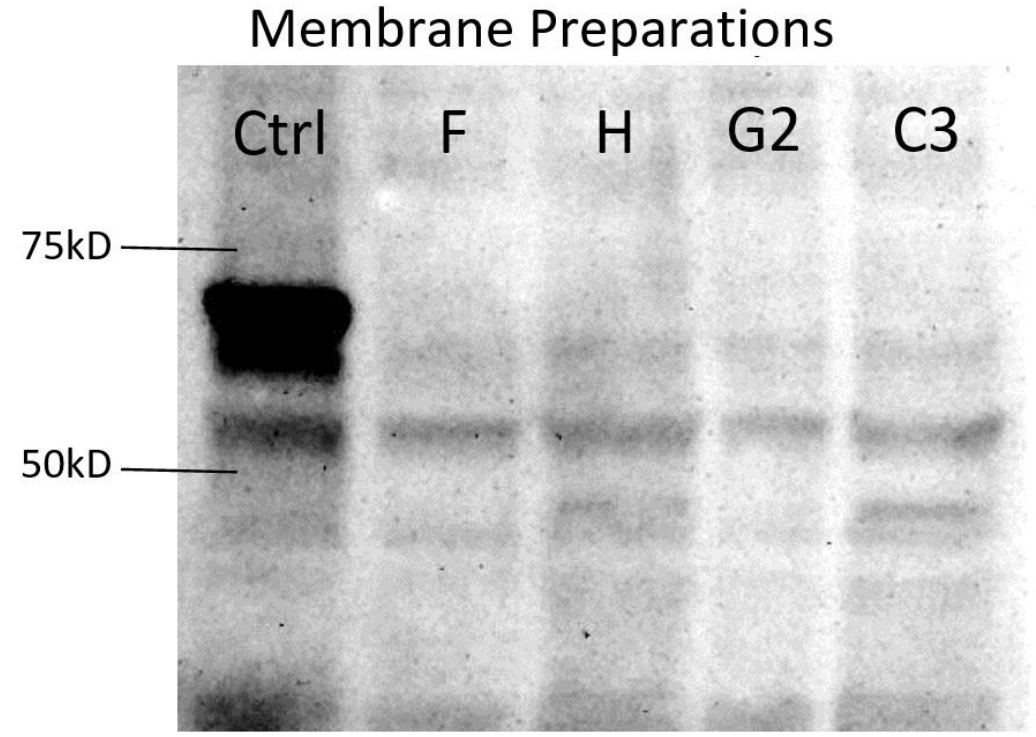
Membrane Preparations
Ctrl
F
H
G2
C3
75kD
50kD

(B)

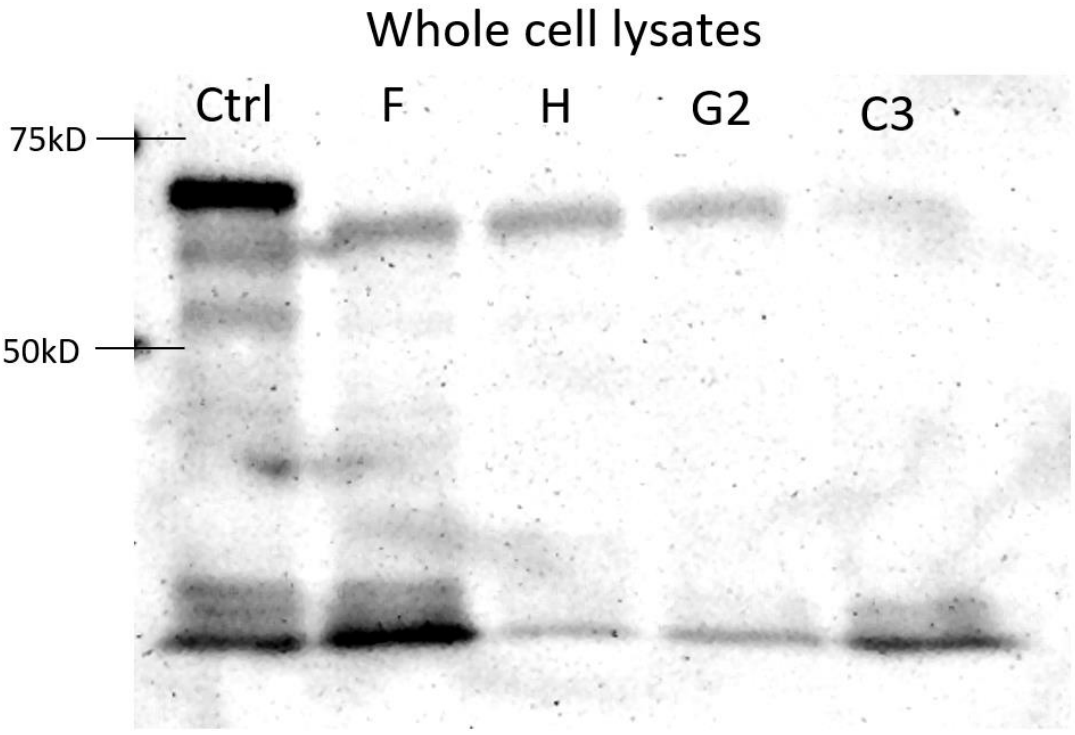
Whole cell lysates
Ctrl
F
H
G2
C3
75kD
50kD

DAGLα/β double knockout generation and characterisation

In tandem with the generation of the DAGLβ KO line, the generation of a DAGLα/β KO line was carried out by other members of the lab (thesis of Rachel Lane Markwick, 2015). DAGLα was first targeted in the parental CB1-Tango cells with the same CRISPR methods using gRNAs designed to exon 14 where the catalytic residue serine is located. After expanding colonies of CRISPR transfected cells and sequencing of DAGLα transcripts from selected colonies, the KO line that showed most disrupted transcripts of DAGLα was taken forward as a DAGLα KO line. Following from that, DAGLβ was then targeted in the DAGLα KO line to generate a dual DAGLα/β KO line. The same DAGLβ CRISPR vector and methods were used as the ones described above.

Genomic sequencing of the CRIPSR site of both DAGLα and DAGLβ was carried out in the DAGLα/β KO cell line to decisively conclude the nature of the CRIPSR mutations (Figure 6.2.7). Only one mutation result of DAGLα was picked up from genomic DNA sequencing which was a 2bp deletion, however through sequencing of over 100 transcripts using RT-PCR it has been concluded that mRNA of DAGLα protein is produced with large deletions within the catalytic domain, effectively rendering the protein catalytically dead. Furthermore, there are no wildtype transcripts, suggesting a successful KO of both alleles of DAGLα (thesis of Rachel Lane Markwick, 2015). DAGLβ has successfully been shown to contain two different mutations, one per allele of the gene. One allele contains 4bp deletion and the other allele shows 1bp insertion. The mRNA of DAGLβ has also been shown to contain large deletions of exons of the catalytic domain.

To confirm the knock out at the protein level, western blot analysis was carried out on the KO cell line probing for DAGLβ. We were not confident that the DAGLα antibody was specific enough for western blot analysis of DAGLα as previous experiments often detected non-specific bands. Membrane preparations of parental CB1-Tango and DAGLα/β KO cells were prepared as described in methods. DAGLβ protein was detected in CB1-Tango cells but not in DAGLα/β KO cells, and β-actin was also detected as a control. Based on the sequencing and western blot results, the DAGLα and DAGLβ transcripts and DAGLβ protein are non-functional in the DAGLα/β KO cell line.

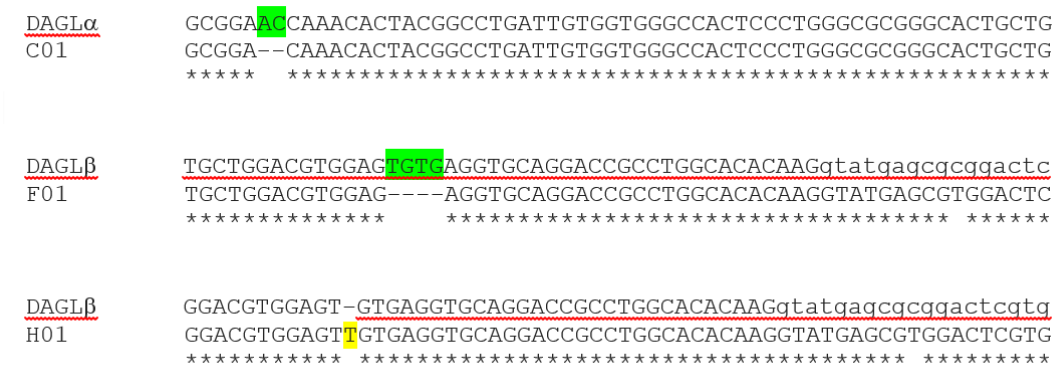

Figure 6.2.7. Sequencing reactions show mutations in genomic DNA of DAGLα and DAGLβ in DAGLα/β KO line.

PCR reactions of DAGLα and DAGLβ flanking the exon of the CRISPR site (DAGLα exon 14, DAGLβ exon 9) was carried out and run on 1% agarose gel. The resolved band was cut from the gel and purified using gel extraction kit according to manufacturer's instructions. The purified PCR product was cloned into TOPO vectors and transformed into bacteria which were sent for Sanger sequencing. Results were aligned against expected amplification sequence (top row sequences) obtained from Ensembl on Clustal Omega. Mutations are highlighted as green for deletions and yellow for insertions.

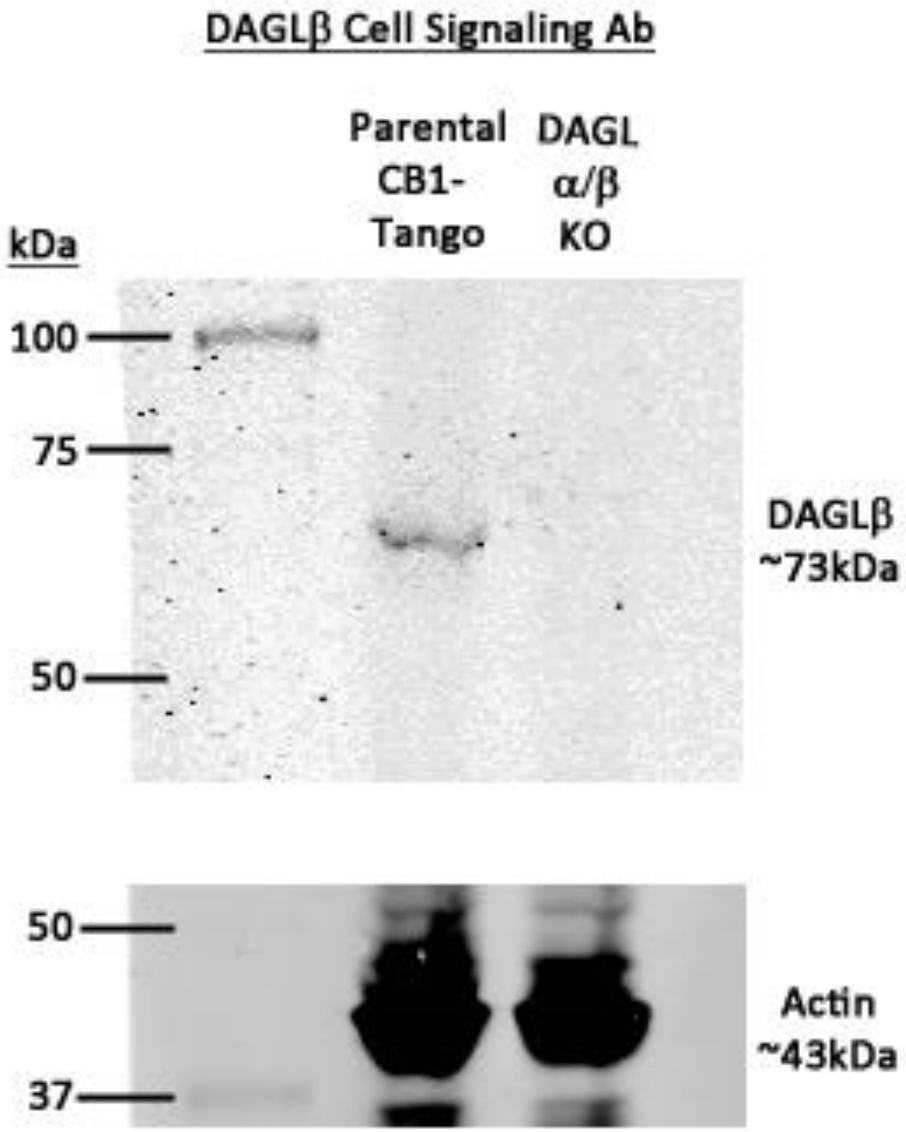

Figure 6.2.8. Western blotting shows lack of expression of DAGLβ in DAGLα/β KO cells

Parental CB1-Tango cells and DAGLα/β KO cells were grown on 10cm dishes until 90% confluent. Cells were then washed with cold PBS and were harvested and membranes were extracted from both cell lines, details in methods. Samples of membranes were then prepared with a total of 20μg of protein in each sample and loaded onto a 7.5% SDS-PAGE gel. The gel was then transferred onto nitrocellulose membrane and blocked with 5% milk for 1 hour. Primary anti-DAGLβ antibody (Cell Signaling) was diluted in milk 1:2500 and incubated with the membrane for 1 hour before being washed. Secondary anti-rabbit antibody was diluted in milk 1:10,000 and incubated with the membrane for 1 hour and then

washed. The blot was visualised on the Odyssey system (Licor) and then stripped and reprobed for actin.

Measurement of 2-AG in the DAGL KO lines show DAGLα is responsible for 2-AG synthesis in the CB1-Tango cells

Having generated three DAGL KO lines, it was prudent to determine the effects this has on the production of 2-AG in the cells, the relative contribution of each DAGL to 2-AG production and to the overall lipid biome in the cells. Lipid levels of 2-AG, AEA and related lipids OEA and PEA were measured from pelleted samples of the parental CB1-Tango line and each DAGL KO cell line and normalised to pg per 10^6 cells.

Levels of lipids were measured from 3-6 independent cell samples from each individual experiment and pooled across three independent experiments for the parental CB1-Tango cells and DAGLα/β KO cells and two independent experiments for the other cell lines with the final level taken as the mean of all of the individual cultures. Levels might fluctuate depending on growth status and batches of cells as the cells could be a heterogenous population with different basal signalling levels.

2-AG can readily be detected in parental CB1-Tango cells (890.69 ± 191.04 pg/10^6 cells) (Figure 6.2.9). Levels of 2-AG were significantly lower in the DAGLα KO cells (194.19 ± 28.57 pg/10^6 cells) and even lower in the dual DAGLα/β KO (108.94 ± 13.20 pg/10^6 cells) which was about 10% of the level seen in parental cells. These results indicate that DAGLα is central in the production of 2-AG in the CB1-Tango cells but that dual KO of both DAGLs produces the most pronounced effect on 2-AG. Interestingly in DAGLβ KO cells, 2-AG levels were significantly higher (1902.61 ± 244.32 pg/10^6 cells) than the level seen in parental cells. This might simply be a clonal artefact, but it does suggest that DAGLα is the dominant enzyme controlling 2-AG levels.

AEA levels were detected in parental CB1-Tango cells at a much lower levels than 2-AG (2.41 ± 0.53 pg/10^6 cells), and showed little change in individual DAGLα or DAGLβ KO lines. However, AEA levels were significantly increased in the DAGLα/β KO cells to 7.21 ± 0.96 pg/10^6 cells. Again, this might be a clonal artefact, but the results clearly show that AEA synthesis does not depend on the DAGLs. Other AEA related lipids OEA and PEA were also measured and showed little changes between the cell lines, however OEA was significantly higher in the in the DAGLα/β KO line.

Figure 6.2.9. Measurements of 2-AG, AEA, OEA and PEA levels in DAGL KO cell lines

Parental CB1-Tango cells and DAGL KO cell lines were grown in regular conditions until 90% confluent. Cells were then harvested and counted to ensure there were more than $6x10^6$ cells present per sample. Cells were then pelleted and immediately frozen in -80^oC and then shipped on dry ice for their lipid levels to be measured by mass spectrometry. 2-AG, AEA, OEA and PEA levels were measured in each sample and normalised to pg per 10^6 cells. Graph shows means and bars represent SEMs across independent samples (n = 12 for parental CB1-Tango cells; n = 9 for DAGLα KO, DAGLβ KO and DAGLα/β KO cells). Significance between groups was calculated using One Way ANOVA.

ns p>0.05; *p<0.05; **p<0.01; ***p<0.001; One Way ANOVA, Dunnett's post-test.

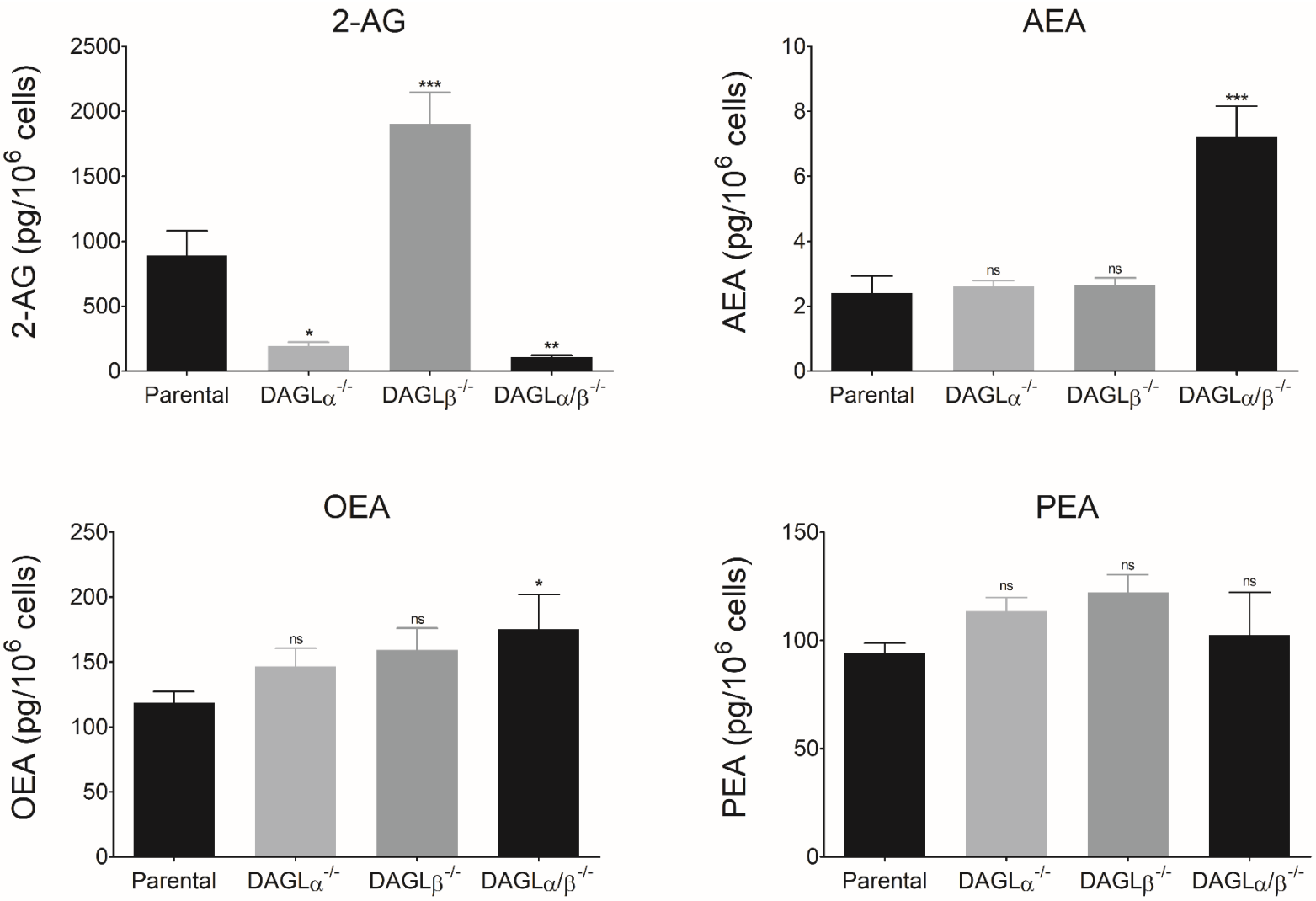
2-AG
2-AG (pg/10^6 cells)
2500
2000
1500
1000
500
0
***
*
**
Parental
DAGLα-/-
DAGLβ-/-
DAGLα/β-/-
AEA
AEA (pg/10^6 cells)
10
8
6
4
2
0
ns
ns
***
Parental
DAGLα-/-
DAGLβ-/-
DAGLα/β-/-
OEA
OEA (pg/10^6 cells)
250
200
150
100
50
0
ns
ns
*
Parental
DAGLα-/-
DAGLβ-/-
DAGLα/β-/-
PEA
PEA (pg/10^6 cells)
150
100
50
0
ns
ns
ns
Parental
DAGLα-/-
DAGLβ-/-
DAGLα/β-/-

Beads assay of DAGLα/β KO cell line show higher NAPEPLD transcript expression

The significantly higher AEA levels in DAGLα/β KO cell line were of interest as it confirmed that the AEA pathway was active in the CB1-Tango cells; this might be a causative effect, however we cannot exclude the possibility that it simply reflects clonal variation. Nonetheless, we once again performed the transcript beads assay on the DAGLα/β KO cells to determine if NAPEPLD levels were also higher and/or FAAH levels lower in this cell line as one of these might explain the higher levels of AEA.

Our probe sets for DAGLα and DAGLβ were not directed to the sites targeted for mutagenesis and as such can still detect mutated transcripts; thus, any changes in expression of these transcripts are not important as the transcripts do not encode functional enzymes.

Whilst most other components showed non-significant changes in transcript expression levels, the NAPEPLD transcript was significantly higher in the DAGLα/β KO line (1.022 ± 0.014 relative expression) (Figure 6.2.10). This is around a 5x increase in this clone over the level seen in the parental cell population (0.192 ± 0.003 relative expression). Thus, it is tempting to speculate that the increased expression of NAPEPLD transcripts might cause an increase in enzyme level and account for the increase in AEA levels, however this has not been directly tested. The transcript levels of FAAH in the DAGLα/β KO cells were around similar levels as those detected in the parental CB1-Tango cells, which is not likely to account for the increase in AEA levels produced in the DAGLα/β KO cells.

Also of interest are the transcript levels of MGLL, ABHD6 and PLA2G4B. MGLL levels were around 1.7x (Parental = 0.023 ± 0.002 relative expression; DAGLα/β KO = 0.041 ± 0.001 relative expression) higher in expression and ABHD6 levels were around 3x higher (Parental = 0.071 ± 0.003 relative expression; DAGLα/β KO = 0.205 ± 0.007 relative expression), both statistically significant. PLA2G4B transcript levels were also slightly, but not significantly, higher in the DAGLα/β KO clone (Parental = 0.313 ± 0.008 relative expression; DAGLα/β KO = 0.423 ± 0.006 relative expression). Again, these changes might reflect an adaptive response to the loss of the DAGLs, however they might simply reflect clonal variation. The most key point is the DAGLα/β KO cell line clearly retains transcripts for the enzymes that serve as gatekeepers in the eCB pathway.

Figure 6.2.10. Beads assay results show DAGLα/β KO cells have higher expression of NAPEPLD, PLA2G4B, MGLL and ABHD6

Parental CB1-Tango cells and DAGLα/β KO RNA was extracted from cells and diluted to 375μg/μl in 20μl for a total RNA amount of 7500ng per well. RNA was incubated with magnetics beads and probes overnight as described in methods. Amplification steps were carried out the next day as instructed by the manufacturer and the plate was read on the Magpix system. Data was analysed by subtracting the background readings from the sample readings and normalising to the expression of two housekeeping genes. Graph shows means and bars represent SEMs of 5 replicates of from one single experiment. Significance between groups was calculated using Student's T-test.

***p<0.001; unpaired Student's T-test, two-tailed.

(A)

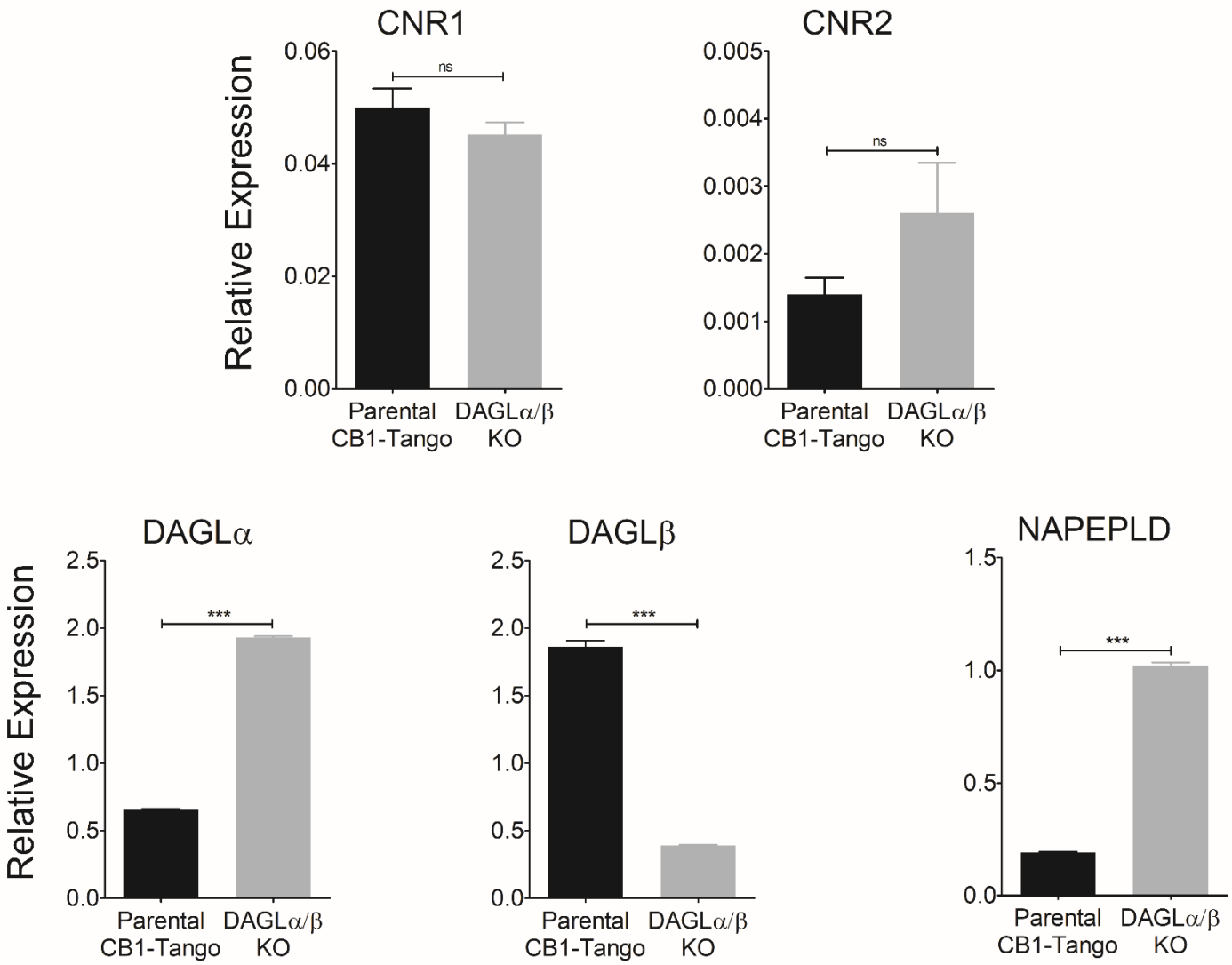
CNR1
Relative Expression
0.06
0.04
0.02
0.00
ns
Parental CB1-Tango
DAGLα/β KO
CNR2
0.005
0.004
0.003
0.002
0.001
0.000
ns
Parental CB1-Tango
DAGLα/β KO
DAGLα
Relative Expression
2.5
2.0
1.5
1.0
0.5
0.0
***
Parental CB1-Tango
DAGLα/β KO
DAGLβ
2.5
2.0
1.5
1.0
0.5
0.0
***
Parental CB1-Tango
DAGLα/β KO
NAPEPLD
1.5
1.0
0.5
0.0
***
Parental CB1-Tango
DAGLα/β KO

(B)

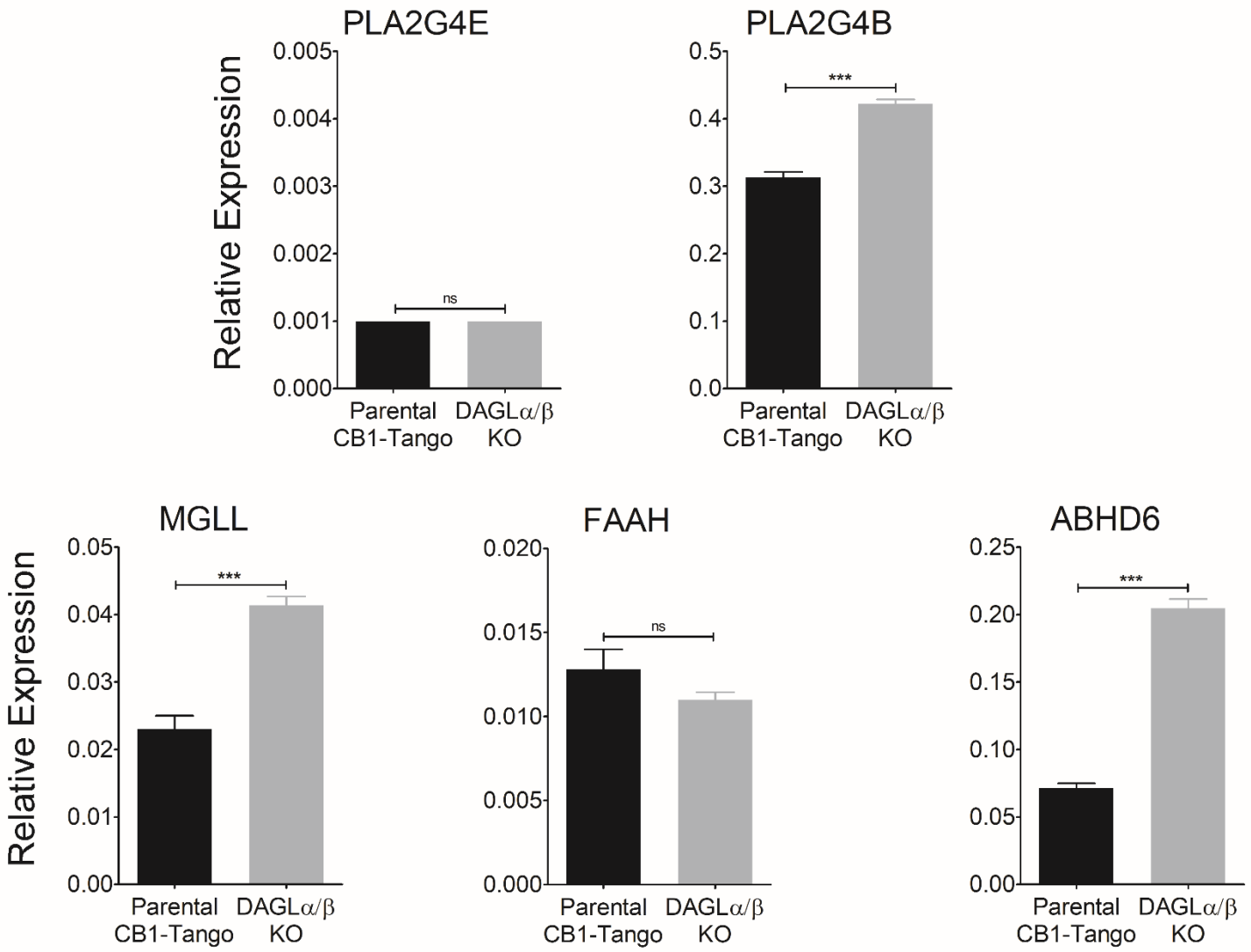
PLA2G4E
Relative Expression
0.005
0.004
0.003
0.002
0.001
0.000
ns
Parental CB1-Tango
DAGLα/β KO
PLA2G4B
0.5
0.4
0.3
0.2
0.1
0.0
***
Parental CB1-Tango
DAGLα/β KO
MGLL
Relative Expression
0.05
0.04
0.03
0.02
0.01
0.00
***
Parental CB1-Tango
DAGLα/β KO
FAAH
0.020
0.015
0.010
0.005
0.000
ns
Parental CB1-Tango
DAGLα/β KO
ABHD6
0.25
0.20
0.15
0.10
0.05
0.00
***
Parental CB1-Tango
DAGLα/β KO

eCB signalling is still present in the DAGLα/β KO cell line in McCoy's assay media

The DAGLα/β KO cells were tested in the CB1-Tango assay to see if the KO of the DAGLs affected eCB signalling. First, the responsiveness of the cells in the assay was tested using ACEA in 0.5% FBS McCoy's assay media. Parental CB1-Tango and DAGLα/β KO cells were plated overnight in McCoy's assay media and treated with ACEA in the presence and absence of AM251 in the standard 4 hour assay (Figure 6.2.11). The DAGLα/β KO cells are still responsive to the maximal ACEA concentration (226.7 ± 12.6% of control) to similar levels reached by parental CB1-Tango cells (245.6 ± 15.4% of control) and this response can be fully antagonised by AM251 to baseline levels suggesting no negative effects of CRISPR on the CB1 reporter assay itself.

Next, we looked to see if the basal eCB tone can still be generated in the DAGLα/β KO clone. The parental CB1-Tango and DAGLα/β KO cells were treated with JZL195 for 4 hours. An eCB tone is still clearly revealed by AM251 under these conditions in the DAGLα/β KO cells (150.6 ± 4.0% of AM251 control) and was actually higher in comparison to that seen in parental cells (129.5% ± 4.8% of AM251 control) (Figure 6.2.12). In non-JZL195 conditions, there was no significant eCB tone in parental CB1-Tango cells and or the DAGLα/β KO cells (Parental = 98.6 ± 3.2% of AM251 control; DAGLα/β KO = 107.5 ± 2.3% of AM251 control) (data not shown), confirming that the eCB tone in both cell lines is consequential to the presence of JZL195. Thus we can conclude that the DAGLs are not responsible for this tone and this is in keeping with the earlier pharmacological results. The apparent increase in the tone in the DAGL knockout line might be consequential to loss of these enzymes, but it might simply reflect clonal variability.

In response to a 4 hour treatment with ionomycin in the presence of JZL195, a CB1 response was still readily detected in the DAGLα/β KO cells (186.9 ± 10.4% of AM251 control) and this was of a similar magnitude to the response seen in the parental CB1-Tango cells (200.1 ± 31.0% on AM251 control) (Figure 6.2.13). Responses in both cell lines are substantially, but again not fully inhibited by AM251. The residual response in both cases might reflect the competitive nature of AM251 that might have failed to fully block an eCB response or as discussed previously, the ionomycin response might also have a non-specific component. The level of the ionomycin response has not reduced to halfway, as predicted previously with the use of DAGL inhibitors, and is on a comparable level to parental CB1-Tango cells, this is evidence for a DAGL-independent calcium induced eCB response.

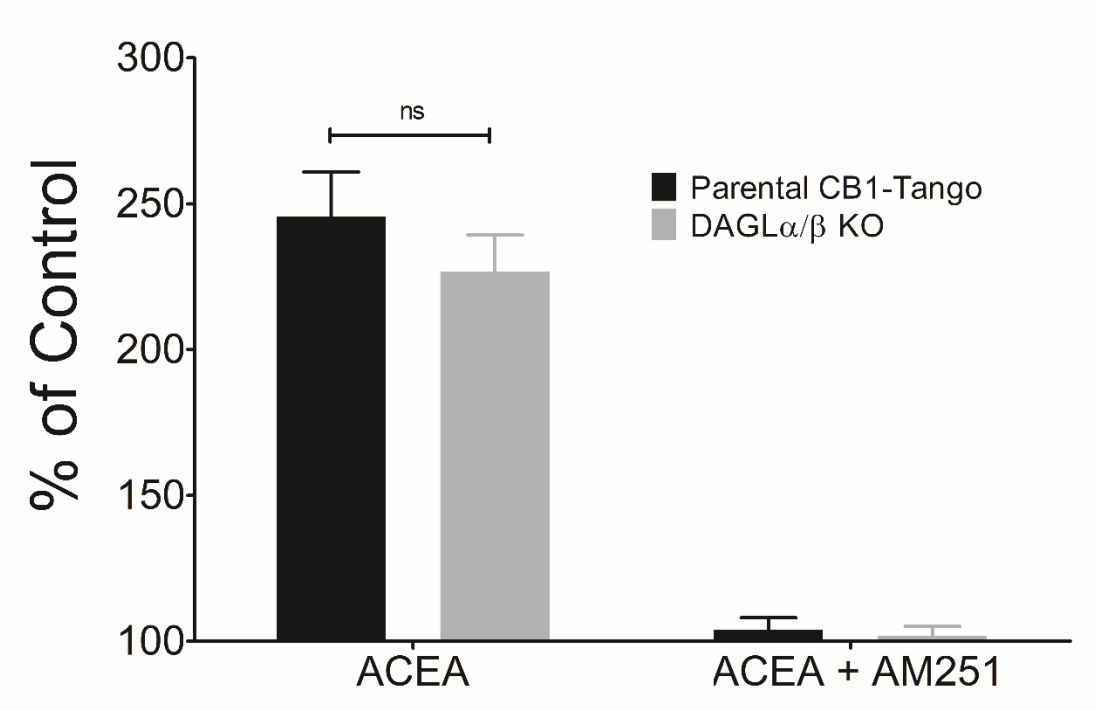

Figure 6.2.11. The ACEA response is present in the DAGLα/β KO cells and comparable to parental CB1-Tango cells

30,000 cells per well were seeded in McCoy's plating media in 96 well black plates and incubated overnight in 37°C. Cells were treated for 4 hours with 5μM ACEA in the presence and absence of AM251 (2.5μM). Assay substrate was combined according to manufacturer's instructions and added to the cells for 90 minutes before being read on the Flexstation. Data was normalised to control wells (set as 100) as % of control. Graph shows means and bars represent SEMs of n = 6 independent experiments, 8 technical replicates in each experiment. Significance between groups was calculated using Student's T-test.

*p<0.05; unpaired Student's T-test, two-tailed.

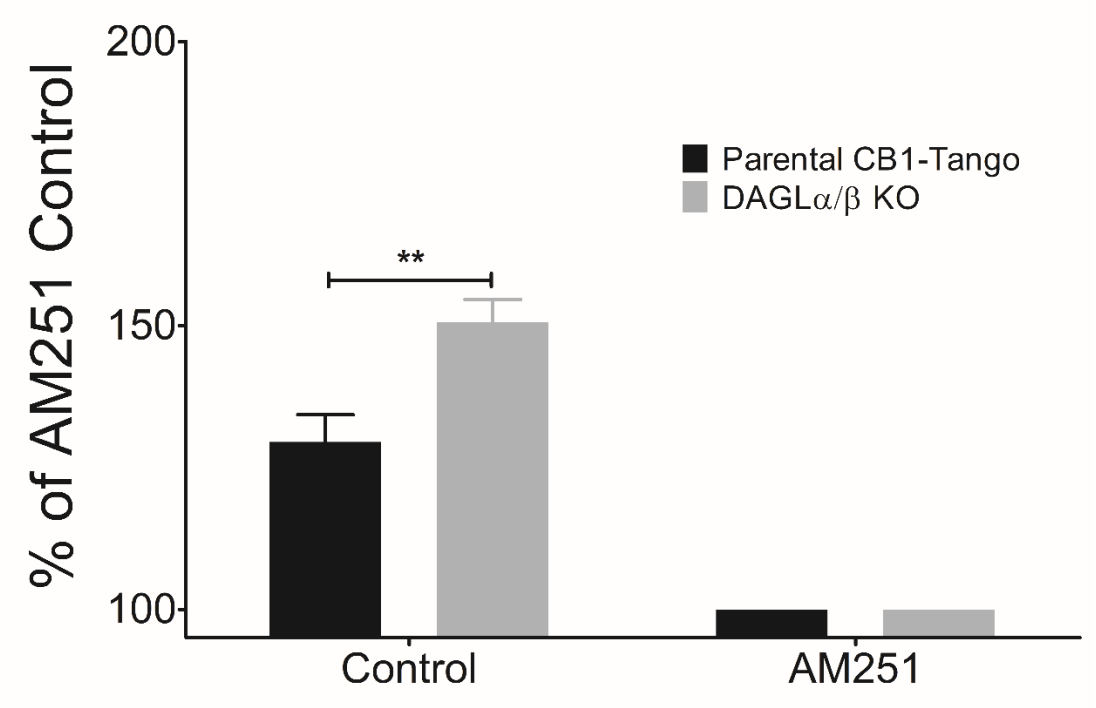

Figure 6.2.12. The eCB tone in DAGLα/β KO cells is elevated compared to parental CB1-Tango cells

30,000 cells per well were seeded in McCoy's plating media in 96 well black plates and incubated overnight in 37°C. Cells were treated for 4 hours with 100nM JZL195 in the presence and absence of AM251 (FAC 2.5μM). Assay substrate was combined according to manufacturer's instructions and added to the cells for 90 minutes before being read on the Flexstation. To best visualise the eCB tone present shown by JZL195, the data was normalised to the wells containing AM251 (set as 100) as % of AM251. Graph shows means and bars represent SEMs of n = 6 independent experiments, 8 technical replicates in each experiment. Significance between groups was calculated using Student's T-test.

**p<0.01; unpaired Student's T-test, two-tailed.

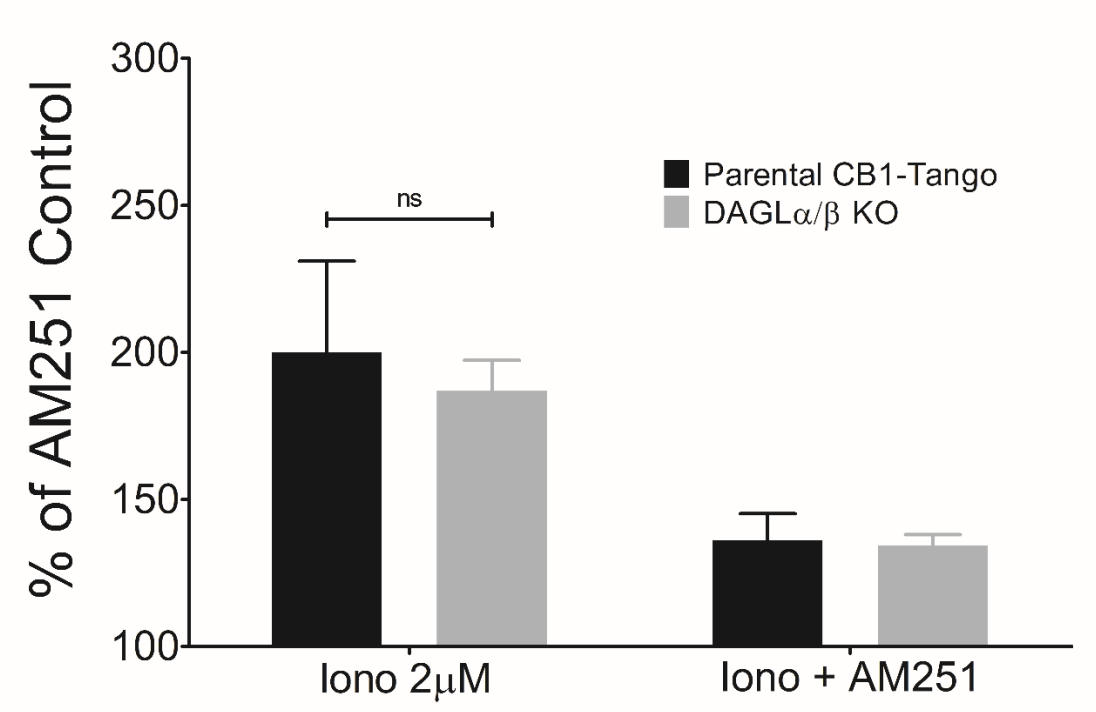

Figure 6.2.13. Ionomycin response in DAGLα/β KO cells and parental CB1-Tango cells are similar

CB1-Tango cells and DAGLα/β KO cells were plated into 96 well black plates in 100μl of McCoy's plating media and incubated overnight. Cells were then treated with ionomycin (2μM) in the presence and absence of AM251 (2.5μM) for 4 hours. 100nM JZL195 was included in all the wells. Substrate was added for 90 minutes at room temperature and read on the Flexstation. Data collected were normalised to wells containing AM251 (set as 100) as % of AM251 control. Graph shows means and bars represent SEMs of n = 4 for parental CB1-Tango and n = 5 for DAGLα/β KO, 8 technical replicates in each experiment. Significance between groups was calculated using Student's T-test.

ns p>0.05; unpaired Student's T-test, two-tailed.

FSK and PMA can still elicit eCB signalling in DAGLα/β KO cells in No Starve Freestyle media

Next, we tested the DAGLα/β KO cells in Freestyle media supplemented with 2mM calcium and 100nM JZL195. Again, the ACEA response was first tested to see if the cells still respond in a comparable manner to parental CB1-Tango cells. The cells were plated and ACEA and AM251 were added immediately afterwards for 24 hours (Figure 6.2.14). Both parental CB1-Tango cells and DAGLα/β KO cells were able to generate a substantial ACEA response in this assay condition (parental CB1-Tango = 612.8 ± 30.6; DAGLα/β KO = 688.1 ± 55.5% of AM251 control). There is no statistically significant difference between the maximal ACEA responses between parental CB1-Tango cells and the DAGLα/β KO cells indicating the expression of similar levels of CB1 receptors. AM251 was also able to largely block the ACEA response in both cell lines.

To test the presence of the eCB tone in the DAGLα/β KO cells in this paradigm, both parental CB1-Tango cells and DAGLα/β KO cells were plated in the same way in No Starve Freestyle media conditions in the presence of 2mM calcium and 100nM JZL195. AM251 was included as the control and data was normalised to the wells containing AM251 only (set to 100%) (Figure 6.2.15). The results show the presence of a significant eCB tone in DAGLα/β KO cells (356.0 ± 14.4% of AM251 control), which is actually higher in comparison to parental CB1-Tango cells (246.2 ± 12.0% of AM251 control), much like in the McCoy's assay media. Thus, in agreement with the pharmacological results this substantial eCB tone does not depend on DAGL function. Possible reasons for the enhanced response in the DAGL knockout cells will be discussed later.

Following from this, the effects of FSK and PMA were tested to see if the cells still have kinase driven eCB signalling. The cells were treated with 10μM FSK for 24 hours in the No Starve Freestyle conditions in the presence and absence of AM251 (Figure 6.2.16). A robust response was detected in both cell lines which was essentially inhibited by AM251 indicating CB1-dependency (parental CB1-Tango = 656.8 ± 40.1%; DAGLα/β KO = 522.3 ± 26.5% of AM251 control). The FSK response in DAGLα/β KO cells was slightly lower when compared to the parental CB1-Tango cells and is not as robust as the ACEA response. However, the main observation is that there is a very substantial FSK response in the knockout cells confirming previous pharmacological results that suggested this is not DAGL dependent.

Lastly, the cells were treated with 25nM PMA in the presence and absence of AM251 in the No Starve Freestyle conditions for 24 hours (Figure 6.2.17). PMA could elicit a CB1 dependent

response in both cell lines which was mostly blocked by AM251 but did show a component which could not be blocked by AM251 in both cell lines. In the DAGLα/β KO cells the PMA response reached 277.8 ± 21.5% of control, which is very robust but significantly lower when compared to the parental CB1-Tango cells response (383.2 ± 7.7% of AM251 control). This comparatively reduced response might be attributable to the KO of the DAGLs, but it might simply reflect clonal variability. However, the important observation is that a robust and substantial PMA response can be elicited in the absence of the DAGLs, and again this is consistent with previous pharmacology results.

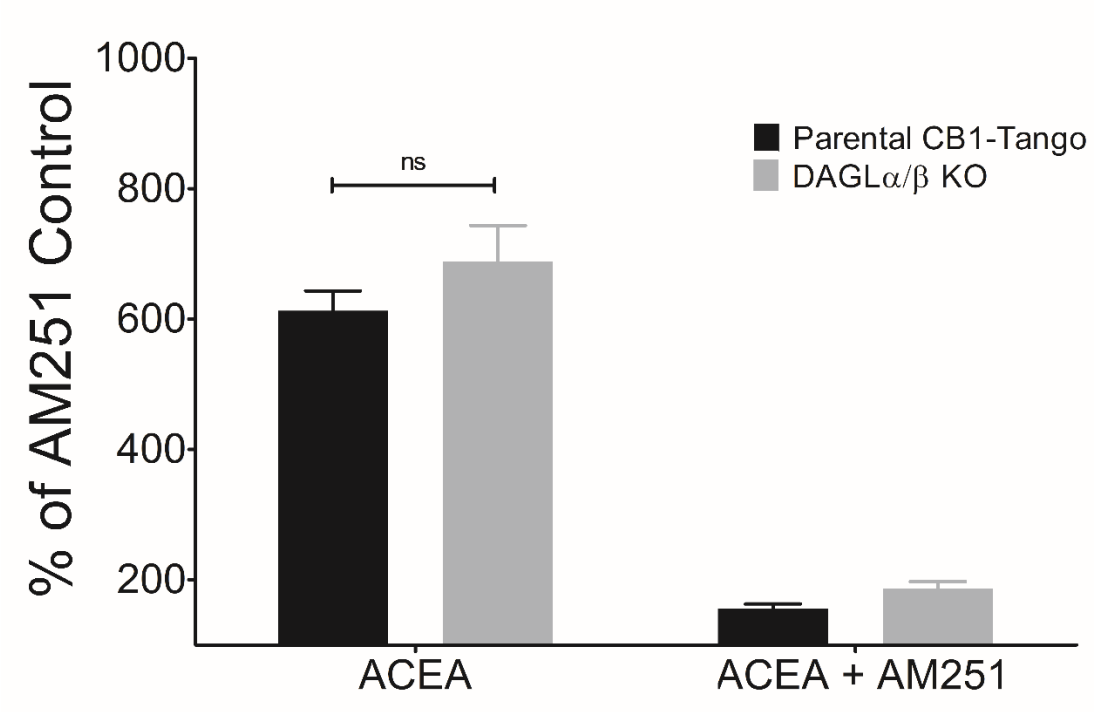

Figure 6.2.14. ACEA responses is comparable between the two cell lines in Freestyle no starve conditions

30,000 of parental CB1-Tango and DAGLα/β KO cells were plated in 100µl of Freestyle media with 2mM Ca^{2+} and 100nM JZL195. 5µM (FAC) ACEA in the presence and absence of 2.5µM (FAC) AM251 was added to the cells shortly after plating and left for 24 hours in the incubator. Substrate was added to the cells the next day for 90 minutes and read on the Flexstation. Data collected was normalised to wells containing AM251 only (set to 100) as % of AM251 control. Graph shows means and bars represent SEMs of n = 3 independent experiments, 8 technical replicates in each experiment. Significance between groups was calculated using Student's T-test.

ns p>0.05; unpaired Student's T-test, two-tailed.

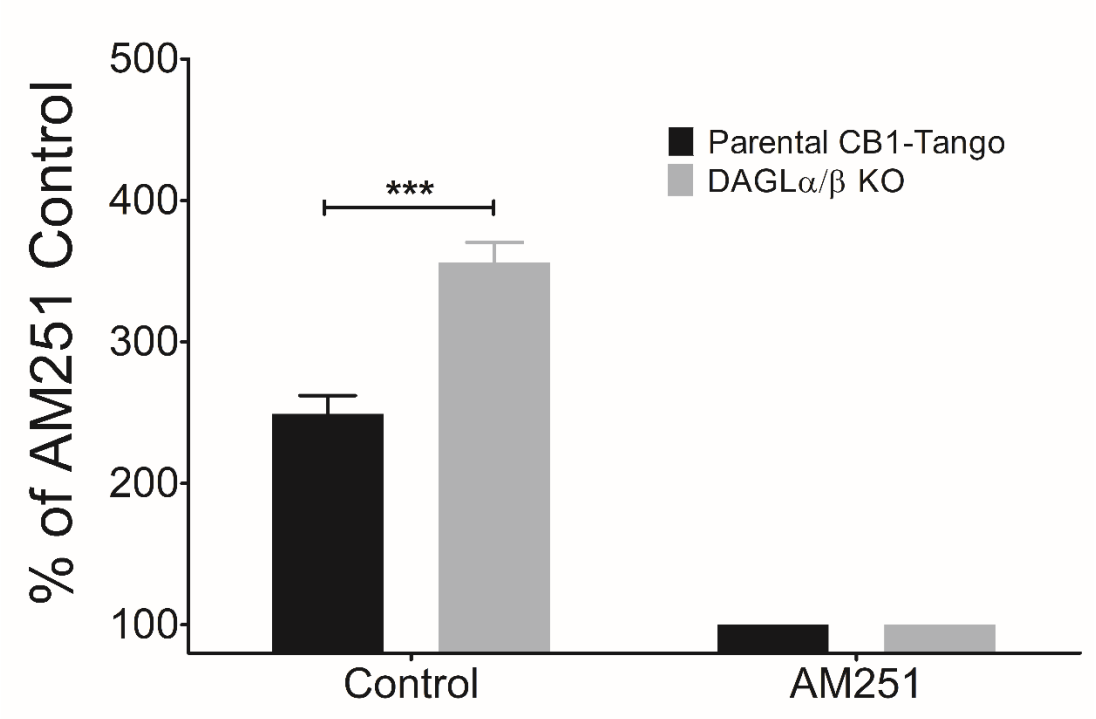

Figure 6.2.15. The eCB tone is enhanced in DAGLα/β KO cells compared to parental CB1-Tango in reduced starve conditions

CB1-Tango cells and DAGLα/β KO cells were plated into 96 well black plates in 100μl of Freestyle media supplemented with 2mM Ca^{2+} and 100nM JZL195. Cells were treated with AM251 (2.5μM) diluted in the plating medium immediately after plating the cells and incubated for 24 hours. Substrate was added for 90 minutes at room temperature and read on the Flexstation. To best display the eCB tone produced in this condition, data collected were normalised to wells containing AM251 (set as 100) as % of AM251 control. Graph shows means and bars represent SEMs of n = 9 for parental CB1-Tango and n = 16 for DAGLα/β KO, 8 technical replicates in each experiment. Significance between groups was calculated using Student's T-test.

***p<0.001; unpaired Student's T-test, two-tailed.

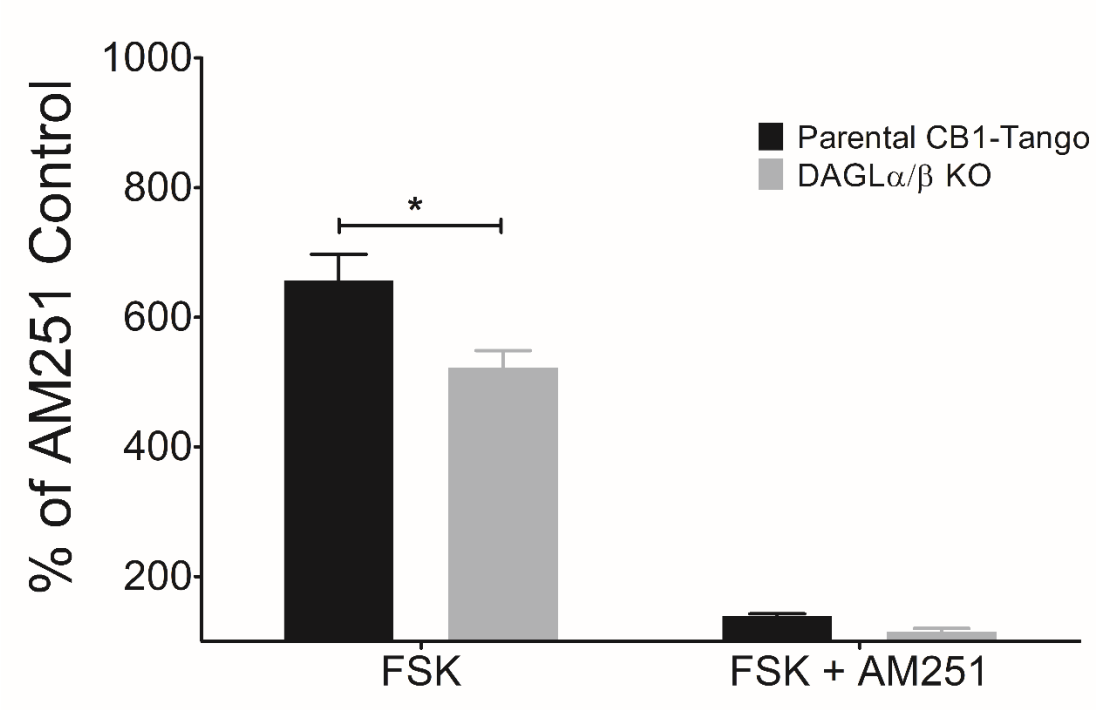

Figure 6.2.16. FSK induced response is reduced in DAGLα/β KO cells

30,000 of parental CB1-Tango and DAGLα/β KO cells were plated in 100µl of Freestyle media supplemented with 2mM Ca^{2+} and 100nM JZL195. FAC 10µM FSK in the presence and absence of FAC 2.5µM AM251 was added to the cells shortly after plating and left for 24 hours in the incubator. Substrate was added to the cells the next day for 90 minutes and read on the Flexstation. Data collected was normalised to wells containing AM251 only (set to 100) as % of AM251 control. Graph shows means and bars represent SEMs of n = 3 independent experiments for parental CB1-Tango and n = 7 for DAGLα/β KO cells, 8 technical replicates in each experiment. Significance between groups was calculated using Student's T-test.

*p<0.05; unpaired Student's T-test, two-tailed.

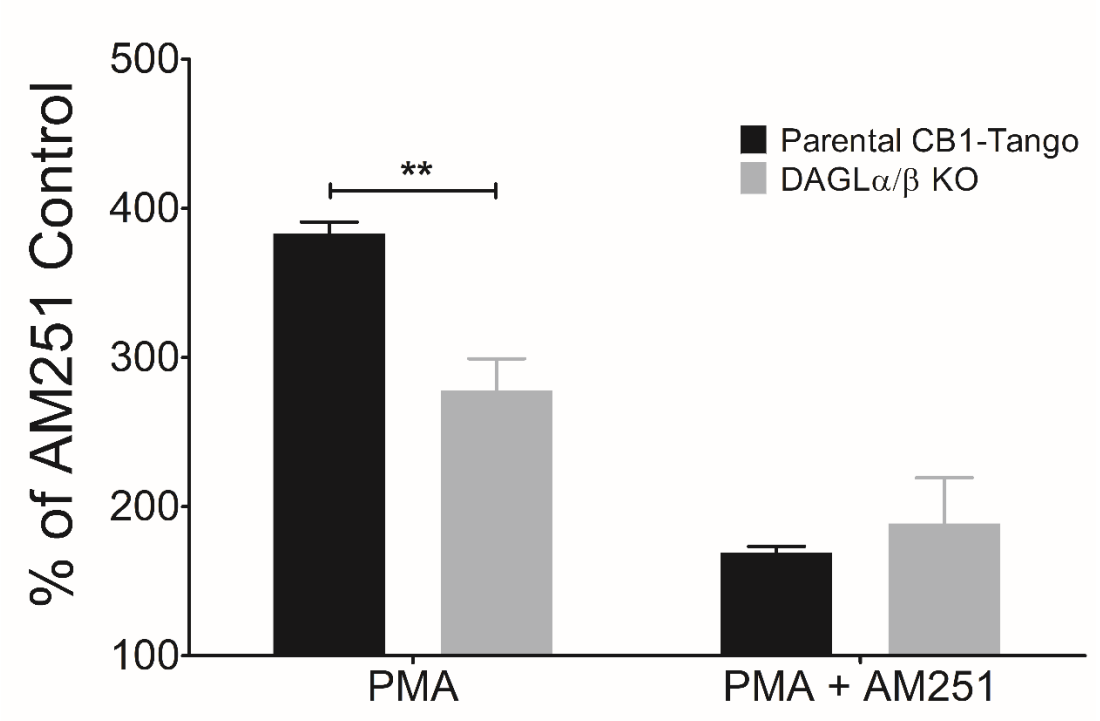

Figure 6.2.17. PMA induced response is reduced in DAGLα/β KO cells

30,000 of parental CB1-Tango and DAGLα/β KO cells were plated in 100µl of Freestyle media supplemented with 2mM Ca^{2+} and 100nM JZL195. FAC 25nM PMA in the presence and absence of 2.5µM AM251 was added to the cells shortly after plating and left for 24 hours in the incubator. Substrate was added to the cells the next day for 90 minutes and read on the Flexstation. Data collected was normalised to wells containing AM251 only (set to 100) as % of AM251 control. Graph shows means and bars represent SEMs of n = 4 independent experiments for parental CB1-Tango and n = 5 for DAGLα/β KO cells, 8 technical replicates in each experiment. Significance between groups was calculated using Student's T-test.

**p<0.01; unpaired Student's T-test, two-tailed.

6.2.3 **Results 4A.** Summary & Conclusions

To complement the pharmacological studies of eCB signalling in the CB1-Tango cell line, a genetic approach was taken to disrupt DAGL function which would give us a platform for studies of the non-DAGL dependent eCB pathway. CRISPR is a relatively new and powerful tool for genome editing which uses gRNA to guide Cas9 nuclease to target sequences which has been utilised to target DAGLα and DAGLβ. As gRNA can be readily replaced within CRISPR vectors, compared to ZNFs and TALENs, CRISPR is a relatively faster and simpler method of genome editing. Viable CRISPR vectors were created targeted to the catalytic domain of DAGLβ and validated by the Surveyor nuclease confirming that our guide sequences can create indel mutations within the genomic DNA.

Following treatment with the CRISPR constructs and the selection of resistant colonies, RT-PCR revealed different PCR band sizes of the catalytic domain, indicative of modified mRNA of DAGLβ. It is worth noting that the control PCR product is a clear single band. As the RT-PCR spans exon 8 to exon 10, this suggests that there are no naturally spliced variant of DAGLβ which skips exon 9 as if this were the case a smaller PCR product (lacking exon 9) would also have been detected. Substantial differences in transcript size were only seen in some colonies, but not others, indicating that CRISPR has induced major as well as more subtle changes in gene structure. This suggests that in those cell lines with a shift in the RT-PCR, it is likely that the mRNA transcripts contain aberrant splicing of exon 9 due to CRISPR interference. This leads to the appearance of a smaller weighted band that has a consistent size across cell lines.

From the sequencing results in Table 6.2.1, it would appear that two knock out cell lines (F and C3) are not likely to be clonal as more than two transcripts were picked up. However, the nature of the mutations in the detected transcripts are intronic and exonic features that tend to occur across different knock out cell lines. Commonly, large deletions and insertions are present – 78bp, 128bp and 209bp deletions correspond to complete bypass of exons 9, 11 and both 10 & 11 respectively; whilst the 299bp insert correspond to retained intron sequences located between exons 8 – 9. These exonic and intronic deletions and insertions are detected at relatively low frequencies indicating the instability of these transcripts, particularly as the host cell line is originally a cancer cell line which may have aberrant splicing due to differentially expressed genes (Fackenthal and Godley, 2008; Eswaran et al., 2013). Thus the presence of more than two transcripts is likely to be a product of aberrant splicing

caused by CRISPR but it could also be possible that the selected colonies were originally not clonal and derived from two or more cell types.

Smaller insertions and deletions tend to occur within the exon sequence which is more likely to be a genuine disruption of the genomic DNA compared to the indel mutations found between exons. Surprisingly the mutation at the CRISPR site was commonly seen across the other cell lines. The same 1bp insertion, located at the CRISPR site may possibly occur because of HDR from a similar template or from one allele using the second allele as a template (Canver et al., 2014). It is of note to point out that the 1bp deletion seen in the first sequencing result from KO line H (Table 6.2.1) was not picked up in the second round of sequencing, but a different 1bp deletion in exon 14 was found (Table 6.2.2). It is uncertain whether this is due to the mutations being present in low frequency within the population or if it is due to sequencing errors.

It is possible to target genes using CRISPR with a slightly altered strategy of using two double strand breaks to induce a large deletion of the intervening segment (Canver et al., 2014). This method may prove more reliable as only 2/3 of indel mutations would give rise to a frameshift mutation, as shown in Table 6.2.1 – certain clones can produce in frame mutations, and alternative splicing may compensate for the gene disruption. This method would rely on major disruptions on the genome, which may impact on other genes within the cell such as DAGLα due to its homology with DAGLβ that could potentially impact on the viability of the cell. To mitigate against this, gRNAs would have to be designed to unique stretches of DNA to prevent off target effects. Nonetheless, western blot analysis shows a very a substantial reduction in the expression of wild type DAGLβ from cell membranes and lysate.

The DAGLα/β KO line was also generated using the same strategy as the DAGLβ KO line (thesis of Rachel Lane Markwick, 2015). From the sequencing results, DAGLα and DAGLβ are both mutated in ways that if protein product is expressed it would not be enzymatically active as the catalytic domain is functionally compromised. Western blot analysis of DAGLβ was carried out as the antibody can consistently detect DAGLβ, however the DAGLα antibody proved to be unreliable and often detects non-specific bands, thus DAGLα protein function was not determined until lipid measurements were carried out from the parental CB1-Tango line and the three KO cell lines.

Lipid measurements revealed the large depletion of 2-AG from the DAGLα KO line which was only slightly lower in the dual DAGLα/β KO line. This confirms the KO of DAGLα, and also suggests that DAGLα is the key enzyme contributing to 2-AG synthesis in the cell line. This is surprising as DAGLβ transcripts were detected much more highly in the CB1-Tango cells but do not seem to be contributing much to 2-AG synthesis. This was observed previously in studies with commercially available DAGL surrogate substrates (Pedicord et al., 2011), namely p-nitrophenyl butyrate (PNPB) and 6,8-difluoro-4-methylumbelliferyl octanoate (DiFMUO). The substrates were used on CB1-Tango cell lines stably overexpressing DAGLs with a V5 tag for use in a live cell assay (Singh et al., 2016). Overexpressed DAGLα-V5 was far more (~5 fold) active than overexpressed DAGLβ-V5 in hydrolysing the surrogate substrates despite DAGLβ-V5 having higher expression levels in western blot analysis (thesis of Praveen K Singh, 2013). Thus, despite the very high homology between the DAGLs, and the fact that they catalyse the same physiological reaction, there are in fact clear differences between the catalytic properties of DAGLα and DAGLβ.

From the lipid measurements of the DAGLβ KO line, 2-AG levels are significantly higher than those seen in parental cells. This is unexpected and the reasons for the significantly higher 2-AG levels in DAGLβ KO cells are unknown. As the DAGLβ KO cells were generated separately from the DAGLα and DAGLα/β KO cells, it could be likely that due to clonal differences between the cell lines that the DAGLβ KO cell line was derived from a cell that had higher endogenous production of 2-AG. However, it is possible that this is a real adaption to the loss of DAGLβ, as mentioned above, DAGLβ might have different catalytic properties to DAGLα. For example, the KO of DAGLβ could essentially increase the free levels of DAG which may be catalysed at a much faster rate by DAGLα, thus causing an increase in the levels of 2-AG. It was outside of the scope of the thesis to investigate this possibility, and it is perhaps noteworthy that similar increase in 2-AG levels are not seen in any brain regions or peripheral organ tissues in DAGLβ knockout animals (Gao et al., 2010; Tanimura et al., 2010; Yoshino et al., 2011). Nonetheless, the results do point to DAGLα as the major contributor to the generation of the basal pool of 2-AG in the CB1-Tango cells and DAGLβ may have a minor contribution. But, as stated our measurements reflect only the basal pool and further studies would be required to determine the contribution of each enzyme to stimulus induced increases in 2-AG levels.

Whilst the majority of the 2-AG levels has been depleted in DAGLα/β KO cells, a small detectable level of 2-AG is still present. This suggests that there may be other synthesis routes of 2-AG, for example through the actions of PLA_1 and lysoPLC (Higgs and Glomset, 1994). Recently, DDHD2 enzyme (previously regarded as a phospholipase A1) was purified from the soluble fraction of rat brain and exhibited *sn*-1 DAGL ability (Aso et al., 2016). This enzyme is ubiquitously expressed, with particularly high detection in the brain in astrocytes and neurons. When DDHD2 was overexpressed in CHO cells, 2-AG release from [^{14}C] SAG increased in a time dependent manner (Araki et al., 2016; Aso et al., 2016). This enzyme may also contribute to the generation of 2-AG, however the importance of this enzyme in cells and tissues for the generation of 2-AG requires further study. The low levels of 2-AG may also indicate the presence of a DAGL-independent signalling pool of 2-AG which may be stored, however this would also mean that the large majority of 2-AG is synthesised on demand as the abolishment of DAGLs reduced the majority of 2-AG levels.

Lipid measurements of AEA were unchanged in the individual KO lines, but were higher in the dual DAGLα/β KO clonal cell line. This again might simply reflect clonal variation, but nonetheless could reflect an adaptive change. Previous studies in KO mice showed surprising reductions in brain levels of AEA in DAGLα KO mice. Around 40-50% reduction of AEA was observed in whole brain (Gao et al., 2010; Ogasawara et al., 2016) with significant reductions in specific regions of the brain e.g. cortex, hippocampus and amygdala (Tanimura et al., 2010; Yoshino et al., 2011; Jenniches et al., 2016). This reduction in AEA levels was not seen in DAGLβ KO mice (Gao et al., 2010; Tanimura et al., 2010; Yoshino et al., 2011) and had no significant reduction in most brain regions in mice lacking both DAGLs (Yoshino et al., 2011). The crosstalk between DAGLα and thus the level of 2-AG and AEA levels observed in KO animals were reproducible using pharmacological blockade of the DAGLs with specific DAGL inhibitors. Blockade of both DAGLα and DAGLβ with selective inhibitors DH376 and DO34 significantly decreased whole brain levels of 2-AG (>80%) and AEA (~40%), mimicking the effects seen from animal KO studies (Ogasawara et al., 2016; Wilkerson et al., 2017). It seems there is crosstalk between DAGLα and thus 2-AG levels with AEA levels in a brain-region specific manner, although the underlying mechanism behind this is inconclusive but likely to be through indirect mechanisms such as maintenance of lipid pools or through the altered activity of cyclooxygenase which both 2-AG and AEA are substrates for (Gao et al., 2010; Di Marzo, 2011).

The increased levels of AEA from the DAGLα/β KO line therefore does not corroborate the majority of the studies mentioned above. However, there are brain specific regions where the KO of DAGLα did not affect AEA levels e.g. striatum (Tanimura et al., 2010; Jenniches et al., 2016). Therefore, the impact of DAGLα KO on AEA levels may differ depending on the degree of crosstalk between the two pathways. Again, the higher levels of AEA could just be reflective of clonal variances between the cell lines as there is little evidence to support the increase of AEA in the absence/inhibition of the DAGLs. It might also be worth noting the DAGLα/β KO clones have changed morphology and slower growth rate following the KO of DAGLs (unpublished observations). There are many reasons why this might be the case: perhaps the KO of DAGLs induced off-target effects which may affect cell morphology; the depletion of DAGLs, which may have other functions, affects cell survival; or the significantly increased levels of AEA may have a negative effect on the survival of the cells (Maccarrone et al., 2000a) – however the levels of AEA increase is relatively low so it is unclear if this is physiologically relevant and this increase is not seen in the CB1-Tango assay in the absence of JZL195.

Related lipids OEA is a proposed ligand for PPARα, TRPV1 and GPR119 receptors (Romano et al., 2014) and PEA is also a ligand for PPARα receptor (Petrosino et al., 2010). PEA showed no significant changes, whilst OEA had a small significant increase, however this slight increase could be due to clonal differences from a heterogenous pool of cells.

The increased AEA levels in the double DAGLα/β knockout cell line is possibly associated with an increase in transcript levels of NAPEPLD, with no change in FAAH transcripts. This increased expression serves as evidence of active pathways that can generate AEA for signalling in the eCB cells in the absence of the DAGLs. This increase in the ability of the cells to make AEA could conceivably account for the increase in eCB tone seen in response to JZL195 treatment in the DAGL deficient cells relative to the parental cells, an interesting possibly that perhaps warrants further investigation. Irrespective of the cause, the higher basal levels of AEA in these cells will be advantageous in further studies into the AEA pathways to determine which enzymes contribute to AEA synthesis. From the results of the QuantiGene beads assay, PLA2G4B transcript levels are also slightly, although significantly higher in this clonal cell line. Interestingly, MGLL and ABHD6 transcript levels are also significantly higher by 2 fold but FAAH transcript levels are similar, it would be of interest to determine if any of these are adaptive changes to loss of the DAGLs, but this was beyond the

scope of the thesis. Nonetheless, the increased expression of MAGL and ABHD6 transcripts could function to maintain the levels of AA and other lipids in the absence of DAGL which contribute greatly to the generation of AA (Gao et al., 2010). The transcripts of the DAGLs were also measured in the beads assay but it is not possible to measure accurate transcript levels using the probe sets on our beads as the probes are targeted to many sites on the gene and are insensitive to indel mutations.

The DAGLα/β KO cells were tested in the assay paradigms that were described in Chapter 5. Results show the expression of CB1 receptors to be similar between the DAGLα/β KO clone and the parental cells and importantly there was no obvious difference in responsiveness to ACEA in McCoy's assay media. A robust JZL195-elicited eCB tone is still present in the DAGLα/β KO cells, which agrees with previous pharmacological experiments with DAGL inhibitors KT107 and KT172 i.e. that the eCB tone produced in the presence of JZL195 is not DAGL dependent. This eCB tone is significantly increased despite the KO of the DAGLs which again might be due to clonal variability or a real adaptive change. If the increase in eCB is an adaptive change, one possible explanation is that it is reflective of the activation of the CB1 receptor by other eCBs which may have different signalling dynamics to 2-AG. For example, measured AEA levels may be much lower than 2-AG but AEA has shown much more potent activity towards the CB1 receptor than 2-AG (Sugiura et al., 1995; Steffens et al., 2005). This is also evidenced in previous CB1-Tango assays where the EC_{50} of AEA is lower than that of 2-AG. Another possibility is perhaps higher levels of eCBs are generated, for example the increased measured AEA levels in the DAGLα/β KO cell line. Despite the increased levels of AEA, there is no eCB tone present in the absence of JZL195, suggesting that perhaps the activity of MAGL, FAAH and ABHD6 is sufficient in limiting the activity of the increased AEA and perhaps any other eCBs produced.

Likewise, after treatment with ionomycin, there is still an inducible eCB signalling which is on comparable levels to parental CB1-Tango cells despite removing the DAGL dependent portion of the response. This increase in eCB tone and the maintenance of the ionomycin response in DAGLα/β KO cells was surprising as it suggests that despite the substantial reduction of 2-AG present in these cells, there is either more eCB signalling or that the DAGL dependent portion can be compensated for. One possibility is the increase in basal AEA levels is reflective of overall increased AEA generation and signalling, or it could also be the action of other possible eCBs that may have either increased synthesis or different signalling dynamics e.g. virodhamine, N-arachidonoyl dopamine or noladin ether.

Similarly, when tested in the No Starve Freestyle conditions, ACEA showed similar maximal responses and the eCB tone is also significantly increased in the DAGLα/β KO cells. When testing FSK and PMA responses, eCB signalling is slightly reduced in the DAGLα/β KO cells compared to parental CB1-Tango cells but there are still large responses that are elicited. The reduction of the responses might reflect the contribution of 2-AG to the responses, or it might be due to clonal variability. It is unknown precisely how the activity of PKA and PKC directly induces eCB signalling. The activity of PKA and PKC may induce synthesis of other eCBs, for example PKC dependent signalling promoted AEA and other NAE synthesis in neuronal cultures (Cadas et al., 1996; Vellani et al., 2008). However, the remaining response is further evidence that activation of PKA and PKC can evoke eCB signalling that is largely not DAGL and 2-AG dependent.

The above results clearly show that loss of the DAGLs has little, if any impact on eCB signalling in response to a wide range of stimuli. Given our sequencing results and the dramatic (~90%) reduction in 2-AG levels in the knockout cells, the conclusion that 2-AG is not responsible for a wide range of eCB signalling can be reached. This is further supported by the pharmacological evidence, for example KT109 and KT172 failed to inhibit the presence of the basal tone induced by JZL195 and in general had no impact on ionomycin, PKA or PKC responses. The one exception was a partial reduction in the enhanced ionomycin response seen in presence of JZL195.

It remains possible that the DAGLs can drive eCB responses stimulated by other agents or pathways. PKA and PKC were hypothesised as the key kinases that can activate DAGL activity, but other kinases may also activate the DAGLs (Reisenberg et al., 2012). Platelets stimulated by thrombin showed accumulation of 2-AG (Prescott and Majerus, 1983) and other stimuli such as ethanol and glutamate have been found to increase 2-AG levels in primary cultures of cerebellar granular neurons (Basavarajappa et al., 2000). Endothelin-1 and ATP can also stimulate 2-AG production from astrocytes via endothelin A receptor and $P2X_7$ receptors, although both stimuli require the presence of extracellular calcium (Walter and Stella, 2003; Walter et al., 2004). In the context of retrograde signalling, excitatory neurotransmitters such as glutamate, activate post synaptic receptors which drives eCB signalling via G-protein or calcium activation of PLCβ (Stella and Piomelli, 2001; Kano, 2014). As most of these stimuli function through receptors which require the extracellular presence of calcium, those stimuli were not tested in the CB1-Tango cells.

It is also possible that DAGL function in these cells is unrelated to eCB signalling. The presence of high transcript levels of the DAGLs appears paradoxal to the minor impact of these enzymes on eCB signalling, however the DAGLs can also generate other related lipid species which may have other signalling roles (Bisogno et al., 2003). This additional role would seem logical as a DAGL homologue is expressed in species such as *Drosophila melanogaster* which do not synthesise AA nor contain CB receptors (Elphick and Egertova, 2001; McPartland et al., 2001; Tortoriello et al., 2013), suggesting that the DAGLs can generate other MAGs for non-CB purposes. As well as this, the measured levels of 2-AG were magnitudes larger than AEA levels in the CB1-Tango cells, which was not unexpected as 2-AG is the most abundant eCB in the developing and adult brain (Mechoulam et al., 1995; Sugiura et al., 1999). The DAGLs were responsible for the generation of ~90% of 2-AG, but the presence of DAGLs and much higher levels of 2-AG had little impact on eCB signalling in the CB1-Tango cells. The presence and continual activity of the eCB degrading enzymes MAGL, ABHD6 and perhaps FAAH limits the signalling activity of the eCBs, but these could also have secondary roles, for instance in liberating the AA from the 2-AG produced by the DAGLs. Indeed, genetic and pharmacological studies of DAGL showed the levels of AA to be substantially reduced alongside 2-AG (Gao et al., 2010; Tanimura et al., 2010; Ogasawara et al., 2016). When viewed this way, the hydrolysis of 2-AG by MAGL/ABHD6 would have the direct function of generating AA as opposed to terminating the action of 2-AG for eCB signalling. The generation of AA could serve as precursors for eicosanoids such as PGE2 (Kozak et al., 2002) which are involved in various pathological processes such as inflammation in macrophages and microglia (Harizi et al., 2008). This function is supported by the presence of DAGLβ expression exclusively in microglia in the brain (Zhang et al., 2014) and has shown active involvement in inflammatory responses (Hsu et al., 2012). This highlights the DAGL/MAGL pathway may have a role in the CB1-Tango cells for the generation/regulation of AA levels, however it was beyond the scope of this thesis to determine contribution of DAGLs to the AA pool.

The DAGL knockout cell lines do have enhanced AEA levels and this is the next obvious candidate to be responsible for the robust eCB signalling that remains in the cells. They also express relatively high levels of NAPEPLD, an enzyme largely attributed to the synthesis of this eCB. However, this is a contentious point as some (but not all) animal KO studies of NAPEPLD have shown that NAPEPLD is dispensable in the synthesis of AEA (Leung et al., 2006; Tsuboi et al., 2011; Leishman et al., 2016), with one possibility being that

compensatory pathways could have emerged due to global deletion of NAPEPLD to maintain physiological levels of AEA. In addition, recent studies have identified other enzymes that might play pivotal roles in the synthesis of this eCB. Having generated a cell line that lacks the DAGLs and has lost ~90% of its basal levels of 2-AG, yet retains robust eCB responses to a variety of stimuli, we have perhaps inadvertently generated a very important model for identifying the pathways responsible for DAGL independent eCB signalling. In the next section of the thesis we will test the importance of NAPEPLD for AEA synthesis and eCB signalling in the DAGLα/β knockout cell line.

6.3 **Results 4B.** Evaluating the role of NAPEPLD in AEA synthesis

6.3.1 **Results 4B.** Introduction

Pharmacological inhibition and genetic knock out of the DAGLs has revealed that eCB signalling can still be robustly generated in a DAGL independent manner in the CB1-Tango cells. It is not known through which eCB this signalling occurs through, but it is speculated to be the second most characterised eCB: AEA. From the lipid measurements of the CRISPR treated cells, basal 2-AG levels were almost completely abolished upon the genetic KO of the DAGLs, highlighting the necessary involvement of the DAGLs in the generation of 2-AG, however basal levels of AEA were significantly higher than in parental CB1-Tango cells. FAAH transcript levels in the DAGLα/β KO cells were of similar levels to the parental CB1-Tango cells, however NAPEPLD transcripts are significantly higher suggesting that this might account for the this increase in AEA. AEA is also a good candidate to be the eCB that can be evoked in the CB1-Tango assay as it can be synthesised in response to various pharmacological stimulations (Di Marzo et al., 1994; Vellani et al., 2008; Ueda et al., 2013), but it is not currently known through which synthesis pathway(s) this occurs through.

AEA has been shown to be a key biological signalling molecule in both the CNS (Elphick and Egertova, 2001; Maccarrone et al., 2014; Di Marzo et al., 2015; Curran et al., 2016) and in the periphery (Berdyshev et al., 1997; Bab et al., 2008; Maccarrone et al., 2015). Due to the ubiquitous presence of AEA in the human body (and other organisms (Elphick, 2012)), focus has been placed on the emerging importance of the AEA as a signalling molecule, as it is a ligand for many receptors aside from CB1 and CB2, for example TRPV1, GPR55, GPR119 and PPARs (Brown and Robin Hiley, 2009; Godlewski et al., 2009; O'Sullivan and Kendall, 2010; Sousa-Valente et al., 2014). It has also therefore been of interest to elucidate through which mechanisms AEA is synthesised and potentially regulated.

NAPEPLD was identified as the enzyme in generating AEA from the precursor NAPE and is highly conserved in sequence from mice to humans (Okamoto et al., 2004). It belongs to the metallohydrolase family, shows calcium sensitivity (Ueda et al., 2001) and the requirement for bile acids for full function has been proposed as a regulation mechanism for NAPEPLD

(Magotti et al., 2015). NAPEPLD is also expressed in many organs in mice, with high expression in the brain and testes where AEA levels are relatively high, placing NAPEPLD as a principle candidate enzyme in AEA generation (Okamoto et al., 2004). However, from various animal KO studies of NAPEPLD, it has been shown that the lack of NAPEPLD enzyme can have little if any impact on AEA levels suggesting that it is not important, or that its loss can be compensated for by alternative routes producing AEA (Leung et al., 2006; Tsuboi et al., 2011; Leishman et al., 2016; Inoue et al., 2017). Most of these studies measured endogenous levels of AEA from the whole brain or large brain regions where compensation mechanisms can occur from different subpopulations of cells, and global deletion of an enzyme that may contribute to the generation of a widely distributed signalling molecule could cause the emergence of alternative pathways that may not normally be active and so should be interpreted with some caution. Based on this, we focused on the extent NAPEPLD is required for eCB signalling in a cell based system where the involvement from secondary pathways might be restricted.

NAPEPLD transcripts were readily detected in the CB1-Tango cells and were significantly higher in the DAGLα/β KO line, which may be connected to the high AEA levels measured in the DAGLα/β KO line. CRISPR strategy was utilised once again to genetically target the NAPEPLD gene from the DAGLα/β KO cells to generate a cell line with three disrupted genes to determine if eCB signalling in the CB1-Tango cells is impacted by the genetic deletion of three major eCB synthesis enzymes. However as mentioned previously, the currently adopted CRISPR technique described by Ran et al. (2013) and used to disrupt the DAGL genes causes relatively subtle changes in the genome thus characterisation of the effects of CRISPR proves relatively inefficient. Therefore, for NAPEPLD a slightly different approach was adopted as described by Canver et al. (2014). Instead of transfecting pools of cells with individual CRISPR vectors and relying on the action of one gRNA, two or more gRNAs are used simultaneously to generate two double strand breaks for the deletion of a defined segment of a gene (Figure 6.3.1) and in this case of NAPEPLD, the region targeted was required for catalytic activity. This method would allow for clearly identifiable successful KO of genes using PCR primers flanking the deletion site, and allows for deletion of whole catalytic regions which may otherwise escape nonsense mediated decay via alternatively spliced variants of the genes. It is also possible to use QuantiGene Multiplex probes designed to the region targeted for deletion and thereby allows for a very simple assay to confirm loss of the transcript.

In this chapter, the generation of a NAPEPLD KO cell line from the DAGLα/β KO cell line using CRISPR will be described. The characterisation of the cell line determined the successful KO of NAPEPLD and the effects of triple gene KO on the measured eCB levels of the cells. The cell line will then be tested in the CB1-Tango assay using previously established paradigms that can generate eCB signalling to determine the necessity of NAPEPLD not only for the synthesis of the basal levels of AEA in the cells, but also for the cells ability to generate a robust eCB response to the various stimuli described previously.

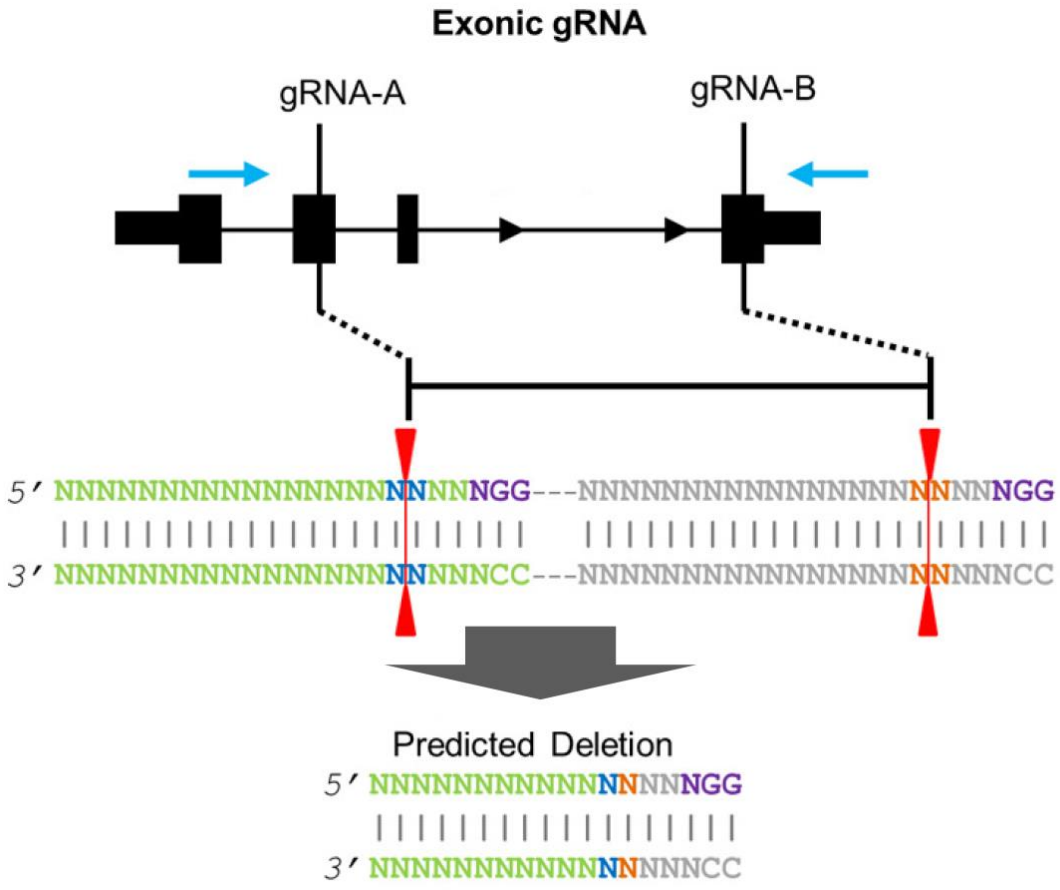

Figure 6.3.1. Schematic of genomic deletion using two or more CRISPR gRNA targets on a single gene

The two gRNA sites are shown located within two different exons of a gene. The gRNA sequences (green and grey) are shown on the top strand located immediately upstream of a subsequent PAM sequence (purple). The red line indicates the predicted Cas9 cleavage site between nucleotide positions 17 and 18 on the gRNA. The blue arrows indicate the position of PCR primers for deletion band amplification.

Adapted from Canver et al. (2014).

6.3.2 **Results 4B.** Results

Design of gRNAs to NAPEPLD catalytic domain and generation of CRISPR vectors

The NAPEPLD gene consists of 6 exons (Figure 6.3.2) coding for 393 amino acid length protein. Previous animal KO models genetically deleted exon 3 of NAPEPLD where the catalytic HXHXDH motif is situated (Okamoto et al., 2004). It was logical to therefore also aim for disruption of exon 3 with CRISPR. This region is 647bp long with the motif positioned in the centre of the exon, gRNAs were designed around the catalytic motif using public gRNA generation websites as described previously (Figure 6.3.2 and Table 2.1.2). For further analysis later using the QuantiGene multiplex assay system, it was also ensured that the Multiplex probes are designed to target the region of the transcript encoded by the stretch of DNA targeted for deletion.

Previous CRISPR experiments aimed to generate indel mutations which would cause frameshift mutations leading to disrupted protein, however with this method it was difficult to characterise the nature of the mutations as they are usually subtle. Instead, 4 gRNAs were selected based on their location prior to and after the HXHXDH motif (Figure 6.3.3) so that upon introduction of two double strand breaks, the two flanking regions would repair and the internal segment would be deleted (Canver et al., 2014). The largest deletion between the two furthest gRNAs is predicted to be around 243bp.

The gRNAs were inserted into the CRISPR backbone vector as previously described and four CRISPR vectors were generated. The vectors were then transfected into plated DAGLα/β KO cells as described in Methods. Pools of cells were transfected with one gRNA vector or all four gRNA vectors together. After transfection and puromycin selection, the remaining cells were seeded at low density to facilitate the growth of individual cells into discrete colonies that could be picked and expanded for full characterisation as previously described.

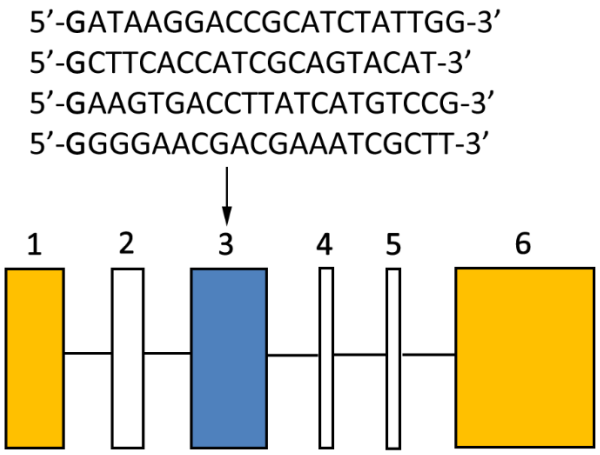

Figure 6.3.2. Selection of gRNA sequences selected for Cas9 recognition of NAPEPLD catalytic domain

Schematic representation of the human NAPEPLD sequence, indicating the exon 1 and 6 UTRs (yellow) and the catalytic domain (blue) in exon 3. Target sequences were designed flanking the catalytic HXHXDH motif necessary for NAPEPLD catalytic action (Daiyasu et al., 2001). Sequences for gRNAs begin with G (bold) for U6 promotor recognition (Ran et al., 2013).

Figure 6.3.3. Targets of exon 3 of NAPEPLD DNA sequence

DNA sequence of exon 3 is displayed above and the corresponding amino acid sequence is displayed in purple below the DNA sequence. The HXHXDH sequence important for catalytic activity of NAPEPLD is highlighted in green and underlined. Guide RNA sequences are highlighted in blue above the sequence and underlined, the 5'-NGG PAM sequence is in red (from left to right gRNA2, gRNA4, gRNA1 and gRNA3) flanking the HXHXDH motif.

```
001 GAACTAGACAAAGAACTCCCAGTGCTTAAGCCATATTTTATCACTAACCCTGAAGAAGCT 060

      E  L  D  K  E  L  P  V  L  K  P  Y  F  I  T  N  P  E  E  A

061 GGAGTGAGGGAAGCTGGCTTAAGAGTCACATGGCTGGGACATGCCACGGTAATGGTGGAA 120

      G  V  R  E  A  G  L  R  V  T  W  L  G  H  A  T  V  M  V  E

                                                  gRNA2-CTTCACCATCGCAG
121 ATGGATGAGCTCATATTTCTCACGGATCCCATCTTTAGCTCTCGTGCTTCACCATCGCAG 180

      M  D  E  L  I  F  L  T  D  P  I  F  S  S  R  A  S  P  S  Q

    TACATGGG CCAAAGCGATTTCGTCGTTCCCC-gRNA4              CCTCCAATA

181 TACATGGGTCCAAAGCGATTTCGTCGTTCCCCGTGCACAATAAGTGAACTCCCTCCAATA 240

      Y  M  G  P  K  R  F  R  R  S  P  C  T  I  S  E  L  P  P  I

    GATGCGGTCCTTAT-gRNA1
241 GATGCGGTCCTTATCAGTCACAACCACTATGACCATCTGGACTACAATTCTGTCATTGCT 300

      D  A  V  L  I  S  H  N  H  Y  D  H  L  D  Y  N  S  V  I  A

301 TTGAATGAGCGATTTGGTAATGAGTTGAGATGGTTTGTGCCTTTGGGTCTCCTTGACTGG 360

      L  N  E  R  F  G  N  E  L  R  W  F  V  P  L  G  L  L  D  W

                                                              C
361 ATGCAAAAATGTGGCTGTGAGAATGTGATTGAGTTGGACTGGTGGGAGGAGAATTGTGTC 420

      M  Q  K  C  G  C  E  N  V  I  E  L  D  W  W  E  E  N  C  V

    CCCGGACATGATAAGGTCACTT-gRNA3
421 CCCGGACATGATAAGGTCACTTTTGTCTTTACACCTTCCCAGCACTGGTGTAAAAGGACT 480

      P  G  H  D  K  V  T  F  V  F  T  P  S  Q  H  W  C  K  R  T

481 CTAATGGATGACAACAAGGTGCTATGGGGCAGCTGGTCTGTCTTGGGGCCTTGGAATCGA 540

      L  M  D  D  N  K  V  L  W  G  S  W  S  V  L  G  P  W  N  R

541 TTTTTTTTCGCAGGAGATACTGGTTATTGCCCTGCTTTTGAAGAGATAGGAAAAAGATTT 600

      F  F  F  A  G  D  T  G  Y  C  P  A  F  E  E  I  G  K  R  F

601 GGACCTTTTGACCTTGCAGCTATTCCCATCGGAGCTTATGAACCGAG             647

      G  P  F  D  L  A  A  I  P  I  G  A  Y  E  P
```

Characterisation of NAPEPLD knockout cell lines

After the colonies had grown to sufficient numbers, RNA was extracted from the cells and converted to cDNA before PCR amplification of the CRISPR site with primers designed to exon 2 and exon 4 (Figure 6.3.4). The parental DAGLα/β KO cell line had a relatively clean band at around the predicted size of 856bp. Colonies which were transfected with single vectors (4B1 – 4B6 and others not shown) showed minor changes in RT-PCR which might be indicative of subtle mutations. Colonies which were transfected with all four CRISPR vectors at once (A41 – A47) showed much more variable transcripts and larger shifts in the RT-PCR band which are indicative of larger mutations. The A43 and A47 cell lines showed large transcript disruptions and produced clean RT-PCR bands at around 600bp mark which would be the expected size if the large targeted region has been disrupted. These two cell lines are likely to have disrupted transcripts in both alleles, although it is not for certain. For further analysis, these lines were selected and renamed NAPEPLD KO1 and NAPEPLD KO2 respectively.

Next, genomic sequencing of the cells were carried out. Genomic DNA was extracted from the cells and PCR was carried out with primers located in the introns flanking exon 3. The PCR product was purified and sent for Sanger sequencing. The sequencing results were clean with only one result obtained, suggesting that both alleles of NAPEPLD could have been cleaved and mutated in the same way although further analysis would need to be carried out to confirm this. The alignment of the sequences in Figure 6.3.5 shows subtle indel mutations present at some of the CRISPR sites, and large deletions beginning and terminating at CRISPR sites flanking the catalytic motif. Analysis of these sequences show that a stop codon has been introduced prior to the catalytic motif (Figure 6.3.6); this indicates the transcripts no longer encode for a functional enzyme.

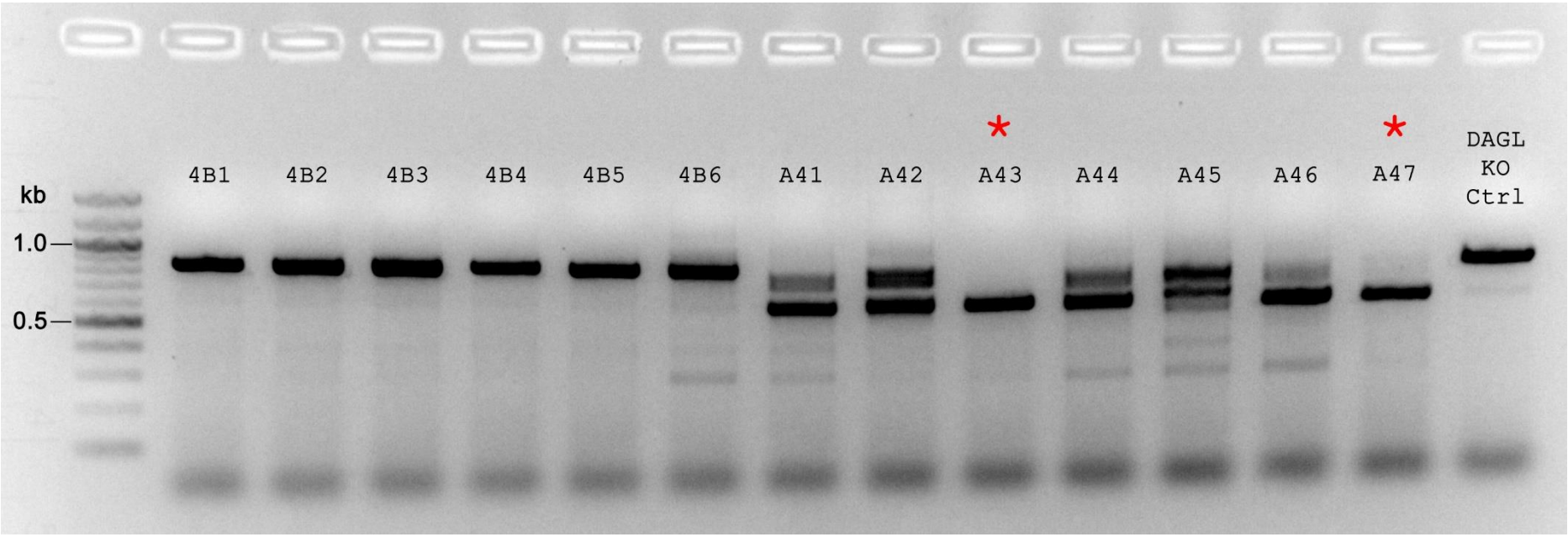

Figure 6.3.4. RT-PCR of NAPEPLD CRISPR treated cells show truncated PCR products

DAGLα/β KO cells that have been transfected with CRISPR vectors were grown from single cell colonies until confluent in T75 flasks where they were pelleted and RNA was extracted and converted to cDNA as described in methods. PCR was carried out with primers flanking the CRISPR sites in exons 2 and 4 as described in methods and loaded on 1% agarose gel (expected band size - 856bp). 4B1 – 4B6 were all treated with CRISPR gRNA4 and individual clones labelled from 1 to 6. A41 – A47 were all treated with 4 CRISPR gRNAs at the same time and individual clones labelled from 1 to 7. DAGLα/β KO RT-PCR was included as a positive control. Red stars indicate cell lines taken forward in the project.

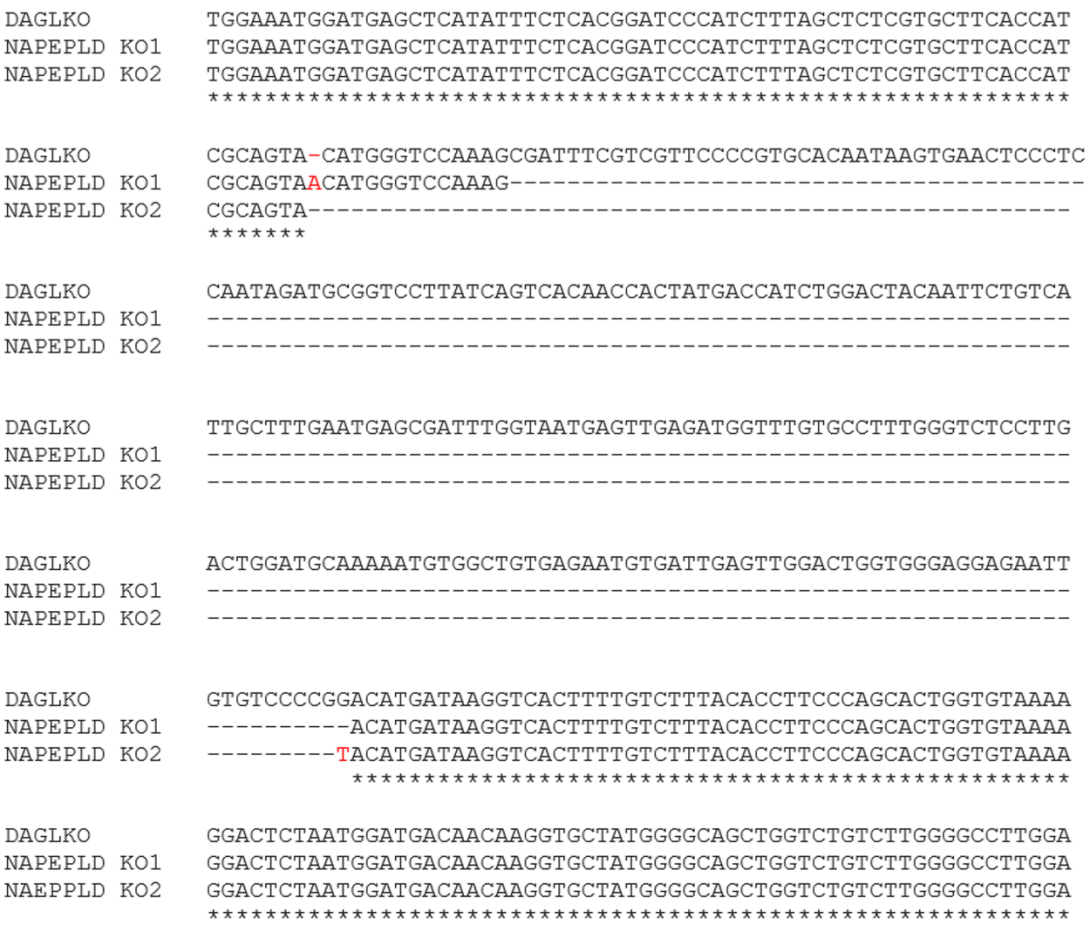

Figure 6.3.5. Genomic DNA sequencing of PCR products reveal large deletions of NAPEPLD between CRISPR sites

NAPEPLD CRISPR treated cells NAPEPLD KO1 and KO2 and DAGLα/β KO cells were grown in T75 flasks until confluent and genomic DNA was extracted from the pelleted cells. PCR was carried out with primers flanking exon 3 as listed in methods. The PCR product was then run on 1% agarose gel and purified from the gel. The purified PCR product and primers were sent for Sanger sequencing, results were aligned in Clustal Omega. Letters in red show indel mutations of single nucleotides.

```
NAPEPLD      ELDKELPVLKPYFITNPEEAGVREAGLRVTWLGHATVMVEMDELIFLTDPIFSSRASPSQ
KO1          ELDKELPVLKPYFITNPEEAGVREAGLRVTWLGHATVMVEMDELIFLTDPIFSSRASPSQ
KO2          ELDKELPVLKPYFITNPEEAGVREAGLRVTWLGHATVMVEMDELIFLTDPIFSSRASPSQ
             ************************************************************

NAPEPLD      YMGPKRFRRSPCTISELPPIDAVLISHNHYDHLDYNSVIALNERFGNELRWFVPLGLLDW
KO1          *HGSKDMIRSLLSLHL-PXXGV-------------------------------------
KO2          YT**GHFCLYTF-----PALV*--KDSNG*QQGAMGQ-------------LVCLGALES
                   :          *

NAPEPLD      MQKCGCENVIELDWWEENCVPGHDKVTFVFTPSQHWCKRTLMDDNKVLWGSWSVLGPWNR
KO1          ---------KGL*WMTTRCYGAAGLS---------------------------------
KO2          -------IFFRRRYWLLPCF*RDRKKIWTF*PCSYS-HRSL*TEVCX--------LPKKT
                           :    *

NAPEPLD      FFFAGDTGYCPAFEEIGKRFGPFDLAAIPIGAYEP
KO1          ------------------------------------
KO2          FLLCDKX------TX-------FKSKA--------
```

Figure 6.3.6. NAPEPLD KO1 and KO2 protein sequences encounter early stop codons shortly after CRISPR site

DNA sequencing results were translated into protein sequences and aligned with wild type NAPEPLD protein sequence. The stars within the sequence indicated stop codons; the stop codons highlighted in red and underlined are the first stop codons encountered in the sequence after the first CRISPR site.

QuantiGene multiplex assay of NAPEPLD KO cell lines confirm undetectable NAPEPLD transcripts

RT-PCR and genome sequencing has shown major disruptions in the NAPEPLD gene. For further evidence of the disruption of both alleles of NAPEPLD in KO1 and KO2 lines the transcriptomes of the cell lines were subject to analysis in the QuantiGene multiplex assay as described in methods (Figure 6.3.7).

NAPEPLD KO1 and NAPEPLD KO2 clones showed complete abolition of detectable NAPEPLD transcripts to below the detectable threshold (KO1 = 4.0 ± 0.3 net MFI; KO2 = 5.1 ± 0.9 net MFI). This confirms that both alleles of NAPEPLD are mutated with a substantial deletion of the catalytic domain.

Expression of CNR2 and PLA2G4E transcripts showed non-significant differences in detected levels when comparing the parental CB1-Tango and DAGLα/β KO cells to the NAPEPLD KO cells. The transcripts levels of CNR1 in the NAPEPLD KO cell lines were not significantly different to the levels detected in both the CB1-Tango and the DAGLα/β KO cells, however the levels of CNR1 transcripts in NAPEPLD KO1 tend to be lower which nears statistical significance when compared to parental CB1-Tango and the DAGLα/β KO cell lines and has a small significance ($p<0.05$) when compared to the NAPEPLD KO2 cell line.

The levels of DAGLα and DAGLβ transcripts were not included for reasons mentioned previously; in brief the more subtle indel mutations introduced into those genes generates transcripts that can still be detected by our DAGL probes.

Interestingly, relative expression of PLA2G4B transcript levels in KO1 and KO2 were 0.51 ± 0.01 and 0.57 ± 0.01 respectively which are both significantly higher, albeit by a relatively small amount, than the relative levels in DAGLα/β KO cells (0.42 ± 0.01 relative expression). FAAH transcripts levels were also detected in both KO1 and KO2 cells (0.017 ± 0.002 relative expression and 0.031 ± 0.001 relative expression respectively) which were relatively higher than the levels in the DAGLα/β KO cells (0.011 ± 0.0004 relative expression). Meanwhile, the levels of MGLL are significantly lower in both NAPEPLD KO lines (0.017 ± 0.001 relative expression and 0.017 ± 0.0008 relative expression KO1 and KO2 respectively) and ABHD6 showed a slight significant reduction in NAPEPLD KO2 cells. However, generally speaking most of these changes are relatively minor (e.g. see PLAG42B result) and importantly variable levels of the transcripts can also be seen between the NAPEPLD KO1 and KO2 lines (e.g. see the FAAH result) and in the case of MGLL the transcript level in the triple KO is similar to the level found in the parental cells. These observations point to simple clonal differences across cell lines, rather than robust adaptive changes, accounting for these differences.

Figure 6.3.7. Results from beads assay show CRISPR has knocked out the catalytic region of NAPEPLD

CRISPR-treated NAPEPLD KO1 and KO2 cells and DAGLα/β KO cells were grown in T75 flasks until confluent and RNA was extracted from the pelleted cells according to manufacturer's instructions. RNA was diluted to a concentration of 375ng/μl and 20μl was added to wells in a 96 well plate, leading to total RNA in each well to be 7500ng. RNA samples and nuclease free water control samples were then incubated with magnetic beads and probes overnight. The beads were then washed and amplified and read on the Magpix system as in the methods section. The background readings from control wells were subtracted from the sample wells and the data was normalised to the expression of two housekeeping genes. Graph shows means and bars represent SEMs of 5 replicates from one single experiment. Significance between groups was calculated using One Way ANOVA.

***p<0.001; One-way ANOVA, Dunnett's post-test.

(A)

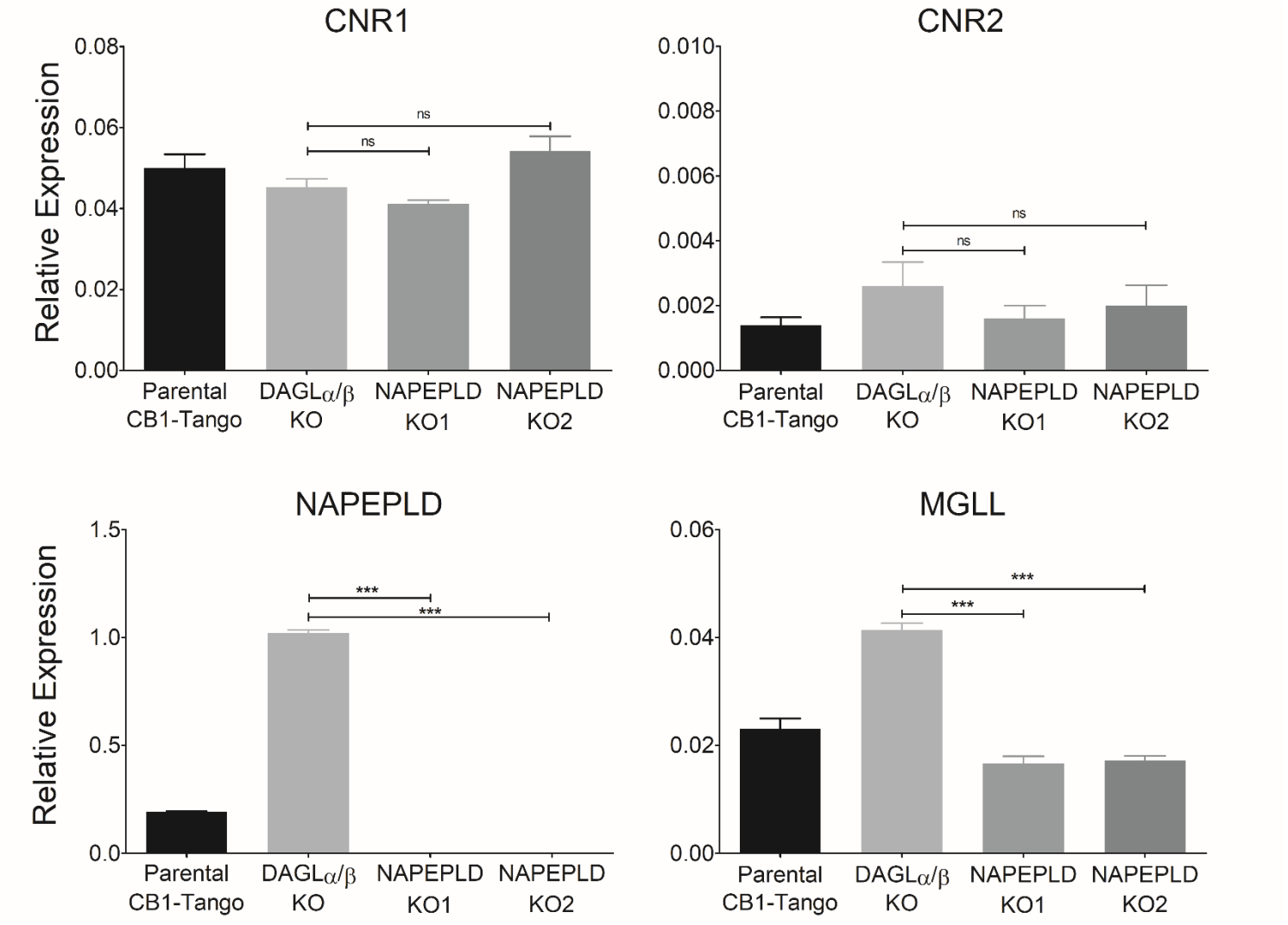
CNR1
Relative Expression
0.08
0.06
0.04
0.02
0.00
ns
ns
Parental CB1-Tango
DAGLα/β KO
NAPEPLD KO1
NAPEPLD KO2
CNR2
0.010
0.008
0.006
0.004
0.002
0.000
ns
ns
Parental CB1-Tango
DAGLα/β KO
NAPEPLD KO1
NAPEPLD KO2
NAPEPLD
Relative Expression
1.5
1.0
0.5
0.0
***
***
Parental CB1-Tango
DAGLα/β KO
NAPEPLD KO1
NAPEPLD KO2
MGLL
0.06
0.04
0.02
0.00
***
***
Parental CB1-Tango
DAGLα/β KO
NAPEPLD KO1
NAPEPLD KO2

(B)

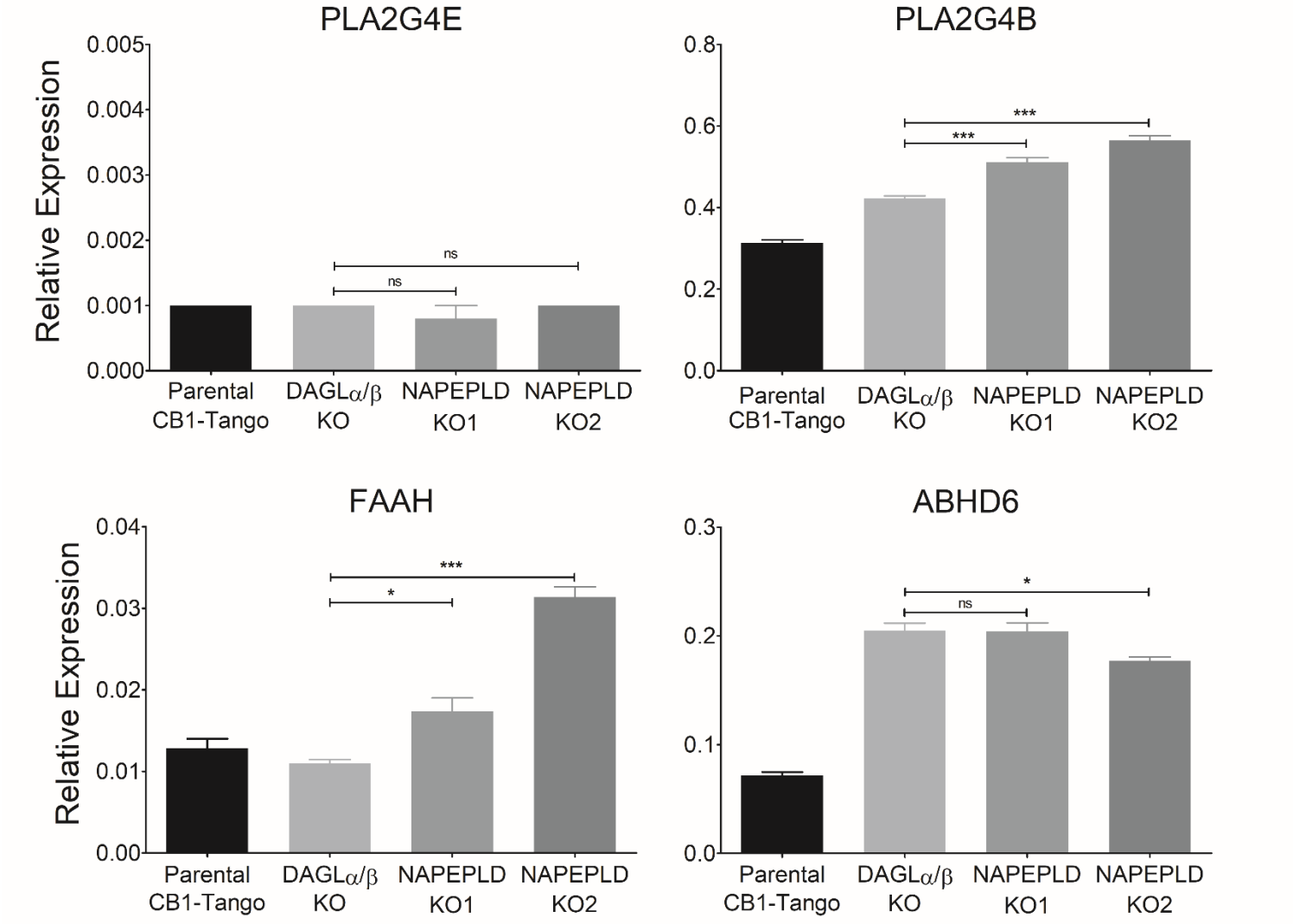
PLA2G4E
Relative Expression
0.005
0.004
0.003
0.002
0.001
0.000
ns
ns
Parental CB1-Tango
DAGLα/β KO
NAPEPLD KO1
NAPEPLD KO2
PLA2G4B
0.8
0.6
0.4
0.2
0.0
***
***
FAAH
Relative Expression
0.04
0.03
0.02
0.01
0.00
***
*
ABHD6
0.3
0.2
0.1
0.0
*
ns

Lipid measurements show insignificant change in AEA levels in NAPEPLD KO lines

Following confirmation of undetectable NAPEPLD transcripts from both cell lines thus confirming successful KO of NAPEPLD in two independent cell lines, the lipid levels of 2-AG, AEA, OEA and PEA were measured from 3 pelleted samples of the NAPEPLD KO cell lines across two independent experiments (Figure 6.3.8).

Low levels of 2-AG were detected in both cell lines (KO1 = 110.8 ± 10.3 and KO2 = 123.8 ± 25.0 pg/10^6 cells) which are consistent with the 2-AG levels from DAGLα/β KO cells these lines were generated from. AEA levels are still readily detectable in the two NAPEPLD KO cell lines (KO1 = 4.74 ± 0.14 and KO2 = 5.82 ± 0.47 pg/10^6 cells), and show no significant difference to the levels in DAGLα/β KO cells (7.21 ± 0.96 pg/10^6 cells) but remain significantly higher than the levels found in parental CB1-Tango cells (2.41 ± 0.53 pg/10^6 cells).

Other related lipids OEA and PEA were also measured. Levels of OEA were detected in both KO lines (KO1 = 131.3 ± 7.2 and KO2 = 113.0 ± 19.7 pg/10^6 cells) and this was not significantly different to the levels detected in parental CB1-Tango (118.6 ± 8.9 pg/10^6 cells) or DAGLα/β KO cells (175.5 ± 26.4 pg/10^6 cells). In both cell lines however, levels of PEA were significantly lower (KO1 = 38.8 ± 2.6 and KO2 = 39.2 ± 3.3 pg/10^6 cells) when compared to parental (94.1 ± 4.5 pg/10^6 cells) and DAGLα/β KO lines (102.6 ± 19.6 pg/10^6 cells).

The results of AEA levels from the cell lines may again be down to clonal variation giving rise to significantly higher levels in comparison to the parental CB1-Tango line, or could be reflective of functional changes in the cell, however the key results suggest that despite the genetic deletion of NAPEPLD, AEA can still be generated in the triple KO cell lines. Nonetheless, it is also interesting that PEA levels were reduced by a similar extent in both NAPEPLD KO lines relative to both the parental CB1-Tango and DAGLα/β KO lines.

Figure 6.3.8. Lipid measurements of triple KO cells NAPEPLD KO 1 and NAPEPLD KO 2

All cell lines were grown in regular conditions until 90% confluent. Cells were then harvested and counted to ensure there were more than $6x10^6$ cells present per sample. Cells were then pelleted and frozen in -80^oC and then shipped on dry ice for their lipid levels to be measured by mass spectrometry. 2-AG, AEA, OEA and PEA levels were measured in each sample and normalised to pg per 10^6 cells. Graph shows means and bars represent SEMs of n = 12 for parental CB1-Tango cells; n = 9 for DAGLα/β KO cells; n = 3 for NAPEPLD KO cells. Significance between DAGLα/β KO cells and NAPEPLD KO cells was calculated using One Way ANOVA.

ns p>0.05; *p<0.05; **p<0.01; One Way ANOVA, Bonferroni's Multiple Comparison post-test.

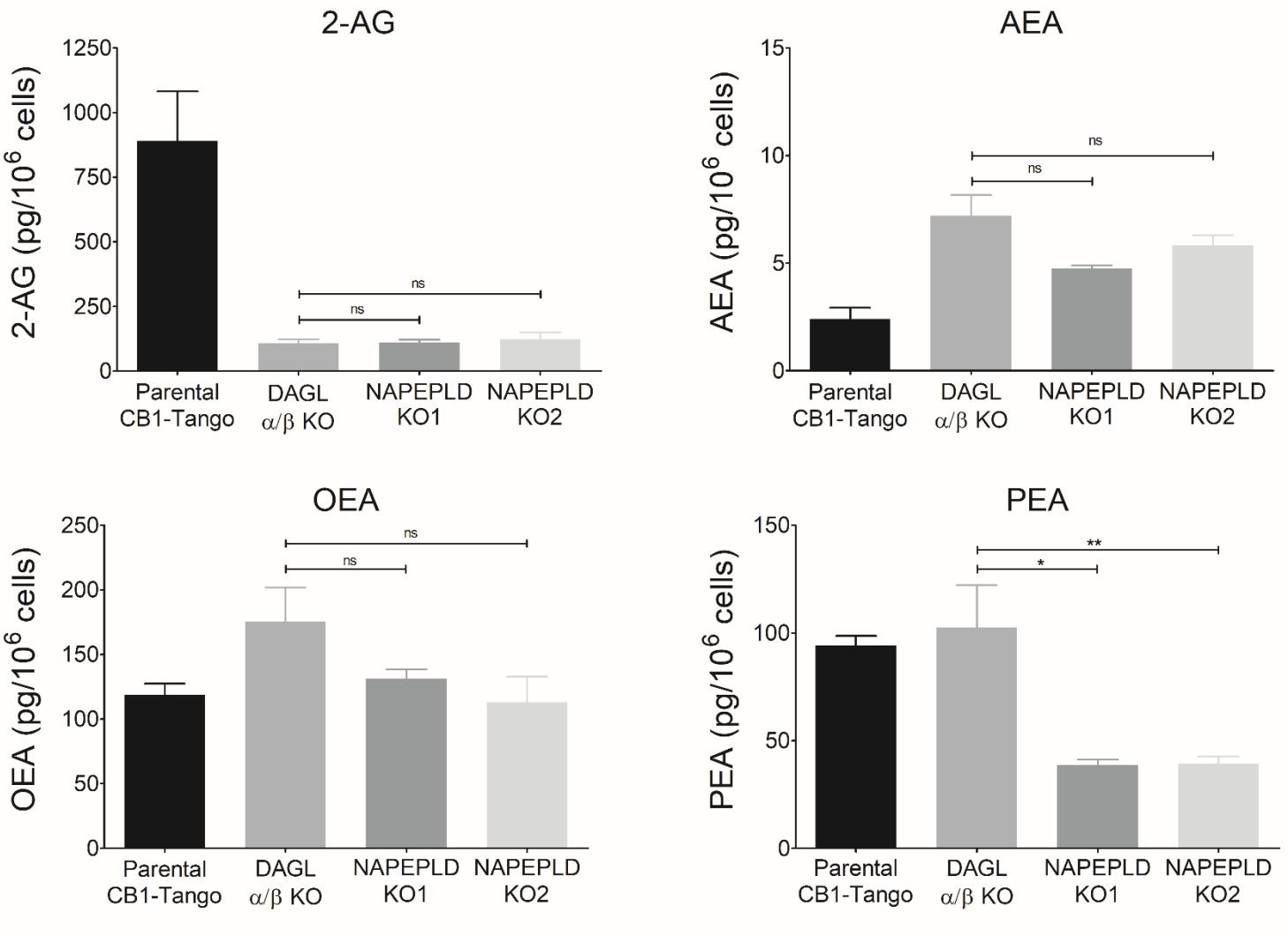
2-AG
2-AG (pg/10^6 cells)
1250
1000
750
500
250
0
ns
ns
Parental CB1-Tango
DAGL α/β KO
NAPEPLD KO1
NAPEPLD KO2
AEA
AEA (pg/10^6 cells)
15
10
5
0
ns
ns
Parental CB1-Tango
DAGL α/β KO
NAPEPLD KO1
NAPEPLD KO2
OEA
OEA (pg/10^6 cells)
250
200
150
100
50
0
ns
ns
Parental CB1-Tango
DAGL α/β KO
NAPEPLD KO1
NAPEPLD KO2
PEA
PEA (pg/10^6 cells)
150
100
50
0
**
*
Parental CB1-Tango
DAGL α/β KO
NAPEPLD KO1
NAPEPLD KO2

eCB signalling is still present in NAPEPLD KO lines in McCoy's assay media

The NAPEPLD KO cell lines were then tested in comparison to the DAGLα/β KO cells in the CB1-Tango assays to determine if there were any changes in eCB signalling as a result of the absence of NAPEPLD which could possibly be involved in a stimulus induced increase in the signalling pool of AEA, or perhaps involved in the synthesis of other eCBs. The cells were first tested in 0.5% FBS McCoy's assay media with ACEA in a standard 4 hour assay. The NAPEPLD KO cells and DAGLα/β KO cells were treated with 5μM ACEA in the presence and absence of 2.5μM AM251 (Figure 6.3.9). The DAGLα/β KO were responsive to ACEA similarly to previously obtained levels (227.6 ± 2.8% of control). NAPEPLD KO2 cells are still responsive to ACEA in the same way as the DAGLα/β KO cells (225.3 ± 13.2% of control). The NAPEPLD KO1 cells are also still responsive to ACEA but showed a significantly lower response when compared to the other two cell lines (179.7 ± 4.2% of control). This suggests that the multiple rounds of mutagenesis and selection might have created a cell line that has become compromised in the CB1 reporter aspect of the assay and this needs to be borne in mind in the following sections.

Next the cells were subject to treatment with JZL195 to determine if an eCB tone is still present in the absence of the three key synthesising enzymes. The cells were treated with 100nM JZL195 in the presence or absence of 2.5μM AM251 for 4 hours (Figure 6.3.10). An eCB tone was present in DAGLα/β KO cell line at similar levels to those obtained previously (142.7 ± 4.1% of AM251 control). The NAPEPLD KO1 cell line still produced a significant eCB tone, although this was slightly but significantly lower than that detected in the DAGLα/β KO line (123.8 ± 4.2% of AM251 control). However, the NAPEPLD KO2 also produced a substantial eCB tone (148.1 ± 6.6% of AM251 control) which was not significantly different to the tone in its parental DAGLα/β KO line.

Finally, the cells were treated with ionomycin to see if eCB signalling can still be induced by the influx of calcium (Figure 6.3.11). The DAGLα/β KO line produced an ionomycin response that was of an expected magnitude (186.1 ± 13.7% of AM251 control) which also contained a portion of response that could not be blocked by AM251 (140.2 ± 2.5% of AM251 control), similar to previously obtained results. The NAPEPLD KO cell lines also produced measurable CB1 dependent responses with the KO2 line again behaving like the parental double DAGLα/β KO line and the KO1 line again showing a significant but muted response (KO1 = 156.0 ± 6.0% of control; KO2 = 198.1 ± 13.9% of control), but had variable sizes of the non-CB1 component of the ionomycin response (Figure 6.3.11A). In this case, the data was re-

normalised to the wells containing ionomycin and AM251 to normalise the data to display only the CB1-dependent portion of the ionomycin response (Figure 6.3.11B). In this case, there were no statistically significant differences between all three cell lines in response to ionomycin (DAGLα/β KO = 132.4 ± 7.3% of control; KO1 = 124.4 ± 4.5% of control; KO2 = 124.7 ± 8.9% of control). Thus, all three cell lines were responsive to 2μM ionomycin, and the responses were able to be partially blocked by AM251.

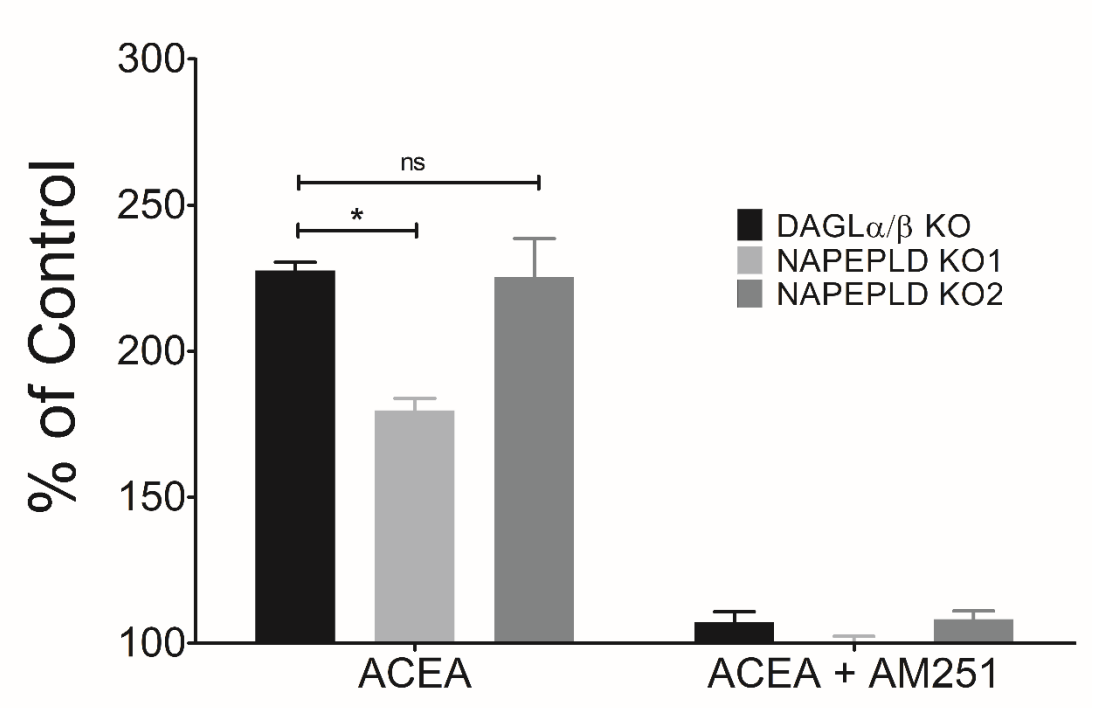

Figure 6.3.9. ACEA response is present in NAPEPLD KO cells

Cells were grown until 90% confluent and plated in black 96 well plates and incubated for 24 hours. The next day cells were treated with 5μM ACEA in the presence or absence of 2.5μM AM251 for 4 hours. Substrate was mixed according to manufacturer's instructions and added to the cells for 90 minutes. The plate was then read on the Flexstation. Data was normalised to wells containing AM251 (set as 100%). Graph shows means and bars represent SEMs of 3 independent experiments, 8 replicates in each individual experiment. Significance between groups was calculated using One Way ANOVA.

ns $p>0.05$; * $p<0.05$; One-way ANOVA, Dunnett's post-test.

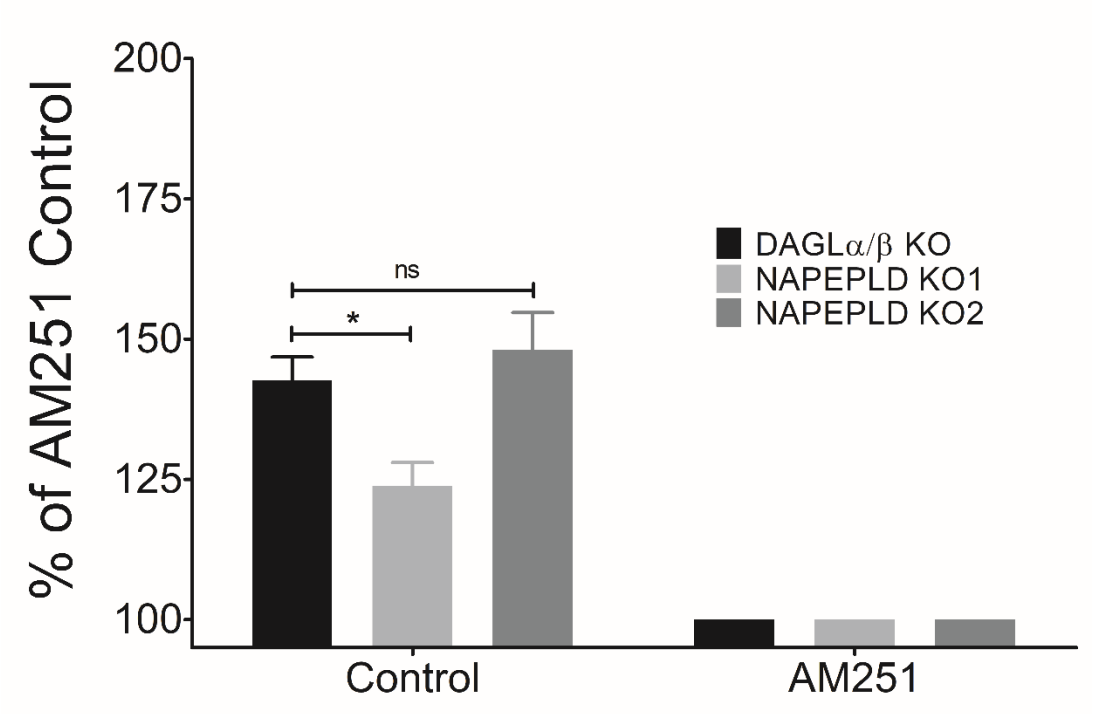

Figure 6.3.10. NAPEPLD KO cells still exhibit eCB tone in the presence of JZL195

30,000 cells were plated in black 96 well plates in 0.5% FBS McCoy's media for 24 hours. The cells were treated the next morning with 100nM JZL195 in the presence and absence of 2.5μM AM251 for 4 hours. The substrate was then mixed according to manufacturer's instructions and added to the wells for 90 minutes. Fluorescent substrate was then read on the Flexstation and the fluorescence ratio calculated. Data was normalised to the wells containing AM251 (set as 100%). Graph shows means and bars represent SEMs of 6 independent experiments, 8 replicates in each individual experiment. Significance between groups was calculated using One Way ANOVA.

ns $p>0.05$; * $p<0.05$; One-way ANOVA, Dunnett's post-test.

Figure 6.3.11. Ionomycin induced response is present in NAPEPLD KO cells

Cells were grown until 90% confluent and plated in black 96 well plates and incubated for 24 hours. The next day cells were treated with 2μM ionomycin in the presence or absence of 2.5μM AM251 for 4 hours. 100nM JZL195 was included in all wells. Substrate was mixed according to manufacturer's instructions and added to the cells for 90 minutes. The plate was then read on the Flexstation. Data was normalised to wells containing AM251 (set as 100%) (A); or the data was normalised to wells containing ionomycin in the presence of AM251 to give the % of ionomycin response (B). Graph shows means and bars represent SEMs of 3 independent experiments, 8 replicates in each individual experiment. Significance between groups was calculated using One Way ANOVA.

ns $p>0.05$; One-way ANOVA, Dunnett's post-test.

(A)

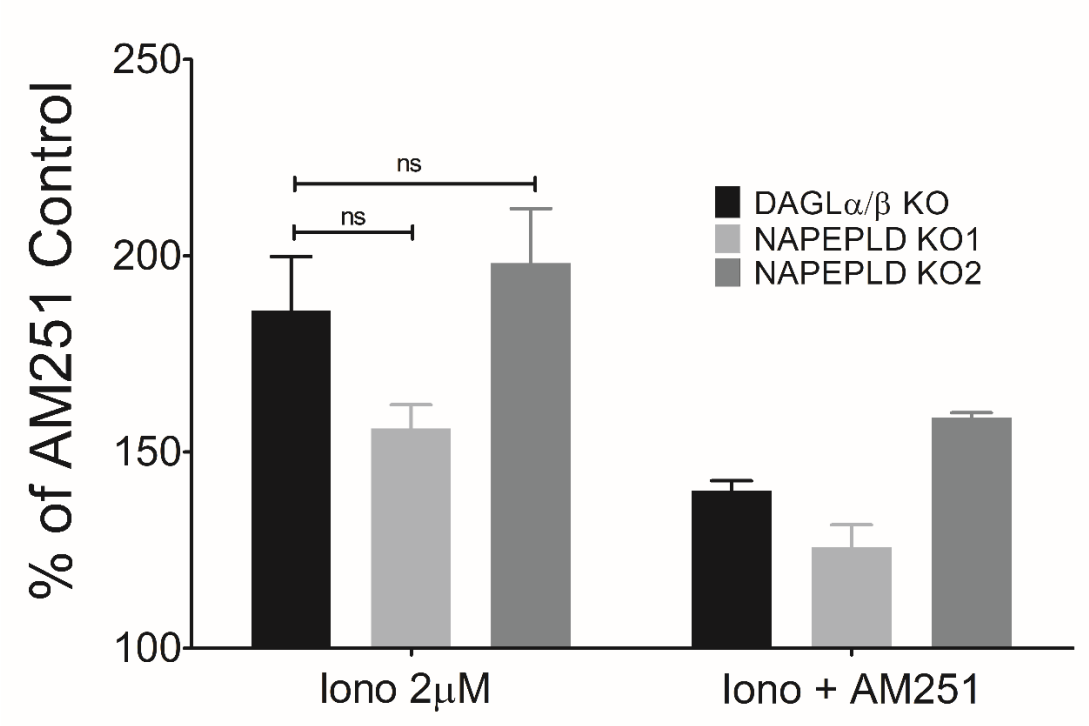
% of AM251 Control
250
200
150
100
ns
ns
DAGLα/β KO
NAPEPLD KO1
NAPEPLD KO2
Iono 2μM
Iono + AM251

(B)

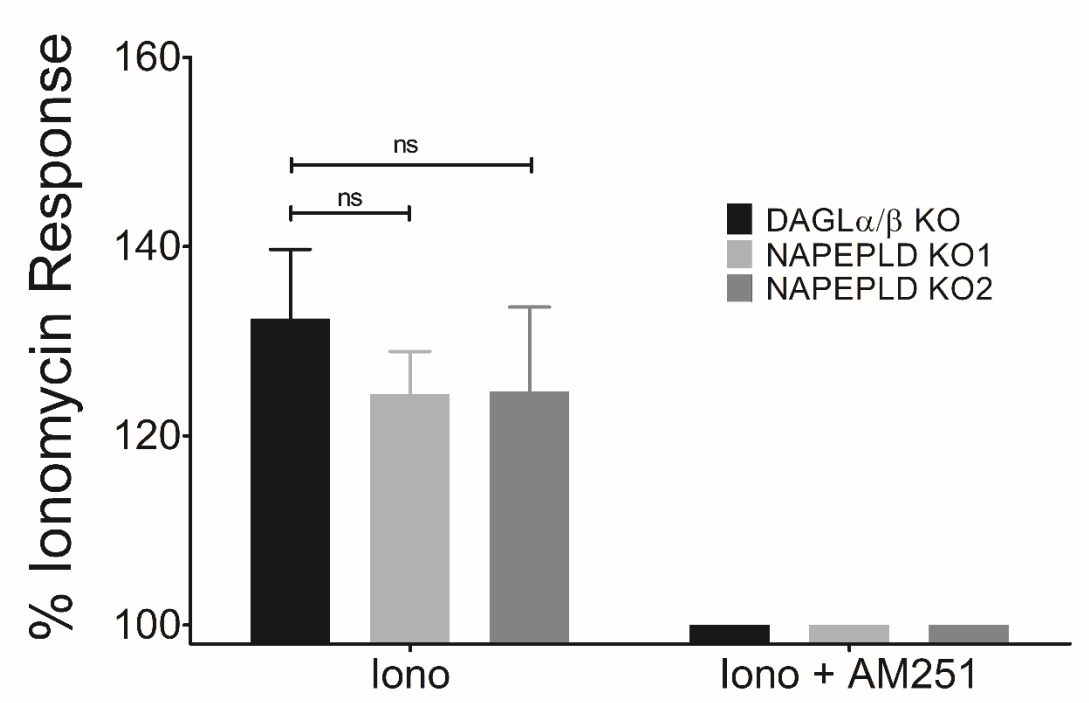
% Ionomycin Response
160
140
120
100
ns
ns
DAGLα/β KO
NAPEPLD KO1
NAPEPLD KO2
Iono
Iono + AM251

FSK and PMA can still elicit eCB signalling in NAPEPLD KO cells in No Starve Freestyle media

Subsequently, the cells were tested in the 24 hour No Starve Freestyle assay conditions to again determine the effect the absence of functional NAPEPLD has on the eCB tone in these conditions and on the FSK and PMA responses. To begin with, the cells were treated with ACEA in the presence and absence of AM251 to determine if CRISPR treatment has affected the expression of the CB1 receptors or the assay system (Figure 6.3.12). The ACEA responses elicited in DAGLα/β KO cells, as expected, are robust reaching 650.5 ± 71.5% of AM251 control. NAPEPLD KO lines are still responsive to ACEA; NAPEPLD KO2 elicited a response reaching 621.2 ± 69.9% of AM251 control which was not statistically different to the response elicited by DAGLα/β KO cells. NAPEPLD KO1 also show responsiveness to ACEA, however the response is again significantly lower than responses evoked by the other two cell lines (421.7 ± 98.6% of AM251 control). Thus it is clear that the NAPEPLD KO1 line is compromised in its sensitivity to CB1 signalling, possibly due to a lower expression of the CB1 receptor. The ACEA responses from all 3 cell lines were largely inhibited by AM251 to near control levels.

The eCB tone was also examined in the NAPEPLD KO cells in this paradigm; the cells were plated in No Starve Freestyle conditions as described in methods in the presence and absence of 2.5μM AM251 (Figure 6.3.13). A substantial eCB tone was detected in DAGLα/β KO cells (373.7 ± 24.2% of AM251 control) which is still significantly higher than the tone detected previously in parental CB1-Tango cells. The NAPEPLD KO2 line showed a very robust response (310.1 ± 13.7% of AM251 control) which was not significantly different from the response of its parental line. Again, the NAPEPLD KO1 cell line showed a substantial and significant response (220.3 ± 24.0% of AM251 control) which, like the ACEA response, was muted when compared to the parental line response. Thus it is clear that NAPEPLD is not required for the generation of the eCB in this paradigm.

To test whether activation of kinases continues to elicit eCB signalling in the NAPEPLD KO cell lines, the cell lines were treated with 10μM FSK in the presence and absence of AM251 (Figure 6.3.14). A robust FSK induced response was measured from the DAGLα/β KO cells (519.0 ± 48.1% of AM251 control) which is on a comparable level to those obtained previously. The NAPEPLD KO2 line gave a robust response to FSK treatment (475.3 ± 14.0% of AM251 control) which was not significantly different to the response of the parental DAGLα/β KO line. The NAPEPLD KO1 line responded to FSK treatment (308.7 ± 68.7% of

AM251 control) however again similarly to the ACEA response, this was muted when compared to the parental DAGLα/β KO line response most likely due to reduced sensitivity of this line to CB1 signalling.

Finally, the cells were treated with 25nM PMA in the presence and absence of AM251 in the No Starve Freestyle conditions for 24 hours to if eCB signalling can still be elicited by PKC in the NAPEPLD KO lines (Figure 6.3.15). PMA elicited a response reaching 289.3 ± 21.4% of AM251 control in the DAGLα/β KO cells which was mostly blocked by AM251 but did show a component that could not be inhibited by AM251, which is in line with previously obtained results. Interestingly, PMA also elicited responses in the NAPEPLD KO cell lines (KO1 = 375.2 ± 76.8%; KO2 = 532.3 ± 15.8% of AM251 control) which lean towards the presence of higher responses in comparison to the DAGLα/β KO line. However, these PMA responses also had higher portions of responses that could not be inhibited by AM251 and therefore may not necessarily be signalling through the CB1 receptor (Figure 6.3.15A). Considering this, the data was instead normalised to PMA in the presence of AM251 to give a clearer indication of the CB1 dependent response (Figure 6.3.15B). When presented this way, the PMA responses from all three cell lines are not significantly different, although the response from NAPEPLD KO2 is of a higher magnitude and nears statistical significance. PMA, along with FSK, still elicits eCB signalling in the NAPEPLD KO cell lines in a very similar manner to the DAGLα/β KO cell line.

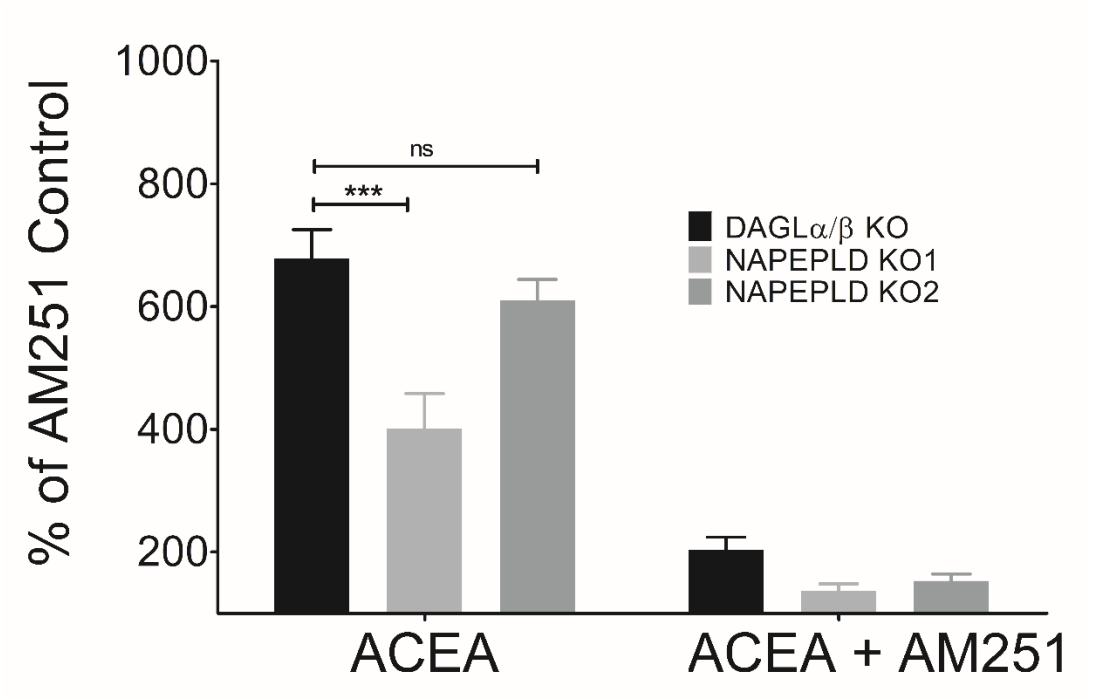

Figure 6.3.12. The NAPEPLD KO cells are still responsive to ACEA in No Starve Freestyle conditions

Cells were grown until 90% confluent and plated in black 96 well plates in Freestyle media supplemented with 2mM Ca^{2+} and 100nM JZL195. Immediately after plating, cells were treated with 5μM ACEA in the presence and absence of 2.5μM AM251 for 24 hours. Substrate was mixed according to manufacturer's instructions and added to the cells for 90 minutes. The plate was then read on the Flexstation. Data was normalised to wells containing AM251 only (set as 100%). Graph shows means and bars represent SEMs of 4 independent experiments, 8 replicates in each individual experiment. Significance between groups was calculated using One Way ANOVA.

ns $p>0.05$; *** $p<0.001$; One-way ANOVA, Dunnett's post-test.

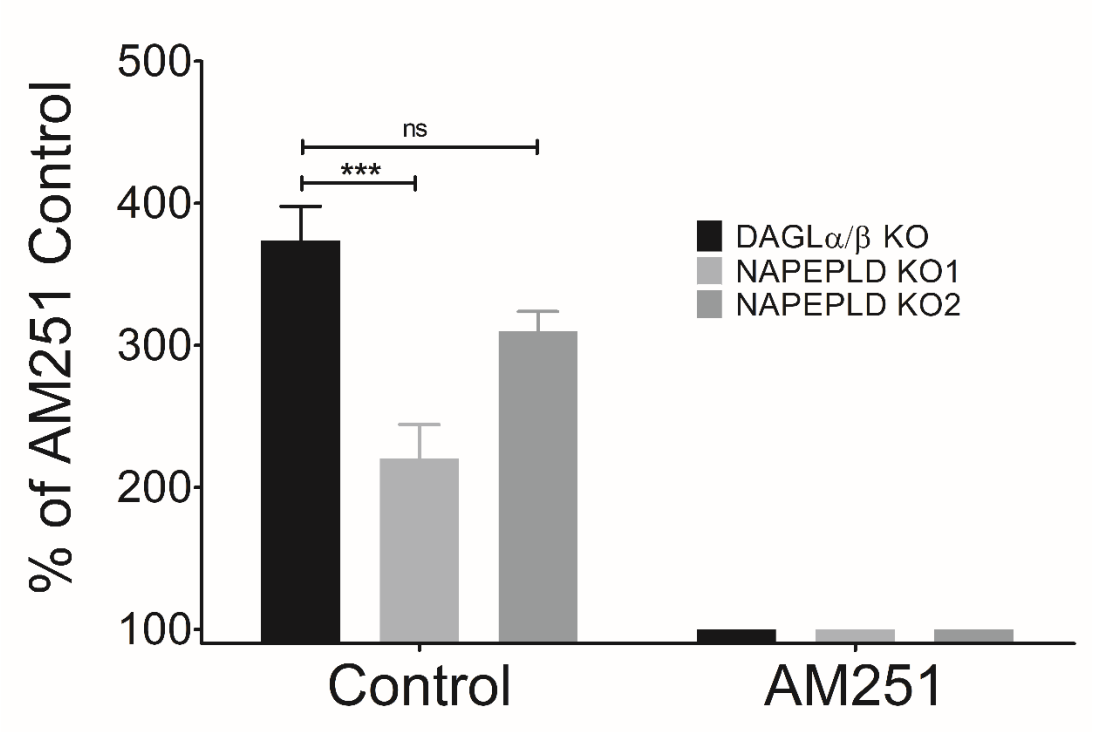

Figure 6.3.13. eCB tone is present in NAPEPLD KO cells in No Starve Freestyle conditions

Cells were grown until 90% confluent and plated in black 96 well plates in Freestyle media supplemented with 2mM Ca^{2+} and 100nM JZL195. Immediately after plating, cells were treated with control media or 2.5μM AM251 for 24 hours. Substrate was mixed according to manufacturer's instructions and added to the cells for 90 minutes. The plate was then read on the Flexstation. Data was normalised to wells containing AM251 (set as 100%). Graph shows means and bars represent SEMs of 4 independent experiments, 8 replicates in each individual experiment. Significance between groups was calculated using One Way ANOVA.

ns $p>0.05$; *** $p<0.001$; One-way ANOVA, Dunnett's post-test.

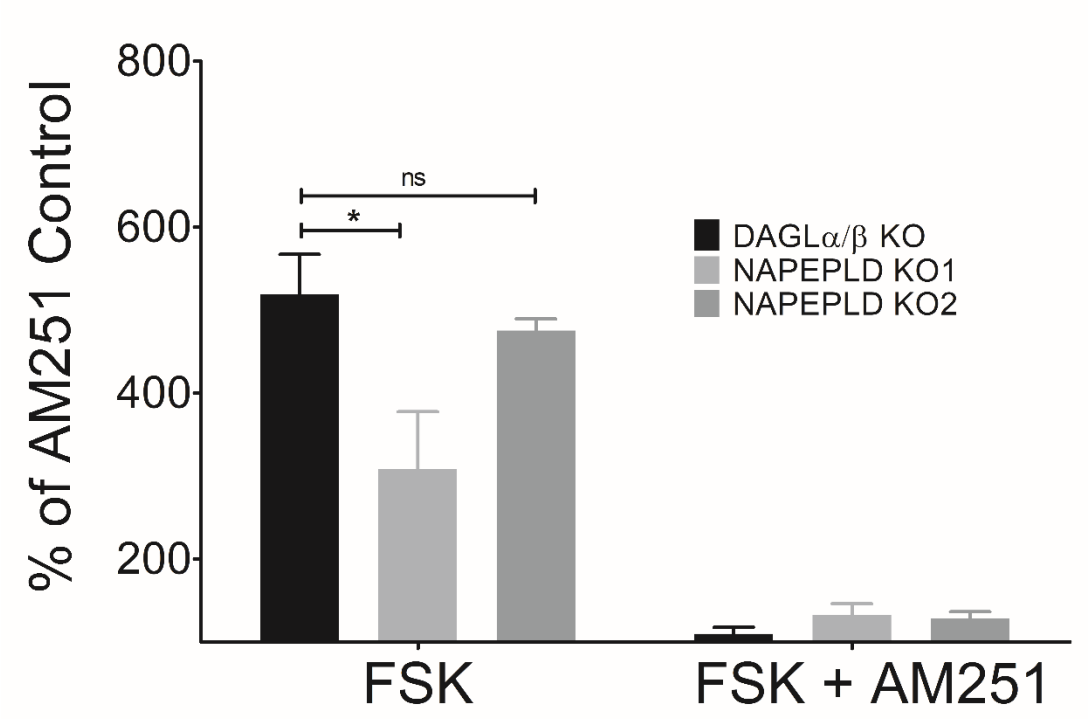

Figure 6.3.14. FSK still elicits a response in NAPEPLD KO cells in No Starve Freestyle conditions

Cells were grown until 90% confluent and plated in black 96 well plates in Freestyle media supplemented with 2mM Ca^{2+} and 100nM JZL195. Immediately after plating, cells were treated with 10μM FSK in the presence and absence of 2.5μM AM251 for 24 hours. Substrate was mixed according to manufacturer's instructions and added to the cells for 90 minutes. The plate was then read on the Flexstation. Data was normalised to wells containing AM251 only (set as 100%). Graph shows means and bars represent SEMs of 4 independent experiments, 8 replicates in each individual experiment. Significance between groups was calculated using One Way ANOVA.

ns $p>0.05$; * $p<0.05$; One-way ANOVA, Dunnett's post-test.

Figure 6.3.15. PMA induced response is unchanged in NAPEPLD KO cells in No Starve Freestyle conditions

Cells were grown until 90% confluent and plated in black 96 well plates in Freestyle media supplemented with 2mM Ca^{2+} and 100nM JZL195. Immediately after plating, cells were treated with 25nM PMA in the presence and absence of 2.5μM AM251 for 24 hours. Data was normalised to wells containing AM251 (set as 100%) (A); or the data was normalised to wells containing PMA in the presence of AM251 to give the % of PMA response (B). Graph shows means and bars represent SEMs of 4 independent experiments, 8 replicates in each individual experiment. Significance between groups was calculated using One Way ANOVA.

ns $p>0.05$; ***$p<0.001$; One-way ANOVA, Dunnett's post-test.

(A)

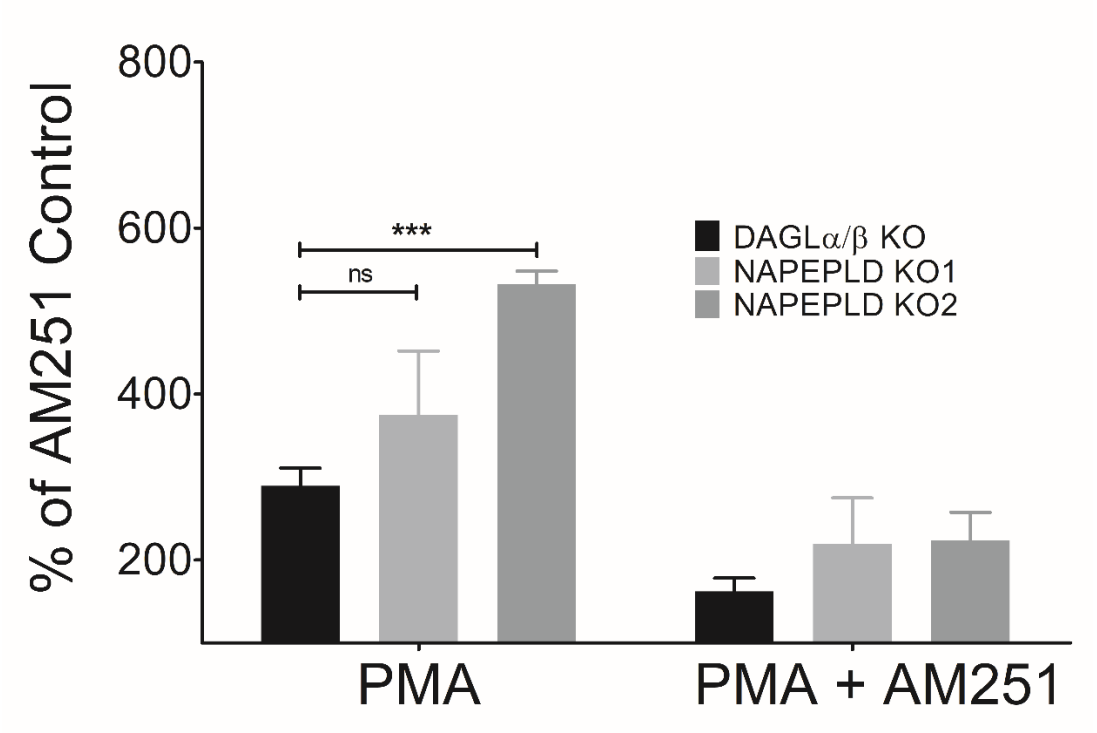
800
600
400
200
% of AM251 Control
***
ns
DAGLα/β KO
NAPEPLD KO1
NAPEPLD KO2
PMA
PMA + AM251

(B)

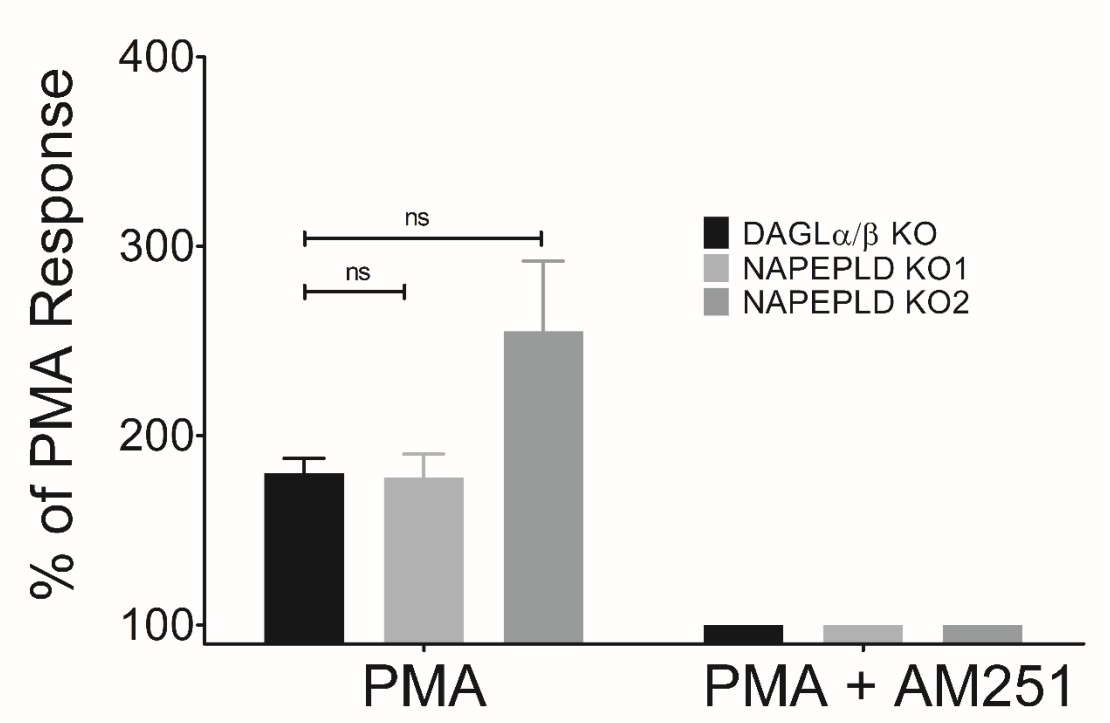
400
300
200
100
% of PMA Response
ns
ns
DAGLα/β KO
NAPEPLD KO1
NAPEPLD KO2
PMA
PMA + AM251

6.3.3 **Results 4B.** Summary & conclusions

Genetic KO of the DAGLs in the CB1-Tango cells revealed significant reduction of 2-AG levels confirming the necessity of the DAGLs in the generation of 2-AG. However, despite the substantial reduction of 2-AG levels, there was little change in JZL195, calcium, PKA and PKC stimulated eCB signalling. AEA is the other well characterised eCB and NAPEPLD remains the best characterised enzyme in the pathway that is generally taken to be responsible for the synthesis of this eCB, and for this reason we have directly tested the requirement for this enzyme for both the synthesis of AEA and stimulus induced eCB signalling in the host cell line.

A CRISPR strategy that uses single gRNAs to introduce small mutations into the genome proved successful for the generation of cell lines that lacked functional DAGLα and DAGLβ gene products. A different CRISPR approach was taken in the generation of NAPEPLD KO lines. As opposed to relying on individual gRNAs in separate pools of cells which had commonly been the technique used (Ran et al., 2013), a new method of combining several CRISPR vectors in one transfection to cause two double strand breaks and thus cause a repair with substantial missing portions of DNA sequence was adopted (Canver et al., 2014). Cell lines generated this way can be predicted to make transcripts will relatively large well defined deletions that would very easily be confirmed by RT-PCR in comparison to subtle mutations that are generated by individual vectors. Genome sequencing could also then be used to confirm the removal of the intermediate DNA flanked by the two CRISPR sites, which in the case of NAPEPLD involves removal of the catalytic motif. Thus, if translated from the compromised transcripts, the truncated protein would be catalytically dead.

Further confirmation of NAPEPLD knockout came from isolating mRNA from two NAPEPLD KO lines for analysis using the QuantiGene multiplex assay. The NAPEPLD probe sets were designed to bind to the region of the transcript corresponding to the catalytic domain that would be missing if the CRISPR strategy was successful. Indeed, the results from the assay showed no detectable levels of NAPEPLD transcripts in both cell lines, indicating the complete knockout of NAPEPLD activity. Unfortunately, a reliable NAPEPLD antibody is unavailable so western blot analysis of NAPEPLD protein expression in the cells was inconclusive. However, from the results of genomic sequencing and transcriptome analysis, we can be certain that there is no NAPEPLD activity in the two selected NAPEPLD KO cell lines.

The QuantiGene multiplex assay also revealed other changes in the transcript levels within the two NAPEPLD KO cell lines. The PLA2G4E transcript levels remained below detectable threshold and the CNR2 transcript levels remained largely unchanged in all of the cell lines. Transcript levels of CNR1 in the NAPEPLD KO1 line was significantly lower in comparison to the NAPEPLD KO2 line and tended to be lower in comparison to the parental CB1-Tango and DAGLα/β KO lines but did not reach statistical significance. This could have been a result of clonal variances, however from the results of the CB1-Tango assay, the responses to ACEA, JZL195 and FSK from the NAPEPLD KO1 line were significantly lower from both media conditions and across several independent experiments. The magnitude of the lowered responses were similar between the ACEA response and JZL195 and/or FSK responses; responses in McCoy's media were ~15-20% lower whilst the responses in No Starve Freestyle media were consistently ~40% lower in comparison the DAGLα/β KO line. In particular, the sustained and consistent muted response to maximally active concentration of ACEA in both media conditions would indicate that there could have been some CRISPR-related side effects on the receptor reporter system, e.g. CRISPR introducing off-target mutations leading to the reduced expression of CB1 receptors, which would be in keeping with the lower levels of CNR1 transcripts. The ACEA response is therefore necessary to ensure the cells maintain similar levels of CB1 activation as a compromised assay system could preclude any changes in eCB signalling and ideally any cell lines generated and taken forward in the project will maintain similar levels of CB1 activation by ACEA. This highlights the importance of selecting and profiling multiple cell clones due to clonal variances and potential CRISPR side effects which could affect responsiveness in the CB1-Tango assay.

Other changes seen in the transcript levels are from the eCB hydrolysing enzymes. First, in comparison to the parental CB1-Tango cell line, the DAGLα/β KO cell line had higher measured levels of AEA and NAPEPLD transcripts despite unchanged transcript levels of FAAH. As well as this, the two NAPEPLD KO lines show the same genetic mutation in NAPEPLD, but have widely different transcript levels of FAAH. This casts doubt on a causal relationship between NAPEPLD and FAAH transcripts and the differences in the FAAH transcript levels between the three KO cell lines are more likely to be caused by clonal variation rather than due to a functional change in AEA synthesis/degradation. Furthermore, transcript levels of MGLL were significantly higher in the DAGLα/β KO cell line, however when measured from the NAPEPLD KO lines, the levels of MGLL transcripts were comparable to the original levels from the parental CB1-Tango cell line. This raises doubt whether the higher transcript levels of MGLL in the DAGLα/β KO line is a real functional change due to the

absence of functional DAGL enzyme as the NAPEPLD KO cells also do not express functional DAGL but the transcript levels of MGLL are similar to those from parental CB1-Tango cells. Finally, transcript levels of ABHD6 remained largely around the same levels between the DAGLα/β KO cell line and the NAPEPLD KO lines which are also significantly higher than levels from the parental CB1-Tango cells. Despite this sustained high level of ABHD6 transcripts, the levels of 2-AG remained unchanged between the three KO cell lines, thus it is unlikely that transcript changes detected from these cell lines truly relate to any functional changes in eCB synthesis and are more likely to be due to clonal variation.

As mentioned above, there was negligible difference in the levels of 2-AG and AEA between the three KO cell lines despite the additional absence of NAPEPLD. AEA levels from NAPEPLD KO cells are still relatively higher than those measured from the parental CB1-Tango cells, and slight differences observed between the KO lines are likely due to clonal differences. This sustained AEA level could be attributed to the activity of a FAAH backwards reaction combining free AA with ethanolamine (Arreaza et al., 1997; Mukhopadhyay et al., 2011), however high levels of AA and ethanolamine are required to tip the equilibrium of the reaction backwards to generate AEA from FAAH (Katayama et al., 1999). Whether this is relevant in our cell line is unknown, but as local concentrations of AA and ethanolamine may reach high enough concentrations, this pathway cannot be rigorously ruled out (Ueda et al., 2000). However, seeing the readily detectable and stable levels of AEA between the three KO cell lines, it is more likely that the other documented synthesis pathways which are not NAPEPLD-dependent are contributing to the generation of AEA (Liu et al., 2008).

Related lipid OEA also showed no differences in the NAPEPLD KO lines. Interestingly, the other related lipid PEA had significantly lower but not complete depletion in the NAPEPLD KO line. Again, this could be a result of clonal variances, but could also be indicative of the partial involvement of NAPEPLD in the generation of PEA, despite showing no changes between the parental CB1-Tango cells and the DAGLα/β KO line with higher NAPEPLD transcript levels. From previous animal KO studies of NAPEPLD, the largest changes were seen in saturated and monounsaturated NAEs such as PEA and OEA (as opposed to AEA which is polyunsaturated), with reductions seen in both PEA and OEA but with more noticeable reductions in PEA levels (Leung et al., 2006; Tsuboi et al., 2011; Leishman et al., 2016). This would suggest there are NAPEPLD-dependent and independent pathways to the generation of these NAEs and that there are overlapping but distinct substrate specificity between these pathways. These pathways could very well be the same pathways described

to be involved in the generation of AEA (Liu et al., 2008). If the change in PEA levels was reflective of a functional change in the NAPEPLD KO cell line, this would fit with the studies of NAPEPLD KO mice and the observation that NAPEPLD is non-selective for the lipid side chain of the substrate (Ueda et al., 2013). It is also possible that NAPEPLD can generate other lipids that might function as an eCB, however due to the scope of the work and the availability of equipment and methods available to us, only the levels of the mentioned lipids were measured from the cell lines.

When tested in the CB1-Tango assays, NAPEPLD KO2 line generally responded in the same manner as the DAGLα/β KO line in the CB1-Tango assays. Treatment with ACEA revealed similar maximal activation levels to the DAGLα/β KO line, a substantial basal eCB tone is still present and evoked eCB signalling with ionomycin, FSK and PMA also generated eCB signalling on comparable levels. The lack of change in the responses and the basal levels of AEA despite the genetic KO of NAPEPLD would suggest that NAPEPLD does not have a pivotal role in the generation of eCBs such as AEA for eCB signalling in NAPEPLD KO2 cell line. The NAPEPLD KO1 line, as mentioned previously, showed muted responses to ACEA, JZL195 and FSK in both media conditions which was present across several experiments and conditions indicating disruption of some of the internal metabolic processes of the cell, thus affecting the responsiveness of the cell to agonists at the CB1 receptor. The absolute magnitude of the response is therefore not fundamental in this cell line due to the off-target effects, but a substantial eCB tone and eCB signalling can still be evoked and detected in the NAPEPLD KO1 cell line despite the KO of NAPEPLD, supporting the generation of eCB signalling through DAGL and NAPEPLD-independent pathways.

The minor role of NAPEPLD towards AEA synthesis is supported by previous studies in NAPEPLD KO mice models (Leung et al., 2006; Liu et al., 2008; Tsuboi et al., 2011; Leishman et al., 2016). Studies differ between different strains of mice used to generate the NAPEPLD KO lines, analytical methods and which lipids were measured, however the general consensus is whilst there are slight reductions in endogenous AEA and other saturated and mono-unsaturated NAE levels in the brain, the attenuation of NAPEPLD does not abolish AEA and NAE levels completely, thus independent mechanisms of AEA generation clearly exist (Liu et al., 2008; Simon and Cravatt, 2010; Tsuboi et al., 2011). These studies generally focused on measuring lipid levels in the brain, but NAE levels (including AEA) were also unaltered in peripheral tissues including the heart, kidney and jejunum (Inoue et al., 2017), consistent with measurements from brain homogenate and the results from the CB1-Tango

cells in this study. However, NAPE levels did generally increase in the NAPEPLD KO animals (Tsuboi et al., 2011; Inoue et al., 2017), and NAPEPLD activity against exogenously applied NAPE was reduced in different tissue areas (Leung et al., 2006). This suggests that NAPEPLD does facilitate the hydrolysis of certain NAPE into NAEs (such as PEA) but other mechanisms also exist to generate and maintain levels of NAEs, particularly of AEA. Therefore, in the NAPEPLD KO cell lines generated in this study, NAPEPLD independent pathways must exist to generate the basal pool of AEA in these cells.

The bulk of AEA synthesis may not be attributable to the action of NAPEPLD, but NAPEPLD is widely expressed and conserved (Okamoto et al., 2004) indicating possible secondary roles of this enzyme that is not eCB signalling. Aside from the generation of NAEs which are biologically active at different receptors, another possible role of NAPEPLD was reported (Guo et al., 2013). NAPEPLD was proposed to degrade potentially harmful aldehyde-modified phosphatidylethanolamines such as isolevuglandin-modified phosphatidylethanolamine (IsoLG-PE). Levels of IsoLG-PE are increased during oxidative stress *in vivo* and can induce a variety of pathological cellular responses (Hoppe et al., 1997; Davies et al., 2002; Fukuda et al., 2005), therefore NAPEPLD may be useful to relieve the pathological effects of oxidative stress. In fact, other NAEs generated by NAPEPLD have protective roles, for example PEA has been suggested to show anti-inflammatory, analgesic, and neuroprotective actions through activity at the PPARα receptor (Hansen, 2010; Petrosino et al., 2010). NAPEPLD might therefore be involved in a protective role against inflammation and oxidative stress by the degradation of harmful modified PE such as IsoLG-PE and the production of protective NEAs such as PEA, which may be physiologically relevant in areas of high oxidative stress such as the brain. Indeed, brain insults such as traumatic brain injury or ischemic conditions cause the increase in NAPE and NAE levels (Moesgaard et al., 1999; Hansen et al., 2001a; Berger et al., 2004) which can have protective effects (Esposito et al., 2014) and NAPEPLD could play a vital role. FAAH has also been implicated in the generation of potentially protective NAEs under ischaemic conditions in a backwards reaction (Lin et al., 2017) which could potentially function in tandem with the actions of NAPEPLD. Other lipids can also be generated by NAPE such as OEA which has also been proposed to bind to PPARα receptor and mediates feeding behaviour (Piomelli, 2013) and SEA also possesses anti-inflammatory and anorexic properties (Astarita and Piomelli, 2009).

Since the generation of NAPEPLD KO mice revealed its slight contribution to AEA levels, other metabolic pathways which can synthesise AEA have been discovered. At least two other

pathways have been suggested for the generation of AEA. First the combined actions of ABHD4 and GDE1 (Simon and Cravatt, 2006) which has shown expression in brain as well as other tissues in the body (Simon and Cravatt, 2008). These enzymes have also been detected at relatively high levels in the U2OS cells from data gathered from the Human Protein Atlas (Thul et al., 2017). However, this pathway is complicated by the result from double NAPEPLD/GDE1 KO mice showing no reduction in AEA levels (Simon and Cravatt, 2010), thus a lysoPLD activity has been attributed to the generation of AEA from the intermediate generated by ABHD4 (Sun et al., 2004). Secondly, the actions of an unidentified PLC and PTPN22 can also generate AEA (Liu et al., 2006). This mechanism is highly localised to macrophages in response to stimulation to lipopolysaccharide (LPS) and thus PTPN22 has very low level of detection in U2OS cells (Thul et al., 2017). It is more likely that the former pathway is present in the NAPEPLD KO cell lines generated, however there are limited pharmacological tools targeting these enzymes, the enzymes themselves may have more than one role, and some enzymes have not been fully characterised for CRISPR treatment. As well as this, it is not likely that the regulatory step of AEA synthesis lies in the hydrolysis step from NAPE to NAEs. Therefore, focus was placed on the calcium sensitive generation step of NAPE as the regulatory step of AEA synthesis.

The calcium sensitive generation of NAPE is mediated through a CaNAT enzyme, which has recently been identified as PLA2G4E (Ogura et al., 2016). This enzyme also displays similar activity in the human isotope (Hussain et al., 2018) and can generate the precursor NAPE to AEA along with other N-AcylPEs. Although there are other proposed enzymes that can generate NAPE (i.e. iNAT and related PLAAT enzymes (Jin et al., 2007; Jin et al., 2009; Hussain et al., 2017)), these enzymes show very limited calcium sensitivity. Since we can evoke eCB signalling through calcium elevation in our cell lines, this suggests a calcium sensitive NAT is present in our CB1-Tango cell lines.

From the results in this chapter, two NAPEPLD KO lines have been generated in which AEA levels are largely unchanged and eCB signalling can still be evoked in both lines to similar levels as DAGLα/β KO line. Between the two cell lines generated, NAPEPLD KO1 shows reduced responsiveness to ACEA, reduced eCB tone and more rounded morphology (unpublished observations), which may be due to either clonal variances or from CRISPR-mediated off-target effects causing metabolic changes on the cells. Because of this, for further downstream applications of CaNAT characterisation, the NAPEPLD KO2 line (later referred to simply as NAPEPLD KO line) was taken forward for further CRISPR treatment.

6.4 **Results 4C.** The role of PLA2G4B in eCB signalling

6.4.1 **Results 4C.** Introduction

The genetic deletion of the DAGLs and NAPEPLD from the CB1-Tango cells revealed that very robust eCB signalling can still be evoked by three different stimuli and that these enzymes are also dispensable in the generation of the a basal eCB tone. The genetic KO of the DAGLs reduced the basal levels of 2-AG by ~90%, identifying them as key enzymes for 2-AG synthesis, however the DAGLs and 2-AG had only a minor contribution to the measured eCB tone. Whilst the lipid(s) responsible for eCB signalling remain uncertain, the second most abundant eCB AEA obviously emerges as the prime candidate, although other unidentified eCBs could also be responsible. The most widely accepted synthesis pathway of AEA is through the hydrolysis of NAPE by NAPEPLD, however conclusions from various animal KO studies and through the results of the previous chapter, an eCB tone including but not limited to AEA, can still be robustly generated in the absence of NAPEPLD in addition to the DAGLs. Thus, other pathways of AEA generation must be present in the CB1-Tango cells.

Since the generation of NAPEPLD KO mice revealed the minor contribution of NAPEPLD to the generation of AEA (Leung et al., 2006; Tsuboi et al., 2011; Leishman et al., 2016), other synthesis pathways have been suggested as the pathways for the generation of AEA in a NAPEPLD independent manner (Liu et al., 2006; Simon and Cravatt, 2006, 2008). The presence of more than one separate pathway complicates the study of AEA synthesis in the CB1-Tango cells as pharmacological tools are limited for these pathways, the enzymes may have more than one role in the cell and some of the enzymes in the pathway are not fully characterised for CRISPR treatment. As well as this, it is not likely that the regulatory step of AEA synthesis lies with the step from NAPE hydrolysis to AEA due to the redundancy of these pathways. It was therefore prudent to focus on the preceding step: NAPE synthesis from membrane lipids catalysed by an N-acyltransferase enzyme.

In the 1980s, a single step N-acyltransferase enzymatic activity was described from dog heart and brain tissue that could transfer an acyl group (including arachidonoyl to generate the precursor for AEA) from PC to PE to generate N-AcylPE (Natarajan et al., 1983; Reddy et al., 1983). This enzymatic activity had been extensively characterised since first described, but the enzyme responsible for the generation of N-AcylPE, the CaNAT, had remained elusive for

many years until its recent discovery. The key features of this enzyme are: (1) its dependence on calcium for activation, (2) its preference for the *sn*-1 position over the *sn*-2 position of the donor lipid and (3) to use phospholipids but not free fatty acid or acyl-CoA as a donor (Natarajan et al., 1981; Schmid et al., 1990; Cadas et al., 1996; Cadas et al., 1997). As well as this, areas of CaNAT activity were characterised in rat tissues. The highest activity was present in the brain, with lower but significant activity in testis and muscles, and low activity in other tissues. Within the brain, the highest activity was detected in brainstem, with intermediate activity in the cortex, striatum, hippocampus, medulla and cerebellum and low levels present in the thalamus, hypothalamus and olfactory bulb (Cadas et al., 1997).

The dependence on calcium for activity would suggest the activation of CaNAT is a regulatory step of NAPE and consequently AEA synthesis. Low levels of arachidonoyl-containing NAPE and AEA are measured from brain homogenate but are markedly increased after stimulation with calcium (Cadas et al., 1996; Sugiura et al., 1996; Astarita et al., 2008). The activity of the CaNAT can also be enhanced by treatment with FSK indicating and involvement of cAMP in activity regulation, however the precise mechanism through which this occurs has not been elucidated (Cadas et al., 1996). The areas of CaNAT activity coincides with the pattern of NAPEPLD expression with prominent levels detected in the brain and testis, areas where AEA is known to be generated, but CaNAT activity is slightly more restricted than NAPEPLD expression (Cadas et al., 1997). Taking together the expression pattern of the CaNAT activity and its dependence on calcium for activation, this places the CaNAT as an interesting enzyme to examine as the potential regulatory step of AEA synthesis pathway and the key enzyme for the generation of AEA for eCB signalling.

In the pursuit to identify the CaNAT enzyme, calcium-insensitive enzymes that have N-acyltransferase activity were identified (i.e. iNAT and related PLAAT enzymes) however these enzymes did not match the enzymological or expression profile of the CaNAT which had been extensively profiled and the physiological role of these enzymes in the generation of AEA uncertain (Jin et al., 2007; Jin et al., 2009; Ueda et al., 2010; Hussain et al., 2017). The enzyme responsible for the CaNAT activity remained elusive for many years but was recently proposed to be the poorly characterised serine hydrolase PLA2G4E (Ogura et al., 2016).

PLA2G4E was identified as the elusive CaNAT through activity-based protein profiling from mouse brain homogenate. Expression of PLA2G4E in HEK293T cells demonstrated N-acyltransferase activity, could generate the NAPE precursor to AEA along with other N-acylPE to NAE derivatives, the activity was dependent on calcium and was not inhibited by THL

(Ogura et al., 2016). Expression of PLA2G4E was revealed by RT-PCR to be present in mouse brain and testis which generally matched areas of CaNAT activity but is also detected predominantly in heart, skeletal muscle, and thyroid (Ohto et al., 2005). The human orthologue of PLA2G4E has recently been functionally characterised in COS7 cells and also shown to exhibit calcium-sensitive NAPE generation (Hussain et al., 2018). Finally, RNA-seq data of sub-populations of cells from mouse cerebral cortex show the highest transcript expression (albeit still relatively low) of PLA2G4E almost exclusively in neurones (Zhang et al., 2014).

However, expression of PLA2G4E is restricted to subpopulations of cells within the brain despite the more ubiquitous expression of NAPEPLD transcripts in other subpopulations of cells such as myelinating oligodendrocytes and endothelial cells (Zhang et al., 2014). Ionomycin also stimulated AEA synthesis from astrocytes despite the lack of PLA2G4E transcripts in astrocytes (Walter et al., 2002). As well as this, previous results from the Quantigene multiplex assay system revealed a lack of PLA2G4E transcripts in the tested cell lines and total RNA from cerebellum and hippocampal brain regions. This raises the possibility that other functionally related enzymes may also generate NAPE and contribute to AEA synthesis in cells and tissues where PLA2G4E appears to be absent. Since PLA2G4E is unlikely to be the enzyme responsible for AEA synthesis in the CB1-Tango cells as the transcripts are not detected, we aimed to search for novel enzymes that could function as the CaNAT.

To begin the search for novel candidate enzymes that could function as an additional CaNAT, focus was placed on the related family of genes to PLA2G4E which may have similar N-acyltransferase function to PLA2G4E. PLA2G4E belongs to the PLA2G4 family (A-F) of which, aside from PLA2G4A, are poorly characterised (Ghosh et al., 2006). These members of the family are all cytosolic proteins but are membrane associated and display calcium sensitivity through the conserved C2 domain (except PLA2G4C) and share homology in the catalytic region (Table 6.4.1). The related enzymes may therefore exhibit similar activity to PLA2G4E and perhaps can also generate NAPE in regions where expression of PLA2G4E is not present. Of the poorly characterised enzymes, PLA2G4C shows no calcium sensitivity and expression patterns of PLA2G4D and PLA2G4F showed abundancy in skin and reproductive organs but were not detected in RNA sequencing of various brain cells (Zhang et al., 2014).

GROUP	SPECIES	TISSUE DISTRIBUTION	CONSERVED DOMAIN	ACTIVE RESIDUES
PLA2G4A	Human	Ubiquitous	C2	R^{200}, S^{228}, D^{549}
	Mouse	Ubiquitous	C2	R^{200}, S^{228}, D^{548}
PLA2G4B	Human	Ubiquitous	JMJC, C2	R^{538}, S^{566}, D^{846}
	Mouse	Not determined	C2	R^{305}, S^{333}, D^{613}
PLA2G4C	Human	Ubiquitous	CAAX	R^{54}, S^{82}, D^{385}
	Mouse	Oocytes	-	R^{55}, S^{83}, D^{417}
PLA2G4D	Human	Psoriatic lesions, fetal skin, cervix	C2	R^{333}, S^{361}, D^{647}
	Mouse	Placenta	C2	R^{342}, S^{370}, D^{654}
PLA2G4E	Human	Skin, GI tract, ovaries		R^{8}, S^{36}, D^{324}
	Mouse	Heart, skeletal muscle, testis, thyroid	C2	R^{392}, S^{420}, D^{708}
PLA2G4F	Human	Skin, lung, muscles	C2	R^{367}, S^{395}, D^{680}
	Mouse	Prostate, stomach, large intestine	C2	R^{365}, S^{393}, D^{685}

Table 6.4.1. Properties of human and mouse PLA2G4 family

Adapted from Ghosh et al. (2006).

PLA2G4B on the other hand shows high expression in cerebellum, heart, pancreas and liver in mice (Ghosh et al., 2006) and is detected relatively ubiquitously in mouse cerebral cortex but is more highly detected in astrocytes, neurons and oligodendrocyte precursor cells (Zhang et al., 2014). From results in the previous chapters, expression of PLA2G4B is readily detected in total RNA from cerebellum and hippocampus and from the CB1-Tango cells in relatively comparable levels, which was maintained through CRISPR treatments and genetic KO of the eCB synthesising enzymes, placing it as a suitable candidate enzyme for CaNAT activity in the CB1-Tango cells. Since PLA2G4B is detected readily in the triple KO cell line generated in the last section, genetic disruption will be adopted in this chapter to elucidate what possible role PLA2G4B may have on eCB signalling.

In this chapter, the expression of PLA2G4E in the CB1-Tango cells will be determined with RT-PCR and its role in AEA synthesis in our cell line will be discussed. The generation of PLA2G4B KO cell line from the triple KO cell line (NAPEPLD KO) will be described in this chapter. The characterisation of the cell line will determine the successful KO of PLA2G4B and the effects on the eCB levels of the cells will be measured. The cell line will then be tested in the CB1-Tango assay using previously established paradigms that can generate eCB signalling to determine the role of PLA2G4B in eCB signalling.

6.4.2 **Results 4C.** Results

PLA2G4E expression is not detected in CB1-Tango cells

Previous results from the QuantiGene multiplex assay revealed no PLA2G4E transcripts were detected in the parental CB1-Tango cell line (Net MFI <10). Subsequent treatments with CRISPR also failed to induce any noticeable changes in transcript levels, despite changes in NAPEPLD transcript levels and AEA lipid levels. Based on this we can conclude that PLA2G4E is not expressed in the CB1-Tango cell line and that it cannot play a role in AEA synthesis. However, given the importance of this point we performed additional studies to confirm the result.

To confirm the results from the QuantiGene multiplex assay, RT-PCR was carried out from the parental CB1-Tango cell line and the DAGLα/β KO cell line. In the original publication by Ogura et al. (2016), total RNA from various organs of C57BL/6J mice was used to detect expression of PLA2G4E, therefore as a control C57BL/6J mouse brain RNA was included in the RT-PCR reaction. The primers used for mouse PLA2G4E were also the same as previously described by Ogura et al. (2016) and the primers were codon matched for the human variant of PLA2G4E (Table 2.1.2). GAPDH was also included as a control and the primers used were also codon matched.

RT-PCR results show detectable levels of PLA2G4E in mouse brain at around the expected size of 403bp (Figure 6.4.1). However, a corresponding band from the CB1-Tango cells at around 400bp is not present. The RT-PCR for GAPDH, which was carried out at the same time, was successful in both mouse brain RNA and RNA from the CB1-Tango cell lines indicating a successful reaction. This result supports the QuantiGene multiplex assay results of a lack of PLA2G4E expression in the CB1-Tango cell line.

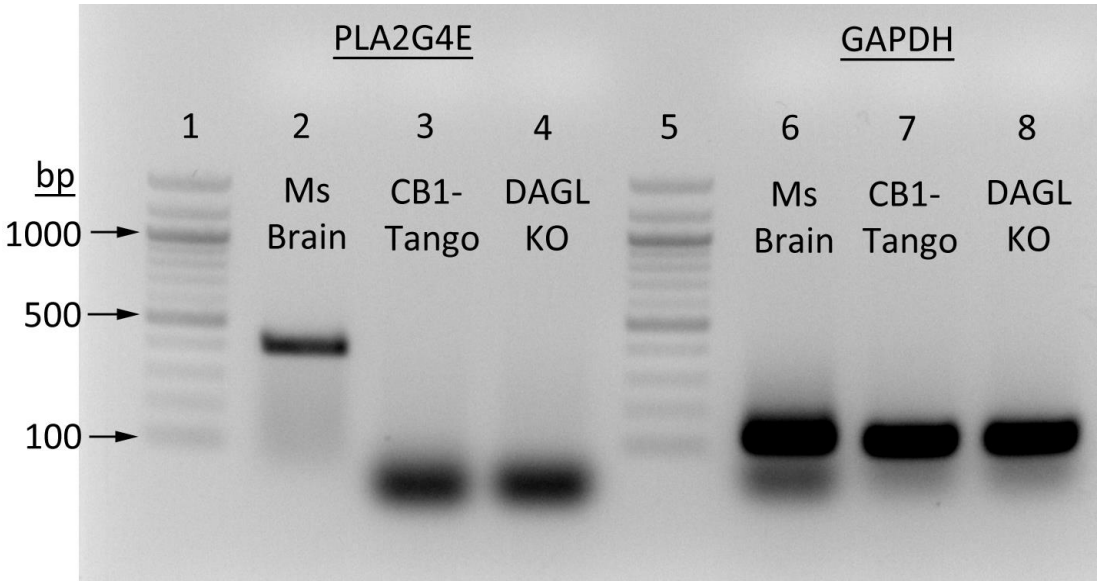

Figure 6.4.1. RT-PCR of PLA2G4E and GADPH in CB1-Tango and DAGLα/β KO cells

CB1-Tango and DAGLα/β KO cells were grown in T75 flasks until 90% confluent, pelleted and RNA was extracted according to manufacturer's instructions. Mouse brain RNA was extracted from brain of a C57BL/6J WT mouse, aged embryonic day 17.5 using TRIzol RNA extraction kit. RNA was then converted to cDNA and mixed with primers to PLA2G4E and GAPDH and PCR mix and the PCR programme was run as previously described by (Ogura et al., 2016). The PCR was then run on 1% agarose gel (expected band sizes: PLA2G4E Ms – 403bp, Hu – 400bp; GAPDH Ms – 123bp, Hu 123bp).

Design of PLA2G4B gRNA and generation of CRISPR vectors

As PLA2G4E transcript expression is not present in the CB1-Tango cell lines, CRISPR treatment of the PLA2G4E gene would be imprudent and could further disrupt expression of other genes or overall cell viability. Therefore, focus was placed on the related yet uncharacterised enzyme PLA2G4B, transcripts of which can be readily detected in the cells and have shown slight increases in transcript levels between CB1-Tango KO lines, although this may be a clonal variance.

The PLA2G4B gene consists of 21 exons, with the catalytic triad residues arginine and serine located in exon 13 and aspartic acid located in exon 19 (Figure 6.4.2). Aside from the catalytic residues, another arginine residue in exon 19 is also required for structural integrity of the catalytic site (Pickard et al., 1999; Song et al., 1999), as highlighted in green in Figure 6.4.2. Thus, the gRNAs were designed to exon 13 and exon 19 to encompass the catalytic triad to completely eradicate catalytic activity of the cells (Figure 6.4.3).

The gRNAs were inserted in the vector backbone as described previously in 2.2 Methods and four separate CRISPR vectors were generated. Pools of cells were transfected with all four CRISPR vectors at once and positively selected with puromycin. The selected cells were then seeded at low density to facilitate isolation of individual cells, left to grow into discrete colonies for picking and expansion for further analysis as previously described.

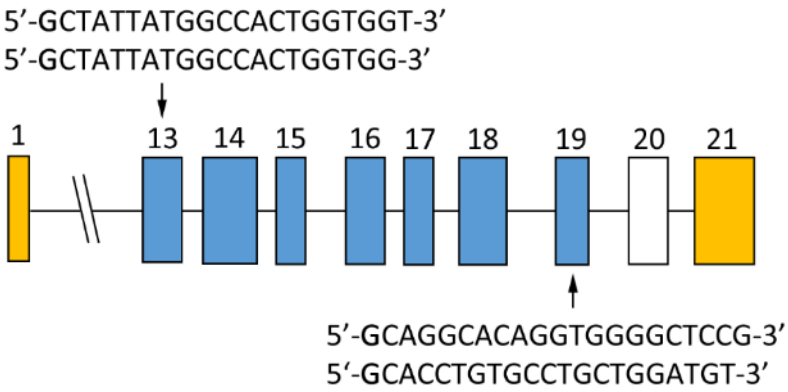

Figure 6.4.2. Selection of gRNA sequences selected for Cas9 recognition of PLA2G4B catalytic domain

Schematic representation of the human PLA2G4B sequence, indicating the UTRs (yellow) and the catalytic domains (blue). Target sequences were designed to exon 13 and exon 19 to target the catalytic triad residues. Sequences for gRNAs begin with G (bold) for U6 promotor recognition (Ran et al., 2013).

(A)

(B)

Figure 6.4.3. Targets of exon 13 and exon 19 of PLA2G4B DNA sequence

DNA sequence of PLA2G4B exon 13 (A) and exon 19 (B) is displayed above and the corresponding amino acid sequence is displayed in purple below the DNA sequence. The sequences important for catalytic activity of PLA2G4B is highlighted in green and underlined. Guide RNA sequences are highlighted in blue above and below the sequence and underlined, the 5'-NGG PAM sequence is in red flanking the catalytic motifs.

Characterisation of PLA2G4B KO cell lines show disrupted transcripts

After the cell colonies were grown to sufficient numbers, genomic DNA was extracted from according to manufacturer's instructions. PCR amplification of the catalytic site was carried out with primers located in the introns flanking exon 13 and 19 (Table 2.1.2) to PCR across the CRISPR sites. The PCR reaction was then run on 1% agarose gel to visualise the bands (Figure 6.4.4).

The NAPEPLD KO parental control line had a prominent band at around 3kbp which is around the expected size of the intact fragment. A few of the tested cell colonies failed to produce a band and others showed more subtle mutations. With the largest deletion of the middle fragment of DNA, the expected band size was predicted to be around 500bp. Three colonies contained a relatively clean band around the predicted size; clone 1, 6 and 8 were therefore taken forward in the project for characterisation renamed PLA2G4B KO1, KO2 and KO3 respectively.

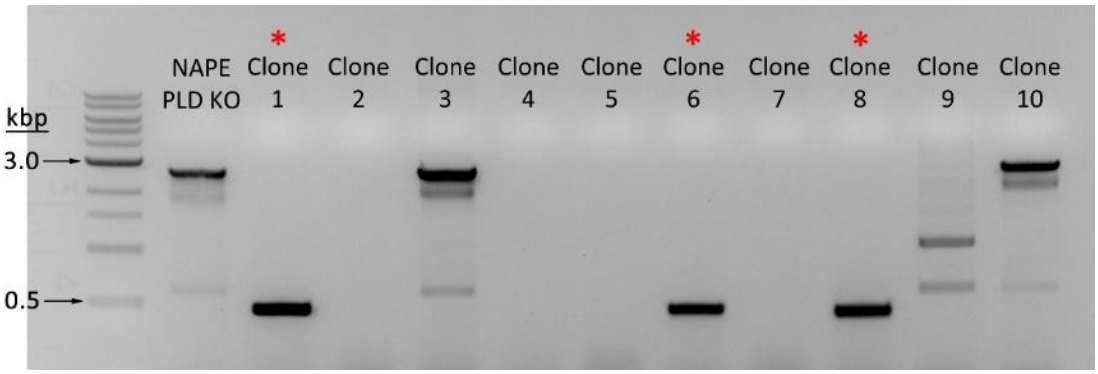

Figure 6.4.4. PCR of PLA2G4B CRISPR treated cells show disruptions in the genomic DNA

NAPEPLD KO cell line, which the PLA2G4B CRISPR treated cells were derived from, and PLA2G4B CRISPR treated cells were grown from individual colonies to 90% confluent T75 flasks and then pelleted and DNA was extracted according to manufacturer's instructions. PCR was run with primers located in introns before exon 13 and after exon 19 of PLA2G4B. The PCR was then run on 1% agarose gel (expected band sizes: PLA2G4B WT – 2704bp; with the widest expected mutations – around 472bp). Red asterisks indicate cell lines taken forward in the project.

The bands from the PCR with genomic DNA was extracted from the gel, purified and then sent for Sanger sequencing. The results for PLA2G4B KO1 and KO2 were clear with only one reading per line, but results for KO3 showed disruption at the first CRISPR gRNA which leads to the detection of two separate sequences (Figure 6.4.5). The presence of two sequences would indicate the presence of two differentially repaired alleles, although it would be difficult to determine the separate sequences after the CRISPR site. The sequences from all three KO lines are aligned against the complete PLA2G4B exon 13 sequence in Figure 6.4.6A and KO1 and KO2 were aligned to the exon 19 sequence in Figure 6.4.6B.

The mutations from the cell lines begin and end at CRISPR targeted areas with minor indel mutations found at the CRISPR sites. The sequence contained within the CRISPR sites are absent in KO1 and KO2 sequences. Translation of the DNA sequences obtained confirm the absence of the catalytic residues of PLA2G4B, despite not reaching a stop codon within the sequence (Figure 6.4.7). Whilst the sequence from KO3 could be aligned to the beginning of exon 13, it was not possible to align KO3 after the CRISPR treated site, therefore it was not confirmed if both alleles of PLA2G4B was disrupted in the PLA2G4B KO3 cell line.

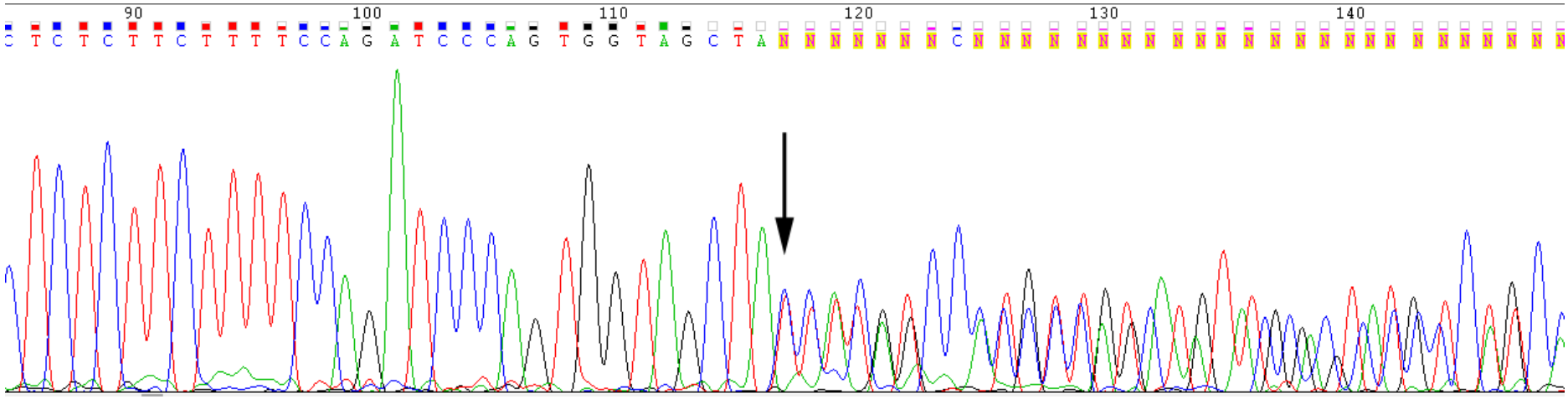
90
100
110
120
130
140
C T C T C T T C T T T T C C A G A T C C C A G T G G T A G C T A N N N N N N N C N N N N N N N

Figure 6.4.6. Sequencing results of PLA2G4B PCR product reveal large deletions between CRISPR sites

PLA2G4B CRISPR treated cells KO1, KO2 and KO3 were grown in T75 flasks until confluent and genomic DNA was extracted from the pelleted cells. PCR was carried out with primers flanking exon 13 and 19 as listed in methods. The PCR product was then run on 1% agarose gel and purified from the gel. The purified PCR product and primers were sent for Sanger sequencing. The results for PLA2G4B KO1, KO2 and KO3 were aligned in Clustal Omega against WT PLA2G4B sequence (AmpSeq). Results show the beginning of alignment (A) and the end of alignment (B).

(A)

```
AmpSeq          ctggtcccaagacctgtgatcaggccttagctgtgggctgggtggccacttgacctgcta
PLA2G4BKO1      ------------------------------NNNNNNNNNNNNNNNCNNTTGNNNTGCNN
PLA2G4BKO2      ------------------------------NNNNNNNNNNNNNNNNNNNNNTTGNCTGCTN
PLA2G4BKO3      ------------------------------NNNNNNNNNNNNNNNNNNNNNNNNNNNGCTA
                                                                        **

AmpSeq          cctcttcttcctgtgacttggccttccccatccctagggcctctacaggcctggctctct
PLA2G4BKO1      CCTCTTCTTCCTGTGACTTGGCCTTCCCCATCCCTAGGGCCTCNCCNGGCCTGGCTCTCT
PLA2G4BKO2      CCTCTTCTTCCTGTGACTTGGCCTTCCCCATCCCTAGGGCCNNNANNGNCNTGGCTCTCT
PLA2G4BKO3      CCTCTTCTTCCTGTGACTTGGCCTTCCCCATCCCTAGGGCCTCTACAGGCCTGGCTCTCT
                ****************************************      * * *********

AmpSeq          tcttttccagATCCCAGTGGTAGCTATTATGGCCACTGGTGGTGGGATCCGGGCAATGAC
PLA2G4BKO1      TCTTTTCCAGATCCCAGTGGTAGCTATTATGGCCACTGGT--------------------
PLA2G4BKO2      TCTTTTCCAGATCCCAGTGGTAGCTATTATGGCCACTGGT--------------------
PLA2G4BKO3      TCTTTTCCAGATCCCAGTGGTAGCTA----------------------------------
                ***************************
```

(B)

```
AmpSeq          ATGGGCTCCCCAACCAGCTGACACCCTCGGAGCCCCACCTGTGCCTGCTGGATGTTGGCT
PLA2G4BKO1      ------------------------------AGCCCCACCTGTGCCTGCTGGATGTTGGCT
PLA2G4BKO2      ------------------------------AGCCCCACCTGTGCCTGCTG--TGTTGGCT
                                              ********************  ********

AmpSeq          ACCTCATCAATACCAGCTGCCTGCCCCTCCTGCAGCCCACTCGGGACGTGGACCTCATCC
PLA2G4BKO1      ACCTCATCAATACCAGCTGCCTGCCCCTCCTGCAGCCCACTCGGGACGTGGACCTCATCC
PLA2G4BKO2      ACCTCATCAATACCAGCTGCCTGCCCCTCCTGCAGCCCACTCGGGACGTGGACCTCATCC
                ************************************************************

AmpSeq          TGTCATTGGACTACAACCTCCACGGAGCCTTCCAGgttgggaagggtgggcagcccacca
PLA2G4BKO1      TGTCATTGGACTACAACCTCCACGGAGCCTTCCAGGTTGAGAAGGGTGGGCAGCCCACCA
PLA2G4BKO2      TGTCATTGGACTACAACCTCCACGGAGCCTTCCAGGTTGAGAAGGGTGGGCAGCCCACCA
                ************************************ ********************

AmpSeq          gggaggcggtgggtggcccctgtcccctgaagagaggggctttggagtccagtgtctggt
PLA2G4BKO1      GGGAGGCGGTGGGTGGCCCCTGTCCCCTGAAGAGAGGGGCTTTGGAGTCCAGTGTCTGGT
PLA2G4BKO2      GGGAGGCGGTGGGTGGCCCCTGTCCCCTGAAGAGAGGGGCTTTGGAGTCCAGTGTCTGGT
                ************************************************************

AmpSeq          tcagcttcctttaggagctgtgattgggacactggaatcttaatttgccaccagaggagc
PLA2G4BKO1      TCAGCTTCCTTTAGGAGCTGTGATTGGGACACTGGAATCTTAATTTGCCACCAGAGGAGC
PLA2G4BKO2      TCAGCTTCCTTTAGGAGCTGTGATTGGGACACTGGAATCTTAATTTGCCACCAGAGGAGC
                ************************************************************

AmpSeq          tcattcttttccggaagttgggaggctggcgaggttctcctggtatcttgtagctgggtc
PLA2G4BKO1      TCATTCTTTTCCGGAAGTTGGGAGGCTGGCGAGGTTCTCCTGGTATCTTGTAGCTGGGTC
PLA2G4BKO2      TCATTCTTTTCCGGAAGTTGGGAGGCTGGCGAGGTTCTCCTGGTATCTTGTAGCTGGGTC
                ************************************************************
```

Figure 6.4.7. Protein sequences of PLA2G4B KO1 and KO2 cells exclude catalytically important motifs

The sequencing results of exons from PLA2G4B KO1 and KO2 cells were translated and aligned with the amino acid sequence of WT PLA2G4B (AmpSeq). Motifs which are important for the catalytic activity of PLA2G4B is highlighted in green.

QuantiGene multiplex assay of PLA2G4B KO cell lines confirm genuine PLA2G4B KO lines

For further evidence of the genetic disruption of PLA2G4B in these three cell lines and to determine the effects of PLA2G4B KO on other transcripts of the key components in eCB signalling, the transcriptome of the three cell lines and NAPEPLD KO line were subjected to the QuantiGene multiplex assay (Figure 6.4.8).

Transcript levels of other key components remained largely unchanged across all the cell lines, CNR1 transcripts in PLA2G4B KO3 are detected at slightly lower levels but this was not statistically significant. There were some statistically significant but relatively minor fluctuations in transcript levels of the eCB degrading enzymes MGLL, FAAH and ABHD6 across the cell lines. The relative levels obtained in NAPEPLD KO line were 0.017 ± 0.001 for MGLL, 0.031 ± 0.001 for FAAH and 0.177 ± 0.004 for ABHD6. PLA2G4B KO2 showed slightly higher levels of MGLL (0.028 ± 0.002) and ABHD6 (0.303 ± 0.004) but decreases in level in FAAH (0.023 ± 0.001). PLA2G4B KO3 had the most similar levels of the eCB degrading enzymes to those obtained from the NAPEPLD KO line (0.018 ± 0.003 for MGLL, 0.038 ± 0.002 for FAAH and 0.237 ± 0.011 for ABHD6).

PLA2G4B transcripts from the NAPEPLD KO line are readily detectable at relatively elevated levels (0.57 ± 0.02 relative expression; 3667.0 ± 124.0 net MFI). The detected transcript levels are significantly reduced in the PLA2G4B KO1 cell line (0.41 ± 0.01 relative expression; 1507.4 ± 47.9 net MFI), but are not completely depleted as expected. Instead, moderate levels of PLA2G4B transcripts are still detected, indicating that the catalytic domain of PLA2G4B is not fully eliminated in this cell line and thus is not a complete knockout. For this reason, the cell line PLA2G4B KO1 is not taken further in the project.

The results from PLA2G4B KO2 show more substantial loss of PLA2G4B transcripts (0.019 ± 0.001 relative expression; 84.8 ± 5.9 net MFI) but this is still within the dynamic detectable range. PLA2G4B KO3 shows complete depletion of PLA2G4B transcripts to below the dynamic detectable range (0.002 ± 0.0005 relative expression; 7.0 ± 1.8 net MFI), indicating that PLA2G4B is likely to be completely eradicated in this cell line despite inconclusive sequencing results. As these two cell lines show substantial KO of PLA2G4B transcripts, they were studied further to determine the effects of PLA2G4B KO on eCB lipid levels.

Figure 6.4.8. Results from the QuantiGene beads assay show PLA2G4B transcripts lack the catalytic domain

NAPEPLD KO cells and PLA2G4B CRISPR treated cells KO1, KO2 and KO3 were grown in T75 flasks until confluent and RNA was extracted from the pelleted cells according to manufacturer's instructions. RNA was diluted to a concentration of 375ng/μl and 20μl was added to wells in a 96 well plate, leading to total RNA in each well to be 7500ng. RNA samples and nuclease free water control samples were then incubated with magnetic beads and probes overnight. The beads were then washed and amplified and read on the Magpix system as in the methods section. The background readings from control wells were subtracted from the sample wells and the data was normalised to the expression of two housekeeping genes. Graph shows to means and bars represent SEMs of 5 replicates of normalised PLA2G4B results from one single experiment. Significance between groups was calculated using One Way ANOVA.

***p<0.001; One-way ANOVA, Dunnett's post-test.

(A)

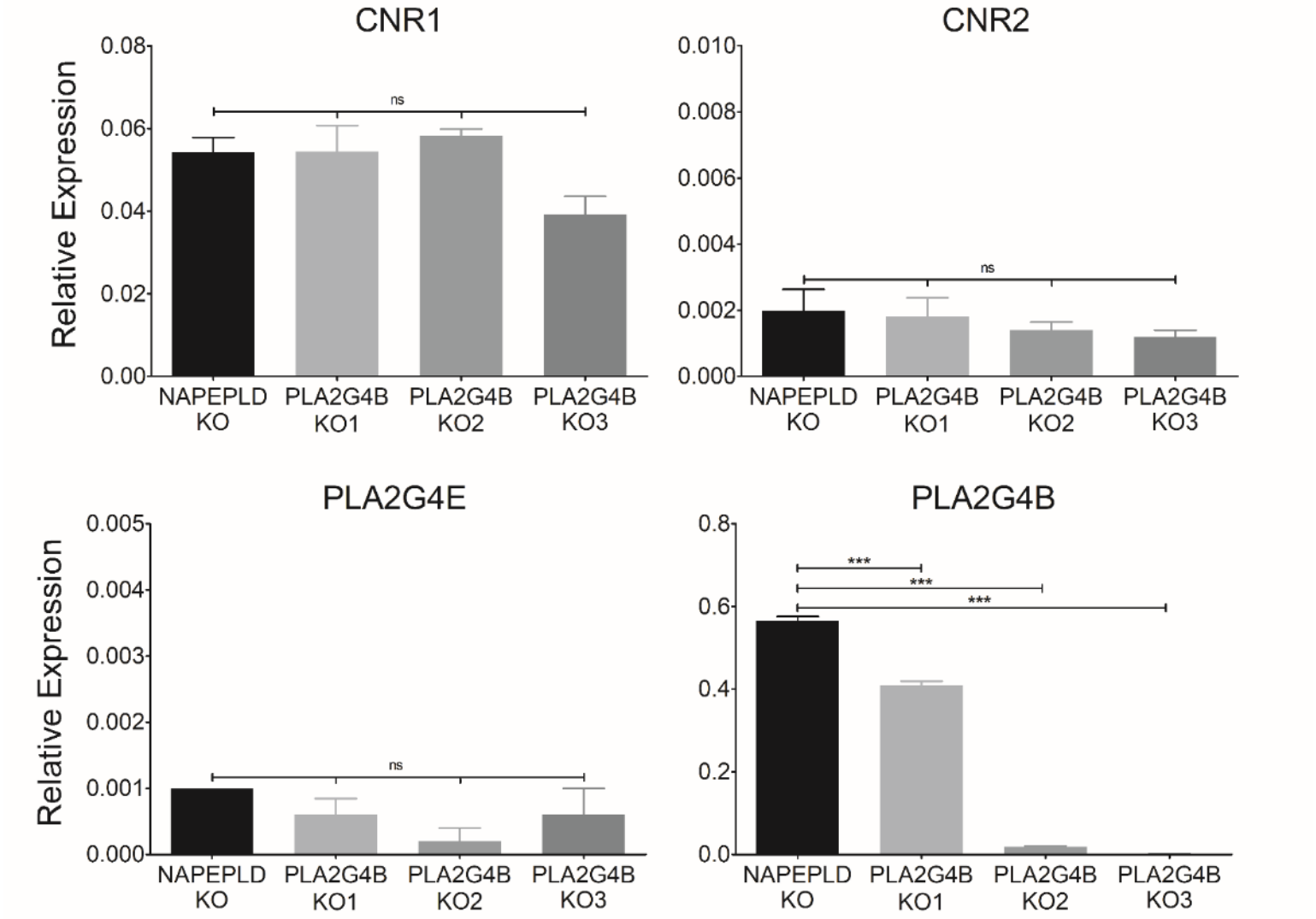
CNR1
Relative Expression
0.08
0.06
0.04
0.02
0.00
ns
NAPEPLD KO
PLA2G4B KO1
PLA2G4B KO2
PLA2G4B KO3
CNR2
0.010
0.008
0.006
0.004
0.002
0.000
ns
NAPEPLD KO
PLA2G4B KO1
PLA2G4B KO2
PLA2G4B KO3
PLA2G4E
Relative Expression
0.005
0.004
0.003
0.002
0.001
0.000
ns
NAPEPLD KO
PLA2G4B KO1
PLA2G4B KO2
PLA2G4B KO3
PLA2G4B
0.8
0.6
0.4
0.2
0.0
***
***
***
NAPEPLD KO
PLA2G4B KO1
PLA2G4B KO2
PLA2G4B KO3

(B)

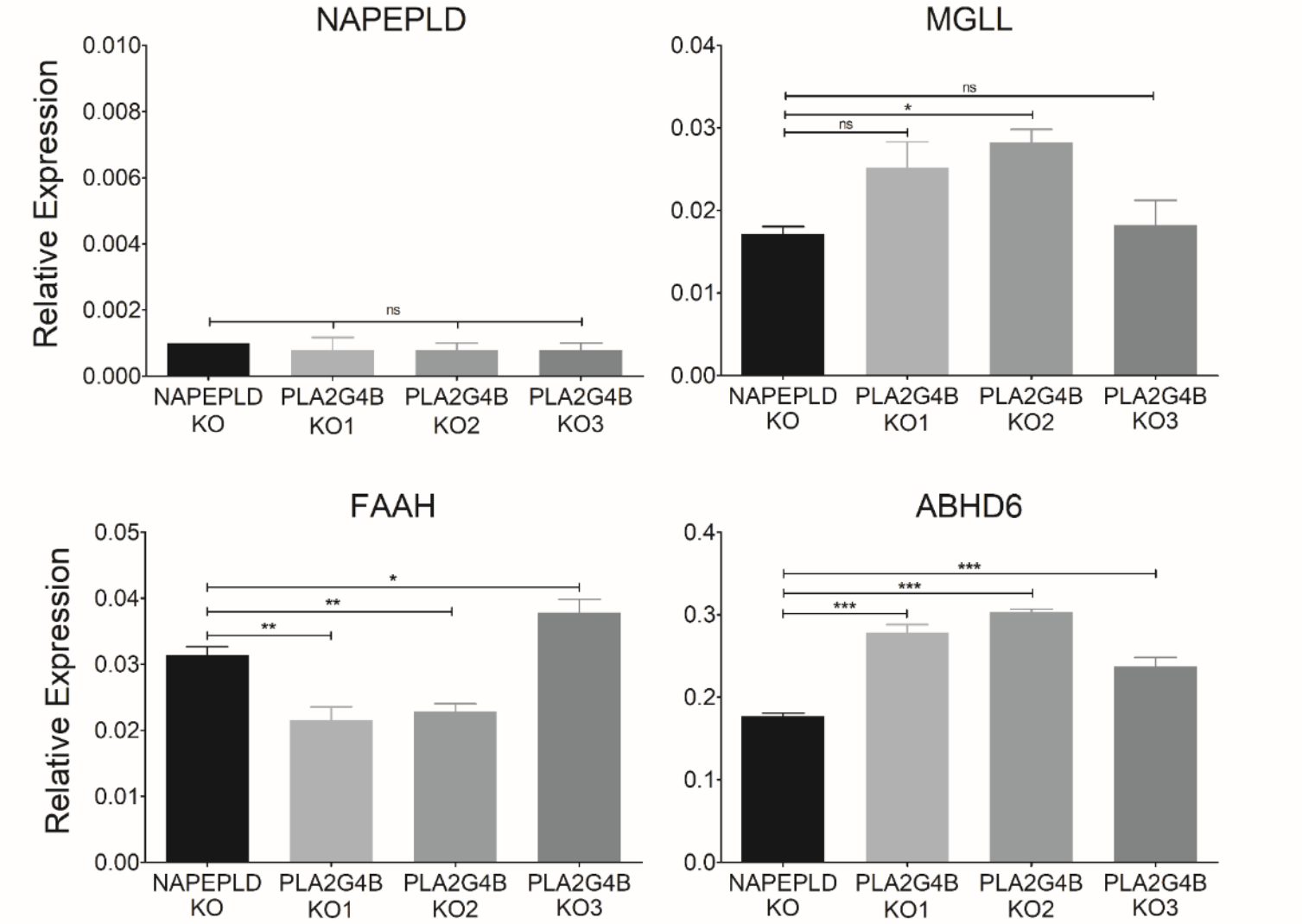
NAPEPLD
Relative Expression
0.010
0.008
0.006
0.004
0.002
0.000
ns
NAPEPLD KO
PLA2G4B KO1
PLA2G4B KO2
PLA2G4B KO3
MGLL
0.04
0.03
0.02
0.01
0.00
ns
*
ns
FAAH
Relative Expression
0.05
0.04
0.03
0.02
0.01
0.00
*
**
**
ABHD6
0.4
0.3
0.2
0.1
0.0
***
***
***

Lipid measurements show insignificant change in AEA levels in PLA2G4B KO lines

After confirmation of successful PLA2G4B KO from the two cell lines: KO2 and KO3, the levels of 2-AG, AEA, OEA and PEA were measured from three independent pelleted samples from each of the PLA2G4B KO cell lines (Figure 6.4.9).

The levels of 2-AG detected in the PLA2G4B KO cell lines remain at a low level (KO2 = 85.69 ± 1.39 pg/10^6 cells, KO3 = 120.95 ± 5.32 pg/10^6 cells) which was not significantly different to the levels mesured from the parental NAPEPLD KO line (123.82 ± 25.06 pg/10^6 cells). The levels of 2-AG from these lines remain at around 10% of the original levels of 2-AG measured from the parental CB1-Tango cell line.

Measured levels of AEA was not significantly different between the NAPEPLD KO (5.82 ± 0.47 pg/10^6 cells) and the PLA2G4B KO cell lines (KO2 = 5.38 ± 0.74 pg/10^6 cells, KO3 = 6.44 ± 0.68 pg/10^6 cells). As well as this, levels of PEA and OEA were also not significantly different between the cell lines, although levels of OEA perhaps were slightly lower in the PLA2G4B KO lines.

Figure 6.4.9. Lipid measurements of PLA2G4B KO2 and KO3 compared to NAPEPLD KO cells

Cell lines were grown in regular conditions until 90% confluent. Cells were then harvested and counted to ensure there were more than $6x10^6$ cells present per sample. Cells were then pelleted and frozen in -80^oC and then shipped on dry ice for their lipid levels to be measured by mass spectrometry. 2-AG, AEA, OEA and PEA levels were measured in each sample and normalised to pg per 10^6 cells. Graph shows means and bars represent SEMs of n = 3. Significance between NAPEPLD KO and PLA2G4B KO2 and KO3 was calculated using One Way ANOVA.

ns p>0.05; One-way ANOVA, Dunnett's post-test.

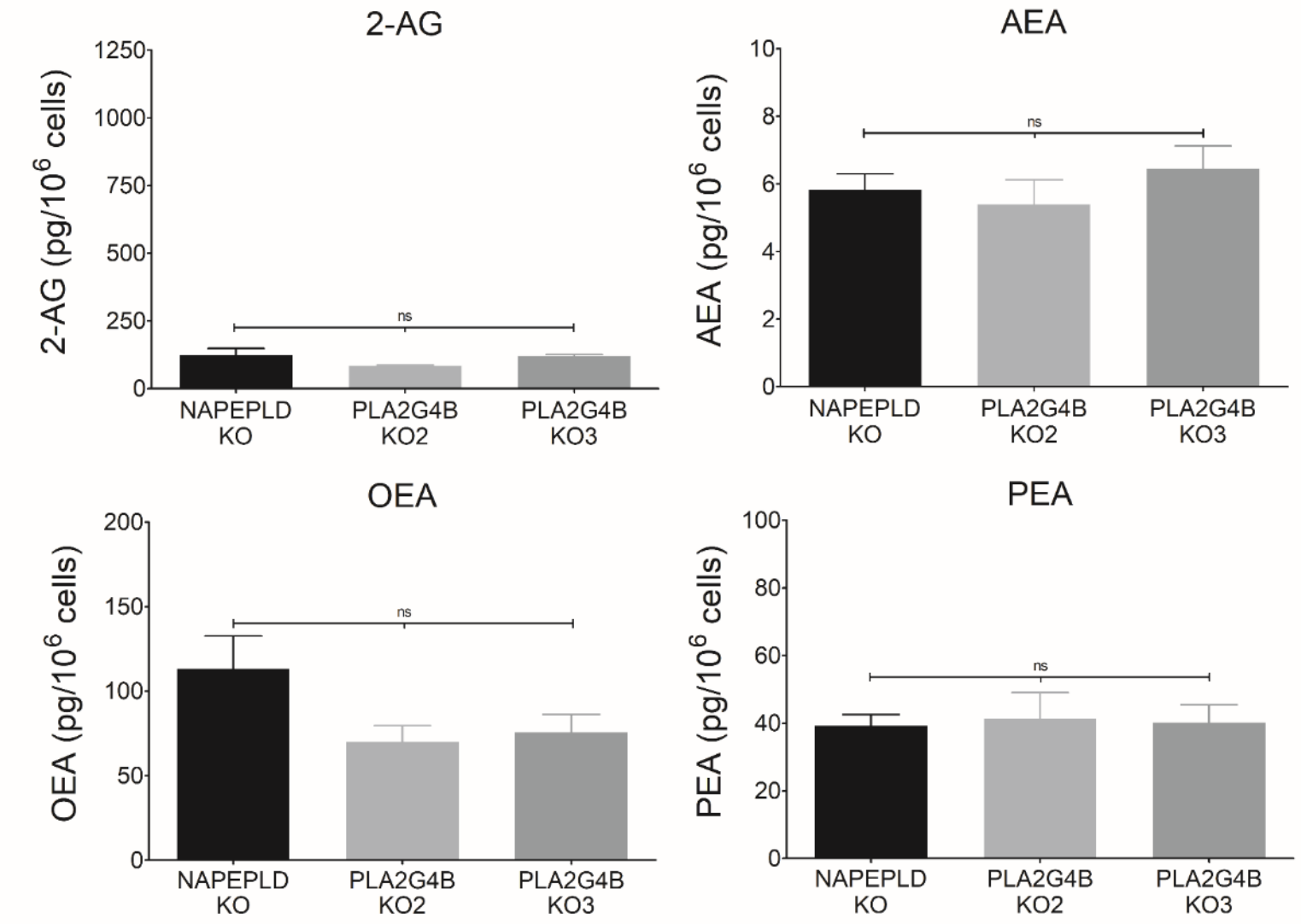
2-AG
2-AG (pg/10^6 cells)
1250
1000
750
500
250
0
ns
NAPEPLD KO
PLA2G4B KO2
PLA2G4B KO3
AEA
AEA (pg/10^6 cells)
10
8
6
4
2
0
ns
NAPEPLD KO
PLA2G4B KO2
PLA2G4B KO3
OEA
OEA (pg/10^6 cells)
200
150
100
50
0
ns
NAPEPLD KO
PLA2G4B KO2
PLA2G4B KO3
PEA
PEA (pg/10^6 cells)
100
80
60
40
20
0
ns
NAPEPLD KO
PLA2G4B KO2
PLA2G4B KO3

eCB signalling is still present in PLA2G4B KO lines in McCoy's assay media

There were no significant changes to the measured lipid levels of 2-AG, AEA, OEA and PEA, however the KO of the PLA2G4B enzyme could potentially impact on stimulus induced changes in AEA or other potential eCBs which could be produced, thus the PLA2G4B KO cells were tested in the CB1-Tango assay alongside the NAPEPLD KO line for comparison. First the cells were subject to treatment with 5μM ACEA in the absence and presence of 2.5μM AM251 in a standard 4 hour assay in 0.5% FBS McCoy's assay media as described in Methods. The NAPEPLD KO cell line evoked a robust ACEA response (248.7 ± 10.1 % of control) which was of comparable magnitudes to results previously obtained with its parental line (Figure 6.4.10). The PLA2G4B KO lines showed slightly lower responses to ACEA (KO2 = 193.2 ± 10.2 % of control, KO3 = 213.6 ± 8.3% of control), however the response from the PLA2G4B KO3 line was not significantly different to the NAPEPLD KO line and the parental CB1-Tango cells (Table 6.4.2). The responses from the two PLA2G4B lines are not significantly different to each other despite the KO2 line having a significantly lower response, which could be a result of clonal variances between the cells. Both cell lines are still responsive to ACEA which can be inhibited by AM251 to the same level near the baseline.

Next, the cells were treated with JZL195 to determine if there are any changes to the basal generation of eCB in the absence of the PLA2G4B enzyme. The cells were treated with 100nM JZL195 in the absence or presence of 2.5μM AM251 (Figure 6.4.11). The NAPEPLD KO line generated a substantial eCB tone (134.0 ± 4.0% of AM251 control) which was in line with previous results. The PLA2G4B KO2 line produced an eCB tone at 119.9 ± 2.5% of AM251 control and the PLA2G4B KO3 line gave a response at 143.4 ± 7.1 % of AM251 control. Both responses from the PLA2G4B KO lines were not significantly different to the NAPEPLD KO line and are still relatively higher than the eCB tone observed from parental CB1-Tango cells (Table 6.4.2). The eCB tones have remained largely unchanged and slight differences may be due to clonal variances.

Finally, responses to ionomycin were tested in the PLA2G4B KO lines to determine if eCB signalling can still be evoked from the cells due to rapid calcium influx. The cells were treated with 2μM ionomycin in the absence or presence of 2.5μM AM251 in the presence of 100nM JZL195 (Figure 6.4.12). The NAPEPLD KO line gave a response reaching 207.5 ± 23.7% of AM251 control, the PLA2G4B KO2 line response was 179.6 ± 21.2% of AM251 control and the PLA2G4B KO3 line response was 202.7 ± 23.1% of AM251 control. These responses were not significantly different to each other and to the response from parental CB1-Tango cells

(Table 6.4.2). AM251 blocked the response partially for all the cell lines (NAPEPLD KO = 134.2 ± 9.0; KO2 = 147.0 ± 17.4; KO3 = 146.6 ± 13.8% of AM251 control) which may indicate a non-specific effect or simply that the concentration of AM251 used was not sufficient to inhibit the response completely. Nonetheless, the eCB response to the influx of calcium was still present in the PLA2G4B KO lines and there were no significant differences in the magnitudes of the responses.

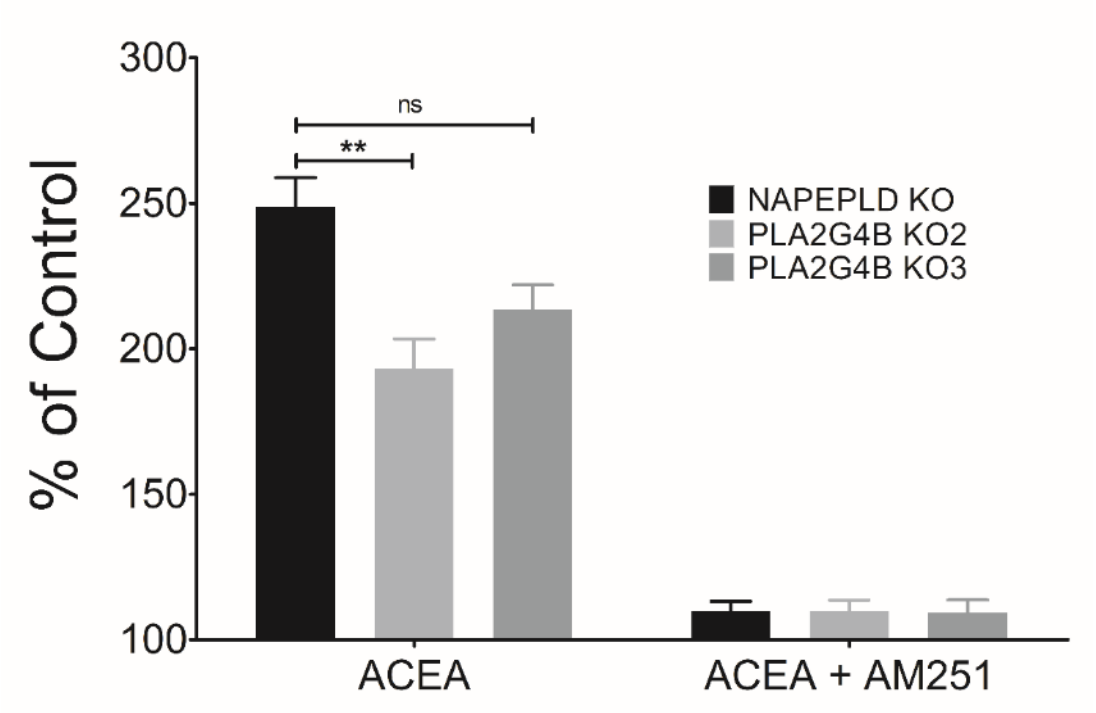

Figure 6.4.10. PLA2G4B KO cells can still respond to ACEA

30,000 cells were plated in black 96 well plates in 0.5% FBS McCoy's media for 24 hours. The cells were treated the next morning with 5μM ACEA in the presence and absence of 2.5μM AM251 for 4 hours. Data was normalised to the control wells (set as 100) as % of control. Graph shows means and bars represent SEMs of 4 independent experiments, 6 replicates in each individual experiment. Significance between groups was calculated using One Way ANOVA.

ns $p>0.05$; **$p<0.01$; One-way ANOVA, Dunnett's post-test.

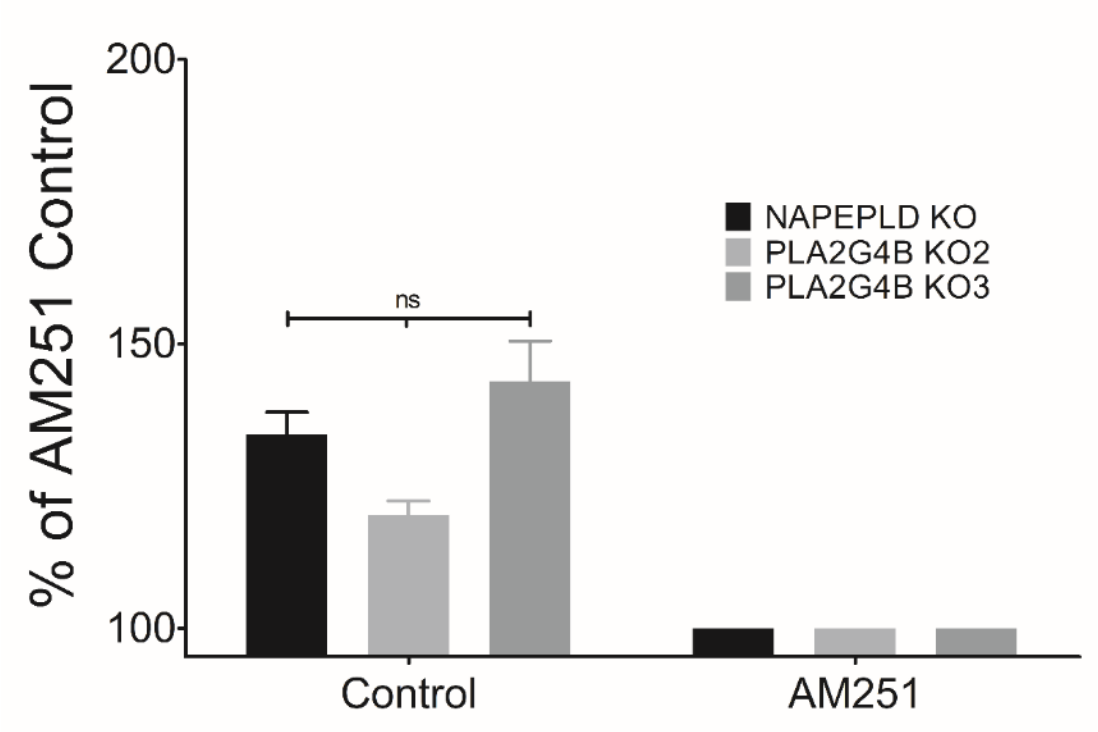

Figure 6.4.11. PLA2G4B KO2 and KO3 cells exhibit eCB tone in the presence of JZL195

30,000 cells were plated in black 96 well plates in 0.5% FBS McCoy's media for 24 hours. The cells were treated the next morning with 100nM JZL195 in the presence and absence of 2.5μM AM251 for 4 hours. Data was normalised to the wells containing AM251 (set as 100) as % of AM251 control. Graph shows means and bars represent SEMs of 4 independent experiments, 6 replicates in each individual experiment. Significance between groups was calculated using One Way ANOVA.

ns $p>0.05$; One-way ANOVA, Dunnett's post-test.

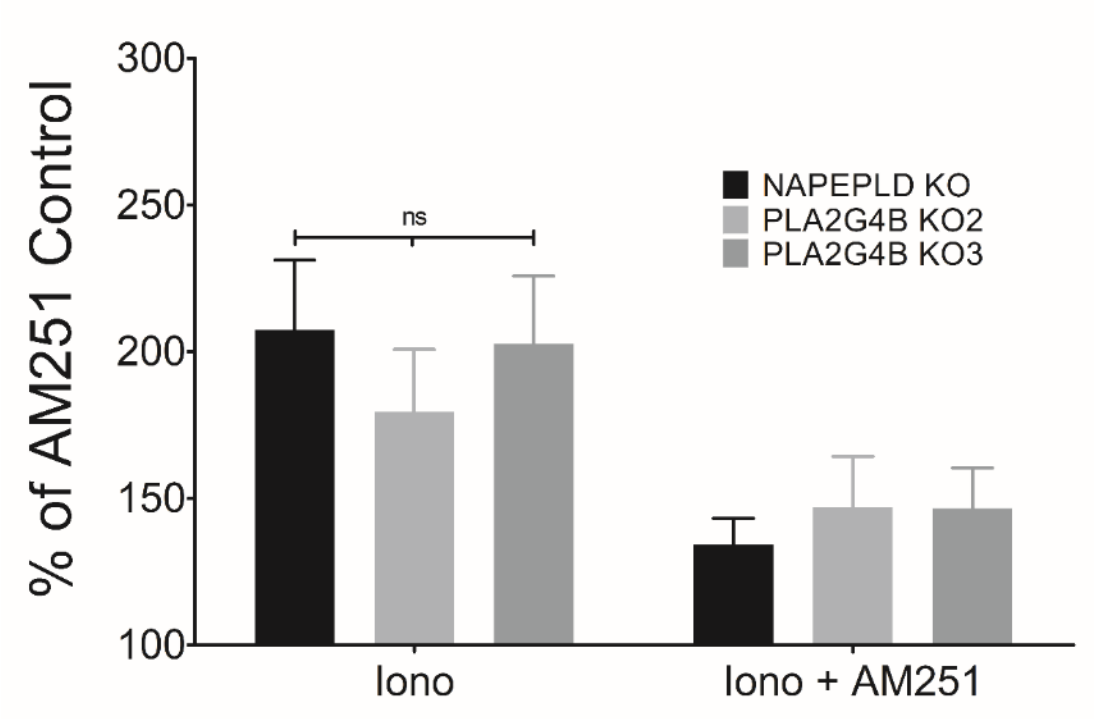

Figure 6.4.12. Ionomycin treatment continue to evoke responses in PLA2G4B KO cell lines

30,000 cells were plated in black 96 well plates in 0.5% FBS McCoy's media for 24 hours. The cells were treated the next morning with 2μM ionomycin in the presence and absence of 2.5μM AM251 for 4 hours. 100nM JZL195 was included in all wells. Data was normalised to the wells with AM251 (set as 100) as % of AM251 control. Graph shows means and bars represent SEMs of 4 independent experiments, 6 replicates in each individual experiment. Significance between groups was calculated using One Way ANOVA.

ns $p>0.05$; *$p<0.05$; One-way ANOVA, Dunnett's post-test.

FSK and PMA can still elicit eCB signalling in PLA2G4B KO cells in No Starve Freestyle media

Next, we tested the PLA2G4B KO cells in Freestyle media supplemented with 2mM calcium and 100nM JZL195 and stimulating eCB signalling with calcium, FSK and PMA in a 24 hour assay. Again, the ACEA response was first tested to see if the cells still respond to CB1 activation in this paradigm. The cells were plated in the No Starve Freestyle media conditions and treated with 5μM ACEA in the absence and presence of 2.5μM AM251 as described in Methods (Figure 6.4.13). The NAPEPLD KO cell line responded to ACEA to comparable levels measured previously (689.5 ± 82.5% of AM251 control). The PLA2G4B KO lines also responded robustly to ACEA to levels which were surprisingly higher than those in the NAPEPLD KO line (KO2 = 1051.6 ± 111.9; KO3 = 890.8 ± 63.0% of AM251 control) and higher than the parental CB1-Tango cells (Table 6.4.2), however this may be due to clonal differences. The ACEA responses in all three cell lines were all largely inhibited by AM251 to near control levels.

The eCB response produced in this paradigm was also examined from all three cell lines in this paradigm. The cells were plated as previously described and treated in the absence or presence of 2.5μM AM251 to inhibit basal eCB activity (Figure 6.4.14). Substantial eCB tones were detected for all three cell lines (NAPEPLD KO = 331.8 ± 31.7%; PLA2G4B KO2 = 439.7 ± 62.2 and KO3 = 429.9 ± 55.4% of AM251 control) which still reflect relatively higher levels of eCB than previously detected in the parental CB1-Tango cells (Table 6.4.2). The magnitudes of the responses are not significantly different to each other, however the PLA2G4B KO lines tend toward higher levels of eCB signalling, which is in keeping with the higher response to ACEA.

The effect of kinase driven eCB signalling was also tested in the PLA2G4B KO cell lines. Firstly, the cells were treated with 10μM FSK in the absence or presence of 2.5μM AM251 in the No Starve Freestyle conditions (Figure 6.4.15). The response to FSK was 511.0 ± 65.8% of AM251 control in the NAPEPLD KO line, which was of comparable levels to previously obtained results. FSK was still able to elicit responses in the PLA2G4B KO lines; the responses were substantially higher (KO2 = 856.0 ± 61.5; KO3 = 810.7 ± 8.7% of AM251 control) even in comparison to the parental CB1-Tango cells (Table 6.4.2), which as mentioned previously, could be a result of functional changes within the cells or are artefacts of clonal differences. All FSK responses were inhibited by AM251 to near basal control levels, indicating a CB1 dependent response.

Secondly, the cell lines were treated with 25nM PMA in the absence or presence of AM251 in the No Starve Freestyle conditions for 24 hours to establish if eCB signalling can still be evoked with PKC activation (Figure 6.4.16). PMA elicited robust responses in the NAPEPLD KO cell line (534.0 ± 75.6% of AM251) which had a nonspecific component when AM251 is present (209.8 ± 26.9% of AM251) and this is in keeping with the results obtained in the previous chapter. The responses from the PLA2G4B KO lines were not significantly different to those obtained in the NAPEPLD KO line (KO2 = 649.8 ± 32.1%; KO3 = 594.4 ± 40.9% of AM251 control) and also contain a relatively similar sized nonspecific component (KO2 = 229.9 ± 22.3%; 193.4 ± 12.9% of AM251 control). The responses to PMA from all three cell lines are at higher levels than detected from the parental CB1-Tango cells (Table 6.4.2). Thus kinase activation by PMA and FSK, still elicits eCB signalling in the PLA2G4B KO cell lines in a very similar manner to the NAPEPLD KO cell line, and the original parental CB1-Tango cell line.

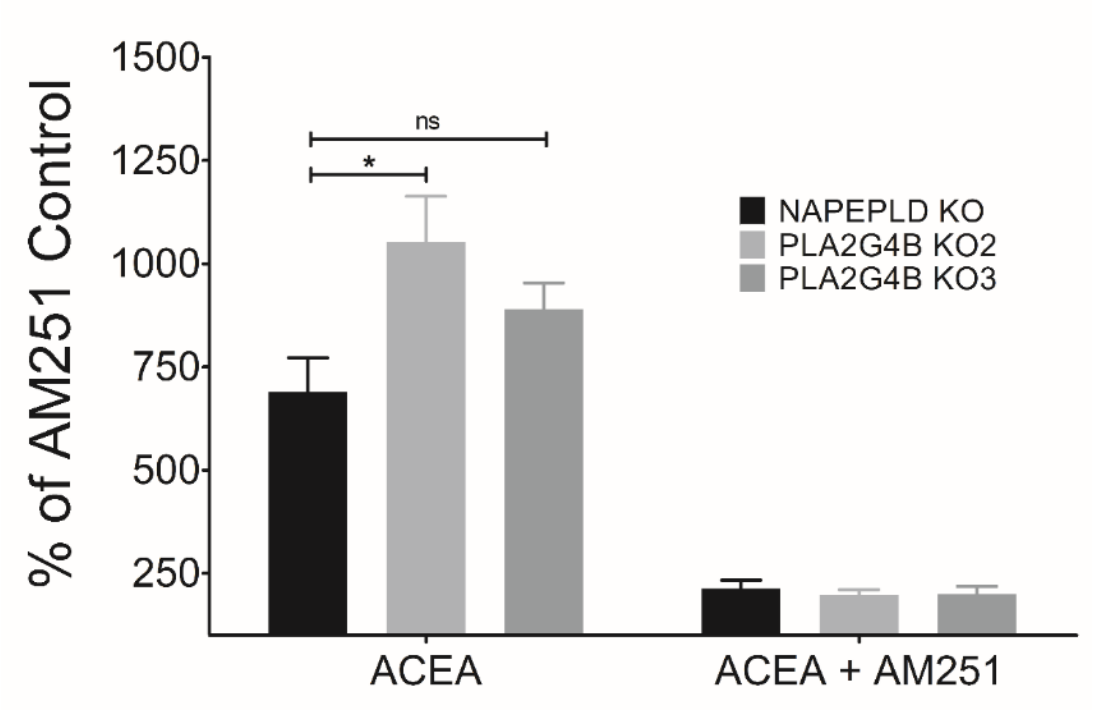

Figure 6.4.13. PLA2G4B KO cells respond to ACEA in No Starve Freestyle conditions

Cells were plated on black 96 well plates at a density of 30,000 cells per well in Freestyle media supplemented with 2mM Ca^{2+} and 100nM JZL195. Immediately after plating, the cells were treated with 5μM ACEA in the presence and absence of 2.5μM AM251. Data was normalised to wells containing AM251 only (set to 100%). Graph shows means and bars represent SEMs of 4 independent experiments, 6 replicates in each individual experiment. Significance between groups was calculated using One Way ANOVA.

ns $p>0.05$; *$p<0.05$; One-way ANOVA, Dunnett's post-test.

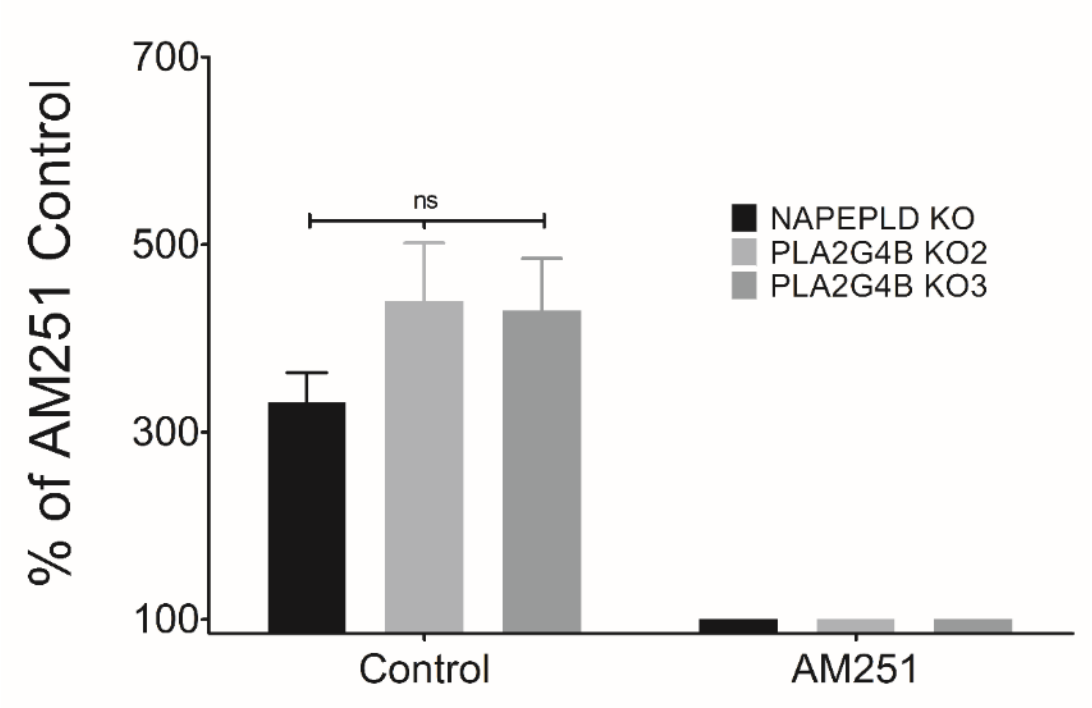

Figure 6.4.14. An eCB tone is still present in PLA2G4B KO cells in No Starve Freestyle conditions

Cells were plated on black 96 well plates at a density of 30,000 cells per well in Freestyle media supplemented with 2mM Ca^{2+} and 100nM JZL195. Immediately after plating, the cells were treated with control media or 2.5μM AM251 for 24 hours. Data was normalised to wells containing AM251 only (set to 100%). Graph shows means and bars represent SEMs of 4 independent experiments, 6 replicates in each individual experiment. Significance between groups was calculated using One Way ANOVA.

ns p>0.05; One-way ANOVA, Dunnett's post-test.

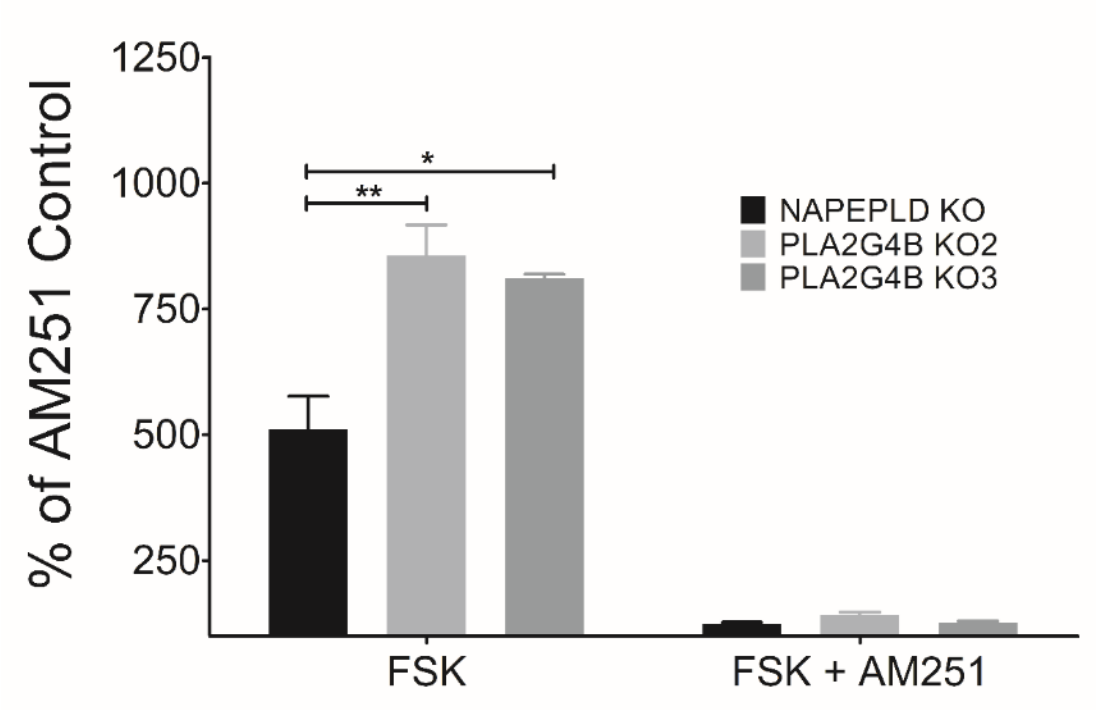

Figure 6.4.15. FSK continues to evoke eCB signalling in PLA2G4B KO cells

Cells were plated on black 96 well plates at a density of 30,000 cells per well in Freestyle media supplemented with 2mM Ca^{2+} and 100nM JZL195. Immediately after plating, the cells were treated with 10μM FSK in the presence or absence of 2.5μM AM251 for 24 hours. Data was normalised to wells containing AM251 only (set to 100%). Graph shows means and bars represent SEMs of 4 independent experiments, 6 replicates in each individual experiment. Significance between groups was calculated using One Way ANOVA.

*p<0.05; **p<0.01; One-way ANOVA, Dunnett's post-test.

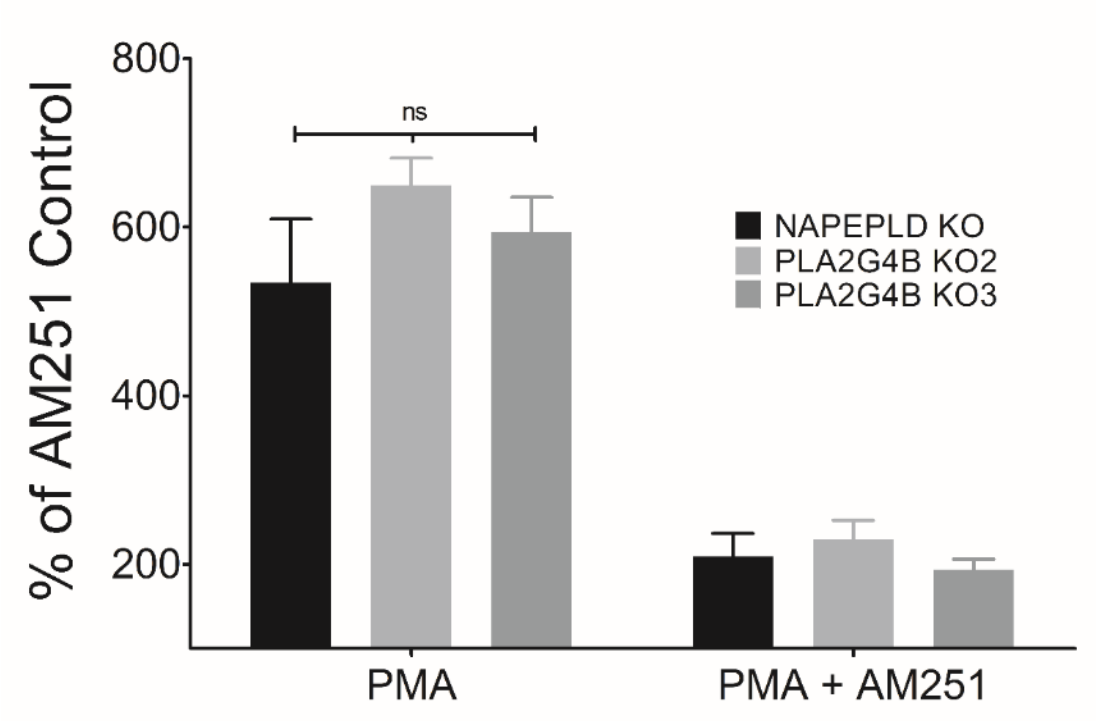

Figure 6.4.16. PMA evoked responses were unchanged in PLA2G4B KO cells

Cells were plated on black 96 well plates at a density of 30,000 cells per well in Freestyle media supplemented with 2mM Ca^{2+} and 100nM JZL195. Immediately after plating, the cells were treated with 25nM PMA in the presence or absence of 2.5μM AM251 for 24 hours. Data was normalised to wells containing AM251 only (set to 100%). Graph shows means and bars represent SEMs of 4 independent experiments, 6 replicates in each individual experiment. Significance between groups was calculated using One Way ANOVA.

ns p>0.05; One-way ANOVA, Dunnett's post-test.

CB1-TANGO ASSAY CONDITIONS AND MEASUREMENT		PARENTAL CB1-TANGO (% OF CONTROL OR AM251 CONTROL)	DAGLα/β KO (% OF CONTROL OR AM251 CONTROL)	NAPEPLD KO (% OF CONTROL OR AM251 CONTROL)	PLA2G4B KO3 (% OF CONTROL OR AM251 CONTROL)
0.5% FBS MCCOY'S ASSAY MEDIA, 4 HOUR ASSAY	ACEA Response	245.6 ± 15.4	226.7 ± 12.6	225.3 ± 13.2	213.6 ± 8.3
	eCB Tone	129.5% ± 4.8	150.6 ± 4.0	148.1 ± 6.6	143.4 ± 7.1
	Ionomycin Response	200.1 ± 31.0	186.9 ± 10.4	198.1 ± 13.9	202.7 ± 23.1
NO STARVE FREESTYLE MEDIA, 24 HOUR ASSAY	ACEA Response	612.8 ± 30.6	688.1 ± 55.5	621.2 ± 69.9	890.8 ± 63.0
	eCB Tone	246.2 ± 12.0	356.0 ± 14.4	310.1 ± 13.7	429.9 ± 55.4
	FSK Response	656.8 ± 40.1	522.3 ± 26.5	475.3 ± 14.0	810.7 ± 8.7
	PMA Response	383.2 ± 7.7	277.8 ± 21.5	532.3 ± 15.8	594.4 ± 40.9

Table 6.4.2. Comparison of responses from the CB1-Tango assay from original parental CB1-Tango cells, DAGLα/β KO cells, NAPEPLD KO cells and PLA2G4B KO3 cells.

6.4.3 **Results 4C.** Summary & Conclusions

The transcript levels of the recently identified CaNAT PLA2G4E measured by the QuantiGene Multiplex assay was below the dynamic detectable range in the CB1-Tango cells suggesting a lack of PLA2G4E expression in the CB1-Tango cells. This was reconfirmed in this chapter with RT-PCR reaction from the CB1-Tango cell lines of PLA2G4E transcripts, the lack of a corresponding PCR band from the CB1-Tango and the DAGLα/β KO cells indicates that PLA2G4E transcripts are not present in the cells. As well as this, PLA2G4E transcripts could not be detected from RNA from other human cell lines and brain regions tested (net MFI <10) but was robustly detected in skin RNA using the QuantiGene multiplex assay system. In support of these results, data from the Human Protein Atlas database documented low PLA2G4E transcript levels in U2OS cells and other cancer cell lines, as well as low expression in brain regions (Thul et al., 2017), casting doubt on the involvement of PLA2G4E in AEA synthesis in these cells and brain regions.

PLA2G4E was previously detected in both neonatal and adult mouse brain with RT-PCR (Ogura et al., 2016) and was confirmed by the RT-PCR results of embryonic mice brain obtained in this chapter, but could not be found from human cell lines or RNA from two human brain regions with prominent AEA synthesis (Felder et al., 1996) which raises the possibility that whilst PLA2G4E could function as a CaNAT regulating AEA synthesis in the mouse brain, this function may not be conserved in humans. In addition, high levels of transcripts were detected using RNA-seq almost exclusively from neurones in the mouse brain samples (Zhang et al., 2014) and yet it is possible for other cells to generate AEA such as mouse astrocytes (Walter et al., 2002) where PLA2G4E expression is not present. Together, the above points to other as yet to be identified CaNATs being present in humans and in cells that do not express PLA2G4E which are most likely responsible for the generation of the NAPE precursor for AEA synthesis. It follows that a major effort needs to be placed on identifying other enzymes that could have a similar N-acyltransferase activity as PLA2G4E with more widespread expression in humans. This led us to focus on the very closely related enzyme PLA2G4B as another possible CaNAT.

Results from the QuantiGene multiplex assay has shown readily detectable levels of PLA2G4B transcripts in the CB1-Tango cells on comparable levels to those found in cerebellum and hippocampus, and is relatively higher in skin RNA. As well as this, levels of PLA2G4B had maintained a relatively steady state across the KO cell lines generated in the study, although there were slight but significantly higher levels in some of the KO lines, perhaps attributable

to clonal variances. Previous characterisation efforts of PLA2G4B revealed associations to neuronal functions including schizophrenia (Tao et al., 2005), autism (Matsunami et al., 2014) and reading disability (Morris et al., 2004). Interestingly, human PLA2G4B contains a JMJC domain from a read-through of the upstream JMJD7 gene creating a conjoined JMJD7-PLA2G4B transcript which may have implications in head and neck squamous cell carcinoma survival (Cheng et al., 2017). JMJC domains are predicted to be metalloenzymes and may have a role in gene transcription or chromatin stability (Clissold and Ponting, 2001). The removal of the JMJC domain has been shown to enhance the activity of PLA2G4B however (Pickard et al., 1999), it could possibly function as a regulator of PLA2G4B activity although the exact role of the domain is unknown. This gene was therefore of interest as a candidate enzyme for the identification of a novel CaNAT.

In order to elucidate if PLA2G4B is involved in eCB signalling in the CB1-Tango cell lines, CRISPR probes were generated to the PLA2G4B gene in the catalytic region (Pickard et al., 1999) and the PLA2G4B KO lines were generated with previously described methods. Three cell lines showed disrupted transcripts in the RT-PCR and sequence thus were taken forward to characterisation in the QuantiGene multiplex assay system. The results from the beads assay highlighted that PLA2G4B KO1 may not have complete disruption of the PLA2G4B gene despite the RT-PCR and sequencing results not detecting any other longer transcript variations. It could be possible that RT-PCR preferentially amplified the shorter mutated transcript, and alongside gel extraction and purification of only the prominent band from the agarose gel would omit any other longer fragments. Thus, the verification of genetic disruptions of CRISPR-treated gene transcripts using the QuantiGene multiplex assay is vital in the generation of KO lines. The other two PLA2G4B KO clones (KO2 and KO3) show low detection of PLA2G4B transcripts and is indicative of successfully mutated PLA2G4B transcripts, thus only these two lines were taken forward further analysis.

Other gene transcripts of the eCB components generally maintained their levels between the KO cell lines, with only clonal variances in the eCB hydrolysing enzymes. Interestingly, despite the partial KO of PLA2G4B in KO1 (as mentioned above), in comparison to PLA2G4B KO2 which had a more substantial depletion of transcripts, their changes in the eCB hydrolysing enzymes were almost identical. This is more evidence that minor changes are reflective of clonal variation between lines and that the KO of PLA2G4B is not likely to affect the expression levels of other enzymes measured in the beads assay panel. The difference in the levels of the eCB hydrolysing enzyme transcripts between cell lines are also relatively small

in comparison to magnitudes seen before, thus significance between these levels are not truly reflective of an adaptive change in function. Nonetheless, the relative expression levels of the eCB hydrolysing enzymes are within a relatively narrow range across cell lines regardless of the presence of functional PLA2G4B.

The lipid levels from the PLA2G4B KO cells were virtually unchanged between cell lines for all measured lipids. These unchanged levels also serve as confirmation that the fluctuations in eCB hydrolysing enzymes are not due to a functional change in the cells as they do not have altered activity levels, but rather are only a consequence of clonal variation or batch differences. It is not known whether PLA2G4B may generate other potential eCBs that could signal at the CB1 receptor, but in terms of the two major eCBs and the two related lipids moieties we measured, PLA2G4B is not involved in the generation of these lipid species.

As it could be possible that PLA2G4B may be involved in the generation of other lipid moieties that could affect eCB signalling either directly or indirectly, the cell lines were tested in the CB1-Tango assay. Despite PLA2G4B KO2 and KO3 showing slightly muted responses in the 4 hour McCoy's assay paradigm, robust responses are present in the 24 hour No Starve Freestyle assay conditions which were on comparably higher levels than the NAPEPLD KO line. Upon comparison of the absolute values of the responses from the PLA2G4B KO3 line which has four separate enzymes genetically deleted, and the parental CB1-Tango cell line, the differences between the responses are of a small magnitude and in fact most responses are higher in the PLA2G4B KO3 line (Table 6.4.2). This really confirms the presence of a robust eCB tone that can be generated in the absence of the DAGLs, NAPEPLD and a candidate enzyme PLA2G4B from the CB1-Tango cells.

As PLA2G4E and PLA2G4B are both unlikely to be involved in eCB signalling and the generation of AEA in the CB1-Tango cells, the presence of a robust eCB tone that can be enhanced by the presence of calcium is indicative of the presence of a novel unidentified CaNAT. As mentioned before, in the pursuit to identify the elusive CaNAT, other N-acyltransferase enzymes were discovered through a bioinformatics search of related enzymes to the N-acyltransferase LRAT (Jin et al., 2007; Ueda et al., 2010). LRAT catalyses the transfer of the *sn*-1 acyl group from PC to vitamin A leading to the formation of retinyl ester which is used in visual processes (Rando, 2002). This acyltransferase activity is functionally similar to the activity of the CaNAT and thus a bioinformatics approach was taken to identify any homologous enzymes related to LRAT. Members of the HRAS-like suppressor (HRASLS) subfamily (also known as phospholipase A/acyltransferase (PLAAT) 1–

5) showed homology to LRAT and are a family of class II tumour suppressors (Jahng et al., 2003; Golczak et al., 2012). HRASLS5 (also known as PLAAT-5) was extensively studied and displayed similar N-acyltransferase activity to form NAPE from PC and PE (Jin et al., 2007; Jin et al., 2009). However, HRASLS5 was most highly expressed in the testis of rat, mouse and human with lower levels in the brain, showed little calcium activity and was not selective of the *sn*-1 position for the donor acyl group, which does not exactly correlate with the described enzymatic activity of the CaNAT, and thus was identified as a calcium-insensitive N-acyltransferase (iNAT) (Jin et al., 2009). Other related members of the family also show varying degrees of N-acyltransferase and PLA1/A2 activity, but all show little calcium sensitivity for activity, and are not activated by FSK or PMA (Shinohara et al., 2011; Uyama et al., 2012; Hussain et al., 2017).

Whilst the physiological contribution of the PLAAT family of enzymes towards AEA synthesis has not been fully elucidated, overexpression PLAATs in COS7 cells led to the accumulation of N-AcylPE and NAE in the absence of any stimuli, indicating that they may contribute to basal turnover of N-AcylPEs (Uyama et al., 2012). As well as this, suppression of endogenous PLAAT1 and PLAAT2 expression from mouse ATDC5 chondrogenic cells and HeLa cells with siRNA partly (~20-50%) reduced N-AcylPE levels (Uyama et al., 2012; Uyama et al., 2013), suggesting some involvement in the generation of NAPE. Moderate expression of only PLAAT1 is detected in the CB1-Tango cells (Thul et al., 2017) but is calcium insensitive (Hussain et al., 2016), thus it is possible that certain members of this family of enzymes are active in the CB1-Tango cells and may generate a continual turnover of N-AcylPEs in unstimulated conditions. However, calcium and activation of kinases can elicit eCB signalling from the CB1-Tango cells and thus that is likely to involve the activity of a CaNAT which has been shown to be calcium sensitive and its activity can be modulated by kinases (Cadas et al., 1996; Cadas et al., 1997). Nonetheless, through extensive characterisation by the efforts of the Ueda group (Jin et al., 2009; Ueda et al., 2010; Hussain et al., 2017; Uyama et al., 2017), the PLAAT family are independent to the activities CaNAT and thus are not candidate enzymes for the CaNAT in the CB1-Tango cells.

To summarise, PLA2G4E is unlikely to be the enzyme responsible for the generation of NAPE for AEA synthesis as transcript levels of PLA2G4E are undetected in the CB1-Tango cells which can generate detectable levels of AEA. In search for novel candidate enzymes that could generate NAPE, focus was first placed on enzymes with homology to PLA2G4E that are poorly characterised with sensitivity to calcium and have relatively similar expression distribution

to the previously described CaNAT. PLA2G4B was therefore the first candidate enzyme to be genetically deleted from the cell line lacking the major eCB synthesis enzymes DAGLs and NAPEPLD to determine its involvement in eCB signalling. The KO of PLA2G4B with CRISPR showed no changes in the levels of AEA and other lipid moieties, and had little effect on eCB signalling in the CB1-Tango cells. The CB1-Tango cells can still elicit robust eCB signalling in the absence of the major eCB synthesis enzymes but serve as valuable tools for further study of AEA synthesis, eCB signalling and the potential identification of the elusive CaNAT.

Chapter 7. Discussion

7.1 Therapeutic potential of the eCBs and CB ligands

The field of eCB signalling has grown extensively since the isolation of Δ^9-THC, the major psychoactive component of *Cannabis sativa* around 50 years ago (Gaoni and Mechoulam, 1964). In the most recent decades, major advances have been made in the field particularly the identification and cloning of the receptors for Δ^9-THC: CB1 and CB2 (Matsuda et al., 1990; Munro et al., 1993) and the identification of the two major endogenous ligands: 2-AG and AEA (Devane et al., 1992; Mechoulam et al., 1995). Since the initial stages of eCB research, many discoveries have linked this signalling pathway with a wide range of physiological CNS processes such as neuronal migration, retrograde synaptic signalling and adult neurogenesis (Goncalves et al., 2008; Oudin et al., 2011a; Kano, 2014) and various disease states (Fowler et al., 2010; Paloczi et al., 2017; Bajwa et al., 2018). The involvement of the eCB system in many processes led to increased interest in targeting the eCB system for therapeutics, however targeting the eCB system has proven difficult, perhaps precisely because of the widespread presence of the eCB system. For example, the anti-obesity drug SR141716A, a CB1 antagonist commercially known as Rimonabant (Christensen et al., 2007; Costa, 2007), was withdrawn from the market following severe side effects such as anxiety and suicide ideation (Moreira and Crippa, 2009), demonstrating the severity of undesired effects associated with targeting the CB1 receptors in the CNS. However, the therapeutic potential of the eCB system is still generating a great deal of interest as more is understood about the metabolic pathways of the eCB ligands, particularly of the synthesis enzymes for two reasons: 1) they can generate other family of molecules which have the potential to modulate the activation of the CB receptors and 2) elucidation of the key enzymes involved in eCB synthesis would provide novel targets for drug discovery efforts, with the idea of designing specific drugs to minimise unwanted effects.

The cloning and characterisation of DAGLα and DAGLβ highlighted the ability of the DAGLs to generate the major eCB 2-AG, plus other 2-acylglycerols such as 2-LG, 2-PG and 2-OG (Bisogno et al., 2003), however the physiological role of these 2-acylglycerols are often overlooked. 2-OG has been proposed to be novel endogenous ligand for GPR119 receptors which may have implications in diet and satiety (Hansen et al., 2011; Syed et al., 2012), whilst

2-LG and 2-PG have been proposed to be entourage molecules for 2-AG (Ben-Shabat et al., 1998) but have also shown antagonistic activity against 2-AG (Murataeva et al., 2016).

It has been shown through the work in this thesis that 2-LG is a novel partial agonist at the CB1 receptor and is capable of signalling on its own and can modulate both 2-AG and AEA signalling with little entourage ability. 2-LG is present in mammalian brain at around 10x lower concentration than 2-AG whilst AEA is around 200x lower than 2-AG (Richardson et al., 2007; Williams et al., 2007), suggesting 2-LG may be at high enough concentrations to exert physiological effects. Whilst concentrations of 2-LG may not be high enough to act as an agonist to the CB1 receptor, it could potentially modulate signalling of 2-AG and/or AEA in distinct areas of the brain such as the hypothalamus where the concentration of 2-LG is higher (Richardson et al., 2007). Levels of 2-LG is around 12x higher than 2-AG in the spleen in a ratio that was reported to be ideal for maximum potentiation of 2-AG (Ben-Shabat et al., 1998; Gallily et al., 2000) and thus may be physiologically relevant to the biological activity of 2-LG. It might also be possible that 2-LG is a ligand for CB2 or an unidentified receptor, much like the case of AEA which was considered a partial agonist of the CB1 receptor but a full agonist of TRPV1 (Smart et al., 2000; Sugiura et al., 2000) but further clarifications of the role of 2-LG in the brain will need to be explored. Nonetheless, the partial agonist activity of 2-LG raises the exciting prospect of the presence of other eCBs/CB ligands that can exert different potencies against the CB receptors to modulate eCB signalling which could perhaps reduce the severity of drug treatments.

Hp was also proposed to be an endogenous ligand of the CB1 receptor with antagonistic activity against the CB1 (Heimann et al., 2007) but more recent contentious studies reported Hp does not exhibit activity towards the CB1 receptor (Hama and Sagen, 2011a; Straiker et al., 2015; Dvoracsko et al., 2016). In support of the more recent publications, Hp did not show any antagonistic effect, nor any modulation against different CB1 ligands in the CB1-Tango assay. Independent sources of both rat and human Hp also failed to show any significant antagonistic effect against the human CB1 receptor. Furthermore, aside from the original studies (Heimann et al., 2007; Gomes et al., 2009), evidence that Hp directly binds to CB1 has not been confirmed.

Additionally, Hp was suggested to be produced endogenously from cleavage of the α_1 chain of haemoglobin (Rioli et al., 2003). However, later studies failed to detect any levels of endogenous Hp in brain and concluded Hp is in fact an artefact of hot acid extraction and thus is not an endogenous ligand of the CB1 receptor (Gomes et al., 2009; Gelman et al.,

2013). As Hp is not an endogenous ligand and only RVD-Hp is suggested to be endogenously produced (Bauer et al., 2012), the therapeutic potential of Hp is restricted as there are no endogenous enzymes that can be the target for drug discovery. Not much is currently known about the degradation of the α_1 chain of haemoglobin and the metabolic pathways of RVD-Hp. Therefore, it is difficult to develop drugs to target the potential enzymes involved in the production of RVD-Hp for any therapeutic benefit until conclusive evidence of the synthesis of RVD-Hp is found.

One major issue is Hp is currently sold as a selective CB1 antagonist when Hp does not show any CB1 activity. The use of Hp as a CB1 antagonist for studies therefore has posed a problem in literature where mistaken conclusions might have been drawn, adding to the growing problem of reproducibility in the biological scientific field (Baker, 2016). Studies of Hp were carried out in animal models with animal preparations of Hp, which exhibited different pharmacological effects *in vivo* (Lippton et al., 2006; Petrovszki et al., 2012; Leone et al., 2017). Despite Hp not acting through the CB receptors, it does still have some desirable pharmacological effects, including attenuation of pain (Dale et al., 2005b; Toniolo et al., 2014), which may still be of therapeutic benefit. It is therefore vital that further study and clarification of the biological effects of Hp should be taken to prevent further mistaken conclusions to be drawn, and to elucidate the real mechanism of action of Hp for the potential generation of therapeutic drugs following full elucidation of the mechanism of action.

7.2 The CB1-Tango cells as a model system to investigate eCB signalling

Originally developed for drug screening and discovery efforts, the CB1-Tango assay was utilised in this work to study eCB signalling. The effects of exogenously applied CB1 ligands such as agonists ACEA, 2-AG and AEA gave measurable activation of the CB1 receptor and antagonist AM251 prevented the activation of the CB1 receptor, as expected. The activities of exogenously applied 2-LG and Hp on the CB1 receptor were clarified using the cell-based assay system, however for the study of eCB signalling, the endogenous production of eCBs were needed from the cells as well as the activation of the CB1 receptor. Many assays study

eCB signalling through electrophysiological responses such as DSI/DSE experiments or quantification of eCB levels following cell stimulation (Balgoma et al., 2013). However, for the study of eCB signalling in the absence of stimuli-dependent release of eCBs such as in peripheral organs, it is not possible to measure eCB through DSI/DSE studies and mass spectrometry studies are usually low throughput. It is also unclear if the measurement of the eCBs from mass spectrometry studies reflect the presence of a signalling pool of eCB or a general metabolic pool which may contribute to a physiological eCB tone under resting conditions (Howlett et al., 2011). We therefore adapted the CB1-Tango assay as a model cell line to study eCB signalling as the CB1-Tango cells express the machinery necessary for the generation and degradation of the two major eCBs.

The CB1-Tango cells revealed an eCB tone in a 4 hour treatment with JZL195 which is much more pronounced following 24 hour drug treatment with JZL195, suggesting there is a constant low turnover of eCBs which is not signalling at the CB1 receptor. It is likely that this eCB tone generated is limited by the activity of MAGL and/or FAAH as a "gatekeeper" to prevent the activation of CB1 receptor. This gatekeeping activity is seen in developing axons where MAGL expression is excluded from the growth cone but is restricted further back along the axon to limit 2-AG signalling from seeping from the localised area around the growth cone (Keimpema et al., 2013). The stimulation of the CB1-Tango cells with known stimuli that enhances eCB signalling such as calcium influx, PKA and PKC activators (Di Marzo et al., 1994; Bisogno et al., 1997; Vellani et al., 2008) in different media conditions led to detectable and reliable CB1 activation which could be antagonised by AM251 and enhanced by JZL195, attributable to eCB signalling.

There are many advantages of the CB1-Tango assay to study eCB signalling. The main advantage is it is a live cell assay which measures the direct activation of the CB1 receptor rather than a binding assays such as binding of the substrate to CB1 or [^{35}S]GTPγS binding, which may be influenced by the expression of other receptors. The CB1-Tango assay is also in a convenient 96-well assay format which does not require isolation of tissues and primary cells from animals thus reducing the cost and timescale of experiments. Lastly, the results are sensitive as it was able to detect responses to a minor eCB tone and partial agonist 2-LG, are less likely to be subject to false positives and reproducibility issues (Barnea et al., 2008).

High transcript levels of the eCB synthesising enzymes DAGLs and NAPEPLD were detected in the CB1-Tango cells, particularly of DAGLβ by the QuantiGene multiplex assay. Unlike conventional techniques to quantify transcript expression such as microarray and RNA

sequencing which is costly, time consuming and may introduce bias and false positives (Boelens et al., 2007; Wang et al., 2009), the QuantiGene multiplex assay amplifies the signal and not the gene transcripts. This removes bias amplification, is relatively faster to conduct and can be customisable in terms of the number of genes to detect and the targeted region (Flagella et al., 2006). The design of the probes to the catalytic regions of genes allowed the beads assay system to be used as a reliable verification system for genetic manipulation using CRISPR. Characterisation of CRISPR treated genes is difficult with subtle mutations using single gRNAs, so multiple gRNAs were used to delete sections of genes (Canver et al., 2014). However, with RT-PCR characterisation of deleted regions that may have repaired unpredictably, biased amplification of the template cDNA could occur (Acinas et al., 2005) leading to false positives KO results as seen with the results from PLA2G4B KO1.

Gene expression in the cells can be manipulated with CRISPR technique and verified with the QuantiGene multiplex beads assay for high throughput screening of potential enzymes involved in eCB signalling. Thus, the CB1-Tango assay and various KO cell lines are valuable research tools which can be used to study the aspects of CB1 receptor activation by exogenously applied ligands and evoked eCB signalling in different conditions.

7.3 Differential synthesis of 2-AG by the DAGLs

The genetic deletion of DAGLα and DAGLβ (Gao et al., 2010; Tanimura et al., 2010) have shown that these enzymes are key regulators of many physiological processes in the body mediated by eCB signalling. Individually, these enzymes are responsible for generating 90% reduction all the 2-AG in the brain (DAGLα) and liver (DAGLβ) (Gao et al., 2010). Importantly, stimulus-driven 2-AG release in the brain is absent from DAGLα KO animals (Tanimura et al., 2010). Various stimuli have been reported to stimulate the release of 2-AG from neurons, including ionomycin, glutamate, NMDA, and ethanol (Bisogno et al., 1997; Stella et al., 1997; Basavarajappa et al., 2000). Ionomycin, ATP and endothelin-1 can stimulate 2-AG release from astrocytes (Walter and Stella, 2003; Walter et al., 2004).

In the CB1-Tango cells, ionomycin could induce CB1-activation which could be enhanced by JZL195 and antagonised by AM251, indicative of eCB signalling. However, this response was only partially DAGL-dependent when JZL195 was included, suggesting DAGLs can generate

2-AG signalling in response to calcium stimulation under normal conditions. However, the 2-AG produced might not be for CB1 signalling but perhaps the secondary role of the generation of AA by DAGL/MAGL pathway. As the CB1-Tango cells are a non-neuronal cell line (Ponten and Saksela, 1967), calcium influx might not induce a rapid release of 2-AG for eCB signalling in the same manner as neurons, possibly due to the specific localisation of the DAGLs and thus 2-AG in neurons (Bisogno et al., 2003).

In previous studies conducted by other members of our lab, it was established that the level of DAGL expression is not the rate-limiting step for eCB signalling and does not contribute to a larger eCB tone as no changes were observed following overexpression of DAGLα or DAGLβ in the CB1-Tango cells (thesis of Rachel Lane Markwick, 2015). Results shown here from DAGLα/β KO cells is in keeping with the conclusion, deletion of the DAGLs resulted in the drastic decrease of basal 2-AG, however this decrease in 2-AG did not reflect any eCB signalling changes. It is possible that despite the basal levels of 2-AG is affected, stimulus-induced release of 2-AG is still present, however this is not likely as *in vivo* studies has shown stimulus-driven 2-AG release in the brain is absent from DAGLα KO animals (Tanimura et al., 2010) and the majority of 2-AG in the CB1-Tango cells is generated by DAGLα rather than DAGLβ.

An interesting observation from DAGL KO cell lines was that DAGLα is largely responsible for the majority of the basal 2-AG synthesis in an osteosarcoma cell background despite expressing much higher transcript levels of DAGLβ. This is further evidence suggesting that the DAGLs might have different enzyme kinetics between them, and this has been observed previously in studies with surrogate substrates whereby DAGLα showed much more hydrolysis activity than DAGLβ within the same time frame (thesis of Praveen Singh, 2013; thesis of Rachel Lane Markwick, 2015; Singh et al., 2016). This finding provides potential for specific therapeutic intervention of one DAGL over the other by developing more selective drugs or drugs which may be metabolised differently by the individual DAGLs.

The eCB system is involved in many physiological processes and in numerous pathophysiological states such as neurodegeneration, cancer, gastrointestinal and metabolic diseases, the eCB tone is dysregulated which may be of potential therapeutic interest (Toczek and Malinowska, 2018), which may be subject to therapeutic intervention. Obesity and type 2 diabetes are associated with altered gut microbiome, low-grade inflammation and increased eCB tone (Muccioli et al., 2010), with more evidence emerging suggesting a link between an increased eCB tone and low-grade inflammation (Scherer and Buettner, 2009;

Muccioli et al., 2010; Olefsky and Glass, 2010; Geurts et al., 2011). The increased eCB tone and connection to low-grade inflammation could be mediated by the kinetically slower activity of DAGLβ rather than DAGLα, as it has been shown that DAGLβ mediates inflammatory responses in macrophages and microglia (Hsu et al., 2012; Viader et al., 2016). Furthermore, recent studies have shown correlations between neuroinflammation and the gut microbiome (Matcovitch-Natan et al., 2016; Sundman et al., 2017). This suggests another possible connection between inflammation and the eCB system in the gut, raising interest in therapeutics targeting the widespread role of DAGLβ in inflammation.

As discussed, the generation of the DAGLα/β KO cell line provided evidence for the differential contribution of DAGLα and DAGLβ to 2-AG generation in the CB1-Tango cells. Despite the large changes in basal 2-AG levels, eCB signalling was still present and could be stimulated by calcium, PKA and PKC. This eCB tone is likely to be comprised of AEA as AEA levels are measurable from the cells. The genetic deletion of the DAGLs have provided a valuable cell line for the study of AEA synthesis pathways.

7.4 Physiological role of NAPEPLD

In contrast to 2-AG and the DAGLs, the identification (Okamoto et al., 2004) and genetic deletion (Leung et al., 2006; Tsuboi et al., 2011; Leishman et al., 2016) of the proposed AEA synthesising enzyme NAPEPLD did not highlight its necessity in the synthesis of AEA and thus secondary pathways were suggested. However, no significant reduction in AEA was seen in the brains of animals lacking the main enzymes thought to be responsible for AEA synthesis: NAPEPLD, GDE1 or both (Leung et al., 2006; Simon and Cravatt, 2010). Thus, the identification of a selective enzyme for AEA production from NAPE has remained elusive.

AEA levels and NAPEPLD transcripts were detected in the CB1-Tango cells, so it was speculated that NAPEPLD might contribute to the generation of AEA in the cells. Genetic KO of NAPEPLD revealed very little change in AEA levels, but did show effect on PEA levels which was generally seen in KO animal studies (Leung et al., 2006; Tsuboi et al., 2011; Leishman et al., 2016). As well as this, little effect was seen in the CB1-Tango assay, with an eCB tone and stimulus-induced eCB signalling intact in the absence of the DAGLs and NAPEPLD. Thus, NAPEPLD is not likely to contribute to eCB signalling in the CB1-Tango cells.

Other pathways are likely to mediate the hydrolysis of NAPE into AEA in the CB1-Tango cells that is independent to NAPEPLD, however these pathways usually contain more than one step and not all the enzymes are fully characterised. The generation of AEA in rat neuron homogenate was observed to occur in one hydrolysis step (Di Marzo et al., 1994), whilst this was attributed to NAPEPLD, it remains possible that it could be mediated by a different enzyme *in vivo*.

The bulk of AEA synthesis may not be attributable to the action of NAPEPLD, but NAPEPLD is widely expressed and conserved (Okamoto et al., 2004) indicating possible secondary roles of NAPEPLD, perhaps in neuroprotection. It was suggested that NAPEPLD may have a role in the breakdown of harmful IsoLG-PE (Guo et al., 2013) alongside generating the neuroprotective NAEs. However, this neuroprotective role of NAPEPLD would require further research as the breakdown of IsoLG-PE is relatively specific in terms of substrate and it would be appealing to determine if NAPEPLD can breakdown other harmful molecules.

The physiological role of NAPEPLD remains to be elucidated. Whilst NAPEPLD KO revealed its involvement in the generation of saturated and mono-unsaturated NAEs in this and other studies (Leung et al., 2006; Tsuboi et al., 2011; Leishman et al., 2016), these NAEs are still detectable and thus generated by other non-NAPEPLD mechanisms. The emergence of a novel NAPEPLD inhibitor (Castellani et al., 2017) may be of interest to study short term/local inhibition of NAPEPLD activity and if it may affect AEA or other NAE synthesis as global KO of NAPEPLD could cause compensatory pathways to emerge. However, further testing with this inhibitor was beyond the scope of this thesis.

7.5 Identification of the CaNAT

As AEA levels can be detected and other reported synthesis pathways for AEA could still be active in the CB1-Tango cells, AEA is likely to be the main eCB contributing to the eCB tone, but it is possible that the eCB tone could be comprised of a novel eCB. As some enzymes facilitating NAPE cleavage to AEA are not fully characterised and are not specific to AEA synthesis (e.g. PLCs, lysoPLD, lysoPLC), it is more feasible that the regulation of AEA synthesis occurs in the generation of NAPE by CaNAT as the presence of a calcium and phosphorylation sensitive pathway remains (Cadas et al., 1996).

Through the results of RT-PCR and the QuantiGene multiplex assay in this work, it was determined that PLA2G4E – the enzyme reported to function as CaNAT (Ogura et al., 2016), is not expressed in the CB1-Tango cells and thus does not contribute to AEA synthesis and eCB signalling in the cells. This was unexpected as the cells lacking the DAGLs and NAPEPLD still clearly show calcium-sensitive eCB signalling and AEA levels can still be detected. As well as this, some expression profiles of PLA2G4E does not correlate with the expression patterns of NAPEPLD and the partially purified CaNAT (Cadas et al., 1997; Okamoto et al., 2004), and PLA2G4E is not present in some cells that can produce AEA such as astrocytes (Walter et al., 2002; Zhang et al., 2014). The activity of PLA2G4E as a CaNAT *in vivo* has not been elucidated, but previous studies have suggested it may regulate recycling in endosomes (Capestrano et al., 2014). Whether the association of PLA2G4E with endosomes may contribute to the accumulation of AEA in liposomes (Oddi et al., 2008) is also unknown. Nonetheless, it was hypothesised that another enzyme is likely to function as the CaNAT in the CB1-Tango cells and perhaps *in vivo*.

PLA2G4B was studied in this work as it is closely related to PLA2G4E, has a poorly characterised function and its expression profile is more in line with the expression of NAPEPLD and the description of CaNAT (Song et al., 1999; Ghosh et al., 2006). However, AEA levels and eCB signalling in PLA2G4B KO cells were unchanged, signifying PLA2G4B is not likely to be involved in eCB signalling. The current role of PLA2G4B is unknown, however some studies have associated PLA2G4B with neuronal functions (Morris et al., 2004; Tao et al., 2005; Matsunami et al., 2014) where it could perhaps interact with the eCB system *in vivo*. It had been highlighted that PLAAT enzymes do not fit the profile of the CaNAT (Jin et al., 2009; Ueda et al., 2013) but the possibility that these enzymes may be modulated by other calcium-sensitive signalling molecules in the CB1-Tango cells exist.

In summary, DAGLα, DAGLβ, NAPEPLD and PLA2G4B were identified as the potential regulatory enzymes of eCB synthesis and have been targeted with CRISPR (Figure 7.5.1). The resulting KO of the DAGLs, NAPEPLD and PLA2G4B in the PLA2G4B KO3 cell line revealed that eCB signalling is still present at comparable levels to the parental cell line which can be evoked by calcium and activation of PKA and PKC. The identity of the CaNAT that is hypothesised to be regulatory step and main generator of AEA is still elusive in our CB1-Tango cells and the remaining 10% of 2-AG levels may be generated by a novel DAGL related enzyme. The generation of a KO line in the absence of the DAGLs and NAPEPLD therefore serves as a valuable tool for the continued study into AEA synthesis pathways.

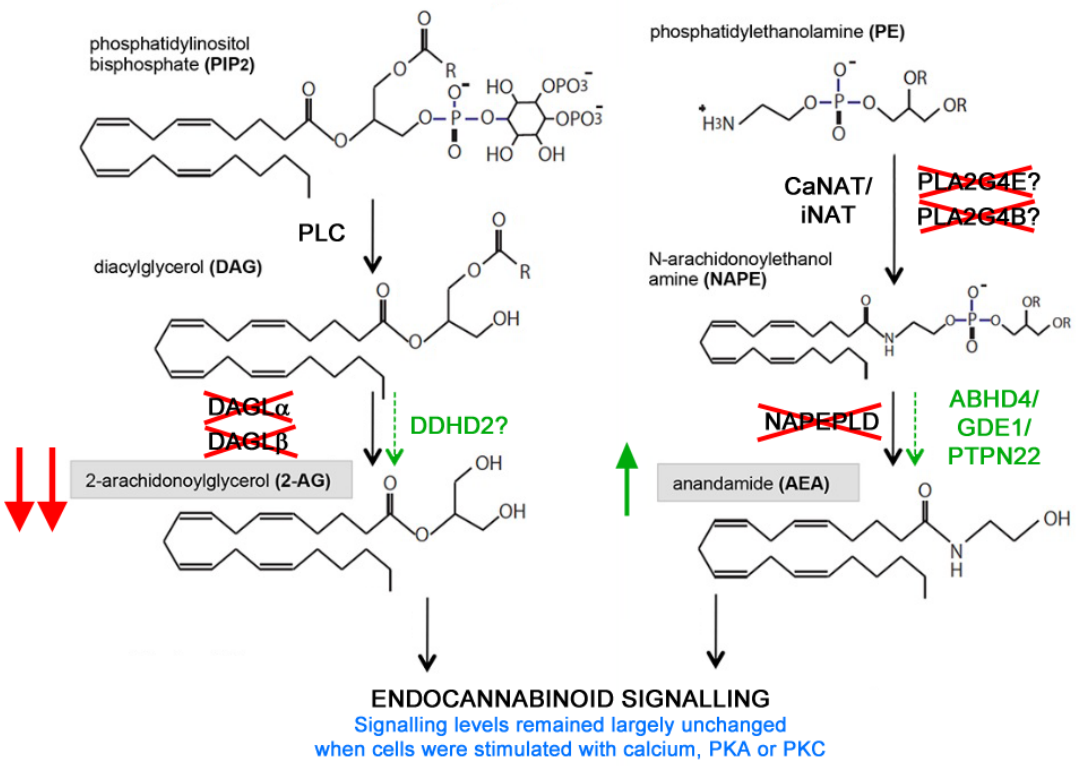

Figure 7.5.1. Summary of the CRISPR KO of key synthesis enzymes involved in eCB signalling in PLA2G4B KO cells.

Genes targeted with CRISPR are denoted with red crosses. KO of both DAGLs caused large reductions in 2-AG levels (~90%), the remaining 2-AG levels detected in the cells may be due to the contribution of DDHD2 in 2-AG synthesis. Slightly higher levels of AEA were detected following the KO of the DAGLs. This AEA level was unaffected by the genetic deletion of NAPEPLD. Secondary synthesis pathways could contribute to the maintained AEA levels which includes ABHD4, GDE1 and PTPN22 enzymes. Proposed CaNAT enzyme PLA2G4E was not detected in the cell line and genetic deletion of proposed CaNAT enzyme PLA2G4B did not alter AEA levels. Endocannabinoid signalling in PLA2G4B KO cells remained largely unchanged in comparison to parental CB1-Tango cells and can be stimulated by calcium and activation of PKA and PKC.

Adapted from Kouchi (2015).

7.6 Future Directions

The identification of PLA2G4E as a CaNAT was elucidated through ABPP (Ogura et al., 2016) but a bioinformatics search could also narrow down possible candidate enzymes for CaNAT based on gene expression from publicly available databases. The primary criteria for the candidate enzyme would be a similar transcript expression profile to CaNAT such as high expression in the brain and testes with low levels in other organs. Computational models of the functions of genes are annotated with gene ontology terms which gives clues about function of uncharacterised enzymes. Genes that have been annotated with closely related terms such as acyltransferase activity or acyl modelling would be high priority, with lower priority for more general terms such as phospholipid binding or calcium sensing. Furthermore, characterised enzymes will have extensively studied functions, another criterion for the candidates would therefore be a poorly characterised function. Finally, the enzymes should be expressed in the CB1-Tango cells.

Following the compilation of a list of candidate enzymes, these candidates would then be genetically knocked out of the PLA2G4B KO line with CRISPR and characterised with the QuantiGene multiplex assay before subject to drug treatment in the CB1-Tango assay to evaluate the contribution of the candidate genes to AEA synthesis and eCB signalling in an effort to identify the CaNAT in the CB1-Tango cells. Further characterisation of the enzymes involved in the AEA synthesis pathways (e.g. PLAAT, iNAT, ABHD4/GDE1 and PTPN22) and in the DAGL synthesis pathway (e.g. DDHD2 (Araki et al., 2016)) (Figure 7.5.1) could also be subject to CRISPR KO and analysis in the CB1-Tango assay.

The generation of a CB1-Tango cell line with no eCB signalling would serve as a good parent line for the reconstitution of any enzymes that could generate eCB signalling and could allow the study of 2-AG and AEA synthesis separately. Mutagenesis studies on the DAGLs or the enzymes from the AEA pathway could highlight regulatory residues on these enzymes involved in the regulation of eCB synthesis once reconstituted back into the parental line. The reconstitution of enzymes of 2-AG or AEA synthesis separately into each parental cell line would also be powerful tools for drug discovery efforts, in particular for a full understanding of AEA synthesis.

References

Abbas T, Shibata E, Park J, Jha S, Karnani N, Dutta A (2010) CRL4(Cdt2) Regulates Cell Proliferation and Histone Gene Expression by Targeting PR-Set7/Set8 for Degradation. Mol Cell 40:9-21.

Abzhanov A, Kaufman TC (2000) Crustacean (malacostracan) Hox genes and the evolution of the arthropod trunk. Development 127:2239-2249.

Acinas SG, Sarma-Rupavtarm R, Klepac-Ceraj V, Polz MF (2005) PCR-induced sequence artifacts and bias: insights from comparison of two 16S rRNA clone libraries constructed from the same sample. Appl Environ Microbiol 71:8966-8969.

Agarwal N et al. (2007) Cannabinoids mediate analgesia largely via peripheral type 1 cannabinoid receptors in nociceptors. Nat Neurosci 10:870-879.

Aguado T, Monory K, Palazuelos J, Stella N, Cravatt B, Lutz B, Marsicano G, Kokaia Z, Guzman M, Galve-Roperh I (2005) The endocannabinoid system drives neural progenitor proliferation. Faseb J 19:1704-1706.

Ahn K, Johnson DS, Mileni M, Beidler D, Long JZ, McKinney MK, Weerapana E, Sadagopan N, Liimatta M, Smith SE, Lazerwith S, Stiff C, Kamtekar S, Bhattacharya K, Zhang Y, Swaney S, Van Becelaere K, Stevens RC, Cravatt BF (2009) Discovery and characterization of a highly selective FAAH inhibitor that reduces inflammatory pain. Chem Biol 16:411-420.

Alger BE (2002) Retrograde signaling in the regulation of synaptic transmission: focus on endocannabinoids. Prog Neurobiol 68:247-286.

Altman J (1969) Autoradiographic and histological studies of postnatal neurogenesis. IV. Cell proliferation and migration in the anterior forebrain, with special reference to persisting neurogenesis in the olfactory bulb. J Comp Neurol 137:433-457.

Altman J, Das GD (1965) Autoradiographic and histological evidence of postnatal hippocampal neurogenesis in rats. J Comp Neurol 124:319-335.

Alvarez-Buylla A, Garcia-Verdugo JM (2002) Neurogenesis in adult subventricular zone. J Neurosci 22:629-634.

Andersson H, D'Antona AM, Kendall DA, Von Heijne G, Chin CN (2003) Membrane assembly of the cannabinoid receptor 1: impact of a long N-terminal tail. Mol Pharmacol 64:570-577.

Araki M, Ohshima N, Aso C, Konishi A, Obinata H, Tatei K, Izumi T (2016) Enzymatic characterization of recombinant rat DDHD2: a soluble diacylglycerol lipase. J Biochem 160:269-279.

Ariuens EJ, Simonis AM (1964) A Molecular Basis for Drug Action. The Interaction of One or More Drugs with Different Receptors. J Pharm Pharmacol 16:289-312.

Arreaza G, Devane WA, Omeir RL, Sajnani G, Kunz J, Cravatt BF, Deutsch DG (1997) The cloned rat hydrolytic enzyme responsible for the breakdown of anandamide also catalyzes its formation via the condensation of arachidonic acid and ethanolamine. Neurosci Lett 234:59-62.

Arvidsson A, Collin T, Kirik D, Kokaia Z, Lindvall O (2002) Neuronal replacement from endogenous precursors in the adult brain after stroke. Nat Med 8:963-970.

Aso C, Araki M, Ohshima N, Tatei K, Hirano T, Obinata H, Kishi M, Kishimoto K, Konishi A, Goto F, Sugimoto H, Izumi T (2016) Protein purification and cloning of diacylglycerol lipase from rat brain. J Biochem 159:585-597.

Astarita G, Piomelli D (2009) Lipidomic analysis of endocannabinoid metabolism in biological samples. J Chromatogr B Analyt Technol Biomed Life Sci 877:2755-2767.

Astarita G, Ahmed F, Piomelli D (2008) Identification of biosynthetic precursors for the endocannabinoid anandamide in the rat brain. J Lipid Res 49:48-57.

Atwood BK, Straiker A, Mackie K (2012) CB(2) cannabinoid receptors inhibit synaptic transmission when expressed in cultured autaptic neurons. Neuropharmacology 63:514-523.
Bab I, Ofek O, Tam J, Rehnelt J, Zimmer A (2008) Endocannabinoids and the regulation of bone metabolism. J Neuroendocrinol 20 Suppl 1:69-74.
Bajwa NM, Kesavan C, Mohan S (2018) Long-term Consequences of Traumatic Brain Injury in Bone Metabolism. Front Neurol 9:115.
Baker D, Pryce G, Giovannoni G, Thompson AJ (2003) The therapeutic potential of cannabis. Lancet Neurol 2:291-298.
Baker D, Pryce G, Davies WL, Hiley CR (2006) In silico patent searching reveals a new cannabinoid receptor. Trends Pharmacol Sci 27:1-4.
Baker M (2016) 1,500 scientists lift the lid on reproducibility. Nature 533:452-454.
Balgoma D, Checa A, Sar DG, Snowden S, Wheelock CE (2013) Quantitative metabolic profiling of lipid mediators. Mol Nutr Food Res 57:1359-1377.
Balsinde J, Winstead MV, Dennis EA (2002) Phospholipase A(2) regulation of arachidonic acid mobilization. FEBS Lett 531:2-6.
Barnea G, Strapps W, Herrada G, Berman Y, Ong J, Kloss B, Axel R, Lee KJ (2008) The genetic design of signaling cascades to record receptor activation. Proc Natl Acad Sci U S A 105:64-69.
Barrangou R, Fremaux C, Deveau H, Richards M, Boyaval P, Moineau S, Romero DA, Horvath P (2007) CRISPR provides acquired resistance against viruses in prokaryotes. Science 315:1709-1712.
Barrow KM, Perez-Campo FM, Ward CM (2006) Use of the cytomegalovirus promoter for transient and stable transgene expression in mouse embryonic stem cells. Methods Mol Biol 329:283-294.
Basavarajappa BS, Saito M, Cooper TB, Hungund BL (2000) Stimulation of cannabinoid receptor agonist 2-arachidonylglycerol by chronic ethanol and its modulation by specific neuromodulators in cerebellar granule neurons. Biochim Biophys Acta 1535:78-86.
Bauer M, Chicca A, Tamborrini M, Eisen D, Lerner R, Lutz B, Poetz O, Pluschke G, Gertsch J (2012) Identification and quantification of a new family of peptide endocannabinoids (Pepcans) showing negative allosteric modulation at CB1 receptors. J Biol Chem 287:36944-36967.
Begbie J, Doherty P, Graham A (2004) Cannabinoid receptor, CB1, expression follows neuronal differentiation in the early chick embryo. J Anat 205:213-218.
Begley CG, Ellis LM (2012) Drug development: Raise standards for preclinical cancer research. Nature 483:531-533.
Ben-Shabat S, Fride E, Sheskin T, Tamiri T, Rhee MH, Vogel Z, Bisogno T, De Petrocellis L, Di Marzo V, Mechoulam R (1998) An entourage effect: inactive endogenous fatty acid glycerol esters enhance 2-arachidonoyl-glycerol cannabinoid activity. Eur J Pharmacol 353:23-31.
Benard G et al. (2012) Mitochondrial CB(1) receptors regulate neuronal energy metabolism. Nat Neurosci 15:558-564.
Berdyshev EV, Boichot E, Germain N, Allain N, Anger JP, Lagente V (1997) Influence of fatty acid ethanolamides and delta9-tetrahydrocannabinol on cytokine and arachidonate release by mononuclear cells. Eur J Pharmacol 330:231-240.
Berger C, Schmid PC, Schabitz WR, Wolf M, Schwab S, Schmid HH (2004) Massive accumulation of N-acylethanolamines after stroke. Cell signalling in acute cerebral ischemia? J Neurochem 88:1159-1167.
Berghuis P, Rajnicek AM, Morozov YM, Ross RA, Mulder J, Urban GM, Monory K, Marsicano G, Matteoli M, Canty A, Irving AJ, Katona I, Yanagawa Y, Rakic P, Lutz B, Mackie K,

Harkany T (2007) Hardwiring the brain: endocannabinoids shape neuronal connectivity. Science 316:1212-1216.
Berrendero F, Garcia-Gil L, Hernandez ML, Romero J, Cebeira M, de Miguel R, Ramos JA, Fernandez-Ruiz JJ (1998) Localization of mRNA expression and activation of signal transduction mechanisms for cannabinoid receptor in rat brain during fetal development. Development 125:3179-3188.
Birdsall NJ (2010) Class A GPCR heterodimers: evidence from binding studies. Trends Pharmacol Sci 31:499-508.
Bisogno T, Sepe N, De Petrocellis L, Di Marzo V (1997) Biosynthesis of 2-arachidonoyl-glycerol, a novel cannabimimetic eicosanoid, in mouse neuroblastoma cells. Adv Exp Med Biol 433:201-204.
Bisogno T, Cascio MG, Saha B, Mahadevan A, Urbani P, Minassi A, Appendino G, Saturnino C, Martin B, Razdan R, Di Marzo V (2006) Development of the first potent and specific inhibitors of endocannabinoid biosynthesis. Biochim Biophys Acta 1761:205-212.
Bisogno T, Howell F, Williams G, Minassi A, Cascio MG, Ligresti A, Matias I, Schiano-Moriello A, Paul P, Williams EJ, Gangadharan U, Hobbs C, Di Marzo V, Doherty P (2003) Cloning of the first sn1-DAG lipases points to the spatial and temporal regulation of endocannabinoid signaling in the brain. J Cell Biol 163:463-468.
Bitinaite J, Wah DA, Aggarwal AK, Schildkraut I (1998) FokI dimerization is required for DNA cleavage. Proc Natl Acad Sci U S A 95:10570-10575.
Blais PA, Cote J, Morin J, Larouche A, Gendron G, Fortier A, Regoli D, Neugebauer W, Gobeil F, Jr. (2005) Hypotensive effects of hemopressin and bradykinin in rabbits, rats and mice. A comparative study. Peptides 26:1317-1322.
Blankman JL, Simon GM, Cravatt BF (2007) A comprehensive profile of brain enzymes that hydrolyze the endocannabinoid 2-arachidonoylglycerol. Chem Biol 14:1347-1356.
Boelens MC, te Meerman GJ, Gibcus JH, Blokzijl T, Boezen HM, Timens W, Postma DS, Groen HJ, van den Berg A (2007) Microarray amplification bias: loss of 30% differentially expressed genes due to long probe - poly(A)-tail distances. BMC Genomics 8:277.
Bomar MG, Galande AK (2013) Modulation of the cannabinoid receptors by hemopressin peptides. Life Sci 92:520-524.
Bomar MG, Samuelsson SJ, Kibler P, Kodukula K, Galande AK (2012) Hemopressin forms self-assembled fibrillar nanostructures under physiologically relevant conditions. Biomacromolecules 13:579-583.
Borgstrom B (1988) Mode of action of tetrahydrolipstatin: a derivative of the naturally occurring lipase inhibitor lipstatin. Biochim Biophys Acta 962:308-316.
Bosier B, Muccioli GG, Hermans E, Lambert DM (2010) Functionally selective cannabinoid receptor signalling: therapeutic implications and opportunities. Biochem Pharmacol 80:1-12.
Bouquet C, Nothias F (2007) Molecular mechanisms of axonal growth. Adv Exp Med Biol 621:1-16.
Brittis PA, Silver J, Walsh FS, Doherty P (1996) Fibroblast Growth Factor Receptor Function Is Required for the Orderly Projection of Ganglion Cell Axons in the Developing Mammalian Retina. Mol Cell Neurosci 8:120-128.
Brose N, Betz A, Wegmeyer H (2004) Divergent and convergent signaling by the diacylglycerol second messenger pathway in mammals. Curr Opin Neurobiol 14:328-340.
Brown AJ, Robin Hiley C (2009) Is GPR55 an anandamide receptor? Vitam Horm 81:111-137.
Brusco A, Tagliaferro P, Saez T, Onaivi ES (2008) Postsynaptic localization of CB2 cannabinoid receptors in the rat hippocampus. Synapse 62:944-949.
Buckley NE, McCoy KL, Mezey E, Bonner T, Zimmer A, Felder CC, Glass M, Zimmer A (2000) Immunomodulation by cannabinoids is absent in mice deficient for the cannabinoid CB(2) receptor. Eur J Pharmacol 396:141-149.

Burke JE, Dennis EA (2009) Phospholipase A2 biochemistry. Cardiovasc Drugs Ther 23:49-59.
Burkey TH, Quock RM, Consroe P, Ehlert FJ, Hosohata Y, Roeske WR, Yamamura HI (1997) Relative efficacies of cannabinoid CB1 receptor agonists in the mouse brain. Eur J Pharmacol 336:295-298.
Burstein S (2005) PPAR-gamma: a nuclear receptor with affinity for cannabinoids. Life Sci 77:1674-1684.
Cadas H, di Tomaso E, Piomelli D (1997) Occurrence and biosynthesis of endogenous cannabinoid precursor, N-arachidonoyl phosphatidylethanolamine, in rat brain. J Neurosci 17:1226-1242.
Cadas H, Gaillet S, Beltramo M, Venance L, Piomelli D (1996) Biosynthesis of an endogenous cannabinoid precursor in neurons and its control by calcium and cAMP. J Neurosci 16:3934-3942.
Calvey TN, Williams NE (2008) Principles and practice of pharmacology for anaesthetists, 5th Edition. Malden, Mass.: Blackwell Pub.
Canver MC, Bauer DE, Dass A, Yien YY, Chung J, Masuda T, Maeda T, Paw BH, Orkin SH (2014) Characterization of genomic deletion efficiency mediated by clustered regularly interspaced palindromic repeats (CRISPR)/Cas9 nuclease system in mammalian cells. J Biol Chem 289:21312-21324.
Capasso A, Milano W, Cauli O (2018) Changes in the Peripheral Endocannabinoid System as a Risk Factor for the Development of Eating Disorders. Endocr Metab Immune Disord Drug Targets.
Capestrano M, Mariggio S, Perinetti G, Egorova AV, Iacobacci S, Santoro M, Di Pentima A, Iurisci C, Egorov MV, Di Tullio G, Buccione R, Luini A, Polishchuk RS (2014) Cytosolic phospholipase A(2)epsilon drives recycling through the clathrin-independent endocytic route. J Cell Sci 127:977-993.
Carta M, Lanore F, Rebola N, Szabo Z, Da Silva SV, Lourenco J, Verraes A, Nadler A, Schultz C, Blanchet C, Mulle C (2014) Membrane lipids tune synaptic transmission by direct modulation of presynaptic potassium channels. Neuron 81:787-799.
Castagna M, Takai Y, Kaibuchi K, Sano K, Kikkawa U, Nishizuka Y (1982) Direct activation of calcium-activated, phospholipid-dependent protein kinase by tumor-promoting phorbol esters. J Biol Chem 257:7847-7851.
Castellani B, Diamanti E, Pizzirani D, Tardia P, Maccesi M, Realini N, Magotti P, Garau G, Bakkum T, Rivara S, Mor M, Piomelli D (2017) Synthesis and characterization of the first inhibitor of N-acylphosphatidylethanolamine phospholipase D (NAPE-PLD). Chem Commun (Camb) 53:12814-12817.
Castillo PE, Younts TJ, Chavez AE, Hashimotodani Y (2012) Endocannabinoid signaling and synaptic function. Neuron 76:70-81.
Centonze D, Finazzi-Agro A, Bernardi G, Maccarrone M (2007) The endocannabinoid system in targeting inflammatory neurodegenerative diseases. Trends Pharmacol Sci 28:180-187.
Chau LY, Tai HH (1981) Release of arachidonate from diglyceride in human platelets requires the sequential action of a diglyceride lipase and a monoglyceride lipase. Biochem Biophys Res Commun 100:1688-1695.
Cheng Y, Wang Y, Li J, Chang I, Wang CY (2017) A novel read-through transcript JMJD7-PLA2G4B regulates head and neck squamous cell carcinoma cell proliferation and survival. Oncotarget 8:1972-1982.
Choi SH, Arai AL, Mou Y, Kang B, Yen CC, Hallenbeck J, Silva AC (2018) Neuroprotective Effects of MAGL (Monoacylglycerol Lipase) Inhibitors in Experimental Ischemic Stroke. Stroke 49:718-726.

Christensen R, Kristensen PK, Bartels EM, Bliddal H, Astrup A (2007) Efficacy and safety of the weight-loss drug rimonabant: a meta-analysis of randomised trials. Lancet 370:1706-1713.
Citri A, Malenka RC (2008) Synaptic plasticity: multiple forms, functions, and mechanisms. Neuropsychopharmacology 33:18-41.
Clissold PM, Ponting CP (2001) JmjC: cupin metalloenzyme-like domains in jumonji, hairless and phospholipase A2beta. Trends Biochem Sci 26:7-9.
Collingridge GL, Peineau S, Howland JG, Wang YT (2010) Long-term depression in the CNS. Nat Rev Neurosci 11:459-473.
Colombo G, Agabio R, Diaz G, Lobina C, Reali R, Gessa GL (1998) Appetite suppression and weight loss after the cannabinoid antagonist SR 141716. Life Sci 63:PL113-117.
Compagnucci C, Di Siena S, Bustamante MB, Di Giacomo D, Di Tommaso M, Maccarrone M, Grimaldi P, Sette C (2013) Type-1 (CB1) cannabinoid receptor promotes neuronal differentiation and maturation of neural stem cells. PLoS One 8:e54271.
Cong L, Ran FA, Cox D, Lin S, Barretto R, Habib N, Hsu PD, Wu X, Jiang W, Marraffini LA, Zhang F (2013) Multiplex genome engineering using CRISPR/Cas systems. Science 339:819-823.
Costa B (2007) Rimonabant: more than an anti-obesity drug? Br J Pharmacol 150:535-537.
Cravatt BF, Giang DK, Mayfield SP, Boger DL, Lerner RA, Gilula NB (1996) Molecular characterization of an enzyme that degrades neuromodulatory fatty-acid amides. Nature 384:83-87.
Cravatt BF, Demarest K, Patricelli MP, Bracey MH, Giang DK, Martin BR, Lichtman AH (2001) Supersensitivity to anandamide and enhanced endogenous cannabinoid signaling in mice lacking fatty acid amide hydrolase. Proc Natl Acad Sci U S A 98:9371-9376.
Curran HV, Freeman TP, Mokrysz C, Lewis DA, Morgan CJ, Parsons LH (2016) Keep off the grass? Cannabis, cognition and addiction. Nat Rev Neurosci 17:293-306.
Daiyasu H, Osaka K, Ishino Y, Toh H (2001) Expansion of the zinc metallo-hydrolase family of the beta-lactamase fold. FEBS Lett 503:1-6.
Dale CS, Pagano Rde L, Rioli V (2005a) Hemopressin: a novel bioactive peptide derived from the alpha1-chain of hemoglobin. Mem Inst Oswaldo Cruz 100 Suppl 1:105-106.
Dale CS, Pagano Rde L, Rioli V, Hyslop S, Giorgi R, Ferro ES (2005b) Antinociceptive action of hemopressin in experimental hyperalgesia. Peptides 26:431-436.
Davies SS, Amarnath V, Montine KS, Bernoud-Hubac N, Boutaud O, Montine TJ, Roberts LJ, 2nd (2002) Effects of reactive gamma-ketoaldehydes formed by the isoprostane pathway (isoketals) and cyclooxygenase pathway (levuglandins) on proteasome function. Faseb J 16:715-717.
Davis MP (2014) Cannabinoids in pain management: CB1, CB2 and non-classic receptor ligands. Expert Opin Investig Drugs 23:1123-1140.
De Petrocellis L, Melck D, Bisogno T, Milone A, Di Marzo V (1999) Finding of the endocannabinoid signalling system in Hydra, a very primitive organism: possible role in the feeding response. Neuroscience 92:377-387.
Deltcheva E, Chylinski K, Sharma CM, Gonzales K, Chao Y, Pirzada ZA, Eckert MR, Vogel J, Charpentier E (2011) CRISPR RNA maturation by trans-encoded small RNA and host factor RNase III. Nature 471:602-607.
Devane WA, Axelrod J (1994) Enzymatic synthesis of anandamide, an endogenous ligand for the cannabinoid receptor, by brain membranes. Proc Natl Acad Sci U S A 91:6698-6701.
Devane WA, Dysarz FA, 3rd, Johnson MR, Melvin LS, Howlett AC (1988) Determination and characterization of a cannabinoid receptor in rat brain. Mol Pharmacol 34:605-613.

Devane WA, Hanus L, Breuer A, Pertwee RG, Stevenson LA, Griffin G, Gibson D, Mandelbaum A, Etinger A, Mechoulam R (1992) Isolation and structure of a brain constituent that binds to the cannabinoid receptor. Science 258:1946-1949.

Deveau H, Garneau JE, Moineau S (2010) CRISPR/Cas system and its role in phage-bacteria interactions. Annu Rev Microbiol 64:475-493.

Devinsky O, Cilio MR, Cross H, Fernandez-Ruiz J, French J, Hill C, Katz R, Di Marzo V, Jutras-Aswad D, Notcutt WG, Martinez-Orgado J, Robson PJ, Rohrback BG, Thiele E, Whalley B, Friedman D (2014) Cannabidiol: pharmacology and potential therapeutic role in epilepsy and other neuropsychiatric disorders. Epilepsia 55:791-802.

Dewey WL (1986) Cannabinoid pharmacology. Pharmacol Rev 38:151-178.

Di Marzo V (1998) 'Endocannabinoids' and other fatty acid derivatives with cannabimimetic properties: biochemistry and possible physiopathological relevance. Biochim Biophys Acta 1392:153-175.

Di Marzo V (2008a) Endocannabinoids: synthesis and degradation. Rev Physiol Biochem Pharmacol 160:1-24.

Di Marzo V (2008b) Targeting the endocannabinoid system: to enhance or reduce? Nat Rev Drug Discov 7:438-455.

Di Marzo V (2011) Endocannabinoid signaling in the brain: biosynthetic mechanisms in the limelight. Nat Neurosci 14:9-15.

Di Marzo V (2018) New approaches and challenges to targeting the endocannabinoid system. Nat Rev Drug Discov 17:623-639.

Di Marzo V, Petrosino S (2007) Endocannabinoids and the regulation of their levels in health and disease. Curr Opin Lipidol 18:129-140.

Di Marzo V, Stella N, Zimmer A (2015) Endocannabinoid signalling and the deteriorating brain. Nat Rev Neurosci 16:30-42.

Di Marzo V, Fontana A, Cadas H, Schinelli S, Cimino G, Schwartz JC, Piomelli D (1994) Formation and inactivation of endogenous cannabinoid anandamide in central neurons. Nature 372:686-691.

Dinh TP, Carpenter D, Leslie FM, Freund TF, Katona I, Sensi SL, Kathuria S, Piomelli D (2002) Brain monoglyceride lipase participating in endocannabinoid inactivation. Proc Natl Acad Sci U S A 99:10819-10824.

Dodd GT, Mancini G, Lutz B, Luckman SM (2010) The peptide hemopressin acts through CB1 cannabinoid receptors to reduce food intake in rats and mice. J Neurosci 30:7369-7376.

Dodd GT, Worth AA, Hodkinson DJ, Srivastava RK, Lutz B, Williams SR, Luckman SM (2013) Central functional response to the novel peptide cannabinoid, hemopressin. Neuropharmacology 71:27-36.

Duff G, Argaw A, Cecyre B, Cherif H, Tea N, Zabouri N, Casanova C, Ptito M, Bouchard JF (2013) Cannabinoid receptor CB2 modulates axon guidance. PLoS One 8:e70849.

Dunn TA, Storm DR, Feller MB (2009) Calcium-dependent increases in protein kinase-A activity in mouse retinal ganglion cells are mediated by multiple adenylate cyclases. PLoS One 4:e7877.

Durai S, Mani M, Kandavelou K, Wu J, Porteus MH, Chandrasegaran S (2005) Zinc finger nucleases: custom-designed molecular scissors for genome engineering of plant and mammalian cells. Nucleic Acids Res 33:5978-5990.

Dvoracsko S, Tomboly C, Berkecz R, Keresztes A (2016) Investigation of receptor binding and functional characteristics of hemopressin(1-7). Neuropeptides 58:15-22.

Eccles JC, McIntyre AK (1951) Plasticity of Mammalian Monosynaptic Reflexes. Nature 167:466.

Egertova M, Elphick MR (2000) Localisation of cannabinoid receptors in the rat brain using antibodies to the intracellular C-terminal tail of CB. J Comp Neurol 422:159-171.

Egertova M, Simon GM, Cravatt BF, Elphick MR (2008) Localization of N-acyl phosphatidylethanolamine phospholipase D (NAPE-PLD) expression in mouse brain: A new perspective on N-acylethanolamines as neural signaling molecules. J Comp Neurol 506:604-615.

El Marroun H, Tiemeier H, Steegers EA, Jaddoe VW, Hofman A, Verhulst FC, van den Brink W, Huizink AC (2009) Intrauterine cannabis exposure affects fetal growth trajectories: the Generation R Study. J Am Acad Child Adolesc Psychiatry 48:1173-1181.

Eljaschewitsch E, Witting A, Mawrin C, Lee T, Schmidt PM, Wolf S, Hoertnagl H, Raine CS, Schneider-Stock R, Nitsch R, Ullrich O (2006) The endocannabinoid anandamide protects neurons during CNS inflammation by induction of MKP-1 in microglial cells. Neuron 49:67-79.

Elphick MR (2012) The evolution and comparative neurobiology of endocannabinoid signalling. Philos Trans R Soc Lond B Biol Sci 367:3201-3215.

Elphick MR, Egertova M (2001) The neurobiology and evolution of cannabinoid signalling. Philos Trans R Soc Lond B Biol Sci 356:381-408.

ElSohly MA, Slade D (2005) Chemical constituents of marijuana: The complex mixture of natural cannabinoids. Life Sci 78:539-548.

Eriksson PS, Perfilieva E, Bjork-Eriksson T, Alborn AM, Nordborg C, Peterson DA, Gage FH (1998) Neurogenesis in the adult human hippocampus. Nat Med 4:1313-1317.

Ernst A, Alkass K, Bernard S, Salehpour M, Perl S, Tisdale J, Possnert G, Druid H, Frisen J (2014) Neurogenesis in the striatum of the adult human brain. Cell 156:1072-1083.

Esposito E, Cordaro M, Cuzzocrea S (2014) Roles of fatty acid ethanolamides (FAE) in traumatic and ischemic brain injury. Pharmacol Res 86:26-31.

Eswaran J, Horvath A, Godbole S, Reddy SD, Mudvari P, Ohshiro K, Cyanam D, Nair S, Fuqua SA, Polyak K, Florea LD, Kumar R (2013) RNA sequencing of cancer reveals novel splicing alterations. Sci Rep 3:1689.

Fackenthal JD, Godley LA (2008) Aberrant RNA splicing and its functional consequences in cancer cells. Dis Model Mech 1:37-42.

Farooqui AA, Taylor WA, Horrocks LA (1984) Separation of bovine brain mono- and diacylglycerol lipases by heparin sepharose affinity chromatography. Biochem Biophys Res Commun 122:1241-1246.

Felder CC, Nielsen A, Briley EM, Palkovits M, Priller J, Axelrod J, Nguyen DN, Richardson JM, Riggin RM, Koppel GA, Paul SM, Becker GW (1996) Isolation and measurement of the endogenous cannabinoid receptor agonist, anandamide, in brain and peripheral tissues of human and rat. FEBS Lett 393:231-235.

Fezza F, Bisogno T, Minassi A, Appendino G, Mechoulam R, Di Marzo V (2002) Noladin ether, a putative novel endocannabinoid: inactivation mechanisms and a sensitive method for its quantification in rat tissues. FEBS Lett 513:294-298.

Fezza F, Bari M, Florio R, Talamonti E, Feole M, Maccarrone M (2014) Endocannabinoids, related compounds and their metabolic routes. Molecules 19:17078-17106.

Fine PG, Rosenfeld MJ (2013) The endocannabinoid system, cannabinoids, and pain. Rambam Maimonides Med J 4:e0022.

Flagella M, Bui S, Zheng Z, Nguyen CT, Zhang A, Pastor L, Ma Y, Yang W, Crawford KL, McMaster GK, Witney F, Luo Y (2006) A multiplex branched DNA assay for parallel quantitative gene expression profiling. Anal Biochem 352:50-60.

Fogaca MV, Sonego AB, Rioli V, Gozzo FC, Dale CS, Ferro ES, Guimaraes FS (2015) Anxiogenic-like effects induced by hemopressin in rats. Pharmacol Biochem Behav 129:7-13.

Fowler CJ, Rojo ML, Rodriguez-Gaztelumendi A (2010) Modulation of the endocannabinoid system: neuroprotection or neurotoxicity? Exp Neurol 224:37-47.

Fu J, Gaetani S, Oveisi F, Lo Verme J, Serrano A, Rodriguez De Fonseca F, Rosengarth A, Luecke H, Di Giacomo B, Tarzia G, Piomelli D (2003) Oleylethanolamide regulates feeding

and body weight through activation of the nuclear receptor PPAR-alpha. Nature 425:90-93.
Fu J, Bottegoni G, Sasso O, Bertorelli R, Rocchia W, Masetti M, Guijarro A, Lodola A, Armirotti A, Garau G, Bandiera T, Reggiani A, Mor M, Cavalli A, Piomelli D (2011) A catalytically silent FAAH-1 variant drives anandamide transport in neurons. Nat Neurosci 15:64-69.
Fukuda K, Davies SS, Nakajima T, Ong BH, Kupershmidt S, Fessel J, Amarnath V, Anderson ME, Boyden PA, Viswanathan PC, Roberts LJ, 2nd, Balser JR (2005) Oxidative mediated lipid peroxidation recapitulates proarrhythmic effects on cardiac sodium channels. Circ Res 97:1262-1269.
Gaj T, Gersbach CA, Barbas CF, 3rd (2013) ZFN, TALEN, and CRISPR/Cas-based methods for genome engineering. Trends Biotechnol 31:397-405.
Galiegue S, Mary S, Marchand J, Dussossoy D, Carriere D, Carayon P, Bouaboula M, Shire D, Le Fur G, Casellas P (1995) Expression of central and peripheral cannabinoid receptors in human immune tissues and leukocyte subpopulations. Eur J Biochem 232:54-61.
Gallily R, Breuer A, Mechoulam R (2000) 2-Arachidonylglycerol, an endogenous cannabinoid, inhibits tumor necrosis factor-alpha production in murine macrophages, and in mice. Eur J Pharmacol 406:R5-7.
Gantz SC, Bean BP (2017) Cell-Autonomous Excitation of Midbrain Dopamine Neurons by Endocannabinoid-Dependent Lipid Signaling. Neuron 93:1375-1387 e1372.
Gao Y et al. (2010) Loss of retrograde endocannabinoid signaling and reduced adult neurogenesis in diacylglycerol lipase knock-out mice. J Neurosci 30:2017-2024.
Gaoni Y, Mechoulam R (1964) Isolation, Structure, and Partial Synthesis of an Active Constituent of Hashish. J Am Chem Soc 86:1646-+.
Garneau JE, Dupuis ME, Villion M, Romero DA, Barrangou R, Boyaval P, Fremaux C, Horvath P, Magadan AH, Moineau S (2010) The CRISPR/Cas bacterial immune system cleaves bacteriophage and plasmid DNA. Nature 468:67-71.
Gelman JS, Dasgupta S, Berezniuk I, Fricker LD (2013) Analysis of peptides secreted from cultured mouse brain tissue. Biochim Biophys Acta 1834:2408-2417.
Gerard CM, Mollereau C, Vassart G, Parmentier M (1991) Molecular cloning of a human cannabinoid receptor which is also expressed in testis. Biochem J 279 (Pt 1):129-134.
Geurts L, Lazarevic V, Derrien M, Everard A, Van Roye M, Knauf C, Valet P, Girard M, Muccioli GG, Francois P, de Vos WM, Schrenzel J, Delzenne NM, Cani PD (2011) Altered gut microbiota and endocannabinoid system tone in obese and diabetic leptin-resistant mice: impact on apelin regulation in adipose tissue. Front Microbiol 2:149.
Ghafouri N, Tiger G, Razdan RK, Mahadevan A, Pertwee RG, Martin BR, Fowler CJ (2004) Inhibition of monoacylglycerol lipase and fatty acid amide hydrolase by analogues of 2-arachidonoylglycerol. Br J Pharmacol 143:774-784.
Ghosh M, Tucker DE, Burchett SA, Leslie CC (2006) Properties of the Group IV phospholipase A2 family. Prog Lipid Res 45:487-510.
Giang DK, Cravatt BF (1997) Molecular characterization of human and mouse fatty acid amide hydrolases. Proc Natl Acad Sci U S A 94:2238-2242.
Godlewski G, Offertaler L, Wagner JA, Kunos G (2009) Receptors for acylethanolamides-GPR55 and GPR119. Prostaglandins Other Lipid Mediat 89:105-111.
Goings GE, Sahni V, Szele FG (2004) Migration patterns of subventricular zone cells in adult mice change after cerebral cortex injury. Brain Res 996:213-226.
Golczak M, Kiser PD, Sears AE, Lodowski DT, Blaner WS, Palczewski K (2012) Structural basis for the acyltransferase activity of lecithin:retinol acyltransferase-like proteins. J Biol Chem 287:23790-23807.

Gomes I, Dale CS, Casten K, Geigner MA, Gozzo FC, Ferro ES, Heimann AS, Devi LA (2010) Hemoglobin-derived peptides as novel type of bioactive signaling molecules. Aaps J 12:658-669.

Gomes I, Grushko JS, Golebiewska U, Hoogendoorn S, Gupta A, Heimann AS, Ferro ES, Scarlata S, Fricker LD, Devi LA (2009) Novel endogenous peptide agonists of cannabinoid receptors. Faseb J 23:3020-3029.

Goncalves MB, Suetterlin P, Yip P, Molina-Holgado F, Walker DJ, Oudin MJ, Zentar MP, Pollard S, Yanez-Munoz RJ, Williams G, Walsh FS, Pangalos MN, Doherty P (2008) A diacylglycerol lipase-CB2 cannabinoid pathway regulates adult subventricular zone neurogenesis in an age-dependent manner. Mol Cell Neurosci 38:526-536.

Gong JP, Onaivi ES, Ishiguro H, Liu QR, Tagliaferro PA, Brusco A, Uhl GR (2006) Cannabinoid CB2 receptors: immunohistochemical localization in rat brain. Brain Res 1071:10-23.

Guo L, Gragg SD, Chen Z, Zhang Y, Amarnath V, Davies SS (2013) Isolevuglandin-modified phosphatidylethanolamine is metabolized by NAPE-hydrolyzing phospholipase D. J Lipid Res 54:3151-3157.

Gupta A, Decaillot FM, Gomes I, Tkalych O, Heimann AS, Ferro ES, Devi LA (2007) Conformation state-sensitive antibodies to G-protein-coupled receptors. J Biol Chem 282:5116-5124.

Hama A, Sagen J (2011a) Activation of spinal and supraspinal cannabinoid-1 receptors leads to antinociception in a rat model of neuropathic spinal cord injury pain. Brain Res 1412:44-54.

Hama A, Sagen J (2011b) Centrally mediated antinociceptive effects of cannabinoid receptor ligands in rat models of nociception. Pharmacol Biochem Behav 100:340-346.

Hampson AJ, Hill WA, Zan-Phillips M, Makriyannis A, Leung E, Eglen RM, Bornheim LM (1995) Anandamide hydroxylation by brain lipoxygenase:metabolite structures and potencies at the cannabinoid receptor. Biochim Biophys Acta 1259:173-179.

Han ZL, Fang Q, Wang ZL, Li XH, Li N, Chang XM, Pan JX, Tang HZ, Wang R (2014) Antinociceptive effects of central administration of the endogenous cannabinoid receptor type 1 agonist VDPVNFKLLSH-OH [(m)VD-hemopressin(alpha)], an N-terminally extended hemopressin peptide. J Pharmacol Exp Ther 348:316-323.

Hansen HH, Ikonomidou C, Bittigau P, Hansen SH, Hansen HS (2001a) Accumulation of the anandamide precursor and other N-acylethanolamine phospholipids in infant rat models of in vivo necrotic and apoptotic neuronal death. J Neurochem 76:39-46.

Hansen HH, Schmid PC, Bittigau P, Lastres-Becker I, Berrendero F, Manzanares J, Ikonomidou C, Schmid HH, Fernandez-Ruiz JJ, Hansen HS (2001b) Anandamide, but not 2-arachidonoylglycerol, accumulates during in vivo neurodegeneration. J Neurochem 78:1415-1427.

Hansen HS (2010) Palmitoylethanolamide and other anandamide congeners. Proposed role in the diseased brain. Exp Neurol 224:48-55.

Hansen HS, Moesgaard B, Hansen HH, Petersen G (2000) N-Acylethanolamines and precursor phospholipids - relation to cell injury. Chem Phys Lipids 108:135-150.

Hansen KB, Rosenkilde MM, Knop FK, Wellner N, Diep TA, Rehfeld JF, Andersen UB, Holst JJ, Hansen HS (2011) 2-Oleoyl glycerol is a GPR119 agonist and signals GLP-1 release in humans. J Clin Endocrinol Metab 96:E1409-1417.

Hanus L, Abu-Lafi S, Fride E, Breuer A, Vogel Z, Shalev DE, Kustanovich I, Mechoulam R (2001) 2-arachidonyl glyceryl ether, an endogenous agonist of the cannabinoid CB1 receptor. Proc Natl Acad Sci U S A 98:3662-3665.

Harbison RD, Mantilla-Plata B (1972) Prenatal toxicity, maternal distribution and placental transfer of tetrahydrocannabinol. J Pharmacol Exp Ther 180:446-453.

Hardie RC, Franze K (2012) Photomechanical responses in Drosophila photoreceptors. Science 338:260-263.

Harizi H, Corcuff JB, Gualde N (2008) Arachidonic-acid-derived eicosanoids: roles in biology and immunopathology. Trends Mol Med 14:461-469.

Harkany T, Mackie K, Doherty P (2008) Wiring and firing neuronal networks: endocannabinoids take center stage. Curr Opin Neurobiol 18:338-345.

Hashimotodani Y, Ohno-Shosaku T, Kano M (2007) Presynaptic monoacylglycerol lipase activity determines basal endocannabinoid tone and terminates retrograde endocannabinoid signaling in the hippocampus. J Neurosci 27:1211-1219.

Hashimotodani Y, Ohno-Shosaku T, Tsubokawa H, Ogata H, Emoto K, Maejima T, Araishi K, Shin HS, Kano M (2005) Phospholipase Cbeta serves as a coincidence detector through its Ca2+ dependency for triggering retrograde endocannabinoid signal. Neuron 45:257-268.

Heifets BD, Castillo PE (2009) Endocannabinoid signaling and long-term synaptic plasticity. Annu Rev Physiol 71:283-306.

Heifets BD, Chevaleyre V, Castillo PE (2008) Interneuron activity controls endocannabinoid-mediated presynaptic plasticity through calcineurin. Proc Natl Acad Sci U S A 105:10250-10255.

Heimann AS, Gomes I, Dale CS, Pagano RL, Gupta A, de Souza LL, Luchessi AD, Castro LM, Giorgi R, Rioli V, Ferro ES, Devi LA (2007) Hemopressin is an inverse agonist of CB1 cannabinoid receptors. Proc Natl Acad Sci U S A 104:20588-20593.

Heng L, Beverley JA, Steiner H, Tseng KY (2011) Differential developmental trajectories for CB1 cannabinoid receptor expression in limbic/associative and sensorimotor cortical areas. Synapse 65:278-286.

Herkenham M, Lynn AB, Little MD, Johnson MR, Melvin LS, de Costa BR, Rice KC (1990) Cannabinoid receptor localization in brain. Proc Natl Acad Sci U S A 87:1932-1936.

Higgs HN, Glomset JA (1994) Identification of a phosphatidic acid-preferring phospholipase A1 from bovine brain and testis. Proc Natl Acad Sci U S A 91:9574-9578.

Hillard CJ, Jarrahian A (2000) The movement of N-arachidonoylethanolamine (anandamide) across cellular membranes. Chem Phys Lipids 108:123-134.

Hillard CJ, Manna S, Greenberg MJ, Dicamelli R, Ross RA, Stevenson LA, Murphy V, Pertwee RG, Campbell WB (1999) Synthesis and characterization of potent and selective agonists of the neuronal cannabinoid receptor (CB1). Journal of Pharmacology and Experimental Therapeutics 289:1427-1433.

Hohmann AG, Herkenham M (1999) Localization of central cannabinoid CB1 receptor messenger RNA in neuronal subpopulations of rat dorsal root ganglia: a double-label in situ hybridization study. Neuroscience 90:923-931.

Hollister LE (1974) Structure-activity relationships in man of cannabis constituents, and homologs and metabolites of delta9-tetrahydrocannabinol. Pharmacology 11:3-11.

Holtmaat A, Svoboda K (2009) Experience-dependent structural synaptic plasticity in the mammalian brain. Nat Rev Neurosci 10:647-658.

Hoover HS, Blankman JL, Niessen S, Cravatt BF (2008) Selectivity of inhibitors of endocannabinoid biosynthesis evaluated by activity-based protein profiling. Bioorg Med Chem Lett 18:5838-5841.

Hoppe G, Subbanagounder G, O'Neil J, Salomon RG, Hoff HF (1997) Macrophage recognition of LDL modified by levuglandin E2, an oxidation product of arachidonic acid. Biochim Biophys Acta 1344:1-5.

Howlett AC (2002) The cannabinoid receptors. Prostaglandins Other Lipid Mediat 68-69:619-631.

Howlett AC, Qualy JM, Khachatrian LL (1986) Involvement of Gi in the inhibition of adenylate cyclase by cannabimimetic drugs. Mol Pharmacol 29:307-313.

Howlett AC, Reggio PH, Childers SR, Hampson RE, Ulloa NM, Deutsch DG (2011) Endocannabinoid tone versus constitutive activity of cannabinoid receptors. Br J Pharmacol 163:1329-1343.

Howlett AC, Barth F, Bonner TI, Cabral G, Casellas P, Devane WA, Felder CC, Herkenham M, Mackie K, Martin BR, Mechoulam R, Pertwee RG (2002) International Union of Pharmacology. XXVII. Classification of cannabinoid receptors. Pharmacol Rev 54:161-202.

Hsu KL, Tsuboi K, Adibekian A, Pugh H, Masuda K, Cravatt BF (2012) DAGLbeta inhibition perturbs a lipid network involved in macrophage inflammatory responses. Nat Chem Biol 8:999-1007.

Hu SS, Bradshaw HB, Benton VM, Chen JS, Huang SM, Minassi A, Bisogno T, Masuda K, Tan B, Roskoski R, Jr., Cravatt BF, Di Marzo V, Walker JM (2009) The biosynthesis of N-arachidonoyl dopamine (NADA), a putative endocannabinoid and endovanilloid, via conjugation of arachidonic acid with dopamine. Prostaglandins Leukot Essent Fatty Acids 81:291-301.

Huang SM, Bisogno T, Trevisani M, Al-Hayani A, De Petrocellis L, Fezza F, Tognetto M, Petros TJ, Krey JF, Chu CJ, Miller JD, Davies SN, Geppetti P, Walker JM, Di Marzo V (2002) An endogenous capsaicin-like substance with high potency at recombinant and native vanilloid VR1 receptors. Proc Natl Acad Sci U S A 99:8400-8405.

Hurd YL, Wang X, Anderson V, Beck O, Minkoff H, Dow-Edwards D (2005) Marijuana impairs growth in mid-gestation fetuses. Neurotoxicol Teratol 27:221-229.

Hussain Z, Uyama T, Tsuboi K, Ueda N (2017) Mammalian enzymes responsible for the biosynthesis of N-acylethanolamines. Biochim Biophys Acta 1862:1546-1561.

Hussain Z, Uyama T, Kawai K, Rahman IA, Tsuboi K, Araki N, Ueda N (2016) Comparative analyses of isoforms of the calcium-independent phosphatidylethanolamine N-acyltransferase PLAAT-1 in humans and mice. J Lipid Res 57:2051-2060.

Hussain Z, Uyama T, Kawai K, Binte Mustafiz SS, Tsuboi K, Araki N, Ueda N (2018) Phosphatidylserine-stimulated production of N-acyl-phosphatidylethanolamines by Ca(2+)-dependent N-acyltransferase. Biochim Biophys Acta 1863:493-502.

Iannotti FA, Di Marzo V, Petrosino S (2016) Endocannabinoids and endocannabinoid-related mediators: Targets, metabolism and role in neurological disorders. Prog Lipid Res 62:107-128.

Idris AI, Ralston SH (2012) Role of cannabinoids in the regulation of bone remodeling. Front Endocrinol (Lausanne) 3:136.

Idris AI, Sophocleous A, Landao-Bassonga E, van't Hof RJ, Ralston SH (2008) Regulation of bone mass, osteoclast function, and ovariectomy-induced bone loss by the type 2 cannabinoid receptor. Endocrinology 149:5619-5626.

Idris AI, van 't Hof RJ, Greig IR, Ridge SA, Baker D, Ross RA, Ralston SH (2005) Regulation of bone mass, bone loss and osteoclast activity by cannabinoid receptors. Nat Med 11:774-779.

Ihunwo AO, Tembo LH, Dzamalala C (2016) The dynamics of adult neurogenesis in human hippocampus. Neural Regen Res 11:1869-1883.

Imperatore R, Morello G, Luongo L, Taschler U, Romano R, De Gregorio D, Belardo C, Maione S, Di Marzo V, Cristino L (2015) Genetic deletion of monoacylglycerol lipase leads to impaired cannabinoid receptor CB(1)R signaling and anxiety-like behavior. J Neurochem 135:799-813.

Inoue M, Tsuboi K, Okamoto Y, Hidaka M, Uyama T, Tsutsumi T, Tanaka T, Ueda N, Tokumura A (2017) Peripheral tissue levels and molecular species compositions of N-acyl-phosphatidylethanolamine and its metabolites in mice lacking N-acyl-phosphatidylethanolamine-specific phospholipase D. J Biochem 162:449-458.

Ishac EJ, Jiang L, Lake KD, Varga K, Abood ME, Kunos G (1996) Inhibition of exocytotic noradrenaline release by presynaptic cannabinoid CB1 receptors on peripheral sympathetic nerves. Br J Pharmacol 118:2023-2028.

Jahng WJ, Xue L, Rando RR (2003) Lecithin retinol acyltransferase is a founder member of a novel family of enzymes. Biochemistry 42:12805-12812.

Jarai Z, Wagner JA, Varga K, Lake KD, Compton DR, Martin BR, Zimmer AM, Bonner TI, Buckley NE, Mezey E, Razdan RK, Zimmer A, Kunos G (1999) Cannabinoid-induced mesenteric vasodilation through an endothelial site distinct from CB1 or CB2 receptors. Proc Natl Acad Sci U S A 96:14136-14141.

Jenniches I, Ternes S, Albayram O, Otte DM, Bach K, Bindila L, Michel K, Lutz B, Bilkei-Gorzo A, Zimmer A (2016) Anxiety, Stress, and Fear Response in Mice With Reduced Endocannabinoid Levels. Biol Psychiatry 79:858-868.

Jhaveri MD, Richardson D, Robinson I, Garle MJ, Patel A, Sun Y, Sagar DR, Bennett AJ, Alexander SP, Kendall DA, Barrett DA, Chapman V (2008) Inhibition of fatty acid amide hydrolase and cyclooxygenase-2 increases levels of endocannabinoid related molecules and produces analgesia via peroxisome proliferator-activated receptor-alpha in a model of inflammatory pain. Neuropharmacology 55:85-93.

Jiang W, Zhang Y, Xiao L, Van Cleemput J, Ji SP, Bai G, Zhang X (2005) Cannabinoids promote embryonic and adult hippocampus neurogenesis and produce anxiolytic- and antidepressant-like effects. J Clin Invest 115:3104-3116.

Jin K, Xie L, Kim SH, Parmentier-Batteur S, Sun Y, Mao XO, Childs J, Greenberg DA (2004) Defective adult neurogenesis in CB1 cannabinoid receptor knockout mice. Mol Pharmacol 66:204-208.

Jin XH, Okamoto Y, Morishita J, Tsuboi K, Tonai T, Ueda N (2007) Discovery and characterization of a Ca2+-independent phosphatidylethanolamine N-acyltransferase generating the anandamide precursor and its congeners. J Biol Chem 282:3614-3623.

Jin XH, Uyama T, Wang J, Okamoto Y, Tonai T, Ueda N (2009) cDNA cloning and characterization of human and mouse Ca(2+)-independent phosphatidylethanolamine N-acyltransferases. Biochim Biophys Acta 1791:32-38.

Jinek M, Chylinski K, Fonfara I, Hauer M, Doudna JA, Charpentier E (2012) A programmable dual-RNA-guided DNA endonuclease in adaptive bacterial immunity. Science 337:816-821.

Jinek M, East A, Cheng A, Lin S, Ma E, Doudna J (2013) RNA-programmed genome editing in human cells. Elife 2:e00471.

Jung KM, Astarita G, Zhu C, Wallace M, Mackie K, Piomelli D (2007) A key role for diacylglycerol lipase-alpha in metabotropic glutamate receptor-dependent endocannabinoid mobilization. Mol Pharmacol 72:612-621.

Kaczocha M, Glaser ST, Deutsch DG (2009) Identification of intracellular carriers for the endocannabinoid anandamide. Proc Natl Acad Sci U S A 106:6375-6380.

Kano M (2014) Control of synaptic function by endocannabinoid-mediated retrograde signaling. Proc Jpn Acad Ser B Phys Biol Sci 90:235-250.

Kano M, Ohno-Shosaku T, Hashimotodani Y, Uchigashima M, Watanabe M (2009) Endocannabinoid-mediated control of synaptic transmission. Physiol Rev 89:309-380.

Kao JP, Alderton JM, Tsien RY, Steinhardt RA (1990) Active involvement of Ca2+ in mitotic progression of Swiss 3T3 fibroblasts. J Cell Biol 111:183-196.

Katayama K, Ueda N, Katoh I, Yamamoto S (1999) Equilibrium in the hydrolysis and synthesis of cannabimimetic anandamide demonstrated by a purified enzyme. Biochim Biophys Acta 1440:205-214.

Katona I, Urban GM, Wallace M, Ledent C, Jung KM, Piomelli D, Mackie K, Freund TF (2006) Molecular composition of the endocannabinoid system at glutamatergic synapses. J Neurosci 26:5628-5637.

Kawamura Y, Fukaya M, Maejima T, Yoshida T, Miura E, Watanabe M, Ohno-Shosaku T, Kano M (2006) The CB1 cannabinoid receptor is the major cannabinoid receptor at excitatory presynaptic sites in the hippocampus and cerebellum. J Neurosci 26:2991-3001.

Keimpema E, Tortoriello G, Alpar A, Capsoni S, Arisi I, Calvigioni D, Hu SS, Cattaneo A, Doherty P, Mackie K, Harkany T (2013) Nerve growth factor scales endocannabinoid signaling by regulating monoacylglycerol lipase turnover in developing cholinergic neurons. Proc Natl Acad Sci U S A 110:1935-1940.

Kim D, Thayer SA (2001) Cannabinoids inhibit the formation of new synapses between hippocampal neurons in culture. J Neurosci 21:RC146.

Kim HS, Kim MS, Hancock AL, Harper JCP, Park JY, Poy G, Perantoni AO, Cam M, Malik K, Lee SB (2007) Identification of novel Wilms' tumor suppressor gene target genes implicated in kidney development. Journal of Biological Chemistry 282:16278-16287.

Kim SR, Lee DY, Chung ES, Oh UT, Kim SU, Jin BK (2005) Transient receptor potential vanilloid subtype 1 mediates cell death of mesencephalic dopaminergic neurons in vivo and in vitro. J Neurosci 25:662-671.

Knoth R, Singec I, Ditter M, Pantazis G, Capetian P, Meyer RP, Horvat V, Volk B, Kempermann G (2010) Murine features of neurogenesis in the human hippocampus across the lifespan from 0 to 100 years. PLoS One 5:e8809.

Kondo S, Kondo H, Nakane S, Kodaka T, Tokumura A, Waku K, Sugiura T (1998) 2-Arachidonoylglycerol, an endogenous cannabinoid receptor agonist: identification as one of the major species of monoacylglycerols in various rat tissues, and evidence for its generation through CA2+-dependent and -independent mechanisms. FEBS Lett 429:152-156.

Koonin EV, Makarova KS, Zhang F (2017) Diversity, classification and evolution of CRISPR-Cas systems. Curr Opin Microbiol 37:67-78.

Kouchi Z (2015) Physiological Role of Endocannabinoid Hydrolyzing Enzymes in Brain Development and Neurodegeneration. Biochemistry & Physiology: Open Access 04.

Kozak KR, Crews BC, Morrow JD, Wang LH, Ma YH, Weinander R, Jakobsson PJ, Marnett LJ (2002) Metabolism of the endocannabinoids, 2-arachidonylglycerol and anandamide, into prostaglandin, thromboxane, and prostacyclin glycerol esters and ethanolamides. J Biol Chem 277:44877-44885.

Kreitzer AC, Regehr WG (2001) Retrograde inhibition of presynaptic calcium influx by endogenous cannabinoids at excitatory synapses onto Purkinje cells. Neuron 29:717-727.

Kruger MC, Coetzee M, Haag M, Weiler H (2010) Long-chain polyunsaturated fatty acids: selected mechanisms of action on bone. Prog Lipid Res 49:438-449.

Kumar RN, Chambers WA, Pertwee RG (2001) Pharmacological actions and therapeutic uses of cannabis and cannabinoids. Anaesthesia 56:1059-1068.

Kunos G, Osei-Hyiaman D, Batkai S, Sharkey KA, Makriyannis A (2009) Should peripheral CB(1) cannabinoid receptors be selectively targeted for therapeutic gain? Trends Pharmacol Sci 30:1-7.

Lampidonis AD, Rogdakis E, Voutsinas GE, Stravopodis DJ (2011) The resurgence of Hormone-Sensitive Lipase (HSL) in mammalian lipolysis. Gene 477:1-11.

Lan RX, Liu Q, Fan PS, Lin SY, Fernando SR, McCallion D, Pertwee R, Makriyannis A (1999) Structure-activity relationships of pyrazole derivatives as cannabinoid receptor antagonists. J Med Chem 42:769-776.

Ledent C, Valverde O, Cossu G, Petitet F, Aubert JF, Beslot F, Bohme GA, Imperato A, Pedrazzini T, Roques BP, Vassart G, Fratta W, Parmentier M (1999) Unresponsiveness to cannabinoids and reduced addictive effects of opiates in CB1 receptor knockout mice. Science 283:401-404.

Leishman E, Mackie K, Luquet S, Bradshaw HB (2016) Lipidomics profile of a NAPE-PLD KO mouse provides evidence of a broader role of this enzyme in lipid metabolism in the brain. Biochim Biophys Acta 1861:491-500.

Leone S, Recinella L, Chiavaroli A, Martinotti S, Ferrante C, Mollica A, Macedonio G, Stefanucci A, Dvoracsko S, Tomboly C, De Petrocellis L, Vacca M, Brunetti L, Orlando G (2017) Emotional disorders induced by Hemopressin and RVD-hemopressin(alpha) administration in rats. Pharmacol Rep 69:1247-1253.

Leung D, Saghatelian A, Simon GM, Cravatt BF (2006) Inactivation of N-acyl phosphatidylethanolamine phospholipase D reveals multiple mechanisms for the biosynthesis of endocannabinoids. Biochemistry 45:4720-4726.

Leung HT, Tseng-Crank J, Kim E, Mahapatra C, Shino S, Zhou Y, An L, Doerge RW, Pak WL (2008) DAG lipase activity is necessary for TRP channel regulation in Drosophila photoreceptors. Neuron 58:884-896.

Li HL (1974) Archeological and Historical Account of Cannabis in China. Econ Bot 28:437-448.

Li XH, Lin ML, Wang ZL, Wang P, Tang HH, Lin YY, Li N, Fang Q, Wang R (2016) Central administrations of hemopressin and related peptides inhibit gastrointestinal motility in mice. Neurogastroenterol Motil 28:891-899.

Li Y, Kim J (2015) Neuronal expression of CB2 cannabinoid receptor mRNAs in the mouse hippocampus. Neuroscience 311:253-267.

Li Y, Kim J (2016) Deletion of CB2 cannabinoid receptors reduces synaptic transmission and long-term potentiation in the mouse hippocampus. Hippocampus 26:275-281.

Lichtman AH, Shelton CC, Advani T, Cravatt BF (2004a) Mice lacking fatty acid amide hydrolase exhibit a cannabinoid receptor-mediated phenotypic hypoalgesia. Pain 109:319-327.

Lichtman AH, Leung D, Shelton CC, Saghatelian A, Hardouin C, Boger DL, Cravatt BF (2004b) Reversible inhibitors of fatty acid amide hydrolase that promote analgesia: evidence for an unprecedented combination of potency and selectivity. J Pharmacol Exp Ther 311:441-448.

Liedhegner ES, Vogt CD, Sem DS, Cunningham CW, Hillard CJ (2014) Sterol carrier protein-2: binding protein for endocannabinoids. Mol Neurobiol 50:149-158.

Ligresti A, Cascio MG, Di Marzo V (2005) Endocannabinoid metabolic pathways and enzymes. Curr Drug Targets CNS Neurol Disord 4:615-623.

Lin L, Metherel AH, Jones PJ, Bazinet RP (2017) Fatty acid amide hydrolase (FAAH) regulates hypercapnia/ischemia-induced increases in n-acylethanolamines in mouse brain. J Neurochem 142:662-671.

Lippton H, Lin B, Gumusel B, Witriol N, Wasserman A, Knight M (2006) Hemopressin, a hemoglobin fragment, dilates the rat systemic vascular bed through release of nitric oxide. Peptides 27:2284-2288.

Liu J, Wang L, Harvey-White J, Osei-Hyiaman D, Razdan R, Gong Q, Chan AC, Zhou Z, Huang BX, Kim HY, Kunos G (2006) A biosynthetic pathway for anandamide. Proc Natl Acad Sci U S A 103:13345-13350.

Liu J, Wang L, Harvey-White J, Huang BX, Kim HY, Luquet S, Palmiter RD, Krystal G, Rai R, Mahadevan A, Razdan RK, Kunos G (2008) Multiple pathways involved in the biosynthesis of anandamide. Neuropharmacology 54:1-7.

Locher RJ, Lunnemann T, Garbe A, Schaser K, Schmidt-Bleek K, Duda G, Tsitsilonis S (2015) Traumatic brain injury and bone healing: radiographic and biomechanical analyses

of bone formation and stability in a combined murine trauma model. J Musculoskelet Neuronal Interact 15:309-315.
Long JZ, Nomura DK, Vann RE, Walentiny DM, Booker L, Jin X, Burston JJ, Sim-Selley LJ, Lichtman AH, Wiley JL, Cravatt BF (2009a) Dual blockade of FAAH and MAGL identifies behavioral processes regulated by endocannabinoid crosstalk in vivo. Proc Natl Acad Sci U S A 106:20270-20275.
Long JZ, Li W, Booker L, Burston JJ, Kinsey SG, Schlosburg JE, Pavon FJ, Serrano AM, Selley DE, Parsons LH, Lichtman AH, Cravatt BF (2009b) Selective blockade of 2-arachidonoylglycerol hydrolysis produces cannabinoid behavioral effects. Nat Chem Biol 5:37-44.
Ma L, Jia J, Niu W, Jiang T, Zhai Q, Yang L, Bai F, Wang Q, Xiong L (2015) Mitochondrial CB1 receptor is involved in ACEA-induced protective effects on neurons and mitochondrial functions. Sci Rep 5:12440.
Maccarrone M (2017) Metabolism of the Endocannabinoid Anandamide: Open Questions after 25 Years. Front Mol Neurosci 10:166.
Maccarrone M, Dainese E, Oddi S (2010) Intracellular trafficking of anandamide: new concepts for signaling. Trends Biochem Sci 35:601-608.
Maccarrone M, Lorenzon T, Bari M, Melino G, Finazzi-Agro A (2000a) Anandamide induces apoptosis in human cells via vanilloid receptors. Evidence for a protective role of cannabinoid receptors. J Biol Chem 275:31938-31945.
Maccarrone M, Guzman M, Mackie K, Doherty P, Harkany T (2014) Programming of neural cells by (endo)cannabinoids: from physiological rules to emerging therapies. Nat Rev Neurosci 15:786-801.
Maccarrone M, Bari M, Lorenzon T, Bisogno T, Di Marzo V, Finazzi-Agro A (2000b) Anandamide uptake by human endothelial cells and its regulation by nitric oxide. J Biol Chem 275:13484-13492.
Maccarrone M, Bab I, Biro T, Cabral GA, Dey SK, Di Marzo V, Konje JC, Kunos G, Mechoulam R, Pacher P, Sharkey KA, Zimmer A (2015) Endocannabinoid signaling at the periphery: 50 years after THC. Trends Pharmacol Sci 36:277-296.
Mackie K, Devane WA, Hille B (1993) Anandamide, an endogenous cannabinoid, inhibits calcium currents as a partial agonist in N18 neuroblastoma cells. Mol Pharmacol 44:498-503.
Maejima T, Hashimoto K, Yoshida T, Aiba A, Kano M (2001) Presynaptic inhibition caused by retrograde signal from metabotropic glutamate to cannabinoid receptors. Neuron 31:463-475.
Magotti P, Bauer I, Igarashi M, Babagoli M, Marotta R, Piomelli D, Garau G (2015) Structure of human N-acylphosphatidylethanolamine-hydrolyzing phospholipase D: regulation of fatty acid ethanolamide biosynthesis by bile acids. Structure 23:598-604.
Makara JK, Mor M, Fegley D, Szabo SI, Kathuria S, Astarita G, Duranti A, Tontini A, Tarzia G, Rivara S, Freund TF, Piomelli D (2005) Selective inhibition of 2-AG hydrolysis enhances endocannabinoid signaling in hippocampus. Nat Neurosci 8:1139-1141.
Makarova KS, Haft DH, Barrangou R, Brouns SJ, Charpentier E, Horvath P, Moineau S, Mojica FJ, Wolf YI, Yakunin AF, van der Oost J, Koonin EV (2011) Evolution and classification of the CRISPR-Cas systems. Nat Rev Microbiol 9:467-477.
Mali P, Yang L, Esvelt KM, Aach J, Guell M, DiCarlo JE, Norville JE, Church GM (2013) RNA-guided human genome engineering via Cas9. Science 339:823-826.
Manolagas SC (2000) Birth and death of bone cells: basic regulatory mechanisms and implications for the pathogenesis and treatment of osteoporosis. Endocr Rev 21:115-137.
Marchalant Y, Brothers HM, Wenk GL (2009) Cannabinoid agonist WIN-55,212-2 partially restores neurogenesis in the aged rat brain. Mol Psychiatry 14:1068-1069.

Markwick RLL (2015) Regulation of DAG Lipase Activity – Implications for 'On-Demand' Endocannabinoid Signalling. In: Wolfson Centre for Age-Related Diseases, p 338. London: King's College London.
Marrs WR et al. (2010) The serine hydrolase ABHD6 controls the accumulation and efficacy of 2-AG at cannabinoid receptors. Nat Neurosci 13:951-957.
Marsicano G, Lutz B (1999) Expression of the cannabinoid receptor CB1 in distinct neuronal subpopulations in the adult mouse forebrain. Eur J Neurosci 11:4213-4225.
Marsicano G, Wotjak CT, Azad SC, Bisogno T, Rammes G, Cascio MG, Hermann H, Tang J, Hofmann C, Zieglgansberger W, Di Marzo V, Lutz B (2002) The endogenous cannabinoid system controls extinction of aversive memories. Nature 418:530-534.
Marsicano G, Goodenough S, Monory K, Hermann H, Eder M, Cannich A, Azad SC, Cascio MG, Gutierrez SO, van der Stelt M, Lopez-Rodriguez ML, Casanova E, Schutz G, Zieglgansberger W, Di Marzo V, Behl C, Lutz B (2003) CB1 cannabinoid receptors and on-demand defense against excitotoxicity. Science 302:84-88.
Martin GG, Landrock D, Dangott LJ, McIntosh AL, Kier AB, Schroeder F (2018) Human Liver Fatty Acid Binding Protein-1 T94A Variant, Nonalcohol Fatty Liver Disease, and Hepatic Endocannabinoid System. Lipids 53:27-40.
Matcovitch-Natan O et al. (2016) Microglia development follows a stepwise program to regulate brain homeostasis. Science 353:aad8670.
Matias I, Di Marzo V (2007) Endocannabinoids and the control of energy balance. Trends Endocrinol Metab 18:27-37.
Matsuda LA, Lolait SJ, Brownstein MJ, Young AC, Bonner TI (1990) Structure of a Cannabinoid Receptor and Functional Expression of the Cloned Cdna. Nature 346:561-564.
Matsunami N et al. (2014) Identification of rare DNA sequence variants in high-risk autism families and their prevalence in a large case/control population. Mol Autism 5:5.
McCarron RM, Shohami E, Panikashvili D, Chen Y, Golech S, Strasser A, Mechoulam R, Spatz M (2003) Antioxidant properties of the vasoactive endocannabinoid, 2-arachidonoyl glycerol (2-AG). Acta Neurochir Suppl 86:271-275.
McHugh D, Page J, Dunn E, Bradshaw HB (2012) Delta(9) -Tetrahydrocannabinol and N-arachidonyl glycine are full agonists at GPR18 receptors and induce migration in human endometrial HEC-1B cells. Br J Pharmacol 165:2414-2424.
McPartland J, Di Marzo V, De Petrocellis L, Mercer A, Glass M (2001) Cannabinoid receptors are absent in insects. J Comp Neurol 436:423-429.
McPartland JM (2004) Phylogenomic and chemotaxonomic analysis of the endocannabinoid system. Brain Res Brain Res Rev 45:18-29.
McPartland JM, Agraval J, Gleeson D, Heasman K, Glass M (2006) Cannabinoid receptors in invertebrates. J Evol Biol 19:366-373.
Mechoulam R, Fride E, Di Marzo V (1998) Endocannabinoids. Eur J Pharmacol 359:1-18.
Mechoulam R, Lander N, University A, Zahalka J (1990) Synthesis of the individual, pharmacologically distinct, enantiomers of a tetrahydrocannabinol derivative. Tetrahedron: Asymmetry 1:315-318.
Mechoulam R, Benshabat S, Hanus L, Ligumsky M, Kaminski NE, Schatz AR, Gopher A, Almog S, Martin BR, Compton DR, Pertwee RG, Griffin G, Bayewitch M, Barg J, Vogel Z (1995) Identification of an Endogenous 2-Monoglyceride, Present in Canine Gut, That Binds to Cannabinoid Receptors. Biochem Pharmacol 50:83-90.
Melamed E, Robinson D, Halperin N, Wallach N, Keren O, Groswasser Z (2002) Brain injury-related heterotopic bone formation: treatment strategy and results. Am J Phys Med Rehabil 81:670-674.
Merida I, Avila-Flores A, Merino E (2008) Diacylglycerol kinases: at the hub of cell signalling. Biochem J 409:1-18.
Meves H (2008) Arachidonic acid and ion channels: an update. Br J Pharmacol 155:4-16.

Mikuriya TH (1969) Marijuana in medicine: past, present and future. Calif Med 110:34-40.
Moesgaard B, Jaroszewski JW, Hansen HS (1999) Accumulation of N-acyl-ethanolamine phospholipids in rat brains during post-decapitative ischemia: a 31p NMR study. J Lipid Res 40:515-521.
Molina-Holgado F, Rubio-Araiz A, Garcia-Ovejero D, Williams RJ, Moore JD, Arevalo-Martin A, Gomez-Torres O, Molina-Holgado E (2007) CB2 cannabinoid receptors promote mouse neural stem cell proliferation. Eur J Neurosci 25:629-634.
Moore JK, Haber JE (1996) Cell cycle and genetic requirements of two pathways of nonhomologous end-joining repair of double-strand breaks in Saccharomyces cerevisiae. Mol Cell Biol 16:2164-2173.
Mor M, Rivara S, Lodola A, Plazzi PV, Tarzia G, Duranti A, Tontini A, Piersanti G, Kathuria S, Piomelli D (2004) Cyclohexylcarbamic acid 3'- or 4'-substituted biphenyl-3-yl esters as fatty acid amide hydrolase inhibitors: synthesis, quantitative structure-activity relationships, and molecular modeling studies. J Med Chem 47:4998-5008.
Morales M, Backman C (2002) Coexistence of serotonin 3 (5-HT3) and CB1 cannabinoid receptors in interneurons of hippocampus and dentate gyrus. Hippocampus 12:756-764.
Morales P, Reggio PH (2017) An Update on Non-CB1, Non-CB2 Cannabinoid Related G-Protein-Coupled Receptors. Cannabis Cannabinoid Res 2:265-273.
Moreira FA, Crippa JA (2009) The psychiatric side-effects of rimonabant. Rev Bras Psiquiatr 31:145-153.
Morgan NH, Stanford IM, Woodhall GL (2009) Functional CB2 type cannabinoid receptors at CNS synapses. Neuropharmacology 57:356-368.
Moriyama T, Urade R, Kito M (1999) Purification and characterization of diacylglycerol lipase from human platelets. J Biochem 125:1077-1085.
Morris DW, Ivanov D, Robinson L, Williams N, Stevenson J, Owen MJ, Williams J, O'Donovan MC (2004) Association analysis of two candidate phospholipase genes that map to the chromosome 15q15.1-15.3 region associated with reading disability. Am J Med Genet B Neuropsychiatr Genet 129B:97-103.
Movahed P, Jonsson BA, Birnir B, Wingstrand JA, Jorgensen TD, Ermund A, Sterner O, Zygmunt PM, Hogestatt ED (2005) Endogenous unsaturated C18 N-acylethanolamines are vanilloid receptor (TRPV1) agonists. J Biol Chem 280:38496-38504.
Muccioli GG, Naslain D, Backhed F, Reigstad CS, Lambert DM, Delzenne NM, Cani PD (2010) The endocannabinoid system links gut microbiota to adipogenesis. Mol Syst Biol 6:392.
Mukhopadhyay B, Cinar R, Yin S, Liu J, Tam J, Godlewski G, Harvey-White J, Mordi I, Cravatt BF, Lotersztajn S, Gao B, Yuan Q, Schuebel K, Goldman D, Kunos G (2011) Hyperactivation of anandamide synthesis and regulation of cell-cycle progression via cannabinoid type 1 (CB1) receptors in the regenerating liver. Proc Natl Acad Sci U S A 108:6323-6328.
Mulder J, Aguado T, Keimpema E, Barabas K, Ballester Rosado CJ, Nguyen L, Monory K, Marsicano G, Di Marzo V, Hurd YL, Guillemot F, Mackie K, Lutz B, Guzman M, Lu HC, Galve-Roperh I, Harkany T (2008) Endocannabinoid signaling controls pyramidal cell specification and long-range axon patterning. Proc Natl Acad Sci U S A 105:8760-8765.
Munro S, Thomas KL, Abushaar M (1993) Molecular Characterization of a Peripheral Receptor for Cannabinoids. Nature 365:61-65.
Murataeva N, Dhopeshwarkar A, Yin D, Mitjavila J, Bradshaw H, Straiker A, Mackie K (2016) Where's my entourage? The curious case of 2-oleoylglycerol, 2-linolenoylglycerol, and 2-palmitoylglycerol. Pharmacological research 110:173-180.

Natarajan V, Schmid PC, Schmid HH (1986) N-acylethanolamine phospholipid metabolism in normal and ischemic rat brain. Biochim Biophys Acta 878:32-41.
Natarajan V, Reddy PV, Schmid PC, Schmid HH (1981) On the biosynthesis and metabolism of N-acylethanolamine phospholipids in infarcted dog heart. Biochim Biophys Acta 664:445-448.
Natarajan V, Schmid PC, Reddy PV, Zuzarte-Augustin ML, Schmid HH (1983) Biosynthesis of N-acylethanolamine phospholipids by dog brain preparations. J Neurochem 41:1303-1312.
Niknami M, Patel M, Witting PK, Dong Q (2009) Molecules in focus: cytosolic phospholipase A2-alpha. Int J Biochem Cell Biol 41:994-997.
Nomura DK, Hudak CS, Ward AM, Burston JJ, Issa RS, Fisher KJ, Abood ME, Wiley JL, Lichtman AH, Casida JE (2008) Monoacylglycerol lipase regulates 2-arachidonoylglycerol action and arachidonic acid levels. Bioorg Med Chem Lett 18:5875-5878.
Nomura DK, Morrison BE, Blankman JL, Long JZ, Kinsey SG, Marcondes MC, Ward AM, Hahn YK, Lichtman AH, Conti B, Cravatt BF (2011) Endocannabinoid hydrolysis generates brain prostaglandins that promote neuroinflammation. Science 334:809-813.
O'Shaughnessy WB (1843) On the Preparations of the Indian Hemp, or gunjah: Cannabis Indica Their Effects on the Animal System in Health, and their Utility in the Treatment of Tetanus and other Convulsive Diseases. Provincial Medical Journal and Retrospect of the Medical Sciences 5:343-347.
O'Sullivan SE, Kendall DA (2010) Cannabinoid activation of peroxisome proliferator-activated receptors: potential for modulation of inflammatory disease. Immunobiology 215:611-616.
Oddi S, Fezza F, Pasquariello N, De Simone C, Rapino C, Dainese E, Finazzi-Agro A, Maccarrone M (2008) Evidence for the intracellular accumulation of anandamide in adiposomes. Cell Mol Life Sci 65:840-850.
Oddi S, Fezza F, Pasquariello N, D'Agostino A, Catanzaro G, De Simone C, Rapino C, Finazzi-Agro A, Maccarrone M (2009) Molecular identification of albumin and Hsp70 as cytosolic anandamide-binding proteins. Chem Biol 16:624-632.
Ofek O, Karsak M, Leclerc N, Fogel M, Frenkel B, Wright K, Tam J, Attar-Namdar M, Kram V, Shohami E, Mechoulam R, Zimmer A, Bab I (2006) Peripheral cannabinoid receptor, CB2, regulates bone mass. Proc Natl Acad Sci U S A 103:696-701.
Ogasawara D, Deng H, Viader A, Baggelaar MP, Breman A, den Dulk H, van den Nieuwendijk AM, Soethoudt M, van der Wel T, Zhou J, Overkleeft HS, Sanchez-Alavez M, Mori S, Nguyen W, Conti B, Liu X, Chen Y, Liu QS, Cravatt BF, van der Stelt M (2016) Rapid and profound rewiring of brain lipid signaling networks by acute diacylglycerol lipase inhibition. Proc Natl Acad Sci U S A 113:26-33.
Ogura Y, Parsons WH, Kamat SS, Cravatt BF (2016) A calcium-dependent acyltransferase that produces N-acyl phosphatidylethanolamines. Nat Chem Biol 12:669-+.
Ohno-Shosaku T, Kano M (2014) Endocannabinoid-mediated retrograde modulation of synaptic transmission. Curr Opin Neurobiol 29:1-8.
Ohno-Shosaku T, Maejima T, Kano M (2001) Endogenous cannabinoids mediate retrograde signals from depolarized postsynaptic neurons to presynaptic terminals. Neuron 29:729-738.
Ohno-Shosaku T, Tanimura A, Hashimotodani Y, Kano M (2012) Endocannabinoids and retrograde modulation of synaptic transmission. Neuroscientist 18:119-132.
Ohno-Shosaku T, Tsubokawa H, Mizushima I, Yoneda N, Zimmer A, Kano M (2002) Presynaptic cannabinoid sensitivity is a major determinant of depolarization-induced retrograde suppression at hippocampal synapses. J Neurosci 22:3864-3872.

Ohto T, Uozumi N, Hirabayashi T, Shimizu T (2005) Identification of novel cytosolic phospholipase A(2)s, murine cPLA(2){delta}, {epsilon}, and {zeta}, which form a gene cluster with cPLA(2){beta}. J Biol Chem 280:24576-24583.

Oka S, Tsuchie A, Tokumura A, Muramatsu M, Suhara Y, Takayama H, Waku K, Sugiura T (2003) Ether-linked analogue of 2-arachidonoylglycerol (noladin ether) was not detected in the brains of various mammalian species. J Neurochem 85:1374-1381.

Okamoto Y, Morishita J, Tsuboi K, Tonai T, Ueda N (2004) Molecular characterization of a phospholipase D generating anandamide and its congeners. J Biol Chem 279:5298-5305.

Okazaki T, Sagawa N, Okita JR, Bleasdale JE, MacDonald PC, Johnston JM (1981) Diacylglycerol metabolism and arachidonic acid release in human fetal membranes and decidua vera. J Biol Chem 256:7316-7321.

Olefsky JM, Glass CK (2010) Macrophages, inflammation, and insulin resistance. Annu Rev Physiol 72:219-246.

Oliver D, Lien CC, Soom M, Baukrowitz T, Jonas P, Fakler B (2004) Functional conversion between A-type and delayed rectifier K+ channels by membrane lipids. Science 304:265-270.

Ortar G, Bisogno T, Ligresti A, Morera E, Nalli M, Di Marzo V (2008) Tetrahydrolipstatin analogues as modulators of endocannabinoid 2-arachidonoylglycerol metabolism. J Med Chem 51:6970-6979.

Oudin MJ, Hobbs C, Doherty P (2011a) DAGL-dependent endocannabinoid signalling: roles in axonal pathfinding, synaptic plasticity and adult neurogenesis. Eur J Neurosci 34:1634-1646.

Oudin MJ, Gajendra S, Williams G, Hobbs C, Lalli G, Doherty P (2011b) Endocannabinoids regulate the migration of subventricular zone-derived neuroblasts in the postnatal brain. J Neurosci 31:4000-4011.

Overton HA, Babbs AJ, Doel SM, Fyfe MC, Gardner LS, Griffin G, Jackson HC, Procter MJ, Rasamison CM, Tang-Christensen M, Widdowson PS, Williams GM, Reynet C (2006) Deorphanization of a G protein-coupled receptor for oleoylethanolamide and its use in the discovery of small-molecule hypophagic agents. Cell Metab 3:167-175.

Oz M (2006) Receptor-independent actions of cannabinoids on cell membranes: focus on endocannabinoids. Pharmacol Ther 111:114-144.

Pagotto U, Marsicano G, Cota D, Lutz B, Pasquali R (2006) The emerging role of the endocannabinoid system in endocrine regulation and energy balance. Endocr Rev 27:73-100.

Palazuelos J, Ortega Z, Diaz-Alonso J, Guzman M, Galve-Roperh I (2012) CB2 cannabinoid receptors promote neural progenitor cell proliferation via mTORC1 signaling. J Biol Chem 287:1198-1209.

Palazuelos J, Aguado T, Egia A, Mechoulam R, Guzman M, Galve-Roperh I (2006) Non-psychoactive CB2 cannabinoid agonists stimulate neural progenitor proliferation. Faseb J 20:2405-2407.

Paloczi J, Varga ZV, Hasko G, Pacher P (2017) Neuroprotection in Oxidative Stress-Related Neurodegenerative Diseases: Role of Endocannabinoid System Modulation. Antioxid Redox Signal.

Pan B, Wang W, Long JZ, Sun D, Hillard CJ, Cravatt BF, Liu QS (2009) Blockade of 2-arachidonoylglycerol hydrolysis by selective monoacylglycerol lipase inhibitor 4-nitrophenyl 4-(dibenzo[d][1,3]dioxol-5-yl(hydroxy)methyl)piperidine-1-carboxylate (JZL184) Enhances retrograde endocannabinoid signaling. J Pharmacol Exp Ther 331:591-597.

Pan JX, Wang ZL, Li N, Han ZL, Li XH, Tang HH, Wang P, Zheng T, Fang Q, Wang R (2014) Analgesic tolerance and cross-tolerance to the cannabinoid receptors ligands

hemopressin, VD-hemopressin(alpha) and WIN55,212-2 at the supraspinal level in mice. Neurosci Lett 578:187-191.
Panikashvili D, Simeonidou C, Ben-Shabat S, Hanus L, Breuer A, Mechoulam R, Shohami E (2001) An endogenous cannabinoid (2-AG) is neuroprotective after brain injury. Nature 413:527-531.
Pardo B, Gomez-Gonzalez B, Aguilera A (2009) DNA repair in mammalian cells: DNA double-strand break repair: how to fix a broken relationship. Cell Mol Life Sci 66:1039-1056.
Parmentier-Batteur S, Jin K, Mao XO, Xie L, Greenberg DA (2002) Increased severity of stroke in CB1 cannabinoid receptor knock-out mice. J Neurosci 22:9771-9775.
Pavon FJ, Serrano A, Perez-Valero V, Jagerovic N, Hernandez-Folgado L, Bermudez-Silva FJ, Macias M, Goya P, de Fonseca FR (2008) Central versus peripheral antagonism of cannabinoid CB1 receptor in obesity: effects of LH-21, a peripherally acting neutral cannabinoid receptor antagonist, in Zucker rats. J Neuroendocrinol 20 Suppl 1:116-123.
Pedicord DL, Flynn MJ, Fanslau C, Miranda M, Hunihan L, Robertson BJ, Pearce BC, Yu XC, Westphal RS, Blat Y (2011) Molecular characterization and identification of surrogate substrates for diacylglycerol lipase alpha. Biochem Biophys Res Commun 411:809-814.
Pernia-Andrade AJ, Kato A, Witschi R, Nyilas R, Katona I, Freund TF, Watanabe M, Filitz J, Koppert W, Schuttler J, Ji G, Neugebauer V, Marsicano G, Lutz B, Vanegas H, Zeilhofer HU (2009) Spinal endocannabinoids and CB1 receptors mediate C-fiber-induced heterosynaptic pain sensitization. Science 325:760-764.
Pertwee RG (1997) Pharmacology of cannabinoid CB1 and CB2 receptors. Pharmacol Ther 74:129-180.
Pertwee RG (2005) Pharmacological actions of cannabinoids. Handb Exp Pharmacol:1-51.
Pertwee RG (2015) Endocannabinoids and Their Pharmacological Actions. Handb Exp Pharmacol 231:1-37.
Petrosino S, Iuvone T, Di Marzo V (2010) N-palmitoyl-ethanolamine: Biochemistry and new therapeutic opportunities. Biochimie 92:724-727.
Petrovszki Z, Kovacs G, Tomboly C, Benedek G, Horvath G (2012) The effects of peptide and lipid endocannabinoids on arthritic pain at the spinal level. Anesth Analg 114:1346-1352.
Petrucci V, Chicca A, Glasmacher S, Paloczi J, Cao Z, Pacher P, Gertsch J (2017) Pepcan-12 (RVD-hemopressin) is a CB2 receptor positive allosteric modulator constitutively secreted by adrenals and in liver upon tissue damage. Sci Rep 7:9560.
Pi-Sunyer FX, Aronne LJ, Heshmati HM, Devin J, Rosenstock J (2006) Effect of rimonabant, a cannabinoid-1 receptor blocker, on weight and cardiometabolic risk factors in overweight or obese patients: RIO-North America: a randomized controlled trial. Jama 295:761-775.
Pickard RT, Strifler BA, Kramer RM, Sharp JD (1999) Molecular cloning of two new human paralogs of 85-kDa cytosolic phospholipase A2. J Biol Chem 274:8823-8831.
Piomelli D (2003) The molecular logic of endocannabinoid signalling. Nat Rev Neurosci 4:873-884.
Piomelli D (2013) A fatty gut feeling. Trends Endocrinol Metab 24:332-341.
Placzek EA, Okamoto Y, Ueda N, Barker EL (2008) Mechanisms for recycling and biosynthesis of endogenous cannabinoids anandamide and 2-arachidonylglycerol. J Neurochem 107:987-1000.
Ponten J, Saksela E (1967) Two established in vitro cell lines from human mesenchymal tumours. International journal of cancer 2:434-447.
Porter AC, Sauer JM, Knierman MD, Becker GW, Berna MJ, Bao J, Nomikos GG, Carter P, Bymaster FP, Leese AB, Felder CC (2002) Characterization of a novel

endocannabinoid, virodhamine, with antagonist activity at the CB1 receptor. J Pharmacol Exp Ther 301:1020-1024.
Powell DR, Gay JP, Wilganowski N, Doree D, Savelieva KV, Lanthorn TH, Read R, Vogel P, Hansen GM, Brommage R, Ding ZM, Desai U, Zambrowicz B (2015) Diacylglycerol Lipase alpha Knockout Mice Demonstrate Metabolic and Behavioral Phenotypes Similar to Those of Cannabinoid Receptor 1 Knockout Mice. Front Endocrinol (Lausanne) 6:86.
Prenderville JA, Kelly AM, Downer EJ (2015) The role of cannabinoids in adult neurogenesis. Br J Pharmacol 172:3950-3963.
Prescott SM, Majerus PW (1983) Characterization of 1,2-diacylglycerol hydrolysis in human platelets. Demonstration of an arachidonoyl-monoacylglycerol intermediate. J Biol Chem 258:764-769.
Psychoyos D, Vinod KY, Cao J, Xie S, Hyson RL, Wlodarczyk B, He W, Cooper TB, Hungund BL, Finnell RH (2012) Cannabinoid receptor 1 signaling in embryo neurodevelopment. Birth Defects Res B Dev Reprod Toxicol 95:137-150.
Qiu P, Shandilya H, D'Alessio JM, O'Connor K, Durocher J, Gerard GF (2004) Mutation detection using Surveyor (TM) nuclease. Biotechniques 36:702-+.
Rahman IA, Tsuboi K, Uyama T, Ueda N (2014) New players in the fatty acyl ethanolamide metabolism. Pharmacological research 86:1-10.
Rahmani MR, Shamsizadeh A, Moghadam-Ahmadi A, Kaeidi A, Allahtavakoli M (2018) Monoacylglycerol lipase inhibitor, JZL-184, confers neuroprotection in the mice middle cerebral artery occlusion model of stroke. Life Sci 198:143-148.
Ramirez BG, Blazquez C, Gomez del Pulgar T, Guzman M, de Ceballos ML (2005) Prevention of Alzheimer's disease pathology by cannabinoids: neuroprotection mediated by blockade of microglial activation. J Neurosci 25:1904-1913.
Ran FA, Hsu PD, Wright J, Agarwala V, Scott DA, Zhang F (2013) Genome engineering using the CRISPR-Cas9 system. Nat Protoc 8:2281-2308.
Randall AS, Liu CH, Chu B, Zhang Q, Dongre SA, Juusola M, Franze K, Wakelam MJ, Hardie RC (2015) Speed and sensitivity of phototransduction in Drosophila depend on degree of saturation of membrane phospholipids. J Neurosci 35:2731-2746.
Rando RR (2002) Membrane-bound lecithin-retinol acyltransferase. Biochem Biophys Res Commun 292:1243-1250.
Reddy PV, Natarajan V, Schmid PC, Schmid HH (1983) N-Acylation of dog heart ethanolamine phospholipids by transacylase activity. Biochim Biophys Acta 750:472-480.
Regehr WG, Carey MR, Best AR (2009) Activity-dependent regulation of synapses by retrograde messengers. Neuron 63:154-170.
Regier JC, Shultz JW, Zwick A, Hussey A, Ball B, Wetzer R, Martin JW, Cunningham CW (2010) Arthropod relationships revealed by phylogenomic analysis of nuclear protein-coding sequences. Nature 463:1079-1083.
Reisenberg M, Singh PK, Williams G, Doherty P (2012) The diacylglycerol lipases: structure, regulation and roles in and beyond endocannabinoid signalling. Philos Trans R Soc Lond B Biol Sci 367:3264-3275.
Remelli M, Ceciliato C, Guerrini R, Kolkowska P, Krzywoszynska K, Salvadori S, Valensin D, Watly J, Kozlowski H (2016) DOES hemopressin bind metal ions in vivo? Dalton Trans 45:18267-18280.
Richardson D, Ortori CA, Chapman V, Kendall DA, Barrett DA (2007) Quantitative profiling of endocannabinoids and related compounds in rat brain using liquid chromatography-tandem electrospray ionization mass spectrometry. Anal Biochem 360:216-226.
Rinaldi-Carmona M, Barth F, Heaulme M, Shire D, Calandra B, Congy C, Martinez S, Maruani J, Neliat G, Caput D, et al. (1994) SR141716A, a potent and selective antagonist of the brain cannabinoid receptor. FEBS Lett 350:240-244.

Rioli V, Gozzo FC, Heimann AS, Linardi A, Krieger JE, Shida CS, Almeida PC, Hyslop S, Eberlin MN, Ferro ES (2003) Novel natural peptide substrates for endopeptidase 24.15, neurolysin, and angiotensin-converting enzyme. J Biol Chem 278:8547-8555.

Rockwell CE, Snider NT, Thompson JT, Vanden Heuvel JP, Kaminski NE (2006) Interleukin-2 suppression by 2-arachidonyl glycerol is mediated through peroxisome proliferator-activated receptor gamma independently of cannabinoid receptors 1 and 2. Mol Pharmacol 70:101-111.

Romanko MJ, Rola R, Fike JR, Szele FG, Dizon ML, Felling RJ, Brazel CY, Levison SW (2004) Roles of the mammalian subventricular zone in cell replacement after brain injury. Prog Neurobiol 74:77-99.

Romano A, Coccurello R, Giacovazzo G, Bedse G, Moles A, Gaetani S (2014) Oleoylethanolamide: a novel potential pharmacological alternative to cannabinoid antagonists for the control of appetite. Biomed Res Int 2014:203425.

Rosenberger TA, Farooqui AA, Horrocks LA (2007) Bovine brain diacylglycerol lipase: substrate specificity and activation by cyclic AMP-dependent protein kinase. Lipids 42:187-195.

Ross RA, Coutts AA, McFarlane SM, Anavi-Goffer S, Irving AJ, Pertwee RG, MacEwan DJ, Scott RH (2001) Actions of cannabinoid receptor ligands on rat cultured sensory neurones: implications for antinociception. Neuropharmacology 40:221-232.

Rouzer CA, Marnett LJ (2011) Endocannabinoid oxygenation by cyclooxygenases, lipoxygenases, and cytochromes P450: cross-talk between the eicosanoid and endocannabinoid signaling pathways. Chem Rev 111:5899-5921.

Rozenfeld R, Devi LA (2008) Regulation of CB1 cannabinoid receptor trafficking by the adaptor protein AP-3. Faseb J 22:2311-2322.

Rubio-Araiz A, Arevalo-Martin A, Gomez-Torres O, Navarro-Galve B, Garcia-Ovejero D, Suetterlin P, Sanchez-Heras E, Molina-Holgado E, Molina-Holgado F (2008) The endocannabinoid system modulates a transient TNF pathway that induces neural stem cell proliferation. Mol Cell Neurosci 38:374-380.

Russo EB, Jiang HE, Li X, Sutton A, Carboni A, del Bianco F, Mandolino G, Potter DJ, Zhao YX, Bera S, Zhang YB, Lu EG, Ferguson DK, Hueber F, Zhao LC, Liu CJ, Wang YF, Li CS (2008) Phytochemical and genetic analyses of ancient cannabis from Central Asia. J Exp Bot 59:4171-4182.

Ryberg E, Larsson N, Sjogren S, Hjorth S, Hermansson NO, Leonova J, Elebring T, Nilsson K, Drmota T, Greasley PJ (2007) The orphan receptor GPR55 is a novel cannabinoid receptor. Br J Pharmacol 152:1092-1101.

Sadikovic B, Yoshimoto M, Al-Romaih K, Maire G, Zielenska M, Squire JA (2008) In Vitro Analysis of Integrated Global High-Resolution DNA Methylation Profiling with Genomic Imbalance and Gene Expression in Osteosarcoma. PLoS One 3.

Salamone JD, McLaughlin PJ, Sink K, Makriyannis A, Parker LA (2007) Cannabinoid CB1 receptor inverse agonists and neutral antagonists: effects on food intake, food-reinforced behavior and food aversions. Physiol Behav 91:383-388.

Sanai N, Tramontin AD, Quinones-Hinojosa A, Barbaro NM, Gupta N, Kunwar S, Lawton MT, McDermott MW, Parsa AT, Manuel-Garcia Verdugo J, Berger MS, Alvarez-Buylla A (2004) Unique astrocyte ribbon in adult human brain contains neural stem cells but lacks chain migration. Nature 427:740-744.

Sanai N, Nguyen T, Ihrie RA, Mirzadeh Z, Tsai HH, Wong M, Gupta N, Berger MS, Huang E, Garcia-Verdugo JM, Rowitch DH, Alvarez-Buylla A (2011) Corridors of migrating neurons in the human brain and their decline during infancy. Nature 478:382-386.

Sander JD, Maeder ML, Reyon D, Voytas DF, Joung JK, Dobbs D (2010) ZiFiT (Zinc Finger Targeter): an updated zinc finger engineering tool. Nucleic Acids Res 38:W462-468.

Sarne Y, Keren O (2004) Are cannabinoid drugs neurotoxic or neuroprotective? Med Hypotheses 63:187-192.
Sarne Y, Mechoulam R (2005) Cannabinoids: between neuroprotection and neurotoxicity. Curr Drug Targets CNS Neurol Disord 4:677-684.
Savinainen JR, Saario SM, Laitinen JT (2012) The serine hydrolases MAGL, ABHD6 and ABHD12 as guardians of 2-arachidonoylglycerol signalling through cannabinoid receptors. Acta Physiol (Oxf) 204:267-276.
Scherer T, Buettner C (2009) The dysregulation of the endocannabinoid system in diabesity-a tricky problem. J Mol Med (Berl) 87:663-668.
Schlicker E, Kathmann M (2001) Modulation of transmitter release via presynaptic cannabinoid receptors. Trends Pharmacol Sci 22:565-572.
Schlosburg JE, Blankman JL, Long JZ, Nomura DK, Pan B, Kinsey SG, Nguyen PT, Ramesh D, Booker L, Burston JJ, Thomas EA, Selley DE, Sim-Selley LJ, Liu QS, Lichtman AH, Cravatt BF (2010) Chronic monoacylglycerol lipase blockade causes functional antagonism of the endocannabinoid system. Nat Neurosci 13:1113-1119.
Schmid HH (2000) Pathways and mechanisms of N-acylethanolamine biosynthesis: can anandamide be generated selectively? Chem Phys Lipids 108:71-87.
Schmid HH, Berdyshev EV (2002) Cannabinoid receptor-inactive N-acylethanolamines and other fatty acid amides: metabolism and function. Prostaglandins Leukot Essent Fatty Acids 66:363-376.
Schmid HH, Schmid PC, Natarajan V (1990) N-acylated glycerophospholipids and their derivatives. Prog Lipid Res 29:1-43.
Scrima M, Di Marino S, Grimaldi M, Mastrogiacomo A, Novellino E, Bifulco M, D'Ursi AM (2010) Binding of the hemopressin peptide to the cannabinoid CB1 receptor: structural insights. Biochemistry 49:10449-10457.
Seamon KB, Daly JW (1986) Forskolin: its biological and chemical properties. Adv Cyclic Nucleotide Protein Phosphorylation Res 20:1-150.
Segula D (2014) Complications of obesity in adults: a short review of the literature. Malawi Med J 26:20-24.
Shen LR, Lai CQ, Feng X, Parnell LD, Wan JB, Wang JD, Li D, Ordovas JM, Kang JX (2010) Drosophila lacks C20 and C22 PUFAs. J Lipid Res 51:2985-2992.
Shen M, Piser TM, Seybold VS, Thayer SA (1996) Cannabinoid receptor agonists inhibit glutamatergic synaptic transmission in rat hippocampal cultures. J Neurosci 16:4322-4334.
Shinohara N, Uyama T, Jin XH, Tsuboi K, Tonai T, Houchi H, Ueda N (2011) Enzymological analysis of the tumor suppressor A-C1 reveals a novel group of phospholipid-metabolizing enzymes. J Lipid Res 52:1927-1935.
Shonesy BC, Bluett RJ, Ramikie TS, Baldi R, Hermanson DJ, Kingsley PJ, Marnett LJ, Winder DG, Colbran RJ, Patel S (2014) Genetic disruption of 2-arachidonoylglycerol synthesis reveals a key role for endocannabinoid signaling in anxiety modulation. Cell Rep 9:1644-1653.
Shonesy BC, Wang X, Rose KL, Ramikie TS, Cavener VS, Rentz T, Baucum AJ, 2nd, Jalan-Sakrikar N, Mackie K, Winder DG, Patel S, Colbran RJ (2013) CaMKII regulates diacylglycerol lipase-alpha and striatal endocannabinoid signaling. Nat Neurosci 16:456-463.
Sierra S, Luquin N, Navarro-Otano J (2017) The endocannabinoid system in cardiovascular function: novel insights and clinical implications. Clin Auton Res.
Simon GM, Cravatt BF (2006) Endocannabinoid biosynthesis proceeding through glycerophospho-N-acyl ethanolamine and a role for alpha/beta-hydrolase 4 in this pathway. J Biol Chem 281:26465-26472.

Simon GM, Cravatt BF (2008) Anandamide biosynthesis catalyzed by the phosphodiesterase GDE1 and detection of glycerophospho-N-acyl ethanolamine precursors in mouse brain. J Biol Chem 283:9341-9349.
Simon GM, Cravatt BF (2010) Characterization of mice lacking candidate N-acyl ethanolamine biosynthetic enzymes provides evidence for multiple pathways that contribute to endocannabinoid production in vivo. Mol Biosyst 6:1411-1418.
Singh PK (2013) Investigating the role of phosphorylation in the regulation of Diacylglycerol Lipase α/β activity. In: Wolfson Centre for Age-Related Diseases, p 284. London: King's College London.
Singh PK, Markwick R, Howell FV, Williams G, Doherty P (2016) A novel live cell assay to measure diacylglycerol lipase alpha activity. Biosci Rep 36.
Smart D, Gunthorpe MJ, Jerman JC, Nasir S, Gray J, Muir AI, Chambers JK, Randall AD, Davis JB (2000) The endogenous lipid anandamide is a full agonist at the human vanilloid receptor (hVR1). Br J Pharmacol 129:227-230.
Smith DR, Stanley CM, Foss T, Boles RG, McKernan K (2017) Rare genetic variants in the endocannabinoid system genes CNR1 and DAGLA are associated with neurological phenotypes in humans. PLoS One 12:e0187926.
Smith PB, Compton DR, Welch SP, Razdan RK, Mechoulam R, Martin BR (1994) The pharmacological activity of anandamide, a putative endogenous cannabinoid, in mice. J Pharmacol Exp Ther 270:219-227.
Snider NT, Walker VJ, Hollenberg PF (2010) Oxidation of the endogenous cannabinoid arachidonoyl ethanolamide by the cytochrome P450 monooxygenases: physiological and pharmacological implications. Pharmacol Rev 62:136-154.
Song B, Kibler PD, Endsley AN, Nayak SK, Galande AK, Jambunathan K (2015) Site-specific Substitutions Eliminate Aggregation Properties of Hemopressin. Chem Biol Drug Des 86:1433-1437.
Song CZ, Chang XJ, Bean KM, Proia MS, Knopf JL, Kriz RW (1999) Molecular characterization of cytosolic phospholipase A(2)-beta. Journal of Biological Chemistry 274:17063-17067.
Song ZH, Zhong M (2000) CB1 cannabinoid receptor-mediated cell migration. J Pharmacol Exp Ther 294:204-209.
Sophocleous A, Marino S, Kabir D, Ralston SH, Idris AI (2017a) Combined deficiency of the Cnr1 and Cnr2 receptors protects against age-related bone loss by osteoclast inhibition. Aging Cell 16:1051-1061.
Sophocleous A, Robertson R, Ferreira NB, McKenzie J, Fraser WD, Ralston SH (2017b) Heavy Cannabis Use Is Associated With Low Bone Mineral Density and an Increased Risk of Fractures. Am J Med 130:214-221.
Sousa-Valente J, Varga A, Ananthan K, Khajuria A, Nagy I (2014) Anandamide in primary sensory neurons: too much of a good thing? Eur J Neurosci 39:409-418.
Spano MS, Ellgren M, Wang X, Hurd YL (2007) Prenatal cannabis exposure increases heroin seeking with allostatic changes in limbic enkephalin systems in adulthood. Biol Psychiatry 61:554-563.
Stefano GB, Liu Y, Goligorsky MS (1996) Cannabinoid receptors are coupled to nitric oxide release in invertebrate immunocytes, microglia, and human monocytes. J Biol Chem 271:19238-19242.
Steffens M, Zentner J, Honegger J, Feuerstein TJ (2005) Binding affinity and agonist activity of putative endogenous cannabinoids at the human neocortical CB1 receptor. Biochem Pharmacol 69:169-178.
Steinberg SF (2008) Structural basis of protein kinase C isoform function. Physiol Rev 88:1341-1378.

Stella N, Piomelli D (2001) Receptor-dependent formation of endogenous cannabinoids in cortical neurons. Eur J Pharmacol 425:189-196.
Stella N, Schweitzer P, Piomelli D (1997) A second endogenous cannabinoid that modulates long-term potentiation. Nature 388:773-778.
Straiker A, Mitjavila J, Yin D, Gibson A, Mackie K (2015) Aiming for allosterism: Evaluation of allosteric modulators of CB1 in a neuronal model. Pharmacological research 99:370-376.
Sugiura T, Kobayashi Y, Oka S, Waku K (2002) Biosynthesis and degradation of anandamide and 2-arachidonoylglycerol and their possible physiological significance. Prostaglandins Leukot Essent Fatty Acids 66:173-192.
Sugiura T, Kishimoto S, Oka S, Gokoh M (2006) Biochemistry, pharmacology and physiology of 2-arachidonoylglycerol, an endogenous cannabinoid receptor ligand. Prog Lipid Res 45:405-446.
Sugiura T, Kondo S, Sukagawa A, Nakane S, Shinoda A, Itoh K, Yamashita A, Waku K (1995) 2-Arachidonoylgylcerol - a Possible Endogenous Cannabinoid Receptor-Ligand in Brain. Biochem Biophys Res Commun 215:89-97.
Sugiura T, Kondo S, Sukagawa A, Tonegawa T, Nakane S, Yamashita A, Ishima Y, Waku K (1996) Transacylase-mediated and phosphodiesterase-mediated synthesis of N-arachidonoylethanolamine, an endogenous cannabinoid-receptor ligand, in rat brain microsomes. Comparison with synthesis from free arachidonic acid and ethanolamine. Eur J Biochem 240:53-62.
Sugiura T, Kondo S, Kishimoto S, Miyashita T, Nakane S, Kodaka T, Suhara Y, Takayama H, Waku K (2000) Evidence that 2-arachidonoylglycerol but not N-palmitoylethanolamine or anandamide is the physiological ligand for the cannabinoid CB2 receptor. Comparison of the agonistic activities of various cannabinoid receptor ligands in HL-60 cells. J Biol Chem 275:605-612.
Sugiura T, Kodaka T, Nakane S, Miyashita T, Kondo S, Suhara Y, Takayama H, Waku K, Seki C, Baba N, Ishima Y (1999) Evidence that the cannabinoid CB1 receptor is a 2-arachidonoylglycerol receptor. Structure-activity relationship of 2-arachidonoylglycerol, ether-linked analogues, and related compounds. J Biol Chem 274:2794-2801.
Sun GY, Shelat PB, Jensen MB, He Y, Sun AY, Simonyi A (2010) Phospholipases A2 and inflammatory responses in the central nervous system. Neuromolecular Med 12:133-148.
Sun YX, Tsuboi K, Okamoto Y, Tonai T, Murakami M, Kudo I, Ueda N (2004) Biosynthesis of anandamide and N-palmitoylethanolamine by sequential actions of phospholipase A2 and lysophospholipase D. Biochem J 380:749-756.
Sundholm-Peters NL, Yang HK, Goings GE, Walker AS, Szele FG (2005) Subventricular zone neuroblasts emigrate toward cortical lesions. J Neuropathol Exp Neurol 64:1089-1100.
Sundman MH, Chen NK, Subbian V, Chou YH (2017) The bidirectional gut-brain-microbiota axis as a potential nexus between traumatic brain injury, inflammation, and disease. Brain Behav Immun 66:31-44.
Svendsen KB, Jensen TS, Bach FW (2004) Does the cannabinoid dronabinol reduce central pain in multiple sclerosis? Randomised double blind placebo controlled crossover trial. Bmj 329:253.
Swartz KJ (2008) Sensing voltage across lipid membranes. Nature 456:891-897.
Syed SK, Bui HH, Beavers LS, Farb TB, Ficorilli J, Chesterfield AK, Kuo MS, Bokvist K, Barrett DG, Efanov AM (2012) Regulation of GPR119 receptor activity with endocannabinoid-like lipids. Am J Physiol Endocrinol Metab 303:E1469-1478.

Szabo B, Dorner L, Pfreundtner C, Norenberg W, Starke K (1998) Inhibition of GABAergic inhibitory postsynaptic currents by cannabinoids in rat corpus striatum. Neuroscience 85:395-403.

Szlavicz E, Perera PS, Tomboly C, Helyes Z, Zador F, Benyhe S, Borsodi A, Bojnik E (2015) Further Characterization of Hemopressin Peptide Fragments in the Opioid and Cannabinoid Systems. Anesth Analg 121:1488-1494.

Takeda S, Elefteriou F, Levasseur R, Liu X, Zhao L, Parker KL, Armstrong D, Ducy P, Karsenty G (2002) Leptin regulates bone formation via the sympathetic nervous system. Cell 111:305-317.

Tam J, Ofek O, Fride E, Ledent C, Gabet Y, Muller R, Zimmer A, Mackie K, Mechoulam R, Shohami E, Bab I (2006) Involvement of neuronal cannabinoid receptor CB1 in regulation of bone mass and bone remodeling. Mol Pharmacol 70:786-792.

Tam J, Trembovler V, Di Marzo V, Petrosino S, Leo G, Alexandrovich A, Regev E, Casap N, Shteyer A, Ledent C, Karsak M, Zimmer A, Mechoulam R, Yirmiya R, Shohami E, Bab I (2008) The cannabinoid CB1 receptor regulates bone formation by modulating adrenergic signaling. Faseb J 22:285-294.

Tanimura A, Uchigashima M, Yamazaki M, Uesaka N, Mikuni T, Abe M, Hashimoto K, Watanabe M, Sakimura K, Kano M (2012) Synapse type-independent degradation of the endocannabinoid 2-arachidonoylglycerol after retrograde synaptic suppression. Proc Natl Acad Sci U S A 109:12195-12200.

Tanimura A, Yamazaki M, Hashimotodani Y, Uchigashima M, Kawata S, Abe M, Kita Y, Hashimoto K, Shimizu T, Watanabe M, Sakimura K, Kano M (2010) The endocannabinoid 2-arachidonoylglycerol produced by diacylglycerol lipase alpha mediates retrograde suppression of synaptic transmission. Neuron 65:320-327.

Tao R, Yu Y, Zhang X, Guo Y, Shi J, Zhang X, Xie L, Liu S, Ju G, Xu Q, Shen Y, Wei J (2005) Cytosolic PLA2 genes possibly contribute to the etiology of schizophrenia. Am J Med Genet B Neuropsychiatr Genet 137B:56-58.

Taschler U, Radner FP, Heier C, Schreiber R, Schweiger M, Schoiswohl G, Preiss-Landl K, Jaeger D, Reiter B, Koefeler HC, Wojciechowski J, Theussl C, Penninger JM, Lass A, Haemmerle G, Zechner R, Zimmermann R (2011) Monoglyceride lipase deficiency in mice impairs lipolysis and attenuates diet-induced insulin resistance. J Biol Chem 286:17467-17477.

Terrazzino S, Berto F, Dalle Carbonare M, Fabris M, Guiotto A, Bernardini D, Leon A (2004) Stearoylethanolamide exerts anorexic effects in mice via down-regulation of liver stearoyl-coenzyme A desaturase-1 mRNA expression. Faseb J 18:1580-1582.

Thul PJ et al. (2017) A subcellular map of the human proteome. Science 356.

Toczek M, Malinowska B (2018) Enhanced endocannabinoid tone as a potential target of pharmacotherapy. Life Sci.

Toniolo EF, Maique ET, Ferreira WA, Jr., Heimann AS, Ferro ES, Ramos-Ortolaza DL, Miller L, Devi LA, Dale CS (2014) Hemopressin, an inverse agonist of cannabinoid receptors, inhibits neuropathic pain in rats. Peptides 56:125-131.

Tortoriello G, Rhodes BP, Takacs SM, Stuart JM, Basnet A, Raboune S, Widlanski TS, Doherty P, Harkany T, Bradshaw HB (2013) Targeted lipidomics in Drosophila melanogaster identifies novel 2-monoacylglycerols and N-acyl amides. PLoS One 8:e67865.

Tsuboi K, Okamoto Y, Ikematsu N, Inoue M, Shimizu Y, Uyama T, Wang J, Deutsch DG, Burns MP, Ulloa NM, Tokumura A, Ueda N (2011) Enzymatic formation of N-acylethanolamines from N-acylethanolamine plasmalogen through N-acylphosphatidylethanolamine-hydrolyzing phospholipase D-dependent and -independent pathways. Biochim Biophys Acta 1811:565-577.

Turcotte C, Chouinard F, Lefebvre JS, Flamand N (2015) Regulation of inflammation by cannabinoids, the endocannabinoids 2-arachidonoyl-glycerol and arachidonoyl-ethanolamide, and their metabolites. J Leukoc Biol.

Ueda H, Kobayashi T, Kishimoto M, Tsutsumi T, Okuyama H (1993) A possible pathway of phosphoinositide metabolism through EDTA-insensitive phospholipase A1 followed by lysophosphoinositide-specific phospholipase C in rat brain. J Neurochem 61:1874-1881.

Ueda N, Liu Q, Yamanaka K (2001) Marked activation of the N-acylphosphatidylethanolamine-hydrolyzing phosphodiesterase by divalent cations. Biochim Biophys Acta 1532:121-127.

Ueda N, Tsuboi K, Uyama T (2010) Enzymological studies on the biosynthesis of N-acylethanolamines. Biochim Biophys Acta 1801:1274-1285.

Ueda N, Tsuboi K, Uyama T (2013) Metabolism of endocannabinoids and related N-acylethanolamines: canonical and alternative pathways. Febs J 280:1874-1894.

Ueda N, Puffenbarger RA, Yamamoto S, Deutsch DG (2000) The fatty acid amide hydrolase (FAAH). Chem Phys Lipids 108:107-121.

Ueda N, Tsuboi K, Uyama T, Ohnishi T (2011) Biosynthesis and degradation of the endocannabinoid 2-arachidonoylglycerol. Biofactors 37:1-7.

Uhlen M et al. (2015) Proteomics. Tissue-based map of the human proteome. Science 347:1260419.

Urquhart P, Nicolaou A, Woodward DF (2015) Endocannabinoids and their oxygenation by cyclo-oxygenases, lipoxygenases and other oxygenases. Biochim Biophys Acta 1851:366-376.

Uyama T, Tsuboi K, Ueda N (2017) An involvement of phospholipase A/acyltransferase family proteins in peroxisome regulation and plasmalogen metabolism. FEBS Lett 591:2745-2760.

Uyama T, Ikematsu N, Inoue M, Shinohara N, Jin XH, Tsuboi K, Tonai T, Tokumura A, Ueda N (2012) Generation of N-acylphosphatidylethanolamine by members of the phospholipase A/acyltransferase (PLA/AT) family. J Biol Chem 287:31905-31919.

Uyama T, Inoue M, Okamoto Y, Shinohara N, Tai T, Tsuboi K, Inoue T, Tokumura A, Ueda N (2013) Involvement of phospholipase A/acyltransferase-1 in N-acylphosphatidylethanolamine generation. Biochim Biophys Acta 1831:1690-1701.

Vadodaria KC, Jessberger S (2014) Functional neurogenesis in the adult hippocampus: then and now. Front Neurosci 8:55.

Valverde O, Torrens M (2012) CB1 receptor-deficient mice as a model for depression. Neuroscience 204:193-206.

van der Lee MM, Blomenrohr M, van der Doelen AA, Wat JW, Smits N, Hanson BJ, van Koppen CJ, Zaman GJ (2009) Pharmacological characterization of receptor redistribution and beta-arrestin recruitment assays for the cannabinoid receptor 1. J Biomol Screen 14:811-823.

van der Stelt M, Di Marzo V (2005a) Anandamide as an intracellular messenger regulating ion channel activity. Prostaglandins Other Lipid Mediat 77:111-122.

van der Stelt M, Di Marzo V (2005b) Cannabinoid receptors and their role in neuroprotection. Neuromolecular Med 7:37-50.

van der Stelt M, van Kuik JA, Bari M, van Zadelhoff G, Leeflang BR, Veldink GA, Finazzi-Agro A, Vliegenthart JF, Maccarrone M (2002) Oxygenated metabolites of anandamide and 2-arachidonoylglycerol: conformational analysis and interaction with cannabinoid receptors, membrane transporter, and fatty acid amide hydrolase. J Med Chem 45:3709-3720.

van der Stelt M, Veldhuis WB, van Haaften GW, Fezza F, Bisogno T, Bar PR, Veldink GA, Vliegenthart JF, Di Marzo V, Nicolay K (2001) Exogenous anandamide protects rat brain against acute neuronal injury in vivo. J Neurosci 21:8765-8771.

Van Sickle MD, Duncan M, Kingsley PJ, Mouihate A, Urbani P, Mackie K, Stella N, Makriyannis A, Piomelli D, Davison JS, Marnett LJ, Di Marzo V, Pittman QJ, Patel KD, Sharkey KA (2005) Identification and functional characterization of brainstem cannabinoid CB2 receptors. Science 310:329-332.

Varma N, Carlson GC, Ledent C, Alger BE (2001) Metabotropic glutamate receptors drive the endocannabinoid system in hippocampus. J Neurosci 21:RC188.

Vellani V, Petrosino S, De Petrocellis L, Valenti M, Prandini M, Magherini PC, McNaughton PA, Di Marzo V (2008) Functional lipidomics. Calcium-independent activation of endocannabinoid/endovanilloid lipid signalling in sensory neurons by protein kinases C and A and thrombin. Neuropharmacology 55:1274-1279.

Viader A, Ogasawara D, Joslyn CM, Sanchez-Alavez M, Mori S, Nguyen W, Conti B, Cravatt BF (2016) A chemical proteomic atlas of brain serine hydrolases identifies cell type-specific pathways regulating neuroinflammation. Elife 5:e12345.

Walsh FS, Doherty P (1997) Neural cell adhesion molecules of the immunoglobulin superfamily: role in axon growth and guidance. Annu Rev Cell Dev Biol 13:425-456.

Walter L, Stella N (2003) Endothelin-1 increases 2-arachidonoyl glycerol (2-AG) production in astrocytes. Glia 44:85-90.

Walter L, Dinh T, Stella N (2004) ATP induces a rapid and pronounced increase in 2-arachidonoylglycerol production by astrocytes, a response limited by monoacylglycerol lipase. J Neurosci 24:8068-8074.

Walter L, Franklin A, Witting A, Moller T, Stella N (2002) Astrocytes in culture produce anandamide and other acylethanolamides. J Biol Chem 277:20869-20876.

Wang J, Ueda N (2009) Biology of endocannabinoid synthesis system. Prostaglandins Other Lipid Mediat 89:112-119.

Wang X, Dow-Edwards D, Keller E, Hurd YL (2003) Preferential limbic expression of the cannabinoid receptor mRNA in the human fetal brain. Neuroscience 118:681-694.

Wang Z, Gerstein M, Snyder M (2009) RNA-Seq: a revolutionary tool for transcriptomics. Nat Rev Genet 10:57-63.

Watson S, Chambers D, Hobbs C, Doherty P, Graham A (2008) The endocannabinoid receptor, CB1, is required for normal axonal growth and fasciculation. Mol Cell Neurosci 38:89-97.

Watson SJ, Benson JA, Jr., Joy JE (2000) Marijuana and medicine: assessing the science base: a summary of the 1999 Institute of Medicine report. Arch Gen Psychiatry 57:547-552.

Wilkerson JL, Donvito G, Grim TW, Abdullah RA, Ogasawara D, Cravatt BF, Lichtman AH (2017) Investigation of Diacylglycerol Lipase Alpha Inhibition in the Mouse Lipopolysaccharide Inflammatory Pain Model. J Pharmacol Exp Ther 363:394-401.

Williams EJ, Walsh FS, Doherty P (1994a) The production of arachidonic acid can account for calcium channel activation in the second messenger pathway underlying neurite outgrowth stimulated by NCAM, N-cadherin, and L1. J Neurochem 62:1231-1234.

Williams EJ, Walsh FS, Doherty P (2003) The FGF receptor uses the endocannabinoid signaling system to couple to an axonal growth response. J Cell Biol 160:481-486.

Williams EJ, Furness J, Walsh FS, Doherty P (1994b) Characterisation of the second messenger pathway underlying neurite outgrowth stimulated by FGF. Development 120:1685-1693.

Williams EJ, Furness J, Walsh FS, Doherty P (1994c) Activation of the FGF receptor underlies neurite outgrowth stimulated by L1, N-CAM, and N-cadherin. Neuron 13:583-594.

Williams J, Wood J, Pandarinathan L, Karanian DA, Bahr BA, Vouros P, Makriyannis A (2007) Quantitative method for the profiling of the endocannabinoid metabolome by LC-atmospheric pressure chemical ionization-MS. Anal Chem 79:5582-5593.

Wilson RI, Nicoll RA (2001) Endogenous cannabinoids mediate retrograde signalling at hippocampal synapses. Nature 410:588-592.

Wu CS, Zhu J, Wager-Miller J, Wang S, O'Leary D, Monory K, Lutz B, Mackie K, Lu HC (2010) Requirement of cannabinoid CB(1) receptors in cortical pyramidal neurons for appropriate development of corticothalamic and thalamocortical projections. Eur J Neurosci 32:693-706.

Xapelli S, Agasse F, Grade S, Bernardino L, Ribeiro FF, Schitine CS, Heimann AS, Ferro ES, Sebastiao AM, De Melo Reis RA, Malva JO (2014) Modulation of subventricular zone oligodendrogenesis: a role for hemopressin? Front Cell Neurosci 8:59.

Xapelli S, Agasse F, Sarda-Arroyo L, Bernardino L, Santos T, Ribeiro FF, Valero J, Braganca J, Schitine C, de Melo Reis RA, Sebastiao AM, Malva JO (2013) Activation of type 1 cannabinoid receptor (CB1R) promotes neurogenesis in murine subventricular zone cell cultures. PLoS One 8:e63529.

Yamaguchi S, Mase T, Takeuchi K (1991) Cloning and structure of the mono- and diacylglycerol lipase-encoding gene from Penicillium camembertii U-150. Gene 103:61-67.

Yoshida T, Fukaya M, Uchigashima M, Miura E, Kamiya H, Kano M, Watanabe M (2006) Localization of diacylglycerol lipase-alpha around postsynaptic spine suggests close proximity between production site of an endocannabinoid, 2-arachidonoyl-glycerol, and presynaptic cannabinoid CB1 receptor. J Neurosci 26:4740-4751.

Yoshino H, Miyamae T, Hansen G, Zambrowicz B, Flynn M, Pedicord D, Blat Y, Westphal RS, Zaczek R, Lewis DA, Gonzalez-Burgos G (2011) Postsynaptic diacylglycerol lipase mediates retrograde endocannabinoid suppression of inhibition in mouse prefrontal cortex. J Physiol 589:4857-4884.

Yu H, Watt H, Mohan S (2014) The negative impact of traumatic brain injury (TBI) on bone in a mouse model. Brain Inj 28:244-251.

Yuan D, Wu Z, Wang Y (2016) Evolution of the diacylglycerol lipases. Prog Lipid Res 64:85-97.

Zarate J, Churruca I, Echevarria E, Casis L, Lopez de Jesus M, Saenz del Burgo L, Salles J (2008) Immunohistochemical localization of CB1 cannabinoid receptors in frontal cortex and related limbic areas in obese Zucker rats: effects of chronic fluoxetine treatment. Brain Res 1236:57-72.

Zhang L, Kolaj M, Renaud LP (2015) Intracellular postsynaptic cannabinoid receptors link thyrotropin-releasing hormone receptors to TRPC-like channels in thalamic paraventricular nucleus neurons. Neuroscience 311:81-91.

Zhang L, Kolaj M, Renaud LP (2016a) Endocannabinoid 2-AG and intracellular cannabinoid receptors modulate a low-threshold calcium spike-induced slow depolarizing afterpotential in rat thalamic paraventricular nucleus neurons. Neuroscience 322:308-319.

Zhang R, Xie X (2012) Tools for GPCR drug discovery. Acta Pharmacol Sin 33:372-384.

Zhang RS, He Z, Jin WD, Wang R (2016b) Effects of the cannabinoid 1 receptor peptide ligands hemopressin, (m)RVD-hemopressin(alpha) and (m)VD-hemopressin(alpha) on memory in novel object and object location recognition tasks in normal young and Abeta1-42-treated mice. Neurobiol Learn Mem 134 Pt B:264-274.

Zhang Y, Chen KN, Sloan SA, Bennett ML, Scholze AR, O'Keeffe S, Phatnani HP, Guarnieri P, Caneda C, Ruderisch N, Deng SY, Liddelow SA, Zhang CL, Daneman R, Maniatis T, Barres BA, Wu JQ (2014) An RNA-Sequencing Transcriptome and Splicing Database of Glia, Neurons, and Vascular Cells of the Cerebral Cortex. Journal of Neuroscience 34:11929-11947.

Zhao C, Deng W, Gage FH (2008) Mechanisms and functional implications of adult neurogenesis. Cell 132:645-660.

Zhou Y, Falenta K, Lalli G (2014) Endocannabinoid signalling in neuronal migration. Int J Biochem Cell Biol 47:104-108.

Zhou Y, Howell FV, Glebov OO, Albrecht D, Williams G, Doherty P (2016) Regulated endosomal trafficking of Diacylglycerol lipase alpha (DAGLalpha) generates distinct cellular pools; implications for endocannabinoid signaling. Mol Cell Neurosci 76:76-86.

Zimmer A, Zimmer AM, Hohmann AG, Herkenham M, Bonner TI (1999) Increased mortality, hypoactivity, and hypoalgesia in cannabinoid CB1 receptor knockout mice. Proc Natl Acad Sci U S A 96:5780-5785.

Zygmunt PM, Petersson J, Andersson DA, Chuang H, Sorgard M, Di Marzo V, Julius D, Hogestatt ED (1999) Vanilloid receptors on sensory nerves mediate the vasodilator action of anandamide. Nature 400:452-457.